



The Role of Cortical Connectivity and Functional Network Analysis of Resting-State EEG in Transient Epileptic Amnesia (TEA)

LESLEY ANNE CHANDRA

A thesis submitted in partial fulfilment of the requirements of
Manchester Metropolitan University
for the degree of Doctor of Clinical Science.

Faculty of Science and Engineering
Manchester Metropolitan University
in collaboration with the University of Exeter

2024

Abstract

Transient epileptic amnesia (TEA) is an underdiagnosed sub-type of temporal lobe epilepsy, associated with recurrent amnesic episodes. There is also more persisting memory dysfunction in the form of accelerated long-term forgetting and autobiographical amnesia. EEG investigations form part of the diagnostic work-up but can often be inconclusive. The current research investigated whether resting-state EEG analysis using quantitative EEG and connectivity analysis could provide new insight into the underlying causes of memory dysfunction in TEA. To date, no research literature has utilised connectivity in resting-state EEG to investigate functional and effective connectivity within TEA.

Resting-state EEG recordings were acquired from the medical records of 28 patients diagnosed with TEA and compared to age and sex-matched healthy controls. Pre-processing and initial analysis were undertaken using MATLAB, and EEGLAB. Connectivity analysis used three connectivity measures: imaginary coherence, weighted phase lag index and phase transfer entropy. All connectivity analysis was performed using Brainstorm.

The results showed functional connectivity alterations across frontal-temporal, frontal-parietal, and temporal-parietal networks within beta, alpha and theta bands. Dysfunction of effective connectivity affecting theta frequencies was seen across all inter-regional networks. Finally, we confirmed that inter-ictal abnormalities were seen more frequently in an independent bi-temporal distribution and were more prevalent during non-REM sleep.

Our research has provided new evidence regarding functional and effective connectivity disturbances in people with TEA. We have demonstrated clear and consistent connectivity dysfunction within memory areas of the temporal lobes and memory networks extending within the cortex. The evidence supports the hypothesis that memory consolidation and recall networks are affected in TEA.

Acknowledgements

I would especially like to acknowledge my academic supervisor at Manchester Metropolitan University, Ian Loram, for his support, advice, and encouragement and for the scripts he created to help with data analysis. I would not have achieved this without his mentorship and guidance.

I would also like to acknowledge my collaborators in the TIME team at the University of Exeter and the University of Edinburgh: to Adam Zeman, who inspired the research idea, helped create a realistic proposal, and provided expert guidance throughout; to Mario Parra Rodriguez and Javier Escudero Rodriguez in Edinburgh who patiently guided my understanding of connectivity and networks analysis. Their advice and guidance have been invaluable, and I have learned so much.

Many thanks to the Neurophysiology Department at the Royal Devon University Hospitals NHS Foundations Trust (RDUH) for all their friendship and support whilst I have focussed on my DClSci and for recording the healthy control EEGs. Also, at RDUH, thanks to the EXTEND team, who helped to recruit suitable healthy volunteers.

Others who have helped me with this achievement have included the admin team and IT team at the University of Exeter, who assisted in getting me access to the TIME database, without which I could not have undertaken the research; those within the TIME team who have already undertaken extensive research which has guided my own work, the NHS Trusts and Neurophysiology departments who have taken the time to locate and send the EEG data.

I cannot close without thanking my husband, Kevin, for his patience (mostly!) and support through this long and, at times, tiring journey. He has been my inspiration and my conscience.

Lesley Chandra

Contents

Abstract	1
Acknowledgements.....	2
Abbreviations	7
Index of Figures.....	10
Index of Tables	17
Introduction	25
What is Electroencephalography (EEG)?.....	25
EEG: A Brief History	25
Overview of Neuronal Mechanisms underlying the EEG	26
Recording an EEG.....	27
Rhythms of the EEG	29
Identifying Abnormal Activities in EEG	34
Recognising Artifacts in EEG	37
EEG Rhythms and Quantitative EEG Analysis	38
Understanding Functional and Effective Network Analysis.....	40
The Different Types of Connectivity and their Uses.....	40
Choice of Connectivity Measure for EEG Analysis.....	42
Memory, Amnesia and Epilepsy.....	50
Memory	50
Amnesia	54
Memory Dysfunction in Temporal Lobe Epilepsy (TLE).....	55
An Overview of Transient Epileptic Amnesia (TEA)	57
Neuroimaging in TEA	61
Scalp EEG Findings in TEA	61

How has Connectivity Analysis been used Memory and Epilepsy Research?	64
Amnestic Syndromes	64
Alzheimer’s Disease (AD) and Mild Cognitive Impairment (MCI)	65
Temporal Lobe Epilepsy (TLE).....	66
Summary	67
Methods.....	69
Research Rationale	69
Research Aims	70
Research Methods Approach	71
Results.....	94
1. Age and Sex Demographics.....	94
1.1. Sex.....	94
1.2. Age	95
2. Visual EEG Analysis Results	99
3. mFREQ Results	101
4. mPSD Results	102
5. Connectivity Analysis – Consistent Findings.....	104
5.1. Global and Intra-Regional Connectivity Differences	104
5.2. Temporal-Frontal and Frontal-Parietal Connectivity	105
5.3. Other Inter-Regional Findings	108
5.4. Consistent Inter-Regional Hemispheric Findings	109
Discussion.....	113
Summary	113
Key Results.....	113
Interpretation.....	116

Reversal of Inter-Regional Theta Frequency Connectivity	118
Functional Connectivity Measure Differences within the Theta Band	123
Significances within Other Frequency Bands	125
mPSD Findings	125
Functional and Effective Connectivity Power within Beta and Alpha Frequency Bands	125
Effective Connectivity	126
Visual Analysis: Significance of sleep-related interictal abnormalities.	127
Implications	129
Limitations	130
Recommendations for Future Research	133
Conclusion	134
References	136
Appendix 1: MATLAB SCRIPTS	152
Resting IAF-Master Scripts (Corcoran <i>et al.</i> , 2018)	153
Appendix 2	171
Full Results	171
i) Mean Frequency (mFREQ)	171
ii) Mean Power (mPSD)	173
iii) Imaginary Coherence (iCoh) connectivity measure	177
iv) Weighted Phase-Lag Index (wPLI) Connectivity Measure	180
v) Phase-Transfer Entropy (PTE) Directional Connectivity Measure	182
First Phase – Spectral Analysis of Mean Frequency (mFREQ)	185
1. Global mFREQ– All Frequencies	185
2. Regional mFREQ – All Frequencies	190
Global mFREQ – Frequency Bands	196

3. Regional mFREQ – Frequency Bands	202
First Phase – Spectral Analysis of Mean Power (mPSD)	210
1. Global mPSD – All Frequencies	210
2. Regional mPSD – All Frequencies.....	214
3. Global mPSD – Frequency Bands	220
4. Regional mPSD – Frequency Bands.....	227
Second Phase – Connectivity Analysis – Imaginary Coherence (iCoh)	235
1. Global iCoh, All Frequencies.....	236
2. Intra-Regional and Inter-Regional iCoh, All Frequencies	238
3. Global iCoh – Frequency Bands.....	242
4. Intra-Regional iCoh – Frequency Bands	245
5. Inter-Regional iCoh – Frequency Bands	252
Second Phase – Connectivity Analysis – Weighted Phase Lag Index (wPLI)	264
1. Global wPLI, All Frequencies	265
2. Intra-Regional and Inter-Regional wPLI, All Frequencies.....	267
3. Global wPLI – Frequency Bands	272
4. Intra-Regional wPLI – Frequency Bands.....	274
5. Inter-Regional wPLI – Frequency Bands.....	281
Second Phase – Connectivity Analysis – Phase Transfer Entropy (PTE).....	290
1. Global PTE, All Frequencies	291
2. Intra-Regional and Inter-Regional PTE, All Frequencies	293
3. Global PTE – Frequency Bands	298
4. Intra-Regional PTE –Frequency Bands	301
5. Inter- Regional PTE –Frequency Bands	306

Abbreviations

AbA	Autobiographical amnesia
AED	Anti-epileptic drug
AH	Alzheimer's disease
Ai	Asymmetry index
ALF	Accelerated long-term forgetting
aMCI	Amnesic mild cognitive impairment
AVG	Average reference
BOLD	Blood oxygenation level dependent
Cf	Coherence function
CT	Computerised tomography
DMN	Default mode network
dMRI	Diffusion magnetic resonance imaging
DTI	Diffusion tensor imaging
ECG	Electrocardiogram
ECoG	Electrocorticography
EDF	European data format
EEG	Electroencephalography
EP	Evoked potential
EPSP	Excitatory post synaptic potential
ERP	Event-related potential
EXTEND	Exeter 10,000 project
FDR	False discovery rate
FFT	Fast Fourier transform

fMRI	Functional magnetic resonance imaging
HFF	High-frequency filter
Hz	Hertz
ICA	Independent component analysis
iCoh	Imaginary coherence
IED	Interictal epileptiform abnormality
IFCN	International Federation of Clinical Neurophysiology
IPSP	Inhibitory post synaptic potential
IQ	Intelligence quotient
IRAS	Integrated Research Application System
LFF	Low-frequency filter
LTM	Long-term monitoring
MCI	Mild cognitive impairment
MEG	Magnetoencephalography
mFREQ	Mean frequency
MI	Mutual information
MMU	Manchester Metropolitan University
MoCA	Montreal Cognitive Assessment scale
MREC	Multi Research Ethics Committee
MRI	Magnetic resonance imaging
NDMA	N-nitrosodimethylamine
NEA	Non-epileptiform abnormality
NHS	National Health Service
NIHR	National Institute for Health and Care Research
NREM	Non rapid eye movement sleep
N1	Non-REM stage 1

N2	Non-REM stage 2
PET	Positron emission tomography
PF	Peak frequency
PLI	Phase lag index
PPHG	Posterior para-hippocampal gyrus
PSD	Power spectral density
PSP	Postsynaptic potential
PTE	Phase transfer entropy
QEEG	Quantitative EEG
REC	Research Ethics Council
REM	Rapid eye movement sleep
REST	Reference electrode standardisation technique
ROI	Region of interest
rsEEG	resting-state electroencephalography
rsMRI	resting-state magnetic resonance imaging
TE	Transfer entropy
TEA	Transient Epileptic Amnesia
TGA	Transient global amnesia
TIME	The Impairment of Memory in Epilepsy
TLE	Temporal lobe epilepsy
UPI	Unique participant identifier
μV	Microvolts
wPLI	Weighted phase lag index

Index of Figures

Figure 1: Effect of pyramidal cell PSPS on EEG signal (Jackson and Bolger, 2014).....	27
Figure 2: The effect of activity location on dipoles Three cases of IED current inflow into a focal cortical patch are illustrated: (A) radial (dark blue), (B) oblique (pink), (C) tangential (red). Dipoles are depicted by arrows in light red to illustrate where they create positive and light blue where they create negative voltages (Scherg et al., 2019).	27
Figure 3: Placement of electrodes in 1958 IFCN 10-20 system A: Lateral, B: frontal, C: from the top (Seeck et al., 2017)	27
Figure 4: 2017 update to the IFCN 10-20 system. Additional electrode sites: F9, T9, P9 on the left and F10, T10, P10 on the right (Seeck et al., 2017)	28
Figure 5: An example of an average reference EEG montage in an anterior-posterior format, displaying typical negative and positive deflections relating to EEG at the scalp. EEG frequency bands are highlighted – Beta in an anterior distribution, alpha in a posterior distribution, underlying theta post-centrally, and underlying delta posteriorly in this example.....	30
Figure 6: Neural Code Organized by Theta and Gamma Oscillations. (A) Simultaneous extracellular (top) and intracellular (bottom) recordings from the hippocampus. Intracellular gamma is due to IPSPs, the amplitude of which is modulated by the phase of theta. (B) Schematic of the theta-gamma code. The ovals at top represent states of the same network during two gamma cycles (active cells are black and constitute the ensemble that codes for a particular item). Different ensembles are active in different gamma cycles. (Lisman and Jensen, 2013).	32
Figure 7: Infographic showing the 6 criteria for identifying IEDs by morphology. The upper representation shows 5 of the IFCN criteria in graphic form. “The voltage maps in window (6) show a tangential orientation (source in the left middle frontal gyrus) and a radial orientation (source in the left superior frontal gyrus); the irregular distribution of the potentials in the last voltage map does not imply a source in the brain (it was an artifact with sharp morphology) and does not fulfil this criterion; negative potentials are in blue, and positive potentials are in red”. (Kural et al., 2020).....	37
Figure 8: A concise list of common sources of EEG noise (Tatum, 2013b).....	38
Figure 9: Infographic depicting the common input problem and the "who's first" problem when using phase-based connectivity measures (Cohen, 2014)	43

Figure 10: The effect of electrode choice on a power spectral map of theta frequencies. From left to right, the references are left ear (LE), LM, AR and REST (Yao et al., 2019)	44
Figure 11: An overview of machine learning techniques and their related algorithms (Matlab, 2022)	49
Figure 12: Memory depicted as stages within memory processes (Stagnor, Accessed 2019)	51
Figure 13: Diagram of the brain structures thought to be especially important for each form of memory. In addition to its central role in emotional learning, the amygdala is able to modulate the strength of both declarative and nondeclarative memory. (Squire and Dede, 2015)	51
Figure 14: The hippocampus and associated structures (https://www.creative-diagnostics.com/blog/index.php/what-is-hippocampus/)	52
Figure 15: Schematic diagram of neuronal circuits involved in theta-gamma (θ - γ) coupling (Nuñez and Buño, 2021).	53
Figure 16: Example of a temporal lobe seizure with right hemisphere onset	62
Figure 17: Standardised electrode placements used for data analysis (EEG Instrumentation, Montage, Polarity, and Localization Neupsy Key)	82
Figure 18: Pre-processing guideline for EEGLAB (Delorme, 2019)	83
Figure 19: Female to Male Ratio for TEA and Healthy Cohorts	94
Figure 20: Boxplot of Age and Sex showing higher mean age in males.	95
Figure 21: Bar Chart of age profiles for TEA and HV cohorts using 3 age categories: $\leq 60y$, 61-70y, and 71y+.....	97
Figure 22: Scatter Plot showing a negative correlation between mean spectral power with increasing age.	98
Figure 23: Scatter Plot showing a negative correlation between global iCoh with increasing age.....	98
Figure 24: Pie Chart breakdown of the proportions of alertness levels seen across TEA EEGs	99
Figure 25: Percentages of epileptic and non-epileptic abnormalities by hemisphere location	100
Figure 26: Non-Epileptiform and Epileptiform Abnormality Occurrence Associated with Alertness Levels Obtained During the EEG	101
Figure 27: mPSD and global/regional connectivity findings (Red indicates increase in	103
Figure 28: Significant frontal-temporal/temporal-frontal connectivity alterations in the TEA cohort.....	106

Figure 29: Significant frontal-parietal/parietal-frontal connectivity alterations in the TEA cohort.....	107
Figure 30: Other significant inter-regional alterations in TEA.....	108
Figure 31: Summary of iCoh mean values for all frequency band within region and inter-regionally. F= frontal region, O= occipital region, P= parietal region, T=temporal region, TF= temporal-frontal networks, TO= temporal-occipital networks, TP= temporal-parietal networks. Significant findings are post FDR corrections and are labelled as follows: ** p= <0.001, * p= >0.001 but <0.05, and ! p= >0.05 prior to FDR correction but show significance following correction.....	110
Figure 32: Summary of wPLI mean values for all frequency band within region and inter-regionally. F= frontal region, O= occipital region, P= parietal region, T=temporal region, TF= temporal-frontal networks, TO= temporal-occipital networks, TP= temporal-parietal networks. Significant findings are post FDR corrections and are labelled as follows: ** p= <0.001, * p= >0.001 but <0.05, and ! p= >0.05 prior to FDR correction but show significance following correction.....	111
Figure 33: Summary of PTE mean values for all frequency band, showing directional networks between regions. TF= temporal to frontal networks, FT= frontal to temporal networks, TO= temporal to occipital networks, OT= occipital to Temporal networks, TP= temporal to parietal networks and PT= parietal to temporal networks. Significant findings are post FDR corrections and are labelled as follows: ** p= <0.001, * p= >0.001 but <0.05, and ! p= >0.05 prior to FDR correction but show significance following correction.....	111
Figure 34: INTER-REGIONAL Theta PTE - (dominance of network flow reversed compared to HV). TEA reversal of dominance of connectivity flow (compared to HV) marked with red arrows. Significant difference in TEA PTE (compared to HV) marked with red stars.....	114
Figure 35: The diagram shows the dominant directional connectivity strength of each frequency band. The dominant direction is signified by the direction of the arrows and has been determined by comparison of the mean value for PTE of each inter-regional. The thickness of the arrows represents the magnitude of the difference in means. The left side of each headstamp represents HV (blue arrows) and the right side TEA (orange arrows). TEA deviations from HV are marked with red arrows. Significant increases or decreases in TEA PTE are marked with stars (pink and blue respectively). The flow patterns are represented for each band: beta, alpha, theta, delta.	119

Figure 36: Diagrammatic representation of the effective connections within the neural network mediating AM retrieval. Arrow thickness represents the strength of the connection (i.e. the value of the path coefficient), as described in the key (Addis et al., 2007)	120
Figure 37: Brain regions associated with recollective memory - a widely distributed network that is selectively sensitive to recollection (Xu et al., 2020).....	120
Figure 38: 18F-FDG-PET findings in TEA patients compared to healthy volunteers (Mosbah et al., 2014)	121
Figure 39: A - a graphical depiction of key brain regions involved in the retrieval of specific autobiographical memories. Ventromedial (vm) and dorsomedial (dm) regions of the prefrontal cortex (PFC) as well as the orbitofrontal cortex (OFC), anterior cingulate, and amygdala play an important role in the processing of self-referential information and in assigning and regulating emotional salience. Temporal regions such as the hippocampus and parahippocampus, and occipital regions such as the cuneus and precuneus, also play an important role in the re-experiencing of the self-relevant sensory, contextual, and temporal details which characterise specific autobiographical memories. Finally, dorsolateral (dl) and ventrolateral (vl) PFC regions enable the controlled retrieval and construction of a memory whilst irrelevant thoughts and memories are inhibited. (Barry et al., 2018). B – a graphical depiction of key brain areas involved in wider episodic memory processing (Stampacchia et al., 2018)	123
Figure 40: Schematic of sleep architecture in humans and associated oscillatory activity and stages of memory consolidation. (A) Sleep stages N2 and SWS are most prominent during the first half of the sleep period and are dominated by thalamic sleep spindles and neocortical slow oscillations (SOs). REM sleep is most prominent during the second half of the sleep period and characterised by ponto-geniculo-occipital waves, increased acetylcholine (ACh) and cortical theta oscillations (reproduced from Vorster and Born, 2015; permission to reuse image is not required from the copyright holder for non-commercial use as determined by RightsLink R). (B) The cyclic occurrence of SWS and REM throughout sleep facilitates memory consolidation. The hierarchical nesting of ripples and spindles within the up state of SOs during SWS facilitates the transfer of information from the hippocampal complex to the neocortex. The neocortically distributed memory representations are strengthened by REM theta oscillations and increases in ACh (Cross et al., 2018).	128
Figure 41: Graphic description of type I and type II statistical errors	130
Figure 42: Mean Frequency Distribution: Comparison across TEA and HV cohorts	171

Figure 43: As expected, mean frequency shows a close correlation across frequency bands.
173

Figure 44: mPSD distribution by cohort.....173

Figure 45: Mean power differences across regions.....175

Figure 46: Inter-hemisphere differences for mean power. Note the split dataset over temporal regions (the analysis is not side-specific regarding asymmetry). 2.0000 represents symmetry between hemispheres.175

Figure 47: Variation of mean spectral power within frequency bands.176

Figure 48: *Inter-hemisphere mean power difference within frequency bands (2.0000 represents symmetry between the hemispheres. Note the split dataset in the delta frequency band).*176

Figure 49: Imaginary Coherence (iCoh), high level distribution across TEA and HV cohorts (all frequencies, all regions).....177

Figure 50: iCoh split by region and by cohort.179

Figure 51: iCoh within frequency band, split by Cohort - Left =HV, Right=TEA179

Figure 52: wPLI high level distribution across TEA and HV cohorts (all frequencies, all regions)180

Figure 53: wPLI regional split by cohort. Left: intra-regional and Right: inter-regional.....181

Figure 54: wPLI within frequency band, split by Cohort - Left =HV, Right=TEA182

Figure 55: PTE high level distribution across TEA and HV cohorts (all frequencies, all regions)182

Figure 56: PTE regional split by cohort. Left: intra-regional and Right: inter-regional184

Figure 57: PTE within frequency band, split by Cohort - Left =HV, Right=TEA.....184

Figure 58: Global mFREQ distribution by cohort187

Figure 59: Global inter-hemispheric mFREQ difference distributions (log) by cohort. +ve values denote a left hemisphere bias and -ve values a right hemisphere bias.....188

Figure 60: Boxplots for HV and TEA Regional mFREQ190

Figure 61: Boxplots for HV and TEA Regional Interhemispheric mFREQ Differences193

Figure 62: Boxplots for HV and TEA Global mFREQ within the beta, alpha, theta, and delta EEG bands196

Figure 63: Boxplots for HV and TEA Global Interhemispheric mFREQ Difference within beta, alpha, theta, and delta EEG bands.....199

Figure 64: Boxplots for HV and TEA Regional Mean Frequencies within beta, alpha, theta, and delta EEG bands203

Figure 65: Boxplots for HV and TEA Regional Interhemispheric mFREQ Differences within beta, alpha, theta, and delta EEG bands	206
Figure 66: Global PSD distribution by cohort	211
Figure 67: Global inter-hemispheric mPSD difference distributions by cohort. +ve values denote a left hemisphere bias and -ve values a right hemisphere bias.....	211
Figure 68 :Boxplots for HV and TEA Regional mPSD Values	214
Figure 69: Boxplots for HV and TEA Regional Interhemispheric mPSD Differences	217
Figure 70: Boxplots for HV and TEA Global mPSD within beta, alpha, theta, and delta EEG bands.....	220
Figure 71: Boxplots for HV and TEA Global Inter-hemispheric mPSD Difference within beta, alpha, theta, and delta EEG bands.....	223
Figure 72: Boxplots for HV and TEA Regional mPSD within the beta, alpha, theta, and delta EEG bands	227
Figure 73: Boxplots for HV and TEA Regional Interhemispheric mPSD Differences within beta, alpha, theta, and delta EEG bands	230
Figure 74: Boxplots for TEA and HV iCoh at Global level, all frequencies (1-40Hz)	236
Figure 75: Intra-Regional iCoh Boxplot, all frequencies (1-40Hz).....	238
Figure 76: Inter-Regional iCoh Boxplot, all frequencies (1-40Hz).....	240
Figure 77: Boxplots for global iCoh, by frequency band. Top left - beta, top right - alpha, bottom left - theta, bottom right - delta.	242
Figure 78: Boxplots for regional iCoh, by frequency band. Top left - beta, top right - alpha, bottom left - theta, bottom right - delta.	245
Figure 79: Boxplots for inter-regional iCoh, by frequency band. Top left - beta, top right - alpha, bottom left - theta, bottom right - delta.	253
Figure 80: Boxplots for TEA and HV wPLI at Global level, all frequencies (1-40Hz)	265
Figure 81: Intra-Regional wPLI Boxplot, all frequencies (1-40Hz)	267
Figure 82: Inter-Regional wPLI Boxplot, all frequencies (1-40Hz)	269
Figure 83: Boxplots for global wPLI, by frequency band. Top left - beta, top right - alpha, bottom left - theta, bottom right - delta.	272
Figure 84: Boxplots for regional wPLI, by frequency band. Top left - beta, top right - alpha, bottom left - theta, bottom right - delta.	274
Figure 85: Boxplots for inter-regional wPLI, by frequency band. Top left - beta, top right - alpha, bottom left - theta, bottom right - delta.	281

Figure 86: Boxplots for global Phase Transfer Entropy data by condition, all frequencies (1-40Hz)	291
Figure 87: Intra-Regional PTE Boxplot, all frequencies (1-40Hz).....	293
Figure 88: Inter-Regional PTE Boxplot, all frequencies (1-40Hz).....	295
Figure 89: Boxplots for global PTE, by frequency band. Top left - beta, top right - alpha, bottom left - theta, bottom right - delta.	298
Figure 90: Boxplots for regional PTE, by frequency band. Top left - beta, top right - alpha, bottom left - theta, bottom right - delta.	301
Figure 91: Boxplots for inter-regional PTE, by frequency band. Top left - beta, top right - alpha, bottom left - theta, bottom right - delta.	306
Figure 92: Paradoxical effect of higher PTE magnitude in the temporal to frontal networks, compared to frontal to temporal networks.	310

Index of Tables

Table 1: Comparison of methods for quantifying brain connectivity using EEG (Cao et al., 2022)	45
Table 2: Clinical, EEG and neuropsychological features from a cohort of 10 TEA subjects (Zeman et al., 1998b)	59
Table 3: Count of Participants for TEA and Healthy Cohorts.....	94
Table 4: Age comparison across TEA and HV cohorts with Age broken down into 3 categories: <= 60y, 61-70y and 71y +	96
Table 5: Pearson Chi-Square tests comparing age profiles across TEA and HV cohorts using age categories: <= 60y, 61-70y and 71y+	97
Table 6: Pearson Correlations between alertness levels and occurrence of NEA and EA.....	101
Table 7: Normality Tests for Mean Frequency, Mean Power, Interhemispheric Mean Frequency difference, and Interhemispheric Mean Power Difference.....	172
Table 8: Data descriptors for Mean Frequency, Mean Power, Interhemispheric Mean Frequency difference, and Interhemispheric Mean Power Difference.....	172
Table 9: Comparison of mPSD by Sex (M/F)	174
Table 10: Data descriptors for imaginary coherence (iCoh)	178
Table 11: Normality Tests for iCoh	178
Table 12: Tests for Normality - wPLI	180
Table 13: Data descriptors for wPLI	181
Table 14: Data descriptors for PTE	183
Table 15: Tests for Normality - PTE data by cohort	183
Table 16: Global Datasets: Shapiro-Wilk tests for normality. mFREQ and mPSD data.	185
Table 17: Global Datasets - Distribution Descriptors. mFREQ and mPSD data.	186
Table 18: Statistical analysis of TEA vs. HV global mFREQ. Mann-Whitney U test.	187
Table 19: Normality tests for Interhemispheric difference of mFREQ (includes frontal, temporal, parietal and occipital regions).....	188
Table 20: Data Descriptors for Interhemispheric difference in mFREQ	189
Table 21: Statistical analysis of TEA vs. HV global inter-hemispheric mFREQ difference. Mann-Whitney U test.	189
Table 22: Tests for Normality for Regional mFREQ Data Distributions	190
Table 23: Regional Datasets – mFREQ Distribution Descriptors	191

Table 24: Regional mFREQ - Multiple Comparisons using False Discovery Rates (FDRs) Adjustments	192
Table 25: Regional Datasets – Interhemispheric mFREQ Difference Descriptors	193
Table 26: Tests for Normality for Regional Interhemispheric mFREQ Difference Distributions	194
Table 27: Regional Interhemispheric mFREQ Differences - Multiple Comparisons using False Discovery Rates (FDRs) Adjustments	195
Table 28: Tests for Normality for Global mFREQ Data within EEG Bands	196
Table 29: Global Datasets – mFREQ within EEG Bands, Distribution Descriptors	197
Table 30: Global mFREQ per EEG Band - Multiple Comparisons using False Discovery Rates (FDRs) Adjustments	198
Table 31: Tests for Normality for Global Inter-hemispheric mFREQ Data within EEG Bands	199
Table 32: Global Datasets – Inter-hemispheric mFREQ Difference within EEG Bands, Distribution Descriptors	200
Table 33: Global Inter-hemispheric mFREQ Difference per EEG Band - Multiple Comparisons using False Discovery Rates (FDRs) Adjustments	201
Table 34: Regional Datasets – mFREQ within EEG Bands, Distribution Descriptors	202
Table 35: Tests for Normality for Regional Mean Frequency Data within EEG Bands	204
Table 36: Regional mFREQ per EEG Band - Multiple Comparisons using False Discovery Rates (FDRs) Adjustments	205
Table 37: Regional Datasets – Interhemispheric mFREQ Difference within EEG Bands, Distribution Descriptors	207
Table 38: Tests for Normality for Regional Interhemispheric mFREQ Difference Data within EEG Bands	209
Table 39: Regional Interhemispheric mFREQ Difference per EEG Band - Multiple Comparisons using False Discovery Rates (FDRs) Adjustments	209
Table 40: Normality tests for Interhemispheric difference of mPSD (includes frontal, temporal, parietal, and occipital regions)	212
Table 41: Data Descriptors for Interhemispheric difference in mPSD. Below: Mann Witney U test Global mPSD	212
Table 42: Statistical analysis of TEA vs. HV global inter-hemispheric mPSD difference. Mann-Whitney U test.	213
Table 43: Tests for Normality for Regional mPSD Data Distributions	214

Table 44: Regional Datasets – mPSD Distribution Descriptors.....	215
Table 45: Regional mPSD - Multiple Comparisons using False Discovery Rates (FDRs) Adjustments.....	216
Table 46: Tests for Normality for Regional Interhemispheric mPSD Difference Distributions	217
Table 47: Regional Datasets – Interhemispheric mPSD Difference Descriptors	218
Table 48: Mean and Median values for TEA and HV cohorts - mPSD temporal inter-hemisphere analysis.....	219
Table 49: T-test results for mPSD temporal inter-hemisphere analysis.....	220
Table 50: Regional Interhemispheric mPSD Differences - Multiple Comparisons using False Discovery Rates (FDRs) Adjustments	220
Table 51: Tests for Normality for Global mPSD Data within EEG Bands	221
Table 52: Global Datasets – PSD within EEG Bands, Distribution Descriptors	221
Table 53: Global mPSD per EEG Band - Multiple Comparisons using False Discovery Rates (FDRs) Adjustments.....	223
Table 54: Tests for Normality for Global Inter-hemispheric mPSD Data within EEG Bands ..	224
Table 55: Global Datasets – Inter-hemispheric mPSD Difference within EEG Bands, Distribution Descriptors.....	224
Table 56: Global Inter-hemispheric PSD Difference per EEG Band - Multiple Comparisons using False Discovery Rates (FDRs) Adjustments	226
Table 57: Regional Datasets – mPSD within EEG Bands, Distribution Descriptors	228
Table 58: Tests for Normality for Regional mPSD Data within EEG Bands.....	229
Table 59: Regional mPSD per EEG Band - Multiple Comparisons using False Discovery Rates (FDRs) Adjustments.....	229
Table 60: Regional Datasets – Interhemispheric mPSD Difference within EEG Bands, Distribution Descriptors.....	231
Table 61: Tests for Normality for Regional Interhemispheric mPSD Difference Data within EEG Bands	232
Table 62: Mean and Median values for TEA and HV cohorts - mPSD temporal inter-hemisphere analysis. Right: Theta frequencies. Left: Delta frequencies.	232
Table 63: Mann Whitney-U test results for mPSD temporal inter-hemisphere analysis, theta frequencies.	233
Table 64: T- test results for mPSD temporal inter-hemisphere analysis, delta frequencies.	233

Table 65: Regional Interhemispheric mPSD Difference per EEG Band - Multiple Comparisons using False Discovery Rates (FDRs) Adjustments	234
Table 66: Tests of Normality for global iCoh, all frequencies (1-40Hz)	236
Table 67: Descriptives for global iCoh, all frequencies (1-40Hz)	237
Table 68: Significant Non-Parametric Findings for Global iCoh.....	237
Table 69: Global iCoh Mean/Median values for TEA and HV cohorts, with lower values for TEA (marked in blue).....	237
Table 70: Tests for normality for Regional iCoh, all frequencies (1-40Hz).....	239
Table 71: Data descriptives for regional iCoh, all frequencies (1-40Hz).....	239
Table 72: FDR q-values for Intra-Regional iCoh, AllFreq.....	239
Table 73: Data descriptives for inter-regional iCoh, all frequencies (1-40Hz).....	241
Table 74: Tests for normality for inter-regional iCoh, all frequencies (1-40Hz).....	241
Table 75: FDR q-values for Inter-Regional iCoh, AllFreq.....	241
Table 76: Data descriptives for global iCoh, by frequency band.	243
Table 77: Tests for normality for global iCoh, by frequency band.	243
Table 78: FDR q-values for Global iCoh within Frequency Bands. Lower mean iCoh in the TEA cohort is marked in blue.	244
Table 79: Descriptives for regional iCoh by frequency band. Top left - frontal, top right - occipital, bottom left - parietal, bottom right – temporal.....	249
Table 80: Tests of normality for regional iCoh by frequency band. Top left - frontal, top right - occipital, bottom left - parietal, bottom right – temporal.	250
Table 81: FDR q-values for Intra-Regional iCoh within Frequency Bands. Lower mean iCoh in the TEA cohort is marked in blue.....	250
Table 82: FDR q-values for Intra-Regional iCoh within Frequency Bands (split by hemisphere, and inter-hemisphere). Lower mean iCoh in the TEA cohort is marked in blue.	251
Table 83: Data descriptives for inter-regional iCoh between temporal and frontal regions, by frequency band	254
Table 84: Tests of normality for inter-regional iCoh between temporal and frontal regions, by frequency band.	255
Table 85: Data descriptives for inter-regional iCoh between temporal and occipital regions, by frequency band	256
Table 86: Tests of normality for inter-regional iCoh between temporal and occipital regions, by frequency band	257

Table 87: Data descriptives for inter-regional iCoh between temporal and parietal regions, by frequency band	258
Table 88: Tests of normality for inter-regional iCoh between temporal and parietal regions, by frequency band	258
Table 89: Data descriptives for inter-regional iCoh between frontal and parietal regions, by frequency band	259
Table 90: Tests of normality for inter-regional iCoh between frontal and parietal regions, by frequency band	260
Table 91: FDR q-values for Inter-Regional iCoh within Frequency Bands. Lower mean iCoh in the TEA cohort is marked in blue.....	260
Table 92: FDR q-values for iCoh between Temporal and Frontal regions, within Frequency Bands (split by hemisphere, and inter-hemisphere). Lower mean iCoh in the TEA cohort is marked in blue.	261
Table 93: FDR q-values for iCoh between Temporal and Occipital regions, within Frequency Bands (split by hemisphere, and inter-hemisphere)	262
Table 94: FDR q-values for iCoh between Temporal and Parietal regions, within Frequency Bands (split by hemisphere, and inter-hemisphere)	262
Table 95: FDR q-values for iCoh between Frontal and Parietal regions, within Frequency Bands (split by hemisphere, and inter-hemisphere)	263
Table 96: Tests of Normality: TEA and HV wPLI at Global level, all frequencies (1-40Hz)	265
Table 97: Data descriptives for TEA and HV wPLI at Global level, all frequencies (1-40Hz) .	266
Table 98: Global wPLI Mean/Median values for TEA and HV cohorts, with lower values for TEA. Lower mean wPLI in the TEA cohort is marked in blue.	266
Table 99: Significant Non-Parametric Findings for Global wPLI.	266
Table 100: Data descriptives for TEA and HV wPLI at regional level, all frequencies (1-40Hz)	268
Table 101: Tests of normality for TEA and HV wPLI at regional level, all frequencies (1-40Hz)	268
Table 102: Data descriptives for TEA and HV wPLI at inter-regional level, all frequencies (1-40Hz)	270
Table 103: Tests for normality for TEA and HV wPLI at inter-regional level, all frequencies (1-40Hz)	270
Table 104: FDR q-values for Intra and Inter-Regional wPLI, AllFreq	271
Table 105: Data descriptives for global wPLI, by frequency band.....	273

Table 106: Mean/Median values for global wPLI, by frequency band. Lower mean wPLI in the TEA cohort is marked in blue.....	273
Table 107: Tests of normality for global wPLI, by frequency band.	273
Table 108: FDR q-values for Global wPLI within Frequency Bands	273
Table 109: Descriptives for regional wPLI by frequency band. Top left - frontal, top right - occipital, bottom left - parietal, bottom right – temporal.....	278
Table 110: Tests of normality for regional wPLI by frequency band. Top left - frontal, top right - occipital, bottom left - parietal, bottom right – temporal.....	279
Table 111: FDR q-values for Intra-Regional wPLI within Frequency Bands. Lower mean wPLI in the TEA cohort is marked in blue.....	279
Table 112: FDR q-values for significant Intra-Regional wPLI - FRONTAL (split by hemisphere, and inter-hemisphere). Lower mean wPLI in the TEA cohort is marked in blue.....	280
Table 113: FDR q-values for significant Intra-Regional wPLI - TEMPORAL (split by hemisphere, and inter-hemisphere). Lower mean wPLI in the TEA cohort is marked in blue.	280
Table 114: Data descriptives for inter-regional wPLI between temporal and frontal regions, by frequency band	282
Table 115: Tests of normality for inter-regional wPLI between temporal and frontal regions, by frequency band	283
Table 116: Data descriptives for inter-regional wPLI between temporal and occipital regions, by frequency band	283
Table 117: Tests of normality for inter-regional wPLI between temporal and occipital regions, by frequency band	284
Table 118: Data descriptives for inter-regional wPLI between temporal and parietal regions, by frequency band	285
Table 119: Tests of normality for inter-regional wPLI between temporal and parietal regions, by frequency band	286
Table 120: Data descriptives for inter-regional wPLI between frontal and parietal regions, by frequency band	287
Table 121: Tests of normality for inter-regional wPLI between frontal and parietal regions, by frequency band	288
Table 122: FDR q-values for Inter-Regional wPLI within Frequency Bands. Lower mean wPLI in the TEA cohort is marked in blue.....	288

Table 123: FDR q-values for wPLI between Temporal and Frontal regions, within Frequency Bands (split by hemisphere, and inter-hemisphere). Lower mean wPLI in the TEA cohort is marked in blue.	289
Table 124: Data Descriptors for global Phase Transfer Entropy data, all frequencies (1-40Hz)	292
Table 125: Tests of normality for global Phase Transfer Entropy data, all frequencies (1-40Hz)	292
Table 126: Mann-Whitney U Test Findings for Global PTE.....	292
Table 127: Data descriptives for intra-regional PTE, AllFreq (1-40Hz)	294
Table 128: Tests of normality for intra-regional PTE, AllFreq (1-40Hz).....	294
Table 129: FDR q-values for Intra-Regional PTE, AllFreq.....	294
Table 130: Data descriptives for inter-regional PTE, AllFreq (1-40Hz)	296
Table 131: Tests of normality for inter-regional PTE, AllFreq (1-40Hz).....	296
Table 132: FDR q-values for Inter-Regional PTE, AllFreq.....	297
Table 133: Mean and median comparisons for inter-regional PTE, AllFreq (1-40Hz). The lower mean PTE in the TEA cohort is marked in blue.....	297
Table 134: Data descriptives for global PTE, by frequency band.	299
Table 135: Tests of normality for global PTE, by frequency band.	299
Table 136: Mann-Whitney U Test Findings for Global PTE within Frequency Bands.....	300
Table 137: Descriptives for regional PTE by frequency band. Top left - frontal, top right - occipital, bottom left - parietal, bottom right – temporal.....	304
Table 138: Tests of normality for regional PTE by frequency band. Top left - frontal, top right - occipital, bottom left - parietal, bottom right – temporal.	305
Table 139: FDR q-values for Intra-Regional PTE, within Frequency Bands	305
Table 140: Data descriptives for directional, inter-regional PTE between temporal and frontal regions, by frequency band	309
Table 141: Tests of normality for directional, inter-regional PTE between temporal and frontal regions, by frequency band	309
Table 142: FDR q-values for Directional Temporal and Frontal PTE within Frequency Bands. The lower mean PTE in the TEA cohort is marked in blue.....	309
Table 143: Mean and Median differences within the temporal to frontal networks, within frequency bands. The lower mean PTE in the TEA cohort is marked in blue.....	309
Table 144: FDR q-values for Directional Temporal and Frontal PTE within Frequency Bands (split by hemisphere, and inter-hemisphere).....	311

Table 145: Data descriptives for directional, inter-regional PTE between temporal and occipital regions, by frequency band.....	313
Table 146: Tests of normality for directional, inter-regional PTE between temporal and occipital regions, by frequency band.....	313
Table 147: FDR q-values for Directional Temporal and Occipital PTE within Frequency Bands. The lower mean PTE in the TEA cohort is marked in blue.....	313
Table 148: Mean and Median differences within the temporal to occipital networks, within frequency bands. The lower mean PTE in the TEA cohort is marked in blue.....	313
Table 149: FDR q-values for Directional Temporal and Occipital PTE within Frequency Bands (split by hemisphere, and inter-hemisphere). The lower mean PTE in the TEA cohort is marked in blue.	314
Table 150: Data descriptives for directional, inter-regional PTE between temporal and parietal regions, by frequency band	317
Table 151: Tests of normality for directional, inter-regional PTE between temporal and parietal regions, by frequency band	317
Table 152: FDR q-values for Directional Temporal and Parietal PTE within Frequency Bands. The lower mean PTE in the TEA cohort is marked in blue.....	317
Table 153: Data descriptives for directional, inter-regional PTE between frontal and parietal regions, by frequency band	319
Table 154: Tests of normality for directional, inter-regional PTE between frontal and parietal regions, by frequency band	319
Table 155: FDR q-values for Directional Frontal and Parietal PTE within Frequency Bands. The lower mean PTE in the TEA cohort is marked in blue.....	320
Table 156: FDR q-values for Directional Frontal and Parietal PTE within Frequency Bands (split by hemisphere, and inter-hemisphere).....	320

Introduction

Electroencephalography (EEG) is often used to assist in the diagnosis and classification of epilepsies. However, unless a seizure is captured, visual inspection of a routine EEG may only yield non-specific or even normal findings in those with the condition. This is often the case in diseases such as transient epileptic amnesia (TEA), where ictal events are infrequent. The growing field of network analysis offers an opportunity to explore the functional connections in conditions such as TEA, to identify less visible changes which could assist an earlier diagnosis, and to improve management of the condition. As TEA is a rare condition, connectivity analysis may help us to further understand the mechanisms underlying the disease. This study aims to assess the usefulness of resting-state EEG (rsEEG) network analysis in this respect.

What is Electroencephalography (EEG)?

EEG: A Brief History

The study of electrophysiology can be traced back to the 1700s and 1800s, to great names such as Galvani, Volta, Ohm, and Faraday. The study of electrophysiology of the brain became possible following the development of the astatic galvanometer by Leopoldo Nobili in 1825. Carlo Matteucci and Emil Du Bois-Raymond began to build on Galvani's initial exploration of bioelectricity in the late 1800s, while Richard Caton started his investigations into the electrophysiology of the brain by recording electrical activity from exposed brains (Collura, 1993; Sutter *et al.*, 2018a).

A major breakthrough on the path to EEG was achieved in 1903 when Willem Einthoven introduced the string galvanometer. By utilising the string galvanometer with moving paper, Vladimir Vladimirovich Parvdich-Neminski published the first photographic EEG recording obtained from a dog in 1912. This was rapidly followed in 1914 by the independent publication of photographic recordings of a canine seizure. It was in 1924 however, that Hans Berger made his landmark recording of the first human EEG, and the first description of alpha rhythm (Sutter *et al.*, 2018a; Collura, 1993; La Vaque, 1999).

The potential of EEG as a diagnostic tool in epilepsy became apparent in 1934, and since the mid-1940s it has remained a central investigation in the assessment and diagnosis of a

variety of neurological disorders, but primarily epilepsy (Schomer and Da Silva, 2018; Adrian and Matthews, 1934; ILAE, Accessed 2019b; Stone and Hughes, 2013).

Overview of Neuronal Mechanisms underlying the EEG

EEG waveforms are a recording predominantly consisting of neuronal and glial cell electrical activity. Routine EEGs in the clinical setting are commonly recorded at the scalp, although recordings can be made from the surface of the brain, or from within the brain itself. Scalp EEG recording is possible due to volume conduction of the collective post-synaptic potentials (PSPs) generated within the brain; these are known as local field potentials (LFPs). The graphical display of EEG waveforms represents the potential difference between two recording electrodes on the scalp, or between a scalp electrode and a given reference (e.g., an averaged reference). Visually, EEG waveforms are displayed as channels of complex variable oscillatory patterns and displayed over time.

There are two types of PSP, excitatory postsynaptic potentials (EPSPs) which produce a negative electrical charge or sink (predominantly generated by a flow of extracellular Na^+ ions into the cellular compartment), and inhibitory postsynaptic potentials (IPSPs) which produce a positive charge or source (these are largely elicited by an intracellular flow of Cl^- ions, or the ejection of K^+ ions from the intracellular compartment). It is not possible to tell from the scalp EEG which type of PSP generated the activity, however. This is because either an IPSP received close to the pyramidal cell soma, or an EPSP received at the pyramidal apical dendrites, will produce a negative (downward) deflection on the scalp EEG; vice versa produces a positive (upward) deflection (Figure 1) (Buzsaki *et al.*, 2003; Creutzfeldt *et al.*, 1966; Schomer and Da Silva, 2018; Jackson and Bolger, 2014). Activities with a radial current with respect to the electrode (from gyri) tend to be more readily, and more prominently recorded at the scalp. However, due to the folding of the brain surface, a large number of activities are picked up from the cortical convexity from gyrus to sulcus producing tangential or more commonly oblique currents at the scalp (Figure 2). These tangential and oblique electrical currents are less easily detected at the scalp. As there are billions of neurons in the human brain producing these bipolar electrical signals, the activities generated become widespread and overlapping by the time they reach the scalp (Buzsaki *et al.*, 2003; Creutzfeldt *et al.*, 1966; Schomer and Da Silva, 2018; Scherg *et al.*, 2019).

Figure 1: Effect of pyramidal cell PSPS on EEG signal (Jackson and Bolger, 2014)

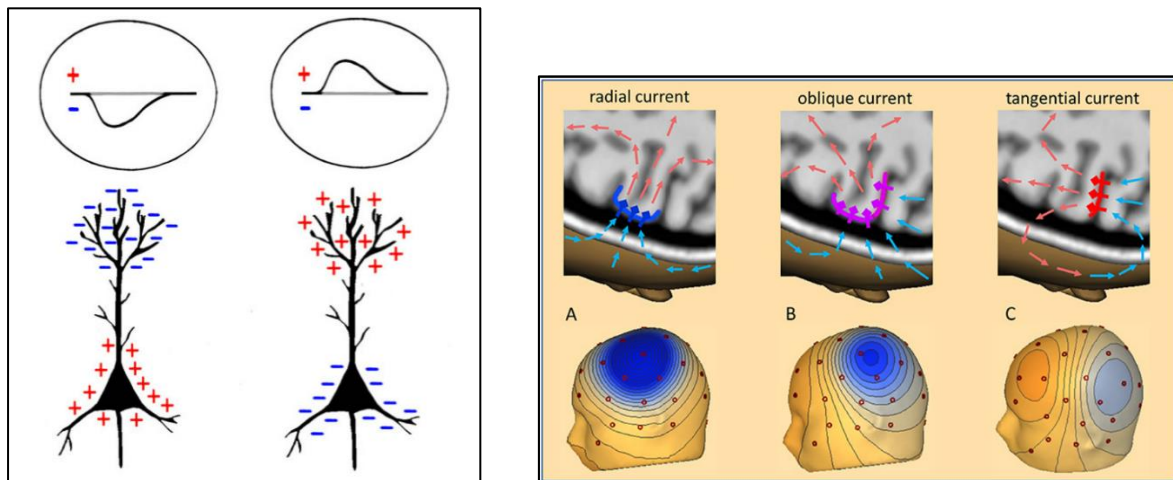


Figure 2: The effect of activity location on dipoles. Three cases of IED current inflow into a focal cortical patch are illustrated: (A) radial (dark blue), (B) oblique (pink), (C) tangential (red). Dipoles are depicted by arrows in light red to illustrate where they create positive and light blue where they create negative voltages (Scherg et al., 2019).

Recording an EEG

The positions on the scalp used to record the EEG are standardised. The most frequently used electrode placement system is the international 10-20 system, which was first proposed in 1958 by the International Federation of Societies for Electroencephalography and Clinical Neurophysiology (IFCN). This consists of 21 EEG recording electrodes positioned at 10% and 20% distances on the scalp (Acharya et al., 2016) (Figure 3). This system has recently been expanded to 25 electrodes to cover the inferior temporal areas of the brain more effectively (Seeck et al., 2017) (Figure 4).

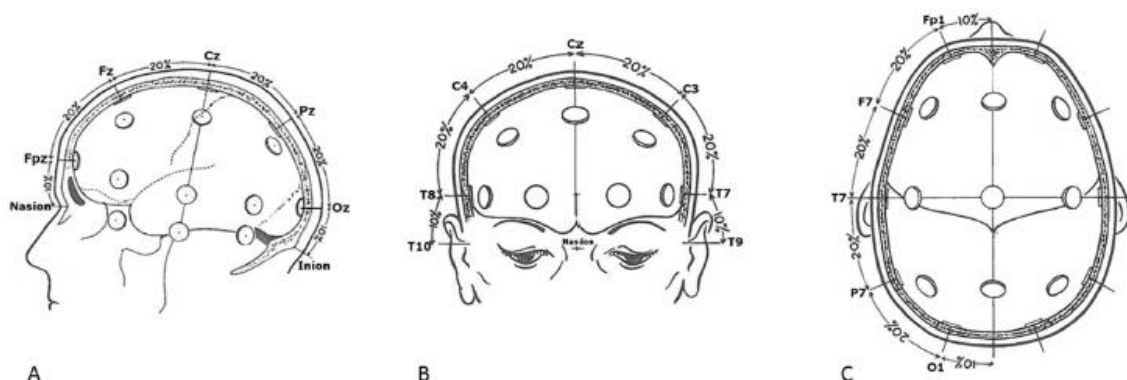


Figure 3: Placement of electrodes in 1958 IFCN 10-20 system A: Lateral, B: frontal, C: from the top (Seeck et al., 2017)

The EEG is recorded using specialised neurodiagnostic equipment. The first EEG machine built by Albert Grass in 1935 was able to record 3 analogue channels. Since this time the technology of EEG equipment has developed, with many more channels, and analogue signals are now digitised. This move from analogue to digital has expanded methods of interpretation, which were previously limited to visual inspection and pattern recognition.

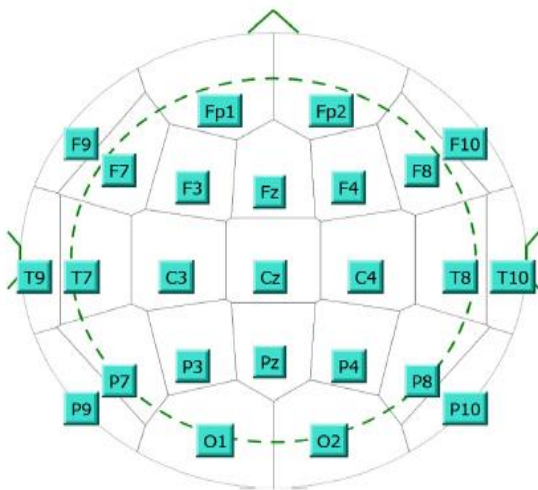


Figure 4: 2017 update to the IFCN 10-20 system. Additional electrode sites: F9, T9, P9 on the left and F10, T10, P10 on the right (Seeck et al., 2017)

Digitised EEG data is accessible for more complex data manipulation and analysis (ILAE, Accessed 2019a; Stone and Hughes, 2013). One of these uses has been within the rapidly expanding field of network analysis where EEG provides a reliable, accessible, and non-invasive source of data. Network analysis can be undertaken on EEG activities acquired as a resting state EEG (rsEEG) i.e., spontaneous ongoing neural activity, or recorded in response to a stimuli or task i.e., evoked and event-related potentials (EPs and ERPs). rsEEG is commonly analysed by dividing the oscillatory waveforms into clinically relevant frequency bands i.e. delta, theta, alpha, beta and gamma, which are described in the next section.

1.1. EEG: The Positives

The scalp EEG has the advantage of being quick and cheap to perform, providing a non-invasive, real-time graphic representation of the electrical activity of the brain. The EEG is capable of covering a wide range of frequencies and provides high temporal resolution in relation to other neuroimaging techniques such as magnetic resonance imaging (MRI), positron emission tomography (PET) and even functional MRI (fMRI). The EEG provides a

dynamic signal, changing over time and with different levels of alertness. The temporal resolution of EEG is excellent, being sensitive to millisecond changes in neural activity. (Amzica and Lopes da Silva, 2017a; Bassett and Bullmore, 2009; Cabral *et al.*, 2014; Jia, 2019; Mahjoory *et al.*, 2017).

1.2. EEG: The Negatives

However, EEG recorded at the scalp has poor spatial resolution i.e., it is poor at differentiating the underlying origins of the neural processes unless they are close to the electrode sites (usually between 1 and 10cm). EEG can also be limited in terms of the number of recording sites, as EEG in clinical practice typically utilises recordings from less than 25 electrode positions. This may be regarded as too low for accurate source localisation in research. However, higher resolution EEG is available and can minimise this problem by incorporating arrays with up to 256 electrodes, although it should be noted that beyond a 64-electrode array, the overall gains with an increase in electrodes become less incremental. Currently, high-density EEG remains used mainly for research. (Sakkalis, 2011; Mahjoory *et al.*, 2017; Crouch *et al.*, 2018; Lai *et al.*, 2018; O'Neill *et al.*, 2018; Sohrabpour *et al.*, 2015; Stoyell *et al.*, 2021; Chu, 2015).

Whilst recording EEG at the scalp is possible due to the volume conduction of electrical activities, this creates difficulties when undertaking in-depth computerised analysis. In network analysis, volume conduction forms part of the common sources problem which will be discussed later (Common Sources Problem) (Jia, 2019).

Rhythms of the EEG

As a graphical representation of ongoing brain activities, the EEG contains a mixture of different frequencies. EEG activities are typically described within bands, determined by their oscillatory frequency. There are classically five main frequency bands: delta (<3.9Hz), theta (4-7.9Hz), alpha (8-12.9Hz), beta (13-30Hz), and gamma (over 30Hz) (Figure 5). Rhythms within these frequency bands can be seen within resting-state EEG recordings.

1.3. Delta Rhythms

Delta activities are commonly associated with sleep and anaesthesia, with strong sources within thalamocortical connections and the cingulate cortex (which lies just above the

corpus callosum and forms part of the limbic system). Delta sources can also be identified during wakefulness and have been associated with long-range co-ordination cross neural networks, and modulation of memory formation and cognitive performance (Amzica and Lopes da Silva, 2018; Abubaker *et al.*, 2021; Lopes da Silva and Halgren, 2018).

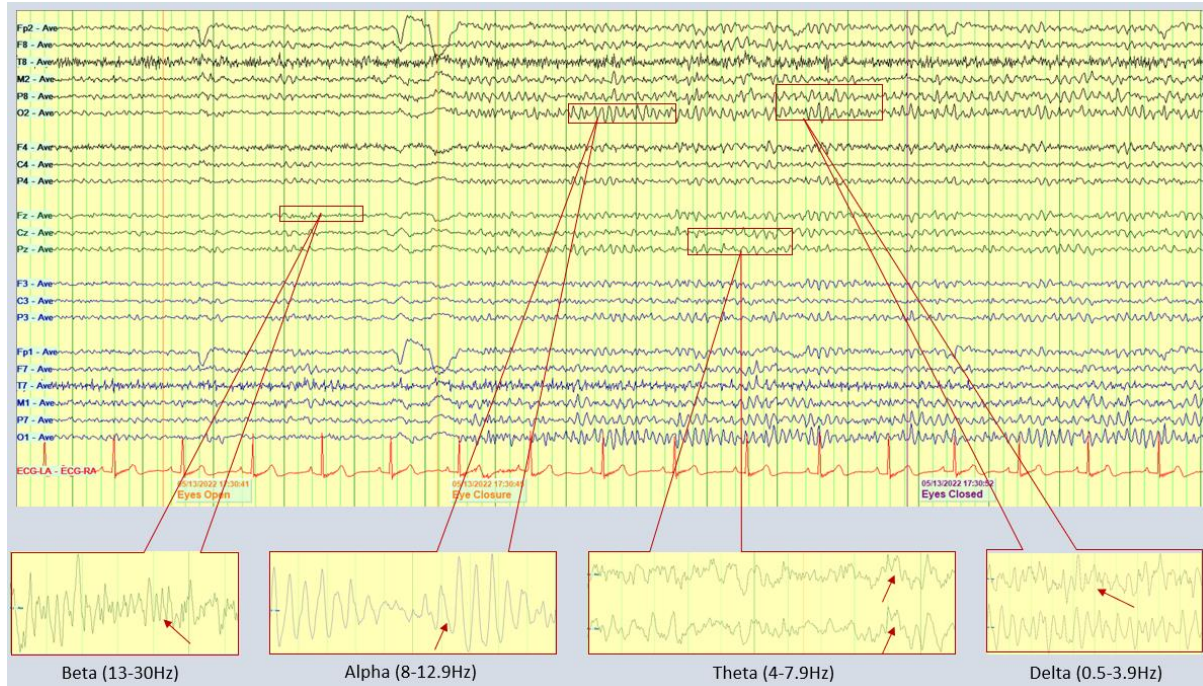


Figure 5: An example of an average reference EEG montage in an anterior-posterior format, displaying typical negative and positive deflections relating to EEG at the scalp. EEG frequency bands are highlighted – Beta in an anterior distribution, alpha in a posterior distribution, underlying theta post-centrally, and underlying delta posteriorly in this example.

1.4. Theta Rhythms

Theta activities are largely associated with memory and cognitive performance and are also the dominant activity seen during rapid eye movement sleep (REM). A high proportion of theta activities are generated in the limbic areas of the brain, in particular the hippocampus. Theta oscillations show alterations in rhythmicity, amplitude and/or frequency associated with activities such as during silent thought before responding to verbal cues, recall of information, co-ordinated movement, during learning and encoding of new information, and in association with multimodal learning tasks such as spatial navigation (Arnolds *et al.*, 1980; Ekstrom *et al.*, 2005; Watrous *et al.*, 2013; Kahana *et al.*, 1999). The hippocampus generates two types of theta rhythms. One type arises from cholinergic inputs which innervate the interneurons and principal cells within the hippocampus (possibly from hippocampal inhibitory interneurons). A non-cholinergic source of hippocampal theta is

generated via glutamatergic inputs from the entorhinal cortex, supplying the n-nitrosodimethylamine (NDMA) synapses of pyramidal cells in CA1 (these are thought to play a mediating role in synaptic plasticity). The CA3 area of the hippocampus and hilar mossy cells are also thought to contribute to theta rhythm generation, via the formation of an intrahippocampal oscillator (Kahana, 1996; Kahana *et al.*, 1999; Raghavachari *et al.*, 2001; Kahana, 2006; Raghavachari *et al.*, 2006; Somogyi and Klausberger, 2005; Buzsáki, 2002; Amzica and Lopes da Silva, 2017b). It has been postulated that there are also local cortical sources of theta activity active during working memory tasks, at a sub-regional level within the neocortex. These have been found primarily in parietal, occipital and temporal regions but not within the frontal lobes (Herweg *et al.*, 2020; Raghavachari *et al.*, 2006).

A strong phase relationship between theta rhythms and gamma oscillations has frequently been reported in the literature concerning memory. Theta/gamma cross-phase coupling has been demonstrated to be modulated by multi-item working memory tasks, with synchrony enhanced with increasing difficulty. Coupling between theta and gamma frequencies has been reported in frontal, parietal, and occipital regions, in addition to the medial temporal lobe structures. The faster gamma frequencies are modulated by the phase of the slower theta rhythms. In effect, the gamma oscillations are nested within the theta waves (Figure 6). This theta-gamma neural code has been demonstrated most clearly within the hippocampus. Current thought posits that this phenomenon optimises the transfer of information throughout the hippocampus, entorhinal cortex and out to the neocortex, thus facilitating encoding, consolidation and retrieval during working and episodic memory functions (Lisman and Jensen, 2013; Raghavachari *et al.*, 2006; Abubaker *et al.*, 2021; Colgin, 2015; Park *et al.*, 2013).

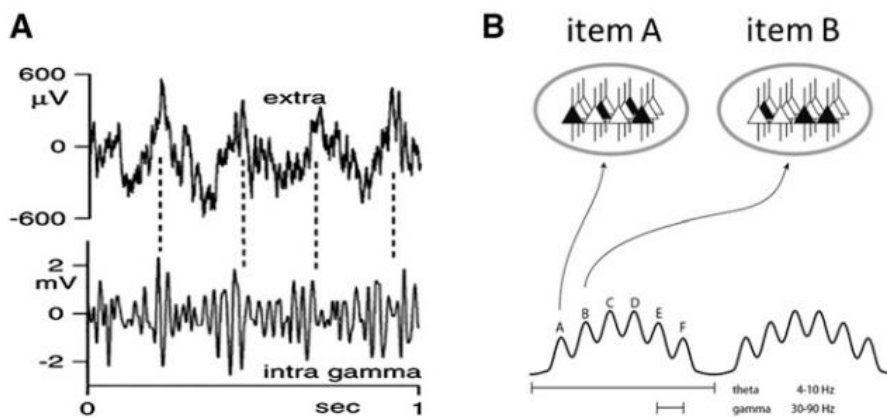


Figure 6: Neural Code Organized by Theta and Gamma Oscillations. (A) Simultaneous extracellular (top) and intracellular (bottom) recordings from the hippocampus. Intracellular gamma is due to IPSPs, the amplitude of which is modulated by the phase of theta. (B) Schematic of the theta-gamma code. The ovals at top represent states of the same network during two gamma cycles (active cells are black and constitute the ensemble that codes for a particular item). Different ensembles are active in different gamma cycles. (Lisman and Jensen, 2013).

1.5. Alpha Rhythms

Alpha frequencies are generated within the cortex, primarily within layers IV and V and, whilst there is some partial influence from thalamic sources, it is the horizontal cortical links which facilitate its spread. The “alpha rhythm” is probably the best-known EEG pattern, occurring over occipital regions during eye closure and with reduced visual attention. Alpha oscillations also occur in the somatosensory cortex (the mu rhythm) and within the temporal lobe (the tau rhythm - this is more readily seen in magnetoencephalography (MEG) rather than scalp EEG). Alpha activities over sensory regions show attenuation when a task related to the region is performed. This is known as “event-related alpha desynchronisation”. Event-related desynchronisation of alpha activity has also been reported to be elicited when consciously controlling or withholding the implementation of a task/response (Karakas, 2020; Amzica and Lopes da Silva, 2018; Klimesch *et al.*, 2007; Lopes da Silva and Halgren, 2018).

Alpha frequency rhythms also include sleep spindles (sigma spindles) as they typically occur at frequencies between 7Hz and 14Hz. Whilst spindles are similar in frequency to the alpha rhythm, their generation and function are different. Sleep spindles are generated by the thalamus and transmitted via thalamocortical networks. These spindles are seen within the EEG over frontal-central areas soon after the onset of non-REM sleep (N2) and have been linked to the blocking of incoming sensory stimuli. Other than this their function is still

debated. A possible inverse reciprocal link with delta activities has been postulated because spindles wane in deep sleep (N3) when delta waves dominate. Sleep spindle occurrence has also been reported to decrease with increasing age (De Gennaro and Ferrara, 2003; Amzica and Lopes da Silva, 2017a; Fernandez and Lüthi, 2020).

Similar to theta frequencies, there is evidence that alpha oscillations also demonstrate synchronisation with gamma rhythms, this may be related to top-down processing of semantic memory. In the past, alpha has been perceived as an “idling rhythm” during relaxed wakefulness, but the more recent research evidence described above recognises alpha activities as representing a “modulating gate” for the flow of information (Karakas, 2020; Amzica and Lopes da Silva, 2018; Klimesch *et al.*, 2007; Lopes da Silva and Halgren, 2018).

1.6. Beta/Gamma Rhythms

Beta frequencies are fast rhythms within the EEG and are sometimes split into beta1 (13-20Hz) and beta2 (20-30Hz). Whilst slower EEG activities are suppressed during waking, fast rhythms such as beta activate. Beta rhythms have generally been observed associated with motor tasks, but more recently it has been postulated that beta coherence may also be altered during cognitive tasks linked to sensorimotor input. Beta rhythms are more diverse in function than first thought and have been recorded within most brain regions. Some beta activities show evidence of a harmonic coupling with alpha rhythms e.g., the classically “notched” appearance of the mu rhythm seen over the sensorimotor cortex at rest (Abubaker *et al.*, 2021; Herrmann *et al.*, 2016; Amzica and Lopes da Silva, 2017a; Lopes da Silva and Halgren, 2018).

Gamma frequencies apply to those above 30Hz and are generated from negative feedback between interneurons and pyramidal neurons. Gamma tends to be more prominent during increased levels of vigilance, and is seen following cholinergic activation, but have also been linked to perception, memory and the consolidation and maintenance of memories (i.e., within the theta-gamma code) (Abubaker *et al.*, 2021; Herrmann *et al.*, 2016; Amzica and Lopes da Silva, 2017a; Lopes da Silva and Halgren, 2018).

For classification purposes we identify EEG activities by their band, however, there is increasing evidence that whilst specific functional roles occur within-band, EEG activities are frequently seen to functionally synchronise and undergo cross-frequency coupling. These findings support the concept that brain networks are not siloed, but function in cooperation.

Identifying Abnormal Activities in EEG

The rhythms previously described provide the basis for EEG interpretation and whilst they represent normal patterns, these activities can also occur as abnormalities if in the wrong place at the wrong time. Good examples of this are the abnormal slowing of background EEG activities associated with neurodegenerative disease, or inter-ictal temporal slow waves associated with temporal lobe epilepsy (Koutroumanidis 1998). The abnormalities discussed in this section refer to those which visually demonstrate a prominent deviation from the underlying background rhythms i.e., they stand out from the background recording. Abnormal activities within EEG can be broadly split into two main groups concerning their morphology – epileptiform and non-epileptiform. Whilst their nomenclature is defined in terms of epilepsy, both can be seen in a variety of other medical conditions. NEA in particular, as their name suggests, do not always provide diagnostic evidence for epilepsy even if the condition is suspected.

1.7. Defining Non-Epileptiform Abnormalities (NEA)

NEA commonly occur in the form of slower waveforms i.e., theta and delta frequencies, however, this is not exclusively the case. Whilst NEA stand out from the background EEG recording their morphology meets the criteria for resting state rhythms. The scope of non-epileptiform abnormalities is broad, therefore the discussion below is limited to the conditions most relevant to the research being undertaken:

- Physiological ageing is generally accompanied by a slight slowing of the background to around 7-8Hz, reduced EEG reactivity associated with opening and closing of the eyes and the appearance of subharmonic theta and delta frequencies more commonly over temporal areas (Krishnan *et al.*, 2018a).

- As described previously, pathological ageing, related to cognitive decline shows the progression of normal ageing patterns. Slowing of the alpha rhythm tends to drop to around 7Hz or below, and increased and abnormal focal theta and delta activities can be seen over the anterior-temporal areas, more so over the left (Babiloni *et al.*, 2018).
- Mild cerebrovascular disease and atrophy are more common with ageing due to a decline in circulation, causing irregular theta/delta frequency abnormalities particularly localising over the vascular watershed areas (central-temporal and parietal/ post-temporal)(Galovic *et al.*, 2018).
- Metabolic disorders also increase in prevalence with ageing. If sub-therapeutic or untreated at the time of the EEG these can give a generalised slowing of EEG activities, which increases in severity with increasing metabolic dysfunction. (Sutter *et al.*, 2018b).
- Localised NEA can be seen associated with underlying structural pathology. The location of the abnormalities will depend on the location of the pathology. For example in the case of hippocampal sclerosis, which is often an epilepsy-related pathology, focal slow waves can be evident over anterior-mid temporal regions (Hartman and Lesser, 2018). Such focal changes can also be seen in focal epilepsy without any visible structural pathology.
- Although not strictly “abnormalities” per se, there may also be medication-related alterations in the EEG. These are variable, dependent on the drug, and cover a range from increased slower activities to excess beta rhythms and even epileptiform abnormalities. It is therefore helpful to be aware of the clinical history and current medications at the time of the EEG recording (Höller *et al.*, 2018).

In summary, NEA can represent a generalised alteration in background frequencies e.g., those seen in neurodegenerative or metabolic conditions, or more localised changes which stand out from the background waveforms e.g., in vascular, and structural pathologies, and focal epilepsy.

1.8. Defining Interictal Epileptiform Discharges (IED)

In addition to NEA which stand out from background rhythms, IEDs are recognisable in the same way. It is often the case that NEAs and IEDs can be seen in association within the same recording. Whilst the nomenclature implies IEDs are confined to epilepsy, it is not that clear cut. IEDs can occur in the EEGs of people without epilepsy, particularly in those with learning and developmental delay, but also in conjunction with some medications. IEDs are also associated with acute infective conditions and neurodegenerative disease, amongst others. For the purposes of the study, the focus of this section is on inter-ictal epileptiform discharges i.e., those seen between seizures in individuals with a diagnosis of epilepsy.

Whilst IEDs may be seen within a resting EEG recording, their morphology falls beyond the EEG frequency band activities described previously. IEDs are typically described as spikes or sharp waves, having a pointed peak, and are clearly distinguishable from the background EEG. IEDs are differentiated from each other by their duration (spikes have a duration of 20-70ms, while sharp waves are 70-200ms in duration). A definition of IED morphology has been internationally agreed and published by the International Federation of Clinical Neurophysiology (IFCN) (Kural *et al.*, 2020; Krishnan *et al.*, 2018b) (Figure 7):

1. "IEDs have two, or three phases with a pointed peak
2. IEDs have a different wave duration than the ongoing background EEG
3. Morphology of the waveform is asymmetric
4. IEDs are followed by a slow wave
5. Background activities are disrupted briefly following the presence of an IED
6. Distribution of the negative and positive potentials on the scalp suggests a source of the signal in the brain (corresponding to a radial, oblique, or tangential orientation of the source)" (Kural *et al.*, 2020).

In summary, IEDs are defined in terms of spikes and sharp waves which are most frequently, but not exclusively, associated with a diagnosis of epilepsy, Clear criteria have been set out to aid the identification of IEDs.

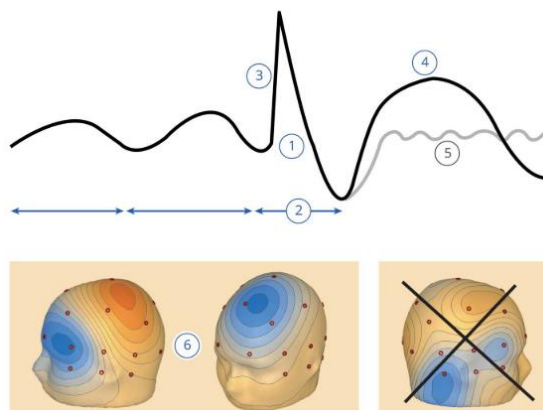


Figure 7: Infographic showing the 6 criteria for identifying IEDs by morphology. The upper representation shows 5 of the IFCN criteria in graphic form. “The voltage maps in window (6) show a tangential orientation (source in the left middle frontal gyrus) and a radial orientation (source in the left superior frontal gyrus); the irregular distribution of the potentials in the last voltage map does not imply a source in the brain (it was an artifact with sharp morphology) and does not fulfil this criterion; negative potentials are in blue, and positive potentials are in red”. (Kural et al., 2020)

Recognising Artifacts in EEG

The EEG rhythms and abnormal waveforms described above provide the electrical information required for the interpretation of brain functionality. However, the activities captured within an EEG also contain signals from sources other than brain generated brain activity. These “unwanted” activities are called artefacts or EEG noise, and they effectively contaminate the recording. For ease of discussion, we will group the concept of artefacts and noise under the common term of EEG noise.

Noise within scalp-EEG recordings is common and can arise from several sources including physiological, electrode and environmental noise (Figure 8). EEG noise can cause problems with interpretation if the reader is inexperienced and is a potential source of contamination and bias within EEG analysis. If not carefully managed by the recordist, noise can obscure the EEG rhythms. Whilst noise can be minimised during acquisition, it cannot be totally eliminated, partly because some EEG noise is produced by other electrophysiological sources e.g. the heart. Also, noise sources can be closer to the recording sites, meaning the signals are of a larger voltage on the recording e.g., muscle activity.

Physiological noise has variable frequency dynamics dependent on the source. For instance, sweat, respiration, tremor, or eye-rolling produce slow-frequency waveforms. On the other hand, muscle activities can produce a variable pattern of fast activities. Eye movements are a common source of physiological noise, producing a complex mix of frequencies which are

distinctive to the experienced EEG interpreter. Both pulse and ECG can be recorded on the EEG as physiological noise, showing a distinctive regularity. Concerning environmental noise, the most common is that of mains interference, which in the UK is seen as a sinusoidal 50Hz signal (Selim R, 2007; Fritz and Benbadis, 2009; Tatum, 2013a; Tatum *et al.*, 2011; Tatum *et al.*, 2018).

In conclusion, EEG noise occurs from a variety of physiological and non-physiological sources which if not accurately identified can lead to misinterpretation of the EEG (Figure 8).

Concerning EEG analysis, pre-processing of the EEG is undertaken partly to minimise the effect of EEG noise, as it can lead to bias and misinterpretation of results.

Nonphysiologic sources	Physiologic sources
Electrodes	Normal
Pop	Eye movements
Impedance mismatch	Cardiac
Lead wires	Myogenic
Machine and connections	Bone defects
Aliasing	Mastication and deglutition
Jackbox	Abnormal
60 Hz	Tremor
Static electricity	Myoclonus
Implanted electrical devices	Movements

Figure 8: A concise list of common sources of EEG noise (Tatum, 2013b)

EEG Rhythms and Quantitative EEG Analysis

The EEG, comprising a mix of the waveforms described above, is clinically interpreted by visual analysis, which remains the gold standard (Kural *et al.*, 2020). However, this can be complemented by the use of quantitative EEG analysis (qEEG).

The use of QEEG is increasing in clinical use. This has been aided by software such as Persyst, which includes features such as EEG trending, artefact reduction, EEG monitoring, and seizure detection (<https://www.persyst.com/>). QEEG is now readily accessible for

assistive analysis of long-term EEG monitoring for epilepsy and in the intensive care environment. QEEG is clinically useful in assisting with the fast detection of trends within EEG, especially when recordings are undertaken over several days, as it gives a compressed overview of the recording (say with respect to amplitude). QEEG is also used within research, to describe and compare EEG findings. This is commonly described in terms of mean amplitude or mean frequency (Osman *et al.*, 2018).

The qEEG tools break down the EEG into key component parts which can be computed in the time domain, the frequency domain, or as a time-frequency analysis. Time domain analysis is based on the amplitude of a signal across a given frequency spectrum. This can then be computed across the EEG frequency bands. Frequency-domain analysis more commonly known as power spectral analysis, is based on frequency and is usually a calculation of frequency and amplitude. Power spectral analysis defines a time-series signal as the summation of a series of sines and cosines (Fourier transform). Power spectral density (PSD) is the total, or mean power, calculated across a given frequency spectrum within the EEG frequency bands, (or for individual frequencies), and is usually described in terms of the mean (Osman *et al.*, 2018; Zhang, 2019).

Spectral and time-frequency analysis can give a useful overview of the frequencies and amplitudes contained within an EEG signal and concerning their power (or dominance) within the total frequency content.

Understanding Functional and Effective Network Analysis

While QEEG can give a macro-level insight regarding EEG changes between conditions, network analysis allows us a more detailed view of brain function.

Network neuroscience is a recent and rapidly growing field of research which is providing novel insights into the structural and functional connectivity of the human brain. It offers new ways of mapping the connections between brain regions. Due to its excellent temporal resolution, EEG provides an ideal dataset with which to analyse the functional dynamics of the brain. Computational methods to map anatomical connections make it possible to examine functional connectivity at rest, during tasks, and functional changes over time within different clinical populations (Medaglia *et al.*, 2015; Fornito *et al.*, 2016; Sakkalis, 2011; McLoughlin *et al.*, 2014; Bullmore and Sporns, 2009; Medaglia and Bassett, 2017).

By comparing network data from a healthy population with that of discrete populations such as those with memory impairment, understanding can be gained regarding the function and dysfunction of the neural networks. In this way, modern network techniques explore both the neural elements (the neuronal activity within brain regions) and the functional interactions between those elements (via circuits, systems and synapses). Whilst the raw surface EEG data from brain regions may be normal or non-specific in TEA, the functional networking behind the neural activity may not (Medaglia *et al.*, 2015; Bassett and Sporns, 2017; Sporns, 2017).

The Different Types of Connectivity and their Uses

Researchers using connectivity analysis now have access to a wide range of connectivity measures with which to work. However, this can appear quite daunting, particularly to a novice. The discussion below is not designed to cover all methods but to focus on those chosen for this research project.

For the context of this research, the term “network” refers to a functionally specific collection of structural brain regions, interconnected by a neuronal framework, which enables the directed flow of information in the form of neural activity. Connectivity analysis describes and quantifies these directed communications, making them measurable. Connectivity within the brain is described in terms of structural, functional, or effective

connectivity. Connectivity analysis can be used in conjunction with a variety of neuroimaging techniques, allowing the study of activations and interactions within and between brain regions, and comparison between healthy and pathological states (Sakkalis, 2011; Brookes *et al.*, 2014; Cohen, 2014; Betzel and Bassett, 2017).

1.1. Structural connectivity

Structural connectivity describes the anatomical organisation of the neuronal framework i.e., the synapses and nerve fibre pathways making up the network. Structural connectivity is best measured by neuroimaging such as magnetic resonance imaging (MRI), diffusion tensor imaging (DTI), diffusion MRI (dMRI) and functional MRI (fMRI). Structural connectivity shapes functional connectivity within the network, therefore the two are interrelated. The latter MRI types i.e., dMRI/fMRI permit co-registration of structural and functional measures and can be utilised alongside EEG for this purpose, providing a more holistic model of brain function (Sakkalis, 2011; Betzel and Bassett, 2017; Cao *et al.*, 2022; Babaeeghazvini *et al.*, 2021).

1.2. Functional connectivity

While fMRI, by using blood oxygenation level-dependent (BOLD) signals, can give an indirect measure of functional connectivity, EEG can provide a direct estimate of functional connectivity (Babaeeghazvini *et al.*, 2021). Magnetoencephalography (MEG) is also a useful functional neuroimaging research tool which is less widely accessible than EEG; whilst mentioned here for completeness, MEG will not be discussed in detail within this study.

Functional connectivity measures the undirected information flow between two brain areas by assessing the correlation, or coherence between them. EEG-based functional connectivity is assessed between time series and can be calculated for specific frequency bands. However, whilst functional connectivity can assess either linear or non-linear dependence between signals (depending on the metric used), it is unable to give any information regarding causality (Crouch *et al.*, 2018; Mahjoory *et al.*, 2017; He *et al.*, 2019; Jia, 2019). To understand causality dynamics between signals, effective connectivity analysis is required.

1.3. Effective connectivity

Effective connectivity enables the researcher to gain an understanding of the directionality of information flow, or the causality, between brain sites. Networked regions have a causal influence on each other via their neural interactions, with the directionality of information transfer dynamically changing over time (Cao *et al.*, 2022; Cabral *et al.*, 2014; He *et al.*, 2019; Rubinov and Sporns, 2010). Causal dynamics provide a further understanding of healthy vs. pathological network communication.

Choice of Connectivity Measure for EEG Analysis

There are numerous connectivity measures which can be used to analyse connectivity data. When using EEG for functional and effective connectivity analysis, care needs to be taken when selecting measures.

1.1. Common Sources Problem

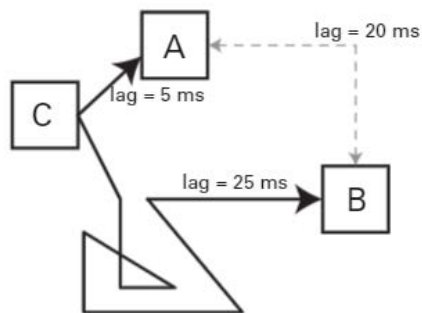
Recording EEG signals at the scalp is possible due to the conductivity of the tissues of the brain, skull, and scalp. However, this poses some problems in analysing connectivity accurately as it makes it difficult to separate true sources from volume-conducted ones. The task of source recognition is also confounded by the choice of reference for the electrode sites.

Volume conduction

Scalp EEG, by nature, depends on volume conduction (the propagation of electromagnetic fields through the brain, skull and then skin) to enable recording. However, volume conduction is a potential cause for error within EEG connectivity analysis as electrical fields spread laterally, affecting the signal at neighbouring electrode sites, creating inaccurate connectivity results and confounding source reconstruction. This is known as the inverse problem (Cohen, 2014; Jia, 2019; O'Neill *et al.*, 2018; Lopez Rincon and Shimoda, 2016). Connectivity measures based on phase are particularly prone to the effects of volume conduction as the variable dipole orientations of an electrical source depend on the electrode position in relation to it. This may influence the magnitude of the phase difference (phase lag) of the signals recorded at the scalp even though they are strongly synchronised at source. The effects of volume conduction can therefore appear to turn phase lags into

phase leads, causing an underestimate in the strength of true connectivity between two signals (Cohen, 2015)(Figure 9).

A) The common input problem



B) The "who's first" problem

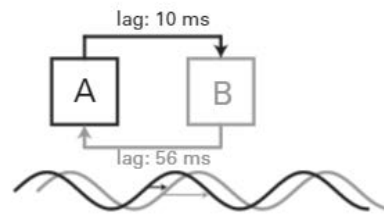


Figure 9: Infographic depicting the common input problem and the "who's first" problem when using phase-based connectivity measures (Cohen, 2014)

Choice of Reference

The choice of a reference standardised across all study EEG data is taken at the pre-processing stage. The selection of an appropriate reference is important as the choice can affect the calculations within PSD and connectivity measures (Figure 10).

Within EEG practice, there is a range of active reference choices. Common reference choices can be split into generalised references e.g., the common average reference, a single active electrode which may be sited on the nose, the vertex or the mastoid, or a linked reference which is usually sited at the mastoids. Each generalised reference has benefits and drawbacks, and different references are used for different neurophysiological techniques. (Jia, 2019; Yao *et al.*, 2019). Average reference has previously been recommended as the reference of choice, however, more recently the use of REST (reference electrode standardization technique) has been proposed as a standard for EEG analysis. REST is described as an infinity reference, and utilises neural current sources from the EEG recording, as these are reference-independent. REST has been compared to other reference choices, including average reference, and has proved superior for connectivity analysis (Yao *et al.*, 2019).

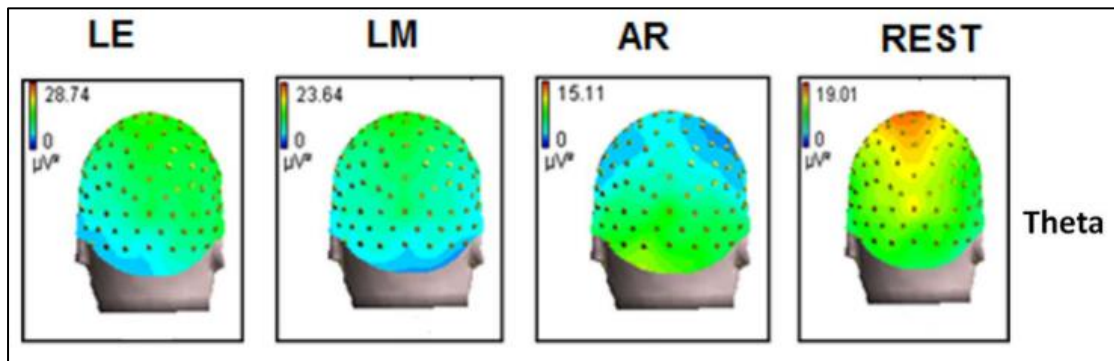


Figure 10: The effect of electrode choice on a power spectral map of theta frequencies. From left to right, the references are left ear (LE), LM, AR and REST (Yao *et al.*, 2019)

1.2. Connectivity Measures in the Study

In addition to measuring functional or effective connectivity, measures can additionally be described in terms of their signal processing method (parametric and non-parametric), whether they measure linear or non-linear interactions, and which domain the connectivity measure uses for its calculations (time domain, frequency domain or, less commonly time-frequency domain). No model is perfect, and each connectivity measure comes with its advantages and disadvantages. For this reason, some research advises the use of more than one measure to validate key results via consistency (Mahjoory *et al.*, 2017; Cohen, 2014).

Cao *et al.* have drawn up a useful comparison of methods suitable for EEG which has been included below (Table 1) (Cao *et al.*, 2022). The functional and effective connectivity measures relevant to this study are discussed in more detail below.

Imaginary Coherence (iCoh)

Coherence measures linear functional connectivity in the frequency domain. It is a bivariate measure, i.e. it assesses the relationship between two signals (or electrode sites). Signals can be analysed within the EEG frequency bands using this method. To do this, fast Fourier Transform (FFT) is used to convert the time-based EEG activities into the frequency domain, i.e., conversion into power spectral densities (PSD). A coherence function (cf) is then calculated; this is the ratio between the cross-PSD (of all frequencies) and the individual PSD of the two signals analysed. The coherence of each frequency band is calculated as $(cf)^2$. Coherence is measured on a scale from 0 to 1. If coherence is 0, there is no linear

dependence between the two signals. Therefore, the larger the relationship between the two signals, the higher the coherence value.

Table 1: Comparison of methods for quantifying brain connectivity using EEG (Cao et al., 2022)

	Linearity		Signal processing		Brain connectivity		Domain		
	Linear	Nonlinear	Parametric	Nonparametric	FC	EC	Time	Frequency	Time-frequency
DCM		√	√			√		√	
MSC	√			√	√			√	
STFC	√			√	√				√
WC	√			√	√				√
PLV		√		√	√			√	
GS		√		√	√		√		
GC	√		√			√	√		
PDC	√		√			√		√	
Corr	√			√	√		√		
SL		√		√	√		√		
TE		√		√	√	√	√		
MI		√		√	√		√		
DTF	√		√			√		√	
PS		√		√	√			√	
SEM	√		√			√			
IPC	√			√	√			√	
PLI		√		√	√			√	
ERR		√	√			√	√		

Abbreviations: Corr, correlation; DCM, dynamic causal modeling; DTF, directed transfer function; EC, effective connectivity; ERR, error reduction ratio; FC, functional connectivity; GC, granger causality; GS, generalized synchronization; IPC, imaginary part of coherency; MI, mutual information; MSC, magnitude squared coherence; PDC, partial directed coherence; PLI, phase lag index; PLV, phase locking value; PS, phase synchronization; SEM, structural equation modeling; SL, synchronization likelihood; STFC, short-time Fourier coherence; TE, transfer entropy; WC, wavelet coherence.

Coherence is a commonly used measure in EEG connectivity analysis but, as stated previously it only detects linear dependence. As the coherence calculation is PSD-based, it is likely to include a representation of the neural mass within the network population alongside the phase relationship. However, coherence is prone to distortion by amplitude variation within the signal. Additionally, coherence does not effectively address the issue of volume conduction. There are several upgrades to the original coherence measure which include imaginary coherence (iCoh) which was proposed by Nolte et al. in 2004.

iCoh minimises the effect of volume conduction by removing correlations which showed zero lag based on the idea that true correlations could not create a zero lag. A remaining drawback of iCoh is its bias for phase-lags of $\pi/4$ (a quarter cycle), as this limits it in detecting coherence in phase with each other, or phase opposition (Cohen, 2014; He *et al.*, 2019; Jia, 2019; Sakkalis, 2011). Therefore, iCoh can over, or under-estimate connectivity, dependent on the signal content.

Weighted phase-lag index (wPLI)

Phase-based connectivity measures are also commonly used in EEG connectivity studies. The focus of phase-based measures is the timing of the oscillations within the network. The prediction is, that if two oscillating signals demonstrate a constant phase shift with respect to each other over time, they have phase synchronisation, and therefore have a connective relationship. There are several different phase-based metrics with variable sensitivity to time lag i.e., how much the magnitude of the lag affects the strength of the connectivity measured. Phase lag index (PLI) was proposed by Stam et al. in 2007 and uses an algorithm which detects asymmetry in phase difference between two signals, with larger asymmetries denoting stronger connectivity. PLI is a robust measure concerning the common sources problem, but its weakness lies in a discontinuity in determining true connectivity when the phase asymmetry is small which leads to a misinterpretation of phase lags and leads.

Weighted phase-lag index (wPLI) is a functional connectivity in the frequency domain which is capable of detecting linear and non-linear connectivity. In comparison to its predecessor, the phase-lag index, wPLI weights phase leads and lags related to the magnitude of the non-zero lag (imaginary component), giving increased statistical power to the metric. WPLI is robust against volume conduction and successfully identifies connectivity. However, with genuine, but small, time lags it can underestimate the connectivity by up to 40%. The output of wPLI can also be affected by non-stationary signals i.e., those that show frequency variation over time. EEG signals are, by nature, dynamically variable over time, and whilst some non-stationary signals within a time series may genuinely represent noise, others can possess a true connective relationship. Again, this can generate an underestimation of true connectivity (Cohen, 2015; Jia, 2019; Cohen, 2014).

Phase Transfer Entropy (PTE)

Transfer entropy (TE) has developed from the mutual information (MI) method, which is used widely in science and engineering. MI originates from Shannon entropy which measures the amount of information a variable holds and the information it provides is based on probabilities and distributions. Unlike the Fourier transform, entropy functions outside of the time domain of the data i.e., the time order of the data does not influence the results. TE however extends the entropy measure, by taking temporally recent signals

into account within its probability calculations (Cohen, 2014; Vicente *et al.*, 2011; Lobier *et al.*, 2014).

Although less popular in neuroscience, both MI and TE provide some real advantages concerning connectivity analysis. Both MI and TE provide a measure of the information shared between two signals and therefore represent bivariate measures. The two signals can arise from two electrode sites, or from the same electrode site, which enables a flexible custom-tailored approach in detecting connectivity for any data distribution type (e.g., linear, non-linear, exponential, circular). Therefore, MI and TE are model-free which gives flexibility but means that if the relationship between signals is purely linear, a linear-based model outperforms both MI and TE. However, the flexibility of MI and TE can create problems with the positivity or negativity of the signal, as MI and TE are blind to these relationships (Vicente *et al.*, 2011; Cohen, 2014).

Another drawback of MI and TE is that it can inflate estimates of connectivity if too little data, or too few sample points are provided. Therefore, a high sampling rate and longer epoch are required to improve the accuracy of the results. It should be noted that increasing the sampling rate also increases the amount of noise within a signal, so it is wise to employ robust pre-processing to remove excess noise from the raw data. The reliability of TE calculations can also be influenced by the presence of strong non-stationaries within the signal (Cohen, 2014; Vicente *et al.*, 2011).

Phase Transfer Entropy (PTE) was introduced to overcome some of the limitations above, particularly concerning oscillatory networks. PTE provides a measure of directed connectivity within neuronal networks and integrates the concept of phase-based information flow into the TE metric. This means that PTE can detect directed phase coupling between signals, and the time-efficiency of this is optimised by the use of a binning method which allows PTE calculation from both trial data (EP/ERP) and continuous EEG data. The PTE metric is robust at detecting directed connectivity in the presence of “realistic” noise and source mixing down to “moderate” coupling strengths, is reliable across a wide range of time lags, and requires less data than the original TE measure. PTE is also shown to be more effective than TE at detecting incidences of cross-band coupling (Lobier *et al.*, 2014).

Due to the constraints of this thesis concerning word count, a full review of connectivity measures was not possible. Therefore, the focus has been on the measures implemented in the research. ICoh, wPLI and PTE are all robust concerning volume conduction and between them cover aspects of connectivity related to power, frequency, phase, and directionality. The measures chosen also provide information regarding both linear and non-linear interactions.

1.3. Beyond Connectivity – Machine Learning

Whilst machine learning algorithms have not been used within this research, I am touching on it here because they provide a natural progression for connectivity data, permitting further pattern analysis, generating insight, and improving predictions drawn from the data. There are wide-ranging, real-world examples of the uses for machine learning, with the most relevant of these being assisting in the diagnosis of medical conditions. An example of the potential use of machine learning in EEG analysis was published by Gemein *et al.*, who applied a feature-based decoding network, to the classification of pathological vs. non-pathological EEG and obtained a high degree of accuracy (Gemein *et al.*, 2020). Machine learning can extract features such as disease biomarkers which have proved useful in the classification and earlier diagnosis of several pathologies such as seizure types, sleep disorders, Alzheimer's disease (AD) and schizophrenia (Cao *et al.*, 2022; Saeidi *et al.*, 2021; Hosseini *et al.*, 2021).

Machine learning can be separated into two types: unsupervised learning where the algorithm builds up a recognition of patterns based on input data only, and supervised learning where the algorithm develops a predictive model based not only on the input data but also from known outputs. There are several common algorithms within each type of machine learning, dependent on the type of data, the data size, and the results required (Figure 11). Common algorithms used in published EEG research are Decision Tree/ Random Forest, Support Vector Machine and K-Nearest Neighbour (Cao *et al.*, 2022; Saeidi *et al.*, 2021; Hosseini *et al.*, 2021; Matlab, 2022).

Machine learning is increasingly offering a meaningful gateway from research findings into clinical practice and provides a viable progression of data analysis for the study results from this thesis.

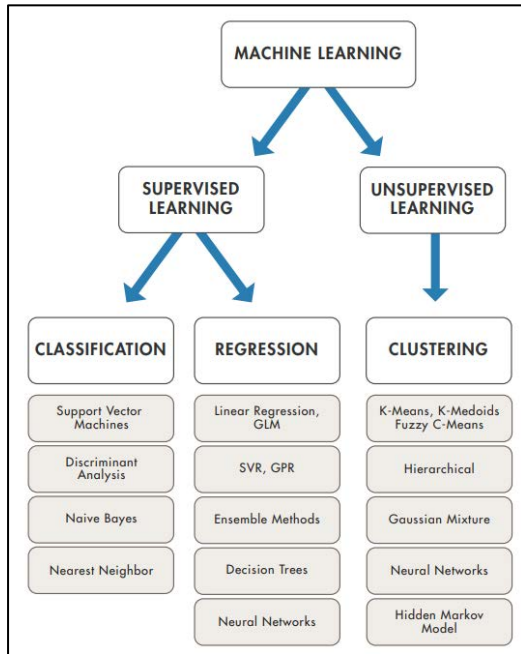


Figure 11: An overview of machine learning techniques and their related algorithms (Matlab, 2022)

Memory, Amnesia and Epilepsy

Memory dysfunction is a key symptom in several neurological conditions including dementia, epilepsy, amnesia, and psychological disorders. It has long been recognised that memory is a complex network of processes involving many areas of the brain.

Memory

To aid understanding, memory can be divided into types, stages, and processes.

- Explicit, or declarative memory represents conscious interaction, generally in the form of facts or experiences that are consciously remembered. Explicit memory can be episodic (or autobiographical) which includes our own experiences (e.g., birthdays, graduation, holidays), or semantic, which encompasses the facts and concepts that we acquire (Figure 13).
- Implicit, or nondeclarative memory consists of knowledge that we cannot access consciously but know that we know. This can be in the form of procedural memory—our knowledge of how to do things (e.g. riding a bike), perceptual learning from experiences we have had, or classical conditioning which includes our emotional and physical responses. Implicit memory can also be non-associative learning such as habits (Figure 13) (Stagnor, Accessed 2019; Squire and Zola-Morgan, 2015; Schwartz, 2014).

Memory can also be described in terms of the stages a sensory input undergoes within the memory process (Figure 12). This may be very brief and then lost (sensory memory), or short-term (temporary storage, which is lost without rehearsal, and sensitive to interference). Maintenance rehearsal leads to a process of encoding memories into long-term memory which is a relatively permanent storage but may be disrupted during retrieval. Material in long-term memory can be retrieved back into short-term memory for reprocessing e.g. when recalling an event (Stagnor, Accessed 2019).

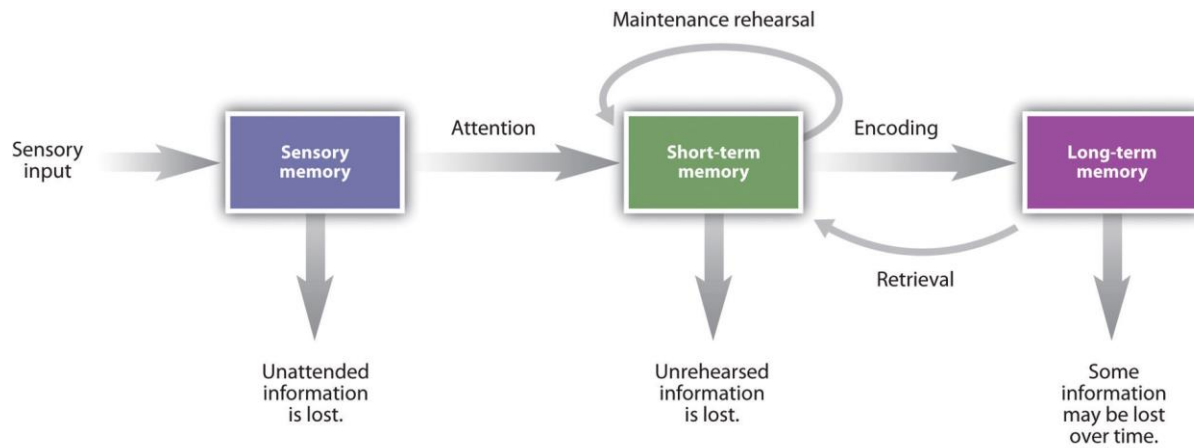


Figure 12: Memory depicted as stages within memory processes (Stagnor, Accessed 2019)

Key Brain Areas

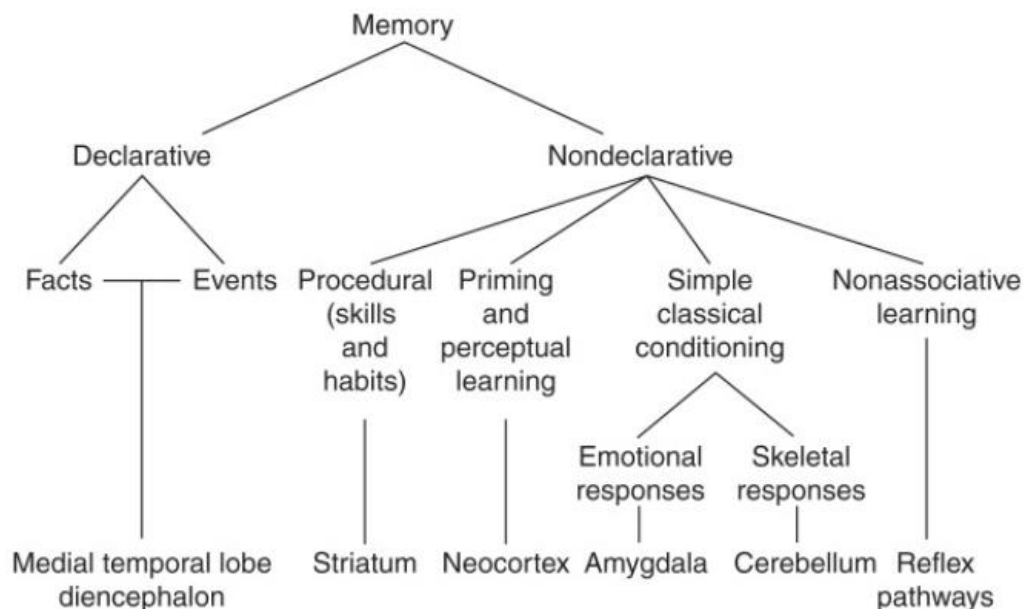


Figure 13: Diagram of the brain structures thought to be especially important for each form of memory. In addition to its central role in emotional learning, the amygdala is able to modulate the strength of both declarative and nondeclarative memory. (Squire and Dede, 2015)

The main structures which support explicit memory lie within the medial temporal lobes, specifically the hippocampus and neighbouring entorhinal, perirhinal and parahippocampal cortices (Figure 13, Figure 14). As stated previously, the theta and gamma EEG rhythms generated within and from the hippocampus are known to play a major role in formation and retrieval of memories. The hippocampus and the entorhinal, perirhinal and parahippocampal cortices function hierarchically and have different roles during the encoding and retrieval processes e.g., the perirhinal cortex is known to relate to encoding of

objects, whereas memories related to scenes are processed by the parahippocampus. The hippocampus has a main role in associations between elements of memories. The perirhinal and parahippocampal cortices have network projections to the neocortical association areas i.e., the frontal, temporal and parietal lobes (Squire and Zola-Morgan, 2015; Stark and Saksida, 2011). The successful formation of memories is associated with a transient increase in the synchronisation of brain activities within the hippocampus-entorhinal cortex network. This coupling/decoupling of activities occurs between theta and gamma frequency bands. This theta/gamma code has been demonstrated as a crucial element in mnemonic processes within the same network. Similar theta/gamma coupling has also been recorded within the medial septum, with strong phase-coupling with the hippocampus-entorhinal cortex network, suggesting that the medial septum co-ordinates network activity within the temporal lobe structures is crucial for memory encoding and retrieval (Király *et al.*, 2023; Nuñez and Buño, 2021) (Figure 15). A desynchronisation of alpha and beta frequencies within the neocortex follows these coupling/decoupling processes within the hippocampus (Chauvière, 2020).

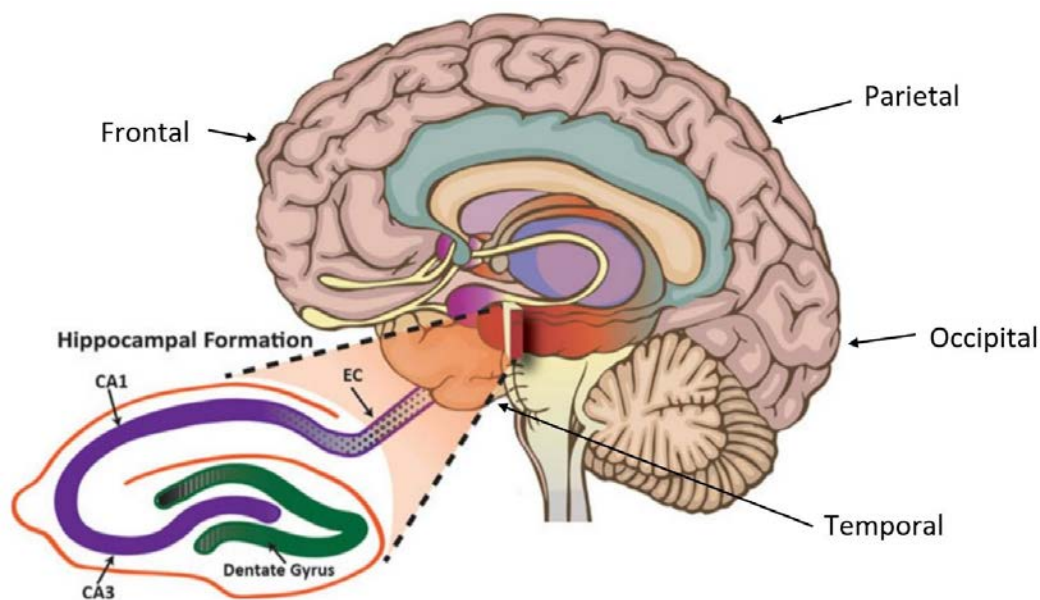
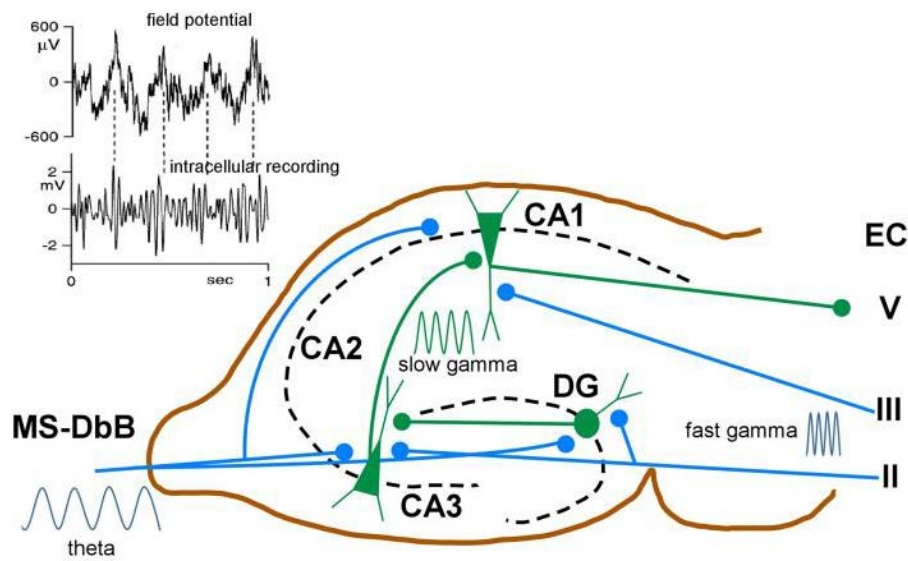


Figure 14: The hippocampus and associated structures (<https://www.creative-diagnostics.com/blog/index.php/what-is-hippocampus/>)



Schematic diagram of neuronal circuits involved in theta-gamma (θ - γ) coupling. Blue traces indicate synaptic inputs from layers II to III of the entorhinal cortex (EC) and from the MS-DdB. The dentate gyrus (DG), CA1, CA3, and EC layer V neuronal connections are also shown. θ - γ coupling in the hippocampus results from the convergence of θ inputs from the MS-DdB and fast γ from the EC. Particularly, θ - γ coupling results in CA1 by the convergence of θ inputs from the MS-DdB and slow γ from the CA3. The inset shows θ - γ interactions in the hippocampus as revealed by the CA1 field activity (upper) and band-pass filtered intracellular γ activity (lower). Note phase locking between both rhythms (θ - γ coupling) and the amplitude modulation of the intracellular γ ; modified from Penttonen et al. (1998).

Figure 15: Schematic diagram of neuronal circuits involved in theta-gamma (θ - γ) coupling (Nuñez and Buño, 2021).

Disruption of Memory

As described previously, the key brain activities involved in facilitating memory processes are theta and gamma EEG rhythms. Temporary or permanent disruption of theta/gamma coupling within memory networks is therefore likely to interrupt memory processes, resulting in poor memory retention, inability to retrieve existing memories (retrograde amnesia), or the inability to retain new ones (anterograde amnesia). Such damage or disruption can occur in conditions such as neurodegenerative disease and epilepsy, or as a result of trauma (Lisman and Jensen, 2013; Raghavachari *et al.*, 2006; Abubaker *et al.*, 2021; Colgin, 2015; Park *et al.*, 2013; Lopes da Silva and Halgren, 2017). Indeed, reduced theta gamma coupling has been demonstrated in degenerative pathologies such as Alzheimer's disease and mild cognitive impairment (Nuñez and Buño, 2021; Goodman *et al.*, 2018). In epileptic mice, a shift in theta synchronisation within the hippocampal-entorhinal network has been demonstrated, whilst other temporal lobe epilepsy (TLE) animal models have shown decreased theta power spectral density. This drop in theta power has been confirmed in-vivo within the affected lobe in patients with TLE. The effect of interictal EEG activity on theta phase stability has also been studied within animal models. These have demonstrated an increase in theta phase stability (implying an increase in synchrony)

alongside theta power decrease lasting up to hours following interictal EEG discharges rather than a time-locked association with the discharge itself (Chauvière, 2020).

The findings described above provide compelling evidence of an association between temporal lobe theta disruption and epileptogenesis in TLE, accompanying an underlying network reorganisation. Unsurprisingly, both transient and long-term cognitive deficits are common in patients with TLE (Chauvière, 2020; Audrain and McAndrews, 2019).

Amnesia

Amnesia simply refers to a loss of memory; this may be in the form of loss of information or experiences. Generally, those with amnesia will remember who they are but will have difficulty remembering prior knowledge during the amnesic episode (retrograde), will temporarily lose the ability to lay down new long-term memories, or will have trouble forming new short-term memories (anterograde). However, amnesia can occasionally also affect established longer-term memories. In isolation, amnesia does not involve any other cognitive problems (Mayo Clinic, 2017).

The best-known form of amnesia is transient global amnesia (TGA), which has an estimated annual incidence of 23.5 to 32/100,000 in those over 50yrs. In TGA, amnesia is an isolated, or low recurrence incidence of temporary loss of memory usually resolving within 24 hours. Memory disruption and profound anterograde amnesia (inability to form new memories), although there may also be some variable impairment of past memory. There may be some disorientation related to the episode, often exhibiting repetitive questioning, but there is no other cognitive impairment. TGA tends to present in middle age and the elderly and can often be precipitated by strenuous exertion, highly stressful or painful experiences, Valsalva manoeuvres, and occasionally migraine. The aetiology of TGA remains elusive, with theories regarding underlying vascular, epileptic and migrainous pathologies predominating. In recent times, researchers increasingly speculate that TGA may be a phenomenon affecting brain networks rather than originating from a single source (Sucholeiki, 2018; Nehring and Kumar, 2018; Sparaco *et al.*, 2022; Nehring *et al.*, 2023). Other than eliminating differential diagnoses, treatment for TGA is generally unnecessary (Nehring *et al.*, 2023).

Memory Dysfunction in Temporal Lobe Epilepsy (TLE)

As discussed previously, both transient and long-term cognitive deficits are common in patients with TLE, and there is growing evidence of an association between temporal lobe theta disruption, network re-organisation and epileptogenesis in TLE.

TLE is the most common form of focal epilepsy. Epilepsy is diagnosed when recurrent epileptic seizures are experienced over a period of time greater than 24 hours, with no identifiable reason. The annual incidence of epilepsy in the UK is around 43/100,000, with TLE representing 60% of focal epilepsy cases (Neligan and Sander, 2015; Diehl and Duncan, 2015; Fisher *et al.*, 2017).

Focal seizures are those where the person remains aware or has impaired awareness during the event, although focal seizures can progress to bilateral seizures where consciousness is lost. The International League Against Epilepsy (ILAE) conceptual definition of seizure is “*an epileptic seizure is a transient occurrence of signs and/or symptoms due to abnormal excessive or synchronous neuronal activity in the brain*”. Focal seizures affect a localised area of the brain, rather than the whole brain (as seen in generalised seizures), with aetiologies including genetic factors, structural pathology and infections (Neligan and Sander, 2015; Diehl and Duncan, 2015; Téllez-Zenteno and Hernández-Ronquillo, 2012; Scheffer *et al.*, 2017; Fisher *et al.*, 2017; Fisher *et al.*, 2005; Patel and De Jesus, 2023).

Clinical signs in temporal lobe seizures often include an aura (warning sensation e.g. déjà-vu, epigastric, autonomic) which can be followed by behavioural arrest, staring, reduced awareness/confusion and automatisms e.g. fumbling or lip-smacking. Following the seizures, the person may be confused or suffer dysphasia. If an EEG captures a temporal lobe seizure, a temporal evolution of rhythmic theta or alpha activity is observed over one, or both temporal regions. Between seizures the EEG may contain non-epileptiform or epileptiform activities over anterior-temporal/mid-temporal regions; these may appear unilaterally, bilaterally, or bilaterally independent. Whilst patients often have no memory of seizures progressing beyond the aura (anterograde amnesia), more persistent cognitive deficits have also been reported associated with TLE including impairments in concentration, episodic memory, mental processing, word-finding and social cognition

(Diehl and Duncan, 2015; Joshi and Klein, 2019; Devinsky, 2004; Elwes, 2012; Ladino *et al.*, 2014; Novak *et al.*, 2022; Bell *et al.*, 2011; Ives-Deliperi and Butler, 2021).

An Overview of Transient Epileptic Amnesia (TEA)

Transient epileptic amnesia (TEA) is a sub-type of TLA. It is a rare condition whose exact prevalence is unknown, with only 250 cases of TEA currently described across the literature (Felician *et al.*, 2015; Savage *et al.*, 2022). TEA is characterised by recurrent, discrete, brief periods of amnesia, typically lasting less than 1 hour. Amnestic events usually occur around 12 per year and are commonly experienced on waking. Between episodes of amnesia, more persisting disturbances in memory are often experienced (Zeman *et al.*, 1998a; Butler *et al.*, 2007a; Zeman and Butler, 2010).

TEA can often go unrecognised leading to delays in diagnosis, or misdiagnosis of the condition. Clinical diagnosis can prove difficult, as TEA events can initially be misdiagnosed as TGA, psychogenic amnesia (no organic cause), or neurodegenerative disease (mild cognitive impairment (MCI), or dementia). Computerised tomography (CT)/MRI and routine EEG are often normal or non-specific in TEA cases, therefore diagnosis remains dependent on history taking and clinical examination. Estimates of the prevalence of misdiagnosis are provided by research undertaken by Del Felice *et al.* and Lanzone *et al.* The Del Felice *et al.*, reviewed 76 patients initially diagnosed with mild cognitive impairment and 4% of the cohort were subsequently found to have TEA (Del Felice *et al.*, 2014). A retrospective clinical review of TGA diagnosis performed by Lanzone *et al.* demonstrated that of 83 patients diagnosed with TGA, 18% (15 patients) were found to fit the diagnostic criteria for TEA (Lanzone *et al.*, 2018). Initial misdiagnosis can lead to significant delays in treatment, particularly for misdiagnoses of TGA, as no treatment is required (Nehring *et al.*, 2023). Concerning neurodegenerative conditions, there are no specific treatments for MCI, whilst dementia medications such as donepezil, rivastigmine and galantamine may help with symptoms of anxiety, and memory, epileptic seizures associated with TEA will remain untreated (Dementia UK, 2022).

In addition to delays in diagnosis, uncertainty regarding diagnosis, particularly the fear of progression to neurodegenerative disease and the neuropsychological effects of cognitive changes can have an adverse effect on quality of life. First-hand accounts from people with TEA describe feelings of isolation and insecurity, and a “weakened sense of self”, which create anxiety and impair social relationships (Chen *et al.*, 2018a; Zeman *et al.*, 2018; Cano-

López *et al.*, 2022). However, when accurately diagnosed, the condition responds well to anti-epileptic drug (AED) monotherapy (Zeman *et al.*, 1998b; Asadi-Pooya, 2014; Butler and Zeman, 2011).

TEA is a type of focal epilepsy arising from the temporal lobe, with amnestic events tending to occur associated with these, either during the seizures (ictal) or following (post-ictal).

TEA is a late-onset epilepsy affecting men more than women, with a mean onset of around 60 years. During the amnestic episode, people with TEA retain awareness, but have a sense of recalling that they could not remember. Amnesia is predominantly retrograde memory dysfunction (affecting recently stored past memories), with some anterograde (new memory) loss. In some cases, there are other subtle signs suggestive of epilepsy, such as lip-smacking, chewing automatisms, or more commonly olfactory or gustatory hallucination. As with other types of amnesia such as transient global amnesia (TGA), there may be some disorientation related to the episode, often exhibiting as repetitive questioning.

The first account of memory loss associated with epileptic seizures was made by the eminent Neurologist, John Hughlings Jackson in 1888. Several researchers described similar cases following this, but it wasn't until 1990 that researcher Narinder Kapur coined the term "Transient Epileptic Amnesia". In his research, Kapur also noted a more persistent change in retrograde memory interictally. (Kapur and Markowitsch, 1990; Kapur, 1993a; Hughlings-Jackson, 1888; Zeman *et al.*, 1998b).

An in-depth study of 10 cases was undertaken by Zeman *et al.* in 1998 which included detailed history and examination, EEG, neuro-imaging and extensive neuropsychological assessment. The study confirmed that the majority of amnestic episodes in people with TEA had a duration of less than an hour (however two patients reported a significantly longer duration), and commonly occurred on waking. Both retrograde and anterograde amnesia were again reported associated with seizures, with confirmation of Kapur's theory that background interictal retrograde memory dysfunction extended beyond the discrete events. EEG findings were again equivocal interictally, but where present tended to be of temporal lobe origin. The clinical, EEG and neuropsychology findings of the study are summarised in Table 2 (Zeman *et al.*, 1998b).

Zeman et al. proposed diagnostic criteria for TEA:

“(1) a history of recurrent witnessed episodes of transient amnesia.

(2) cognitive functions other than memory judged to be intact during typical episodes by a reliable witness.

(3) evidence for a diagnosis of epilepsy based on one or more of the following:

epileptiform abnormalities on EEG, the concurrent onset of other clinical features of epilepsy e.g., lip-smacking, olfactory hallucinations, a clear-cut response to anticonvulsant therapy” (Zeman et al., 1998b; Butler et al., 2007a).

Table 2: Clinical, EEG and neuropsychological features from a cohort of 10 TEA subjects (Zeman et al., 1998b)

Case	Age	Sex	History (duration)	Attacks	Attack (duration)	Repetitive questioning	Sleep related	EEG findings	Rx response	Other epilepsy	TEA aura	Focal retrograde amnesia
1	63	M	3 y	20	1 h	+	+	-	+ CBZ	sps	+/-	+
2	49	M	4 months	12	<1 h	+	+	+Bilateral	+ CBZ	sps	+/-	+
3	68	M	8 months	5	h-days	+	+	+Bilateral	+ SVP	sps,cps	-	+
4	66	F	14	5	<1 h ≥ 1 h	+	+	+L	E CBZ	-	-	-
5	79	M	15 months	3	h-days	+	+	+Bilateral	E CBZ	-	-	+
6	70	M	2 y	13	<1 h	+	+	Polyr	no Rx	sps	+/-	-
7	73	M	6 months	5	1-2 h	-	+	Polyr	+ P	-	-	-
8	60	M	6 months	3	<1 h ≥ 1 h	+	+	-	+ SVP	tcl	-	+
9	69	M	4 months	3	<1 h	+	+	-	+ CBZ	cps	+/-	+
10	56	M	9 months	20	<1 h	+	+	-	+ CBZ	cps, tcl	-	+

Polyr = polyrhythmic abnormalities present; Rx response = treatment response (+ = abolition or substantial reduction of episodes, E = equivocal reduction, CBZ = carbamazepine; P = phenytoin, SVP = sodium valproate); sps = simple partial seizures; cps = complex partial seizures; tcl = tonic-clonic seizures; TEA aura = occurrence of co-occurring seizure type as prodrome of amesic episode (+ = co-occurring seizure type always precedes TEA, +/- = co-occurring seizure type sometimes precedes TEA, - = no co-occurring seizure type).

Several large-scale studies have been undertaken, including a study of 50 patients performed by Butler et al. in 2007 as part of The Impairment of Memory in Epilepsy (TIME) Project. The study uses similar methods to those employed by Zeman et al. and provides support for previous key findings regarding the condition: the findings are consistent regarding average age of onset, recurrence and duration of attacks, main symptoms during attacks and good response to AED (Zeman et al., 1998b; Pritchard et al., 1985; Kapur, 1993b; Gallassi et al., 1992; Gallassi, 2006; Felician et al., 2015; Butler et al., 2007b; Hodges and Warlow, 1990; Mosbah et al., 2014; Lapenta et al., 2014). An update of the TIME project and associated literature review undertaken by Baker et al. in the 2021 study sheds further light on TEA as a condition and the associated interictal memory changes. The mean intelligence quotient (IQ) of people with TEA is reported as higher than the general population, with executive memory remaining intact. Slight changes are seen on standard memory tests in some studies. Slight impairments were noted in anterograde memory and

semantic memory recall after 30 mins., with a sharp decline in recall noted over 30 mins. to 1 week, and a lesser extent over 1 to 3 weeks of recall (Baker *et al.*, 2021; Manes *et al.*, 2005b; Blain *et al.*, 2021). This has been termed accelerated long-term forgetting (ALF). There was also significant impairment noted interictally concerning episodic memory, in particular patchy loss of recall for significant autobiographical events e.g., birthdays, holidays etc. – autobiographical amnesia (AbA). A study by Blain *et al.* describes ALF occurring in 87% of a TEA group with hippocampal calcification, however, this pathology showed no correlation with any specific cognitive complaint (Blain *et al.*, 2021; Baker *et al.*, 2021; Manes *et al.*, 2001; Manes *et al.*, 2005b; Butler *et al.*, 2007a). In contrast to Gallassi's findings (Gallassi, 2006), interictal memory difficulties were shown to be persistent even following AED treatment, although some improvement in ALF has been reported following the cessation of seizures (Baker *et al.*, 2021; Savage *et al.*, 2022; Savage *et al.*, 2019a).

More recent studies into TEA have explored detailed aspects of impairment associated with the condition, such as picture recognition and olfactory disturbances (Dewar *et al.*, 2015; Savage *et al.*, 2017d). A follow-up study performed as part of the TIME Project in 2016; revisited the 10 patients initially reported in 1998 by Zeman *et al.* and again in 2007 by Butler *et al.* as part of their 50-patient cohort (Zeman *et al.*, 1998b; Butler *et al.*, 2007a; Savage *et al.*, 2017a). The aim was to investigate the long-term clinical and cognitive effects of TEA and demonstrate that the memory difficulties seen in 2007 persisted, but there was no significant additional cognitive decline noted over time. Further longer-term research by the Impairment of Memory in Epilepsy (TIME) team has concluded that there is no reduction in life expectancy in people with TEA, and no evidence of progression to dementia (Savage *et al.*, 2017b; Savage *et al.*, 2022).

The emphasis of most TEA studies has been to further understand the condition; other than clinical examination and history taking there is little evidence to date regarding improving diagnosis. Symptomatology suggests pathophysiology in TEA is likely to involve the hippocampus and in some cases the amygdala, limbic system, or neighbouring temporal lobe structures. There have also been reports of TEA symptoms in patients with limbic encephalitis but, as stated earlier standard CT and MRI studies have not demonstrated any consistent abnormalities. However, when abnormalities have been present, these tend to

be over the temporal, hippocampal and amygdala structures (Zeman *et al.*, 1998b; Kapur, 1993a; Blain *et al.*, 2021; Oagawa *et al.*, 2021; Cretin *et al.*, 2020; Chiba *et al.*, 2020; Savage *et al.*, 2019b; Pizzanelli *et al.*, 2022; Chakravarty *et al.*, 2021).

Neuroimaging in TEA

Some more sophisticated neuroimaging techniques have been performed in a small number of studies. Volumetric analysis of the MRI has demonstrated subtle volume loss over the hippocampi bilaterally and also over the perirhinal and orbitofrontal regions (Butler *et al.*, 2013). Milton *et al.* used fMRI comparing TEA patients to normal controls using memory tasks, with people with TEA showing reduced activation of the right posterior parahippocampal gyrus (pPHG), the right temporal-parietal junction and the right cerebellum during recall. The study also demonstrated comparatively reduced effective connectivity between the right pPHG and the right middle temporal gyrus (Milton *et al.*, 2012). TEA Research using positron emission tomography (F18-FDG PET) has revealed hypometabolism over bilateral middle frontal gyrus and mesial temporal lobe, with the latter statistically significant concerning anterograde and retrograde memory dysfunction (Mosbah *et al.* 2014); these findings were not specific to TEA.

Scalp EEG Findings in TEA

The sensitivity of visual inspection of routine interictal EEG is often too low to provide a robust diagnostic tool for TEA. However, EEG recordings incorporating sleep are more successful in providing diagnostic evidence in the form of epileptiform activities over anterior or mid-temporal regions during non-REM sleep (Pukropski *et al.*, 2022; Blain *et al.*, 2021; Baker *et al.*, 2021; Ramanan *et al.*, 2019; Lanzone *et al.*, 2018; Lapenta *et al.*, 2014; Mosbah *et al.*, 2014).

There are also several case studies of ictal EEG recordings. Gallassi documented a seizure associated with automatisms followed by an amnesic episode: the EEG showed rhythmic theta activity over the anterior-temporal regions followed by bilateral attenuation of the EEG; a 15-minute amnesic event followed where the EEG appeared similar to the pre-ictal recording (Gallassi, 2006). Previously Tassinari *et al.* described a similar seizure followed by amnesia where the EEG demonstrated a focal temporal seizure (Figure 16), with post-ictal

amnesia (Tassinari *et al.*, 1991). There are several reports from long-term monitoring of numerous seizures being recorded which appear to occur in N1 or N2 sleep; amnesia did not appear to be associated at the time but patients presented with amnesic events subsequently (Burkholder *et al.*, 2017).

Other accounts of ictal EEG during amnesia report ictal EEG abnormalities during the amnesic event, however, these tend to be limited to longer episodes lasting several hours – the EEG descriptions in some cases appear to be that of non-convulsive status epilepticus (Vuilleumier *et al.*, 1996; Butler and Zeman, 2008; Dasheiff, 1997; Meo *et al.*, 1995). A recent report documents two cases of TEA associated with frequent subclinical focal onset temporal lobe seizures arising from sleep, in patients with a history of amnesia on waking. The author suggests these subclinical nocturnal seizures may explain the transient cognitive impairments typical of TEA (Burkholder *et al.*, 2017). These studies reveal that amnesia associated with TEA appears post-ictal or ictal in nature, with episodes of longer duration, likely representing non-convulsive status epilepticus.

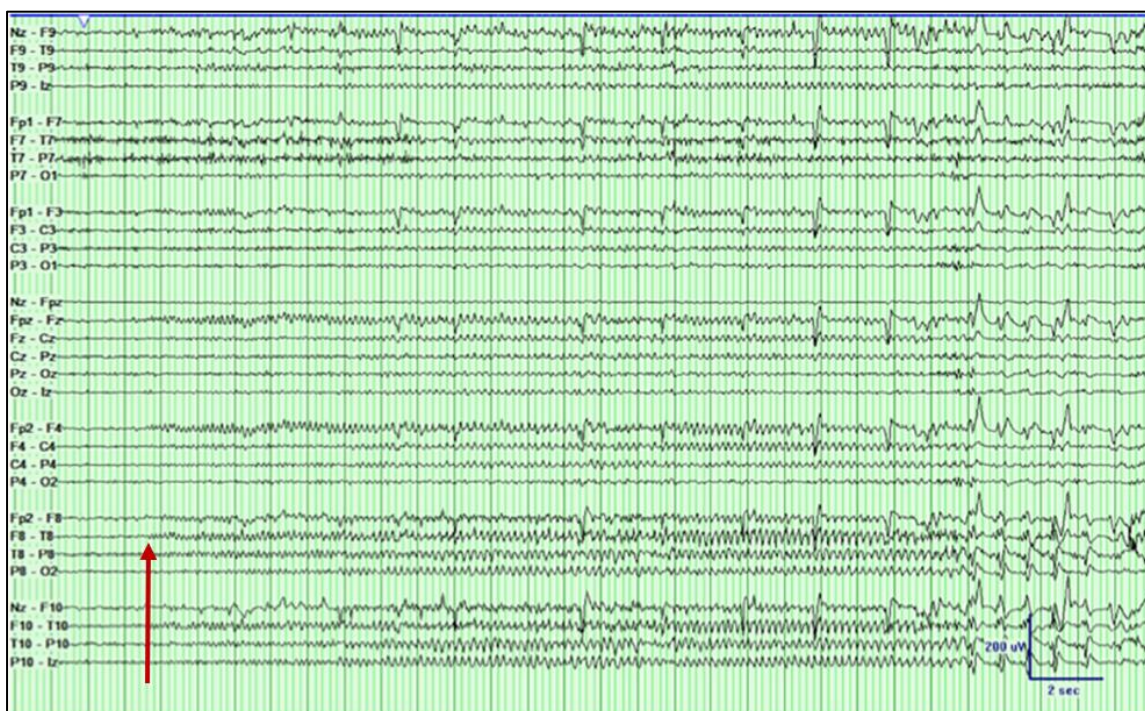


Figure 16: Example of a temporal lobe seizure with right hemisphere onset

In summary, TEA is a type of late-onset temporal lobe epilepsy with associated recurrent ictal/post-ictal amnestic events and more persistent interictal memory dysfunction in the form of ALF and AbA. TEA is underdiagnosed or can be misdiagnosed, leading to a delay in diagnosis and treatment. Once treated with antiepileptic drugs, there is generally good remission of seizures, but memory dysfunction often remains an ongoing problem.

How has Connectivity Analysis been used Memory and Epilepsy Research?

As mentioned previously, the study of brain networks and connectivity has expanded rapidly over the last few years. Whilst we have provided an overview of connectivity and how EEG has been integrated within research, this section seeks to provide examples of how network and connectivity research is furthering medical knowledge regarding a selection of relevant conditions.

Amnestic Syndromes

1.4. TEA/TGA

It seems appropriate to first discuss EEG research currently existing within the field of our chosen condition, TEA. However, a literature search yielded very few results. Research reported by Lanzone et al. in 2020 and Sancetta et al. in 2022 were the only literature found directly related to qEEG findings in TEA and there was no research currently available about connectivity using EEG.

Both studies mentioned above originate from the same research group and explore mPSD analysis findings from TEA and TGA patients. Lanzone et al. took a TEA approach within their paper, and Sancetta et al. focussed more on TGA. Lanzone et al. utilise the TGA group as a “normal” EEG control (Lanzone *et al.*, 2020). The author acknowledges that there are no pre-existing qEEG studies involving TEA. PSD analysis was undertaken using exact Low-Resolution Brain Electromagnetic Tomography (eLORETA) and demonstrated an increase in beta power over the hemisphere containing the epileptogenic focus, localising to the mesial temporal lobe. The authors speculate that the findings may correlate with memory impairment in epilepsy, due to the region of interest (ROI) being involved in memory functions such as episodic memory and recall. The authors postulate that the findings may represent a compensatory mechanism to sustain memory function (Lanzone *et al.*, 2020).

From a TGA perspective, Sancetta et al. reported that compared to TEA, the TGA group showed a significantly increased relative theta mPSD, with no regional differences or changes within other frequency bands found (Sancetta *et al.*, 2022). This finding has been confirmed in other TGA studies, although additional findings were also described, including decreased absolute alpha and beta power, increased absolute delta power, increased left

parietal-occipital theta mPSD, decreased frontal-temporal theta, and decreased parietal-occipital and parietal beta mPSD (Primavera *et al.*, 1993; Ukai and Watanabe, 2017; Park *et al.*, 2016b; Park *et al.*, 2016a; Jung *et al.*, 2022). Many of these findings were seen during the acute phase of the TGA episode, however, Primavera *et al.* report an ongoing marked reduction of absolute beta and alpha power in the temporal-parietal regions 1-week following the resolution of an episode (Primavera *et al.*, 1993).

1.5. Amnestic Mild Cognitive Impairment (aMCI)

Some forms of mild cognitive impairment (MCI) are associated with amnesia and have been shown more susceptible to progress to AD (Zhu *et al.*, 2021). Zhu *et al.* describe increased connectivity over frontal-temporal, frontal-parietal and temporal-parietal networks using Resting-state functional magnetic resonance imaging (rs-fMRI) (Zhu *et al.*, 2021). More specifically, Li *et al.* reported significantly reduced functional connectivity strength over the left middle temporal gyrus in aMCI (Li *et al.*, 2021). In a further rs-fMRI study, Zhang *et al.* described lower connectivity in the default mode network (DMN), alongside significant connectivity increases in the sensorimotor network. Remote DMN connectivity reduction was associated with lower cognitive performance, specifically, within the delayed Auditory Verbal Learning Test (Zhang *et al.*, 2017). However, this finding has been contradicted in a recent study by Liang *et al.* who reported increased connectivity in the DMN and the central executive network (CEN) (Liang *et al.*, 2020).

Alzheimer's Disease (AD) and Mild Cognitive Impairment (MCI)

The pathological cognitive decline within conditions such as mild cognitive impairment (MCI) and Alzheimer's disease (AD) is associated with episodic and working memory decline in the earliest stages of the disease, including accelerated long-term forgetting (ALF). In AD, this is often associated with medial temporal lobe pathology (Bondi *et al.*, 2017; Abubaker *et al.*, 2021). Whilst it is recognised, from long-term follow-up of TEA patients, that TEA appears relatively benign with no evidence of increased prevalence of dementia within the condition compared to the general population (Savage *et al.*, 2017c; Savage *et al.*, 2017b; Savage *et al.*, 2017a), similar electrophysiological mechanisms may underlie both conditions.

Common mPSD alterations associated with pathological cognitive decline include a well-documented reduction in mPSD of beta and posterior alpha, with a shift in maximum alpha

and beta power anteriorly (Dierks *et al.*, 1993; Dierks *et al.*, 2000; Huang *et al.*, 2000; Babiloni *et al.*, 2016; Jeong, 2004; Giustiniani *et al.*, 2023). Within the theta and delta frequency bands a widespread increase in mPSD in patients with Alzheimer's compared to the "normal" old (Nold) (Jeong, 2004; Babiloni *et al.*, 2006a; Rossini *et al.*, 2007; Babiloni *et al.*, 2016; Babiloni *et al.*, 2021a; Giustiniani *et al.*, 2023).

Connectivity studies of AD and MCI have included coherence and synchronisation. There appears to be a consensus that in these conditions, a reduction in both coherence and synchronisation concerning alpha and beta frequencies (Giustiniani *et al.*, 2023; Fischer *et al.*, 2023; Rossini *et al.*, 2007; Jeong, 2004; Stam and van Dijk, 2002). Findings regarding slower frequencies are more contentious, with studies reporting both increases and decrease in coherence both intra- and inter-regionally (Babiloni *et al.*, 2009; Escudero *et al.*, 2011; Tóth *et al.*, 2014b; Vecchio *et al.*, 2014). With regard to inter-hemispheric coherence, a reduction in alpha and beta coherence has been described between frontal, temporal, and parietal regions, whilst parietal-occipital coherence within these bands may be increased (Giustiniani *et al.*, 2023). With the use of synchronisation likelihood measures, lower coupling has been seen within frontal-parietal networks across delta-alpha bands (Babiloni *et al.*, 2006a). Central-occipital synchronisation reduction within delta frequencies has also been reported in several AD studies (Giustiniani *et al.*, 2023).

Temporal Lobe Epilepsy (TLE)

Connectivity analysis has been extensively utilised for the epilepsies. The focus of this section will be on focal epilepsy, due to its relevance within the project. People with focal epilepsy can suffer from widespread and debilitating neuro-cognitive dysfunctions. Resting state EEG can demonstrate ongoing inter-ictal abnormalities not just around the ictal onset zone but also further afield. Evidence now suggests that interictal network alterations contribute to cognitive deficits (Burman and Parrish, 2018; Englot *et al.*, 2016; Van Diessen *et al.*, 2014).

fMRI and electrocorticography (ECoG) based connectivity studies are the most performed concerning focal epilepsies, and most studies tend to use resting-state analysis. There are a significant number of connectivity studies in temporal lobe epilepsy describing increased functional connectivity across the mesial temporal structures, including the hippocampus,

and other limbic regions such as the insula and thalamus. Other research points to more widespread or generalised alterations in connectivity interictally. These include the disruption of cross-hemispheric networks and increased ipsilateral functional connectivity with these patients more likely to achieve seizure freedom). (Englot *et al.*, 2016; Liao *et al.*, 2010; Haneef *et al.*, 2014; Dinkelacker *et al.*, 2015; Morgan *et al.*, 2011) (Omidvarnia *et al.*, 2017).

The research strongly points to increased functional connectivity around the ictal onset zone of the temporal lobe, including the hippocampus and other limbic structures, but also to more widespread network changes not directly adjacent to the epileptogenic focus. These findings suggest a shift in functional connectivity patterns which may be due to seizure-related synaptic changes (Omidvarnia *et al.*, 2017)

Summary

The clinical symptoms of TEA can be very distressing for both patients and family causing anxiety, particularly when the cause is unknown or not understood. By seeking to advance current methods of diagnosis of TEA, the study aims to increase understanding of the condition, aid diagnosis and improve quality of life.

The use of networking and connectivity analysis of resting-state EEG improves the spatial resolution previously offered by EEG. Its use has improved the understanding and treatment of conditions such as AD by demonstrating localised alterations in network characteristics. Currently, no studies are exploring the network dynamics of TEA, therefore this study aims to further knowledge of the disease through the study of pathophysiological networks and connectivity mechanisms within the brain. Due to the consistency of network measures employed in AD research, similar methods will be employed within this study: Graph theory, with resting-state EEG, and connectivity measures e.g. cluster co-efficient and network metrics including centrality evaluations.

Principle hypothesis for this study: Networks and connectivity analysis of resting-state EEG in TEA will demonstrate distinct functional alterations compared to healthy volunteers.

Current literature provides consistent evidence regarding the symptoms and treatment of TEA. EEG research with regards to TEA, however, provides conflicting evidence with regards

to whether the amnestic element is ictal or post-ictal in nature. It is known that interictal EEG abnormalities are often non-specific in TEA, but there is no clear evidence to date regarding the frequency of occurrence compared to healthy controls. Therefore, the study will also seek to shed further light regarding the ictal nature of amnesia in TEA and to assess the prevalence of interictal abnormalities compared to an age-matched healthy population, both using visual analysis of the raw EEG.

Methods

Research Rationale

This research is a sub-study within the TIME project (The Impairment of Memory in Epilepsy) run by Exeter University. The TIME project is a programme of research projects with the following aim: to learn more about Transient Epileptic Amnesia (TEA), a form of temporal lobe epilepsy which causes temporary and persistent memory problems. The research projects cover three problems that may contribute to the understanding of impaired memory functioning in epilepsy (Zeman and Butler, 2022a):

- Seizures causing attacks of memory loss
- Accelerated long-term forgetting (ALF)
- Autobiographical amnesia

Routine EEG, sleep EEG and long-term EEG monitoring are recommended procedures in the diagnosis of epilepsy (NICE, 2022). The resting-state EEG (rsEEG) is included as part of the diagnostic criteria for TEA and is used for this research project, as it is a readily available ~~and~~ retrospective source of data (Butler *et al.*, 2007b; Ukai *et al.*, 2021).

Patients considered for the diagnosis of TEA usually fall in the “young old” category at around 60 years of age. It is well recognised that rsEEG activities alter during the ageing process, including a shift to the lower end of the normal spectrum of the posterior dominant alpha rhythm, with less reactivity on eye-opening, plus a general reduction of background EEG amplitudes (Babiloni *et al.*, 2021a; Schomer and Da Silva, 2018; Rossini *et al.*, 2007; Babiloni *et al.*, 2006a; Widdess-Walsh *et al.*, 2005). It has also long been recognised that non-specific focal polymorphic slowing occurs more commonly in healthy volunteers as age progresses, with such waveforms seen in approximately 30-50% of those over 60yrs (Peltz *et al.*, 2010; Klass and Brenner, 1995). These waveforms can be classed as borderline, non-epileptiform, abnormalities and are thought most likely due to cerebrovascular or neurodegenerative changes associated with ageing (Widdess-Walsh *et al.*, 2005; Peltz *et al.*, 2010; Schomer and Da Silva, 2018).

For this reason, EEG findings in those being investigated for TEA are often inconclusive or borderline, due to the limited sensitivity of rsEEG as a diagnostic tool. This can necessitate further investigation before diagnostic evidence of seizures is obtained, causing a delay in diagnosis (Zeman and Butler, 2022b).

EEG changes often exist in older people, and delineation of any changes specific to TEA can be difficult using current “gold standard” visual analysis. The development of QEEG analysis, including the aspects of connectivity and networking, raises the possibility that potentially key diagnostic information may be uncovered from within the EEG waveforms which have previously been inaccessible. This has begun to be demonstrated with pathological neurodegenerative conditions such as Mild Cognitive Impairment (MCI) and Alzheimer’s disease (Franciotti *et al.*, 2022; Babiloni *et al.*, 2021b; Eyer *et al.*, 2019; Blinowska *et al.*, 2017; Teipel *et al.*, 2016). This study aims to investigate whether this is the case for the TEA population, as there are currently no rsEEG connectivity studies specific to this emerging condition.

Research Aims

1. Primary Objective

Using resting state EEG, to compare qEEG, networking and connectivity in patients with TEA with healthy age-matched controls.

Hypothesis: The network analysis of resting-state EEG activities reveals distinctive qEEG, or networking and connectivity patterns in TEA patients compared to age-matched healthy controls.

Null Hypothesis: There is no statistical difference between qEEG or networking and connectivity in TEA patients and healthy age-matched controls.

Confirmation of the primary outcome will provide further knowledge and understanding of TEA as a condition and improve diagnosis times.

2. Secondary Objectives

Using visual EEG analysis, to compare background activities and non-specific EEG abnormalities in TEA patients with healthy age-matched controls.

To further explore a visual analysis of the EEG recordings:

- Determine whether background activities and borderline scalp EEG abnormalities are more common or differ in any way in TEA than in age and sex-matched healthy controls.
- Where activities differ significantly, to determine in what frequency bands and distributions this occurs.
- Determine what scalp EEG changes are seen during clinical events in TEA.

3. Primary endpoint/outcome

The expected primary outcome is a statistically relevant alteration of brain networking and connectivity in TEA patients. The significance of any alterations is assessed by comparing the analysed data with an age and sex-matched control group.

4. Secondary endpoint/outcome

If the primary outcome of the study is achieved, it would be of clinical importance to:

- Compare the findings to published data regarding networking and connectivity changes associated with other disorders involving cognitive impairment such as mild cognitive impairment (MCI) and Alzheimer's disease (AD).
- Assess whether the networking and connectivity changes in TEA differ in any statistically significant way from those seen in temporal lobe epilepsy without amnesia.

Research Methods Approach

1. Ethics

IRAS application submitted to the NHS Health Research Authority – REC reference 20/NW/0376, IRAS project ID 272304.

Assessed and received a favourable ethical opinion from the North-West-Greater Manchester East Research Ethics Committee on the basis described in the application form, protocol and supporting documentation. The following conditions were met before the start of the study:

- Confirmation of capacity and capability was sought for all NHS organisations EEGs were obtained from, these included NHS organisations in both England and Scotland. This included the provision of all required REC-approved documents

REC reporting requirements were adhered to throughout the study.

Academic Ethics approval was gained via the Academic Ethics Committee at Manchester Metropolitan University.

Approval to access healthy volunteers through the Exeter 10,000 project (EXTEND), was gained via National Institute for Health and Care Research (NIHR)/ Exeter Clinical Research Facility. This included a presentation of the research aims to the Peninsula Research Bank (PRB) steering committee before acceptance.

Permission to use the Montreal Cognitive Assessment Scale (MoCA) as an assessment of eligibility within this study was gained before use.

2. Subjects

EEG data was obtained from the following patient and participant groups:

- TEA patients who were existing participants of the TIME project (project ID 69738).
- Healthy participants (age and gender-matched subjects) were recruited from:
 - Existing research using EEG data: (the Memory and Learning: Cognitive processes underlying disorders of memory research project; IRAS ID 33500; MREC Reference: 06/MRE07/40).
 - Exeter 10,000 project (EXTEND) research volunteers; these were new EEGs performed as part of this research. The project is run by the NIHR Exeter Clinical Research Facility, a partnership between the University of Exeter Medical School and the Royal Devon & Exeter NHS Foundation

Trust. It is funded by the National Institute for Health Research. The project has collected data and samples of blood and urine from 10,000 people who have agreed for this to be used anonymously in health research. Most project participants have also agreed to be contacted again if their profiles match the requirements of future research studies. Consent for participation in further studies has been given as part of the EXTEND recruitment process, with details of this held on the Exeter 10,000 project database.

3. Inclusion/Exclusion Criteria

3.1. Inclusion Criteria

TEA group:

- All TEA recruits had a formal diagnosis of TEA, meeting Zeman et al. diagnostic criteria:
 - “A history of recurrent witnessed episodes of transient amnesia.
 - Cognitive functions other than memory judged to be intact during typical episodes by a reliable witness.
 - Evidence for a diagnosis of epilepsy based on one or more of the following:
 - Epileptiform abnormalities on EEG,
 - The concurrent onset of other clinical features of epilepsy e.g., lip-smacking, olfactory hallucinations
 - A clear-cut response to anticonvulsant therapy” (Zeman *et al.*, 1998b; Butler *et al.*, 2007a).
- Adults (Male and Female)
- There were no age restrictions, although TEA generally occurs in older adults, around an average age of 60 years.
- Existing EEG data had been obtained as part of their clinical care plan.

Healthy Participants

- Participants were gender and age-matched to include TEA participants.

- Healthy volunteers recruited via the Exeter 10,000 project (EXTEND) were required to undertake the Montreal Cognitive Assessment (MoCA). A score of who score greater than 26 was required to be eligible to participate (Alzheimer's Society, 2015).

3.2. Exclusion Criteria

- Those still in the process of being investigated for TEA
- TEA candidates with an additional diagnosis of AD/MCI at the time of the EEG recording
- TEA candidates with additional central neurological disease, cardiac disease or peripheral vascular disease at the time of the EEG recording.
- TEA patients with no existing EEG data.
- Those lacking the capacity to give consent themselves.
- Healthy controls with a history of central neurological disease, cardiac disease or peripheral vascular disease.
- Healthy controls scoring 26 or less on MoCA. Where potential healthy control participants scored less than 26, the finding was reviewed by a Neurologist on the study team. If the findings were considered significant, this was communicated to the General Practitioner (GP) and the individual was informed.

4. Recruitment

A total of 50 TEA study participants had already been recruited as part of the TIME project (project ID 69738 – the start of the project predates IRAS). Retrospective EEG Data had been recorded from patients diagnosed with TEA as part of their normal care pathway.

Permission was sought via Research and Development Departments within relevant NHS Trusts across England and Scotland. Permission was granted following an assessment of the capacity and capability of the Trusts and their Neurophysiology departments to undertake the work. EEG data for 28 of the TEA study participants were subsequently obtained.

Healthy control data from the Edinburgh research project: *Memory and Learning: Cognitive processes underlying disorders of memory research project* was selected from age and sex matched participants.

4.1. Recruitment of additional participants

Recruitment of healthy participants from EXTEND was undertaken by the Exeter 10,000 project team. Details of the inclusion and exclusion criteria were supplied, along with the sex and age demographic required to match potential candidates to TEA participants. The EXTEND project team undertook a database search for volunteers meeting the EEG project criteria and gained initial consent for the TEA project team to make contact.

5. Consents

Consents for the TIME project EEG data were already in place, as part of recruitment to the overarching TIME project. This included access to medical records (which includes the EEG data) for the initial and further research undertaken as part of the TIME project.

Consents for healthy control EEG data obtained from the Edinburgh research project *Memory and Learning: Cognitive processes underlying disorders of memory research project* (IRAS ID 33500; MREC Reference: 06/MRE07/40) had already been obtained as part of the original study. This included the use of data in further relevant research.

Consent to contact potential healthy participants from EXTEND was gained by the Exeter 10,000 project team and the contact details of consenting participants were communicated to named staff within the Neurophysiology department via secure NHS email. Potential participants were contacted by email or via telephone (dependent on the participant's wishes) to discuss the project further and allow for questions. Consent discussions and consent-taking included an option for collected pseudonymised data to be used for further research. If interpretation services were required, this was booked using the usual procedures, as per the RDEFT Interpretation and Translation Policy and Procedure. An informed consent form (ICF) (along with a further copy of the patient information sheet (PIS)) was sent via post or email (depending on the participant's wishes). At this stage, if the potential participant verbally confirmed their willingness to participate, the date and time of the EEG appointment was agreed with the participant. The EEGs were undertaken in the Neurophysiology department at RDEFT, with written consent taken and MoCA assessment being undertaken before the EEG was performed.

6. Data Collection

EEG data from 28 patients diagnosed with TEA and 28 healthy controls were collected from several sources as follows:

6.1. Collection of EEG data from existing TIME project TEA participants

EEG data for 28 TIME project TEA participants had previously been acquired as part of the normal care pathway for TEA and patient consent already exists for the TEA cohort. Some TEA participants also underwent repeat EEGs. The TIME database holds information regarding which NHS Trusts hold the original EEG data. Once permissions were granted by the relevant Research and Development team, Neurophysiology departments were contacted by email initially, to request the EEG data. Once confirmation of data accessibility was received, the relevant consent forms were forwarded.

A copy of the EEG data, including any repeat studies, was obtained by the hosting Neurophysiology department and sent via encrypted email, or shared via their Trust-approved secure route (e.g. Microsoft OneDrive). If email or secure data sharing was not possible, the data was uploaded to an encrypted memory stick (provided as part of the project) and sent to the EEG project team via Royal Mail Special Delivery. The EEG data was provided in European Data File Format (EDF) using a common reference (rather than a bipolar EEG montage) Once received by the EEG project team, the participant's details were added to the EEG research database and a unique participant number (UPN) allocated. The EEG files were uploaded to the Principal Investigator's (P.I.) Manchester Metropolitan University OneDrive. An anonymised file of each EEG file was created using the corresponding UPN. All traces of patient-identifiable data were removed, including those held in the file header. Sex, and age at the time of EEG were retained on the EEG research database for age and sex matching purposes. Any data residing on encrypted memory sticks was securely held through the TIME project in a locked cabinet.

6.2. Collection of healthy volunteer EEG data from the Memory and Learning research study

This was existing data held at Edinburgh University. Eighteen suitable age and sex-matched EEG data were identified by the Principal Investigation for the Edinburgh project. The 18

data-matched EEG files were shared via the Edinburgh project OneDrive and copied directly to the P.I.'s Manchester Metropolitan University OneDrive. The file information i.e., Edinburgh project ID number, participant age and sex, were added to the EEG research database and a UPI was allocated. Files accessed were in EDF or Neuroscan file (.cnt), all with a common EEG reference electrode. One Neuroscan file was found to be unreadable and was therefore excluded from the study

6.3. Collection of additional healthy volunteer EEG data

This cohort of eleven participants was recruited through the Exeter 10,000 project (EXTEND). Following recruitment and verbal consent, the participants were contacted via telephone and an appointment to have a routine EEG performed was arranged; any further questions they had at this time were answered.

Written consent was obtained before the EEG was performed and a MoCA assessment was undertaken.

The EEG investigations were performed in the Neurophysiology department at the RDEFT, after the normal NHS hours.

The raw EEG data was stored on the department's secure EEG database, which is maintained by the Trust Informatics department. The participant's name, age at the time of EEG, and sex were added to the EEG research database and a UPI was allocated. An anonymised EDF data file for each EEG was copied directly to the P.I.'s MMU OneDrive, using the UPI as the filename.

The possibility that healthy volunteer EEGs may reveal some incidental abnormalities was considered and processes were put in place to mitigate this. There is a low risk that unexpected abnormalities may be found on the EEG. It is recognised however, that subtle irregularities and abnormalities can develop within the EEG activity as we age. In most cases, these do not indicate an underlying medical problem and would be regarded as within the normal range for age. However, in the situation that a volunteer's EEG revealed unexpected abnormalities the following process was used:

- The possibility of incidental findings was discussed with every participant as part of the consent process. Formal consent was taken before the EEG was performed.
- If such changes were identified, these were reviewed by a Neurologist to determine the significance of the findings. The Neurologist reviewed the abnormalities with the following in mind:
 - the potential severity of the abnormalities and the certainty with which this is known
 - The nature of the test, for example, the predictive value of the test and the chance of false positives
 - Whether the abnormalities were clinically actionable i.e. whether there are available and accessible strategies for prevention, management or treatment of any potential underlying condition.
- If the Neurologist recommended further action, the participant was contacted and referred to the Neurology clinic.

7. Blinding

All EEG data was anonymised using a UPI before data cleansing was performed, to avoid bias.

8. Data Types

- Raw EEG Data (EDF files)
- Categorical Nominal
 - Sex
 - Study Groups (TEA, Healthy)
 - Brain Regions
 - Frequency Bands
 - Electrodes
- Categorical Ordinal
 - Age Categories (3 bins)
- Numerical Discrete
 - Number of participants

- Numerical Continuous
 - Mean Frequency/ Log10 Mean Frequency
 - Log10 Mean Frequency - Inter-hemisphere difference (to accommodate negative numbers, a standard value of 100 was added before undertaking Log10 transformation).
 - Mean Power Spectral Density/ Log10 Mean Power Spectral Density.
 - Log10 Mean Power Spectral Density - Inter-hemisphere difference (to accommodate negative numbers, a standard value of 100 was added before undertaking Log10 transformation).
 - Imaginary coherence (iCoh)
 - iCoh – Inter-hemisphere difference
 - Weighted Phase Lag Index (wPLI)
 - wPLI – Inter-hemisphere difference
 - Phase Transfer Entropy (PTE)
 - PTE – Inter-hemisphere difference

The inter-hemisphere difference was calculated using the asymmetry index (A_i) recommended by IFCN ($A_i = (Leftr - Rightr) \div (Leftr + Rightr) \times 100$) (Babiloni *et al.*, 2020), positive values (> 0) denote a left hemisphere emphasis, whilst negative values (< 0) denote a right hemisphere emphasis.

9. Data pre-processing

EEG signals are a graphic representation of fluctuating local field potentials, recorded at scalp level over time. These field potentials are created by extracellular ionic currents flowing within the cerebral cortex, primarily from within layers IV (the internal granular layer) and V (the ganglionic layer). The extracellular generators of these currents are predominantly excitatory and inhibitory post-synaptic potentials (EPSPs and IPSPs), with local field potentials (LFP) caused by the summation of the electrical currents from large populations of activated neurons. The fluctuations in LFPs can be recorded at the scalp due to a phenomenon called volume conduction, where the electrical signals are transmitted

through the brain, meninges and skull to the electrodes on the scalp (Beniczky and Schomer, 2020; Schomer and Da Silva, 2018; Brienza and Mecarelli, 2019; Jackson and Bolger, 2014). The transmission process through the various brain layers and skull attenuates the electrical signals, and by the time the electrical activities reach the scalp, the electrical EEG signals detected are in the order of microvolts (μV).

In addition to electrical generators within the brain, there are several other electrical sources within the human body and from external sources, which can be detected within an EEG recording. These include the electrocardiogram (ECG), respiration, sweat, muscle activity, eye blinking, movement, the electrodes, and mains electrical interference (i.e. 50/60Hz depending on the country). Non-cortical electrical activities detected within the EEG recording are described as artefacts which, if not minimised, contaminate the cortical activities seen at the scalp, leading to misinterpretation (Beniczky and Schomer, 2020; Hartman and Lesser, 2018; Brienza *et al.*, 2019).

As mentioned previously, the EEG data used for the study was resting state EEG recorded for scalp electrodes over a period of time. Typically a routine clinical EEG is around 20 minutes in length and will include periods of eye opening, closure and activation procedures such as hyperventilation and photic stimulation; a routine recording may also capture periods of drowsiness and perhaps sleep (Schomer and Da Silva, 2018; Sinha *et al.*, 2016; Peltola *et al.*, 2022).

The EEG data obtained varied in length from 20 minutes to 48 hours. All EEGs included portions of eye-opening and eye-closure. Shorter 20-minute recordings generally included hyperventilation and photic stimulation, whilst longer EEGs included drowsiness and sleep. TEA data had also been obtained from a variety of hospitals around the UK, which may lead to practice variation regarding reference placement, order and naming of electrode locations, sampling rate and montage selection. Any variation in filters and montages used during the recording of the EEG was negated by the EEG data being obtained in raw digital format. Whilst sampling rates varied depending on the recording site, all had sampling rates of 250Hz and above. As EEGs for TEA participants had been performed for diagnostic purposes, some recordings may also contain epileptiform activities and possibly epileptic

seizures (whose morphology does not fall within the frequency bands which make up resting state EEG activities); this would not be the case for HV EEG data.

For the reasons described above, pre-processing the EEG data before analysis is performed, is essential. It is important to ensure the data files are standardised, non-cortical activities are minimised, and EEG segments with the appropriate state of consciousness are selected. Portions of relaxed, awake EEG containing eyes open, and eyes closed state were used. As the morphology of IEAs and seizure activity falls outside the resting state EEG frequency band descriptions, these were excluded from the quantitative and connectivity analysis.

For these reasons, a standardised pre-processing pipeline was used for healthy and TEA data files, to extract study-relevant information. There are no agreed national or international standards currently in place specific to EEG pre-processing, but there are several examples of suggested pipelines. These include a semi-automated pipeline for EEGLAB suggested by Delorme and Makeig, an automated EEG pre-processing script by Rodrigues et al., a summary of common pre-processing procedures by Peng in Hu and Zhang's book *EEG Signal Processing and Feature Extraction*, IFCN recommendations for referencing, recording parameters and preliminary data analysis, plus joint ILAE/IFCN draft minimum standards for EEG (Delorme, 2019; Peng, 2019; Rodrigues *et al.*, 2021; Babiloni *et al.*, 2020; Delorme and Makeig, 2004; Peltola *et al.*, 2022).

To utilise the current clinical practice of visual EEG analysis, which is still widely regarded as a "gold standard" (Tatum *et al.*, 2016), the semi-automated pipeline recommendations by Delorme and Makeig were used for this study (Figure 18), with some minor changes in process order. The programming platform used was MATLAB ver. R2021b (MathWorks, Accessed 2021), alongside EEGLAB 2022.0, an interactive MATLAB toolbox for processing electrophysiological data, including resting state EEG (Delorme and Makeig, 2004). The automated MATLAB script used for pre-processing was written and supplied by Javier Escudero, utilised by Kinney-Lang et al. (Kinney-Lang *et al.*, 2019), and is included in Appendix 1: MATLAB SCRIPTS.

The following standardised EEG pre-processing pipeline was employed for all EEG datafiles:

1. Import EEG files (EDF/cnt) to EEGLAB

2. Convert files (EDF/cnt) to SET files
3. Import channel locations.
4. Standardise channel locations to pre-2017, 10-20 nomenclature.
5. Select data (removing any empty or unrequired channels)
6. Visual inspection of each EEG file to remove sections with excessive biological and/or electrode artefacts, IEAs, periods of drowsiness and sleep, and any seizures. This was performed by a state-registered Clinical Scientist (Neurophysiology).
7. Put through a pre-processing script (describe elements of this) – TEA_Preproc.m (Appx1)
 - a. Selection and re-ordering of channel names and channel locations 'Fp1'; 'Fp2'; 'F3'; 'F4'; 'C3'; 'C4'; 'P3'; 'P4'; 'O1'; 'O2'; 'F7'; 'F8'; 'T3'; 'T4'; 'T5'; 'T6'; 'Fz'; 'Cz'; 'Pz'; 'A1'; 'A2' (Figure 17).

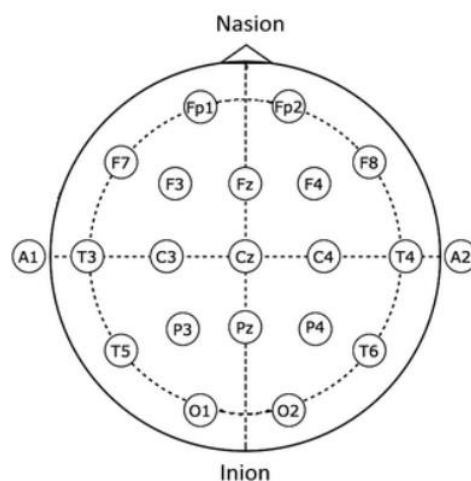


Figure 17: Standardised electrode placements used for data analysis ([EEG Instrumentation, Montage, Polarity, and Localization | Neupsy Key](#)).

- b. Re-reference to Average reference (AVG)
 - c. Re-Sample to 256Hz
 - d. Set filters: Low-frequency filter (LFF) – 1Hz, High-frequency filter (HFF) – 40Hz
 - e. Run Independent Component Analysis (ICA) to separate the individual sources making up the data signals (Delorme, Accessed 2022)
 - f. Epoching data (0-5s)
 - g. Save as new filename
8. Visually inspection of ICA, removing components with a high percentage of non-brain content.

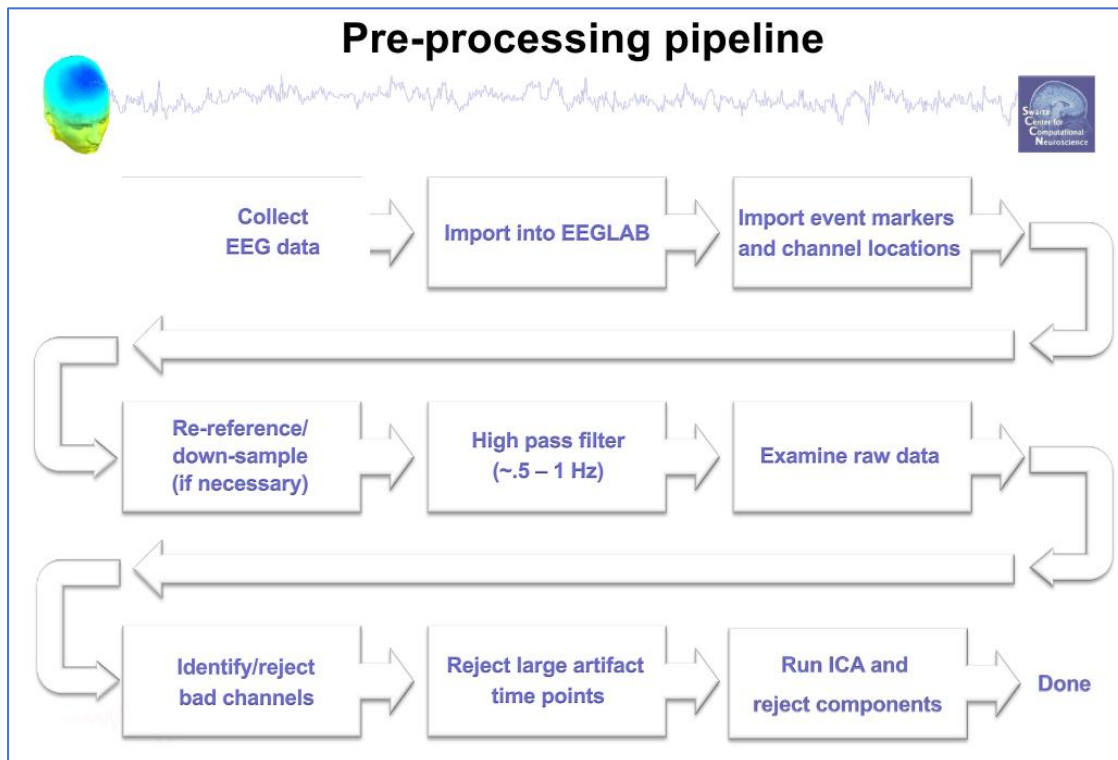


Figure 18: Pre-processing guideline for EEGLAB (Delorme, 2019)

10. Re-processed and Excluded Data

10.1. TEA Data

- Participant 7:** The pre-processed data contained a large amount of outlying data. The file was visually re-analysed to exclude any previously included artefacts, with the reader blinded to the previous selections. The file was then reprocessed as per the methods (Data Pre-processing section), with a reduction in outliers seen. The project ID TEA4 was allocated to the new data file.
- Participant 12:** There was an error when the Preproc script was run (line 52). EEG channels T4, T3, T6, T5, A2, and A1 had channel labels T8, T7, P8, P7, M2, and M1 respectively, which prevented the script from processing past this point. These are modifications to the 10-20 nomenclature recommended by the American Clinical Neurophysiology Society in 2016 (Acharya et al., 2016b). As electrode nomenclature needs to be consistent between files within channel locations, the electrode names

were converted to T4, T3, T6, T5, A2, and A1 for consistency. File pre-processing was then able to be completed. The project ID TEA7 was allocated to the new data file.

- **Participant 18:** There was an error when the Preproc script was run (line 52); this was resolved using the same technique as Participant 12. The processed data file also contained a significant number of outliers. On reviewing the EEG, it was noted to be low in amplitude, contained 50Hz and the participant was drowsy through much of the recording. The file was visually re-analysed to exclude any previously included artefacts and/or drowsiness, with the reader blinded to the previous selections. The file was then reprocessed as per TEA participant 7, with a reduction in outliers seen. The project ID TEA11 was allocated to the new data file.
- **Participant 19:** Following initial analysis using the restingIAF script and data import from Excel to SPSS, Z-scores of Mean power and Interhemispheric mean power showed an unusually extreme outlier within frontal regions, in the delta band. The corresponding two single data elements within these datasets were removed for this participant. The project ID for this participant is TEA12.
- **Participant 26:** On initial pre-processing, the electrode positions in the data file omitted channels A2 and A1. This participant had undergone two separate EEGs; therefore, the second file was examined. Both files omitted A2 and A1, so the participant was excluded from the study.
- **Participant 35:** The pre-processed data contained a large amount of outlying data. On reviewing the EEG, the participant was drowsy for much of the recording. The file was visually re-analysed and re-processed as per TEA Participant 7, with a reduction in outliers seen. The project ID TEA20 was allocated to the new data file.
- **Participant 44:** The pre-processed data contained a large amount of outlying data. On reviewing the EEG, it was noted to be low in amplitude, and there was a significant amount of muscle artefact in the recording. The file was visually re-analysed and re-processed as per TEA Participant 7, with a reduction in outliers seen. The project ID TEA20 was allocated to the new data file.
- **Participant 49:** The pre-processed data contained a large amount of outlying data. The participant had undergone 2 EEGs, and the second file contained significantly

less outlying data. The second file was therefore used for analysis instead of the initial recording. The project ID TEA25 was allocated to the 2nd data file.

10.2. HV Data

- **Participant 9:** The pre-processed data contained a large amount of outlying data. On reviewing the EEG, the participant was drowsy for much of the recording. The file was visually re-analysed to exclude any previously included artefacts/drowsiness, with the reader blinded to the previous selections. The file was then reprocessed as per the methods (Data Pre-processing section), with a reduction in outliers seen. The project ID HV9 was allocated to the new data file.
- **Participant 12:** On initial review of the EEG, it was ascertained that the data within the file did not represent EEG data. The participant was therefore excluded from the study.
- **Participant 15:** The pre-processed data contained a large amount of outlying data. On reviewing the EEG there was no clear cause for this. The file was therefore re-analysed and re-processed as per HV participant 9, with a reduction in outliers seen. The project ID HV15 was allocated to the new data file.
- **Participant 20:** The pre-processed data contained a large amount of outlying data. The pre-processed data contained a large amount of outlying data. On reviewing the EEG there was no clear cause for this. The file was therefore re-analysed and re-processed as per HV participant 9, with a reduction in outliers seen. The project ID HV20 was allocated to the new data file.
- **Participant 29:** The pre-processed data contained a large amount of outlying data. The pre-processed data contained a large amount of outlying data. On reviewing the EEG there was no clear cause for this. The file was therefore re-analysed and re-processed as per HV participant 9, with a reduction in outliers seen. The project ID HV12 was allocated to the new data file (in place of the excluded data above).

11. Data Analysis

11.1. First Phase Analysis – Visual EEG analysis

11.1.1. Visual EEG Interpretation

The aim of the first phase of visual EEG analysis was to analyse the TEA EEGs using the current gold standard visual interpretation, to quantify the prevalence of normality, non-epileptiform, and epileptiform abnormalities, including the location of any abnormalities found.

The anonymised raw TEA EDF files were uploaded into the Xltek Neuroworks database at the Royal Devon and Exeter NHS Foundation Trust. Visual interpretation was undertaken by a Consultant Scientist qualified in EEG interpretation. A standardised reporting tool was devised in Excel to capture normal and abnormal findings and their location. The fields used were as follows:

- Participant TEA identifier
- Sex
- Age at the time of the EEG
- Date of EEG
- EEG Type (routine, sleep, long-term monitoring (LTM))
- Length of recording in minutes
- Levels of alertness recorded (wakefulness, drowsiness, sleep)
- Description of background (normal, abnormal)
- Presence of any non-epileptiform abnormalities (NEA) (yes, no)
- Presence of any interictal epileptiform discharges (IED) (yes, no)
- Type of NEA (n/a, irregular theta/delta, sharpened theta/delta)
- Type of IED (n/a, spikes, sharp waves, spike and wave complexes, sharp and slow wave complexes, polyspikes)
- Hemisphere location of NEA and IED (n/a, right, left, bilateral, bilateral independent R>L, bilateral independent L>R)
- Regional occurrence of NEA and IED (frontal, temporal, anterior temporal, posterior temporal, central, parietal, occipital, multifocal, variable)

Epileptiform activities (i.e. sharp waves, spikes, sharp and slow-wave complexes, spike and wave complexes, and polyspikes) were identified as per the glossary of EEG terms recently updated by Kane et.al. (Kane *et al.*, 2017).

11.1.2. SPSS Analysis

The findings for the 28 TEA EEGs were uploaded into SPSS

The SPSS Descriptive Statistics *Frequencies* analysis and *Chart Builder* were used to test hypothesis data:

- Descriptives, with percentage of occurrence
- Cross tabs, with Chi-square correlations
- Bivariate Correlations
- Data bar charts
- Data pie-charts

11.2. First Phase Analysis – Peak Frequencies and Power Spectral Densities

This first phase analysis aimed to determine the effects TEA may have on the mean frequency and mean spectral power, considering variation within the frequency band, brain regions, and any effects of sex and age.

11.2.1. MATLAB/EEGLAB Analysis

Initial data analysis was employed to ascertain the peak frequency (PF) and the power spectral density (PSD) for global and regional cortical activity (frontal, temporal, parietal, occipital). For both global and regional PF and PSD, an interhemispheric difference was calculated using an asymmetry index (A_i) as recommended by the International Federation of Clinical Neurophysiology (IFCN) in their paper *EEG research workgroup:*

Recommendations on the frequency and topographic analysis of resting state EEG rhythms.

Part 1: Applications in clinical research studies ((Babiloni *et al.*, 2020). Relative PF, PSD, PFA_i , and $PSDA_i$ were then calculated for the following EEG bands: Full Spectrum (1Hz-40Hz), Beta (13-40Hz), Alpha (8-12.9Hz), Theta (4-7.9Hz) and Delta (0.5-3.9Hz), both globally and regionally.

Regional data was analysed using the following electrode configurations:

- Frontal (FP1, FP2, F3, Fz, F4)
- Temporal (F7, F8, T3, T4, A1, A1, T5, T6)
- Parietal (C3, Cz, C4, P3, Pz, P4)
- Occipital (O1, O2)

The asymmetry index (A_i) was obtained using the following formula: $A_i = (Leftr - Rightr) \div (Leftr + Rightr) \times 100$, where r represents the region of interest (i.e. global, and regional (frontal, temporal, parietal, occipital)). As A_i contains both positive and negative values (+ve indicating values larger on the left and, -ve indicating values larger on the right), a factor of 100 was added to each A_i score before transforming using Log10.

MATLAB scripts used for PF and PSD calculation were modified from open source corcorana/restingIAF scripts published on GitHub (Corcoran *et al.*, 2018). The restingIAF scripts were modified in 2022 to include PF for all frequency bands, and to accommodate different selections of electrodes in the calculations; these are attached in Appendix 1. The data output from the PF and PSD analysis were saved as Excel files. Data was interrogated to identify and correct any errors during the manual data re-organisation. Extreme outlier data was identified using Z-scores and data was excluded when over 50% of the data within the study were identified as extreme. The final datasets were then imported into SPSS for statistical analysis.

11.2.2. SPSS Analysis

The following TEA participant PF and PSD data were compared to the Healthy Participant data, to determine any significant differences between the two datasets:

- Peak Frequency (beta, alpha, theta, delta bands and all frequencies)
 - Frontal (FP1, FP2, F3, Fz, F4)
 - Temporal (F7, F8, T3, T4, A1, A1, T5, T6)
 - Parietal (C3, Cz, C4, P3, Pz, P4)
 - Occipital (O1, O2)

- Regional inter-hemispheric mean frequency differences, for the 4 frequency bands
- Mean Power (beta, alpha, theta, delta bands and all frequencies)
 - Frontal (FP1, FP2, F3, Fz, F4)
 - Temporal (F7, F8, T3, T4, T5, T6)
 - Parietal (C3, Cz, C4, P3, Pz, P4)
 - Occipital (O1, O2)
 - Regional inter-hemispheric mean frequency differences, for the 4 frequency bands

The SPSS Descriptive Statistics *Explore* analysis and *Chart Builder* were used to test hypothesis data:

- Descriptives, with a 95% confidence level for Mean.
- Data histogram (factor levels together)
- Normality statistics - Shapiro-Wilk
- Normality plots - QQ-plots
- Boxplots
- Population Pyramid Frequency graphs

Where data were normally distributed, the independent Samples T-test was used to compare means between TEA and HV data. For data that did not meet the criteria for normality (i.e., Shapiro-Wilk tests for either TEA, HV or both datasets showed p-values of ≤ 0.05), non-parametric tests relevant to two independent samples were used (the Mann-Whitney U non-parametric-test). The effect of age within cohorts was analysed using a Linear Mixed Model.

As two-sample statistics do not incorporate post-hoc correction methods to offset type I errors related to multiple comparisons, the false discovery rate (FDR) correction method, proposed by Benjamini (Benjamini *et al.*, 2006; Benjamini and Hochberg, 2000; Benjamini and Hochberg, 1995; Pike, 2011), was employed to counteract false null hypothesis rejections.

11.3. Second Phase Analysis – Connectivity

A second phase of analysis was implemented to examine connectivity between brain regions i.e., communication between different areas of the brain. Several EEG connectivity measures have been described in the literature, some of which are better suited to scalp-level EEG recordings as they seek to minimise the inherent problem of volume conduction. All however have strengths and weaknesses within their application. Imaginary coherence (iCoh) was selected to detect linear dependencies; however, it is recognised that this does not provide any causal information about the activities analysed. Weighted phase lag index was selected as a phase-based measure, capable of detecting both linear and non-linear dependencies. To detect directionality and to provide causal information regarding connectivity, phase transfer entropy (PTE) was selected (Nolte *et al.*, 2004; Hu and Zhang, 2019; Jia, 2019; Lobier *et al.*, 2014; He *et al.*, 2019; Babiloni *et al.*, 2021b; Kaminski and Blinowska, 2022).

Several open-source packages were considered, with which to perform connectivity analysis, including SIFT (an EEGLAB plugin), LORETA, fieldtrip, and Brainstorm. Brainstorm was chosen for its ease of use, intuitive interface, and international recognition (Jia, 2019; Babiloni *et al.*, 2020).

11.3.1. Brainstorm Analysis

In Brainstorm, a protocol was created with TEA and HV subset folders. As MRI scans had not been undertaken on HV participants and MRI image files were not available for TEA participants, the Brainstorm default anatomy was utilised for both HV and TEA files. Pre-processed EEGLAB *.set* files were then imported into the appropriate subset folders along with the EEG channel files. Brainstorm automatically converts the *.set* files to Brainstorm sub-files, breaking down each EEG file into its 5-second epochs.

Imaginary coherence analysis (iCoh) was undertaken for each 5-second epoch within each of the HV and TEA participant sub-folders, and an averaged iCoh analysis was undertaken for each TEA and HV file at the participant level and group level. Process options were selected as follows:

- Imaginary Coherence (2019) - $IC = |\text{imag}(C)|$

- Window length for PSD estimation = 1sec
- Overlap for PSD estimation = 50%
- Highest frequency of interest = 40Hz

Weighted phase-lag index (wPLI) was undertaken by processing into frequency bands using Hilbert transformation, then concatenating the 5-second files and producing an averaged wPLI analysis for each TEA and HV file at the participant level, and for each cohort at the group level. Process options were selected as follows:

- Frequency bands
 - Delta / 0.5, 3.9 / mean
 - Theta / 4, 7.9 / mean
 - Alpha / 8, 12.9 / mean
 - Beta / 13, 40 / mean
- wPLI: Weighted phase lag index – selected.
- Measure = Magnitude.
- Output Option = Concatenate input files before processing (one file).

Phase transfer entropy (PTE) was undertaken by processing into frequency bands using Hilbert transformation, then concatenating the 5-second files before processing at the participant level, and at the group level. Process options were selected as follows:

- Frequency bands
 - Delta / 0.5, 3.9 / mean
 - Theta / 4, 7.9 / mean
 - Alpha / 8, 12.9 / mean
 - Beta / 13, 40 / mean
- Return normalised phase transfer entropy – Yes.
- Output Option = Concatenate input files before processing (one file).

The patient-level and cohort-level iCoh, wPLI and PTE analyses were then exported as MATLAB files, imported into Excel, restructured into a usable form, and then imported into SPSS for statistical analysis.

11.3.2. SPSS Analysis

Stage 1 analysis and previous connectivity literature within memory and focal epilepsy research were used to inform regarding areas of interest within TEA iCoh data. These were then compared to healthy participant data, to determine any significant differences between the two datasets. The following analyses were used:

- Global iCoh, wPLI and PTE
- Intra-regional iCoh, wPLI and PTE (all frequencies, beta, alpha, theta, delta bands)
 - Frontal (FP1, FP2, F3, Fz, F4)
 - Temporal (F7, F8, T3, T4, A1, A1, T5, T6)
 - Parietal (C3, Cz, C4, P3, Pz, P4)
- Inter-hemispheric regional networks for significant findings (all frequencies, beta, alpha, theta, delta bands)
- Inter-hemispheric network connectivity between regions (all frequencies, beta, alpha, theta, delta bands):
 - Temporal and frontal (F7, F8, T3, T4, A1, A2, T5, T6, FP1, FP2, F3, Fz, F4)
 - Temporal and parietal (F7, F8, T3, T4, A1, A2, T5, T6, C3, Cz, C4, P3, Pz, P4)
 - Temporal and occipital (F7, F8, T3, T4, A1, A2, T5, T6, O1, O2)
 - Frontal and parietal (FP1, FP2, F3, Fz, F4, C3, Cz, C4, P3, Pz, P4)
 - Frontal and occipital (FP1, FP2, F3, Fz, F4, O1, O2)

The SPSS Descriptive Statistics *Frequencies* and *Chart Builder* were used to test hypothesis data:

- Descriptives, with a 95% confidence level for Mean.
- Data histogram and boxplots.
- Normality statistics - Shapiro-Wilk.
- Means.
- Population Pyramid Frequency graphs.

Where data were normally distributed, the independent Samples T-test was used to compare means between TEA and HV data. For data that did not meet the criteria for normality (i.e., Shapiro-Wilk tests for either TEA, HV or both datasets showed p-values of \leq

0.05), non-parametric tests relevant to two independent samples were used (the Mann-Whitney U non-parametric-test).

As per stage 1 analysis, FDR post-hoc correction was used to offset type I errors related to multiple comparisons (Benjamini *et al.*, 2006; Benjamini and Hochberg, 2000; Benjamini and Hochberg, 1995; Pike, 2011).

Results

Due to the constraints of thesis word count, a full breakdown of the mFREQ, mPSD and connectivity analysis results is found in Appendix 2.

1. Age and Sex Demographics

1.1. Sex

Crosstabs data analysis demonstrates there is an equal sex distribution across TEA and Healthy volunteer cohorts (Table 3, Figure 19).

Table 3: Count of Participants for TEA and Healthy Cohorts

Sex * Condition Crosstabulation				
Count		Condition		Total
		Healthy	TEA	
Sex	F	7 _a	7 _a	14
	M	21 _a	21 _a	42
Total		28	28	56

Each subscript letter denotes a subset of Condition categories whose column proportions do not differ significantly from each other at the .05 level.

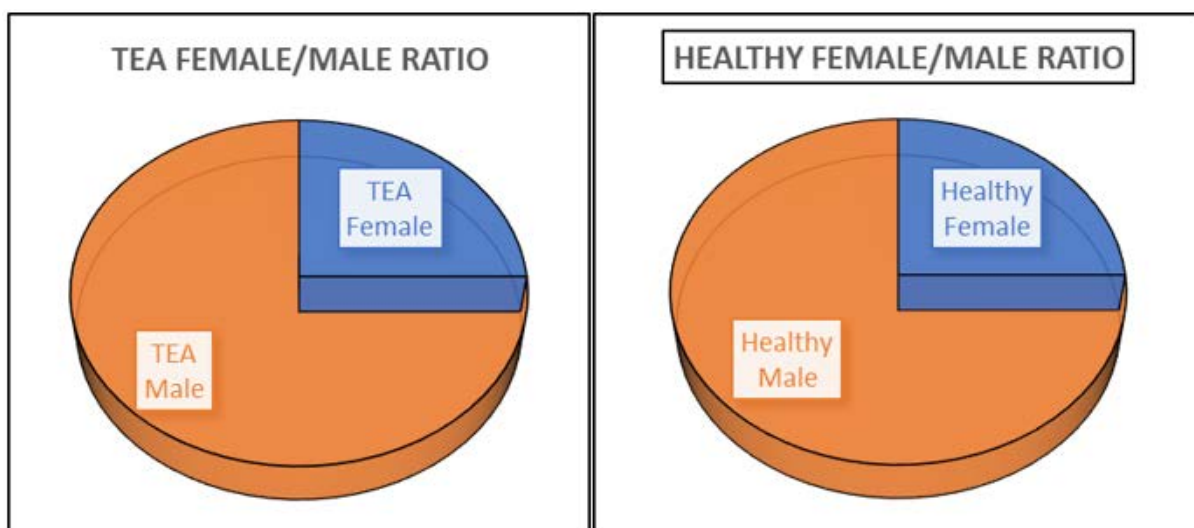


Figure 19: Female to Male Ratio for TEA and Healthy Cohorts

Pearson's correlation was used to test for relationships between data variables, with correlation being significant at $p=0.001$ level (two-tailed) and 95% confidence intervals (CI).

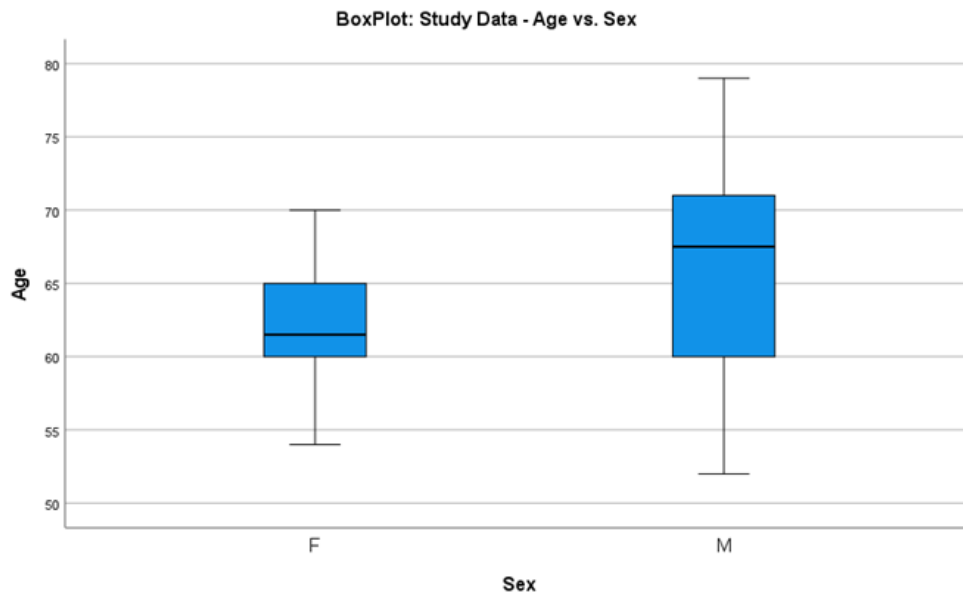


Figure 20: Boxplot of Age and Sex showing higher mean age in males.

Sex and age show a correlation coefficient of 0.22 ($p<0.001$, 95% CI 0.157 to 0.281), with mean age within the dataset being higher in males (Figure 20).

A negative correlation coefficient of -0.157 ($p<0.001$, 95% CI -0.220 to -0.93) is seen concerning age and mean power, i.e., mean power shows an overall decrease with increasing age (Figure 22). A similar negative correlation with age is seen concerning global imaginary coherence (iCoh) (Pearson Correlation -0.1, $P<0.001$, 95% CI 10.136 to -0.065) – (Figure 23).

1.2. Age

Crosstabs and Pearson Chi-Square analysis demonstrate that whilst there are some minor age differences across the TEA and HV groups, there is no significant difference at $p<0.05$ level (

Table 4,

Table 5, Figure 21).

Table 4: Age comparison across TEA and HV cohorts with Age broken down into 3 categories: <= 60y, 61-70y and 71y +

		Condition * Age (3 Bins) Crosstabulation				
		Age (3 Bins)			Total	
		<= 60	61 - 70	71+		
Condition	Healthy	Count	8 _a	15 _a	5 _a	28
		% within Condition	28.6%	53.6%	17.9%	100.0%
TEA	Count	7 _a	13 _a	8 _a	28	
		% within Condition	25.0%	46.4%	28.6%	100.0%
Total	Count	15	28	13	56	
		% within Condition	26.8%	50.0%	23.2%	100.0%

Each subscript letter denotes a subset of Age (3 Bins) categories whose column proportions do not differ significantly from each other at the .05 level.

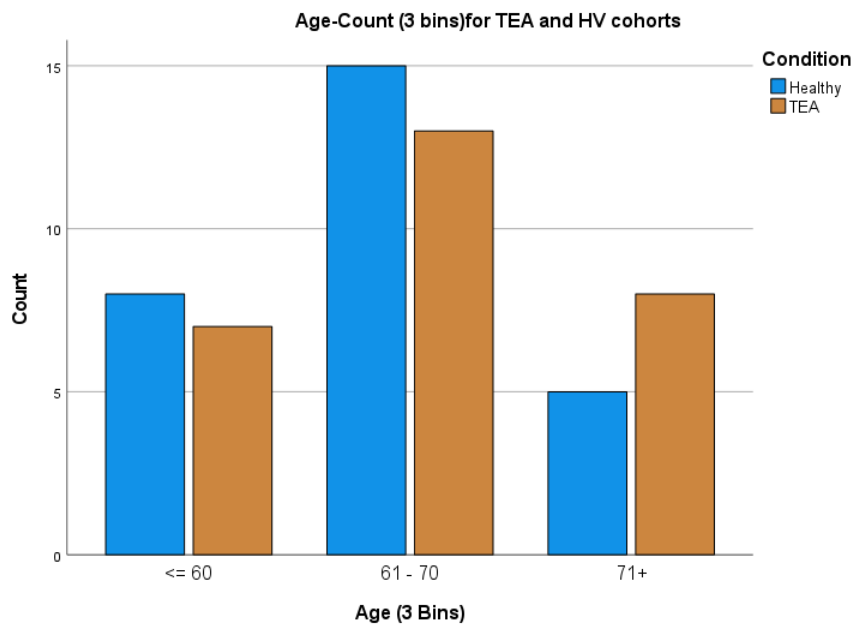


Figure 21: Bar Chart of age profiles for TEA and HV cohorts using 3 age categories: <=60y, 61-70y, and 71y+

Table 5: Pearson Chi-Square tests comparing age profiles across TEA and HV cohorts using age categories: <= 60y, 61-70y and 71y+

Chi-Square Tests			
	Value	df	Asymptotic Significance (2-sided)
Pearson Chi-Square	.902 ^a	2	.637
Likelihood Ratio	.908	2	.635
Linear-by-Linear Association	.563	1	.453
N of Valid Cases	56		

a. 0 cells (.0%) have expected count less than 5. The minimum expected count is 6.50.

Pearson’s correlation was used to test for relationships between data variables, with correlation being significant at p=0.001 level (two-tailed) and 95% confidence intervals (CI).

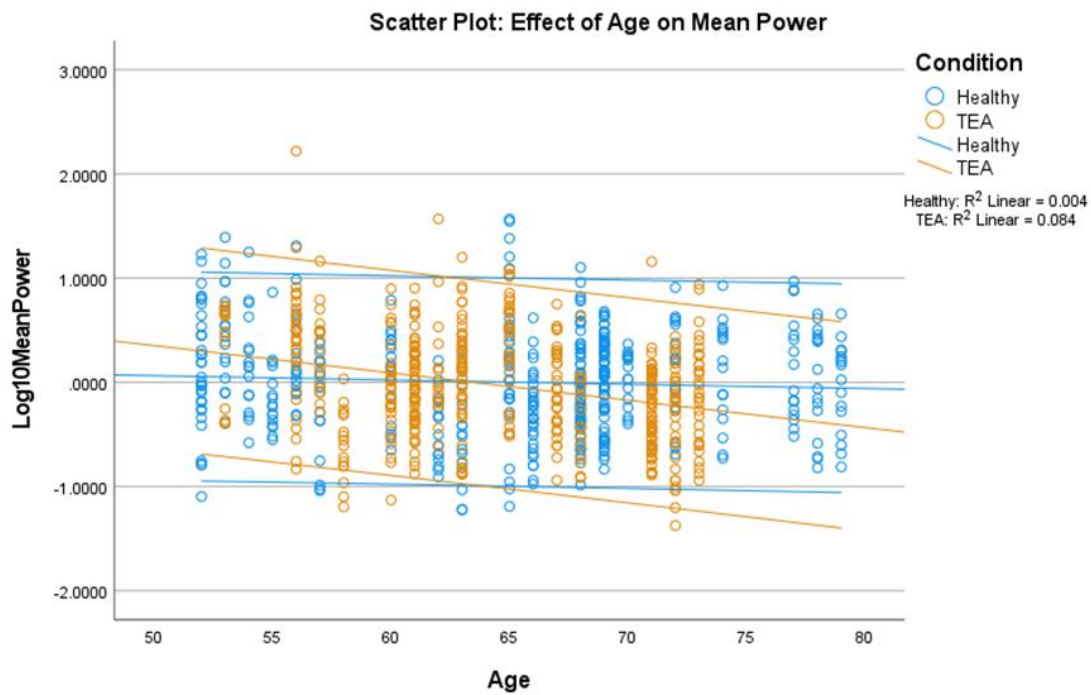


Figure 22: Scatter Plot showing a negative correlation between mean spectral power with increasing age.

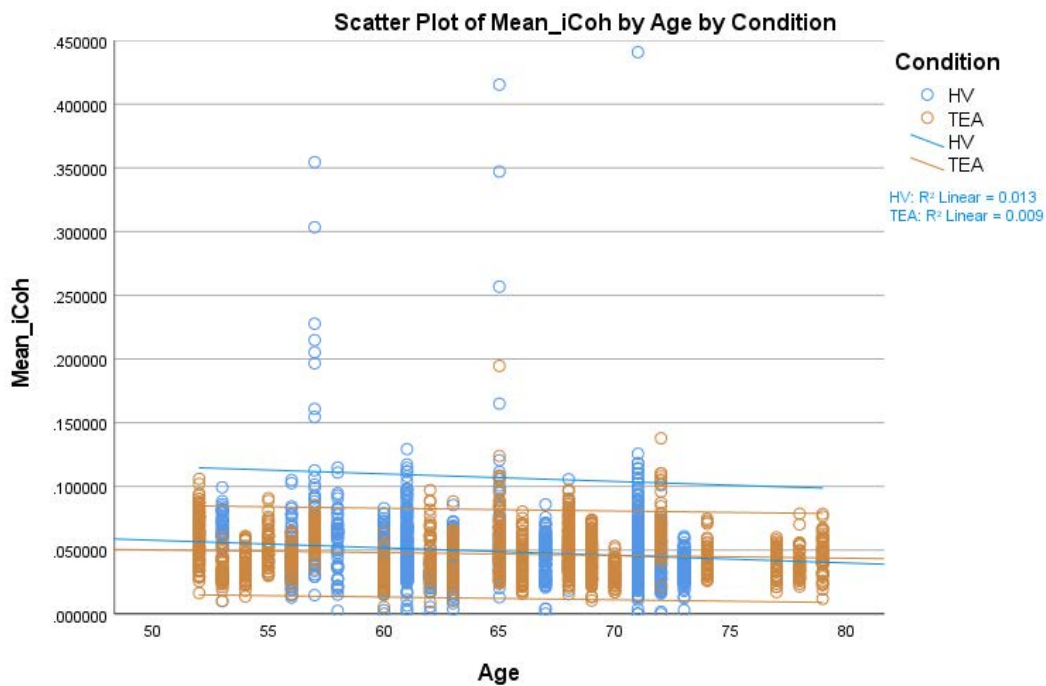


Figure 23: Scatter Plot showing a negative correlation between global iCoh with increasing age.

In line with most larger-scale TEA research studies, there is a higher proportion of males within the TEA cohort (Baker *et al.*, 2021; Ramanan *et al.*, 2019; Lapenta *et al.*, 2014; Mosbah *et al.*, 2014; Hodges and Warlow, 1990). The proportion of males to females within

our TEA cohort is 3:1. The mean age of males within the study is higher than female participants, although this may be skewed by the limited number of females (7 participants).

Analysing age effects reveals an inverse linear relationship concerning global mean power across both cohorts i.e., spectral density decreases with increasing age. This reflects the findings of Babiloni et al. (Babiloni *et al.*, 2006a). The inverse linear relationship between age and PSD appears more marked within the TEA cohort ($p=0.044$).

2. Visual EEG Analysis Results

Data appearing as “not applicable” (n/a) were classified as missing data, and as such were excluded from statistical analysis.

Visual EEG analysis was not undertaken on HV EEGs. All 28 TEA EEGs were visually interpreted. Of these, 19 (68%) were routine EEGs, 7 (25%) were sleep EEGs, and 2 (7%) were long-term monitoring. The shortest recording was 7 minutes and the longest was 1395 minutes, with a median value of 26 minutes. States of alertness were recorded for all EEGs with 10 (36%) containing wakefulness only, 10 (36%) containing both wakefulness and drowsiness and 8 (28%) also capturing sleep (Figure 24). Background activities within 27 of the 28 EEGs were normal, with one participant showing slightly slow background activities (TEA20). 75% of the EEGs reviewed contained abnormal activity.

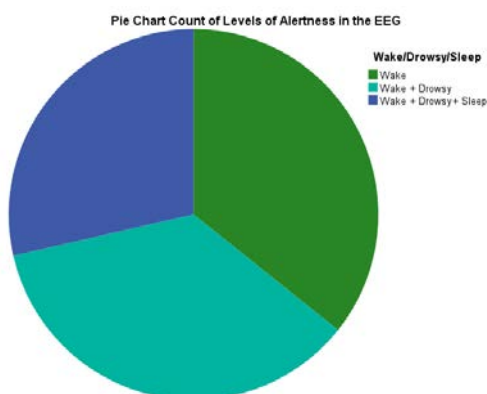


Figure 24: Pie Chart breakdown of the proportions of alertness levels seen across TEA EEGs

The terminology set out by Kane et.al was used to distinguish EA waveforms from NEA (Kane *et al.*, 2017). The presence of both non-epileptiform (NEA) and epileptiform activities (EA) was documented. 16 EEGs (57%) contained NEA, and 12 EEGs (42%) contained EA.

Using *Crosstabs* to compare the two categories, there were 7 EEGs (25%) showing neither NEA nor EA which would be interpreted as normal. 9 EEGs (32%) contained only NEA and 5 (18%) contained only EA, whilst 7 EEGs (25%) contained both NEA and EA changes within the recording. All NEA and EA abnormalities were seen either within the anterior-temporal region or across temporal regions as a whole.

Of the EEGs containing NEA abnormalities, where these occurred unilaterally, there was an increased prevalence over the left hemisphere (31% compared to 13% right-sided). 56% of NEA were seen bilaterally, occurring either simultaneously or independently. 25% of these were bilaterally equal across the hemispheres, 19% were bilaterally independent with a left-sided prevalence, and 13% were bilaterally independent with a right-sided prevalence (Figure 25). Of the 16 EEGs with NEA, in 7 cases (44%) the NEA were described as having a sharpened appearance.

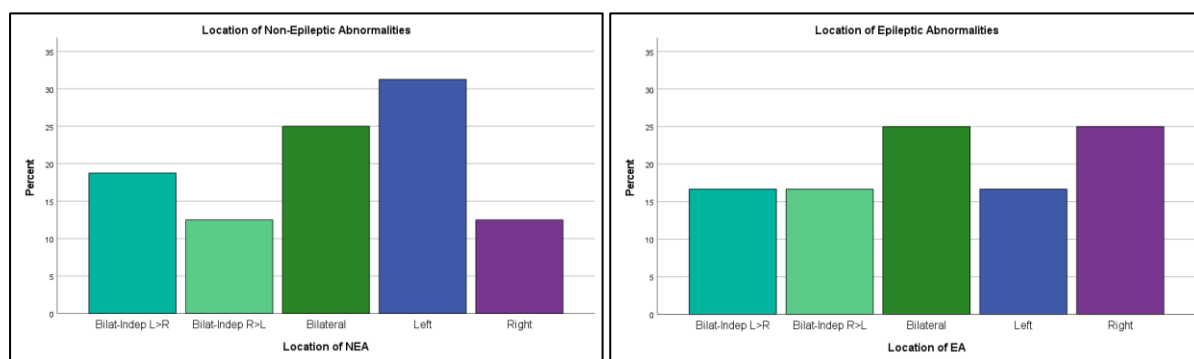


Figure 25: Percentages of epileptic and non-epileptic abnormalities by hemisphere location

Of the EEGs containing EA abnormalities, where these occurred unilaterally, there was a slightly increased prevalence over the right hemisphere (2 (17%) left-sided and 3 (25%) right-sided). 58% of EEGs show EA over both hemispheres, with an even distribution across the right and left hemispheres overall (Figure 25). Of the 12 EEGs with EA, the largest proportion were described as having a “sharp” morphology (either sharp waves or sharp and slow wave complexes). These were described in 7 of the 12 EEGs (58%), and spikes in 5 (42%).

The Pearson Correlation was used to assess any correlations between EEG factors, particularly regarding NEA and EA. There is no correlation between EEG type, or length of the EEG and occurrence of NEA or EA. However, there is a correlation between the

occurrence of drowsiness and sleep and the appearance of NEA ($p=0.05$), and to a lesser extent EA (weak correlation at $p=0.69$) (Figure 26, Table 6).

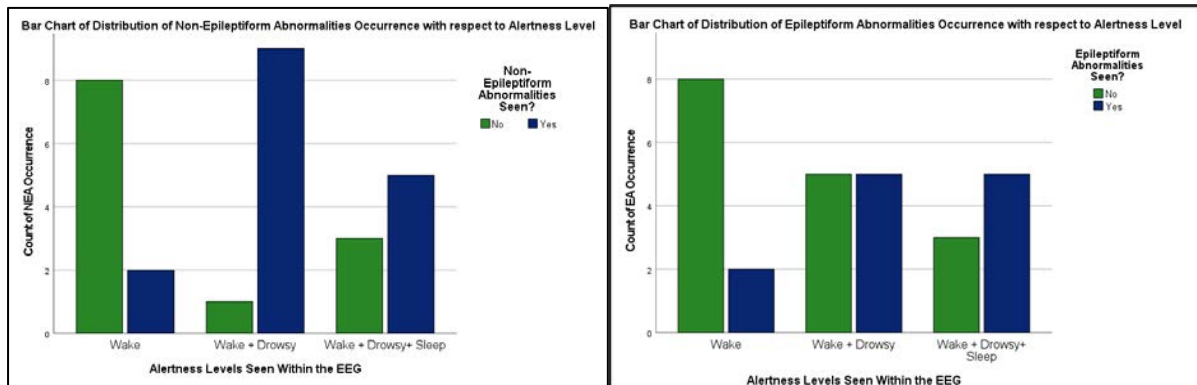


Figure 26: Non-Epileptiform and Epileptiform Abnormality Occurrence Associated with Alertness Levels Obtained During the EEG

Table 6: Pearson Correlations between alertness levels and occurrence of NEA and EA.

Pearson Correlations with Confidence Intervals				
	Pearson Correlation	Sig. (2-tailed)	95% Confidence Intervals (2-tailed) ^a	
			Lower	Upper
Wake/Drowsy/Sleep - Non Epileptiform Abn	.374	.050	-.005	.652
Wake/Drowsy/Sleep - Epileptiform Abn	.349	.069	-.035	.635
Non Epileptiform Abn - Epileptiform Abn	.021	.916	-.355	.391

a. Estimation is based on Fisher's r-to-z transformation with bias adjustment.

3. mFREQ Results

Once FDR corrections have been applied, there are no significant mFREQ differences (at the alpha threshold of 0.05) between TEA patients and healthy volunteers.

There are however several significant *p-values* which, when FDR adjusted, do not subsequently show significance as *q-values*:

- Beta mFREQ difference over frontal regions, with beta frequencies higher in the TEA cohort compared to HV ($p=0.03$). Medication effects should be considered when interpreting this finding.
- A slight interhemispheric difference in mFREQ is seen in the TEA cohort, compared to HV, with higher mean frequencies seen over the right frontal region within the TEA group ($p=0.004$).

4. mPSD Results

From a regional perspective, the most striking features are seen in mPSD inter-hemisphere difference ($Ai = (Leftr - Rightr) \div (Leftr + Rightr) \times 100$). There is relative mPSD symmetry between the hemispheres within most regions, across most frequency bands within both groups. In healthy volunteers, mean theta and delta mPSD tend to be slightly higher over the right temporal region in comparison to the left, compared to TEA but this is a non-significant finding. On the other hand, the TEA cohort has a higher mean theta and delta mPSD over the left temporal region compared to HV. This asymmetry reaches statistical significance concerning delta mPSD over the left temporal region, inter-hemisphere delta mPSD difference, and inter-hemisphere theta mPSD difference ($p=0.037$, $p=0.006$ and $p=0.002$ respectively). This suggests that TEA delta mPSD is higher over the left hemisphere (when compared to their right hemisphere within the cohort, and when compared to the left hemisphere data of healthy volunteers). Additionally, there is an increased inter-hemisphere mPSD difference within delta and theta frequency bands in TEA, when compared to healthy data (with higher mPSD seen over the left temporal region in TEA). Once the FDR multiple comparisons adjustment is made, statistical significance remains within inter-hemisphere delta mPSD difference, and inter-hemisphere theta mPSD difference ($q=0.048$ and $q=0.032$ respectively) (Figure 27).

Previous focal epilepsy research papers have identified mPSD spectra increases associated with the epileptogenic zone (Bourel-Ponchel *et al.*, 2019; Adebimpe *et al.*, 2015; Quraan *et al.*, 2013).

There are several other significant p -values which, when FDR adjusted, do not subsequently show significance as q -values:

- Interhemispheric difference in alpha mPSD over temporal regions, with higher mPSD seen over the left hemisphere in the TEA cohort, compared to HV ($p=0.04$). This appears in keeping with the effects seen within the theta and delta bands, and in focal epilepsy research.
- Over frontal regions, there is a mPSD difference between TEA and HV cohorts, with alpha power being lower in the TEA cohort compared to HV ($p=0.04$).
- Alpha mPSD difference over frontal regions, with alpha power being lower in the TEA cohort compared to HV ($p=0.04$).

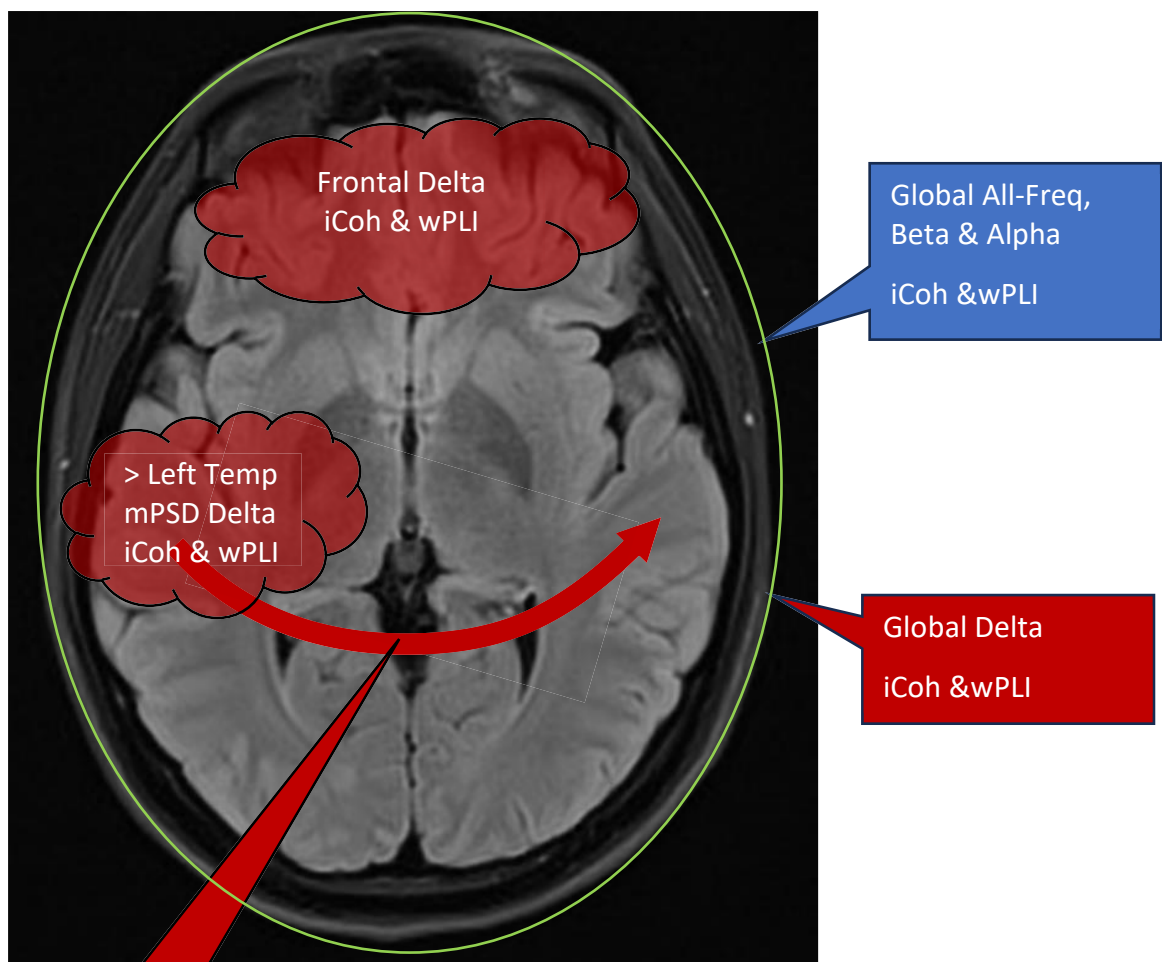


Figure 27: mPSD and global/regional connectivity findings (Red indicates increase in TEA compared to HV. Blue indicates lower in TEA compared to HV)

Temporal
INTER-H mPSD
Delta & Theta

5. Connectivity Analysis – Consistent Findings

As stated previously, individual connectivity measures have inherent benefits and drawbacks. The selection of measures chosen for this study encompasses those based on spectral power density (coherence-based) phase-synchronisation, and information theory. Both the coherence-based and phase synchronisation-based measures were used, and linear and non-linear connectivity captured (iCoh detects linear connectivity whilst wPLI is capable of detecting both linear and non-linear connectivity) are linear measures. Both iCoh and wPLI measure functional connectivity. The information-theory-based PTE measure was also used in the study for its ability to measure effective connectivity i.e., to assess the causal network relationships between regions (Jia, 2019; Lobier *et al.*, 2014; Vinck *et al.*, 2011). Due to the number of significant findings within the connectivity data as a whole, only consistent findings occurring in both functional analyses or all three measures are summarised below.

5.1. Global and Intra-Regional Connectivity Differences

At a global and regional level, PTE directional analysis (TEA vs. healthy control) does not show any areas of significance. This is likely due to its lack of sensitivity for closer regional analysis (Ursino *et al.*, 2020).

Both iCoh and wPLI demonstrate global changes in connectivity (TEA vs. healthy control), at all frequency levels (1-40Hz) and within frequency bands (beta, alpha, theta, delta):

- At the macro level (global, all frequency), connectivity is shown to have lower strength within the TEA group when compared to HV. Broad spectrum phase lag index has been associated with a history of epilepsy, being negatively correlated with epilepsy duration and with the use of multiple anti-epileptic drugs but unrelated to the frequency of seizure occurrence (Van Dellen *et al.*, 2009).
- Global beta and alpha frequencies have lower connectivity strength in the TEA cohort compared to HV. Such reductions in coherence in alpha and beta bands have been reported in patients with Alzheimer's disease (Babiloni *et al.*, 2021b)
- Global delta frequencies have higher connectivity strength in the TEA cohort compared to HV.

- Global theta frequency iCoh and wPLI show a significant difference between TEA and HV but show differing results. iCoh suggests significantly higher connectivity strength in the TEA cohort, whilst wPLI (a phase-based metric) suggests significantly lower connectivity strength in TEA when compared to HV.
- Intra-regionally, the only alteration consistent using both iCoh and wPLI is within the frontal region. Delta frequency connectivity within the frontal region has higher network strength in the TEA group compared to HV (Figure 27)

5.2. Temporal-Frontal and Frontal-Parietal Connectivity

The most compelling area of significant difference is within temporal-frontal and frontal-parietal networks, where all three measures show consistent differences between TEA and HV cohorts.

5.2.1. Temporal and Frontal Network Alterations

- Alpha and beta band frequencies (encompassing frequencies from 8Hz-40Hz) have significantly lower connectivity within the TEA cohort in comparison to healthy participants using iCoh and wPLI analysis. Directional PTE analysis suggests that in these frequency bands frontal to temporal network strength is lower in TEA than seen in HV, whilst temporal to frontal network strength is higher in TEA compared to HV. The alpha band dominant direction of flow i.e., “posterior” to anterior is consistent with the findings of Wang et. Al (Wang *et al.*, 2019a; Wang *et al.*, 2019b).
- Delta band frequencies exhibit significantly higher connectivity within the TEA cohort in comparison to healthy participants – this is seen in both iCoh and wPLI analysis, but no significant difference is seen within directed PTE analysis (Figure 28, Figure 31, Figure 32).
- Theta band frequencies show significance using all connectivity measures, but there is a discrepancy between measures regarding the direction of the changes. ICoh measures show higher connectivity in TEA subjects compared to HV, while wPLI shows lower connectivity in the TEA group in comparison to healthy participants (Figure 28, Figure 31, Figure 32). Directional analysis using PTE demonstrates higher

levels of connectivity flowing from frontal-to-temporal regions within the TEA cohort compared to HV, whilst temporal regions-to-frontal areas show significantly lower connectivity flow in TEA compared to HV (Figure 28, Figure 33). The theta band dominant direction of flow i.e., anterior to “posterior” is consistent with the findings of Wang et. Al (Wang *et al.*, 2019a; Wang *et al.*, 2019b).

- There is a paradoxical effect within TEA theta-band networks compared to HV, with higher PTE flow dominance within the frontal-to-temporal network in the TEA cohort compared to a temporal-to-frontal flow dominance seen in the HV cohort (Figure 28).

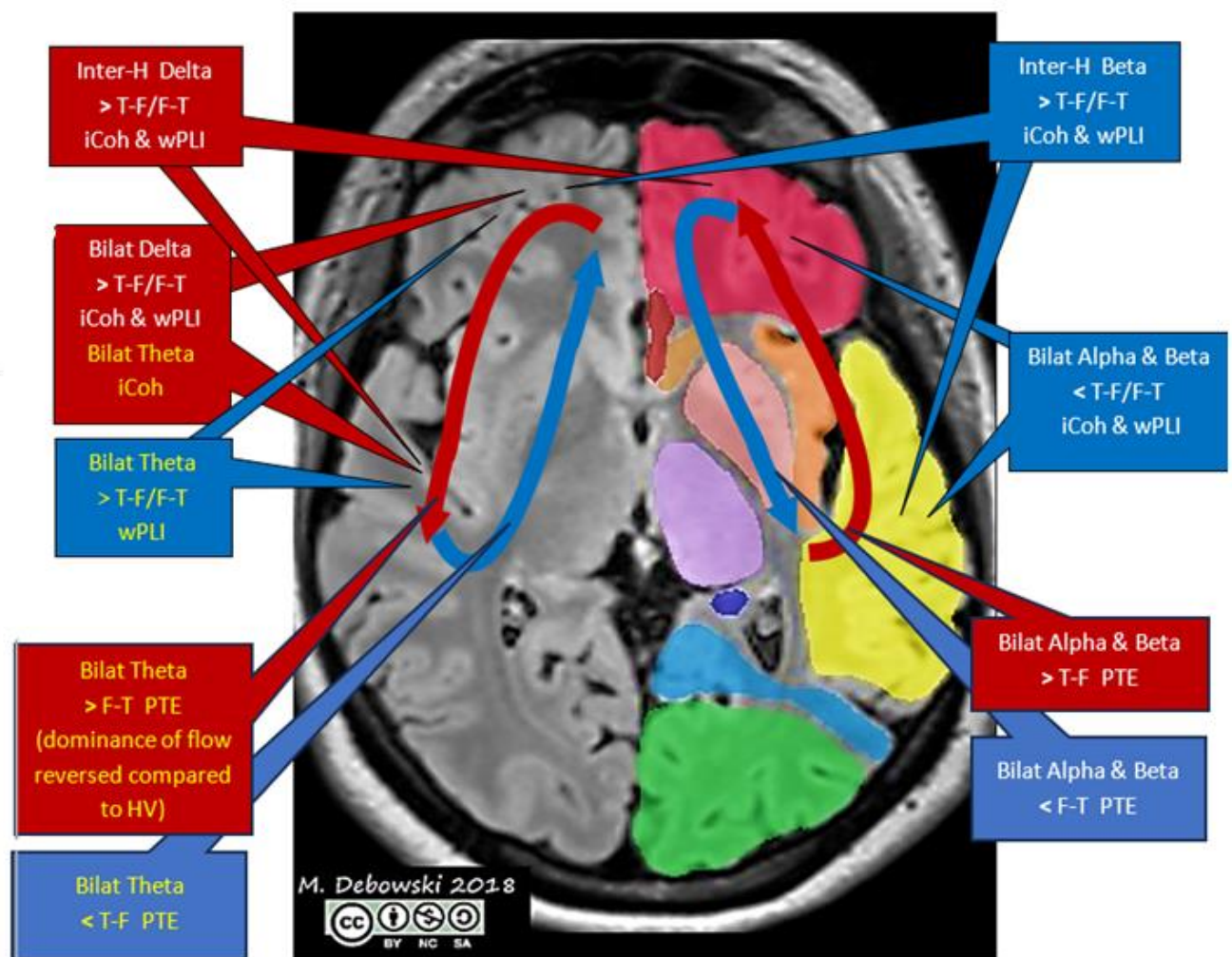


Figure 28: Significant frontal-temporal/temporal-frontal connectivity alterations in the TEA cohort

5.2.2. Frontal and Parietal Network Alterations

Frontal-to-parietal and parietal-to-frontal networks demonstrate a similar pattern of findings to those seen in temporal and frontal connections (Figure 29, Figure 31, Figure 32, Figure 33). The only pattern differences seen are within alpha band results, where wPLI analysis does not demonstrate any significant difference within the frontal-parietal networks. The same paradoxical effect within TEA concerning HV theta-band PTE is also noted with dominance of network flow being from frontal to parietal in TEA, rather than the parietal to frontal dominance seen in the HV cohort. A paradoxical flow dominance reversal effect is also noted within alpha PTE findings: network flow dominance in TEA is from parietal to frontal, rather than the frontal to parietal dominant direction of flow present in HV participants. Figure 29.

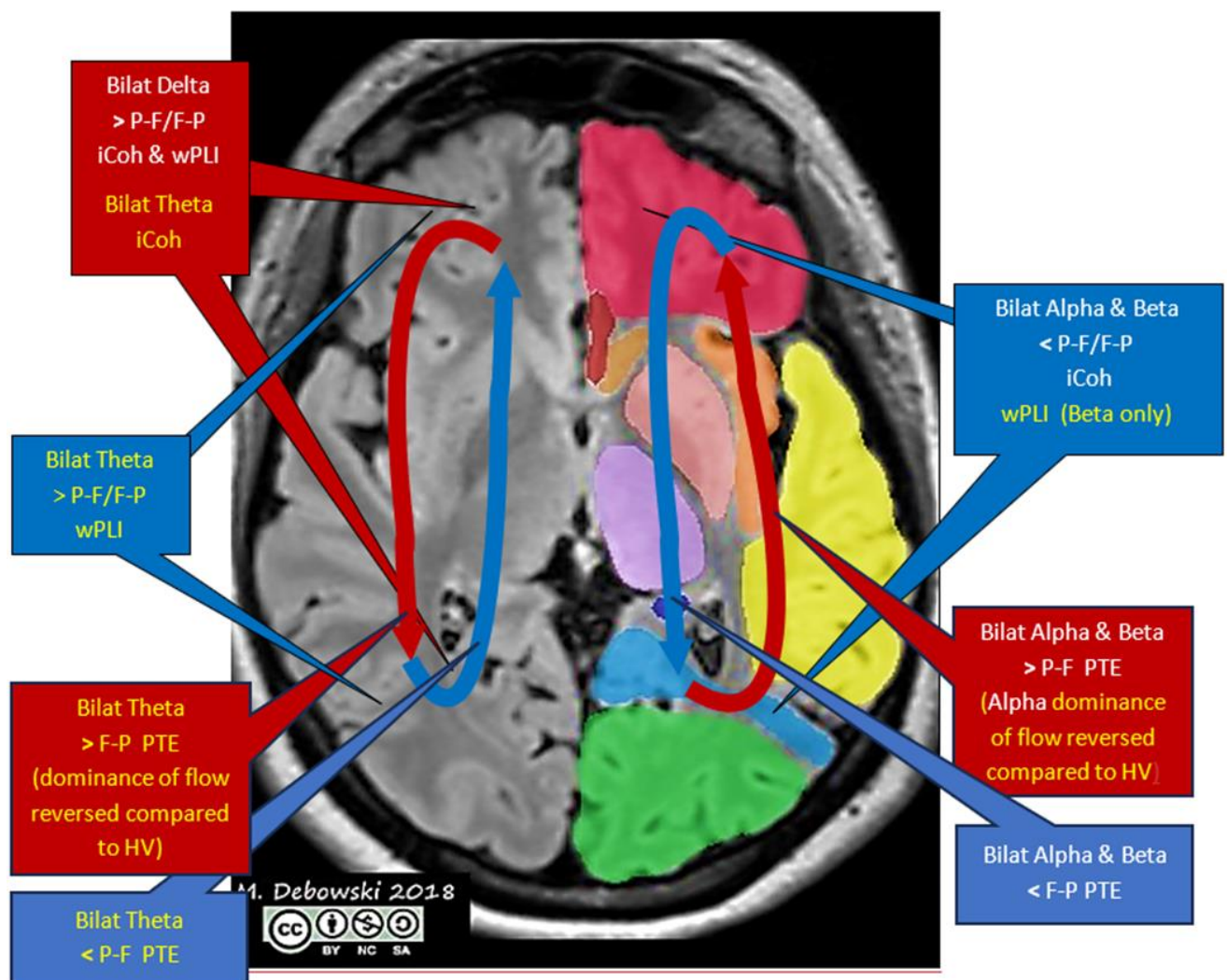


Figure 29: Significant frontal-parietal/parietal-frontal connectivity alterations in the TEA cohort

5.3. Other Inter-Regional Findings

Network connectivity within theta band frequencies shows the most consistent changes in other inter-regional connections, with the temporal-occipital and temporal-parietal networks both showing significant differences between TEA and HV using all three connectivity metrics. Figure 30.

The pattern of these findings is again similar to those seen within temporal-frontal and frontal-parietal results i.e., there is a discrepancy between measures regarding the direction of the changes with ICoh measures showing higher connectivity in TEA subjects compared to HV, while wPLI shows lower connectivity in the TEA group than in HV (Figure 30, Figure 31, Figure 32).

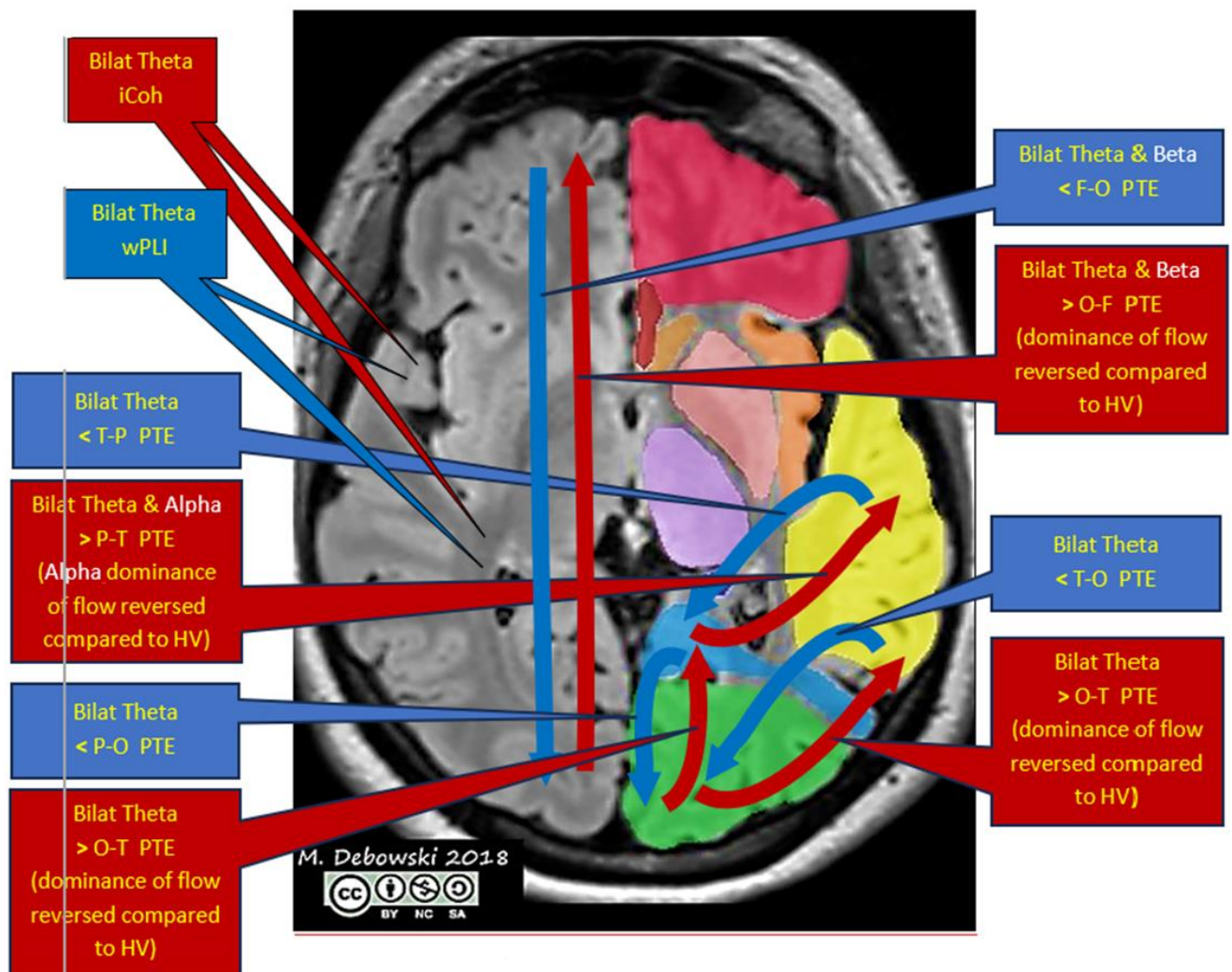


Figure 30: Other significant inter-regional alterations in TEA

Directional analysis using PTE demonstrates higher levels of theta connectivity flowing from occipital to temporal, and occipital to parietal regions within the TEA cohort compared to higher levels of theta connectivity flow from temporal to occipital, and parietal to occipital network flow noted within the HV cohort. Similarly, the TEA theta and beta PTE network flow dominance between frontal and occipital regions are noted to be reversed compared to that of HV i.e., network dominance is from occipital to frontal in TEA, compared to frontal to occipital in HV (Figure 33).

Other inter-regional differences affecting two of the three connectivity metrics are as follows:

- Lower network power is seen in the TEA group compared to HV within beta and alpha band temporal-parietal connectivity. This finding is seen using both iCoh and wPLI analysis.
- Beta band inter-regional differences between temporal and occipital regions are seen using iCoh and PTE. iCoh shows lower power within the TEA cohort compared to HV. Directional PTE differences demonstrate lower temporal-to-occipital flow, but higher occipital-to-temporal network flow in the TEA group; this is reversed compared to HV directional flow patterns.

5.4. Consistent Inter-Regional Hemispheric Findings

Only inter-regional hemispheric analyses across temporal-frontal networks show any consistent significant differences between the two cohorts, where changes are seen with both iCoh and wPLI metrics.

- TEA cohort connectivity within the left hemisphere temporal-frontal networks is significantly different from that of the HV cohort. This is seen across all frequency bands (beta, alpha, theta, delta).
- Inter-hemisphere functional connectivity within temporal-frontal networks shows significant differences between cohorts within beta and delta frequency bands.
- There is a difference in delta band functional connectivity within the right hemisphere temporal frontal networks, between TEA and HV cohorts.

The pattern of iCoh/wPLI frequency band changes is identical to inter-regional findings i.e., beta and alpha frequency network flow is significantly lower in the TEA cohort compared to TEA. Delta frequency network flow is significantly higher in TEA in comparison to HV, and theta frequencies demonstrate higher TEA connectivity activity with iCoh compared to HV, whilst wPLI shows lower TEA connectivity compared to HV (Figure 31, Figure 32).

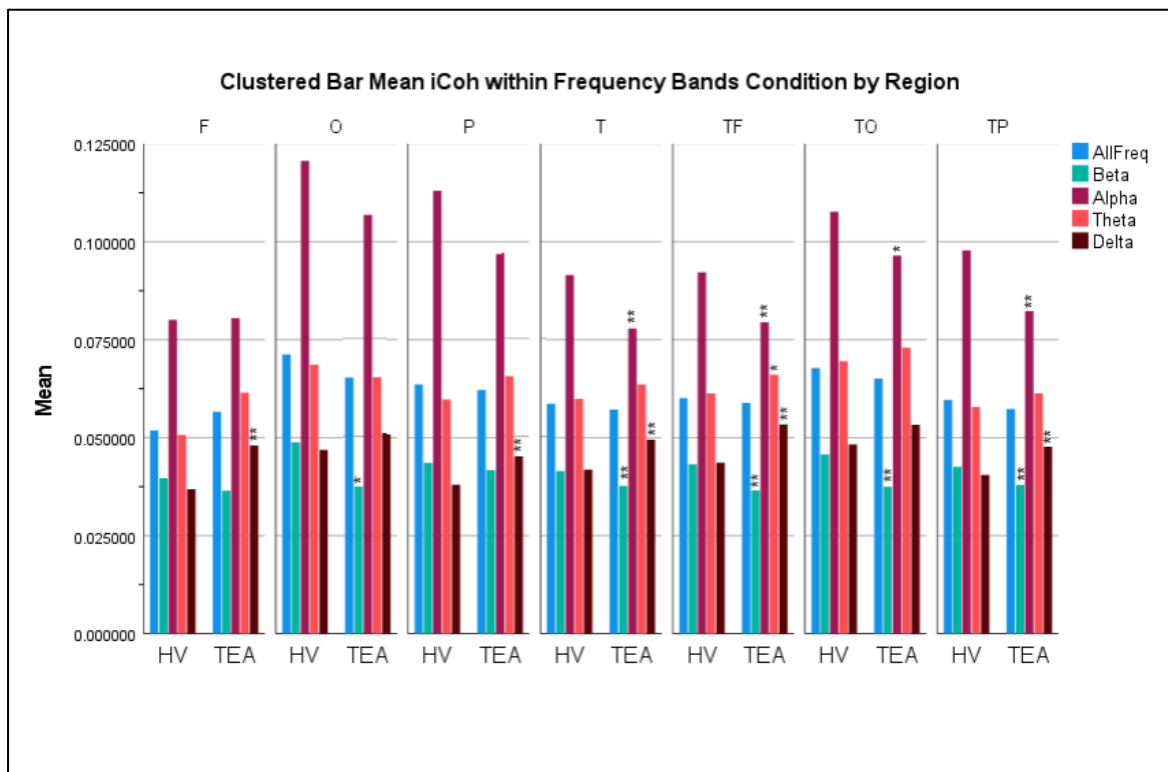


Figure 31: Summary of iCoh mean values for all frequency band within region and inter-regionally. F= frontal region, O= occipital region, P= parietal region, T=temporal region, TF= temporal-frontal networks, TO= temporal-occipital networks, TP= temporal-parietal networks. Significant findings are post FDR corrections and are labelled as follows: ** $p < 0.001$, * $p > 0.001$ but < 0.05 , and ! $p > 0.05$ prior to FDR correction but show significance following correction.

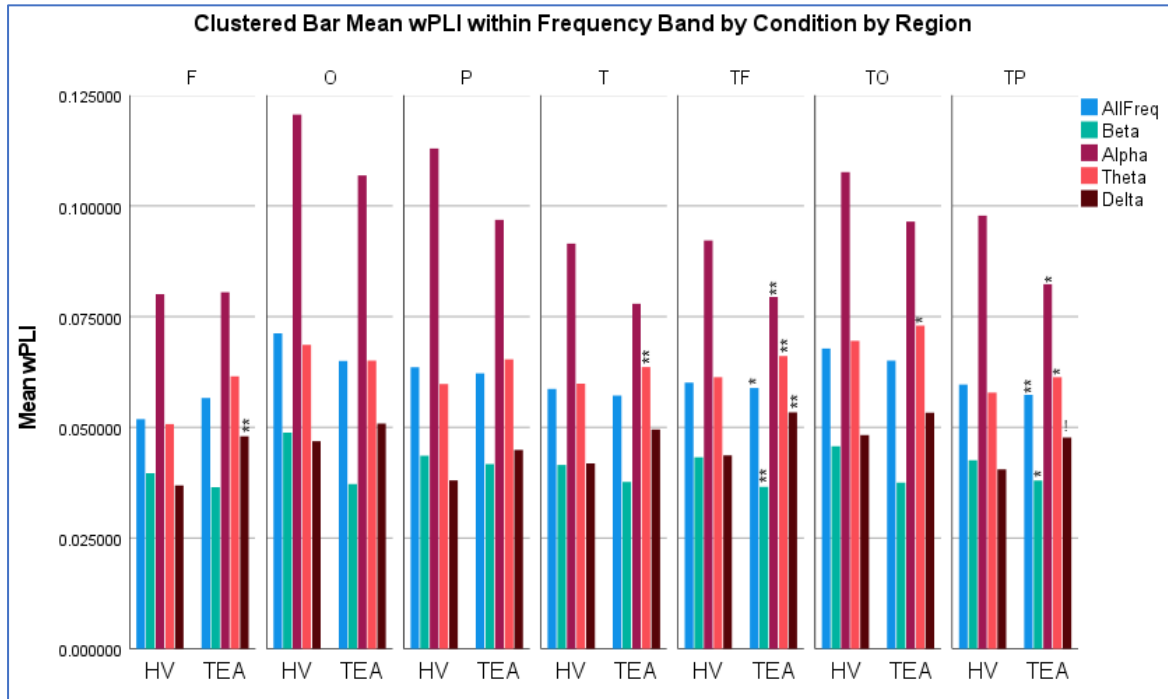


Figure 32: Summary of wPLI mean values for all frequency band within region and inter-regionally. F= frontal region, O= occipital region, P= parietal region, T=temporal region, TF= temporal-frontal networks, TO= temporal-occipital networks, TP= temporal-parietal networks. Significant findings are post FDR corrections and are labelled as follows: ** $p < 0.001$, * $p > 0.001$ but < 0.05 , and ! $p > 0.05$ prior to FDR correction but show significance following correction.

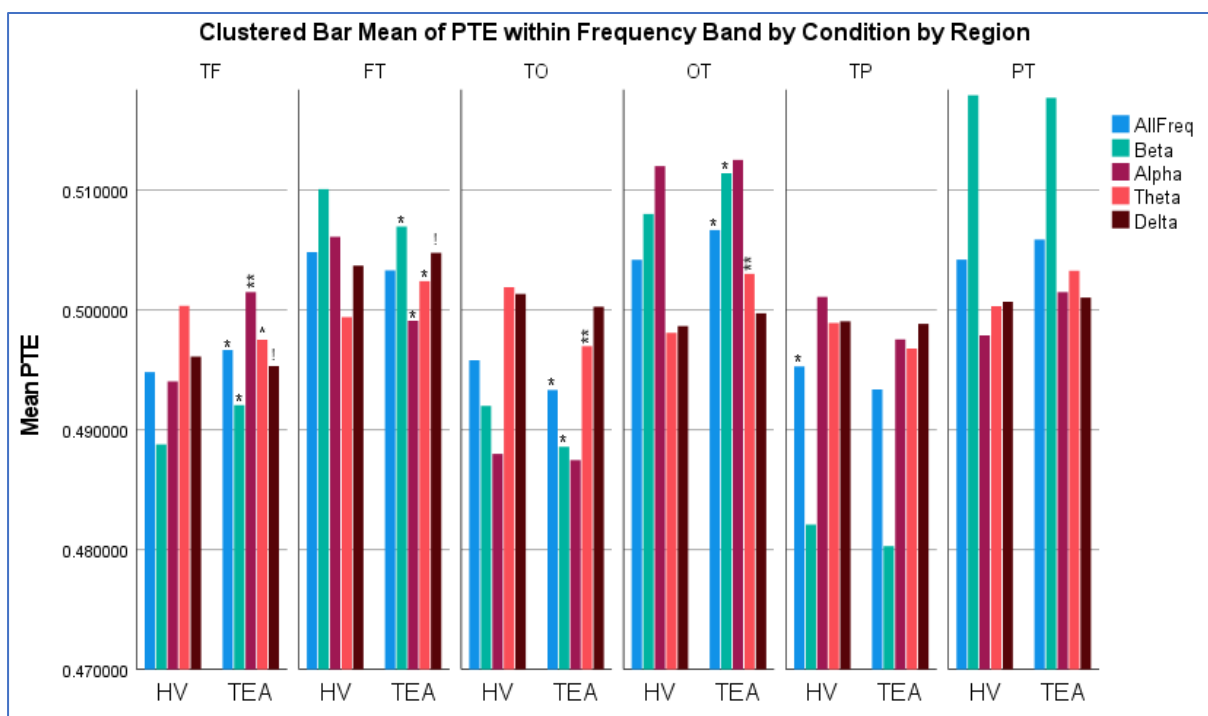


Figure 33: Summary of PTE mean values for all frequency band, showing directional networks between regions. TF= temporal to frontal networks, FT= frontal to temporal networks, TO= temporal to occipital networks, OT= occipital to Temporal networks, TP= temporal to parietal networks and PT= parietal to temporal networks. Significant findings are post FDR corrections and are labelled as follows: ** $p < 0.001$, * $p > 0.001$ but < 0.05 , and ! $p > 0.05$ prior to FDR correction but show significance following correction.

Discussion

Summary

Whilst the results of visual EEG interpretation is a key element in the diagnosis of transient epileptic amnesia (TEA) (Zeman *et al.*, 1998a; Butler *et al.*, 2007a), findings can be normal or non-specific (Seo *et al.*, 2023). Lanzone *et al.* suggest that quantitative analysis (qEEG) of the EEG could further aid the diagnosis of neurological disorder by identifying aspects of the EEG which may be difficult to recognise using visual analysis alone (Lanzone *et al.*, 2020). To our knowledge, only one previous piece of research exists exploring qEEG findings in TEA, comparing the findings to a transient global amnesia (TGA) cohort (Lanzone *et al.*, 2020).

Our research aims are to evaluate differences in qEEG, functional, and effective connectivity in resting-state EEG (rsEEG) recorded from patients diagnosed with TEA and compared to healthy age-matched controls.

The primary objective is to compare the resting-state EEG-derived brain network and connectivity patterns of 28 patients diagnosed with transient epileptic amnesia with 28 healthy controls. The findings are discussed and compared to similar published work from other relevant conditions with memory deficits, such as transient global amnesia (TGA), mild cognitive impairment (MCI) Alzheimer's disease, and temporal lobe epilepsy.

Key Results

Key results from the resting-state EEG analysis undertaken in this study are as follows:

- Linear frequency-based iCoh and phase-synchronisation-based wPLI connectivity measures demonstrate a global decrease in broad spectrum (0.5Hz-40Hz) connectivity strength in TEA, with frequency bands showing consistent dynamics:
 - A global reduction in beta and alpha band connectivity strength (Figure 27)
 - A global increase in delta band connectivity strength. Intra-regionally, this is particularly noticeable over frontal regions (Figure 27). Similar findings have been reported associated with MCI and Alzheimer's disease (Babiloni *et al.*, 2006b).
 - Altered global network connectivity activity in theta band frequencies, which presents as higher mean connectivity values using iCoh and lower mean

values with wPLI – both highly significant (adjusted p -values= <0.0001) (Figure 27).

- Marked disruption of theta frequency networks is evident within all inter-regional analyses undertaken (frontal-temporal, frontal-parietal temporal-occipital, and temporal-parietal), occurring in all metrics (iCoh, wPLI and PTE). The findings carry a specific hallmark, as seen in global theta analysis i.e., higher mean values than HV with iCoh and lower with wPLI (Figure 28, Figure 29, Figure 30).
- Directionality of connectivity inter-regionally, as assessed using PTE, shows marked derangement of theta frequency strength, resulting in a reversal in directionality between all inter-regions other than parietal-temporal (Figure 34).

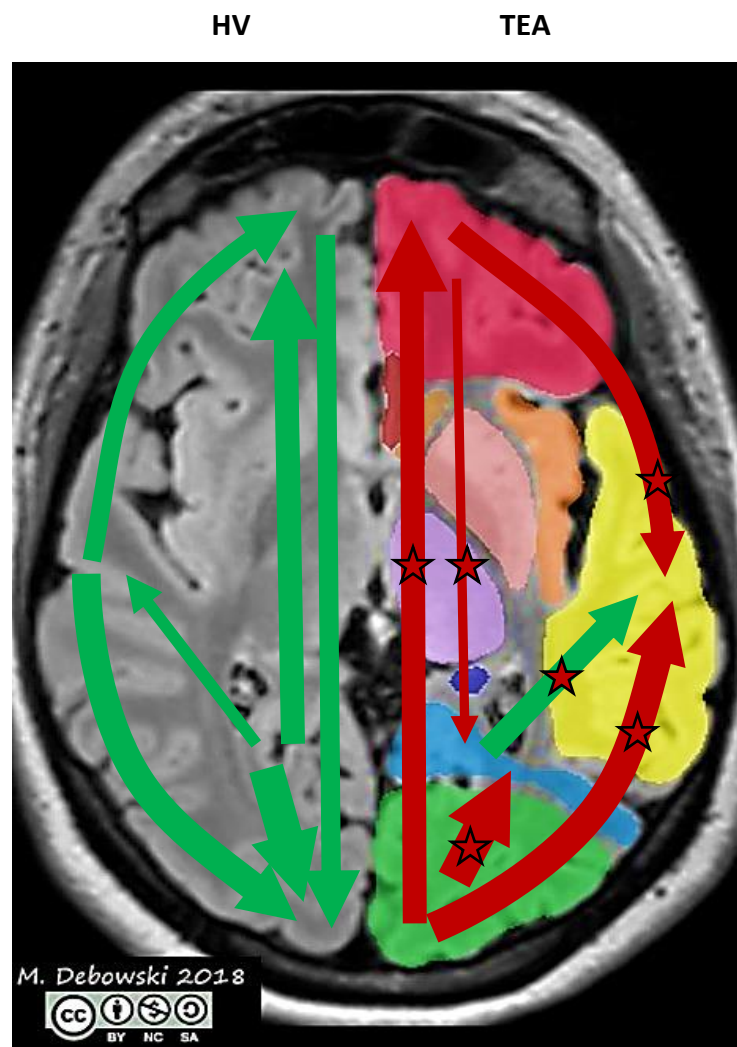


Figure 34: INTER-REGIONAL Theta PTE - (dominance of network flow reversed compared to HV). TEA reversal of dominance of connectivity flow (compared to HV) marked with red arrows. Significant difference in TEA PTE (compared to HV) marked with red stars.

- Frontal-temporal and frontal-parietal networks additionally demonstrate a cross-band reduction of connectivity between the regions in TEA, affecting beta and alpha frequency bands across all metrics (iCoh, wPLI and PTE) (Figure 28, Figure 29).
- Data demonstrates higher delta band mPSD over the left temporal region in TEA compared with healthy controls, and an increased asymmetry compared to the right temporal region within the TEA cohort compared to HV. The study demonstrates a correlation between this delta band mPSD asymmetry, and the presence of increased inter-ictal non-epileptiform abnormalities seen over the same region during visual EEG analysis (Figure 27). Similar non-epileptiform findings have been documented over the epileptogenic region in focal epilepsy (Pellegrino *et al.*, 2018). There is, however, no correlation with the distribution of epileptiform abnormalities following visual analysis of the raw EEG, which demonstrates a right-sided dominance. This is unsurprising, as epileptiform abnormalities were extracted during pre-processing.
- Rather than being related to the length of the EEG recording, epileptiform abnormalities noted during visual analysis were more likely to be found in EEG recordings including a period of sleep. Similar findings were demonstrated by Tramoni *et al.* (Tramoni and Felician, 2017) and by Lanzone *et al.*, however, Lanzone *et al.* attributed the increased occurrence of interictal abnormalities to the performance of long-term monitoring (Lanzone *et al.*, 2018).

Interpretation

Our analysis targeted the effects of TEA on the qEEG and rsEEG, comparing these results to healthy age-matched controls. As an epilepsy syndrome, TEA is amenable to treatment with antiepileptic medication which yields effective seizure control in 70-97% of people with TEA (Pukropski *et al.*, 2022; Blain *et al.*, 2021; Baker *et al.*, 2021; Ramanan *et al.*, 2019; Lanzone *et al.*, 2018; Mosbah *et al.*, 2014). Yet even when treated, TEA represents a long-term condition with a proportion of patients experiencing persisting memory deficits, in the form of accelerated long-term forgetting (ALF) and autobiographical amnesia (AbA) (Savage *et al.*, 2022; Savage *et al.*, 2019a). From an EEG perspective, one has to look below the surface rhythms, to the substrate of qEEG and connectivity within networks for further answers.

To meaningfully interpret the study results, a background knowledge of the effect of ageing on qEEG and brain networks is required. Changes in functional connectivity occur throughout maturation and as part of a healthy ageing process. Inevitably this leads to normal structural and functional decline, including the disruption of memory functions (Pappalettera *et al.*, 2023; Perinelli *et al.*, 2022; Alù *et al.*, 2021; Tóth *et al.*, 2014a; Ishii *et al.*, 2017). Resting state studies include EEG and magnetoencephalography (MEG), as both provide superior temporal resolution compared to functional MRI (fMRI) (Ishii *et al.*, 2017). Healthy ageing-related EEG/MEG findings include:

- An overall reduction in the amplitude and mean power of the posterior alpha rhythm, and reduced reactivity to eye opening. Impairment of reactivity is progressive from healthy ageing to pathological ageing, correlating with cognitive decline (Ishii *et al.*, 2017; Babiloni *et al.*, 2021a).
- Slowing of background activity and the posterior dominant rhythm (alpha rhythm), although studies show inconsistent findings particularly about theta and delta rhythms (Babiloni *et al.*, 2006a; Ishii *et al.*, 2017).
- Global increase in mean power within theta and delta bands, covering frequencies between 0.5Hz and 7.9Hz (Ishii *et al.*, 2017).
- Localised delta mean power reduction over occipital regions (Babiloni *et al.*, 2006a)
- Reduction in mean power within beta frequencies (13-30Hz) and alpha frequencies (Pappalettera *et al.*, 2023; Babiloni *et al.*, 2006a)

- Inter-regional disruption of frontal-parietal, frontal-temporal and parietal-temporal connectivity has also been reported (Perinelli *et al.*, 2022)

As healthy volunteers (HV) within the study were age-matched to the TEA cohort, it is reasonable to assume that both cohorts start from the same baseline concerning the healthy ageing findings above.

In TEA, a significant deviation from this status quo concerns the *increase* of inter-regional connectivity between frontal-parietal, frontal-temporal and parietal-temporal regions reported by Perinelli *et al.* within alpha and theta bands (Perinelli *et al.*, 2022). This pattern is not replicated in our TEA cohort but rather, an overall *decrease* in inter-regional connectivity being evidenced between these regions with respect to HV. Perinelli *et al.* attribute their findings to the posterior to anterior shift in ageing (PASA) which is reported across a range of connectivity literature (Perinelli *et al.*, 2022; Eyer *et al.*, 2011; Davis *et al.*, 2007; Babiloni *et al.*, 2006a). It is thought that the increasing frontal dominance described by the PASA model is a compensatory response to an age-related waning of posterior functional integrity (Perinelli *et al.*, 2022; Eyer *et al.*, 2011; Davis *et al.*, 2007). Concerning the PASA model, our findings suggest that this compensatory process has been disrupted in the TEA group, possibly due to malfunctioning plasticity within the network systems (Babiloni *et al.*, 2016).

Further support for the PASA model compensatory mechanism being dysfunctional in TEA, lies within a clear deviation from healthy controls in inter-regional PTE findings. Each frequency band shows a distinct directional connectivity dominance pattern in healthy controls. However, there is a marked deviation from HV patterns concerning theta frequencies and to a lesser extent, alpha frequencies within the TEA group (Figure 35). The healthy control PTE maps largely follow the predictions of the PASA model, with delta, beta and theta frequencies performing similarly. In our HV data, these frequencies additionally demonstrate an outward PTE flow from parietal regions (including central electrodes in this study) to frontal, occipital and temporal areas. This is unlikely to be the result of active sensory input, due to the resting-state nature of the EEGs. It is perhaps more likely to result from resting-state activity within one or more of the brain network systems.

The beta, alpha and theta TEA PTE maps show significant alterations from the healthy normal, particularly within theta-band frequencies. There are more subtle alterations in PTE within the beta and alpha frequencies, in frontal inter-regional networks and temporal-parietal networks. Delta inter-region PTE patterns are matched between the cohorts, suggesting that delta networks are largely unaffected in TEA (Figure 35).

Reversal of Inter-Regional Theta Frequency Connectivity

As stated previously, there are significant alterations in the theta PTE maps within the TEA cohort when compared to HV. These alterations appear across most aspects of inter-region directional flow, with an almost complete reversal of theta connectivity flow magnitude in contradiction to the PASA model (Figure 35). Theta PTE power from occipital to frontal, occipital to temporal, frontal to parietal, frontal to temporal, and parietal to temporal are significantly increased compared to healthy controls. This is accompanied by a significant PTE decrease, compared to healthy, in the opposite direction i.e., frontal-to-occipital, temporal-to-occipital, parietal-to-frontal, temporal-to-frontal, and temporal-to-parietal. The above alterations in network strength effectively reverse the dominant resting state network flow pattern (Figure 35).

Our study also shows that the most widespread intra-band changes are seen within the theta range (4-7.9Hz). All inter-regional connections examined (frontal-temporal, frontal-parietal temporal-occipital, and temporal-parietal) show the same pattern of alteration, with phase and amplitude affected in different ways, as shown by the divergent iCoh and wPLI significances. wPLI, a purely phase-synchronisation-based measure exhibits reduced connectivity strength in TEA. iCoh however demonstrates an increased value.

5.5. Can Inter-Regional Theta Dysfunction Disrupt Memory?

Theta band frequencies (4-7.9Hz) have frequently been associated with memory and learning, with successful memory facilitated by theta oscillations, including encoding, retrieval and associative memory involving multiple items (Kahana *et al.*, 1999; Sederberg *et al.*, 2003; Guderian and Düzel, 2005; Kahana, 2006; Raghavachari *et al.*, 2006; Jacobs *et al.*, 2006; Nyhus and Curran, 2010; Hasselmo and Stern, 2014; Herweg *et al.*, 2020; Karakaş, 2020; Abubaker *et al.*, 2021). It is suggested that accelerated long-term (ALF) forgetting is due to

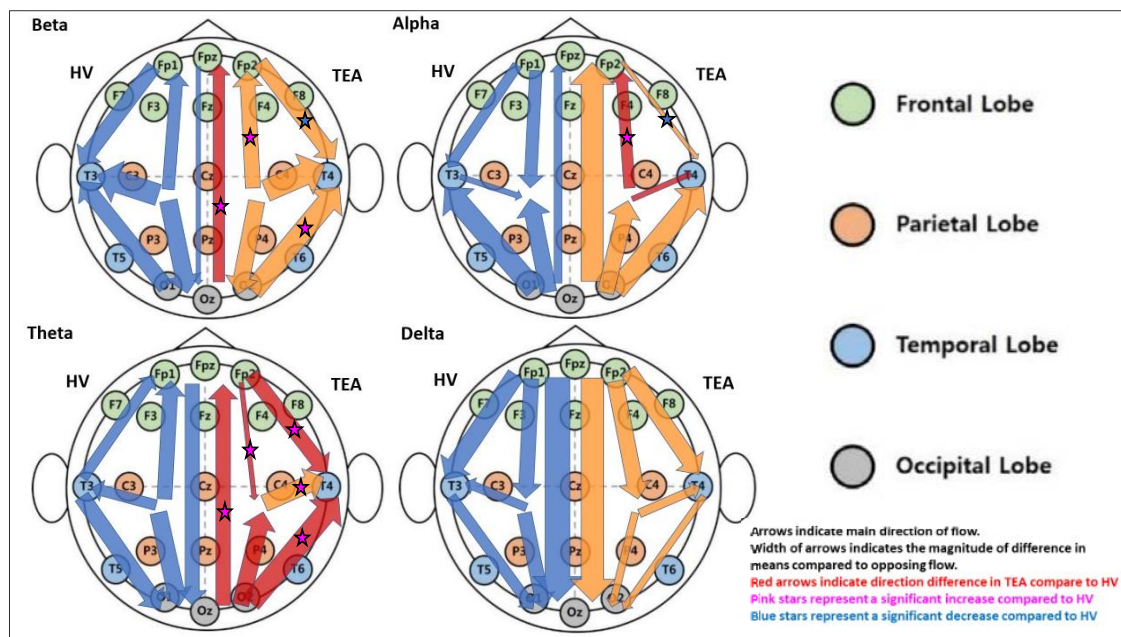


Figure 35: The diagram shows the dominant directional connectivity strength of each frequency band. The dominant direction is signified by the direction of the arrows and has been determined by comparison of the mean value for PTE of each inter-regional. The thickness of the arrows represents the magnitude of the difference in means. The left side of each headstamp represents HV (blue arrows) and the right side TEA (orange arrows). TEA deviations from HV are marked with red arrows. Significant increases or decreases in TEA PTE are marked with stars (pink and blue respectively). The flow patterns are represented for each band: beta, alpha, theta, delta.

dysfunction of consolidation rather than acquisition (Hoefijzers *et al.*, 2013), whilst autobiographical amnesia is related to disruption in recollection (Milton *et al.*, 2012).

Autobiographical memory utilises a wide group of brain regions including the hippocampus and associated regions, the lateral temporal lobes, the temporoparietal junction, and areas of the frontal lobe (Milton *et al.*, 2012; Xu *et al.*, 2020)(Figure 37). These are in keeping with the areas of theta network disruption within our findings. Studies including connectivity analysis have also demonstrated interconnections between these regions, forming an autobiographical memory network (Addis *et al.*, 2007; McAndrews, 2012)(Figure 36). Therefore, the inter-regional network alterations within our study provide a possible explanation for the phenomena of ALF and AbA.

5.6. Are Temporal Lobe Theta alterations related to Amnestic seizures, AbA, and ALF?

As previously discussed, the hippocampus, which forms part of the medial temporal lobe, plays a key role in episodic memory function including consolidation and recollection (Butler *et al.*, 2012; Amin and Malik, 2014; Tramoni and Felician, 2017). It acts both downstream

and upstream as an integrator with the cortical regions of association (Sweatt, 2009). Memory disturbance is common in epilepsy, in particular in those with temporal lobe epilepsy (Elwes, 2012).

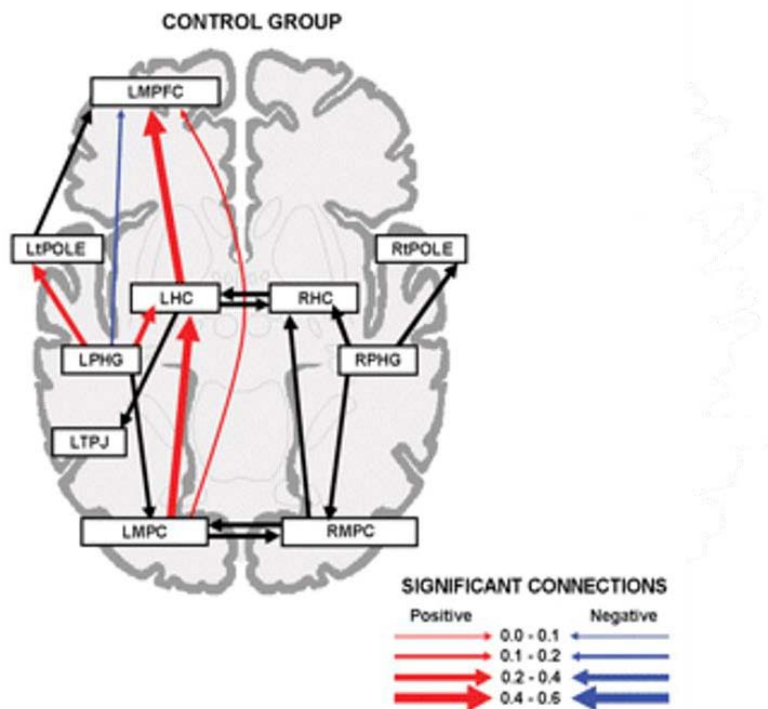


Figure 36: Diagrammatic representation of the effective connections within the neural network mediating AM retrieval. Arrow thickness represents the strength of the connection (i.e. the value of the path coefficient), as described in the key (Addis et al., 2007)

Remember Network

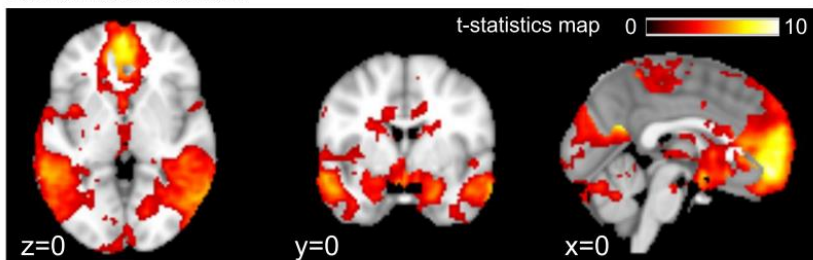
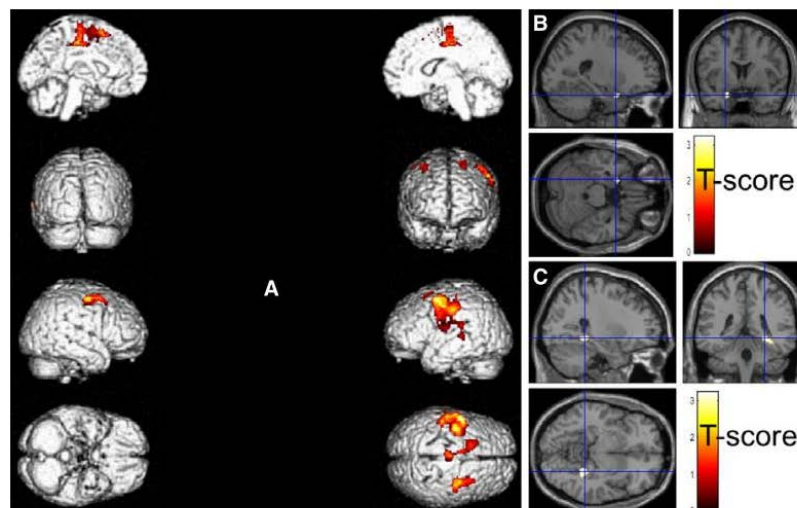


Figure 37: Brain regions associated with recollective memory - a widely distributed network that is selectively sensitive to recollection (Xu et al., 2020).

Medial temporal lobe epilepsy is the most common form of temporal lobe epilepsy and the syndrome of transient epileptic amnesia sits within this diagnosis (Elwes, 2012; Zeman and Butler, 2010; Milton et al., 2012). Mesial temporal sclerosis or hippocampal pathology can often, but not always, be associated (Elwes, 2012). In TEA, 18F-FDG-PET and fMRI studies have shown hypometabolism within the hippocampal-neocortical network supporting

episodic memory function, even in those without associated pathology (Figure 38) (Mosbah *et al.*, 2014; Tramonì and Felician, 2017; Milton *et al.*, 2012). Theta frequency oscillations are widely recognised as originating within the hippocampus and associated medial temporal lobe networks, but also further afield within the neocortex (Herweg *et al.*, 2020; Raghavachari *et al.*, 2006; Karakaş, 2020). The above findings may suggest that theta disruption found in TEA may represent a decrease in theta network activity within theta networks projecting out from the temporal lobe, rather than increased activity being received into temporal areas from other regions. However, this hypothesis alone, would not explain theta disruptions within frontal-occipital, frontal parietal and parietal-occipital networks.

One of the main criteria for TEA diagnosis is the relative preservation of cognitive functioning during attacks, except memory (Zeman *et al.*, 1998a). Memory dysfunction is generally in the form of amnesia during or following seizures, alongside persisting accelerated long-term forgetting and autobiographical amnesia (Zeman and Butler, 2010; Muhlert *et al.*, 2010; Milton *et al.*, 2010).



Anatomic localization of area of hypometabolism in patients, in comparison to healthy subjects. In comparison to healthy subjects, patients with TEA showed significant hypometabolism within bilateral middle frontal gyri (BA6), and within left medial, superior, precentral, and paracentral gyri (BA6, BA31; $p < 0.05$, corrected) (A). Additional hypometabolism was found using medial temporal mask within the left uncus (BA28) (B) and right posterior parahippocampus (BA36) (C).
Epilepsia © ILAE

Figure 38: 18F-FDG-PET findings in TEA patients compared to healthy volunteers (Mosbah *et al.*, 2014)

Theta frequency rhythms are well known to play a major role in the encoding and recall of memories, particularly those with multiple cognitive and sensory elements. This has been

demonstrated through research into spatial navigation and episodic memory-related tasks (Lopes da Silva and Halgren, 2018; Kahana *et al.*, 1999; Raghavachari *et al.*, 2001; Herweg *et al.*, 2020; Kemp *et al.*, 2012).

It stands to reason that if theta activities increase during the successful formation of new episodic memories, disruption of theta-driven networks could result in the disruption of memory encoding. A high proportion of theta waves arise in the medial temporal lobe, particularly within the hippocampus networks and the hippocampus itself, which are entrained during learning, but more so during recall (Kahana, 2006; Herweg *et al.*, 2020). Theta waves are also found in the neocortex, with many memory models suggesting this is driven by the hippocampus via its projections (Herweg *et al.*, 2020).

As theta rhythms are strongly related to memory processing in key regions within the temporal lobe, combined with evidence from other research, this suggests that resting-state temporal lobe theta connectivity dysfunction is likely to be a contributory factor for ALF and AbA within people with TEA. Whilst our study lacks the spatial detail of the PET and fMRI studies, previous TIME research included such neuroimaging, demonstrating hypometabolism within the hippocampus and reduced effective connectivity between the right pPHG and the right middle temporal gyrus (Milton *et al.*, 2012; Butler *et al.*, 2013). The combined evidence supports the theory that theta network dysfunction, seen at a more macro level within this study, extends to, or is possibly sourced from hippocampal regions. It is unclear however whether the network alterations exist before epilepsy onset, and/or are exacerbated by seizures, or occur as a result of temporal lobe seizures.

In summary, our findings of theta network disruptions between temporal, frontal, and parietal areas appear highly significant concerning memory problems experienced by people with TEA, namely epileptic amnesia, persisting accelerated long-term forgetting, and autobiographical amnesia. Based on the evidence above, the pattern of disruption of theta connectivity in TEA is likely to underlie the impairment of episodic memory processes (Figure 39).

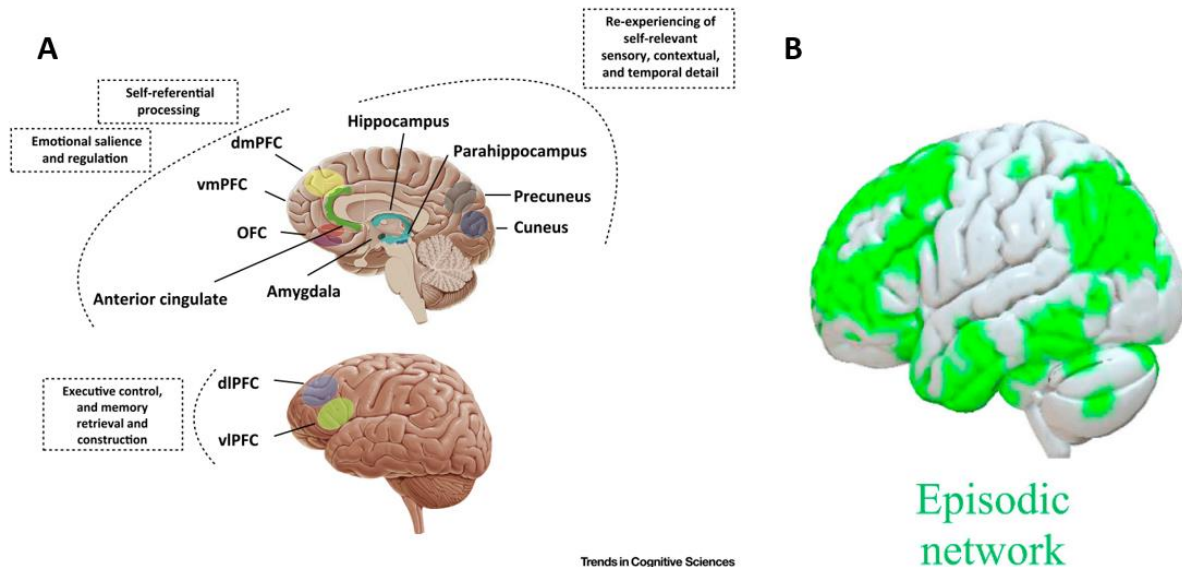


Figure 39: **A** – a graphical depiction of key brain regions involved in the retrieval of specific autobiographical memories. Ventromedial (vm) and dorsomedial (dm) regions of the prefrontal cortex (PFC) as well as the orbitofrontal cortex (OFC), anterior cingulate, and amygdala play an important role in the processing of self-referential information and in assigning and regulating emotional salience. Temporal regions such as the hippocampus and parahippocampus, and occipital regions such as the cuneus and precuneus, also play an important role in the re-experiencing of the self-relevant sensory, contextual, and temporal details which characterise specific autobiographical memories. Finally, dorsolateral (dl) and ventrolateral (vl) PFC regions enable the controlled retrieval and construction of a memory whilst irrelevant thoughts and memories are inhibited. (Barry et al., 2018). **B** – a graphical depiction of key brain areas involved in wider episodic memory processing (Stampacchia et al., 2018).

Functional Connectivity Measure Differences within the Theta Band

It was noted previously that theta frequency functional connectivity results consistently show the disparity between iCoh and wPLI results, which makes a judgement concerning an increased significance or decreased significance compared to HV difficult.

With regard to these contradictory iCoh/wPLI findings, whilst both measures are robust concerning volume conduction, PLI (the predecessor of wPLI) tends to underestimate true connectivity strength through misinterpretation of small phase changes. wPLI however uses a weighting algorithm which is designed to minimise this error. Additionally, it is unclear, if there is an underestimate by wPLI, why this should only affect theta frequencies.

There are other technical considerations which might account for the consistent difference in theta connectivity. Firstly, iCoh detects linear connectivity whilst wPLI is capable of detecting both linear and non-linear interactions (Cohen, 2015; Jia, 2019; Cohen, 2014). Secondly, iCoh tends to be less sensitive to phase synchronisation, being selective at a phase

lag of a quarter cycle (Cohen, 2014; He *et al.*, 2019; Jia, 2019; Sakkalis, 2011). Thirdly, iCoh is thought to be more susceptible to noise compared to wPLI and can be influenced by signal amplitude changes (Vinck *et al.*, 2011; Jia, 2019). iCoh therefore tends to positive bias when detecting connectivity, whereas wPLI is described as “debiased” by its developers (Vinck *et al.*, 2011). However, as stated above, according to other authors wPLI may underestimate connectivity strength due to missing connectivity with small phase lags, or through the deselection of frequency non-stationary signals (Cohen, 2014; Cohen, 2015).

If the discrepancies in iCoh/wPLI strength are related to the choice of metric, why only the theta band is affected is not clear. If the iCoh/wPLI difference was due to an increased prevalence of non-linear connectivity within the theta frequency band (detected by wPLI), this would lead to increased connectivity wPLI compared to iCoh. In contradiction to this the opposite is the case as increased iCoh and decreased wPLI connectivity are noted. It is also unlikely that the inconsistency is due to noise which, as described above, might affect iCoh measure preferentially. This is because theta activities (4-7.9Hz) do not typically fall within the frequency range which commonly constitutes noise, which tends to consist of faster frequencies i.e. contamination by muscle. Additionally, the EEG data was pre-processed to minimise potential contaminants (Jia, 2019; Wendling and Lopes da Silva, 2017). The influence of amplitude variation within the EEG on iCoh, compared to wPLI which does not use amplitude within its calculation, may provide a possible explanation. However, a significant difference in mPSD between TEA and HV cohorts is predominantly noted within delta frequencies, with significant theta difference only seen within the left temporal area. As the theta band iCoh/wPLI discrepancy occurs across all inter-regions, not just those involving temporal areas, this explanation is less plausible. Other possible theories may lie within the phase of the EEG waveforms. As described above iCoh is less sensitive to phase synchronisation, whilst wPLI can miss true connectivity with small phase lags and non-stationary waveforms. The phase changes would need to be specific to the theta frequency band, with phase differences related to the type of dysfunction clinically e.g. disruption of memory.

Unfortunately, the cause of the iCoh/wPLI discrepancy is not satisfactorily resolvable from our study data, but it does provide insight into the reporting of contradictory findings

concerning connectivity increases or decreases across studies (Babiloni *et al.*, 2021b; Babiloni *et al.*, 2009; Escudero *et al.*, 2011; Tóth *et al.*, 2014b; Vecchio *et al.*, 2014). Our study provides support for connectivity measure effects being the root cause, rather than the overall significance being an error per se. Ultimately, therefore, it is clear from our study results that theta functional connectivity is significantly different from healthy volunteers in people with TEA. Further investigation is required to resolve the significance, by using a multimodal approach for instance.

Significances within Other Frequency Bands

mPSD Findings

Of interest is the reduction in mPSD within beta and alpha frequencies (13-30Hz, and 8-12.9Hz respectively) occurring with healthy ageing. One would expect the two age-matched groups to behave similarly in this respect, and our mPSD findings confirm this. There are, however, localised changes in theta and delta mPSD within the TEA group, which is confined to the temporal regions, in particular within the left hemisphere. These focal changes demonstrate a pattern similar to the prevalence of interictal non-epileptiform abnormalities noted during visual EEG interpretation (note, epileptiform discharges were seen relatively evenly across hemispheres often within the same recording – these have been removed during pre-processing). As noted previously, PET and fMRI studies undertaken on TEA patients revealed hypometabolism within the hippocampus and reduced effective connectivity between the right pPHG and the right middle temporal gyrus (Milton *et al.*, 2012; Butler *et al.*, 2013). Similar findings have been previously described as associated with TLE and attributed to the topographic distribution of the epileptogenic area, thus providing reliable lateralising value (Koutroumanidis *et al.*, 1998; Tao *et al.*, 2011). Our findings, combined with the research findings above suggest a left temporal focus is more prevalent in our cohort of TEA patients.

Functional and Effective Connectivity Power within Beta and Alpha Frequency Bands

Whilst mPSD is similar between the two groups, TEA data does show a significant reduction in functional connectivity within alpha and beta frequencies, in comparison to healthy

controls. This occurs in relation to global and inter-regional connectivity. The reduction in alpha and beta connectivity strength is seen across both coherence (iCoh) and synchronisation-based (wPLI) metrics, whilst intra-regional iCoh and wPLI show inconsistent findings concerning significance compared to HV.

In contrast to faster frequencies, delta functional connectivity is seen to increase in TEA with respect to healthy controls, both globally and within the frontal lobe. Similarly, increased functional connectivity increases within the delta band are also apparent between frontal-temporal and frontal-parietal inter-regions. The inter-regional functional connectivity reductions within the alpha/beta bands are visible across frontal-temporal, frontal-parietal, and parietal-temporal regions.

These findings are similar to those often reported within MCI/AD research, which is ascribed to dysfunctional transmission in long cortico-cortical network connections (Babiloni *et al.*, 2016; Pijnenburg *et al.*, 2004; Stam *et al.*, 2005; Giustiniani *et al.*, 2023; Stam *et al.*, 2006). On the other hand, antagonistic increases in delta coherence are seen between the same regions within TEA, which is not a consistent finding in MCI/AD. Increased frontal delta connectivity over frontal regions was related specifically to frontal-temporal dementia in a study by Yu *et al.* (Yu *et al.*, 2016) According to Babiloni *et al.* a global increase in delta band source activity and functional connectivity comes under the broad spectrum of brain dysfunction (Babiloni *et al.*, 2021b). This research points to the possibility of a more localised delta network dysfunction within frontal networks in TEA.

Effective Connectivity

Compared to the marked effective connectivity dysfunction seen with theta frequencies, there is considerably less derangement of beta and alpha networks from a directionality perspective, despite a significant reduction in connectivity power within these frequencies, both globally and inter-regionally. Delta inter-regional networks are very similar to HV concerning PTE directionality, although there is increased connectivity strength. The strongest and most consistent beta and alpha PTE findings in our study were seen within the frontal-temporal and frontal-parietal networks, although temporal-parietal networks also have a consistent reduction in alpha and beta functional connectivity using iCoh and wPLI metrics. Additionally alpha band PTE directionality between frontal-parietal and temporal-

parietal shows reversal of directionality strength in TEA. This suggests that dysfunction throughout frontal-temporal-parietal networks is more extensive than merely theta frequency connectivity.

In summary, global and inter-regional alpha and beta connectivity demonstrate similar patterns to that found within MCI/AD conditions, whilst the slower theta and delta frequency networks may behave differently. It is worth noting that similar alpha/beta inter-regional alterations in connectivity have also been reported in healthy ageing (Perinelli *et al.*, 2022), therefore this phenomenon could be part of a natural ageing process which becomes more progressive in pathological ageing.

Visual Analysis: Significance of sleep-related interictal abnormalities.

Other key findings likely to impact effective memory function are the increased non-epileptiform and epileptiform abnormalities seen during visual analysis which are seen more frequently during sleep, and over temporal areas.

It is well known that interictal abnormalities are seen more frequently during sleep in patients with epilepsy, in particular those with temporal lobe epilepsy - TLE (Elwes, 2012; Didato *et al.*, 2015; Ergene *et al.*, 2000; Krishnan *et al.*, 2018b). In medial temporal lobe epilepsy, interictal abnormalities include irregular focal temporal theta and delta activities (non-epileptiform - NEAs) and focal sharp waves and spikes maximal over anterior-temporal and mid-temporal regions (epileptiform discharges - IEDs) (Krishnan *et al.*, 2018b; Elwes, 2012) NEAs and IEDs in TLE can be unilateral, or bitemporal - most commonly independently over left and right hemispheres. Independent bitemporal IEDs tend to occur more during non-REM (NREM) sleep. Prevalence is more frequent than previously thought, presumably due to the now widespread use of long-term EEG monitoring recorded over one or more nights (Ergene *et al.*, 2000; Malow *et al.*, 1999). In most cases of independent bitemporal IEDs in TLE, the seizure onset zone includes the hippocampus (Di Vito *et al.*, 2016) and amnesia associated with seizures and the post-ictal period is common (Schulz *et al.*, 1995).

It is also well known that disturbances in sleep affect the retention of memory (Walker, 2017; Peigneux and Smith, 2010; Rasch and Born, 2013). Recent theories and research

support the importance of slow-wave sleep in the consolidation of memories, suggesting that the slow waves generated in slow-wave sleep prompt repeated activation of recently encoded memory representations within the hippocampus. This process is linked with the production of hippocampal gamma frequency ripples and thalamocortical sleep spindles which promote neural plasticity within the neocortex. Less evidenced, is the theory that synaptic consolidation, to stabilise these changes, occurs within the subsequent REM periods (Figure 40) (Cross *et al.*, 2018; Rasch and Born, 2013).

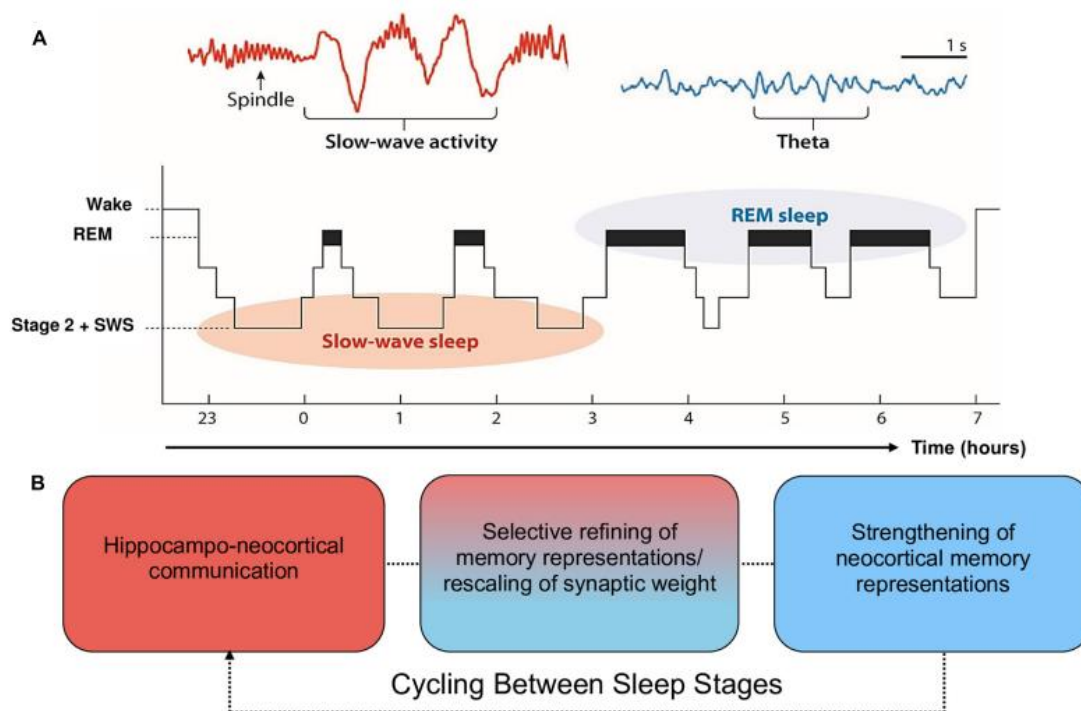


Figure 40: Schematic of sleep architecture in humans and associated oscillatory activity and stages of memory consolidation. (A) Sleep stages N2 and SWS are most prominent during the first half of the sleep period and are dominated by thalamic sleep spindles and neocortical slow oscillations (SOs). REM sleep is most prominent during the second half of the sleep period and characterised by ponto-geniculo-occipital waves, increased acetylcholine (ACh) and cortical theta oscillations (reproduced from Vorster and Born, 2015; permission to reuse image is not required from the copyright holder for non-commercial use as determined by RightsLink R). (B) The cyclic occurrence of SWS and REM throughout sleep facilitates memory consolidation. The hierarchical nesting of ripples and spindles within the up state of SOs during SWS facilitates the transfer of information from the hippocampal complex to the neocortex. The neocortically distributed memory representations are strengthened by REM theta oscillations and increases in ACh (Cross *et al.*, 2018).

There is some evidence in support of IED-disrupted memory maintenance and recall (Kleen *et al.*, 2013; Henin *et al.*, 2021), but this is not conclusive (Latreille *et al.*, 2022).

Disturbances in memory consolidation during sleep via the occurrence of frequent IEDs involving the hippocampus, and thus competing with and disrupting hippocampal spindles

during reactivation and consolidation, is a possible explanation for the occurrence of accelerated long-term forgetting in TEA. The combination of theta network dysfunctions and increased interictal EEG abnormalities (NEAs and IEDs) during sleep, evidenced in this research, provide evidence for possible underlying causes of disruption in memory consolidation and retrieval of complex memories in TEA, resulting in accelerated long-term forgetting and autobiographical amnesia.

Implications

The results of the study provide clear evidence of network and connectivity alterations beyond those seen as part of a normal ageing process.

Our surface EEG findings show consistency with other TLE and TEA research regarding the distribution and occurrence of interictal abnormalities (Krishnan *et al.*, 2018b; Elwes, 2012; Butler *et al.*, 2007a; Mosbah *et al.*, 2014; Baker *et al.*, 2021), providing additional support that TEA is a mesial temporal lobe epilepsy sub-type.

Concerning connectivity findings within the study, i.e., widespread derangement of theta band networks inter-regionally, and reduced functional connectivity strength of alpha and beta frequencies, the results provide the first EEG-based connectivity evidence within current literature for the syndrome of TEA. The functional connectivity findings within this study build on existing EEG evidence collated from scalp EEG, long-term EEG monitoring, high-density EEG and quantitative EEG regarding TEA (Hodges and Warlow, 1990; Kapur, 1993b; Zeman *et al.*, 1998a; Manes *et al.*, 2005a; Butler *et al.*, 2007a; Zeman and Butler, 2010; Lapenta *et al.*, 2014; Mosbah *et al.*, 2014; Del Felice *et al.*, 2014; Burkholder *et al.*, 2017; Lanzone *et al.*, 2018; Ramanan *et al.*, 2019; Lanzone *et al.*, 2020; Baker *et al.*, 2021; Blain *et al.*, 2021; Pukropski *et al.*, 2022; Sancetta *et al.*, 2022) to strengthen understanding the role of EEG in TEA.

Other than EEG, other neuroimaging techniques have been employed including positron emission tomography (PET) and fMRI (Milton *et al.*, 2012; Mosbah *et al.*, 2014), with fMRI studies providing some limited information regarding functional connectivity (Milton *et al.*, 2012). Our rsEEG connectivity study adds a further dimension to this evidence, contributing

to a clearer understanding of network dynamics in TEA, directionality alterations within inter-region network alterations and the activities affected within them.

Limitations

Every consideration was made within the methods to minimise variation between the two research cohorts to reduce type I and type II errors within the study. However, it should be noted that all statistical analysis carries a risk of over-interpretation (Type I error) or under-interpretation (type II error) of significance (Figure 41). Additionally, EEG by nature contains considerable variation over time and with the level of alertness, even within the same participant. This may introduce further risk of occurrence of errors within the study results. Again, the methods used sought to reduce the risk of type I and II errors by standardisation wherever possible.





	Null Hypothesis is TRUE	Null Hypothesis is FALSE
Reject null hypothesis	 Type I Error (False positive)	 Correct Outcome! (True positive)
Fail to reject null hypothesis	 Correct Outcome! (True negative)	 Type II Error (False negative)

Figure 41: Graphic description of type I and type II statistical errors

Although this study has revealed some robust findings, there are several limitations which restrict their scope.

As TEA is a fairly rare syndrome and EEGs needed to be obtained from a variety of clinical Neurophysiology departments, the sample size was limited to 28 patients. This is likely to affect the impact of the results, as a larger sample size would inevitably provide more robust findings.

Whilst the use of a variety of metrics significantly assisted in focussing on the common areas of significance, a second effective connectivity measure may have provided a more robust results comparison. For example, the additional use of a Grainger Causality measure would

provide an effective connectivity measure within the time domain. All methods used were bivariate (assessing the connectivity between two sources). The use of a multivariate measure in addition may have given more robust and refined results.

We analysed resting state EEG which provides the advantage of being independent of any task specificity, thus allowing more general assumptions (Perinelli *et al.*, 2022; Cabral *et al.*, 2014). However, rsEEG has the drawback of not specifically assessing connectivity in relation to memory, and of potentially producing more variation across studies, as the participant's mind is free to wander. Due to the selection of rsEEG, the study results cannot confirm the effect of specific memory tasks on global and inter-regional connectivity.

We used retrospective EEG data from several Neurophysiology departments around the UK. Inevitably this increases the risk of variation within the data with regard to environment, equipment used, sampling rate, filter settings, reference placement, electrical interference, physiological noise and recording standards. There are several mitigations for these variations, including the general use of the International 10-20 system for electrode placement, national guidance of 256Hz sampling rate and reduction of skin impedance to below 5K Ω . Further mitigations were employed within pre-processing by rejecting affected sections during visual inspection, rejection at the ICA analysis stage of pre-processing, standardising sampling rate at 256Hz and standardisation to an average reference.

The TEA data files included significant variation in record length when compared to HV data, where EEGs were all 20 minutes in duration. TEA EEGs often included activation techniques i.e. hyperventilation and photic stimulation. Longer TEA files were more prone to movement, muscle artefacts, and epileptiform activities and more likely to include periods of drowsiness and sleep, as well as periods of restful eye opening and eye closure. The effects of these differences were minimised by the removal of sections of non-resting EEG, drowsiness, sleep and epileptiform abnormalities. The increased variation in file length within the TEA cohort compared to the HV cohort was difficult to avoid and therefore may have impacted the results gained, in the form of type II errors.

The use of average reference rather than the now recommended REST may have introduced some spurious results compared to the use of what is recognised as more robust referencing.

EEGs recorded for clinical purposes are, by nature, limited in the number of electrodes applied. In our study, EEGs required 21 electrodes, which included inferior temporal electrodes at A1 and A2. This clearly creates some limits regarding the regional preciseness of connectivity metrics, limiting the study to the regions of frontal, temporal, parietal, and occipital. High-density EEG would provide more detailed results but is currently only used in research environments, however, its use may have enabled a more in-depth investigation of the temporal lobe structures. The methodological choices were constrained by time as the use of high-density EEG would require the collection of prospective data.

Whilst we were able to match healthy volunteers by age and sex, we did not match for educational level, this was due to time constraints on the study and the availability of suitable education-matched healthy volunteers. As patients with TEA tend to have a slightly higher IQ than average, this could cause connectivity effects in the temporal-frontal and frontal-parietal regions. However, previous study findings are inconclusive regarding IQ or educational level effects, as both increase or decrease in connectivity strength have been reported (Arenaza-Urquijo *et al.*, 2013; Chen *et al.*, 2018b).

Due to IT issues with remote connection to the TIME project patient files, we have been unable to properly explore the possible effects of medication or co-existing conditions on our study results. Anti-epileptic drugs (AEDs) acting on sodium channel function as a blocker are particularly effective in TLE/TEA. These include CBZ, lamotrigine and phenytoin. Inevitably these affect brain networks and connectivity. A review of AED effects on the EEG demonstrates that these AEDs generally cause an increase in background theta and delta activities, although lamotrigine is more likely to give a reduction in activity within all frequency bands (Höller *et al.*, 2018). This may have created some bias in the results, particularly of mPSD but could also have implications regarding connectivity strengths. However, if present, changes are likely to have affected global connectivity values rather than more specific regional or inter-regional results.

As discussed previously, non-invasive scalp-EEG recordings are recordable due to the phenomenon of volume conduction, which transmits electrical brain activity through the skull and scalp and enables detection at the scalp level. Volume conduction creates difficulties with source detection in EEG connectivity studies (Jia, 2019). This means that

some connectivity metrics are more suitable for use with scalp EEG than others. We mitigated this by using connectivity measures which are known to be robust to the effects of volume conduction, and by using a spectrum of connectivity metrics to enable correlation of findings within the study (Moezzi *et al.*, 2019).

Due to time limitations, we were unfortunately unable to explore ictal findings within TEA, which was one of our secondary objectives.

Recommendations for Future Research

Reinforced the need for sleep and longer-term EEG recordings to be incorporated into diagnostic work-up.

This current research provides a robust base for connectivity differences between TEA and healthy volunteers. Further study comparing TEA with lesional and non-lesional TLE, and mild neurodegenerative conditions such as MCI/aMCI could provide further delineation of network modifications between neurological conditions.

Further research is needed to explore our research findings in more depth, and perhaps to establish the effects of memory-based specific tasks on the altered connectivity found within TEA. Certainly, future TEA studies in this area would benefit from considering the academic level/IQ of participants, along with co-existing conditions within the TEA cohort and medications at the time of the EEG.

Multimodal studies including high-density EEG combined with fMRI are likely to give a more detailed understanding by providing structural network data, alongside more detailed functional connectivity to allow more accurate source localisation. Including the analysis of different resting states i.e., both wake and NREM and REM sleep states would provide a more holistic approach to research of conditions affecting memory.

Effective connectivity measures within this study have provided valuable insight into the directional dynamics of information flow within inter-regional networks. Other avenues to explore include the use of machine learning and deep learning methods, which may aid the differentiation of TEA from other cognitive/epileptic conditions and promote earlier diagnosis of the condition.

Conclusion

The current research aimed to provide further knowledge of the underlying causes of transient epileptic amnesia, a medial temporal lobe epilepsy syndrome, and the often-persisting memory difficulties associated with the condition. To date, no research has utilised EEG media to explore potential alterations in functional and effective connectivity within TEA.

Resting-state EEG recordings were acquired from the medical records of 28 patients diagnosed with TEA and compared to age and sex-matched healthy controls. All TEA recordings were visually analysed before pre-processing to record abnormality types seen, their location and their prevalence i.e., in wake or sleep. Noisy and unsuitable data (e.g., sections of drowsiness and sleep, as the data we are using is restful waking EEG) were discarded, and all EEGs were pre-processed using a standardised MATLAB script before analysing with EEGLAB and Brainstorm. Mean frequency and mean power were calculated for the two groups across a 1Hz-40Hz frequency range and grouped into EEG bands (beta, alpha, theta, and delta). Global, regional, and inter-regional functional connectivity was obtained using imaginary coherence and weighted phase lag index, whilst phase transfer entropy assessed effective connectivity.

The results showed no significant difference concerning mean frequency, but regional slow wave alterations in mean power were seen, which were localised to temporal areas. There were functional connectivity differences predominantly between frontal and temporal, frontal and parietal, and temporal and parietal regions within beta, alpha and theta bands. Effective connectivity showed significant changes within the same frequency bands, with widespread derangement of network directionality additionally seen inter-regionally for theta frequencies. Further to this, and in line with previous literature evidence, inter-ictal abnormalities were predominantly seen in an independent bilateral pattern and were more prevalent during non-REM sleep.

This research has provided new evidence regarding functional and effective connectivity disturbances in TEA, shedding further light on the possible underlying causes for persisting memory dysfunction in the form of accelerated long-term forgetting and autobiographical amnesia. We have demonstrated clear and consistent disruptions of connectivity, both

within memory networks of the temporal lobes, and further afield within cortical connectivity. The evidence supports the hypothesis of dysfunctional memory consolidation and recall networks within TEA.

The high incidence of independent bilateral inter-ictal EEG abnormalities during NREM sleep may also contribute to the increased prevalence of ineffective memory consolidation within TEA, in the form of accelerated long-term forgetting.

References

- Abubaker, M., Al Qasem, W. and Kvašňák, E. (2021) 'Working Memory and Cross-Frequency Coupling of Neuronal Oscillations.' *Front Psychol*, 12, p. 756661.
- Acharya, J. N., Hani, A. J., Cheek, J., Thirumala, P. and Tsuchida, T. N. (2016) 'American clinical neurophysiology society guideline 2: guidelines for standard electrode position nomenclature.' *The Neurodiagnostic Journal*, 56(4), pp. 245-252.
- Addis, D. R., Moscovitch, M. and McAndrews, M. P. (2007) 'Consequences of hippocampal damage across the autobiographical memory network in left temporal lobe epilepsy.' *Brain*, 130(Pt 9), pp. 2327-2342.
- Adebimpe, A., Aarabi, A., Bourel-Ponchel, E., Mahmoudzadeh, M. and Wallois, F. (2015) 'Functional brain dysfunction in patients with benign childhood epilepsy as revealed by graph theory.' *PLoS One*, 10(10), p. e0139228.
- Adrian, E. D. and Matthews, B. H. C. (1934) 'The Berger Rhythm: Potential changes from the occipital lobes in man.' *Brain*, 57(4), pp. 355-385.
- Alù, F., Orticoni, A., Judica, E., Cotelli, M., Rossini, P. M., Miraglia, F. and Vecchio, F. (2021) 'Entropy modulation of electroencephalographic signals in physiological aging.' *Mechanisms of Ageing and Development*, 196, p. 111472.
- Alzheimer's Society. (2015) Helping you to assess cognition: A practical toolkit for clinicians. https://www.alzheimers.org.uk/sites/default/files/migrate/downloads/alzheimers_society_cognitive_assessment_toolkit.pdf: Alzheimer's Society.
- Amin, H. U. and Malik, A. (2014) 'Memory Retention and Recall Process.' *In* pp. 219-237.
- Amzica, F. and Lopes da Silva, F. H. (2017a) 'Chapter 2: Cellular Substrates of Brain Rhythms.' *In* Schomer, D. L. and Lopes da Silva, F. H. (eds.) *Niedermeyer's Electroencephalography: Basic Principles, Clinical Applications, and Related Fields*. Seventh ed., New York: Oxford University Press, pp. 20-62.
- Amzica, F. and Lopes da Silva, F. H. (2017b) 'Chapter 2: Cellular Substrates of Brain Rhythms.' *In* Schomer, D. L., Lopes da Silva, F. H., Schomer, D. L. and Lopes da Silva, F. H. (eds.) *Niedermeyer's Electroencephalography: Basic Principles, Clinical Applications, and Related Fields*. Oxford University Press, p. 0.
- Amzica, F. and Lopes da Silva, F. H. (2018) 'Chapter 2: Cellular Substrates of Brain Rhythms.' *In* Schomer, D. L. and Lopes da Silva, F. H. (eds.) *Niedermeyer's Electroencephalography: Basic Principles, Clinical Applications, and Related Fields*. Oxford University Press,
- Arenaza-Urquijo, E. M., Landeau, B., La Joie, R., Mevel, K., Mézenge, F., Perrotin, A., Desgranges, B., Bartrés-Faz, D., Eustache, F. and Chételat, G. (2013) 'Relationships between years of education and gray matter volume, metabolism and functional connectivity in healthy elders.' *NeuroImage*, 83, pp. 450-457.
- Arnolds, D. E., Lopes da Silva, F. H., Aitink, J. W., Kamp, A. and Boeijinga, P. (1980) 'The spectral properties of hippocampal EEG related to behaviour in man.' *Electroencephalogr Clin Neurophysiol*, 50(3-4), pp. 324-328.
- Asadi-Pooya, A. A. (2014) 'Transient epileptic amnesia: a concise review.' *Epilepsy Behav*, 31, pp. 243-245.
- Audrain, S. and McAndrews, M. P. (2019) 'Cognitive and functional correlates of accelerated long-term forgetting in temporal lobe epilepsy.' *Cortex*, 110, pp. 101-114.
- Babaeeghazvini, P., Rueda-Delgado, L. M., Gooijers, J., Swinnen, S. P. and Daffertshofer, A. (2021) 'Brain Structural and Functional Connectivity: A Review of Combined Works of Diffusion Magnetic Resonance Imaging and Electro-Encephalography.' *Front Hum Neurosci*, 15, p. 721206.
- Babiloni, C., Del Percio, C. and Bujan, A. (2018) 'Chapter 16: EEG in Dementing Disorders.' *In* Schomer, D. L. and Lopes da Silva, F. H. (eds.) *Niedermeyer's Electroencephalography*. Seventh ed., New York: Oxford University Press, pp. 266-316.

- Babiloni, C., Lizio, R., Marzano, N., Capotosto, P., Soricelli, A., Triggiani, A. I., Cordone, S., Gesualdo, L. and Del Percio, C. (2016) 'Brain neural synchronization and functional coupling in Alzheimer's disease as revealed by resting state EEG rhythms.' *Int J Psychophysiol*, 103, pp. 88-102.
- Babiloni, C., Barry, R. J., Başar, E., Blinowska, K. J., Cichocki, A., Drinkenburg, W., Klimesch, W., Knight, R. T., Lopes da Silva, F., Nunez, P., Oostenveld, R., Jeong, J., Pascual-Marqui, R., Valdes-Sosa, P. and Hallett, M. (2020) 'International Federation of Clinical Neurophysiology (IFCN) - EEG research workgroup: Recommendations on frequency and topographic analysis of resting state EEG rhythms. Part 1: Applications in clinical research studies.' *Clin Neurophysiol*, 131(1), pp. 285-307.
- Babiloni, C., Ferri, R., Binetti, G., Vecchio, F., Frisoni, G. B., Lanuzza, B., Miniussi, C., Nobili, F., Rodriguez, G., Rundo, F., Cassarino, A., Infarinato, F., Cassetta, E., Salinari, S., Eusebi, F. and Rossini, P. M. (2009) 'Directionality of EEG synchronization in Alzheimer's disease subjects.' *Neurobiology of Aging*, 30(1), pp. 93-102.
- Babiloni, C., Binetti, G., Cassarino, A., Dal Forno, G., Del Percio, C., Ferreri, F., Ferri, R., Frisoni, G., Galderisi, S., Hirata, K., Lanuzza, B., Miniussi, C., Mucci, A., Nobili, F., Rodriguez, G., Luca Romani, G. and Rossini, P. M. (2006a) 'Sources of cortical rhythms in adults during physiological aging: a multicentric EEG study.' *Hum Brain Mapp*, 27(2), pp. 162-172.
- Babiloni, C., Binetti, G., Cassetta, E., Forno, G. D., Percio, C. D., Ferreri, F., Ferri, R., Frisoni, G., Hirata, K., Lanuzza, B., Miniussi, C., Moretti, D. V., Nobili, F., Rodriguez, G., Romani, G. L., Salinari, S. and Rossini, P. M. (2006b) 'Sources of cortical rhythms change as a function of cognitive impairment in pathological aging: a multicenter study.' *Clinical Neurophysiology*, 117(2), pp. 252-268.
- Babiloni, C., Ferri, R., Noce, G., Lizio, R., Lopez, S., Lorenzo, I., Tucci, F., Soricelli, A., Nobili, F., Arnaldi, D., Famà, F., Orzi, F., Buttinelli, C., Giubilei, F., Cipollini, V., Marizzoni, M., Güntekin, B., Aktürk, T., Hanoğlu, L., Yener, G., Özbek, Y., Stocchi, F., Vacca, L., Frisoni, G. B. and Del Percio, C. (2021a) 'Resting State Alpha Electroencephalographic Rhythms Are Differently Related to Aging in Cognitively Unimpaired Seniors and Patients with Alzheimer's Disease and Amnesic Mild Cognitive Impairment.' *Journal of Alzheimer's Disease*, 82(3), pp. 1085-1114.
- Babiloni, C., Arakaki, X., Azami, H., Bennys, K., Blinowska, K., Bonanni, L., Bujan, A., Carrillo, M. C., Cichocki, A., Frutos-Lucas, J., Del Percio, C., Dubois, B., Edelmayer, R., Egan, G., Epelbaum, S., Escudero, J., Evans, A., Farina, F., Fargo, K., Fernández, A., Ferri, R., Frisoni, G., Hampel, H., Harrington, M. G., Jelic, V., Jeong, J., Jiang, Y., Kaminski, M., Kavcic, V., Kilborn, K., Kumar, S., Lam, A., Lim, L., Lizio, R., Lopez, D., Lopez, S., Lucey, B., Maestú, F., McGeown, W. J., McKeith, I., Moretti, D. V., Nobili, F., Noce, G., Olichney, J., Onofrij, M., Osorio, R., Parra-Rodriguez, M., Rajji, T., Ritter, P., Soricelli, A., Stocchi, F., Tarnanas, I., Taylor, J. P., Teipel, S., Tucci, F., Valdes-Sosa, M., Valdes-Sosa, P., Weiergräber, M., Yener, G. and Güntekin, B. (2021b) 'Measures of resting state EEG rhythms for clinical trials in Alzheimer's disease: Recommendations of an expert panel.' *Alzheimer's & Dementia*, 17(9), pp. 1528-1553.
- Baker, J., Savage, S., Milton, F., Butler, C., Kapur, N., Hodges, J. and Zeman, A. (2021) 'The syndrome of transient epileptic amnesia: a combined series of 115 cases and literature review.' *Brain Communications*, 3(2),
- Barry, T. J., Chiu, C. P. Y., Raes, F., Ricarte, J. and Lau, H. (2018) 'The Neurobiology of Reduced Autobiographical Memory Specificity.' *Trends in Cognitive Sciences*, 22(11), pp. 1038-1049.
- Bassett, D. S. and Bullmore, E. T. (2009) 'Human brain networks in health and disease.' *Current Opinion in Neurology*, 22(4), pp. 340-347.
- Bassett, D. S. and Sporns, O. (2017) 'Network neuroscience.' *Nat Neurosci*, 20(3), pp. 353-364.
- Bell, B., Lin, J. J., Seidenberg, M. and Hermann, B. (2011) 'The neurobiology of cognitive disorders in temporal lobe epilepsy.' *Nature Reviews Neurology*, 7(3), pp. 154-164.
- Beniczky, S. and Schomer, D. L. (2020) 'Electroencephalography: basic biophysical and technological aspects important for clinical applications.' *Epileptic Disorders*, 22(6), pp. 697-715.
- Benjamini, Y. and Hochberg, Y. (1995) 'Controlling the False Discovery Rate: A Practical and Powerful Approach to Multiple Testing.' *Journal of the Royal Statistical Society.*, 57(Series B (Methodological)), pp. 289-300.

- Benjamini, Y. and Hochberg, Y. (2000) 'On the Adaptive Control of the False Discovery Rate in Multiple Testing with Independent Statistics.' *Journal of Educational and Behavioral Statistics*, 25(1), p. 60.
- Benjamini, Y., Krieger, A. M. and Yekutieli, D. (2006) 'Adaptive linear step-up procedures that control the false discovery rate.' *Biometrika*, 93(3), pp. 491-507.
- Betzel, R. F. and Bassett, D. S. (2017) 'Multi-scale brain networks.' *Neuroimage*, 160, pp. 73-83.
- Blain, A., Sellal, F., Philippi, N., Blanc, F. and Cretin, B. (2021) 'Transient epileptic amnesia is significantly associated with discrete CA1-located hippocampal calcifications but not with atrophic changes on brain imaging.' *Epilepsy Research*, 176, p. 106736.
- Blinowska, K. J., Rakowski, F., Kaminski, M., De Vico Fallani, F., Del Percio, C., Lizio, R. and Babiloni, C. (2017) 'Functional and effective brain connectivity for discrimination between Alzheimer's patients and healthy individuals: A study on resting state EEG rhythms.' *Clin Neurophysiol*, 128(4), pp. 667-680.
- Bondi, M. W., Edmonds, E. C. and Salmon, D. P. (2017) 'Alzheimer's Disease: Past, Present, and Future.' *J Int Neuropsychol Soc*, 23(9-10), pp. 818-831.
- Bourel-Ponchel, E., Mahmoudzadeh, M., Adebimpe, A. and Wallois, F. (2019) 'Functional and Structural Network Disorganizations in Typical Epilepsy With Centro-Temporal Spikes and Impact on Cognitive Neurodevelopment.' *Front Neurol*, 10, p. 809.
- Brienza, M. and Mecarelli, O. (2019) 'Chapter 2: Neurophysiological Basis of EEG.' In Mecarelli, O. (ed.) *Clinical Electroencephalography*. Switzerland: Springer Nature Switzerland AG, pp. 9-21.
- Brienza, M., Davassi, C. and Mecarelli, O. (2019) 'Chapter 8: Artifacts.' In Mecarelli, O. (ed.) *Clinical Electroencephalography*. Switzerland: Springer Nature Switzerland AG, pp. 109-130.
- Brookes, M. J., O'Neill, G. C., Hall, E. L., Woolrich, M. W., Baker, A., Palazzo Corner, S., Robson, S. E., Morris, P. G. and Barnes, G. R. (2014) 'Measuring temporal, spectral and spatial changes in electrophysiological brain network connectivity.' *NeuroImage*, 91, pp. 282-299.
- Bullmore, E. and Sporns, O. (2009) 'Complex brain networks: graph theoretical analysis of structural and functional systems.' *Nature reviews neuroscience*, 10(3), p. 186.
- Burkholder, D. B., Jones, A. L., Jones, D. T., Fabris, R. R., Britton, J. W., Lagerlund, T. D., So, E. L., Cascino, G. D., Worrell, G. A., Shin, C. and St Louis, E. K. (2017) 'Frequent sleep-related bitemporal focal seizures in transient epileptic amnesia syndrome: Evidence from ictal video-EEG.' *Epilepsia Open*, 2(2), pp. 255-259.
- Burman, R. J. and Parrish, R. R. (2018) 'The Widespread Network Effects of Focal Epilepsy.' *The Journal of Neuroscience*, 38(38), pp. 8107-8109.
- Butler, C., Kapur, N., Zeman, A., Weller, R. and Connelly, A. (2012) 'Epilepsy-related long-term amnesia: anatomical perspectives.' *Neuropsychologia*, 50(13), pp. 2973-2980.
- Butler, C., van Erp, W., Bhaduri, A., Hammers, A., Heckemann, R. and Zeman, A. (2013) 'Magnetic resonance volumetry reveals focal brain atrophy in transient epileptic amnesia.' *Epilepsy Behav*, 28(3), pp. 363-369.
- Butler, C. R. and Zeman, A. Z. (2008) 'Recent insights into the impairment of memory in epilepsy: transient epileptic amnesia, accelerated long-term forgetting and remote memory impairment.' *Brain*, 131(Pt 9), pp. 2243-2263.
- Butler, C. R. and Zeman, A. (2011) 'The causes and consequences of transient epileptic amnesia.' *Behav Neurol*, 24(4), pp. 299-305.
- Butler, C. R., Graham, K. S., Hodges, J. R., Kapur, N., Wardlaw, J. M. and Zeman, A. Z. (2007a) 'The syndrome of transient epileptic amnesia.' *Ann Neurol*, 61(6), pp. 587-598.
- Butler, C. R., Graham, K. S., Hodges, J. R., Kapur, N., Wardlaw, J. M. and Zeman, A. Z. J. (2007b) 'The syndrome of transient epileptic amnesia.' *Annals of Neurology*, 61(6), pp. 587-598.
- Buzsáki, G., Traub, R. D. and Pedley, A. P. (2003) 'The cellular basis of EEG activity.' In Ebersole, J. S. and Pedley, T. A. (eds.) *Current practice of Clinical Electroencephalography*. 3rd Edition ed., Philadelphia, USA: Lippincott Williams and Wilkins,
- Buzsáki, G. (2002) 'Theta Oscillations in the Hippocampus.' *Neuron*, 33(3), pp. 325-340.

- Cabral, J., Kringelbach, M. L. and Deco, G. (2014) 'Exploring the network dynamics underlying brain activity during rest.' *Prog Neurobiol*, 114, pp. 102-131.
- Cano-López, I., Lozano-García, A., Catalán-Aguilar, J., Hampel, K. G., Villanueva, V. and González-Bono, E. (2022) 'The relationship between memory and quality of life is mediated by trait anxiety in patients with temporal lobe epilepsy.' *Quality of Life Research*,
- Cao, J., Zhao, Y., Shan, X., Wei, H. L., Guo, Y., Chen, L., Erkoyuncu, J. A. and Sarrigiannis, P. G. (2022) 'Brain functional and effective connectivity based on electroencephalography recordings: A review.' *Human Brain Mapping*, 43(2), pp. 860-879.
- Chakravarty, K., Ray, S., Kharbanda, P. S., Lal, V. and Baishya, J. (2021) 'Temporal lobe epilepsy with amygdala enlargement: A systematic review.' *Acta Neurol Scand*, 144(3), pp. 236-250.
- Chauvière, L. (2020) 'Update on temporal lobe-dependent information processing, in health and disease.' *European Journal of Neuroscience*, 51(11), pp. 2159-2204.
- Chen, Y.-y., Huang, S., Wu, W.-y., Liu, C.-r., Yang, X.-y., Zhao, H.-t., Wu, L.-c., Tan, L.-z., Long, L.-l. and Xiao, B. (2018a) 'Associated and predictive factors of quality of life in patients with temporal lobe epilepsy.' *Epilepsy & Behavior*, 86, pp. 85-90.
- Chen, Y., Qi, D., Qin, T., Chen, K., Ai, M., Li, X., Li, H., Zhang, J., Mao, H., Yang, Y. and Zhang, Z. (2018b) 'Brain Network Connectivity Mediates Education-related Cognitive Performance in Healthy Elderly Adults.' *Current Alzheimer Research*, 16(1), pp. 19-28.
- Chiba, T., Henmi, N., Neshige, S., Takada, K., Ikeda, A., Takahashi, R. and Yokoe, M. (2020) '[Ictal EEG pattern of transient epileptic amnesia in acute phase of non-herpetic limbic encephalitis].' *Rinsho shinkeigaku = Clinical neurology*, 60(6), pp. 446-451.
- Chu, C. J. (2015) 'High density EEG—What do we have to lose?' *Clinical Neurophysiology*, 126(3), pp. 433-434.
- Cohen, M. X. (2014) *Analyzing neural time series data: theory and practice*. MIT press.
- Cohen, M. X. (2015) 'Effects of time lag and frequency matching on phase-based connectivity.' *Journal of Neuroscience Methods*, 250, pp. 137-146.
- Colgin, L. L. (2015) 'Theta–gamma coupling in the entorhinal–hippocampal system.' *Current Opinion in Neurobiology*, 31, pp. 45-50.
- Collura, T. F. (1993) 'History and Evolution of Electroencephalographic Instruments and Techniques.' *Journal of Clinical Neurophysiology*, 10(4),
- Corcoran, A. W., Alday, P. M., Schlesewsky, M. and Bornkessel-Schlesewsky, I. (2018) 'Toward a reliable, automated method of individual alpha frequency (IAF) quantification.' *Psychophysiology*, 55(7), p. e13064.
- Cretin, B., Bilger, M., Philippi, N. and Blanc, F. (2020) 'CASPR2 antibody encephalitis presenting as transient epileptic amnesia.' *Seizure*, 81, pp. 175-177.
- Creutzfeldt, O. D., Watanabe, S. and Lux, H. D. (1966) 'Relations between EEG phenomena and potentials of single cortical cells. II. Spontaneous and convulsoid activity.' *Electroencephalogr Clin Neurophysiol*, 20(1), pp. 19-37.
- Cross, Z. R., Kohler, M. J., Schlesewsky, M., Gaskell, M. G. and Bornkessel-Schlesewsky, I. (2018) 'Sleep-Dependent Memory Consolidation and Incremental Sentence Comprehension: Computational Dependencies during Language Learning as Revealed by Neuronal Oscillations.' *Frontiers in Human Neuroscience*, 12,
- Crouch, B., Sommerlade, L., Veselcic, P., Riedel, G., Schelter, B. and Platt, B. (2018) 'Detection of time-, frequency- and direction-resolved communication within brain networks.' *Scientific Reports*, 8(1),
- Dasheiff, R. M. (1997) 'Pure transient amnesia during nonconvulsive status epilepticus.' *Neurology*, 48(6), pp. 1736-1737.
- Davis, S. W., Dennis, N. A., Daselaar, S. M., Fleck, M. S. and Cabeza, R. (2007) 'Qué PASA? The Posterior–Anterior Shift in Aging.' *Cerebral Cortex*, 18(5), pp. 1201-1209.
- De Gennaro, L. and Ferrara, M. (2003) 'Sleep spindles: an overview.' *Sleep Medicine Reviews*, 7(5), pp. 423-440.

- Del Felice, A., Broggio, E., Valbusa, V., Gambina, G., Arcaro, C. and Manganotti, P. (2014) 'Transient epileptic amnesia mistaken for mild cognitive impairment? A high-density EEG study.' *Epilepsy Behav*, 36, pp. 41-46.
- Delorme, A. (2019) *EEG Preprocessing in EEGLAB*.
https://sccn.ucsd.edu/github/wiki/files/eeGLAB2019_aspet_artifact_and_ica.pdf: SCCN (Swartz Centre for Computational Neuroscience). [Online] [Accessed
- Delorme, A. (Accessed 2022) *Infomax Independent Component Analysis for dummies*.
https://arnauddelorme.com/ica_for_dummies/: Arnaud Delorme. [Online] [Accessed
- Delorme, A. and Makeig, S. (2004) 'EEGLAB: an open source toolbox for analysis of single-trial EEG dynamics including independent component analysis.' *Journal of Neuroscience Methods*, 134(1), pp. 9-21.
- Dementia UK. (2022) *Medication for people living with dementia*.
<https://www.dementiauk.org/information-and-support/health-advice/medication-for-people-living-with-dementia/>: Dementia UK. [Online] [Accessed on 20/01/2024]
- Devinsky, O. (2004) 'Diagnosis and treatment of temporal lobe epilepsy.' *Rev Neurol Dis*, 1(1), pp. 2-9.
- Dewar, M., Hoefjeijzers, S., Zeman, A., Butler, C. and Della Sala, S. (2015) 'Impaired picture recognition in transient epileptic amnesia.' *Epilepsy Behav*, 42, pp. 107-116.
- Di Vito, L., Mauguière, F., Catenoix, H., Rheims, S., Bourdillon, P., Montavont, A. and Isnard, J. (2016) 'Epileptic networks in patients with bitemporal epilepsy: the role of SEEG for the selection of good surgical candidates.' *Epilepsy Research*, 128, pp. 73-82.
- Didato, G., Chiesa, V., Villani, F., Pelliccia, V., Deleo, F., Gozzo, F., Canevini, M. P., Mai, R., Spreafico, R., Cossu, M. and Tassi, L. (2015) 'Bitemporal epilepsy: A specific anatomo-electro-clinical phenotype in the temporal lobe epilepsy spectrum.' *Seizure*, 31, pp. 112-119.
- Diehl, B. and Duncan, J. (2015) *Temporal lobe epilepsy*.
https://epilepsysociety.org.uk/sites/default/files/2020-08/Chapter13Diehl2015_0.pdf: Epilepsy Society. [Online] [Accessed on 20/01/2024]
- Dierks, T., Ihl, R., Frölich, L. and Maurer, K. (1993) 'Dementia of the Alzheimer type: effects on the spontaneous EEG described by dipole sources.' *Psychiatry Research: Neuroimaging*, 50(3), pp. 151-162.
- Dierks, T., Jelic, V., Pascual-Marqui, R. D., Wahlund, L.-O., Julin, P., Linden, D. E., Maurer, K., Winblad, B. and Nordberg, A. (2000) 'Spatial pattern of cerebral glucose metabolism (PET) correlates with localization of intracerebral EEG-generators in Alzheimer's disease.' *Clinical Neurophysiology*, 111(10), pp. 1817-1824.
- Dinkelacker, V., Valabregue, R., Thivard, L., Lehericy, S., Baulac, M., Samson, S. and Dupont, S. (2015) 'Hippocampal-thalamic wiring in medial temporal lobe epilepsy: enhanced connectivity per hippocampal voxel.' *Epilepsia*, 56(8), pp. 1217-1226.
- Ekstrom, A. D., Caplan, J. B., Ho, E., Shattuck, K., Fried, I. and Kahana, M. J. (2005) 'Human hippocampal theta activity during virtual navigation.' *Hippocampus*, 15(7), pp. 881-889.
- Elwes, R. D. C. (2012) 'Chapter 26: Temporal Lobe Epilepsy.' In Alarcon, G. and Valentin, A. (eds.) *Introduction to Epilepsy*. Cambridge, UK: Cambridge University Press, pp. 168-173.
- Englot, D. J., Konrad, P. E. and Morgan, V. L. (2016) 'Regional and global connectivity disturbances in focal epilepsy, related neurocognitive sequelae, and potential mechanistic underpinnings.' *Epilepsia*, 57(10), pp. 1546-1557.
- Ergene, E., Shih, J. J., Blum, D. E. and So, N. K. (2000) 'Frequency of Bitemporal Independent Interictal Epileptiform Discharges in Temporal Lobe Epilepsy.' *Epilepsia*, 41(2), pp. 213-218.
- Escudero, J., Sanei, S., Jarchi, D., Abásolo, D. and Hornero, R. (2011) 'Regional coherence evaluation in mild cognitive impairment and Alzheimer's disease based on adaptively extracted magnetoencephalogram rhythms.' *Physiological measurement*, 32(8), p. 1163.
- Eyler, L. T., Sherzai, A., Kaup, A. R. and Jeste, D. V. (2011) 'A Review of Functional Brain Imaging Correlates of Successful Cognitive Aging.' *Biological Psychiatry*, 70(2), pp. 115-122.

- Eyler, L. T., Elman, J. A., Hatton, S. N., Gough, S., Mischel, A. K., Hagler, D. J., Franz, C. E., Docherty, A., Fennema-Notestine, C., Gillespie, N., Gustavson, D., Lyons, M. J., Neale, M. C., Panizzon, M. S., Dale, A. M. and Kremen, W. S. (2019) 'Resting State Abnormalities of the Default Mode Network in Mild Cognitive Impairment: A Systematic Review and Meta-Analysis.' *J Alzheimers Dis*, 70(1), pp. 107-120.
- Felician, O., Tramoni, E. and Bartolomei, F. (2015) 'Transient epileptic amnesia: Update on a slowly emerging epileptic syndrome.' *Rev Neurol (Paris)*, 171(3), pp. 289-297.
- Fernandez, L. M. J. and Lüthi, A. (2020) 'Sleep Spindles: Mechanisms and Functions.' *Physiological Reviews*, 100(2), pp. 805-868.
- Fischer, M. H. F., Zibrandtsen, I. C., Høgh, P. and Musaeus, C. S. (2023) 'Systematic Review of EEG Coherence in Alzheimer's Disease.' *J Alzheimers Dis*,
- Fisher, R. S., Boas, W. V. E., Blume, W., Elger, C., Genton, P., Lee, P. and Engel, J. (2005) 'Epileptic Seizures and Epilepsy: Definitions Proposed by the International League Against Epilepsy (ILAE) and the International Bureau for Epilepsy (IBE).' *Epilepsia*, 46(4), pp. 470-472.
- Fisher, R. S., Cross, J. H., French, J. A., Higurashi, N., Hirsch, E., Jansen, F. E., Lagae, L., Moshé, S. L., Peltola, J., Roulet Perez, E., Scheffer, I. E. and Zuberi, S. M. (2017) 'Operational classification of seizure types by the International League Against Epilepsy: Position Paper of the ILAE Commission for Classification and Terminology.' *Epilepsia*, 58(4), pp. 522-530.
- Fornito, A., Zalesky, A. and Bullmore, E. (2016) *Fundamentals of brain network analysis*. Academic Press.
- Franciotti, R., Moretti, D. V., Benussi, A., Ferri, L., Russo, M., Carrarini, C., Barbone, F., Arnaldi, D., Falasca, N. W., Koch, G., Cagnin, A., Nobili, F. M., Babiloni, C., Borroni, B., Padovani, A., Onofri, M. and Bonanni, L. (2022) 'Cortical network modularity changes along the course of frontotemporal and Alzheimer's dementing diseases.' *Neurobiology of Aging*, 110, pp. 37-46.
- Fritz, S. C. and Benbadis, S. R. (2009) 'Errors in EEG interpretation: the viewpoint of a technologist.' *Am J Electroneurodiagnostic Technol*, 49(3), pp. 289-294.
- Gallassi, R. (2006) 'Epileptic Amnesic Syndrome: An Update and Further Considerations.' *Epilepsia*, 47(s2), pp. 103-105.
- Gallassi, R., Morreale, A., Di Sarro, R. and Lugaresi, E. (1992) 'Epileptic amnesic syndrome.' *Epilepsia*, 33 Suppl 6, pp. S21-25.
- Galovic, M., Schmitz, B. and Tettgenborn, B. (2018) 'Chapter 15: EEG in Inflammatory Disorders, Cerebrovascular Diseases, Trauma, and Migraine.' In Schomer, D. L. and Lopes da Silva, F. H. (eds.) *Niedermeyer's Electroencephalography*. Seventh ed., New York: Oxford University Press, pp. 266-316.
- Gemein, L. A. W., Schirrmeyer, R. T., Chrabąszcz, P., Wilson, D., Boedecker, J., Schulze-Bonhage, A., Hutter, F. and Ball, T. (2020) 'Machine-learning-based diagnostics of EEG pathology.' *NeuroImage*, 220, p. 117021.
- Giustiniani, A., Danesin, L., Bozzetto, B., Macina, A., Benavides-Varela, S. and Burgio, F. (2023) 'Functional changes in brain oscillations in dementia: a review.' *Rev Neurosci*, 34(1), pp. 25-47.
- Goodman, M. S., Kumar, S., Zomorodi, R., Ghazala, Z., Cheam, A. S. M., Barr, M. S., Daskalakis, Z. J., Blumberger, D. M., Fischer, C., Flint, A., Mah, L., Herrmann, N., Bowie, C. R., Mulsant, B. H. and Rajji, T. K. (2018) 'Theta-Gamma Coupling and Working Memory in Alzheimer's Dementia and Mild Cognitive Impairment.' *Frontiers in Aging Neuroscience*, 10,
- Guderian, S. and Düzel, E. (2005) 'Induced theta oscillations mediate large-scale synchrony with mediotemporal areas during recollection in humans.' *Hippocampus*, 15(7), pp. 901-912.
- Haneef, Z., Lenartowicz, A., Yeh, H. J., Levin, H. S., Engel Jr, J. and Stern, J. M. (2014) 'Functional connectivity of hippocampal networks in temporal lobe epilepsy.' *Epilepsia*, 55(1), pp. 137-145.
- Hardmeier, M., Hatz, F., Bousleiman, H., Schindler, C., Stam, C. J. and Fuhr, P. (2014) 'Reproducibility of functional connectivity and graph measures based on the phase lag index (PLI) and weighted phase lag index (wPLI) derived from high resolution EEG.' *PLoS One*, 9(10), p. e108648.

- Hartman, A. L. and Lesser, R. P. (2018) 'Chapter 14: Brain Tumors and Other Space-Occupying Lesions.' In Schomer, D. L. and Lopes da Silva, F. H. (eds.) *Niedermeyer's Electroencephalography*. Seventh ed., New York: Oxford University Press, pp. 266-316.
- Hasselmo, M. E. and Stern, C. E. (2014) 'Theta rhythm and the encoding and retrieval of space and time.' *NeuroImage*, 85, pp. 656-666.
- He, B., Astolfi, L., Valdes-Sosa, P. A., Marinazzo, D., Palva, S. O., Benar, C.-G., Michel, C. M. and Koenig, T. (2019) 'Electrophysiological Brain Connectivity: Theory and Implementation.' *IEEE Transactions on Biomedical Engineering*, 66(7), pp. 2115-2137.
- Henin, S., Shankar, A., Borges, H., Flinker, A., Doyle, W., Friedman, D., Devinsky, O., Buzsáki, G. and Liu, A. (2021) 'Spatiotemporal dynamics between interictal epileptiform discharges and ripples during associative memory processing.' *Brain*, 144(5), pp. 1590-1602.
- Herrmann, C. S., Strüber, D., Helfrich, R. F. and Engel, A. K. (2016) 'EEG oscillations: From correlation to causality.' *International Journal of Psychophysiology*, 103, pp. 12-21.
- Herweg, N. A., Solomon, E. A. and Kahana, M. J. (2020) 'Theta Oscillations in Human Memory.' *Trends in Cognitive Sciences*, 24(3), pp. 208-227.
- Hodges, J. and Warlow, C. (1990) 'Syndromes of transient amnesia: towards a classification. A study of 153 cases.' *Journal of Neurology, Neurosurgery & Psychiatry*, 53(10), pp. 834-843.
- Hoefeijzers, S., Dewar, M., Della Sala, S., Zeman, A. and Butler, C. (2013) 'Accelerated long-term forgetting in transient epileptic amnesia: an acquisition or consolidation deficit?' *Neuropsychologia*, 51(8), pp. 1549-1555.
- Höller, Y., Helmstaedter, C. and Lehnertz, K. (2018) 'Quantitative Pharmacoelectroencephalography in Antiepileptic Drug Research.' *CNS Drugs*, 32(9), pp. 839-848.
- Hosseini, M.-P., Hosseini, A. and Ahi, K. (2021) 'A Review on Machine Learning for EEG Signal Processing in Bioengineering.' *IEEE Reviews in Biomedical Engineering*, 14, pp. 204-218.
- Hu, L. and Zhang, Z. (2019) *EEG signal processing and feature extraction*. Singapore: Springer Nature.
- Huang, C., Wahlund, L., Dierks, T., Julin, P., Winblad, B. and Jelic, V. (2000) 'Discrimination of Alzheimer's disease and mild cognitive impairment by equivalent EEG sources: a cross-sectional and longitudinal study.' *Clin Neurophysiol*, 111(11), pp. 1961-1967.
- Hughlings-Jackson, J. (1888) 'On a particular variety of epilepsy ("intellectual aura"), one case with symptoms of organic brain disease.' *Brain*, 11(2), pp. 179-207.
- ILAE. (Accessed 2019a) *The Growth of EEG*. https://www.ilae.org/files/dmfile/Epi_poster17-26_PRESS7_000.pdf: International League Against Epilepsy. [Online] [Accessed 20/01/2024]
- ILAE. (Accessed 2019b) *The Birth of EEG*. https://www.ilae.org/files/dmfile/Epi_poster17-26_PRESS6.pdf: International League Against Epilepsy. [Online] [Accessed 20/01/2024]
- Ishii, R., Canuet, L., Aoki, Y., Hata, M., Iwase, M., Ikeda, S., Nishida, K. and Ikeda, M. (2017) 'Healthy and Pathological Brain Aging: From the Perspective of Oscillations, Functional Connectivity, and Signal Complexity.' *Neuropsychobiology*, 75(4), pp. 151-161.
- Ives-Deliperi, V. and Butler, J. T. (2021) 'Mechanisms of cognitive impairment in temporal lobe epilepsy: A systematic review of resting-state functional connectivity studies.' *Epilepsy & Behavior*, 115, p. 107686.
- Jackson, A. F. and Bolger, D. J. (2014) 'The neurophysiological bases of EEG and EEG measurement: A review for the rest of us.' *Psychophysiology*, 51(11), pp. 1061-1071.
- Jacobs, J., Hwang, G., Curran, T. and Kahana, M. J. (2006) 'EEG oscillations and recognition memory: Theta correlates of memory retrieval and decision making.' *NeuroImage*, 32(2), pp. 978-987.
- Jeong, J. (2004) 'EEG dynamics in patients with Alzheimer's disease.' *Clinical Neurophysiology*, 115(7), pp. 1490-1505.
- Jia, H. (2019) 'Chapter 12: Connectivity Analysis.' In Hu, L. and Zhang, Z. (eds.) *EEG Signal Processing and Feature Extraction*. Springer Singapore, pp. 241-266.
- Joshi, C. and Klein, H. (2019) *Temporal Lobe Epilepsy (TLE)*. [https://www.epilepsy.com/what-is-epilepsy/syndromes/temporal-lobe-epilepsy#What-Is-Temporal-Lobe-Epilepsy-\(TLE\)?](https://www.epilepsy.com/what-is-epilepsy/syndromes/temporal-lobe-epilepsy#What-Is-Temporal-Lobe-Epilepsy-(TLE)?): Epilepsy Foundation. [Online] [Accessed on 20/01/2024]

- Jung, K.-H., Kang, D.-j., Lee, W.-J., Son, H.-S., Kim, S. and Kang, S. W. (2022) 'Pathophysiological insight into transient global amnesia from quantitative electroencephalography.' *Neurobiology of Disease*, 170, p. 105778.
- Kahana, M. J. (1996) 'Associative retrieval processes in free recall.' *Memory & cognition*, 24(1), pp. 103-109.
- Kahana, M. J. (2006) 'The Cognitive Correlates of Human Brain Oscillations.' *The Journal of Neuroscience*, 26(6), pp. 1669-1672.
- Kahana, M. J., Sekuler, R., Caplan, J. B., Kirschen, M. and Madsen, J. R. (1999) 'Human theta oscillations exhibit task dependence during virtual maze navigation.' *Nature*, 399(6738), pp. 781-784.
- Kaminski, M. and Blinowska, K. J. (2022) 'From Coherence to Multivariate Causal Estimators of EEG Connectivity.' *Front Physiol*, 13, p. 868294.
- Kane, N., Acharya, J., Benickzy, S., Caboclo, L., Finnigan, S., Kaplan, P. W., Shibasaki, H., Pressler, R. and van Putten, M. (2017) 'A revised glossary of terms most commonly used by clinical electroencephalographers and updated proposal for the report format of the EEG findings. Revision 2017.' *Clin Neurophysiol Pract*, 2, pp. 170-185.
- Kapur, N. (1993a) 'Transient epileptic amnesia--a clinical update and a reformulation.' *J Neurol Neurosurg Psychiatry*, 56(11), pp. 1184-1190.
- Kapur, N. (1993b) 'Transient epileptic amnesia--a clinical update and a reformulation.' *Journal of Neurology, Neurosurgery & Psychiatry*, 56(11), pp. 1184-1190.
- Kapur, N. and Markowitsch, H. (1990) 'Transient epileptic amnesia: a clinically distinct form of neurological memory disorder.' *Transient global amnesia and related disorders. New York: Hogrefe and Huber*, pp. 140-151.
- Karakaş, S. (2020) 'A review of theta oscillation and its functional correlates.' *International Journal of Psychophysiology*, 157, pp. 82-99.
- Kemp, S., Illman, N. A., Moulin, C. J. and Baddeley, A. D. (2012) 'Accelerated long-term forgetting (ALF) and transient epileptic amnesia (TEA): two cases of epilepsy-related memory disorder.' *Epilepsy Behav*, 24(3), pp. 382-388.
- Kinney-Lang, E., Yoong, M., Hunter, M., Kamath Tallur, K., Shetty, J., McLellan, A., Fm Chin, R. and Escudero, J. (2019) 'Analysis of EEG networks and their correlation with cognitive impairment in preschool children with epilepsy.' *Epilepsy & Behavior*, 90, pp. 45-56.
- Király, B., Domonkos, A., Jelitai, M., Lopes-dos-Santos, V., Martínez-Bellver, S., Kocsis, B., Schlingloff, D., Joshi, A., Salib, M., Fiáth, R., Barthó, P., Ulbert, I., Freund, T. F., Viney, T. J., Dupret, D., Varga, V. and Hangya, B. (2023) 'The medial septum controls hippocampal supra-theta oscillations.' *Nature Communications*, 14(1), p. 6159.
- Klass, D. W. and Brenner, R. P. (1995) 'Electroencephalography of the Elderly.' *Journal of Clinical Neurophysiology*, 12(2), pp. 116-131.
- Kleen, J. K., Scott, R. C., Holmes, G. L., Roberts, D. W., Rundle, M. M., Testorf, M., Lenck-Santini, P. P. and Jobst, B. C. (2013) 'Hippocampal interictal epileptiform activity disrupts cognition in humans.' *Neurology*, 81(1), pp. 18-24.
- Klimesch, W., Sauseng, P. and Hanslmayr, S. (2007) 'EEG alpha oscillations: the inhibition-timing hypothesis.' *Brain Res Rev*, 53(1), pp. 63-88.
- Koutroumanidis, M., Binnie, C. D., Elwes, R. D., Polkey, C. E., Seed, P., Alarcon, G., Cox, T., Barrington, S., Marsden, P. and Maisey, M. N. (1998) 'Interictal regional slow activity in temporal lobe epilepsy correlates with lateral temporal hypometabolism as imaged with¹⁸F¹⁸FDG PET: neurophysiological and metabolic implications.' *Journal of Neurology, Neurosurgery & Psychiatry*, 65(2), pp. 170-176.
- Krishnan, V., Chang, B. S. and Schomer, D. L. (2018a) 'Chapter 8: Normal EEG in Wakefulness and sleep: Adults and Elderly.' In Schomer, D. L. and Lopes da Silva, F. H. (eds.) *Niedermeyer's Electroencephalography*. Seventh ed., New York: Oxford University Press, pp. 202-228.
- Krishnan, V., Chang, B. S. and Schomer, D. L. (2018b) 'Chapter 19: The Application of EEG to Epilepsy in Adults and the Elderly.' In Schomer, D. L. and Lopes da Silva, F. H. (eds.) *Niedermeyer's*

- Electroencephalography: Basic Principles, Clinical Applications, and Related Fields*. Oxford University Press,
- Kural, M. A., Duez, L., Sejer Hansen, V., Larsson, P. G., Rampp, S., Schulz, R., Tankisi, H., Wennberg, R., Bibby, B. M., Scherg, M. and Beniczky, S. (2020) 'Criteria for defining interictal epileptiform discharges in EEG.' *Neurology*, 94(20), pp. e2139-e2147.
- La Vaque, T. J. (1999) 'The History of EEG Hans Berger.' *Journal of Neurotherapy*, 3(2), pp. 1-9.
- Ladino, L. D., Moien-Afshari, F. and Téllez-Zenteno, J. F. (2014) 'A comprehensive review of temporal lobe epilepsy.' *Neurological Disorders: Clinical Methods*, pp. 1-35.
- Lai, M., Demuru, M., Hillebrand, A. and Fraschini, M. (2018) 'A comparison between scalp- and source-reconstructed EEG networks.' *Scientific Reports*, 8(1),
- Lanzone, J., Ricci, L., Assenza, G., Ulivi, M., Di Lazzaro, V. and Tombini, M. (2018) 'Transient epileptic and global amnesia: Real-life differential diagnosis.' *Epilepsy & Behavior*, 88, pp. 205-211.
- Lanzone, J., Imperatori, C., Assenza, G., Ricci, L., Farina, B., Di Lazzaro, V. and Tombini, M. (2020) 'Power Spectral Differences between Transient Epileptic and Global Amnesia: An eLORETA Quantitative EEG Study.' *Brain Sciences*, 10(9), p. 613.
- Lapenta, L., Brunetti, V., Losurdo, A., Testani, E., Giannantoni, N. M., Quaranta, D., Di Lazzaro, V. and Della Marca, G. (2014) 'Transient epileptic amnesia: clinical report of a cohort of patients.' *Clin EEG Neurosci*, 45(3), pp. 179-183.
- Latreille, V., Schiller, K., Peter-Derex, L. and Frauscher, B. (2022) 'Does epileptic activity impair sleep-related memory consolidation in epilepsy? A critical and systematic review.' *Journal of Clinical Sleep Medicine*, 18(10), pp. 2481-2495.
- Li, H., Gao, S., Jia, X., Jiang, T. and Li, K. (2021) 'Distinctive Alterations of Functional Connectivity Strength between Vascular and Amnesic Mild Cognitive Impairment.' *Neural Plasticity*, 2021, pp. 1-8.
- Liang, J., Li, Y., Liu, H., Zhang, S., Wang, M., Chu, Y., Ye, J., Xi, Q. and Zhao, X. (2020) 'Increased intrinsic default-mode network activity as a compensatory mechanism in aMCI: a resting-state functional connectivity MRI study.' *Aging*, 12(7), pp. 5907-5919.
- Liao, W., Zhang, Z., Pan, Z., Mantini, D., Ding, J., Duan, X., Luo, C., Lu, G. and Chen, H. (2010) 'Altered functional connectivity and small-world in mesial temporal lobe epilepsy.' *PLoS one*, 5(1), p. e8525.
- Lisman, J. E. and Jensen, O. (2013) 'The Theta-Gamma Neural Code.' *Neuron*, 77(6), pp. 1002-1016.
- Lobier, M., Siebenhüner, F., Palva, S. and Palva, J. M. (2014) 'Phase transfer entropy: A novel phase-based measure for directed connectivity in networks coupled by oscillatory interactions.' *NeuroImage*, 85, pp. 853-872.
- Lopes da Silva, F. H. and Halgren, E. (2017) 'Chapter 48: Neurocognitive Processes.' In Schomer, D. L., Lopes da Silva, F. H., Schomer, D. L. and Lopes da Silva, F. H. (eds.) *Niedermeyer's Electroencephalography: Basic Principles, Clinical Applications, and Related Fields*. Oxford University Press, p. 0.
- Lopes da Silva, H. F. and Halgren, E. (2018) 'Chapter 48: Neurocognitive Processes.' In Schomer, D. L. and Lopes da Silva, F. H. (eds.) *Niedermeyer's Electroencephalography: Basic Principles, Clinical Applications, and Related Fields*. Oxford University Press,
- Lopez Rincon, A. and Shimoda, S. (2016) 'The inverse problem in electroencephalography using the bidomain model of electrical activity.' *Journal of Neuroscience Methods*, 274, pp. 94-105.
- Mahjoory, K., Nikulin, V. V., Botrel, L., Linkenkaer-Hansen, K., Fato, M. M. and Haufe, S. (2017) 'Consistency of EEG source localization and connectivity estimates.' *NeuroImage*, 152, pp. 590-601.
- Malow, B. A., Selwa, L. M., Ross, D. and Aldrich, M. S. (1999) 'Lateralizing Value of Interictal Spikes on Overnight Sleep-EEG Studies in Temporal Lobe Epilepsy.' *Epilepsia*, 40(11), pp. 1587-1592.
- Manes, F., Hodges, J. R., Graham, K. S. and Zeman, A. (2001) 'Focal autobiographical amnesia in association with transient epileptic amnesia.' *Brain*, 124(3), pp. 499-509.
- Manes, F., Graham, K. S., Zeman, A., de Lujan Calcagno, M. and Hodges, J. (2005a) 'Autobiographical amnesia and accelerated forgetting in transient epileptic amnesia.' *Journal of Neurology, Neurosurgery & Psychiatry*, 76(10), pp. 1387-1391.

- Manes, F., Graham, K. S., Zeman, A., de Lujan Calcagno, M. and Hodges, J. R. (2005b) 'Autobiographical amnesia and accelerated forgetting in transient epileptic amnesia.' *J Neurol Neurosurg Psychiatry*, 76(10), pp. 1387-1391.
- MathWorks. (Accessed 2021) 'MATLAB.' The MathWorks Inc. R2021b R2021b. [Accessed Matlab. (2022) Machine Learning with MATLAB. <https://uk.mathworks.com/content/dam/mathworks/ebook/gated/machine-learning-ebook-all-chapters.pdf>: The MathWorks, Inc.
- Mayo Clinic. (2017) *Amnesia*. Patient Care & Health Information - Diseases & Conditions. <https://www.mayoclinic.org/diseases-conditions/amnesia/symptoms-causes/syc-20353360>: Mayo Foundation for Medical Education and Research. [Online] [Accessed
- McAndrews, M. P. (2012) 'Chapter 13: Remote memory and temporal lobe epilepsy.' In Zeman, A., Kapur, N. and Jones-Gotman, M. (eds.) *Epilepsy and memory*. Oxford University Press, pp. 227-243.
- McLoughlin, G., Makeig, S. and Tsuang, M. T. (2014) 'In search of biomarkers in psychiatry: EEG-based measures of brain function.' *American Journal of Medical Genetics Part B: Neuropsychiatric Genetics*, 165(2), pp. 111-121.
- Medaglia, J. D. and Bassett, D. S. (2017) *Network analyses and nervous system disorders*. arXiv preprint arXiv:1701.01101. <https://arxiv.org/pdf/1701.01101.pdf>: University of Pennsylvania. [Online] [Accessed
- Medaglia, J. D., Lynall, M. E. and Bassett, D. S. (2015) 'Cognitive network neuroscience.' *J Cogn Neurosci*, 27(8), pp. 1471-1491.
- Meo, R., Bilo, L., Striano, S., Ruosi, P., Estraneo, A. and Nocerino, C. (1995) 'Transient global amnesia of epileptic origin accompanied by fever.' *Seizure*, 4(4), pp. 311-317.
- Milton, F., Butler, C. R., Benattayallah, A. and Zeman, A. Z. (2012) 'The neural basis of autobiographical memory deficits in transient epileptic amnesia.' *Neuropsychologia*, 50(14), pp. 3528-3541.
- Milton, F., Muhlert, N., Pindus, D. M., Butler, C. R., Kapur, N., Graham, K. S. and Zeman, A. Z. (2010) 'Remote memory deficits in transient epileptic amnesia.' *Brain*, 133(Pt 5), pp. 1368-1379.
- Moezzi, B., Pratti, L. M., Hordacre, B., Graetz, L., Berryman, C., Lavrencic, L. M., Ridding, M. C., Keage, H. A. D., McDonnell, M. D. and Goldsworthy, M. R. (2019) 'Characterization of Young and Old Adult Brains: An EEG Functional Connectivity Analysis.' *Neuroscience*, 422, pp. 230-239.
- Morgan, V. L., Rogers, B. P., Sonmez Turk, H. H., Gore, J. C. and Abou-Khalil, B. (2011) 'Cross hippocampal influence in mesial temporal lobe epilepsy measured with high temporal resolution functional magnetic resonance imaging.' *Epilepsia*, 52(9), pp. 1741-1749.
- Mosbah, A., Tramonì, E., Guedj, E., Aubert, S., Daquin, G., Ceccaldi, M., Félician, O. and Bartolomei, F. (2014) 'Clinical, neuropsychological, and metabolic characteristics of transient epileptic amnesia syndrome.' *Epilepsia*, 55(5), pp. 699-706.
- Muhlert, N., Milton, F., Butler, C. R., Kapur, N. and Zeman, A. Z. (2010) 'Accelerated forgetting of real-life events in Transient Epileptic Amnesia.' *Neuropsychologia*, 48(11), pp. 3235-3244.
- Nehring, S., Spurling, B. and Kumar, A. (2023) *Transient Global Amnesia*. <https://www.ncbi.nlm.nih.gov/books/NBK442001/>: StatPearls [Internet]. [Online] [Accessed on 20/1/2024]
- Nehring, S. M. and Kumar, A. (2018) 'Transient Global Amnesia.' In *StatPearls*. Treasure Island (FL): StatPearls Publishing LLC.,
- Neligan, A. and Sander, J. (2015) *The incidence and prevalence of epilepsy*. https://epilepsysociety.org.uk/sites/default/files/2020-08/Chapter01Neligan-2015_0.pdf: Epilepsy Society. [Online] [Accessed on 20/1/24]
- NICE. (2022) 'NICE guideline [NG217]: Epilepsies in children, young people and adults.' [Online]. [Accessed on 13/11/2022]
- Nichols, K. (2007) 'CHAPTER 20 - False Discovery Rate procedures.' In Friston, K., Ashburner, J., Kiebel, S., Nichols, T. and Penny, W. (eds.) *Statistical Parametric Mapping: The Analysis of Functional Brain Images*. London: Elsevier, pp. 246-252.

- Nolte, G., Bai, O., Wheaton, L., Mari, Z., Vorbach, S. and Hallett, M. (2004) 'Identifying true brain interaction from EEG data using the imaginary part of coherency.' *Clinical Neurophysiology*, 115(10), pp. 2292-2307.
- Novak, A., Vizjak, K. and Rakusa, M. (2022) 'Cognitive impairment in people with epilepsy.' *Journal of Clinical Medicine*, 11(1), p. 267.
- Nuñez, A. and Buño, W. (2021) 'The Theta Rhythm of the Hippocampus: From Neuronal and Circuit Mechanisms to Behavior.' *Frontiers in Cellular Neuroscience*, 15,
- Nyhus, E. and Curran, T. (2010) 'Functional role of gamma and theta oscillations in episodic memory.' *Neuroscience & Biobehavioral Reviews*, 34(7), pp. 1023-1035.
- O'Neill, G. C., Tewarie, P., Vidaurre, D., Liuzzi, L., Woolrich, M. W. and Brookes, M. J. (2018) 'Dynamics of large-scale electrophysiological networks: A technical review.' *NeuroImage*, 180, pp. 559-576.
- Oagawa, S., Uchida, Y., Kobayashi, S., Takada, K., Terada, K. and Matsukawa, N. (2021) 'GABA B receptor autoimmune encephalitis presenting as transient epileptic amnesia.' *Rinsho shinkeigaku = Clinical neurology*, 61(1), pp. 6-11.
- Omidvarnia, A., Pedersen, M., Rosch, R. E., Friston, K. J. and Jackson, G. D. (2017) 'Hierarchical disruption in the Bayesian brain: Focal epilepsy and brain networks.' *Neuroimage Clin*, 15, pp. 682-688.
- Osman, G. M., Riviello, J. J. and Hirsch, L. J. (2018) 'Chapter 22: EEG in the Intensive Care Unit: Anoxia, Coma, Brain Death and Related Disorders.' In Schomer, D. L. and Lopes da Silva, F. H. (eds.) *Niedermeyer's Electroencephalography: Basic Principles, Clinical Applications, and Related Fields*. Oxford University Press,
- Pappalettera, C., Cacciotti, A., Nucci, L., Miraglia, F., Rossini, P. M. and Vecchio, F. (2023) 'Approximate entropy analysis across electroencephalographic rhythmic frequency bands during physiological aging of human brain.' *GeroScience*, 45(2), pp. 1131-1145.
- Park, J. Y., Jhung, K., Lee, J. and An, S. K. (2013) 'Theta-gamma coupling during a working memory task as compared to a simple vigilance task.' *Neuroscience Letters*, 532, pp. 39-43.
- Park, Y. H., Kim, J.-Y., Yi, S., Lim, J.-S., Jang, J.-W., Im, C.-H. and Kim, S. (2016a) 'Transient Global Amnesia Deteriorates the Network Efficiency of the Theta Band.' *PLOS ONE*, 11(10), p. e0164884.
- Park, Y. H., Jeong, H.-Y., Jang, J.-W., Park, S. Y., Lim, J.-S., Kim, J.-Y., Im, C.-H., Ahn, S., Park, S.-H. and Kim, S. (2016b) 'Disruption of the Posterior Medial Network during the Acute Stage of Transient Global Amnesia: A Preliminary Study.' *Clinical EEG and Neuroscience*, 47(1), pp. 69-74.
- Patel, P. and De Jesus, O. (2023) *Partial Epilepsy*. <https://www.ncbi.nlm.nih.gov/books/NBK564376/>: StatPearls [Internet]. [Online] [Accessed on 20/01/2024]
- Peigneux, P. and Smith, C. (2010) 'Chapter 29: Memory Processing in Relation to Sleep.' In Kryger, M. H., Roth, T. and Dement, W. C. (eds.) *Principles and Practice of Sleep Medicine E-Book*. Elsevier Health Sciences,
- Pellegrino, G., Mecarelli, O., Pulitano, P., Tombini, M., Ricci, L., Lanzone, J., Brienza, M., Davassi, C., Di Lazzaro, V. and Assenza, G. (2018) 'Eslicarbazepine Acetate Modulates EEG Activity and Connectivity in Focal Epilepsy.' *Front Neurol*, 9, p. 1054.
- Peltola, M., Leitinger, M., Halford, J., Vinayan, K., Kobayash, i. K., Pressler, R., Mindruta, I., Mayor, L., Lauronen, L. and Beniczky, S. (2022) 'Proposed Guideline: Joint ILAE and IFCN minimum standards for recording routine and sleep EEG.' [Online]. [Accessed on 2022]
- Peltz, C. B., Kim, H. L. and Kawas, C. H. (2010) 'Abnormal EEGs in Cognitively and Physically Healthy Oldest Old: Findings From The 90+ Study.' *Journal of Clinical Neurophysiology*, 27(4), pp. 292-295.
- Peng, W. (2019) 'Chapter 5: EEG Preprocessing and Denoising.' In Hu, L. and Zhang, Z. (eds.) *EEG Signal Processing and Feature Extraction*. Singapore: Springer Nature Singapore Pte Ltd.,
- Perinelli, A., Asseondi, S., Tagliabue, C. F. and Mazza, V. (2022) 'Power shift and connectivity changes in healthy aging during resting-state EEG.' *NeuroImage*, 256, p. 119247.

- Pijnenburg, Y. A. L., vd Made, Y., van Cappellen van Walsum, A. M., Knol, D. L., Scheltens, P. and Stam, C. J. (2004) 'EEG synchronization likelihood in mild cognitive impairment and Alzheimer's disease during a working memory task.' *Clinical Neurophysiology*, 115(6), pp. 1332-1339.
- Pike, N. (2011) 'Using false discovery rates for multiple comparisons in ecology and evolution.' *Methods in Ecology and Evolution*, 2(3), pp. 278-282.
- Pizzanelli, C., Pesaresi, I., Milano, C., Cecchi, P., Fontanelli, L., Giannoni, S., Giorgi, F. S., Cosottini, M. and Bonanni, E. (2022) 'Distinct limbic connectivity in left and right benign mesial temporal lobe epilepsy: Evidence from a resting state functional MRI study.' *Front Neurol*, 13, p. 943660.
- Primavera, A., Novello, P. and Stara, S. (1993) 'Transient global amnesia: a quantified electroencephalographic study.' *Acta neurologica scandinavica*, 87(2), pp. 115-117.
- Pritchard, P., Holmstrom, V., Roitzsch, J. and Giacinto, J. (1985) 'Epileptic amnesic attacks: benefit from antiepileptic drugs.' *Neurology*, 35(8), pp. 1188-1188.
- Pukropski, J., von Wrede, R., Helmstaedter, C. and Surges, R. (2022) '[Transient epileptic amnesia-A rare phenomenon in temporal lobe epilepsies].' *Nervenarzt*, 93(12), pp. 1193-1205.
- Quraan, M. A., McCormick, C., Cohn, M., Valiante, T. A. and McAndrews, M. P. (2013) 'Altered Resting State Brain Dynamics in Temporal Lobe Epilepsy Can Be Observed in Spectral Power, Functional Connectivity and Graph Theory Metrics.' *PLoS ONE*, 8(7), p. e68609.
- Raghavachari, S., Lisman, J. E., Tully, M., Madsen, J. R., Bromfield, E. and Kahana, M. J. (2006) 'Theta oscillations in human cortex during a working-memory task: evidence for local generators.' *Journal of neurophysiology*, 95(3), pp. 1630-1638.
- Raghavachari, S., Kahana, M. J., Rizzuto, D. S., Caplan, J. B., Kirschen, M. P., Bourgeois, B., Madsen, J. R. and Lisman, J. E. (2001) 'Gating of Human Theta Oscillations by a Working Memory Task.' *The Journal of Neuroscience*, 21(9), pp. 3175-3183.
- Ramanan, V. K., Morris, K. A., Graff-Radford, J., Jones, D. T., Burkholder, D. B., Britton, J. W., Josephs, K. A., Boeve, B. F. and Savica, R. (2019) 'Transient Epileptic Amnesia: A Treatable Cause of Spells Associated With Persistent Cognitive Symptoms.' *Front Neurol*, 10, p. 939.
- Rasch, B. and Born, J. (2013) 'About sleep's role in memory.' *Physiol Rev*, 93(2), pp. 681-766.
- Rodrigues, J., Weiß, M., Hewig, J. and Allen, J. J. B. (2021) 'EPOS: EEG Processing Open-Source Scripts.' *Front Neurosci*, 15, p. 660449.
- Rossini, P. M., Rossi, S., Babiloni, C. and Polich, J. (2007) 'Clinical neurophysiology of aging brain: from normal aging to neurodegeneration.' *Prog Neurobiol*, 83(6), pp. 375-400.
- Rubinov, M. and Sporns, O. (2010) 'Complex network measures of brain connectivity: uses and interpretations.' *Neuroimage*, 52(3), pp. 1059-1069.
- Saeidi, M., Karwowski, W., Farahani, F. V., Fiok, K., Taiar, R., Hancock, P. A. and Al-Juaid, A. (2021) 'Neural Decoding of EEG Signals with Machine Learning: A Systematic Review.' *Brain Sciences*, 11(11), p. 1525.
- Sakkalis, V. (2011) 'Review of advanced techniques for the estimation of brain connectivity measured with EEG/MEG.' *Computers in biology and medicine*, 41(12), pp. 1110-1117.
- Sancetta, B. M., Ricci, L., Assenza, G., Boscarino, M., Narducci, F., Vico, C., Di Lazzaro, V. and Tombini, M. (2022) 'EPIAMNE: A New Scoring System for Differentiating Transient Epileptic Amnesia from Transient Global Amnesia.' *Brain Sciences*, 12(12), p. 1632.
- Savage, S., Baker, J., Butler, C., Hodges, J. and Zeman, A. (2017a) 'Long-term prognosis of transient epileptic amnesia: Evidence from the time project.' *Journal of the Neurological Sciences*, 381, p. 156.
- Savage, S., Hoefjezers, S., Milton, F., Streatfield, C., Dewar, M. and Zeman, A. (2019a) 'The evolution of accelerated long-term forgetting: Evidence from the TIME study.' *Cortex*, 110, pp. 16-36.
- Savage, S. A., Irani, S. R., Leite, M. I. and Zeman, A. Z. (2019b) 'NMDA receptor antibody encephalitis presenting as Transient Epileptic Amnesia.' *J Neuroimmunol*, 327, pp. 41-43.
- Savage, S. A., Butler, C., Baker, J., Hodges, J. R. and Zeman, A. Z. (2017b) 'Investigating the prognosis of Transient Epileptic Amnesia: Does it lead to Alzheimer's Disease?' *Alzheimer's & Dementia: The Journal of the Alzheimer's Association*, 13(7), p. P1341.

- Savage, S. A., Butler, C. R., Baker, J., Hodges, J. R. and Zeman, A. Z. (2017c) 23 Long-term follow-up in transient epileptic amnesia: prognosis over 10–20 years. BMJ Publishing Group Ltd.
- Savage, S. A., Butler, C. R., Milton, F., Han, Y. and Zeman, A. Z. (2017d) 'On the nose: Olfactory disturbances in patients with transient epileptic amnesia.' *Epilepsy Behav*, 66, pp. 113-119.
- Savage, S. A., Baker, J., Milton, F., Butler, C. and Zeman, A. (2022) 'Clinical outcomes in Transient Epileptic Amnesia: a 10-year follow-up cohort study of 47 cases.' *Epilepsia*,
- Scheffer, I. E., Berkovic, S., Capovilla, G., Connolly, M. B., French, J., Guilhoto, L., Hirsch, E., Jain, S., Mathern, G. W. and Moshé, S. L. (2017) 'ILAE classification of the epilepsies: position paper of the ILAE Commission for Classification and Terminology.' *Epilepsia*, 58(4), pp. 512-521.
- Scherg, M., Berg, P., Nakasato, N. and Beniczky, S. (2019) 'Taking the EEG Back Into the Brain: The Power of Multiple Discrete Sources.' *Frontiers in Neurology*, 10,
- Schomer, D. L. and Da Silva, F. L. (2018) *Niedermeyer's electroencephalography: basic principles, clinical applications, and related fields*. 7th ed.: Oxford University Press.
- Schulz, R., Lüders, H. O., Noachtar, S., May, T., Sakamoto, A., Holthausen, H. and Wolf, P. (1995) 'Amnesia of the epileptic aura.' *Neurology*, 45(2), pp. 231-235.
- Schwartz, B. L. (2014) 'Memory and the Brian.' *In Memory - Foundations and Applications*. https://uk.sagepub.com/sites/default/files/upm-binaries/35762_Chapter2.pdf: Sage Publications Inc.,
- Sederberg, P. B., Kahana, M. J., Howard, M. W., Donner, E. J. and Madsen, J. R. (2003) 'Theta and Gamma Oscillations during Encoding Predict Subsequent Recall.' *The Journal of Neuroscience*, 23(34), pp. 10809-10814.
- Seeck, M., Koessler, L., Bast, T., Leijten, F., Michel, C., Baumgartner, C., He, B. and Beniczky, S. (2017) 'The standardized EEG electrode array of the IFCN.' *Clinical Neurophysiology*, 128(10), pp. 2070-2077.
- Selim R, B. (2007) 'Errors in EEGs and the misdiagnosis of epilepsy: Importance, causes, consequences, and proposed remedies.' *Epilepsy & Behavior*, 11(3), pp. 257-262.
- Seo, Y. D., Lee, D. A. and Park, K. M. (2023) 'Can Artificial Intelligence Diagnose Transient Global Amnesia Using Electroencephalography Data?' *Journal of Clinical Neurology*, 19(1), p. 36.
- Sinha, S. R., Sullivan, L., Sabau, D., San-Juan, D., Dombrowski, K. E., Halford, J. J., Hani, A. J., Drislane, F. W. and Stecker, M. M. (2016) 'American Clinical Neurophysiology Society Guideline 1.' *Journal of Clinical Neurophysiology*, 33(4), pp. 303-307.
- Sohrabpour, A., Lu, Y., Kankirawatana, P., Blount, J., Kim, H. and He, B. (2015) 'Effect of EEG electrode number on epileptic source localization in pediatric patients.' *Clinical Neurophysiology*, 126(3), pp. 472-480.
- Somogyi, P. and Klausberger, T. (2005) 'Defined types of cortical interneurone structure space and spike timing in the hippocampus.' *The Journal of Physiology*, 562(1), pp. 9-26.
- Sparaco, M., Pascarella, R., Muccio, C. F. and Zedde, M. (2022) 'Forgetting the Unforgettable: Transient Global Amnesia Part I: Pathophysiology and Etiology.' *Journal of Clinical Medicine*, 11(12), p. 3373.
- Sporns, O. (2017) 'The future of network neuroscience.' *Netw Neurosci*, 1(2), pp. 1-2.
- Squire, L. R. and Zola-Morgan, M. (1991) 'The brain and memory: a new synthesis.' *Oxford Surveys on the Mind*, 10, pp. 1-90.
- Squire, L. R. and Zola-Morgan, M. (1991) 'The brain and memory: a new synthesis.' *Cold Spring Harbor Perspect Biol*, 7(3), p. a021667.
- Stagnor, C. (Accessed 2019) 9.1 Memories as Types and Stages. Introduction to Psychology – 1st Canadian Edition. <https://opentextbc.ca/introductiontopsychology/chapter/8-1-memories-as-types-and-stages/>: [Online] [Accessed
- Stam, C. J. and van Dijk, B. W. (2002) 'Synchronization likelihood: an unbiased measure of generalized synchronization in multivariate data sets.' *Physica D: Nonlinear Phenomena*, 163(3), pp. 236-251.
- Stam, C. J., Montez, T., Jones, B. F., Rombouts, S. A. R. B., van der Made, Y., Pijnenburg, Y. A. L. and Scheltens, P. (2005) 'Disturbed fluctuations of resting state EEG synchronization in Alzheimer's disease.' *Clinical Neurophysiology*, 116(3), pp. 708-715.

- Stam, C. J., Jones, B. F., Manshanden, I., van Cappellen van Walsum, A. M., Montez, T., Verbunt, J. P. A., de Munck, J. C., van Dijk, B. W., Berendse, H. W. and Scheltens, P. (2006) 'Magnetoencephalographic evaluation of resting-state functional connectivity in Alzheimer's disease.' *NeuroImage*, 32(3), pp. 1335-1344.
- Stampacchia, S., Thompson, H. E., Ball, E., Nathaniel, U., Hallam, G., Smallwood, J., Lambon Ralph, M. A. and Jefferies, E. (2018) 'Shared processes resolve competition within and between episodic and semantic memory: Evidence from patients with LIFG lesions.' *Cortex*, 108, pp. 127-143.
- Staresina, B. P., Duncan, K. D. and Davachi, L. (2011) 'Perirhinal and parahippocampal cortices differentially contribute to later recollection of object- and scene-related event details.' *J Neurosci*, 31(24), pp. 8739-8747.
- Stone, J. L. and Hughes, J. R. (2013) 'Early history of electroencephalography and establishment of the American Clinical Neurophysiology Society.' *Journal of Clinical Neurophysiology*, 30(1), pp. 28-44.
- Stoyell, S. M., Wilmskoetter, J., Dobrota, M. A., Chinappen, D. M., Bonilha, L., Mintz, M., Brinkmann, B. H., Herman, S. T., Peters, J. M., Vulliemoz, S., Seeck, M., Hämäläinen, M. S. and Chu, C. J. (2021) 'High-Density EEG in Current Clinical Practice and Opportunities for the Future.' *J Clin Neurophysiol*, 38(2), pp. 112-123.
- Sucholeiki, R. (2018) *Transient Global Amnesia*. Neurology.
<https://emedicine.medscape.com/article/1160964-overview#a4>: MedScape - WebMD LLC. [Online] [Accessed
- Sutter, R., Kaplan, P. W. and Schomer, D. L. (2018a) 'Chapter 1: Historical aspects of Electroencephalography.' In Schomer, D. L. and Lopes da Silva, F. H. (eds.) *Niedermeyer's Electroencephalography*. Seventh ed., New York: Oxford University Press, pp. 202-228.
- Sutter, R., Pang, T. and Kaplan, P. W. (2018b) 'Chapter 17: EEG in Metabolic Disorders, Intoxications, and Epileptic Encephalopathies.' In Schomer, D. L. and Lopes da Silva, F. H. (eds.) *Niedermeyer's Electroencephalography*. Seventh ed., New York: Oxford University Press, pp. 266-316.
- Sweatt, J. D. (2009) *Mechanisms of memory*. Academic Press.
- Tao, J. X., Chen, X.-J., Baldwin, M., Yung, I., Rose, S., Frim, D., Hawes-Ebersole, S. and Ebersole, J. S. (2011) 'Interictal regional delta slowing is an EEG marker of epileptic network in temporal lobe epilepsy.' *Epilepsia*, 52(3), pp. 467-476.
- Tassinari, C. A., Ciarmatori, C., Alesi, C., Cardinaletti, L., Salvi, F., Rubboli, G., Plasmati, R., Forti, A. and Michelucci, R. (1991) 'Transient global amnesia as a postictal state from recurrent partial seizures.' *Epilepsia*, 32(6), pp. 882-885.
- Tatum, W. O. (2013a) 'Artifact-related epilepsy.' *Neurology*, 80(1 Suppl 1), pp. S12-25.
- Tatum, W. O. (2013b) 'Artifact-related epilepsy.' *Neurology*, 80(1 Supplement 1), pp. S12-S25.
- Tatum, W. O., Dworetzky, B. A. and Schomer, D. L. (2011) 'Artifact and recording concepts in EEG.' *J Clin Neurophysiol*, 28(3), pp. 252-263.
- Tatum, W. O., Reinsberger, C. and Dworetzky, B. A. (2018) 'Chapter 11: Artifacts of Recording and Common Errors in Interpretation.' In Schomer, D. L. and Lopes da Silva, F. H. (eds.) *Niedermeyer's Electroencephalography*. Seventh ed., New York: Oxford University Press, pp. 266-316.
- Tatum, W. O., Olga, S., Ochoa, J. G., Munger Clary, H., Cheek, J., Drislane, F. and Tsuchida, T. N. (2016) 'American Clinical Neurophysiology Society Guideline 7: Guidelines for EEG Reporting.' *Journal of Clinical Neurophysiology*, 33(4),
- Teipel, S., Grothe, M. J., Zhou, J., Sepulcre, J., Dyrba, M., Sorg, C. and Babiloni, C. (2016) 'Measuring Cortical Connectivity in Alzheimer's Disease as a Brain Neural Network Pathology: Toward Clinical Applications.' *J Int Neuropsychol Soc*, 22(2), pp. 138-163.
- Télliez-Zenteno, J. F. and Hernández-Ronquillo, L. (2012) 'A Review of the Epidemiology of Temporal Lobe Epilepsy.' *Epilepsy Research and Treatment*, 2012, pp. 1-5.
- Tóth, B., Kardos, Z., File, B., Boha, R., Stam, C. J. and Molnár, M. (2014a) 'Frontal midline theta connectivity is related to efficiency of WM maintenance and is affected by aging.' *Neurobiology of Learning and Memory*, 114, pp. 58-69.

- Tóth, B., File, B., Boha, R., Kardos, Z., Hidasi, Z., Gaál, Z. A., Csibri, É., Salacz, P., Stam, C. J. and Molnár, M. (2014b) 'EEG network connectivity changes in mild cognitive impairment — Preliminary results.' *International Journal of Psychophysiology*, 92(1), pp. 1-7.
- Tramoni, E. and Felician, O. (2017) 'Memory and consolidation: contribution of transient epileptic amnesia.' *Revue de neuropsychologie*, 9(4), pp. 243-252.
- Ukai, K. and Watanabe, M. (2017) 'Transient epileptic amnesia without epileptic seizures: proposal of a new entity.' *Psychogeriatrics*, 17(6), pp. 491-492.
- Ukai, K., Ito, M. and Watanabe, M. (2021) 'A proposal for a new clinical entity: transient epileptic amnesia complex syndrome (TEACS).' *Psychogeriatrics*, 21(6), pp. 920-925.
- Ursino, M., Ricci, G. and Magosso, E. (2020) 'Transfer Entropy as a Measure of Brain Connectivity: A Critical Analysis With the Help of Neural Mass Models.' *Frontiers in Computational Neuroscience*, 14, Van Dellen, E., Douw, L., Baayen, J. C., Heimans, J. J., Ponten, S. C., Vandertop, W. P., Velis, D. N., Stam, C. J. and Reijneveld, J. C. (2009) 'Long-Term Effects of Temporal Lobe Epilepsy on Local Neural Networks: A Graph Theoretical Analysis of Corticography Recordings.' *PLoS ONE*, 4(11), p. e8081.
- Van Diessen, E., Zweiphenning, W. J. E. M., Jansen, F. E., Stam, C. J., Braun, K. P. J. and Otte, W. M. (2014) 'Brain Network Organization in Focal Epilepsy: A Systematic Review and Meta-Analysis.' *PLoS ONE*, 9(12), p. e114606.
- Vecchio, F., Miraglia, F., Marra, C., Quaranta, D., Vita, M. G., Bramanti, P. and Rossini, P. M. (2014) 'Human brain networks in cognitive decline: a graph theoretical analysis of cortical connectivity from EEG data.' *J Alzheimers Dis*, 41(1), pp. 113-127.
- Vicente, R., Wibral, M., Lindner, M. and Pipa, G. (2011) 'Transfer entropy—a model-free measure of effective connectivity for the neurosciences.' *Journal of Computational Neuroscience*, 30(1), pp. 45-67.
- Vinck, M., Oostenveld, R., van Wingerden, M., Battaglia, F. and Pennartz, C. M. (2011) 'An improved index of phase-synchronization for electrophysiological data in the presence of volume-conduction, noise and sample-size bias.' *Neuroimage*, 55(4), pp. 1548-1565.
- Vuilleumier, P., Despland, P. A. and Regli, F. (1996) 'Failure to recall (but not to remember): pure transient amnesia during nonconvulsive status epilepticus.' *Neurology*, 46(4), pp. 1036-1039.
- Walker, M. (2017) *Why we sleep: The new science of sleep and dreams*. Penguin UK.
- Wang, J., Wang, J., Sun, J., Tong, S. and Hong, X. (2019a) *Phase Transfer Entropy between Frontal and Posterior Regions during Visual Spatial Attention*. 2019. IEEE.
- Wang, R., Ge, S., Zommará, N. M., Ravienna, K., Espinoza, T. and Iramina, K. (2019b) 'Consistency and dynamical changes of directional information flow in different brain states: A comparison of working memory and resting-state using EEG.' *NeuroImage*, 203, p. 116188.
- Wang, Y. and Chen, W. (2021) *A modified phase transfer entropy for cross-frequency directed coupling estimation in brain network*. 2021. IEEE.
- Watrous, A. J., Tandon, N., Conner, C. R., Pieters, T. and Ekstrom, A. D. (2013) 'Frequency-specific network connectivity increases underlie accurate spatiotemporal memory retrieval.' *Nature Neuroscience*, 16(3), pp. 349-356.
- Wendling, F. and Lopes da Silva, F. H. (2017) 'Chapter 3: Dynamics of EEGs as Signals of Neuronal Populations: Models and Theoretical Considerations.' In Schomer, D. L. and Lopes da Silva, F. H. (eds.) *Niedermeyer's Electroencephalography: Basic Principles, Clinical Applications, and Related Fields*. Oxford University Press,
- Widdess-Walsh, P., Sweeney, B. J., Galvin, R. and McNamara, B. (2005) 'Utilization and Yield of EEG in the Elderly Population.' *Journal of Clinical Neurophysiology*, 22(4), pp. 253-255.
- Xu, Q., Zhang, J., Grandjean, J., Tan, C., Subbaraju, V., Li, L., Lee, K. J., Hsieh, P.-J. and Lim, J.-H. (2020) 'Neural correlates of retrieval-based enhancement of autobiographical memory in older adults.' *Scientific Reports*, 10(1),
- Yao, D., Qin, Y., Hu, S., Dong, L., Bringas Vega, M. L. and Valdés Sosa, P. A. (2019) 'Which Reference Should We Use for EEG and ERP practice?' *Brain Topography*, 32(4), pp. 530-549.

- Yu, M., Gouw, A. A., Hillebrand, A., Tijms, B. M., Stam, C. J., van Straaten, E. C. W. and Pijnenburg, Y. A. L. (2016) 'Different functional connectivity and network topology in behavioral variant of frontotemporal dementia and Alzheimer's disease: an EEG study.' *Neurobiology of Aging*, 42, pp. 150-162.
- Zeman, A. and Butler, C. (2010) 'Transient epileptic amnesia.' *Curr Opin Neurol*, 23(6), pp. 610-616.
- Zeman, A. and Butler, C. (2022a) *The TIME Project*. <https://projects.exeter.ac.uk/time/index.php>: University of Exeter Medical School. [Online] [Accessed
- Zeman, A. and Butler, C. (2022b) *Clinical Features of TEA*. https://projects.exeter.ac.uk/time/research_areas.php?cat=tea: University of Exeter Medical School. [Online] [Accessed
- Zeman, A., Byrck, M., Tallis, P., Vossel, K. and Tranel, D. (2018) 'Touching the void - First and third person perspectives in two cases of autobiographical amnesia linked to temporal lobe epilepsy.' *Neuropsychologia*, 110, pp. 55-64.
- Zeman, A. Z., Boniface, S. J. and Hodges, J. R. (1998a) 'Transient epileptic amnesia: a description of the clinical and neuropsychological features in 10 cases and a review of the literature.' *J Neurol Neurosurg Psychiatry*, 64(4), pp. 435-443.
- Zeman, A. Z. J., Boniface, S. J. and Hodges, J. R. (1998b) 'Transient epileptic amnesia: a description of the clinical and neuropsychological features in 10 cases and a review of the literature.' *Journal of Neurology, Neurosurgery & Psychiatry*, 64(4), pp. 435-443.
- Zhang, Y.-W., Zhao, Z.-L., Qi, Z., Hu, Y., Wang, Y.-S., Sheng, C., Sun, Y., Wang, X., Jiang, L.-L., Yan, C.-G., Li, K., Li, H.-J. and Zuo, X.-N. (2017) 'Local-to-remote cortical connectivity in amnesic mild cognitive impairment.' *Neurobiology of Aging*, 56, pp. 138-149.
- Zhang, Z. (2019) 'Chapter 6: Spectral and Time-Frequency Analysis.' In Hu, L. and Zhang, Z. (eds.) *EEG Signal Processing and Feature Extraction*. Singapore: Springer Nature,
- Zhu, Y., Zang, F., Wang, Q., Zhang, Q., Tan, C., Zhang, S., Hu, T., Qi, L., Xu, S., Ren, Q. and Xie, C. (2021) 'Connectome-based model predicts episodic memory performance in individuals with subjective cognitive decline and amnesic mild cognitive impairment.' *Behavioural Brain Research*, 411, p. 113387.

Appendix 1: MATLAB SCRIPTS

Pre-processing Script

TEA_Preproc script

```

clear all;
close all;
clc;

ActualPath = 'C:\Users\lchan\OneDrive\Desktop\Data Analysis\Reprocessed Files with high ZScores\HV';
ActualFileName = 'HV20_reduced_chanlocs_vis inspected_2nd.set';

%% Open EEGLab and Set File
[ALLEEG EEG CURRENTSET ALLCOM] = eeglab;
EEG = pop_loadset('filename',ActualFileName,'filepath',ActualPath);
[ALLEEG, EEG, CURRENTSET] = eeg_store( ALLEEG, EEG, 0 );
EEG = eeg_checkset( EEG );

%% Reordering
standardOrder={'Fp1';'Fp2';'F3';'F4';'C3';'C4';'P3';'P4';'O1';'O2';'F7';'F8';'T3';'T4';'T5';'T6';'Fz';
'Cz';'Pz';'A1';'A2'};
newOrder=[];
for index = 1:21
    newOrder(index)=find(strcmpi({EEG.chanlocs.labels},standardOrder{index}));
end
EEG.data = EEG.data(newOrder,:);
EEG.chanlocs = EEG.chanlocs(newOrder);

%% Rereference
EEG = pop_reref( EEG, [], 'exclude',[1 2 17] );
[ALLEEG EEG CURRENTSET] = pop_newset(ALLEEG, EEG, 1, 'setname',[ActualFileName '_ReRef'], 'gui', 'off');
EEG = eeg_checkset( EEG );

%% Resample
EEG = pop_resample( EEG, 256);
[ALLEEG EEG CURRENTSET] = pop_newset(ALLEEG, EEG, 2, 'setname',[ActualFileName
'_ReRef_resampled'], 'gui', 'off');
EEG = eeg_checkset( EEG );

%% Filter
EEG = pop_eegfiltnew(EEG, 'locutoff',1,'plotfreqz',1);
[ALLEEG EEG CURRENTSET] = pop_newset(ALLEEG, EEG, 3, 'setname',[ActualFileName
'_ReRef_resampled_Filt'], 'gui', 'off');
EEG = eeg_checkset( EEG );
EEG = pop_eegfiltnew(EEG, 'hicutoff',40,'plotfreqz',1);
[ALLEEG EEG CURRENTSET] = pop_newset(ALLEEG, EEG, 4, 'gui', 'off');
EEG = eeg_checkset( EEG );
%[ALLEEG EEG CURRENTSET] = pop_newset(ALLEEG, EEG, 5, 'retrieve',1, 'study',0);
%EEG = eeg_checkset( EEG );

%% Run ICA
EEG = pop_runica(EEG, 'icatype', 'runica', 'extended',1, 'interrupt', 'on');
[ALLEEG EEG] = eeg_store(ALLEEG, EEG, CURRENTSET);
EEG = eeg_checkset( EEG );
EEG = pop_iclabel(EEG, 'default');
[ALLEEG EEG] = eeg_store(ALLEEG, EEG, CURRENTSET);

%% Epoching EEG Data
EEGout = eeg_repepochs(EEG, 'recurrence', 5, 'limits',[0 5], 'extractepochs', 'on');
EEG = EEGout;
[ALLEEG EEG] = eeg_store(ALLEEG, EEG, CURRENTSET);
EEG = eeg_checkset( EEG );

%% Save pre-processed Set File
EEG = pop_saveset( EEG, 'filename',[ActualFileName '_Preproc.set'], 'filepath',ActualPath);
[ALLEEG EEG] = eeg_store(ALLEEG, EEG, CURRENTSET);

eeglab redraw;

```

Resting IAF-Master Scripts (Corcoran *et al.*, 2018)

5.7. Resting IAF

Resting IAF

```

%% setup inputParser
p = inputParser;
p.addRequired('data',...
    @(x) validateattributes(x, {'numeric'}, ...
    {'2d', 'nonempty'}));
p.addRequired('nchan',...
    @(x) validateattributes(x, {'numeric'}, ...
    {'scalar', 'integer', 'positive'}));
p.addRequired('cmin',...
    @(x) validateattributes(x, {'numeric'}, ...
    {'scalar', 'integer', 'positive', '<=', size(data, 1)}));
p.addRequired('fRange',...
    @(x) validateattributes(x, {'numeric'}, ...
    {'integer', 'nonnegative', 'increasing', 'size', [1,2]}));
p.addRequired('Fs',...
    @(x) validateattributes(x, {'numeric'}, ...
    {'scalar', 'integer', 'positive', '>=', 2*fRange(2)}));
p.addRequired('w',...
    @(x) validateattributes(x, {'numeric'}, ...
    {'nonnegative', 'increasing', 'size', [1,2], '>', fRange(1), '<',
fRange(2)}));
p.addRequired('Fw',...
    @(x) validateattributes(x, {'numeric'}, ...
    {'scalar', 'integer', 'positive', 'odd'}));
p.addRequired('k',...
    @(x) validateattributes(x, {'numeric'}, ...
    {'scalar', 'integer', 'positive', '<', Fw }));

p.addOptional('mpow', 1,...
    @(x) validateattributes(x, {'numeric'}, ...
    {'scalar', 'positive'}));
p.addOptional('mdiff', .20,...
    @(x) validateattributes(x, {'numeric'}, ...
    {'scalar', '>=', 0, '<=', 1}));
p.addOptional('taper', 'hamming',...
    @(x) validateattributes(x, {'char'}, ...
    {}));
p.addOptional('tlen', (Fs*4),...
    @(x) validateattributes(x, {'numeric'}, ...
    {'scalar', 'integer', 'positive'}));
p.addOptional('tover', [],...
    @(x) validateattributes(x, {'numeric'}, ...
    {'integer', 'nonnegative'}));
p.addOptional('nfft', [],...
    @(x) validateattributes(x, {'numeric'}, ...
    {'integer', 'positive'}));
p.addOptional('norm', true,...
    @(x) validateattributes(x, {'logical'}, ...
    {'scalar'}));

p.parse(data, nchan, cmin, fRange, Fs, w, Fw, k, varargin{:})

mpow = p.Results.mpow;
mdiff = p.Results.mdiff;

```

```

taper    = p.Results.taper;
tlen     = p.Results.tlen;
tover    = p.Results.tover;
nfft     = p.Results.nfft;
norm     = p.Results.norm;
%%
% struct for channel data (PSD estimates & derivatives, some additional info)
pChans = struct('pxx', [], 'minPow', [], 'd0', [], 'd1', [], 'd2', [],...
    'peaks', [], 'pos1', [], 'pos2', [], 'f1', [], 'f2', [], 'inf1', [], 'inf2',
    [],...
    'Q', [], 'Qf', [], 'gravs', [], 'selP', [], 'selG', [] );

for kx = 1:nchan
    if sum(isnan(data(kx,:)))==0      % ensure no channel NaNs

        % perform pwelch routine to extract PSD estimates by channel
        fh = str2func(taper);
        [pxx, f] = pwelch(data(kx,:), fh(tlen), tover, nfft, Fs);
        pxx_AllChannels(:,kx)=pxx;

        % delimit range of freq bins to be included in analysis
        frex = dsearchn(f, fRange(1)):dsearchn(f, fRange(2));
        f = f(frex);
        pxx = pxx(frex);          % truncate PSD to frex range

        % normalise truncated PSD
        if norm == true
            pChans(kx).pxx = pxx / mean(pxx);
        else
            pChans(kx).pxx = pxx;
        end

        % calculate minPower vector
        [pfit, sig] = polyfit(f, log10(pChans(kx).pxx), 1);      % fit 1st order
        poly (regression line) to normalised spectra (log-scaled)
        [yval, del] = polyval(pfit, f, sig);                    % derive yval
        coefficients of fitted polynomial and delta (std dev) error estimate
        pChans(kx).minPow = yval + (mpow * del);                % takes
        [minPowThresh * Std dev] as upper error bound on background spectral noise

        % apply Savitzky-Golay filter to fit curves to spectra & estimate 1st and
        2nd derivatives
        [pChans(kx).d0, pChans(kx).d1, pChans(kx).d2] = sgfDiff(pChans(kx).pxx,
        Fw, k, Fs, tlen);

        % calculate frequency resolution
        exp_tlen = nextpow2(tlen);
        fres = Fs/2.^exp_tlen;

        % take derivatives, find peak(s) and boundaries of alpha band
        [pChans(kx).peaks, pChans(kx).pos1, pChans(kx).pos2, pChans(kx).f1,
        pChans(kx).f2,...
        pChans(kx).inf1, pChans(kx).inf2, pChans(kx).Q, pChans(kx).Qf]...
        = peakBounds(pChans(kx).d0, pChans(kx).d1, pChans(kx).d2, f, w,...
        pChans(kx).minPow, mdiff, fres);
    end
end

```

```
    else
        warning('Row #kx contains NaNs, skipping channel...', num2str(kx))
        nchan = nchan-1;    % trim nchans for cx loop later on
    end
end

end

meanAcrossChannels_pxx=nanmean(pxx_AllChannels,2);
medianAcrossChannels_pxx=nanmedian(pxx_AllChannels,2);

% estimate gravities for smoothed spectra (average IAF window across channels)
[ gravs, selG, iaw ] = chanGravs([pChans(:).d0], f, [pChans(:).f1], [pChans(:).f2]
);

% calculate average pt estimates/spectra across k-th channels for each j-th
recording
[ selP, pSum ] = chanMeans(gravs, selG, [pChans(:).peaks], [pChans(:).d0],
[pChans(:).Qf], cmin);

% retain gravity estimates and selected channels in channel data struct
% (only loop through trimmed channels)
for cx = 1:nchan
    pChans(cx).gravs = gravs(cx);
    pChans(cx).selP = selP(cx);
    pChans(cx).selG = selG(cx);
end

% get total number of chans that contributed to PAF/CoG estimation
pSum.pSel = sum(selP);
pSum.gSel = sum(selG);
pSum.iaw = iaw;

end
```

5.8. chanGravs

chanGravs

```

%% setup inputParser
p = inputParser;
p.addRequired('d0',...
    @(x) validateattributes(x, {'numeric'}, ...
    {'2d'}));
p.addRequired('f',...
    @(x) validateattributes(x, {'numeric'}, ...
    {'vector', 'nonnegative', 'increasing'}));
p.addRequired('f1',...
    @(x) validateattributes(x, {'numeric'}, ...
    {'vector'}));
p.addRequired('f2',...
    @(x) validateattributes(x, {'numeric'}, ...
    {'vector'}));
p.parse(d0, f, f1, f2)
%%

% trim off any NaNs in f1/f2 vectors
trim_f1 = f1(~isnan(f1));
trim_f2 = f2(~isnan(f2));

% derive average f1 & f2 values across chans, then look for nearest freq bin
mean_f1 = dsearchn(f, mean(f(trim_f1)));
mean_f2 = dsearchn(f, mean(f(trim_f2)));
iaw = [mean_f1, mean_f2];

% calculate CoG for each channel spectra on basis of averaged alpha window
cogs = zeros(1,size(d0,2));
for d = 1:length(cogs)
    if isempty(trim_f1) || isempty(trim_f2)
        cogs(d) = NaN;
    else
        cogs(d) = nansum(d0(mean_f1:mean_f2,d).*f(mean_f1:mean_f2)) /
sum(d0(mean_f1:mean_f2,d));
    end
end

% report which channels contribute to averaged window
sel = ~isnan(f1);

end

```

5.9. chanMeans

chanMeans

```

%% setup inputParser
p = inputParser;
p.addRequired('chanCogs',...
    @(x) validateattributes(x, {'numeric'}, ...
        {'vector', 'positive'}));
p.addRequired('selG',...
    @(x) validateattributes(x, {'logical'}, ...
        {'vector'}));
p.addRequired('peaks',...
    @(x) validateattributes(x, {'numeric'}, ...
        {'vector', 'positive'}));
p.addRequired('qf',...
    @(x) validateattributes(x, {'numeric'}, ...
        {'vector', 'positive'}));
p.addRequired('cmin',...
    @(x) validateattributes(x, {'numeric'}, ...
        {'scalar', 'integer', 'positive'}));
p.parse(chanCogs, selG, peaks, qf, cmin)
%%

% channel selection and weights
selP = ~isnan(peaks);           % evaluate whether channel provides estimate
of PAF

% qWt = nansum(qf)/sum(selP);   % average area under peak (Qf) across viable
channels (depricated: was used when calculating cross-recording comparisons)
chanWts = qf/max(qf);          % channel weightings scaled in proportion to
Qf value of channel manifesting highest Qf

% average across peaks
if sum(selP) < cmin             % if number of viable channels < cmin
threshold, don't calculate cross-channel mean & std
    sums.paf = NaN;
    sums.pafStd = NaN;
    sums.muSpec = NaN;
else                             % else compute (weighted) cross-channel
average PAF estimate and corresponding std of channel PAFs
    sums.paf = nansum(bsxfun(@times, peaks, chanWts))/nansum(chanWts);
    sums.pafStd = nanstd(peaks);
    % estimate averaged spectra for plotting
    wtSpec = bsxfun(@times, specs, chanWts);
    sums.muSpec = nansum(wtSpec, 2)/nansum(chanWts);
end

% now for the gravs (no channel weighting, all channels included if cmin
satisfied)
if sum(selG) < cmin
    sums.cog = NaN;
    sums.cogStd = NaN;
else
    sums.cog = nanmean(chanCogs, 2);
    sums.cogStd = nanstd(chanCogs);
end

end

end

```

FindF1

FindF1

```

%% setup inputParser
p = inputParser;
p.addRequired('f',...
    @(x) validateattributes(x, {'numeric'}, ...
    {'vector', 'nonnegative', 'increasing'}));
p.addRequired('d0',...
    @(x) validateattributes(x, {'numeric'}, ...
    {'vector'}));
p.addRequired('d1',...
    @(x) validateattributes(x, {'numeric'}, ...
    {'vector'}));
p.addRequired('negZ',...
    @(x) validateattributes(x, {'numeric'}, ...
    {'2d', 'nonempty'}));
p.addRequired('minPow',...
    @(x) validateattributes(x, {'numeric'}, ...
    {'vector'}));
p.addRequired('slen',...
    @(x) validateattributes(x, {'numeric'}, ...
    {'scalar', 'integer', 'positive', '>', 1}));
p.addRequired('bin',...
    @(x) validateattributes(x, {'numeric'}, ...
    {'scalar', 'integer', 'positive'}));
p.parse(f, d0, d1, negZ, minPow, slen, bin)
%%

posZ1 = zeros(1,4);

% contingency for multiple peaks - aim to identify left-most peak in range for
upper bound of k in next loop (avoid falling into local minimum)
if size(negZ, 1) > 1
    negZ = sortrows(negZ, 3);      % sort by frequency (ascending)
    for z = 1:size(negZ, 1)
        if log10(negZ(z, 4)) > minPow(negZ(1,2)) || negZ(z, 4) > (0.5* d0(bin)) %
relax power constraint, as may result in excessively narrow alpha window in noisy
spectra with shallow peakF (i.e. precisely where we want CoG to take breadth into
account)
            leftPeak = negZ(z, 2);
            break          % break off search when conditions satisfied
        else leftPeak = bin;      % if fail to satisfy search conditions, default
to bin (sub)peak
            end
        end
    else leftPeak = bin;          % if no other peaks were identified, take bin
(sub)peak as boundary
    end

cnt = 0;                        % start counter at 0
for k = 2:leftPeak-1           % step through frequency bins up to left-most peak
in search window
    if sign(d1(k)) < sign(d1(k+1))      % look for switch from negative to
positive derivative values (i.e. upward/positive zero-crossing)
        [~, mink] = min(abs([d0(k-1), d0(k), d0(k+1)])); % search around
crossing for local minimum in d0 (indexing 1st derivative sometimes results in
small errors)
        if mink == 1
            minim = k-1;
        end
    end
end

```



```
    minim = k;
    else
        minim = k+1;
    end

    cnt = cnt+1;           % advance counter by 1
    posZ1(cnt,1) = cnt;    % zero-crossing count
        posZ1(cnt,2) = minim; % zero-crossing frequency bin
    posZ1(cnt,3) = f(minim); % zero-crossing frequency

    % look for consistent low d1 values for signs of shallow slope (levelling
off)
    elseif abs(d1(k)) < 1 && lessThan1(d1(k+1:k+slen))
        minim = k;
        cnt = cnt+1;           % advance counter by 1
        posZ1(cnt,1) = cnt;    % zero-crossing count
            posZ1(cnt,2) = minim; % zero-crossing frequency bin
        posZ1(cnt,3) = f(minim); % zero-crossing frequency
    end
end

end

% sort out appropriate estimates for output
if size(posZ1, 1) == 1 % if singular crossing --> report frequency
    f1 = posZ1(1, 2);
    posZ1 = posZ1(1, 3);
else % else sort by frequency values (descending),
take highest frequency (bin nearest to peak)
    posZ1 = sortrows(posZ1, -3);
    f1 = posZ1(1, 2);
    posZ1 = posZ1(1, 3);
end

end
```

FindF2

FindF2

```

%% setup inputParser
p = inputParser;
p.addRequired('f',...
    @(x) validateattributes(x, {'numeric'}, ...
    {'vector', 'nonnegative', 'increasing'}));
p.addRequired('d0',...
    @(x) validateattributes(x, {'numeric'}, ...
    {'vector'}));
p.addRequired('d1',...
    @(x) validateattributes(x, {'numeric'}, ...
    {'vector'}));
p.addRequired('negZ',...
    @(x) validateattributes(x, {'numeric'}, ...
    {'2d', 'nonempty'}));
p.addRequired('minPow',...
    @(x) validateattributes(x, {'numeric'}, ...
    {'vector'}));
p.addRequired('slen',...
    @(x) validateattributes(x, {'numeric'}, ...
    {'scalar', 'integer', 'positive', '>', 1}));
p.addRequired('bin',...
    @(x) validateattributes(x, {'numeric'}, ...
    {'scalar', 'integer', 'positive'}));
p.parse(f, d0, d1, negZ, minPow, slen, bin)
%%

posZ2 = zeros(1,4);

% contingency for multiple peaks - try to identify right-most peak in range for
upper bound of k in next loop (avoid falling into local minima)
if size(negZ, 1) > 1
    negZ = sortrows(negZ, -3);      % sort by frequency (descending)
    for z = 1:size(negZ, 1)
        if log10(negZ(z, 4)) > minPow(negZ(1,2)) || negZ(z, 4) > (0.5* d0(bin))
            rightPeak = negZ(z, 2);
            break                % break search when conditions satisfied
        else rightPeak = bin;    % if fail to satisfy search conditions, default
    to bin (sub)peak
    end
end
else rightPeak = bin;          % if no other peaks identified, take bin
(sub)peak as boundary
end

cnt = 0;                       % start counter at 0
for k = rightPeak+1:length(d1) - slen % step through frequency bins following
right-most peak (trim end of range to allow for following conditional search of d1
values < 1)
    if sign(d1(k)) < sign(d1(k+1)) % look for switch from negative to
positive derivative values (i.e. upward/positive zero-crossing)
        [~, mink] = min(abs([d0(k-1), d0(k), d0(k+1)])); % search around
crossing for local minimum in d0 (indexing 1st derivative sometimes results in
small errors)
        if mink == 1
            minim = k-1;
        elseif mink == 2
            minim = k;
        end
    end
end

```

```

    minim = k+1;
    end

    cnt = cnt+1;           % advance counter by 1
    posZ2(cnt,1) = cnt;    % zero-crossing count
    posZ2(cnt,2) = minim;  % zero-crossing frequency bin
    posZ2(cnt,3) = f(minim); % zero-crossing frequency

    % look for consistent low d1 values for signs of shallow slope (levelling off)
    elseif abs(d1(k)) < 1 && lessThan1(d1(k+1:k+slen))
        minim = k;
        cnt = cnt+1;           % advance counter by 1
        posZ2(cnt,1) = cnt;    % zero-crossing count
        posZ2(cnt,2) = minim;  % zero-crossing frequency bin
        posZ2(cnt,3) = f(minim); % zero-crossing frequency
    end
end

f2 = posZ2(1, 2);
posZ2 = posZ2(1, 3);           % can simply take first estimate for output

end

```

5.10. *LessThan1*

LessThan1

```

%% Output:
%   tval = logical
%
%% Required input:
%   d1 = segment of 1st derivative spanning approx. 1 Hz

%% setup variable check
if ~exist('d1', 'var')
    error('Provide vector containing series of 1st derivative values for slope
analysis')
elseif length(d1) < 2
    error('Length of 1st derivative segment < 2');
end
%%

t = zeros(1, length(d1));
for kx = 1:length(d1)
    t(kx) = abs(d1(kx) < 1);
end

if all(t == 1)
    tval = 1;
else
    tval = 0;
end

end

```

5.11. MeanIAF

MeanIAF

```
%% setup variable check
if ~exist('sums', 'var')
    error('Provide structure containing PAF and CoG estimate fields');
end
if ~exist('nchan', 'var')
    error('Provide vector containing number of channels in each recording')
end
%%

% peaks
nSelect = [sums.pSel] >= cmin;
if sum(nSelect) == 0
    paf = NaN;
else
    paf = sum([sums(nSelect).paf].*([sums(nSelect).pSel]./nchan(nSelect)))...
        / sum([sums(nSelect).pSel]./nchan(nSelect));
end

% gravs
nSelect = [sums.gSel] >= cmin;
if sum(nSelect) == 0
    cog = NaN;
else
    cog = sum([sums(nSelect).cog].*([sums(nSelect).gSel]./nchan(nSelect)))...
        / sum([sums(nSelect).gSel]./nchan(nSelect));
end

end
```

PeakBounds

PeakBounds

```

%% setup inputParser
p = inputParser;
p.addRequired('d0',...
    @(x) validateattributes(x, {'numeric'}, ...
    {'vector'}));
p.addRequired('d1',...
    @(x) validateattributes(x, {'numeric'}, ...
    {'vector'}));
p.addRequired('d2',...
    @(x) validateattributes(x, {'numeric'}, ...
    {'vector'}));
p.addRequired('f',...
    @(x) validateattributes(x, {'numeric'}, ...
    {'vector', 'nonnegative', 'increasing'}));
p.addRequired('w',...
    @(x) validateattributes(x, {'numeric'}, ...
    {'nonnegative', 'increasing', 'size', [1 2]}));
p.addRequired('minPow',...
    @(x) validateattributes(x, {'numeric'}, ...
    {'vector'}));
p.addRequired('minDiff',...
    @(x) validateattributes(x, {'numeric'}, ...
    {'scalar', '>=', 0, '<=', 1}));
p.addRequired('fres',...
    @(x) validateattributes(x, {'numeric'}, ...
    {'scalar', 'positive'}));
p.parse(d0, d1, d2, f, w, minPow, minDiff, fres)
%%

% evaluate derivative for zero-crossings

[~, lower_alpha] = min(abs(f-w(1)));    % set lower bound for alpha band
[~, upper_alpha] = min(abs(f-w(2)));    % set upper bound for alpha band

negZ = zeros(1,4);                      % initialise for zero-crossing
count & frequency bin
cnt = 0;                                 % start counter at 0
for k = lower_alpha-1:upper_alpha+1     % step through frequency bins in
alpha band (start/end at bound +/- 1 to make sure don't miss switch)
    if sign(d1(k)) > sign(d1(k+1))      % look for switch from positive to
negative derivative values (i.e. downward zero-crossing)
        [~, maxk] = max([d0(k), d0(k+1)]);    % ensure correct frequency
bin is picked out (find larger of two values either side of crossing (in the
smoothed signal))
        if maxk == 1
            maxim = k;
        elseif maxk == 2
            maxim = k+1;
        end
        cnt = cnt+1;                      % advance counter by 1
        negZ(cnt,1) = cnt;                % zero-crossing (i.e. peak) count
        negZ(cnt,2) = maxim;             % keep bin index for later
        negZ(cnt,3) = f(maxim);          % zero-crossing frequency
        negZ(cnt,4) = d0(maxim);         % power estimate
    end
end
end

```

```

% sort out appropriate estimates for output
if negZ(1,1) == 0 % if no zero-crossing detected --> report NaNs
    peakF = NaN;
    subBin = NaN;
elseif size(negZ, 1) == 1 % if singular crossing...
    if log10(negZ(1, 4)) > minPow(negZ(1,2)) % ...and peak power is > minimum
        threshold --> report frequency
        peakBin = negZ(1, 2);
        peakF = negZ(1, 3);
    else
        peakF = NaN; % ...otherwise, report NaNs
        subBin = NaN;
    end
else negZ = sortrows(negZ, -4); % if >1 crossing, re-sort from largest to
    smallest peak...
    if log10(negZ(1, 4)) > minPow(negZ(1,2)) % ...if highest peak exceeds
        min threshold...
        if negZ(1, 4)*(1-minDiff) > negZ(2, 4) % ...report frequency of this
            peak.
                peakBin = negZ(1, 2);
                peakF = negZ(1, 3);
            else % ...if not...
                peakF = NaN;
                subBin = negZ(1, 2); % ... index as a subpeak for
            starting alpha bound search.
        end
    else
        peakF = NaN; % ...otherwise, report NaNs
        subBin = NaN;
    end
end
end

%% search for positive (upward going) zero-crossings (minima / valleys) either
side of peak/subpeak(s)
slen = round(1/fres); % define number of bins included in shallow
slope search (approximate span = 1 Hz)

if isnan(peakF) && isnan(subBin); % if no evidence of peak activity, no
parameter estimation indicated

    posZ1 = NaN;
    posZ2 = NaN;
    f1 = NaN;
    f2 = NaN;
    inf1 = NaN;
    inf2 = NaN;
    Q = NaN;
    Qf = NaN;

elseif isnan(peakF) % deal with spectra lacking a clear primary peak (similar
strategy to peak; take highest subpeak as start point, look for minima)

    [f1, posZ1] = findF1(f, d0, d1, negZ, minPow, slen, subBin);
    [f2, posZ2] = findF2(f, d0, d1, negZ, minPow, slen, subBin);

    % inflections / Q values not calculated as these spectra won't be included in
    averaged channel peak analyses
    inf1 = NaN;

```



```

inf2 = NaN;
Q = NaN;
Qf = NaN;

else % now for the primary peak spectra

[f1, posZ1] = findF1(f, d0, d1, negZ, minPow, slen, peakBin);
[f2, posZ2] = findF2(f, d0, d1, negZ, minPow, slen, peakBin);

% define boundaries by inflection points (requires 2nd derivative of smoothed
signal)
inf1 = zeros(1,2); % initialise for zero-crossing count &
frequency
cnt = 0; % start counter at 0
for k = 1:peakBin-1 % step through frequency bins prior peak
    if sign(d2(k)) > sign(d2(k+1)) % look for switch from
        positive to negative derivative values (i.e. downward zero-crossing)
            [~, mink] = min(abs([d2(k), d2(k+1)])); % ensure correct frequency
            bin is picked out (find smaller of two values either side of crossing)
            if mink == 1
                min1 = k;
            else
                min1 = k+1;
            end
            cnt = cnt+1; % advance counter by 1
            inf1(cnt,1) = cnt; % zero-crossing count
            inf1(cnt,2) = f(min1); % zero-crossing frequency
        end
    end

% sort out appropriate estimates for output
if size(inf1, 1) == 1 % if singular crossing --> report
    frequency
    inf1 = inf1(1, 2);
else
    inf1 = sortrows(inf1, -2); % sort by frequency values (descending)...
    inf1 = inf1(1, 2); % take highest frequency (bin nearest to
peak)
end

for k = peakBin+1:length(d2)-1 % step through frequency
    bins post peak
    if sign(d2(k)) < sign(d2(k+1)) % look for upward zero-
crossing
        [~, mink] = min(abs([d2(k), d2(k+1)])); % ensure frequency bin
nearest zero-crossing point picked out (find smaller of two values either side of
crossing)
        if mink == 1
            min2 = k;
        else
            min2 = k+1;
        end
        inf2 = f(min2); % zero-crossing frequency
        break % break loop (only need to record first
crossing)
    end

end

end

```

```

% estimate approx. area under curve between inflection points either
% side of peak, scale by inflection band width
Q = trapz(f(min1:min2), d0(min1:min2));
Qf = Q / (min2-min1);

```

```
end
```

```
end
```

5.12. *PlotAvSpec*

PlotAvSpec

```

figure
if log == 1          % log-scaled plots
    plot(f, 10*log10(pSpec(ix,1).sums.muSpec), 'Color', [0 .3 .7], 'LineWidth',2)
    hold on
    plot(f, 10*log10(pSpec(ix,2).sums.muSpec), 'Color', [1 .2 0], 'LineWidth',2)
elseif log == 0     % linear-scaled plots
    plot(f, pSpec(ix,1).sums.muSpec, 'Color', [0 .3 .7], 'LineWidth',2)
    hold on
    plot(f, pSpec(ix,2).sums.muSpec, 'Color', [1 .2 0], 'LineWidth',2)
end

xlim([2 25])
xlabel('Frequency (Hz)')
ylabel('Power (normalised)')
set(gca, 'FontSize', 14)

```

5.13. *PlotSpec*

PlotSpec

```

%%
nchan = length(pSpec(ix, jx).chans);    % calculate number of included channels

figure
if log == 1          % log-scaled plots
    for kx = 1:nchan
        plot(f, 10*log10(eval(sprintf(['pSpec(' num2str(ix) ',' num2str(jx)
        ').chans(' num2str(kx) ').' psd]'))))
        hold on
    end
elseif log == 0     % linear-scaled plots
    for kx = 1:nchan
        plot(f, eval(sprintf(['pSpec(' num2str(ix) ',' num2str(jx) ').chans('
        num2str(kx) ').' psd]'))))
        hold on
    end
end

xlim([2 25])
xlabel('Frequency (Hz)')
ylabel('Power (normalised)')
set(gca, 'FontSize', 14)

```

5.14. *sgfDiff*

```
sgfDiff
```

```
%% setup inputParser
p = inputParser;
p.addRequired('x',...
    @(x) validateattributes(x, {'numeric'}, ...
    {'vector'}));
p.addRequired('Fw',...
    @(x) validateattributes(x, {'numeric'}, ...
    {'scalar', 'integer', 'positive', 'odd'}));
p.addRequired('poly',...
    @(x) validateattributes(x, {'numeric'}, ...
    {'scalar', 'integer', 'positive', '<', Fw }));
p.addRequired('Fs',...
    @(x) validateattributes(x, {'numeric'}, ...
    {'scalar', 'integer', 'positive'}));
p.addRequired('tlen',...
    @(x) validateattributes(x, {'numeric'}, ...
    {'scalar', 'integer', 'positive'}));
p.parse(x, Fw, poly, Fs, tlen)
%%

[~, g] = sgolay(poly, Fw);

dt = Fs/tlen;
dx = zeros(length(x),3);
for p = 0:2 % p determines order of estimated derivatives
    dx(:,p+1) = conv(x, factorial(p)/(-dt)^p * g(:,p+1), 'same');
end

d0 = dx(:,1); % smoothed signal post S-G diff filt
d1 = dx(:,2); % 1st derivative
d2 = dx(:,3); % 2nd derivative

end
```

Appendix 2

Full Results

i) Mean Frequency (mFREQ)

The data distribution is complex due to the frequency bands used (Beta, Alpha, Theta Delta) but is similar across both cohorts (Figure 42).

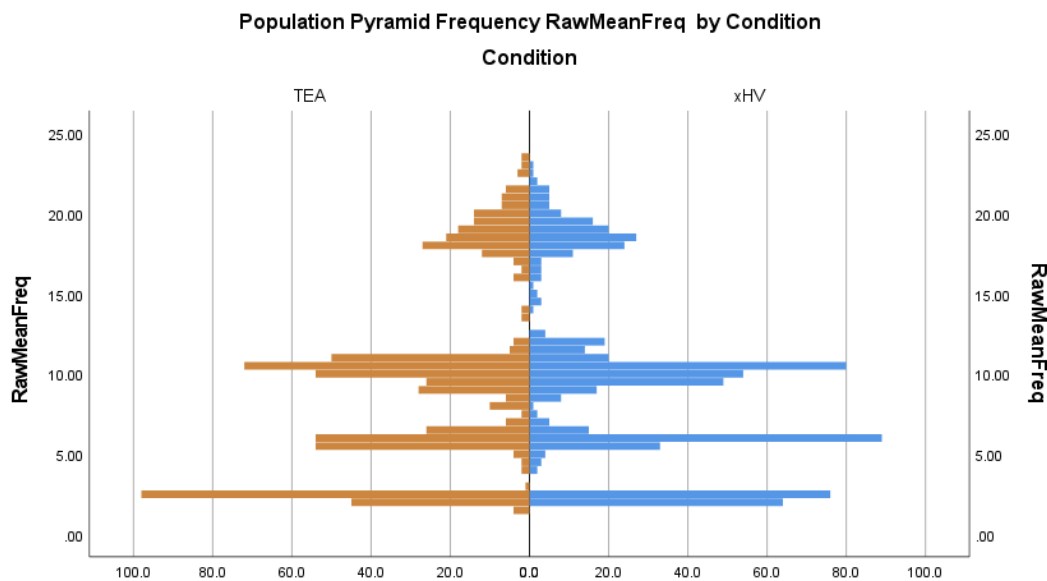


Figure 42: Mean Frequency Distribution: Comparison across TEA and HV cohorts

The mean across all data is 9.27, with a standard error (SE) of 0.15 and a standard deviation (SD) of 5.69. The interquartile range is 5.55 and the range is 22.0, whilst the variance is 32.35. There is a moderate positive skew, and the data shows a platykurtic tendency overall (Table 8). Unsurprisingly, the dataset does not meet the test criteria for normality (Table 7).

Table 7: Normality Tests for Mean Frequency, Mean Power, Interhemispheric Mean Frequency difference, and Interhemispheric Mean Power Difference.

Tests of Normality - Continuous Variables							
	Condition	Kolmogorov-Smirnov ^a			Shapiro-Wilk		
		Statistic	df	Sig.	Statistic	df	Sig.
RawMeanFreq	TEA	.160	699	<.001	.907	699	<.001
	xHV	.132	700	<.001	.913	700	<.001
RawMeanPower	TEA	.283	699	<.001	.471	699	<.001
	xHV	.291	700	<.001	.458	700	<.001
InterHemisphere_RawMeanFreq	TEA	.307	699	<.001	.454	699	<.001
	xHV	.310	700	<.001	.333	700	<.001
InterHemisphere_RawMeanPower	TEA	.184	699	<.001	.844	699	<.001
	xHV	.178	700	<.001	.801	700	<.001

a. Lilliefors Significance Correction

Table 8: Data descriptors for Mean Frequency, Mean Power, Interhemispheric Mean Frequency difference, and Interhemispheric Mean Power Difference.

		Statistics			
		RawMeanFreq	RawMeanPower	InterHemisphere_RawMeanFreq	InterHemisphere_RawMeanPower
N	Valid	1400	1399	1400	1399
	Missing	0	1	0	1
Mean		9.2798	1.812076	-.140137	-.169390
Std. Error of Mean		.15203	.0836239	.0998206	.3368066
Median		9.3800 ^a	.890766 ^a	.001224 ^a	-.014689 ^a
Std. Deviation		5.68845	3.1278007	3.7349460	12.5976489
Variance		32.358	9.783	13.950	158.701
Skewness		.554	6.398	-3.884	-1.316
Std. Error of Skewness		.065	.065	.065	.065
Kurtosis		-.643	58.653	82.767	9.383
Std. Error of Kurtosis		.131	.131	.131	.131
Range		22.00	41.4597	96.9388	140.3050
Minimum		1.50	.0424	-50.0000	-88.0060
Maximum		23.50	41.5021	46.9388	52.2989
Percentiles	25	5.4368 ^b	.438672 ^b	-.214815 ^b	-2.360751 ^b
	50	9.3800	.890766	.001224	-.014689
	75	10.9821	1.927769	.215422	3.060760

a. Calculated from grouped data.
 b. Percentiles are calculated from grouped data.

As expected, the frequency band shows a close correlation with mean frequency in the order beta, alpha, theta, delta (high to low) - correlation coefficient -0.539, $p < 0.001$, 95% CI -0.584 to -0.047 (Figure 43).

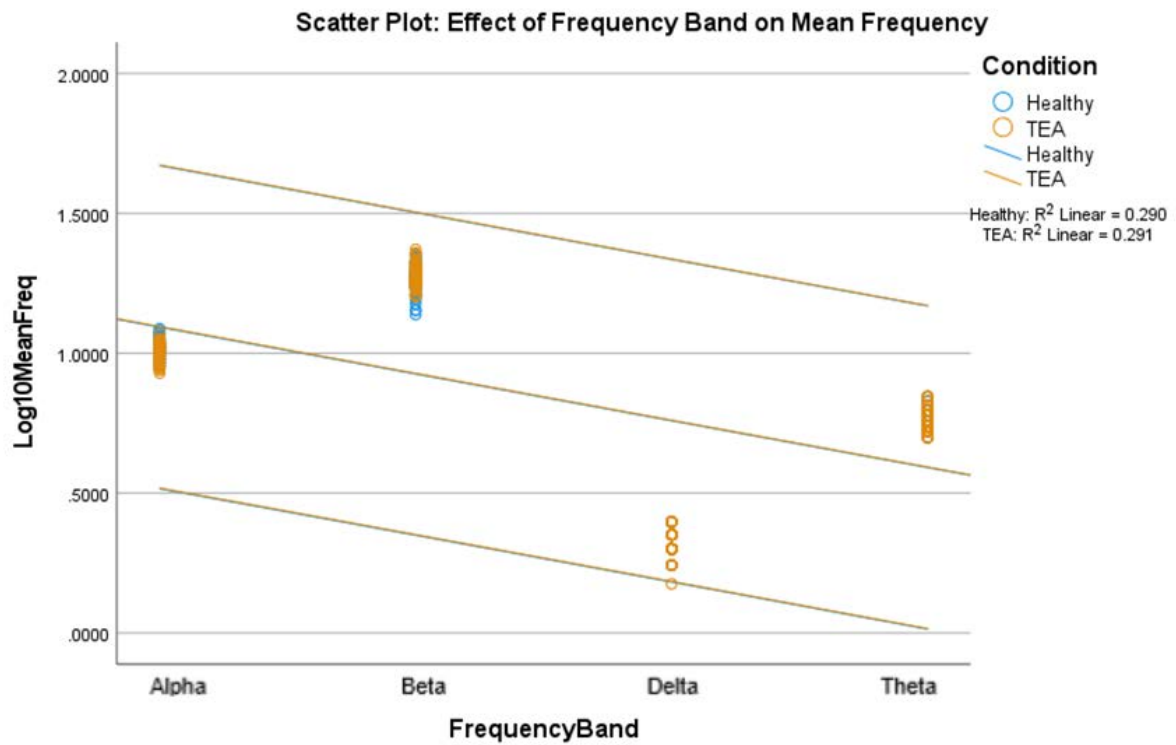


Figure 43: As expected, mean frequency shows a close correlation across frequency bands.

ii) Mean Power (mPSD)

The data distribution is similar across the TEA and HV cohorts (Figure 44).

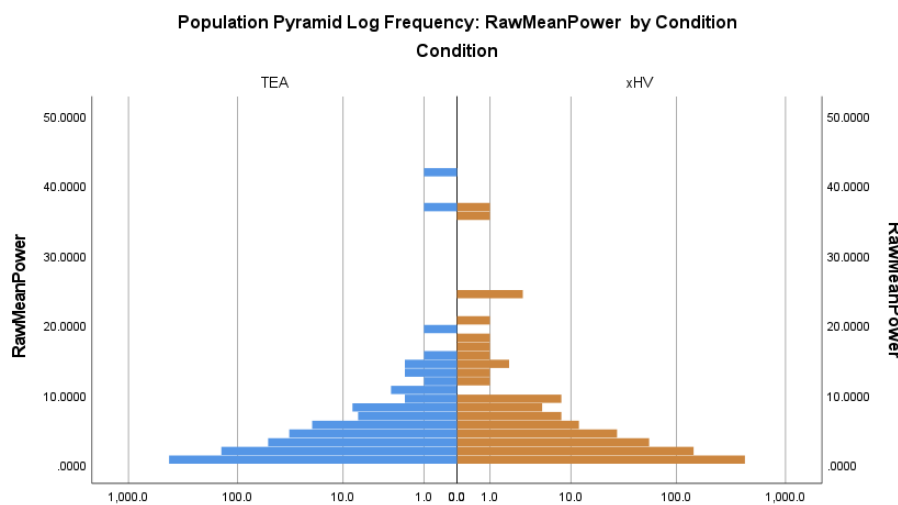


Figure 44: mPSD distribution by cohort

The dataset has one missing value, which was excluded (TEA12, frontal region, delta frequency band). The mean across all data is 1.81, with a standard error (SE) of 0.08 and a standard deviation (SD) of 3.13. The interquartile range is 1.89 and the range is 41.46, whilst the variance is 9.78. There is a marked positive skew, and the data shows a strong leptokurtic tendency overall (Table 8). Unsurprisingly, the dataset does not meet the test criteria for normality (Table 7).

Table 9: Comparison of mPSD by Sex (M/F)

Report - mPSD vs Sex		
RawMeanPower		
Sex	Mean	Median
F	2.374595	1.228768
M	1.624391	.797668
Total	1.812076	.890766

There is a correlation of sex with mean power, with females within the group showing a higher mean power overall (correlation coefficient -0.126, $p < 0.001$, 95% CI -0.190 to -0.061) (Table 9).

mPSD demonstrates a relationship concerning the region, with frontal and occipital regions having slightly higher spectral power than parietal and temporal regions overall (correlation coefficient -0.114, $p < 0.001$, 95% CI -0.178 to -0.049) (Figure 45).

Inter-hemisphere mean power is relatively symmetrical over frontal, parietal and occipital regions (where symmetry is represented by 2.0) however, whilst several participants show symmetry over the temporal region, some demonstrate asymmetry indicating an inter-hemisphere difference between temporal regions (correlation coefficient -0.335, $p < 0.001$, 95% CI -0.391 to -0.275) Figure 46. The data displayed at this level does not allow for side specificity regarding asymmetry.

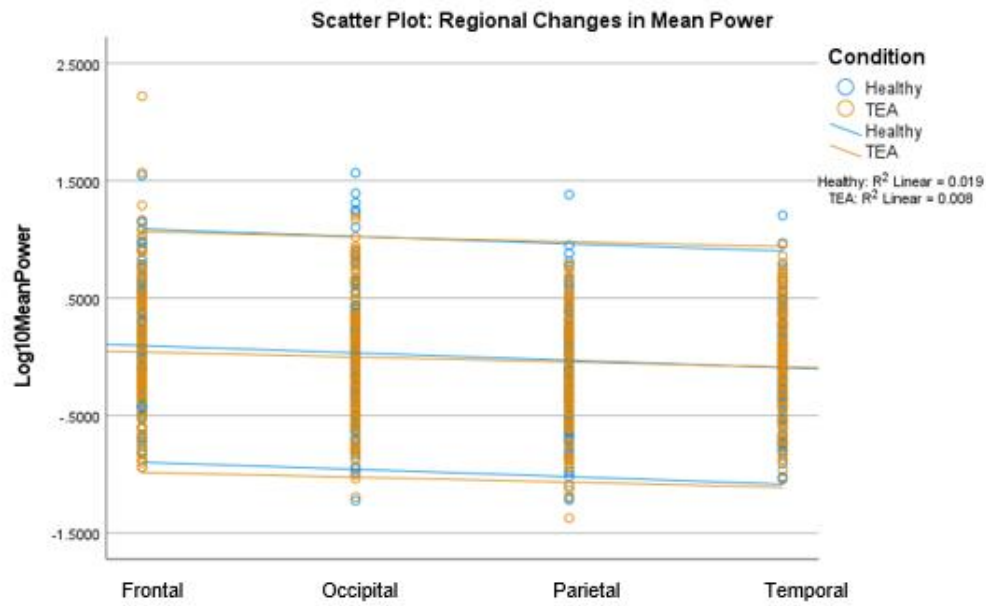


Figure 45: Mean power differences across regions

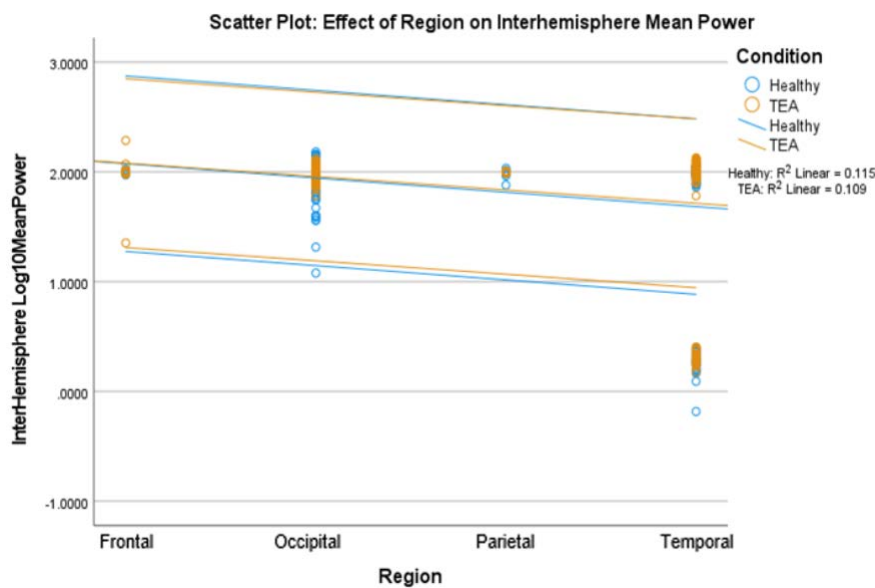


Figure 46: Inter-hemisphere differences for mean power. Note the split dataset over temporal regions (the analysis is not side-specific regarding asymmetry). 2.0000 represents symmetry between hemispheres.

Mean spectral power and inter-hemisphere mean power also show significant correlation concerning frequency band, with correlation coefficients of -0.112 and -0.107, $p < 0.001$ and $p = 0.001$ and, 95% CI of -0.176 to -0.047 and -0.171 to -0.042 respectively. A progressive reduction in mean spectral power is seen through alpha, delta, and theta to beta frequency bands (Figure 47). Regarding inter-hemisphere correlation, alpha, beta, and theta bands

show relative symmetry (where symmetry is represented by 2.0), but a split in the delta band data is seen with some participants showing symmetry and others an asymmetry in delta power between left and right hemisphere

Figure 48).

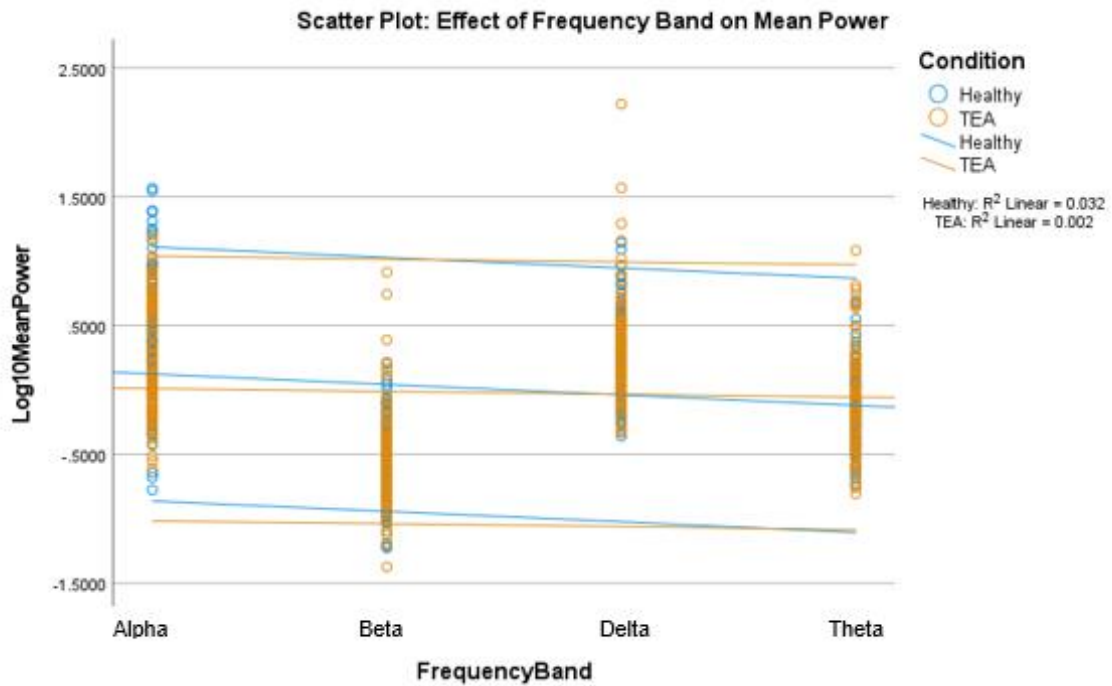


Figure 47: Variation of mean spectral power within frequency bands.

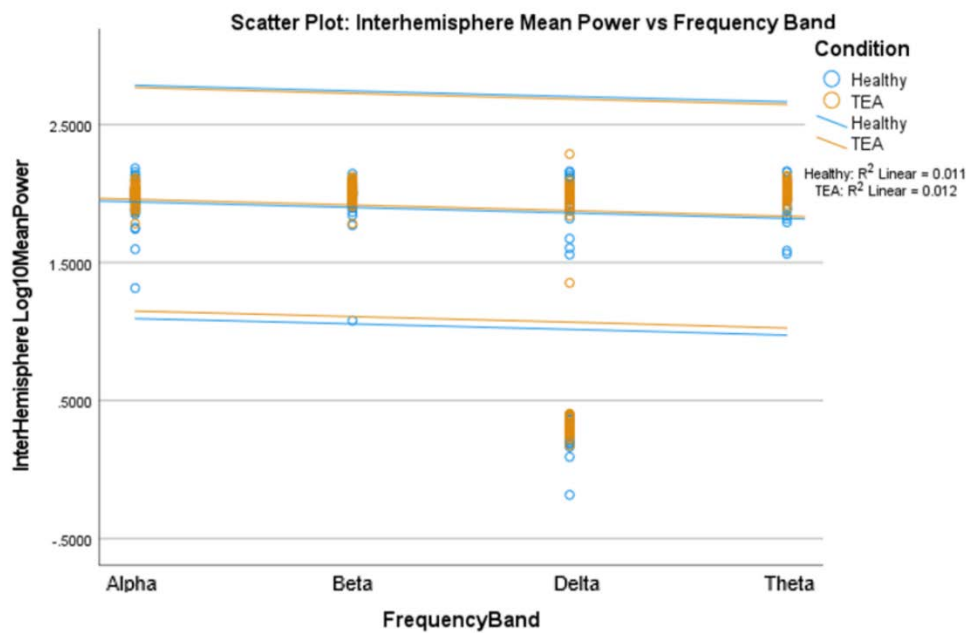


Figure 48: Inter-hemisphere mean power difference within frequency bands (2.0000 represents symmetry between the hemispheres. Note the split dataset in the delta frequency band).

iii) Imaginary Coherence (iCoh) connectivity measure

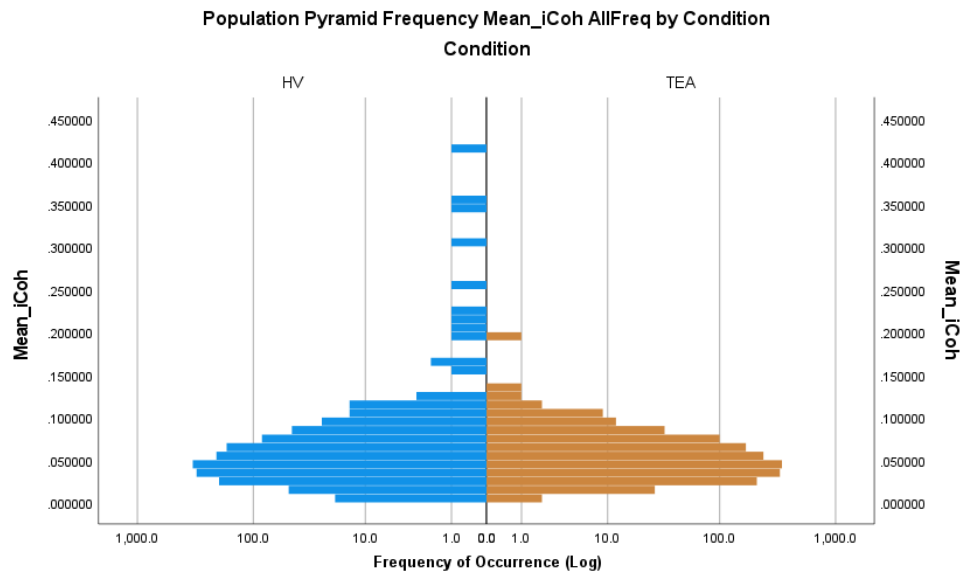


Figure 49: Imaginary Coherence (iCoh), high level distribution across TEA and HV cohorts (all frequencies, all regions)

The iCoh data distribution profile is similar across TEA and HV cohorts, with some higher iCoh outliers in the HV data (Figure 49). The mean iCoh across all data is 0.048, with a standard error (SE) of 0.0004 and a standard deviation (SD) of 0.024. The interquartile range is 0.025 and the range is 0.415, whilst the variance is 0.001 (Table 10). The iCoh dataset, including all frequencies and all regions, has a marked positive skew and is very highly leptokurtic (Figure 49, Table 10). Both TEA and HV cohort distributions do not meet the criteria for normality at the global level (Table 11).

Table 10: Data descriptors for imaginary coherence (iCoh)

Statistics		
Mean_iCoh		
N	Valid	3024
	Missing	0
Mean		.04813528
Std. Error of Mean		.000446492
Std. Deviation		.024553016
Variance		.001
Skewness		5.130
Std. Error of Skewness		.045
Kurtosis		61.074
Std. Error of Kurtosis		.089
Range		.440635
Percentiles	25	.03366274
	50	.04440853
	75	.05855277

Table 11: Normality Tests for iCoh

Tests of Normality							
	Condition	Kolmogorov-Smirnov ^a			Shapiro-Wilk		
		Statistic	df	Sig.	Statistic	df	Sig.
Mean_iCoh	HV	.124	1512	<.001	.668	1512	<.001
	TEA	.062	1512	<.001	.949	1512	<.001

a. Lilliefors Significance Correction

Examining the iCoh data, within the region and between the regions of interest, shows the lowest iCoh variation over occipital regions (more marked in HV) and occipital connections intra-regionally. Frontal areas show the greatest iCoh variation intra-regionally (more noticeable in TEA data), while parietal/temporal connectivity has more variation inter-regionally (Figure 53).

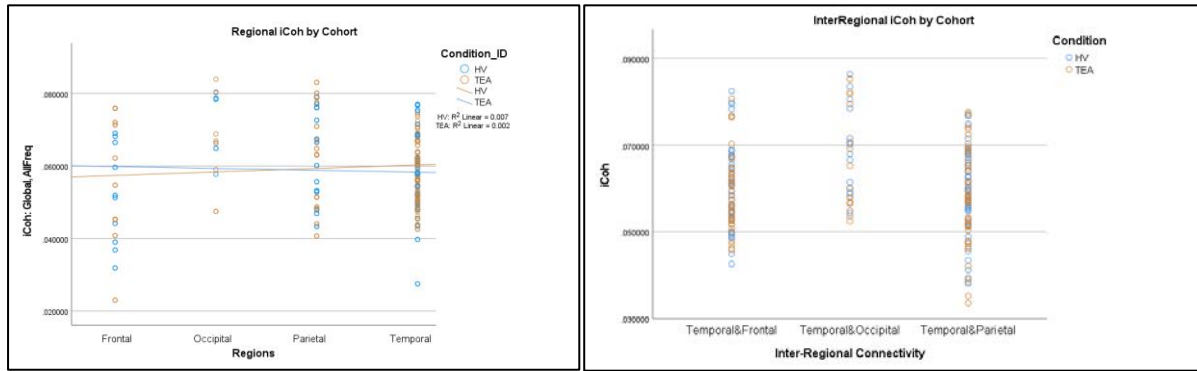


Figure 50: iCoh split by region and by cohort.

Exploring iCoh within frequency bands, alpha frequencies show the highest iCoh in both datasets. In HV subjects both delta and beta activities have the lowest iCoh, with data from the two bands mixed. The TEA cohort clearly shows beta frequencies having the lowest iCoh within the band. This difference between the cohorts appears to be due to TEA subjects having higher delta iCoh than HV, separating the two frequency bands, rather than any beta variation between the cohorts. (Figure 51).

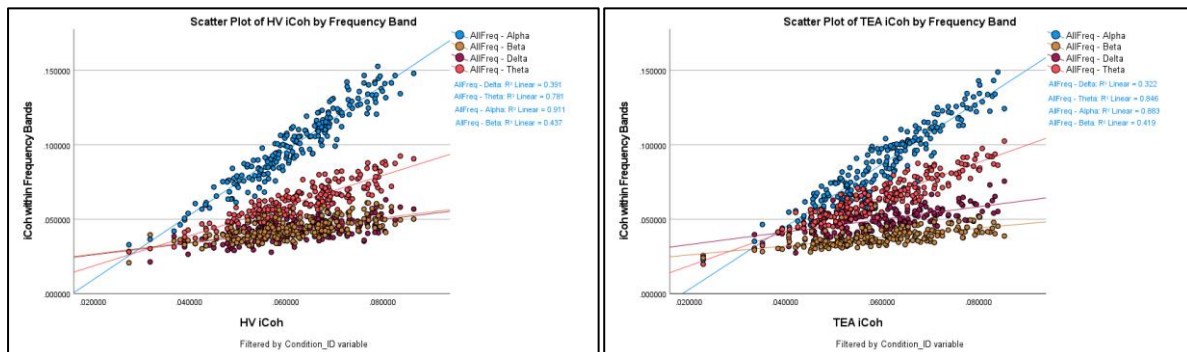


Figure 51: iCoh within frequency band, split by Cohort - Left =HV, Right=TEA

iv) Weighted Phase-Lag Index (wPLI) Connectivity Measure

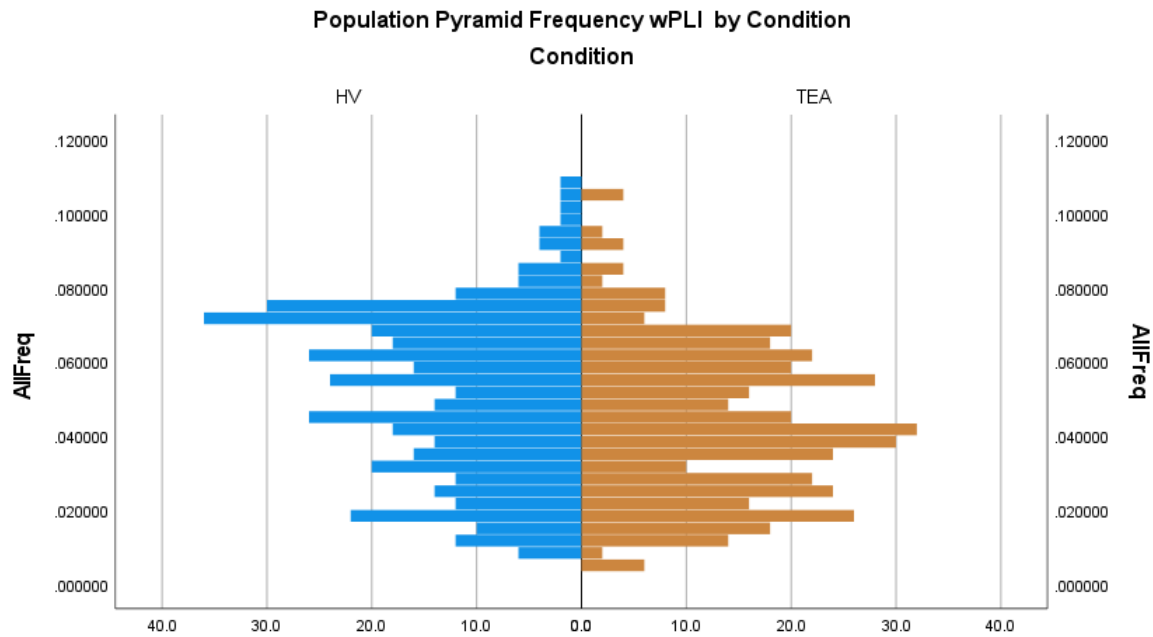


Figure 52: wPLI high level distribution across TEA and HV cohorts (all frequencies, all regions)

The wPLI data distribution profile shows visual differences, with HV data tending towards slightly higher wPLI values overall, and TEA data showing slightly lower global wPLI compared to HV data (Figure 52). The mean wPLI across all data is 0.047, with a standard error (SE) of 0.0008 and a standard deviation (SD) of 0.022. The interquartile range is 0.0181 and the range is 0.104, whilst the variance is 0.000 (Table 10). The wPLI dataset, including all frequencies and all regions, has only a slight positive skew and is leptokurtic (Figure 52, Table 13). Both TEA and HV cohort distributions do not meet the criteria for normality at the global level (Table 12).

Table 12: Tests for Normality - wPLI

Tests of Normality							
Condition	Kolmogorov-Smirnov ^a			Shapiro-Wilk			
	Statistic	df	Sig.	Statistic	df	Sig.	
AllFreq HV	.067	420	<.001	.977	420	<.001	
AllFreq TEA	.055	420	.004	.980	420	<.001	

a. Lilliefors Significance Correction

Statistics - wPLI		
AllFreq		
N	Valid	840
	Missing	42
Mean		.04747617
Std. Error of Mean		.000759973
Median		.04646030
Std. Deviation		.022026098
Variance		.000
Skewness		.177
Std. Error of Skewness		.084
Kurtosis		-.629
Std. Error of Kurtosis		.169
Range		.104855
Percentiles	25	.02943200
	50	.04646030
	75	.06455771

Table 13: Data descriptors for wPLI

Examining the wPLI data, within the region and between the regions of interest, shows the least wPLI variation over occipital regions (more marked in HV) and occipital connections interregionally. Parietal areas show the greatest wPLI variation (more marked in HV), which is reflected to a lesser extent in parietal connections interregionally (Figure 53).

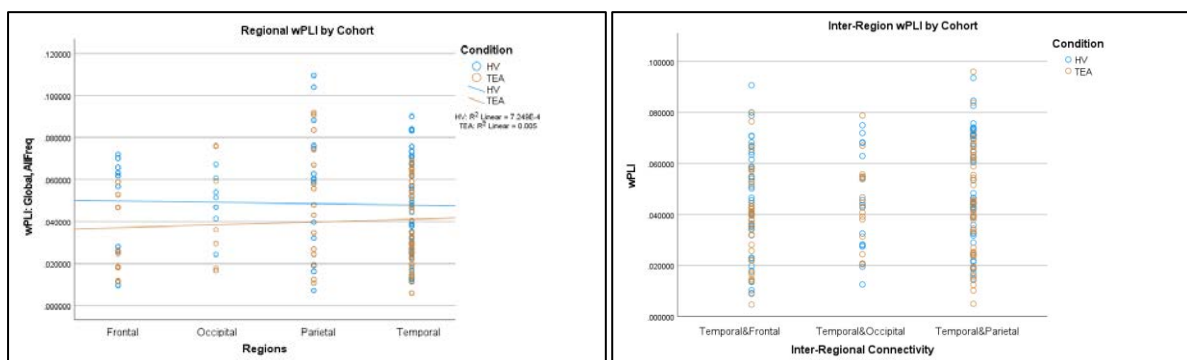


Figure 53: wPLI regional split by cohort. Left: intra-regional and Right: inter-regional

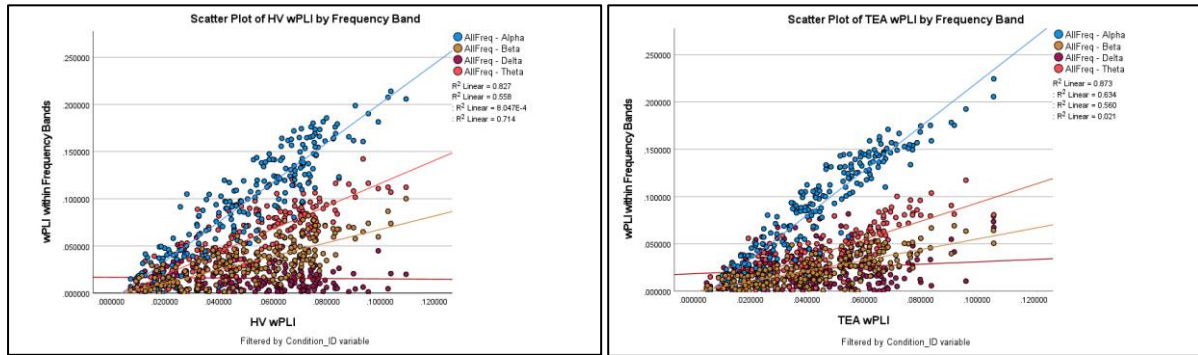


Figure 54: wPLI within frequency band, split by Cohort - Left =HV, Right=TEA

Exploring wPLI within frequency bands, alpha frequencies show the highest wPLI and delta the lowest wPLI. This finding is seen in both HV and TEA cohorts, although TEA participants show less variation overall with regards to alpha and more variation with higher wPLI within delta frequencies. Slightly lower wPLI is noted overall in the Theta band, and slightly higher in the delta band in TEA subjects (Figure 54).

v) Phase-Transfer Entropy (PTE) Directional Connectivity Measure

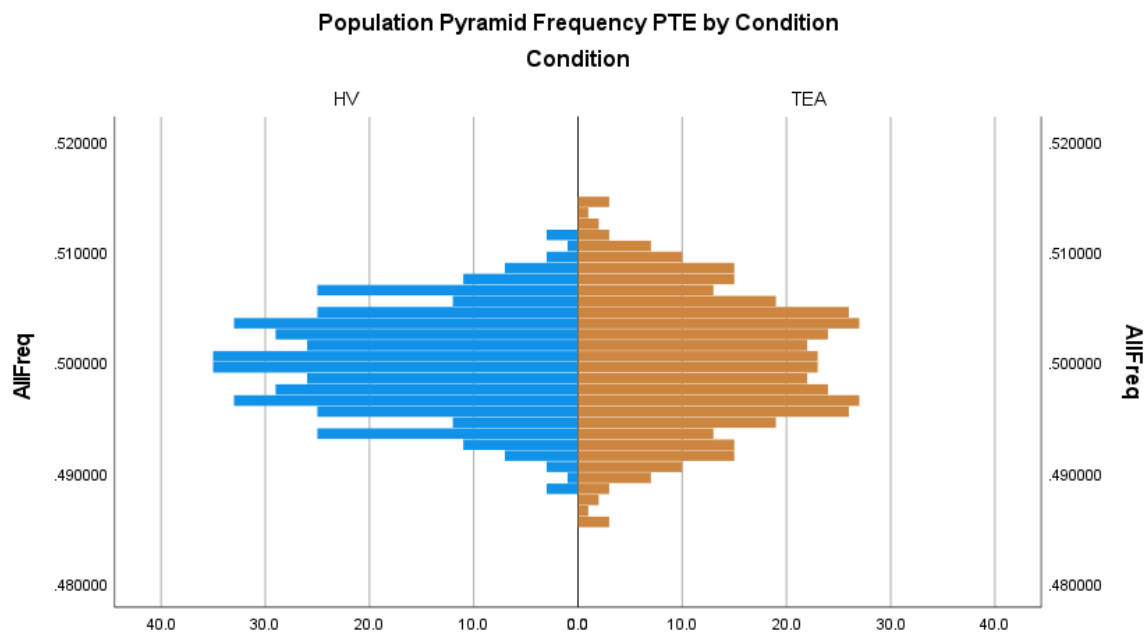


Figure 55: PTE high level distribution across TEA and HV cohorts (all frequencies, all regions)

The PTE dataset distribution profile shows some visual differences, with HV data tending towards higher PTE values around 0.5 overall, and TEA data showing a slightly broader bimodal range of PTE values compared to HV data (Figure 55). The mean PTE across all data is 0.5, with a standard error (SE) of 0.0002 and a standard deviation (SD) of 0.0053. The interquartile range is 0.0078 and the range is 0.0297, whilst the variance is 0.000 (Table 14). The PTE dataset, including all frequencies and all regions, shows no skew and is platykurtic (Figure 55, Table 14). At a global level, the TEA distribution meets the criteria for normality, whilst HV data does not (Table 15).

Table 14: Data descriptors for PTE

Statistics - PTE		
AllFreq		
N	Valid	840
	Missing	42
Mean		.50000000
Std. Error of Mean		.000183007
Median		.50000000
Std. Deviation		.005304050
Variance		.000
Skewness		.000
Std. Error of Skewness		.084
Kurtosis		-.436
Std. Error of Kurtosis		.169
Range		.029710
Percentiles	25	.49610314
	50	.50000000
	75	.50389686

Table 15: Tests for Normality - PTE data by cohort

Tests of Normality							
	Condition	Kolmogorov-Smirnov ^a			Shapiro-Wilk		
		Statistic	df	Sig.	Statistic	df	Sig.
AllFreq	HV	.041	420	.086	.993	420	.035
	TEA	.037	420	.191	.994	420	.069

a. Lilliefors Significance Correction

Exploring PTE within regions, both parietal and temporal regions show the greatest variation in PTE values (more so in the TEA cohort), whilst occipital regions show the least. (Figure 56). As PTE is a directional connectivity measure, it shows the different network distributions going into and out of the temporal lobe. Generally, network activity has lower PTE out from the temporal lobe to all regions of interest (frontal, parietal, occipital). The lowest PTE values tend to be from the TEA cohort, as do most of the highest, suggesting a wider range of PTE magnitude generally within TEA data (Figure 56).

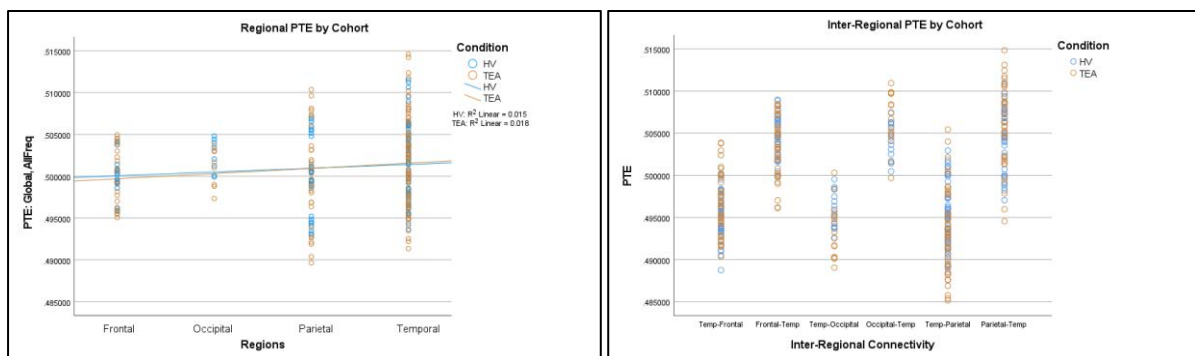


Figure 56: PTE regional split by cohort. Left: intra-regional and Right: inter-regional

Examining PTE data from a frequency band perspective, both HV and TEA datasets cluster around a mean of around 0.5. Overall, HV participant PTE values show less variation than those from TEA subjects. This is particularly noticeable within the beta band, but the effect is seen in all frequency bands (Figure 57).

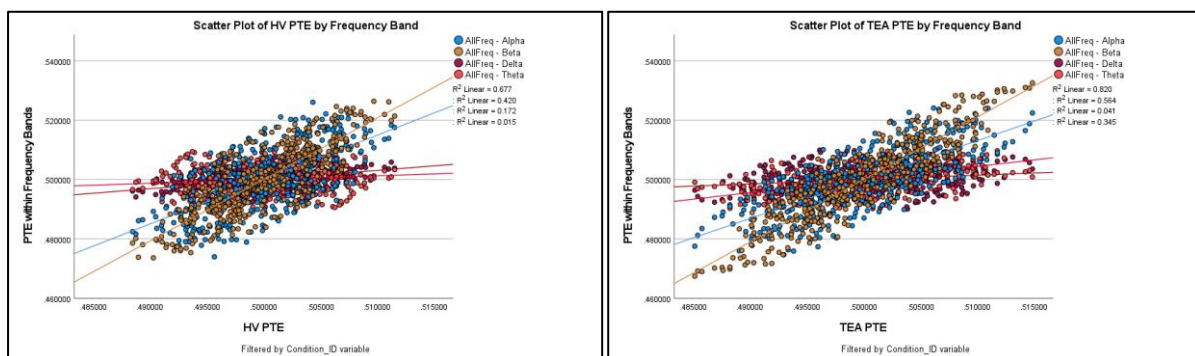


Figure 57: PTE within frequency band, split by Cohort - Left =HV, Right=TEA

First Phase – Spectral Analysis of Mean Frequency (mFREQ)

The analysis aimed to determine the effects TEA may have on mean frequency (mFREQ), considering variation within the frequency band and brain regions.

mFREQ, and inter-hemisphere mFREQ spectra were computed for global and regional cortical activities. Relative frequency analysis was calculated within frequency bands (beta, alpha, theta, delta) for both global and regional spectra.

Dataset distributions were assessed using SPSS explore and Shapiro-Wilk tests were performed to check for normality. Comparison of TEA and HV cohorts was undertaken using a parametric Independent Samples T-Test for normal distributions; otherwise, a non-parametric Independent Samples Mann-Whitney U test was performed. Statistical significance was set at $p = <0.05$. To control for type I errors generated by the false rejection of the null hypothesis through multiple comparisons within the regional, and frequency band analysis, False Discovery Rate (FDR) adjustments using the classic one-stage, and two-stage sharpened methods were undertaken (Benjamini and Hochberg, 1995; Benjamini and Hochberg, 2000; Benjamini *et al.*, 2006; Pike, 2011; Nichols, 2007) with before p -values, and after correction q -values being reported within the results.

1. Global mFREQ– All Frequencies

Shapiro-Wilk tests for normality showed that within the global dataset, both mFREQ distributions fall outside the criteria for normality (Table 16).

Table 16: Global Datasets: Shapiro-Wilk tests for normality. mFREQ and mPSD data.

Tests of Normality							
	Condition	Kolmogorov-Smirnov ^a			Shapiro-Wilk		
		Statistic	df	Sig.	Statistic	df	Sig.
Total_mf_ALL	Healthy	.155	28	.083	.879	28	.004
	TEA	.225	28	<.001	.844	28	<.001
Total_mp_ALL	Healthy	.232	28	<.001	.714	28	<.001
	TEA	.233	28	<.001	.761	28	<.001
Total_mf_LT/RT ALL	Healthy	.326	28	<.001	.553	28	<.001
	TEA	.252	28	<.001	.665	28	<.001
Total_mp_LT/RT ALL	Healthy	.101	28	.200*	.985	28	.942
	TEA	.172	28	.033	.848	28	<.001

*. This is a lower bound of the true significance.
a. Lilliefors Significance Correction

Table 17: Global Datasets - Distribution Descriptors. mFREQ and mPSD data.

		Statistics			
		Total_mf_ALL	Total_mp_ALL	Total_mf_LT/RT ALL	Total_mp_LT/RT ALL
N	Valid	56	56	56	56
	Missing	0	0	0	0
Mean		9.3884	1.06702379	-1.507530	-1.341825
Std. Error of Mean		.36373	.123629924	1.2652094	1.3762632
Median		9.7500	.72691554	.000000	-.807564
Std. Deviation		2.72193	.925161636	9.4679602	10.2990105
Variance		7.409	.856	89.642	106.070
Skewness		-.142	2.196	-1.909	-.570
Std. Error of Skewness		.319	.319	.319	.319
Kurtosis		5.552	5.130	11.555	3.081
Std. Error of Kurtosis		.628	.628	.628	.628
Range		18.50	4.295278	74.6296	66.7922
Minimum		1.50	.192001	-45.0000	-39.5158
Maximum		20.00	4.487280	29.6296	27.2764
Percentiles	25	9.0000	.48278421	-2.171734	-7.493036
	50	9.7500	.72691554	.000000	-.807564
	75	10.5000	1.32755765	1.031677	4.332140

1.1. mFREQ

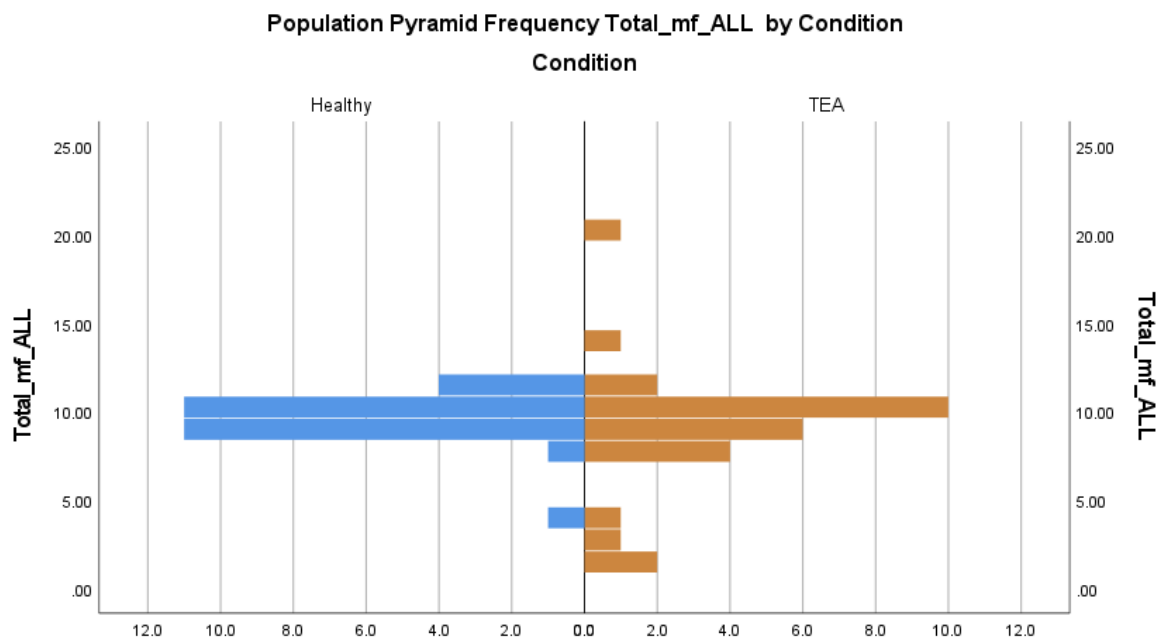


Figure 58: Global mFREQ distribution by cohort

Global mFREQ has a leptokurtic data distribution with negligible skew (Table 17, Figure 58). The mean across all data is 9.39, with a standard error (SE) of 0.36 and a standard deviation (SD) of 2.72. The interquartile range is 1.50 the range 18.5, and the variance is 7.40 (Table 17).

As both cohorts do not show a normal distribution (Table 16, Figure 58), the non-parametric Mann-Whitney U test was performed demonstrating there is no significant difference in the mFREQ profiles between the cohorts at a global level ($p = 0.393$) –Table 18.

Table 18: Statistical analysis of TEA vs. HV global mFREQ. Mann-Whitney U test.

Test Statistics^a	
	Total_mf_ALL
Mann-Whitney U	340.000
Wilcoxon W	746.000
Z	-.854
Asymp. Sig. (2-tailed)	.393
Exact Sig. (2-tailed)	.398
Exact Sig. (1-tailed)	.199
Point Probability	.002

a. Grouping Variable: Condition

1.2. Inter-hemisphere mFREQ Difference

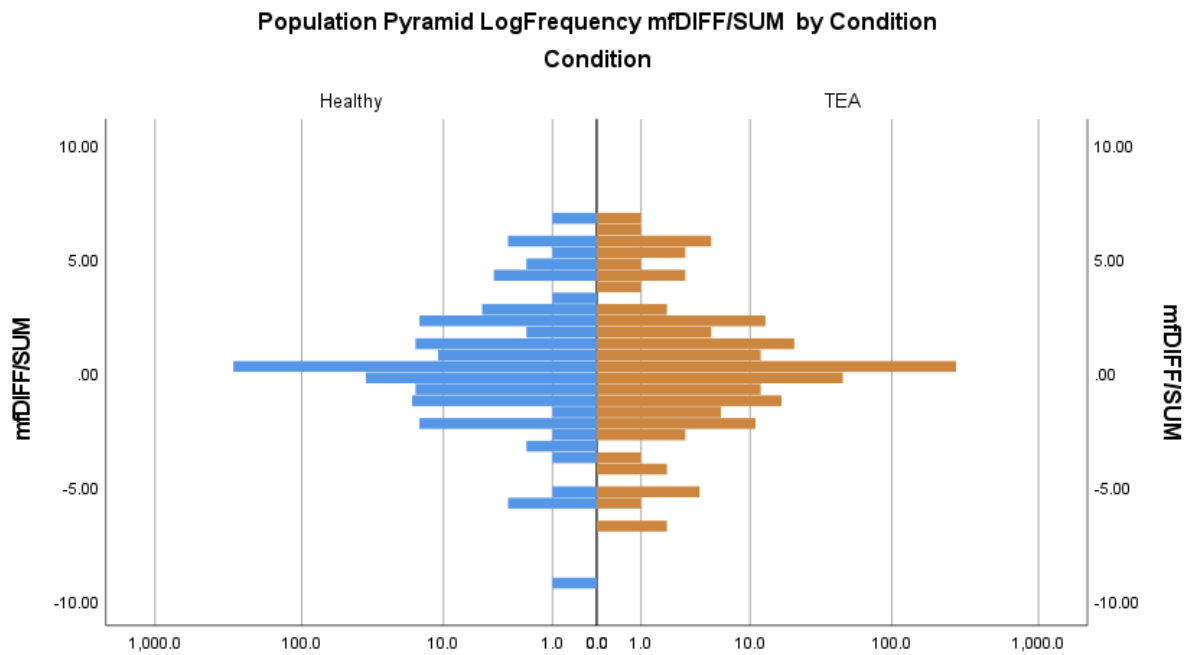


Figure 59: Global inter-hemispheric mFREQ difference distributions (log) by cohort. +ve values denote a left hemisphere bias and -ve values a right hemisphere bias.

Global inter-hemisphere mFREQ difference data is highly leptokurtic in distribution and has negligible skew (Figure 59). The mean across all data is 0.0511, with a standard error (SE) of 0.047 and a standard deviation (SD) of 1.418. The interquartile range is 0, the range is 15.76, and the variance is 2.013 (Table 20).

As neither cohort shows a normal distribution (Figure 59, Table 19), the non-parametric Man-Whitney U test was performed demonstrating there is no significant difference in the inter-hemispheric mFREQ difference profiles between the cohorts at a global level ($p = 0.525$) – Table 21.

Table 19: Normality tests for Interhemispheric difference of mFREQ (includes frontal, temporal, parietal and occipital regions)

Tests of Normality							
Condition	Kolmogorov-Smirnov ^a			Shapiro-Wilk			
	Statistic	df	Sig.	Statistic	df	Sig.	
mfDIFF/SUM							
Healthy	.307	448	<.001	.681	448	<.001	
TEA	.293	448	<.001	.704	448	<.001	

a. Lilliefors Significance Correction

Table 20: Data Descriptors for Interhemispheric difference in mFREQ

Statistics		
mfDIFF/SUM		
N	Valid	896
	Missing	0
Mean		.0511
Std. Error of Mean		.04740
Median		.0000
Std. Deviation		1.41891
Variance		2.013
Skewness		.198
Std. Error of Skewness		.082
Kurtosis		9.435
Std. Error of Kurtosis		.163
Range		15.76
Percentiles	25	.0000
	50	.0000
	75	.0000

Independent-Samples Mann-Whitney U Test Summary	
Total N	896
Mann-Whitney U	98103.500
Wilcoxon W	198679.500
Test Statistic	98103.500
Standard Error	3533.982
Standardized Test Statistic	-.636
Asymptotic Sig.(2-sided test)	.525

Table 21: Statistical analysis of TEA vs. HV global inter-hemispheric mFREQ difference. Mann-Whitney U test.

2. Regional mFREQ – All Frequencies

2.1. mFREQ

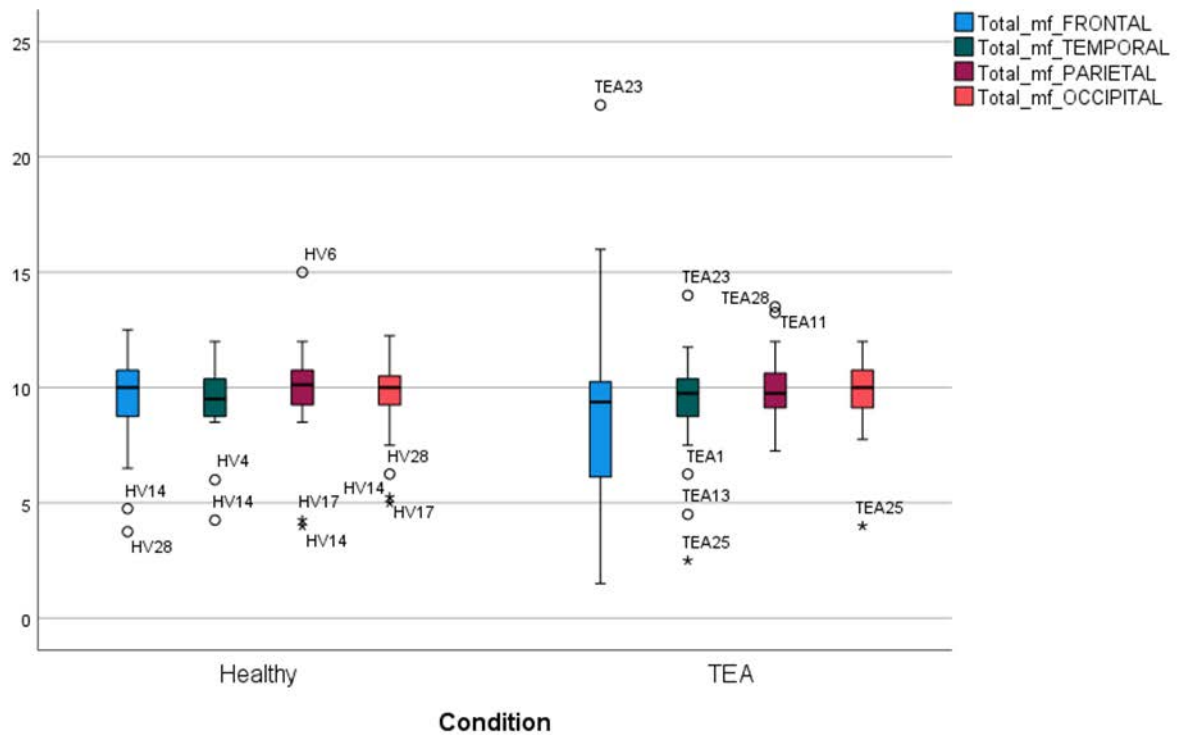


Figure 60: Boxplots for HV and TEA Regional mFREQ

Table 22: Tests for Normality for Regional mFREQ Data Distributions

Tests of Normality							
	Condition	Kolmogorov-Smirnov ^a			Shapiro-Wilk		
		Statistic	df	Sig.	Statistic	df	Sig.
Total_mf_FRONTAL	Healthy	.146	28	.129	.899	28	.011
	TEA	.204	28	.004	.881	28	.004
Total_mf_TEMPORAL	Healthy	.193	28	.009	.855	28	.001
	TEA	.217	28	.002	.855	28	.001
Total_mf_PARIETAL	Healthy	.220	28	.001	.835	28	<.001
	TEA	.137	28	.192	.955	28	.269
Total_mf_OCCIPITAL	Healthy	.202	28	.005	.869	28	.002
	TEA	.164	28	.052	.831	28	<.001

a. Lilliefors Significance Correction

Table 23: Regional Datasets – mFREQ Distribution Descriptors

		Statistics			
		Total_mf_FRONTAL	Total_mf_TEMPORAL	Total_mf_PARIETAL	Total_mf_OCCIPITAL
N	Valid	56	56	56	56
	Missing	0	0	0	0
Mean		9.1027	9.3973	9.9464	9.6563
Std. Error of Mean		.44811	.24884	.23800	.21963
Median		9.7500	9.6250	10.0000	10.0000
Std. Deviation		3.35335	1.86217	1.78103	1.64356
Variance		11.245	3.468	3.172	2.701
Skewness		.403	-1.457	-.644	-1.521
Std. Error of Skewness		.319	.319	.319	.319
Kurtosis		4.102	4.211	3.725	3.021
Std. Error of Kurtosis		.628	.628	.628	.628
Range		20.75	11.50	11.00	8.25
Percentiles	25	8.2500	8.7500	9.2500	9.2500
	50	9.7500	9.6250	10.0000	10.0000
	75	10.4375	10.4375	10.6875	10.6875

- mFREQ within the frontal region has a leptokurtic data distribution with negligible skew. The mean across all data is 9.01, with a standard error (SE) of 0.45 and a standard deviation (SD) of 3.35 (Figure 60, Table 23). The interquartile range is 2.19, the range is 20.75, and the variance is 11.25 (Table 23). As neither cohort show a normal distribution (Table 22), a non-parametric Man-Whitney U test was performed demonstrating there is no significant difference between cohorts, within mFREQ over frontal regions ($p = 0.16$ and, using FDR two-stage sharpened method, $q=0.67$) – Table 24.
- mFREQ within the temporal region has a leptokurtic data distribution with a negative skew. The mean across all data is 9.40, with a standard error (SE) of 0.25 and a standard deviation (SD) of 1.86 (Figure 60, Table 23). The interquartile range is 1.69, the range is 11.50, and the variance is 3.47 (Table 23).
- As neither cohort show a normal distribution (Table 22), a non-parametric Man-Whitney U test was performed demonstrating there is no significant difference between cohorts, within mFREQ over temporal regions ($p = 0.90$ and, using FDR two-stage sharpened method, $q=0.94$) (Table 24).
- mFREQ data within the parietal region is relatively mesokurtic with a moderate negative skew. The mean across all data is 9.95, with a standard error (SE) of 0.24

and a standard deviation (SD) of 1.64 (Figure 60, Table 23). The interquartile range is 1.44, the range is 11.00, and the variance is 3.17 (Table 23). As only the TEA cohort shows normal distribution within parietal regions (Table 22), a non-parametric Man-Whitney U test was performed demonstrating there is no significant difference between cohorts, within mFREQ over parietal regions ($p = 0.58$ and, using FDR two-stage sharpened method, $q=0.94$) (Table 24).

- mFREQ data within the occipital region is mesokurtic with a negative skew. The mean across all data is 9.66, with a standard error (SE) of 0.22 and a standard deviation (SD) of 1.64 (Figure 60,). The interquartile range is 1.44, the range is 8.25, and the variance is 2.70 (Table 23).
- As neither cohort show a normal distribution (Table 22), a non-parametric Man-Whitney U test was performed demonstrating there is no significant difference between cohorts, within mFREQ over occipital regions ($p = 0.86$ and, using FDR two-stage sharpened method, $q=0.94$) (Table 24).

Table 24: Regional mFREQ - Multiple Comparisons using False Discovery Rates (FDRs) Adjustments

FDR		Hypothesis name	Parametric	Classical one-stage method*		Two-stage sharpened method†		
Order	Ascending p -values			FDR-derived significance thresholds	FDR-adjusted p -values a.k.a. q -values	Stage 1 significance thresholds	Stage 2 significance thresholds	FDR-adjusted p -values a.k.a. q -values
1	0.16030	Total_mf_FRONTAL		0.0125	0.641212	0.0119048	0.0119048	0.6732726
2	0.58192	Total_mf_PARIETAL		0.025	0.895267	0.0238095	0.0238095	0.94003035
3	0.85639	Total_mf_OCCIPITAL		0.0375	0.895267	0.0357143	0.0357143	0.94003035
4	0.89527	Total_mf_TEMPORAL		0.05	0.895267	0.047619	0.047619	0.94003035

2.2. Interhemispheric mFREQ Difference

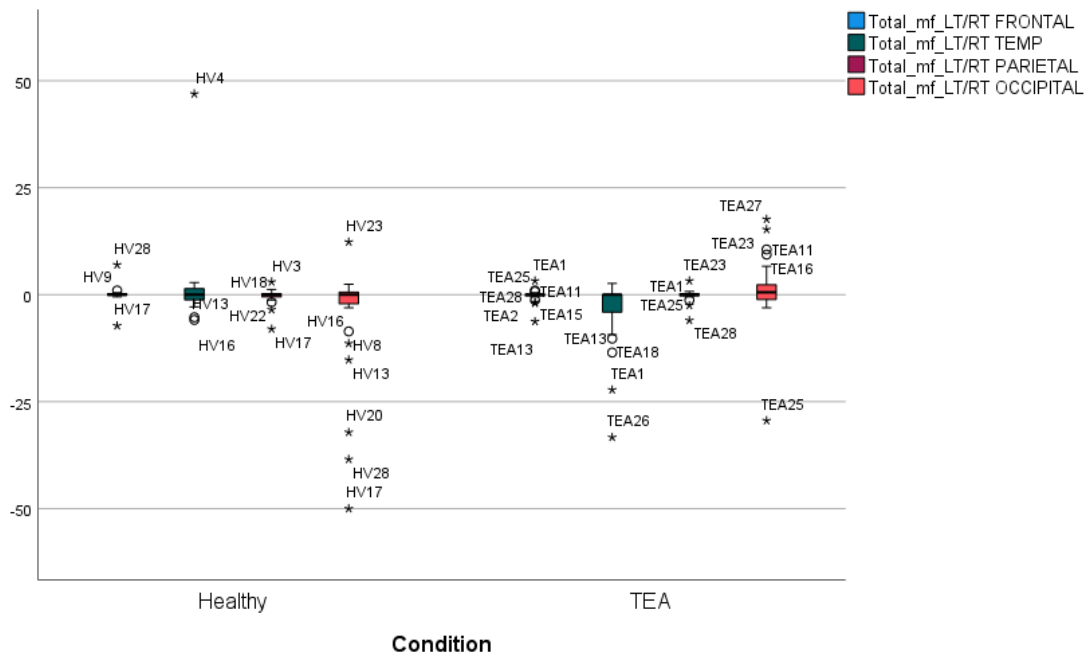


Figure 61: Boxplots for HV and TEA Regional Interhemispheric mFREQ Differences

Table 25: Regional Datasets – Interhemispheric mFREQ Difference Descriptors

		Statistics			
		Total_mf_LT/RT FRONTAL	Total_mf_LT/RT TEMP	Total_mf_LT/RT PARIETAL	Total_mf_LT/RT OCCIPITAL
N	Valid	56	56	56	56
	Missing	0	0	0	0
Mean		-.107143	-.958451	-.276786	-1.911502
Std. Error of Mean		.2309158	1.1885773	.2197326	1.5204972
Median		.000000	.000000	.000000	.000000
Std. Deviation		1.7280159	8.8944981	1.6443281	11.3783595
Variance		2.986	79.112	2.704	129.467
Skewness		-.760	1.688	-2.570	-2.454
Std. Error of Skewness		.319	.319	.319	.319
Kurtosis		12.138	18.234	10.849	7.601
Std. Error of Kurtosis		.628	.628	.628	.628
Range		14.2500	80.2721	11.2500	67.6471
Percentiles	25	-.250000	-1.360731	-.250000	-1.204819
	50	.000000	.000000	.000000	.000000
	75	.250000	1.220044	.250000	1.258009

Table 26: Tests for Normality for Regional Interhemispheric mFREQ Difference Distributions

Tests of Normality							
	Condition	Kolmogorov-Smirnov ^a			Shapiro-Wilk		
		Statistic	df	Sig.	Statistic	df	Sig.
Total_mf_LT/RT FRONTAL	Healthy	.371	28	<.001	.493	28	<.001
	TEA	.290	28	<.001	.686	28	<.001
Total_mf_LT/RT TEMP	Healthy	.409	28	<.001	.387	28	<.001
	TEA	.283	28	<.001	.656	28	<.001
Total_mf_LT/RT PARIETAL	Healthy	.275	28	<.001	.687	28	<.001
	TEA	.307	28	<.001	.679	28	<.001
Total_mf_LT/RT OCCIPITAL	Healthy	.362	28	<.001	.636	28	<.001
	TEA	.293	28	<.001	.712	28	<.001

a. Lilliefors Significance Correction

Inter-hemispheric mFREQ difference data within the frontal region has a very highly leptokurtic data distribution with a negative skew. The mean across all data is -0.11, with a standard error (SE) of 0.23 and a standard deviation (SD) of 1.73 (Figure 61, Table 25). The interquartile range is 0.50, the range is 14.25, and the variance is 2.99 (Table 25). As neither cohort shows a normal distribution (Table 26), a non-parametric Man-Whitney U test was performed demonstrating there is no significant difference in the inter-hemispheric mFREQ difference profiles between the cohorts at a global level ($p = 0.41$ and, using FDR two-stage sharpened method, $q=0.58$) – Table 27.

Inter-hemispheric mFREQ difference data within the temporal region has a very highly leptokurtic data distribution and is highly positively skewed. The mean across all data is -0.96, with a standard error (SE) of 1.19 and a standard deviation (SD) of 8.89 (Figure 61, Table 25). The interquartile range is 2.58, the range is 80.27, and the variance is 79.11 (Table 25). As neither cohort shows a normal distribution (Table 26), a non-parametric Man-Whitney U test was performed demonstrating there is no significant difference in the inter-hemispheric mFREQ difference profiles between the cohorts at a global level ($p = 0.07$, using FDR two-stage sharpened method $q=0.15$) –Table 27.

Inter-hemispheric mFREQ difference data within the parietal region is highly leptokurtic with a significant negative skew. The mean across all data is -0.28, with a standard error (SE) of 0.22 and a standard deviation (SD) of 1.64 (Figure 61, Table 25). The interquartile range is 0.50, the range is 11.25, and the variance is 2.70 (Table 25). As neither cohort shows a

normal distribution (Table 26), a non-parametric Man-Whitney U test was performed demonstrating there is no significant difference in the inter-hemispheric mFREQ difference profiles between the cohorts at a global level ($p = 0.87$ and, using FDR two-stage sharpened method, $q=0.92$) – Table 27.

Inter-hemispheric mFREQ difference data within the occipital region is highly leptokurtic with a significant negative skew. The mean across all data is -1.91, with a standard error (SE) of 1.52 and a standard deviation (SD) of 11.38 (Figure 61, Table 25). The interquartile range is 2.46, the range is 67.64, and the variance is 129.47 (Table 25). As neither cohort shows a normal distribution (Table 26), a non-parametric Man-Whitney U test was performed demonstrating there is no significant difference in the inter-hemispheric mFREQ difference profiles between the cohorts at a global level ($p = 0.07$ and, using FDR two-stage sharpened method, $q=0.15$) – Table 27.

Table 27: Regional Interhemispheric mFREQ Differences - Multiple Comparisons using False Discovery Rates (FDRs) Adjustments

FDR			Classical one-stage method*		Two-stage sharpened method†		
Order	Ascending p -values	Hypothesis name	Parametric FDR-derived significance thresholds	FDR-adjusted p -values a.k.a. q -values	Stage 1 significance thresholds	Stage 2 significance thresholds	FDR-adjusted p -values a.k.a. q -values
1	0.06746	Total_mf_LT/RT OCCIPITAL	0.0125	0.146376	0.0119048	0.0119048	0.1536948
2	0.07319	Total_mf_LT/RT TEMP	0.025	0.146376	0.0238095	0.0238095	0.1536948
3	0.41093	Total_mf_LT/RT FRONTAL	0.0375	0.547905333	0.0357143	0.0357143	0.5753006
4	0.87408	Total_mf_LT/RT PARIETAL	0.05	0.874084	0.047619	0.047619	0.9177882

Global mFREQ – Frequency Bands

2.3. mFREQ

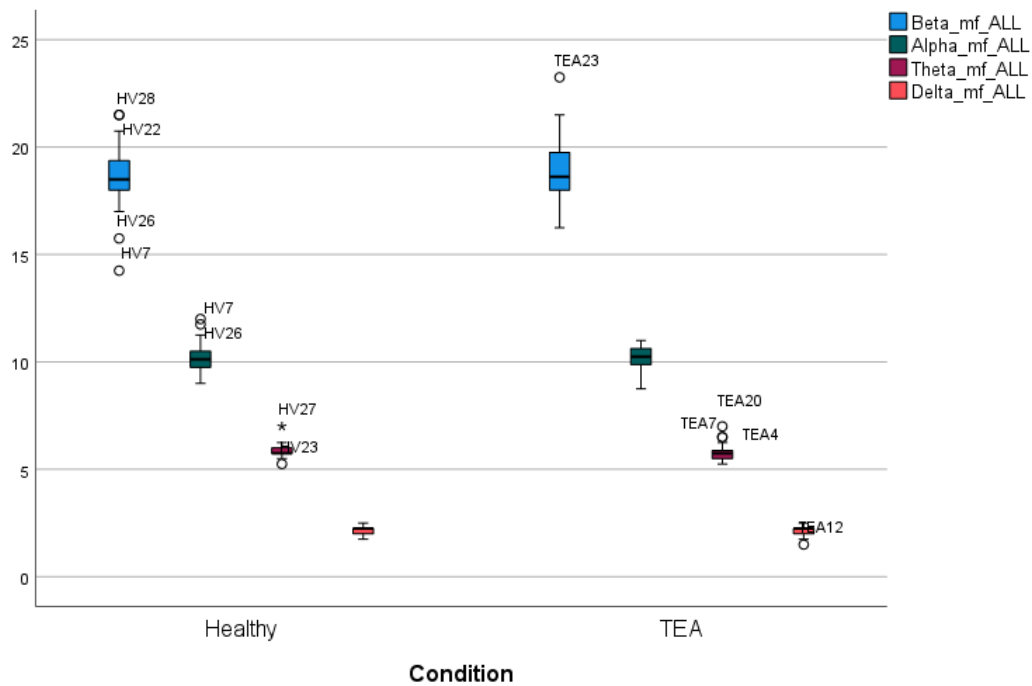


Figure 62: Boxplots for HV and TEA Global mFREQ within the beta, alpha, theta, and delta EEG bands

Table 28: Tests for Normality for Global mFREQ Data within EEG Bands

Tests of Normality							
	Condition	Kolmogorov-Smirnov ^a			Shapiro-Wilk		
		Statistic	df	Sig.	Statistic	df	Sig.
Beta_mf_ALL	Healthy	.149	28	.115	.931	28	.063
	TEA	.152	28	.094	.927	28	.051
Alpha_mf_ALL	Healthy	.155	28	.084	.943	28	.130
	TEA	.207	28	.003	.895	28	.009
Theta_mf_ALL	Healthy	.222	28	.001	.844	28	<.001
	TEA	.250	28	<.001	.872	28	.003
Delta_mf_ALL	Healthy	.268	28	<.001	.828	28	<.001
	TEA	.374	28	<.001	.760	28	<.001

a. Lilliefors Significance Correction

Table 29: Global Datasets – mFREQ within EEG Bands, Distribution Descriptors

		Statistics			
		Beta_mf_ALL	Alpha_mf_ALL	Theta_mf_ALL	Delta_mf_ALL
N	Valid	56	56	56	56
	Missing	0	0	0	0
Mean		18.8214	10.1696	5.8036	2.1518
Std. Error of Mean		.19848	.09079	.05164	.02602
Median		18.5000	10.2500	5.7500	2.2500
Std. Deviation		1.48532	.67942	.38646	.19469
Variance		2.206	.462	.149	.038
Skewness		.143	.071	1.067	-.850
Std. Error of Skewness		.319	.319	.319	.319
Kurtosis		1.907	.404	1.782	1.478
Std. Error of Kurtosis		.628	.628	.628	.628
Percentiles	25	18.0000	9.7500	5.5000	2.0000
	50	18.5000	10.2500	5.7500	2.2500
	75	19.5000	10.5000	6.0000	2.2500

Global mFREQ data within the beta band (13Hz – 40Hz) has a platykurtic data distribution with negligible skew. The mean across all data is 18.82, with a standard error (SE) of 0.20 and a standard deviation (SD) of 1.49 (Figure 62, Table 29). The interquartile range is 1.50, and the variance is 2.21 (Table 29). As both cohorts show a normal distribution (Table 28), a parametric independent samples T-test was performed demonstrating there is no significant difference between cohorts for global mFREQ within the beta EEG band profiles ($p = 0.21$ and, using FDR two-stage sharpened method, $q=0.44$) – Table 30.

Global mFREQ data within the alpha band (8Hz - 12.9Hz) has a platykurtic data distribution and has negligible skew. The mean across all data is 10.17, with a standard error (SE) of 0.9 and a standard deviation (SD) of 0.68 (Figure 62, Table 29). The interquartile range is 0.75, and the variance is 0.46 (Table 29). As only the HV cohort shows a normal distribution (Table 28), a non-parametric Mann-Whitney U test was performed demonstrating there is no significant difference between cohorts for global mFREQ data within the alpha EEG band profiles ($p = 0.69$, using FDR two-stage sharpened method $q=0.73$) – Table 30.

Global mFREQ data within the theta (4Hz – 7.9Hz) is platykurtic with a significant positive skew. The mean across all data is 5.80, with a standard error (SE) of 0.05 and a standard

deviation (SD) of 0.66 (Figure 62, Table 29). The interquartile range is 0.50, and the variance is 0.15 (Table 29). As neither cohort shows a normal distribution (Table 28), a non-parametric Mann-Whitney U test was performed demonstrating there is no significant difference between cohorts for global mFREQ data within the theta EEG band ($p = 0.09$ and, using FDR two-stage sharpened method, $q=0.36$) – Table 30.

Global mFREQ data within the delta band (1Hz – 3.9Hz) is platykurtic with a moderate negative skew. The mean across all data is 2.15, with a standard error (SE) of 0.03 and a standard deviation (SD) of 0.19 (Figure 62, Table 29). The interquartile range is 0.25, and the variance is 0.04 (Table 29). As neither cohort shows a normal distribution (Table 28), a non-parametric Mann-Whitney U test was performed demonstrating there is no significant difference between cohorts for global mFREQ data within the delta EEG band ($p = 0.37$ and, using FDR two-stage sharpened method, $q = 0.52$) – Table 30.

Table 30: Global mFREQ per EEG Band - Multiple Comparisons using False Discovery Rates (FDRs) Adjustments

FDRs			Classical one-stage method*		Two-stage sharpened method†			
Order	Ascending <i>p</i> -values	Hypothesis name	Parametric FDR-derived significance thresholds	FDR-adjusted <i>p</i> -values a.k.a. <i>q</i> -values	Stage 1 significance thresholds	Stage 2 significance thresholds	FDR-adjusted <i>p</i> -values a.k.a. <i>q</i> -values	
1	0.08686	Theta_mf_ALL		0.0125	0.347452	0.0119048	0.0119048	0.3648246
2	0.21079	Beta_mf_ALL	P	0.025	0.421588	0.0238095	0.0238095	0.4426674
3	0.36996	Delta_mf_ALL		0.0375	0.493282667	0.0357143	0.0357143	0.5179468
4	0.69171	Alpha_mf_ALL		0.05	0.691714	0.047619	0.047619	0.7262997

2.4. Interhemispheric mFREQ Difference

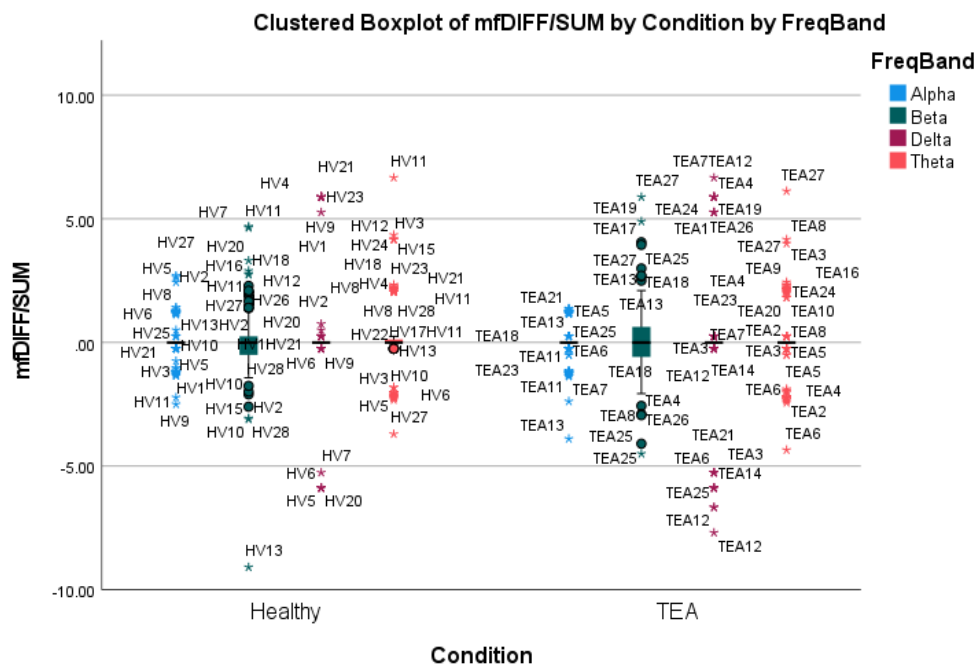


Figure 63: Boxplots for HV and TEA Global Interhemispheric mFREQ Difference within beta, alpha, theta, and delta EEG bands

Table 31: Tests for Normality for Global Inter-hemispheric mFREQ Data within EEG Bands

Tests of Normality							
	Condition	Kolmogorov-Smirnov ^a			Shapiro-Wilk		
		Statistic	df	Sig.	Statistic	df	Sig.
Beta_mf_LT/RT ALL	Healthy	.166	28	.048	.960	28	.342
	TEA	.219	28	.001	.882	28	.005
Alpha_mf_LT/RT ALL	Healthy	.320	28	<.001	.812	28	<.001
	TEA	.288	28	<.001	.819	28	<.001
Theta_mf_LT/RT ALL	Healthy	.321	28	<.001	.795	28	<.001
	TEA	.402	28	<.001	.682	28	<.001
Delta_mf_LT/RT ALL	Healthy	.446	28	<.001	.605	28	<.001
	TEA	.424	28	<.001	.651	28	<.001

a. Lilliefors Significance Correction

Table 32: Global Datasets – Inter-hemispheric mFREQ Difference within EEG Bands, Distribution Descriptors

		Statistics			
		Beta_mf_LT/RT ALL	Alpha_mf_LT/R T ALL	Theta_mf_LT/RT ALL	Delta_mf_LT/RT ALL
N	Valid	56	56	56	56
	Missing	0	0	0	0
Mean		-.036086	.064849	.233766	.177763
Std. Error of Mean		.1561486	.1065009	.1636367	.3771152
Median		.000000	.000000	.000000	.000000
Std. Deviation		1.1685091	.7969801	1.2245450	2.8220716
Variance		1.365	.635	1.500	7.964
Skewness		-.302	-.057	.034	-.066
Std. Error of Skewness		.319	.319	.319	.319
Kurtosis		2.521	-.449	.266	2.151
Std. Error of Kurtosis		.628	.628	.628	.628
Percentiles	25	-.677989	.000000	.000000	.000000
	50	.000000	.000000	.000000	.000000
	75	.668919	.000000	.000000	.000000

Global interhemispheric mFREQ difference data within the beta band (13Hz – 40Hz) is marginally leptokurtic but reasonably symmetrical around the mean. The mean across all data is -0.04, with a standard error (SE) of 0.16 and a standard deviation (SD) of 1.17 (Figure 63, Table 32). The interquartile range is 1.35, and the variance is 1.37 (Table 32). As only the HV cohort shows a normal distribution (Table 31), a non-parametric Mann-Whitney U test was performed demonstrating there is no significant difference between cohorts for global inter-hemispheric mFREQ difference within the beta EEG band profile ($p = 0.63$ and, using FDR two stage sharpened method, $q=0.88$) – Table 33.

Global inter-hemispheric mFREQ difference data within the alpha band (8Hz - 12.9Hz) is platykurtic but symmetrical around the mean. The mean across all data is 0.06, with a standard error (SE) of 0.10 and a standard deviation (SD) of 0.80 (Figure 63, Table 32). The interquartile range is 0, and the variance is 0.64 (Table 32). As neither cohort shows a normal distribution (Table 31), a non-parametric Mann-Whitney U test was performed demonstrating there is no significant difference between cohorts for global inter-hemispheric mFREQ difference data within the alpha EEG band profile ($p = 0.54$, using FDR two-stage sharpened method $q=0.88$) – Table 33.

Global inter-hemispheric mFREQ difference data within the theta band (4Hz – 7.9Hz) is platykurtic but symmetrical around the mean. The mean across all data is 0.23, with a standard error (SE) of 0.16 and a standard deviation (SD) of 1.22 (Figure 63, Table 32). The interquartile range is 0, and the variance is 1.50 (Table 32). As neither cohort shows a normal distribution (Table 31), a non-parametric Mann-Whitney U test was performed demonstrating there is no significant difference between cohorts for global inter-hemispheric mFREQ difference within the theta EEG band ($p = 0.97$ and, using FDR two stage sharpened method, $q=1.02$) – Table 33.

Global inter-hemispheric mFREQ difference data within the delta band (1Hz – 3.9Hz) is marginally leptokurtic but symmetrical around the mean. The mean across all data is 0.18, with a standard error (SE) of 0.38 and a standard deviation (SD) of 2.82 (Figure 63, Table 32). The interquartile range is 0, and the variance is 8.00 (Table 32). As neither cohort shows a normal distribution (Table 31), a non-parametric Mann-Whitney U test was performed demonstrating there is no significant difference between cohorts for global inter-hemispheric mFREQ difference within the delta EEG band ($p = 0.08$ and, using FDR two-stage sharpened method, $q = 0.35$) – Table 33.

Table 33: Global Inter-hemispheric mFREQ Difference per EEG Band - Multiple Comparisons using False Discovery Rates (FDRs) Adjustments

FDRs		Classical one-stage method*			Two-stage sharpened method†		
Order	Ascending <i>p</i> -values	Hypothesis name	Parametric FDR-derived significance thresholds	FDR-adjusted <i>p</i> -values a.k.a. <i>q</i> -values	Stage 1 significance thresholds	Stage 2 significance thresholds	FDR-adjusted <i>p</i> -values a.k.a. <i>q</i> -values
1	0.08404	Delta_mf_LT/RT ALL	0.0125	0.336148	0.0119048	0.0119048	0.3529554
2	0.53806	Alpha_mf_LT/RT ALL	0.025	0.833814667	0.0238095	0.0238095	0.8755054
3	0.62536	Beta_mf_LT/RT ALL	0.0375	0.833814667	0.0357143	0.0357143	0.8755054
4	0.96846	Theta_mf_LT/RT ALL	0.05	0.968456	0.047619	0.047619	1.0168788

3. Regional mFREQ – Frequency Bands

3.1. mFREQ

Table 34: Regional Datasets – mFREQ within EEG Bands, Distribution Descriptors

		Statistics															
		Beta_mf_FRONTAL	Alpha_mf_FRONTAL	Theta_mf_FRONTAL	Delta_mf_FRONTAL	Beta_mf_TEMPORAL	Alpha_mf_TEMPORAL	Theta_mf_TEMPORAL	Delta_mf_TEMPORAL	Beta_mf_PARIETAL	Alpha_mf_PARIETAL	Theta_mf_PARIETAL	Delta_mf_PARIETAL	Beta_mf_OCCIPITAL	Alpha_mf_OCCIPITAL	Theta_mf_OCCIPITAL	Delta_mf_OCCIPITAL
N	Valid	56	56	56	56	56	56	56	56	56	56	56	56	56	56	56	56
	Missing	0	0	0	0	0	0	0	0	0	0	0	0	0	0	0	0
Mean		19.3571	10.2232	5.7545	2.1429	18.8170	10.0670	5.7679	2.1741	18.4063	10.2411	5.8661	2.1607	18.2902	10.2902	5.8393	2.1607
Std. Error of Mean		.23118	.09549	.05821	.02456	.18600	.08606	.05091	.02377	.17912	.08757	.05404	.02582	.19342	.09249	.05074	.02335
Std. Deviation		1.72999	.71459	.43561	.18376	1.39193	.64401	.38096	.17786	1.34042	.65534	.40442	.19323	1.44739	.69213	.37968	.17470
Variance		2.993	.511	.190	.034	1.937	.415	.145	.032	1.797	.429	.164	.037	2.095	.479	.144	.031
Skewness		.039	.097	.656	-1.110	.469	-.010	.962	-.423	-.058	.003	.988	-.500	-.201	.206	.622	.626
Std. Error of Skewness		.319	.319	.319	.319	.319	.319	.319	.319	.319	.319	.319	.319	.319	.319	.319	.319
Kurtosis		.902	.140	1.021	1.920	.419	.097	1.434	.258	1.699	.392	.948	.037	1.474	.658	1.049	-.729
Std. Error of Kurtosis		.628	.628	.628	.628	.628	.628	.628	.628	.628	.628	.628	.628	.628	.628	.628	.628
Percentiles	25	18.2500	9.7500	5.5000	2.0000	18.0000	9.5625	5.5000	2.0000	17.7500	9.8125	5.5625	2.0000	17.5000	10.0000	5.5625	2.0000
	50	19.2500	10.2500	5.7500	2.2500	18.6250	10.2500	5.7500	2.2500	18.2500	10.2500	5.7500	2.2500	18.2500	10.2500	5.7500	2.2500
	75	20.5000	10.6875	6.0000	2.2500	19.5000	10.5000	6.0000	2.2500	19.0000	10.7500	6.0000	2.2500	19.1875	10.6875	6.0000	2.2500

All regional mFREQ datasets show varying degrees of platykurtosis All theta datasets (frontal, temporal, parietal, occipital), and delta occipitally demonstrate moderate positive skew, whilst the delta dataset over frontal regions is highly negatively skewed. Otherwise, datasets are symmetrical around the mean (Table 34).

Means fall in the following ranges (Figure 64, Table 34):

- Beta: means range from 18.29Hz (occipital) to 19.36Hz (frontal)
- Alpha: means range from 10.07Hz (temporal) to 10.29Hz (occipital)
- Theta: means range from 5.75 (frontal) to 5.87Hz (parietal)
- Delta: means range from 2.14Hz (frontal) to 2.17 (temporal)

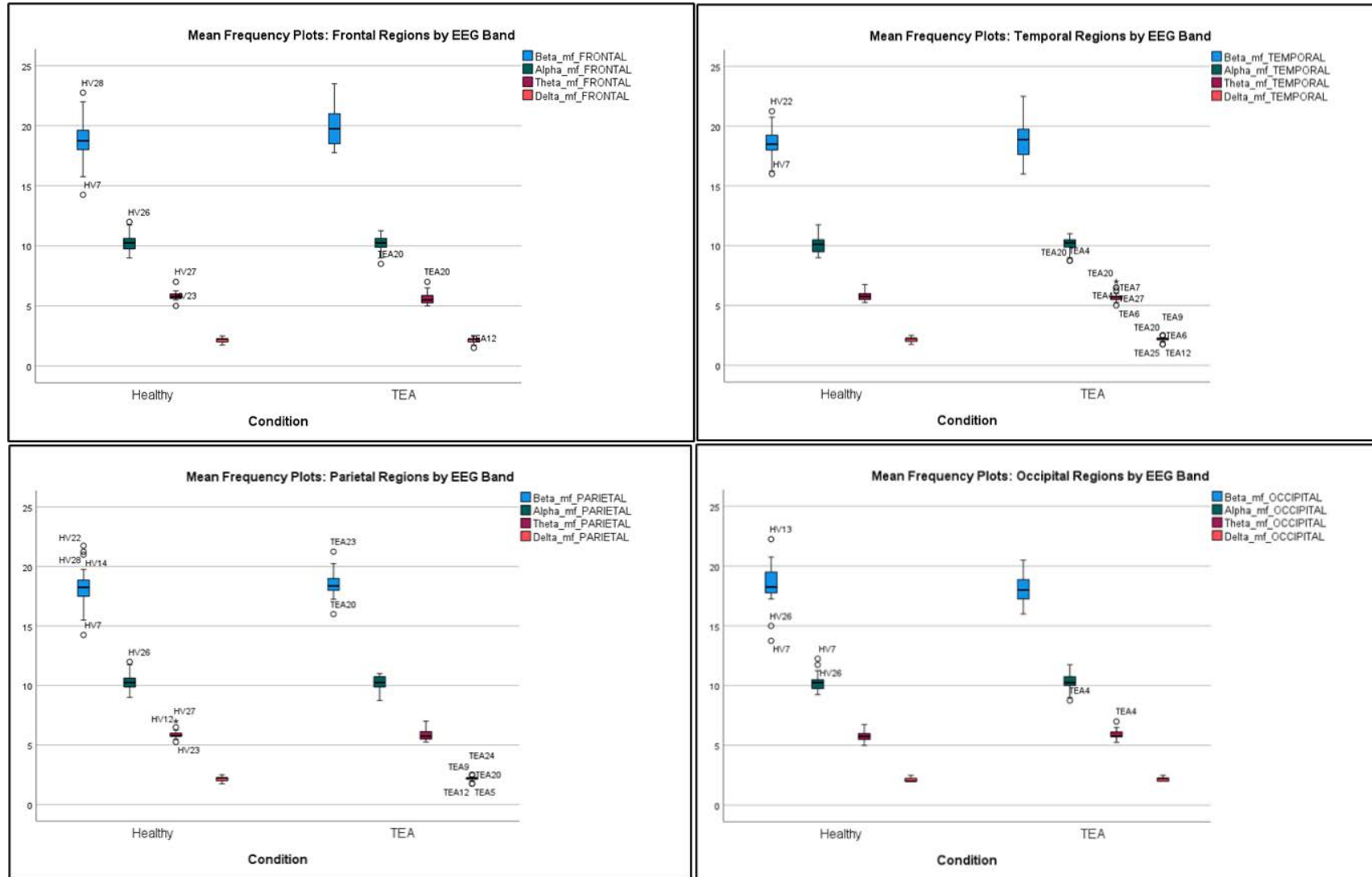


Figure 64: Boxplots for HV and TEA Regional Mean Frequencies within beta, alpha, theta, and delta EEG bands

Beta activities tend to show the highest standard errors for the mean (max being 0.23Hz over frontal areas), with delta frequencies showing the lowest (0.02Hz). Beta datasets also have the largest standard deviation, variance, and interquartile range (particularly over the frontal areas), whilst delta band datasets show the lowest (temporal/occipital regions representing the lowest) (Figure 64, Table 34).

Table 35: Tests for Normality for Regional Mean Frequency Data within EEG Bands

Tests of Normality							
	Condition	Kolmogorov-Smirnov ^a			Shapiro-Wilk		
		Statistic	df	Sig.	Statistic	df	Sig.
Beta_mf_FRONTAL	Healthy	.121	28	.200 [*]	.963	28	.412
	TEA	.134	28	.200 [*]	.934	28	.078
Alpha_mf_FRONTAL	Healthy	.141	28	.159	.962	28	.390
	TEA	.163	28	.056	.953	28	.232
Theta_mf_FRONTAL	Healthy	.209	28	.003	.875	28	.003
	TEA	.193	28	.009	.921	28	.036
Delta_mf_FRONTAL	Healthy	.341	28	<.001	.782	28	<.001
	TEA	.353	28	<.001	.766	28	<.001
Beta_mf_TEMPORAL	Healthy	.144	28	.142	.959	28	.334
	TEA	.096	28	.200 [*]	.959	28	.328
Alpha_mf_TEMPORAL	Healthy	.129	28	.200 [*]	.951	28	.205
	TEA	.221	28	.001	.906	28	.016
Theta_mf_TEMPORAL	Healthy	.169	28	.039	.922	28	.040
	TEA	.269	28	<.001	.864	28	.002
Delta_mf_TEMPORAL	Healthy	.288	28	<.001	.826	28	<.001
	TEA	.364	28	<.001	.785	28	<.001
Beta_mf_PARIETAL	Healthy	.141	28	.164	.950	28	.202
	TEA	.146	28	.129	.943	28	.130
Alpha_mf_PARIETAL	Healthy	.131	28	.200 [*]	.965	28	.461
	TEA	.214	28	.002	.918	28	.032
Theta_mf_PARIETAL	Healthy	.259	28	<.001	.863	28	.002
	TEA	.263	28	<.001	.891	28	.007
Delta_mf_PARIETAL	Healthy	.271	28	<.001	.858	28	.001
	TEA	.364	28	<.001	.785	28	<.001
Beta_mf_OCCIPITAL	Healthy	.164	28	.052	.938	28	.100
	TEA	.093	28	.200 [*]	.979	28	.836
Alpha_mf_OCCIPITAL	Healthy	.181	28	.019	.933	28	.072
	TEA	.170	28	.038	.941	28	.118
Theta_mf_OCCIPITAL	Healthy	.174	28	.030	.939	28	.102
	TEA	.272	28	<.001	.900	28	.011
Delta_mf_OCCIPITAL	Healthy	.332	28	<.001	.742	28	<.001
	TEA	.270	28	<.001	.784	28	<.001

*. This is a lower bound of the true significance.
a. Lilliefors Significance Correction

Beta datasets across all regions fit the criteria for normal distribution using Shapiro-Wilk, as do the frontal and occipital alpha datasets (Table 35). For these datasets, TEA and HV cohorts were compared using a parametric independent samples T-test. The remaining data were compared using the non-parametric Mann-Whitney U test (Table 36). Only frontal beta activities show a significant p-value ($p=0.03$) however, once multiple comparisons FDR

adjustments are made, the resulting q-values are not significant for either the classic one-stage or the two-stage sharpened method (Table 36).

Table 36: Regional mFREQ per EEG Band - Multiple Comparisons using False Discovery Rates (FDRs) Adjustments

FDRs		Classical one-stage method*			Two-stage sharpened method†		
Order	Ascending p -values	Hypothesis name	Parametric FDR-derived significance thresholds	FDR-adjusted p -values a.k.a. q -values	Stage 1 significance thresholds	Stage 2 significance thresholds	FDR-adjusted p -values a.k.a. q -values
1	0.02920	Beta_mf_FRONTAL	P 0.003125	0.467152	0.0029762	0.0029762	0.4905096
2	0.06973	Theta_mf_FRONTAL	0.00625	0.557808	0.0059524	0.0059524	0.5856984
3	0.13073	Delta_mf_PARIETAL	0.009375	0.663712	0.0089286	0.0089286	0.6968976
4	0.23422	Delta_mf_TEMPORAL	0.0125	0.663712	0.0119048	0.0119048	0.6968976
5	0.26862	Theta_mf_TEMPORAL	0.015625	0.663712	0.014881	0.014881	0.6968976
6	0.34553	Theta_mf_PARIETAL	0.01875	0.663712	0.0178571	0.0178571	0.6968976
7	0.35415	Beta_mf_TEMPORAL	P 0.021875	0.663712	0.0208333	0.0208333	0.6968976
8	0.36181	Beta_mf_PARIETAL	P 0.025	0.663712	0.0238095	0.0238095	0.6968976
9	0.37334	Beta_mf_OCCIPITAL	P 0.028125	0.663712	0.0267857	0.0267857	0.6968976
10	0.42747	Delta_mf_OCCIPITAL	0.03125	0.668410182	0.0297619	0.0297619	0.701830691
11	0.45953	Alpha_mf_FRONTAL	P 0.034375	0.668410182	0.0327381	0.0327381	0.701830691
12	0.65414	Theta_mf_OCCIPITAL	0.0375	0.872192	0.0357143	0.0357143	0.9158016
13	0.81181	Alpha_mf_OCCIPITAL	P 0.040625	0.977615	0.0386905	0.0386905	1.02649575
14	0.91436	Alpha_mf_TEMPORAL	0.04375	0.977615	0.0416667	0.0416667	1.02649575
15	0.94069	Alpha_mf_PARIETAL	0.046875	0.977615	0.0446429	0.0446429	1.02649575
16	0.97762	Delta_mf_FRONTAL	0.05	0.977615	0.047619	0.047619	1.02649575

5.15. 4.2. Interhemispheric mFREQ Difference

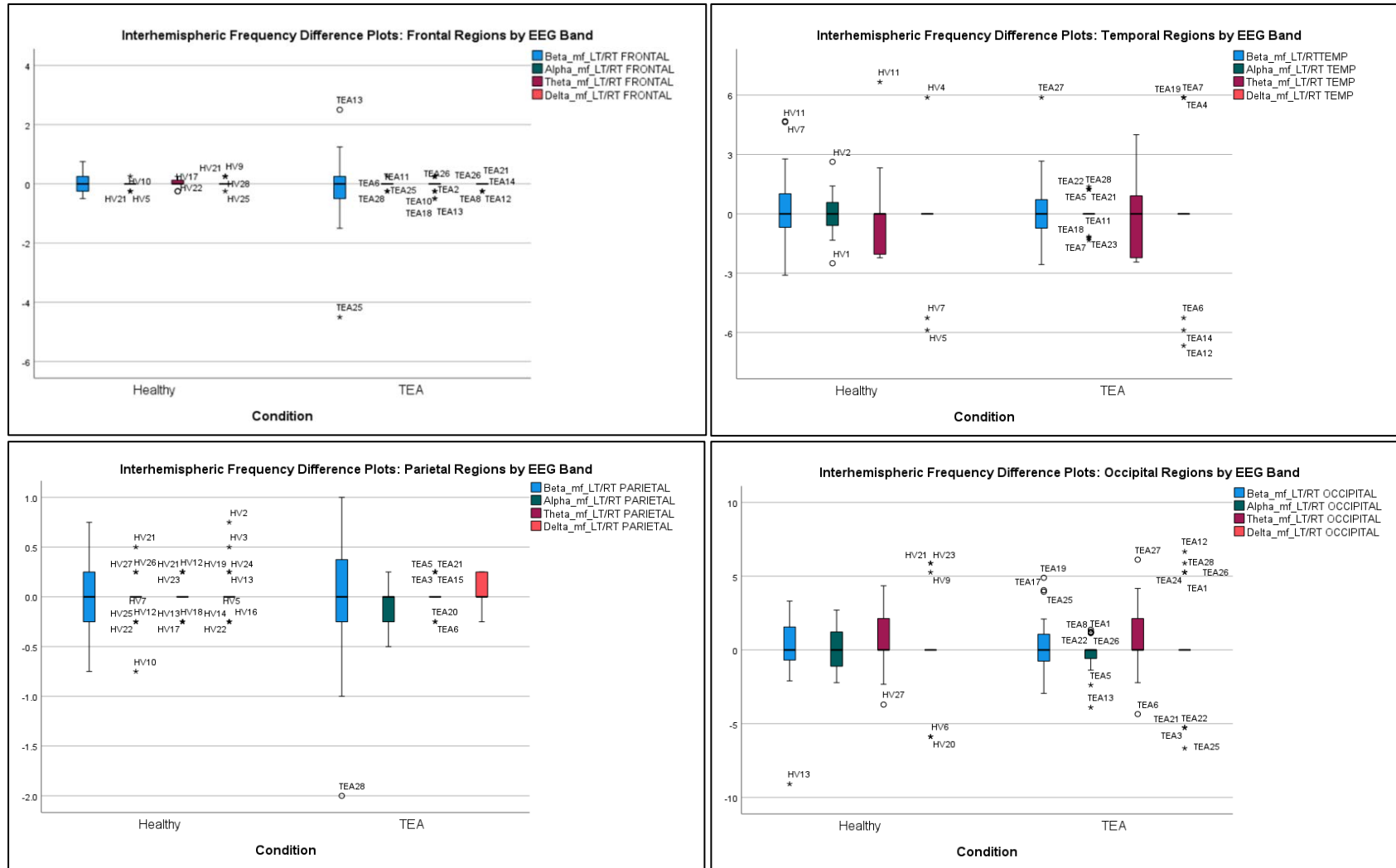


Figure 65: Boxplots for HV and TEA Regional Interhemispheric mFREQ Differences within beta, alpha, theta, and delta EEG bands

Table 37: Regional Datasets – Interhemispheric mFREQ Difference within EEG Bands, Distribution Descriptors

		Statistics															
		Beta_mf_LT/RT FRONTAL	Alpha_mf_LT/RT FRONTAL	Theta_mf_LT/RT FRONTAL	Delta_mf_LT/RT FRONTAL	Beta_mf_LT/RT TEMP	Alpha_mf_LT/RT TEMP	Theta_mf_LT/RT TEMP	Delta_mf_LT/RT TEMP	Beta_mf_LT/RT PARIETAL	Alpha_mf_LT/RT PARIETAL	Theta_mf_LT/RT PARIETAL	Delta_mf_LT/RT PARIETAL	Beta_mf_LT/RT OCCIPITAL	Alpha_mf_LT/RT OCCIPITAL	Theta_mf_LT/RT OCCIPITAL	Delta_mf_LT/RT OCCIPITAL
N	Valid	56	56	56	56	56	56	56	56	56	56	56	56	56	56	56	56
	Missing	0	0	0	0	0	0	0	0	0	0	0	0	0	0	0	0
Mean		-.071429	-.026786	.013393	-.008929	.222961	.025607	-.111047	-.096934	-.031250	-.040179	.013393	.053571	.163198	-.054620	.567706	.199027
Std. Error of Mean		.1102893	.0137796	.0233373	.0155582	.2358559	.1222760	.2542394	.3156792	.0718106	.0283307	.0184853	.0235921	.2757640	.1557248	.2733475	.3837557
Std. Deviation		.8253295	.1031170	.1746402	.1164268	1.7649840	.9150295	1.9025532	2.3623270	.5373811	.2120076	.1383313	.1765470	2.0636285	1.1653376	2.0455455	2.8717648
Variance		.681	.011	.030	.014	3.115	.837	3.620	5.581	.289	.045	.019	.031	4.259	1.358	4.184	8.247
Skewness		-2.298	-.786	-.737	-.134	.914	.032	-.737	-.131	-.766	-.609	.032	1.275	-1.213	-.427	.271	.062
Std. Error of Skewness		.319	.319	.319	.319	.319	.319	.319	.319	.319	.319	.319	.319	.319	.319	.319	.319
Kurtosis		16.058	2.501	1.376	1.919	1.770	.848	1.521	3.758	2.465	1.933	4.31	3.834	6.653	1.454	.526	1.343
Std. Error of Kurtosis		.628	.628	.628	.628	.628	.628	.628	.628	.628	.628	.628	.628	.628	.628	.628	.628
Percentiles	25	-.250000	.000000	.000000	.000000	-.714394	.000000	-2.040816	.000000	-.250000	-.250000	.000000	.000000	-.689655	-1.119801	.000000	.000000
	50	.000000	.000000	.000000	.000000	.000000	.000000	.000000	.000000	.000000	.000000	.000000	.000000	.000000	.000000	.000000	.000000
	75	.250000	.000000	.000000	.000000	.719424	.000000	.000000	.000000	.250000	.000000	.000000	.187500	1.423541	.862069	2.127660	.000000

All regional interhemispheric mFREQ difference datasets are leptokurtic, with frontal beta and parietal alpha data having the most significant leptokurtosis and occipital beta and delta showing the least. All regional interhemispheric mFREQ difference datasets show significant positive skew (Table 37).

Occipital theta activities have the highest left hemisphere mFREQ difference (0.57) whilst temporal theta activities show the highest right hemisphere mFREQ difference (-0.11). The frontal delta shows the lowest interhemispheric mFREQ difference i.e., is the most symmetrical between the hemispheres (Figure 65, Table 37). Delta activities in occipital and temporal areas tend to show the highest standard errors for the mean, whereas frontal alpha, frontal delta and parietal theta datasets have the lowest. A similar pattern is seen for standard deviation, variance, and interquartile range. (Figure 65, Table 37).

Only temporal beta data for the HV cohort and parietal beta data for the TEA cohort meet the criteria for normal distribution using Shapiro-Wilk (Table 38). Therefore, all datasets were compared using the non-parametric Mann-Whitney U test (Table 39). Only frontal delta activities

show a significant p-value ($p=0.004$) however, once multiple comparisons FDR adjustments are made, the resulting q-values are not significant for either the classic one-stage or the two-stage sharpened method (Table 39).

Table 38: Tests for Normality for Regional Interhemispheric mFREQ Difference Data within EEG Bands

Tests of Normality							
	Condition	Kolmogorov-Smirnov ^a			Shapiro-Wilk		
		Statistic	df	Sig.	Statistic	df	Sig.
Beta_mf_LT/RT FRONTAL	Healthy	.239	28	<.001	.892	28	.007
	TEA	.264	28	<.001	.791	28	<.001
Alpha_mf_LT/RT FRONTAL	Healthy	.459	28	<.001	.565	28	<.001
	TEA	.459	28	<.001	.565	28	<.001
Theta_mf_LT/RT FRONTAL	Healthy	.378	28	<.001	.720	28	<.001
	TEA	.321	28	<.001	.819	28	<.001
Delta_mf_LT/RT FRONTAL	Healthy	.446	28	<.001	.605	28	<.001
	TEA	.482	28	<.001	.508	28	<.001
Beta_mf_LT/RTTEMP	Healthy	.155	28	.084	.943	28	.131
	TEA	.195	28	.008	.890	28	.007
Alpha_mf_LT/RT TEMP	Healthy	.250	28	<.001	.904	28	.015
	TEA	.349	28	<.001	.763	28	<.001
Theta_mf_LT/RT TEMP	Healthy	.279	28	<.001	.813	28	<.001
	TEA	.210	28	.003	.871	28	.003
Delta_mf_LT/RT TEMP	Healthy	.468	28	<.001	.456	28	<.001
	TEA	.394	28	<.001	.655	28	<.001
Beta_mf_LT/RT PARIETAL	Healthy	.208	28	.003	.901	28	.012
	TEA	.209	28	.003	.932	28	.069
Alpha_mf_LT/RT PARIETAL	Healthy	.355	28	<.001	.752	28	<.001
	TEA	.259	28	<.001	.871	28	.003
Theta_mf_LT/RT PARIETAL	Healthy	.308	28	<.001	.785	28	<.001
	TEA	.418	28	<.001	.636	28	<.001
Delta_mf_LT/RT PARIETAL	Healthy	.388	28	<.001	.721	28	<.001
	TEA	.382	28	<.001	.701	28	<.001
Beta_mf_LT/RT OCCIPITAL	Healthy	.261	28	<.001	.768	28	<.001
	TEA	.198	28	.006	.924	28	.043
Alpha_mf_LT/RT OCCIPITAL	Healthy	.240	28	<.001	.916	28	.028
	TEA	.313	28	<.001	.829	28	<.001
Theta_mf_LT/RT OCCIPITAL	Healthy	.281	28	<.001	.890	28	.007
	TEA	.258	28	<.001	.892	28	.008
Delta_mf_LT/RT OCCIPITAL	Healthy	.423	28	<.001	.596	28	<.001
	TEA	.347	28	<.001	.779	28	<.001

a. Lilliefors Significance Correction

Table 39: Regional Interhemispheric mFREQ Difference per EEG Band - Multiple Comparisons using False Discovery Rates (FDRs) Adjustments

Order	Ascending	Hypothesis name	FDR-derived	FDR-adjusted	Stage 1	Stage 2	FDR-adjusted
	p-values		significance thresholds	p-values a.k.a. q-values	significance thresholds	significance thresholds	p-values a.k.a. q-values
1	0.00400	FRONTAL Delta mfDIFF/SUM	0.003125	0.064	0.0029762	0.0029762	0.0672
2	0.15000	PARIETAL Delta mfDIFF/SUM	0.00625	0.966	0.0059524	0.0059524	1.0143
3	0.27800	FRONTAL Theta mfDIFF/SUM	0.009375	0.966	0.0089286	0.0089286	1.0143
4	0.36000	PARIETAL Alpha mfDIFF/SUM	0.0125	0.966	0.0119048	0.0119048	1.0143
5	0.53700	OCCIPITAL Alpha mfDIFF/SUM	0.015625	0.966	0.014881	0.014881	1.0143
6	0.60100	FRONTAL Beta mfDIFF/SUM	0.01875	0.966	0.0178571	0.0178571	1.0143
7	0.60800	TEMPORAL Theta mfDIFF/SUM	0.021875	0.966	0.0208333	0.0208333	1.0143
8	0.72700	TEMPORAL Alpha mfDIFF/SUM	0.025	0.966	0.0238095	0.0238095	1.0143
9	0.76000	TEMPORAL Delta mfDIFF/SUM	0.028125	0.966	0.0267857	0.0267857	1.0143
10	0.78700	PARIETAL Beta mfDIFF/SUM	0.03125	0.966	0.0297619	0.0297619	1.0143
11	0.84000	PARIETAL Theta mfDIFF/SUM	0.034375	0.966	0.0327381	0.0327381	1.0143
12	0.84700	OCCIPITAL Theta mfDIFF/SUM	0.0375	0.966	0.0357143	0.0357143	1.0143
13	0.87600	OCCIPITAL Beta mfDIFF/SUM	0.040625	0.966	0.0386905	0.0386905	1.0143
14	0.88800	TEMPORAL Beta mfDIFF/SUM	0.04375	0.966	0.0416667	0.0416667	1.0143
15	0.91500	FRONTAL Alpha mfDIFF/SUM	0.046875	0.966	0.0446429	0.0446429	1.0143
16	0.96600	OCCIPITAL Delta mfDIFF/SUM	0.05	0.966	0.047619	0.047619	1.0143

First Phase – Spectral Analysis of Mean Power (mPSD)

The analysis aimed to determine the effects TEA may have on mean power (mPSD), considering variation within frequency band and brain regions.

mPSD and mPSD interhemispheric spectra were computed for global and regional cortical activities. Relative power analysis was calculated within frequency bands (beta, alpha, theta, delta) for both global and regional spectra.

Dataset distributions were assessed using SPSS explore and Shapiro-Wilk tests were performed to check for normality. Comparison of TEA and HV cohorts was undertaken using a parametric Independent Samples T-Test for normal distributions; otherwise, a non-parametric Independent Samples Mann-Whitney U test was performed. Statistical significance was set at $p = <0.05$. To control for type I errors generated by the false rejection of the null hypothesis through multiple comparisons within the regional, and frequency band analysis, False Discovery Rate (FDR) adjustments using the classic one-stage, and two-stage sharpened methods were undertaken (Benjamini and Hochberg, 1995; Benjamini and Hochberg, 2000; Benjamini *et al.*, 2006; Pike, 2011; Nichols, 2007) with before p -values, and after correction q -values being reported within the results.

1. Global mPSD – All Frequencies

1.1. Power Spectral Density (mPSD)

Global mPSD has a leptokurtic data distribution with a strong positive skew (Figure 66, Table 17). The mean across all data is 1.07, with a standard error (SE) of 0.10 and a standard deviation (SD) of 0.93. The interquartile range is 0.84, the range is 4.30, and the variance is 0.86 (Table 17).

As both cohorts are not normally distributed (Figure 66, Table 16), the non-parametric Man-Whitney U test was performed demonstrating there is no significant difference in mPSD profiles between the cohorts at a global level ($p = 0.974$) – Table 41

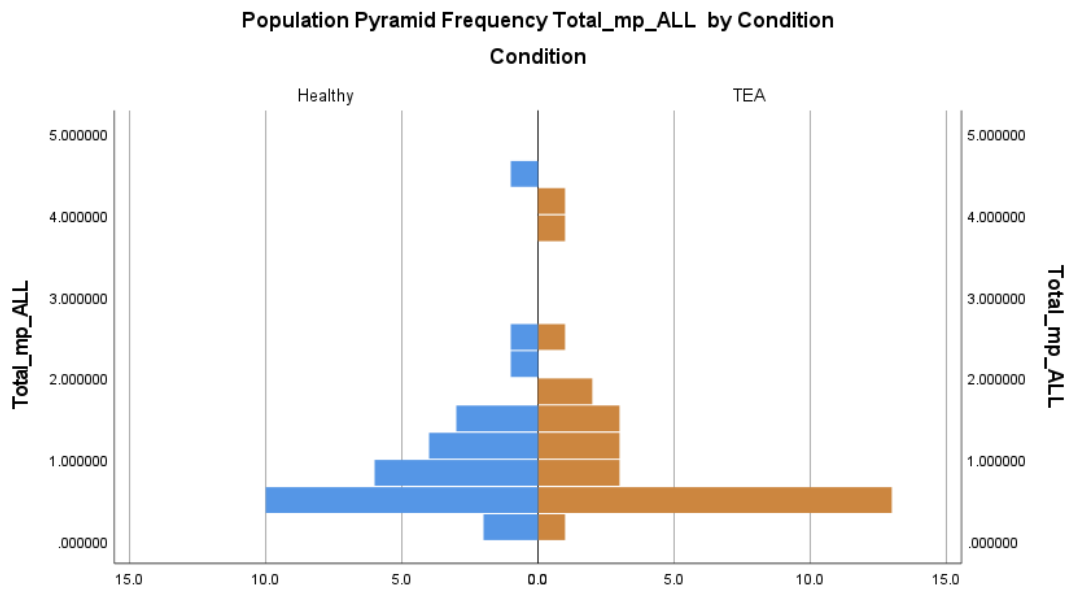


Figure 66: Global PSD distribution by cohort

1.2. Inter-hemispheric mPSD Difference

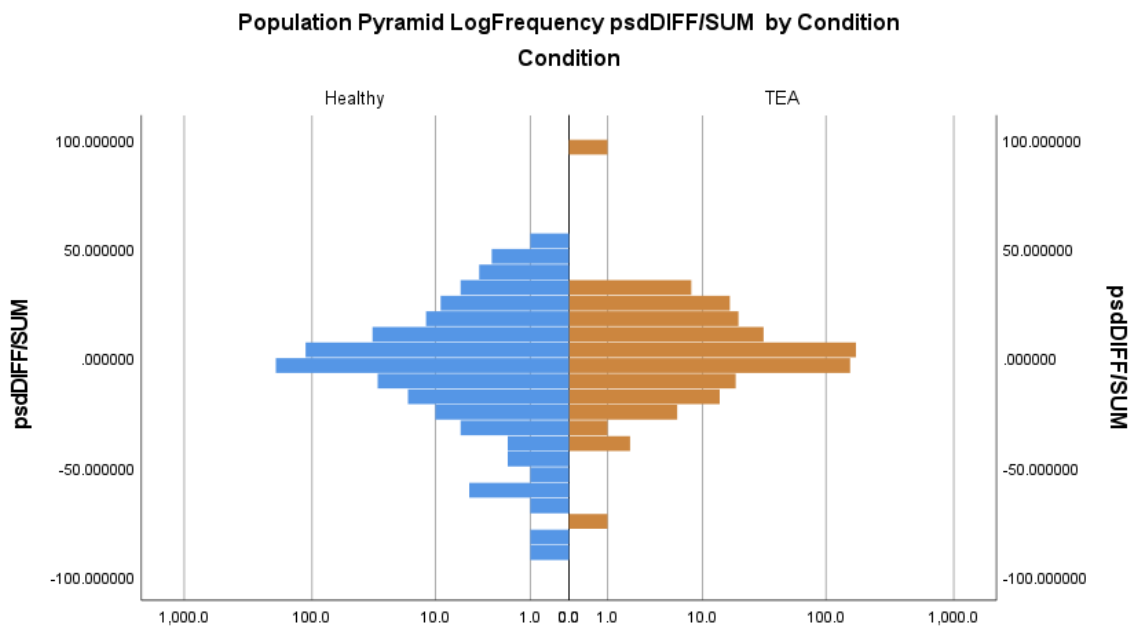


Figure 67: Global inter-hemispheric mPSD difference distributions by cohort. +ve values denote a left hemisphere bias and -ve values a right hemisphere bias.

Global interhemispheric mPSD difference data is leptokurtic in distribution and has a slight negative skew (Figure 67, Table 41). The mean across all data is 0.187, with a standard error (SE) of 0.45 and a standard deviation (SD) of 13.46. The interquartile range is 3.066, the range is 181.28, and the variance is 181.11 (Table 41).

As neither cohort data is normally distributed (Table 40), the non-parametric Mann-Whitney U test was performed. This demonstrates a significant difference in the inter-hemispheric mPSD difference profiles between the cohorts at a global level ($p = 0.020$) with mPSD being higher than HV. Examining the mean power hemispheric mean/median values in more depth (Table 41), there is no significant difference for either the right or left mPSD in isolation –Table 42.

Table 40: Normality tests for Interhemispheric difference of mPSD (includes frontal, temporal, parietal, and occipital regions)

Tests of Normality							
Condition	Kolmogorov-Smirnov ^a			Shapiro-Wilk			
	Statistic	df	Sig.	Statistic	df	Sig.	
psdDIFF/SUM	Healthy	.213	448	<.001	.774	448	<.001
	TEA	.217	448	<.001	.771	448	<.001

a. Lilliefors Significance Correction

Table 41: Data Descriptors for Interhemispheric difference in mPSD. Below: Mann Witney U test Global mPSD

Statistics		
psdDIFF/SUM		
N	Valid	896
	Missing	0
Mean		.18722101
Std. Error of Mean		.449584302
Median		-.01153988
Std. Deviation		13.45752341
Variance		181.105
Skewness		-.868
Std. Error of Skewness		.082
Kurtosis		10.885
Std. Error of Kurtosis		.163
Range		181.284729
Percentiles	25	-1.03054307
	50	-.01153988
	75	2.03587658

Report: mPSD Global, AllFreq				
Condition		psdRIGHT	psdLEFT	psdDIFF/SUM
Healthy	Mean	1.05845074	.97305438	-3.96456392
	Median	.80010584	.70058162	-3.10787300
TEA	Mean	1.15116341	1.18204097	1.28091439
	Median	.70941123	.74816770	1.56101705
Total	Mean	1.10480707	1.07754767	-1.34182476
	Median	.73064413	.72945256	-.80756435

Table 42: Statistical analysis of TEA vs. HV global inter-hemispheric mPSD difference. Mann-Whitney U test.

Hypothesis Test Summary - Mean PSD Global, AllFreq				
	Null Hypothesis	Test	Sig. ^{a,b}	Decision
1	The distribution of psdRIGHT is the same across categories of Condition.	Independent-Samples Mann-Whitney U Test	.768	Retain the null hypothesis.
2	The distribution of psdLEFT is the same across categories of Condition.	Independent-Samples Mann-Whitney U Test	.756	Retain the null hypothesis.
3	The distribution of psdDIFF/SUM is the same across categories of Condition.	Independent-Samples Mann-Whitney U Test	.020	Reject the null hypothesis.

a. The significance level is .050.
 b. Asymptotic significance is displayed.

2. Regional mPSD – All Frequencies

2.1. mPSD

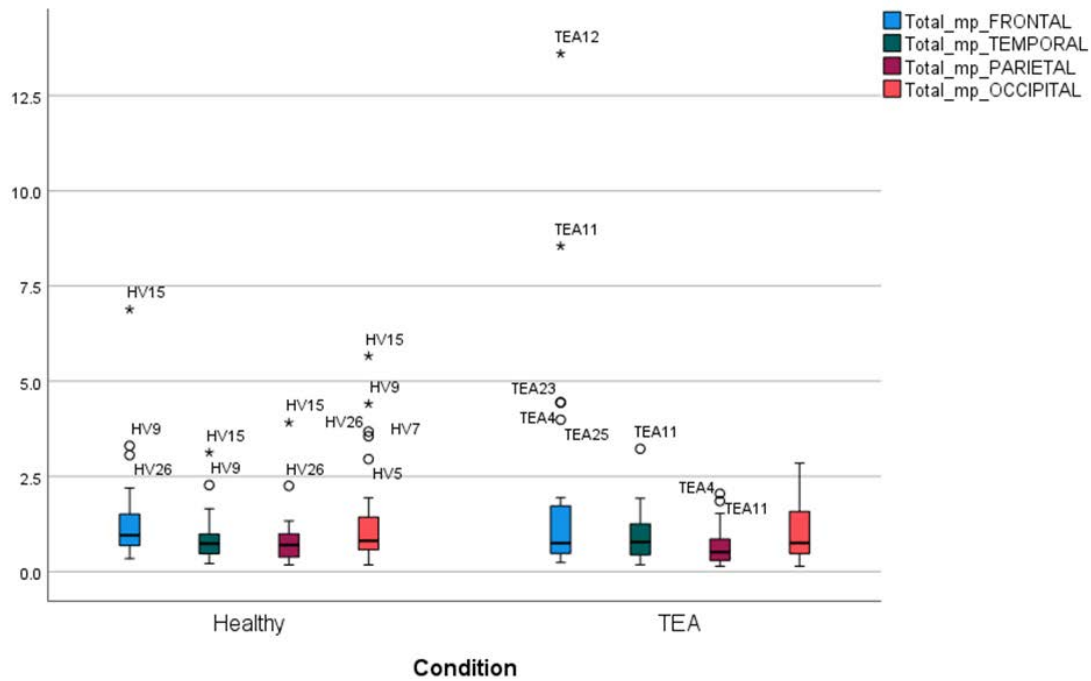


Figure 68 :Boxplots for HV and TEA Regional mPSD Values

Table 43: Tests for Normality for Regional mPSD Data Distributions

Tests of Normality							
	Condition	Kolmogorov-Smirnov ^a			Shapiro-Wilk		
		Statistic	df	Sig.	Statistic	df	Sig.
Total_mp_FRONTAL	Healthy	.236	28	<.001	.663	28	<.001
	TEA	.320	28	<.001	.584	28	<.001
Total_mp_TEMPORAL	Healthy	.212	28	.002	.783	28	<.001
	TEA	.144	28	.144	.849	28	<.001
Total_mp_PARIETAL	Healthy	.205	28	.004	.685	28	<.001
	TEA	.239	28	<.001	.817	28	<.001
Total_mp_OCCIPITAL	Healthy	.272	28	<.001	.736	28	<.001
	TEA	.220	28	.001	.865	28	.002

a. Lilliefors Significance Correction

Table 44: Regional Datasets – mPSD Distribution Descriptors

		Statistics			
		Total_mp_FRONTAL	Total_mp_TEMPORAL	Total_mp_PARIETAL	Total_mp_OCCIPITAL
N	Valid	56	56	56	56
	Missing	0	0	0	0
Mean		1.65229518	.89889434	.74795171	1.23357932
Std. Error of Mean		.302425133	.085072838	.085769389	.149918653
Median		.85828920	.73804250	.56986649	.77897651
Std. Deviation		2.263142464	.636626822	.641839332	1.121888471
Variance		5.122	.405	.412	1.259
Skewness		3.576	1.904	2.695	1.992
Std. Error of Skewness		.319	.319	.319	.319
Kurtosis		15.074	4.432	10.168	4.319
Std. Error of Kurtosis		.628	.628	.628	.628
Range		13.359056	3.045537	3.769240	5.520446
Percentiles	25	.54613085	.44664856	.32215059	.49096772
	50	.85828920	.73804250	.56986649	.77897651
	75	1.64426305	1.17202018	.91349657	1.51374153

- mPSD within the frontal region has a very highly leptokurtic data distribution with a marked positive skew. The mean across all data is 1.65, with a standard error (SE) of 0.30 and a standard deviation (SD) of 2.26 (Figure 68, Table 44). The interquartile range is 1.09, the range is 13.36, and the variance is 5.12 (Table 44). As neither cohort shows a normal distribution (Table 43), a non-parametric Man-Whitney U test was performed demonstrating there is no significant difference between the cohorts for mPSD within the frontal regions ($p = 0.53$ and, using FDR two-stage sharpened method, $q=0.74$) – Table 45.
- mPSD within the temporal region has a leptokurtic data distribution and is highly positively skewed. The mean across all data is 0.90, with a standard error (SE) of 0.09 and a standard deviation (SD) of 0.64 (Figure 68, Table 44). The interquartile range is 0.72, the range is 3.05, and the variance is 0.41 (Table 44). As neither cohort shows a normal distribution (Table 43), a non-parametric Man-Whitney U test was performed demonstrating there is no significant difference between the cohorts for mPSD

within the temporal regions ($p = 0.71$, using FDR two-stage sharpened method $q=0.74$) – Table 45.

- mPSD data within the parietal region is highly leptokurtic with a significant positive skew. The mean across all data is 0.75, with a standard error (SE) of 0.86 and a standard deviation (SD) of 0.64 (Figure 68, Table 44). The interquartile range is 0.59, the range is 3.77, and the variance is 0.41 (Table 44). As neither cohort shows a normal distribution (Table 43), a non-parametric Man-Whitney U test was performed demonstrating there is no significant difference between the cohorts for mPSD within the parietal regions ($p = 0.17$ and, using FDR two-stage sharpened method, $q=0.71$) – Table 45.
- mPSD data within the occipital region is slightly leptokurtic with a positive skew. The mean across all data is 1.23, with a standard error (SE) of 0.15 and a standard deviation (SD) of 1.12 (Figure 68, Table 44). The interquartile range is 1.02, the range is 5.52, and the variance is 1.26 (Table 44). As neither cohort shows a normal distribution (Table 43), a non-parametric Man-Whitney U test was performed demonstrating there is no significant difference between the cohorts for mPSD within the occipital regions ($p = 0.54$ and, using FDR two-stage sharpened method, $q=0.74$) – Table 45.

Table 45: Regional mPSD - Multiple Comparisons using False Discovery Rates (FDRs) Adjustments

FDR			Classical one-stage method*		Two-stage sharpened method†		
Order	Ascending p -values	Hypothesis name	Parametric FDR-derived significance thresholds	FDR-adjusted p -values a.k.a. q -values	Stage 1 significance thresholds	Stage 2 significance thresholds	FDR-adjusted p -values a.k.a. q -values
1	0.16867	Total_mp_PARIETAL	0.0125	0.674676	0.0119048	0.0119048	0.7084098
2	0.53348	Total_mp_FRONTAL	0.025	0.70625	0.0238095	0.0238095	0.7415625
3	0.54431	Total_mp_OCCIPITAL	0.0375	0.70625	0.0357143	0.0357143	0.7415625
4	0.70625	Total_mp_TEMPORAL	0.05	0.70625	0.047619	0.047619	0.7415625

2.2. Interhemispheric mPSD Difference

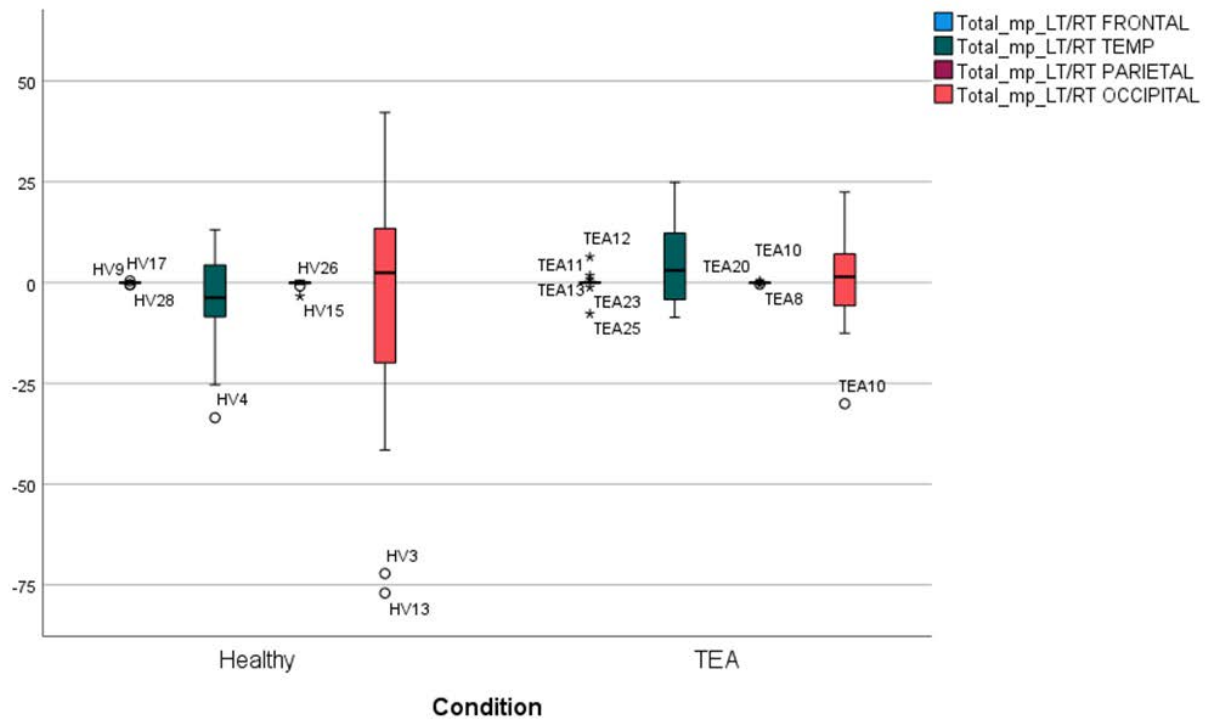


Figure 69: Boxplots for HV and TEA Regional Interhemispheric mPSD Differences

Table 46: Tests for Normality for Regional Interhemispheric mPSD Difference Distributions

Tests of Normality							
Condition	Kolmogorov-Smirnov ^a			Shapiro-Wilk			
	Statistic	df	Sig.	Statistic	df	Sig.	
Total_mp_LT/RT FRONTAL	Healthy	.162	28	.058	.922	28	.039
	TEA	.378	28	<.001	.523	28	<.001
Total_mp_LT/RT TEMP	Healthy	.134	28	.200*	.946	28	.161
	TEA	.136	28	.200*	.930	28	.062
Total_mp_LT/RT PARIETAL	Healthy	.286	28	<.001	.560	28	<.001
	TEA	.205	28	.004	.896	28	.009
Total_mp_LT/RT OCCIPITAL	Healthy	.134	28	.200*	.935	28	.085
	TEA	.084	28	.200*	.971	28	.609

*. This is a lower bound of the true significance.
a. Lilliefors Significance Correction

Table 47: Regional Datasets – Interhemispheric mPSD Difference Descriptors

		Statistics			
		Total_mp_LT/RT FRONTAL	Total_mp_LT/RT TEMP	Total_mp_LT/RT PARIETAL	Total_mp_LT/RT OCCIPITAL
N	Valid	56	56	56	56
	Missing	0	0	0	0
Mean		-.021367	.438905	-.111406	-1.436315
Std. Error of Mean		.1860986	1.4922166	.0672163	2.8886374
Median		-.007633	.054082	-.039046	2.027208
Std. Deviation		1.3926343	11.1667267	.5030005	21.6165832
Variance		1.939	124.696	.253	467.277
Skewness		-1.344	-.335	-5.248	-1.284
Std. Error of Skewness		.319	.319	.319	.319
Kurtosis		24.879	.922	34.371	3.465
Std. Error of Kurtosis		.628	.628	.628	.628
Range		14.0935	58.3949	4.0147	119.1816
Percentiles	25	-.091500	-6.342003	-.154083	-9.208594
	50	-.007633	.054082	-.039046	2.027208
	75	.068868	9.170808	.063926	9.397199

- Inter-hemispheric mPSD difference data within the frontal region has a very highly leptokurtic data distribution with a negative skew. The mean across all data is -0.02, with a standard error (SE) of 0.19 and a standard deviation (SD) of 1.39 (Figure 69, Table 47). The interquartile range is 0.50, the range is 14.09, and the variance is 1.94 (Table 47). As neither cohort shows a normal distribution (Table 46), a non-parametric Man-Whitney U test was performed demonstrating there is no significant difference in the inter-hemispheric mPSD difference profiles between the cohorts at a global level ($p = 0.09$ and, using FDR two-stage sharpened method, $q=0.013$) – Table 50.
- Inter-hemispheric mPSD difference data within the temporal region has a platykurtic data distribution and has a moderate negative skew. The mean across all data is 0.44, with a standard error (SE) of 1.49 and a standard deviation (SD) of 11.17 (Figure 69, Table 47). The interquartile range is 15.51, the range is 58.39, and the variance is 124.70 (Table 47). As both cohorts show a normal distribution (Table 46), a

parametric independent samples T-test was performed demonstrating a significant difference in the inter-hemispheric PSD difference profiles between the cohorts at a global level ($p = 0.01$, using FDR two-stage sharpened method $q=0.02$), with mPSD being higher in the TEA cohort – Table 50. Examining the hemispheric mean power mean/median values in more depth (Table 48), there is no significant difference in the right or left mPSD in isolation (Table 49).

- Inter-hemispheric mPSD difference data within the parietal region is highly leptokurtic with a significant negative skew. The mean across all data is -0.11, with a standard error (SE) of 0.07 and a standard deviation (SD) of 0.50 (Figure 69, Table 47). The interquartile range is 0.50, the range is 4.01, and the variance is 0.25 (Table 47). As neither cohort shows a normal distribution (Table 46), a non-parametric Man-Whitney U test was performed demonstrating there is no significant difference in the inter-hemispheric mPSD difference profiles between the cohorts at a global level ($p = 0.95$ and, using FDR two-stage sharpened method, $q=0.75$) – Table 50.
- Inter-hemispheric mPSD difference data within the occipital region is relatively mesokurtic with a significant negative skew. The mean across all data is -1.44, with a standard error (SE) of 2.89 and a standard deviation (SD) of 21.62 (Figure 69, Table 47). The interquartile range is 18.61, the range is 119.18, and the variance is 467.28 (Table 47). As both cohorts show a normal distribution (Table 46), a parametric independent samples T-test was performed demonstrating there is no significant difference in the inter-hemispheric mPSD difference profiles between the cohorts at a global level ($p = 0.52$ and, using FDR two-stage sharpened method, $q=0.54$) – Table 50.

Table 48: Mean and Median values for TEA and HV cohorts - mPSD temporal inter-hemisphere analysis

Report mPSD IHD TEMPORAL, AllFreq				
Condition		psdRIGHT	psdLEFT	psdDIFF/SUM
Healthy	Mean	.88863882	.84665015	-3.63479458
	Median	.73280246	.67996196	-3.72600376
TEA	Mean	.89052091	.96976748	4.51260495
	Median	.83696607	.78236921	3.01449095
Total	Mean	.88957986	.90820882	.43890519
	Median	.74431077	.69087715	.05408242

Table 49: T-test results for mPSD temporal inter-hemisphere analysis

Independent Samples Test: mPSD IHD TEMPORAL, AllFreq										
		Levene's Test for Equality of Variances		t-test for Equality of Means				95% Confidence Interval of the Difference		
		F	Sig.	t	df	Sig. (2-tailed)	Mean Difference	Std. Error Difference	Lower	Upper
psdRIGHT	Equal variances assumed	.054	.817	-.011	54	.991	-.001882087	.168014892	-.338731663	.334967490
	Equal variances not assumed			-.011	53.930	.991	-.001882087	.168014892	-.338741678	.334977505
psdLEFT	Equal variances assumed	.425	.517	-.688	54	.495	-.123117323	.179040759	-.482072432	.235837786
	Equal variances not assumed			-.688	53.977	.495	-.123117323	.179040759	-.482075932	.235841285
psdDIFF/SUM	Equal variances assumed	.032	.858	-2.909	54	.005	-8.147399528	2.800450281	-13.7619643	-2.532834762
	Equal variances not assumed			-2.909	53.462	.005	-8.147399528	2.800450281	-13.7632585	-2.531540583

Table 50: Regional Interhemispheric mPSD Differences - Multiple Comparisons using False Discovery Rates (FDRs) Adjustments

FDR	Ascending Hypothesis		Parametric	Classical one-stage method*		Two-stage sharpened method†		
	p-values	name		FDR-derived significance thresholds	FDR-adjusted p-values a.k.a. q-values	Stage 1 significance thresholds	Stage 2 significance thresholds	FDR-adjusted p-values a.k.a. q-values
1	0.00527	Total_mp_LT/RT TEMP	P	0.0125*	0.021072	0.0119048	0.015873*	0.0165942
2	0.08532	Total_mp_LT/RT FRONTAL		0.025	0.17064	0.0238095	0.031746	0.134379
3	0.51652	Total_mp_LT/RT OCCIPITAL	P	0.0375	0.688693333	0.0357143	0.047619	0.542346
4	0.94774	Total_mp_LT/RT PARIETAL		0.05	0.947738	0.047619	0.0634921	0.746343675

3. Global mPSD – Frequency Bands

3.1. mPSD

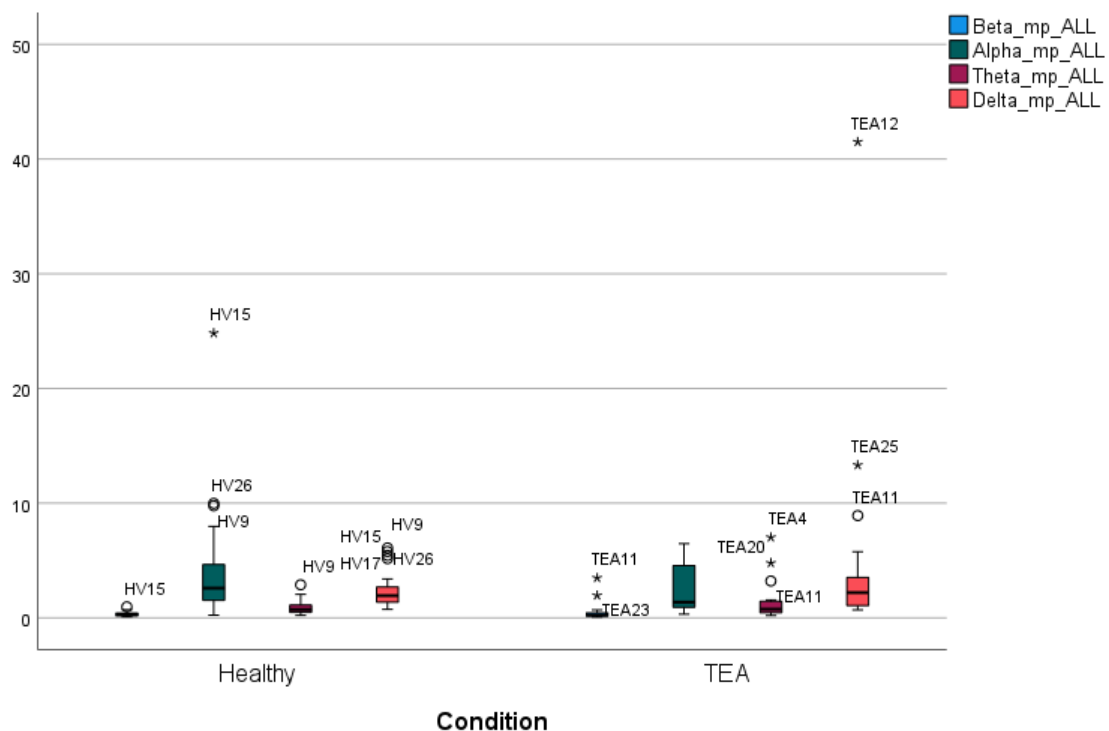


Figure 70: Boxplots for HV and TEA Global mPSD within beta, alpha, theta, and delta EEG bands

Table 51: Tests for Normality for Global mPSD Data within EEG Bands

Tests of Normality							
	Condition	Kolmogorov-Smirnov ^a			Shapiro-Wilk		
		Statistic	df	Sig.	Statistic	df	Sig.
Beta_mp_ALL	Healthy	.172	28	.034	.882	28	.004
	TEA	.305	28	<.001	.517	28	<.001
Alpha_mp_ALL	Healthy	.243	28	<.001	.654	28	<.001
	TEA	.262	28	<.001	.833	28	<.001
Theta_mp_ALL	Healthy	.163	28	.054	.811	28	<.001
	TEA	.307	28	<.001	.616	28	<.001
Delta_mp_ALL	Healthy	.193	28	.009	.828	28	<.001
	TEA	.349	28	<.001	.424	28	<.001

a. Lilliefors Significance Correction

Table 52: Global Datasets – PSD within EEG Bands, Distribution Descriptors

		Statistics			
		Beta_mp_ALL	Alpha_mp_ALL	Theta_mp_ALL	Delta_mp_ALL
N	Valid	56	56	56	56
	Missing	0	0	0	0
Mean		.40772375	3.30752822	1.06013155	3.33068141
Std. Error of Mean		.068337600	.503487494	.151020909	.752611730
Median		.29468649	2.34689048	.74867940	2.05757242
Std. Deviation		.511391769	3.767755402	1.130136998	5.632030479
Variance		.262	14.196	1.277	31.720
Skewness		4.646	3.693	3.597	5.973
Std. Error of Skewness		.319	.319	.319	.319
Kurtosis		25.417	18.976	15.452	39.853
Std. Error of Kurtosis		.628	.628	.628	.628
Percentiles	25	.17047603	1.00952925	.48430791	1.23646953
	50	.29468649	2.34689048	.74867940	2.05757242
	75	.44073838	4.60253697	1.21897438	3.06002215

- Global mPSD data within the beta band (13Hz – 40Hz) is very highly leptokurtic with a marked positive skew. The mean across all data is 0.41, with a standard error (SE) of 0.07 and a standard deviation (SD) of 0.51 (Figure 70, Table 52). The interquartile range is 0.27, and the variance is 0.26 (Table 52). As neither cohort shows a normal distribution (Table 51), a non-parametric Mann-Whitney U test was performed demonstrating there is no significant difference between cohorts for global mPSD within the beta EEG band profiles ($p = 0.99$ and, using FDR two-stage sharpened method, $q=1.04$) – Table 53.
- Global mPSD data within the alpha band (8Hz - 12.9Hz) is very highly leptokurtic with a marked positive skew. The mean across all data is 3.31, with a standard error (SE) of 0.50 and a standard deviation (SD) of 3.77 (Figure 70, Table 52). The interquartile range is 3.59, and the variance is 14.20 (Table 52). As neither cohort shows a normal distribution (Table 51), a non-parametric Mann-Whitney U test was performed demonstrating there is no significant difference between cohorts for global mPSD data within the alpha EEG band profiles ($p = 0.16$, using FDR two-stage sharpened method $q=0.67$) – Table 53.
- Global mPSD data within the theta (4Hz – 7.9Hz) is very highly leptokurtic with a marked positive skew. The mean across all data is 1.06, with a standard error (SE) of 0.15 and a standard deviation (SD) of 1.13 (Figure 70, Table 52). The interquartile range is 0.74, and the variance is 1.28 (Table 52). As neither cohort shows a normal distribution (Table 51), a non-parametric Mann-Whitney U test was performed demonstrating there is no significant difference between cohorts for global mPSD data within the theta EEG band ($p = 0.82$ and, using FDR two-stage sharpened method, $q=1.04$) – Table 53.
- Global mPSD data within the delta band (1Hz – 3.9Hz) is very highly leptokurtic with a marked positive skew. The mean across all data is 3.33, with a standard error (SE) of 0.75 and a standard deviation (SD) of 5.63 (Figure 70, Table 52). The interquartile range is 1.82, and the variance is 31.72 (Table 52). As neither cohort shows a normal distribution (Table 51), a non-parametric Mann-Whitney U test was performed demonstrating there is no significant difference between cohorts for global mPSD

data within the delta EEG band ($p = 0.49$ and, using FDR two-stage sharpened method, $q = 1.03$) – Table 53.

Table 53: Global mPSD per EEG Band - Multiple Comparisons using False Discovery Rates (FDRs) Adjustments

FDRs		Classical one-stage method*			Two-stage sharpened method†			
Order	Ascending p -values	Hypothesis name	Parametric FDR-derived significance thresholds	FDR-adjusted p -values a.k.a. q -values	Stage 1 significance thresholds	Stage 2 significance thresholds	FDR-adjusted p -values a.k.a. q -values	
1	0.15876	Alpha_mp_ALL		0.0125	0.635024	0.0119048	0.0119048	0.6667752
2	0.49130	Delta_mp_ALL		0.025	0.982594	0.0238095	0.0238095	1.0317237
3	0.81855	Theta_mp_ALL		0.0375	0.986926	0.0357143	0.0357143	1.0362723
4	0.98693	Beta_mp_ALL		0.05	0.986926	0.047619	0.047619	1.0362723

3.2. Interhemispheric mPSD Difference

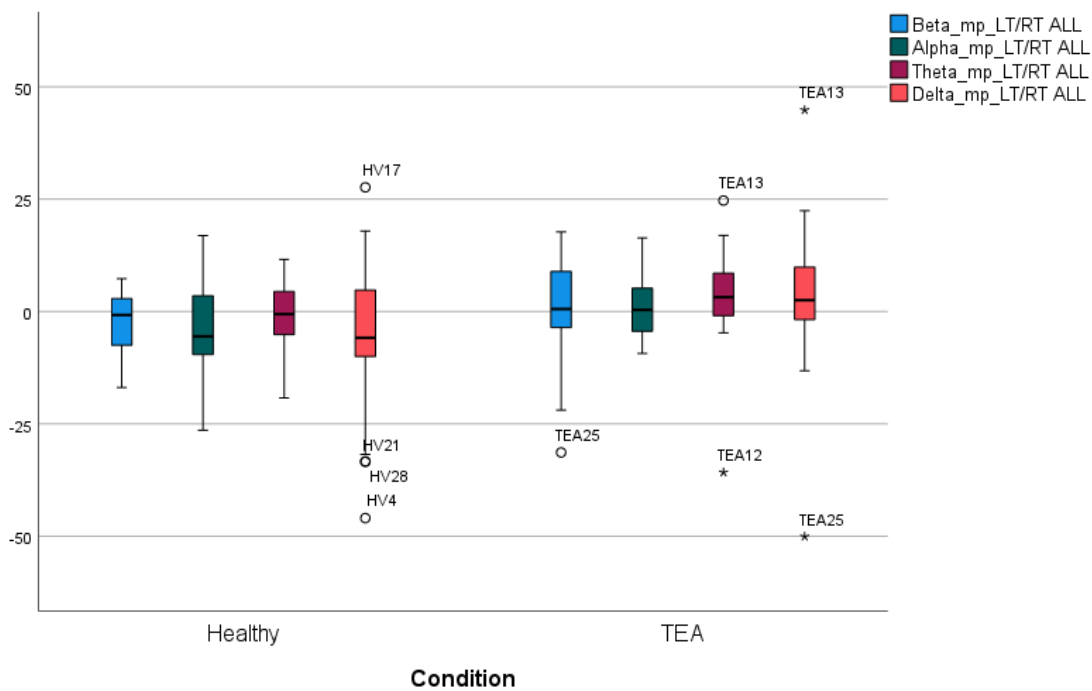


Figure 71: Boxplots for HV and TEA Global Inter-hemispheric mPSD Difference within beta, alpha, theta, and delta EEG bands

Table 54: Tests for Normality for Global Inter-hemispheric mPSD Data within EEG Bands

Tests of Normality							
	Condition	Kolmogorov-Smirnov ^a			Shapiro-Wilk		
		Statistic	df	Sig.	Statistic	df	Sig.
Beta_mp_LT/RT ALL	Healthy	.118	28	.200 [*]	.953	28	.231
	TEA	.152	28	.095	.945	28	.144
Alpha_mp_LT/RT ALL	Healthy	.098	28	.200 [*]	.990	28	.994
	TEA	.112	28	.200 [*]	.968	28	.525
Theta_mp_LT/RT ALL	Healthy	.102	28	.200 [*]	.965	28	.447
	TEA	.187	28	.013	.845	28	<.001
Delta_mp_LT/RT ALL	Healthy	.196	28	.007	.943	28	.133
	TEA	.150	28	.110	.885	28	.005

*. This is a lower bound of the true significance.
a. Lilliefors Significance Correction

Table 55: Global Datasets – Inter-hemispheric mPSD Difference within EEG Bands, Distribution Descriptors

		Statistics			
		Beta_mp_LT/RT ALL	Alpha_mp_LT/RT ALL	Theta_mp_LT/RT ALL	Delta_mp_LT/RT ALL
N	Valid	56	56	56	56
	Missing	0	0	0	0
Mean		-.957539	-1.624731	.914301	-1.421601
Std. Error of Mean		1.2415148	1.1504669	1.2657968	2.2523849
Median		-.372155	-1.774720	.703522	-.026441
Std. Deviation		9.2906463	8.6093057	9.4723557	16.8553048
Variance		86.316	74.120	89.726	284.101
Skewness		-.560	-.228	-.914	-.576
Std. Error of Skewness		.319	.319	.319	.319
Kurtosis		1.485	.460	3.701	1.784
Std. Error of Kurtosis		.628	.628	.628	.628
Percentiles	25	-6.976245	-6.556091	-3.494995	-9.255307
	50	-.372155	-1.774720	.703522	-.026441
	75	3.764540	4.244227	5.970660	8.001218

- Global inter-hemispheric mPSD difference data within the beta band (13Hz – 40Hz) is platykurtic and has a moderate negative skew. The mean across all data is -0.96, with a standard error (SE) of 1.24 and a standard deviation (SD) of 9.29 (Figure 71, Table 55). The interquartile range is 10.74, and the variance is 86.32 (Table 55). As both datasets show a normal distribution (Table 54), a parametric independent

samples T-test was performed demonstrating there is no significant difference between cohorts for global inter-hemispheric mPSD difference data within the beta EEG band profile ($p = 0.33$, using FDR two-stage sharpened method $q=0.35$) – Table 56.

- Global inter-hemispheric mPSD difference data within the alpha band (8Hz - 12.9Hz) is platykurtic but reasonably symmetric around the mean. The mean across all data is -1.62, with a standard error (SE) of 1.15 and a standard deviation (SD) of 8.61 (Figure 71, Table 55). The interquartile range is 10.80, and the variance is 74.12 (Table 55). As both datasets show a normal distribution (Table 54), a parametric independent samples T-test was performed demonstrating there is no significant difference between cohorts for global inter-hemispheric mPSD difference data within the alpha EEG band profile ($p = 0.06$, using FDR two-stage sharpened method $q=0.08$) – Table 56.
- Global inter-hemispheric mPSD difference data within the theta band (4Hz – 7.9Hz) is mesokurtic but shows a moderate negative skew. The mean across all data is 0.91, with a standard error (SE) of 1.27 and a standard deviation (SD) of 9.47 (Figure 71, Table 55). The interquartile range is 9.46, and the variance is 89.73 (Table 55). As only the HV cohort shows a normal distribution (Table 54), a non-parametric Mann-Whitney U test was performed demonstrating there is a significant difference between cohorts for global inter-hemispheric mPSD difference within the theta EEG band profile ($p = 0.03$). However, this is not verified using the FDR two-stage sharpened method, ($q = 0.07$) – Table 56.
- Global inter-hemispheric mPSD difference data within the delta band (1Hz – 3.9Hz) is slightly platykurtic with a moderate negative skew. The mean across all data is -1.42, with a standard error (SE) of 2.25 and a standard deviation (SD) of 16.86 (Figure 71, Table 55). The interquartile range is 17.26, and the variance is 284.10 (Table 55). As only the HV cohort shows a normal distribution (Table 54), a non-parametric Mann-Whitney U test was performed demonstrating there is a significant difference between cohorts for global inter-hemispheric mPSD difference within the delta EEG band profile ($p = 0.03$). However, this is not verified using the FDR two-stage sharpened method, ($q=0.07$) – Table 56.

Table 56: Global Inter-hemispheric PSD Difference per EEG Band - Multiple Comparisons using False Discovery Rates (FDRs) Adjustments

FDRs			Classical one-stage method*		Two-stage sharpened method†		
Order	Ascending <i>p</i> -values	Hypothesis name	Parametric FDR-derived significance thresholds	FDR-adjusted <i>p</i> -values a.k.a. <i>q</i> -values	Stage 1 significance thresholds	Stage 2 significance thresholds	FDR-adjusted <i>p</i> -values a.k.a. <i>q</i> -values
1	0.02584	Theta_mp_LT/RT ALL		0.069048	0.0119048	0.0119048	0.0725004
2	0.03452	Delta_mp_LT/RT ALL		0.069048	0.0238095	0.0238095	0.0725004
3	0.05672	Alpha_mp_LT/RT ALL	P	0.075624	0.0357143	0.0357143	0.0794052
4	0.33056	Beta_mp_LT/RT ALL	P	0.330561	0.047619	0.047619	0.34708905

4. Regional mPSD – Frequency Bands

4.1. mPSD

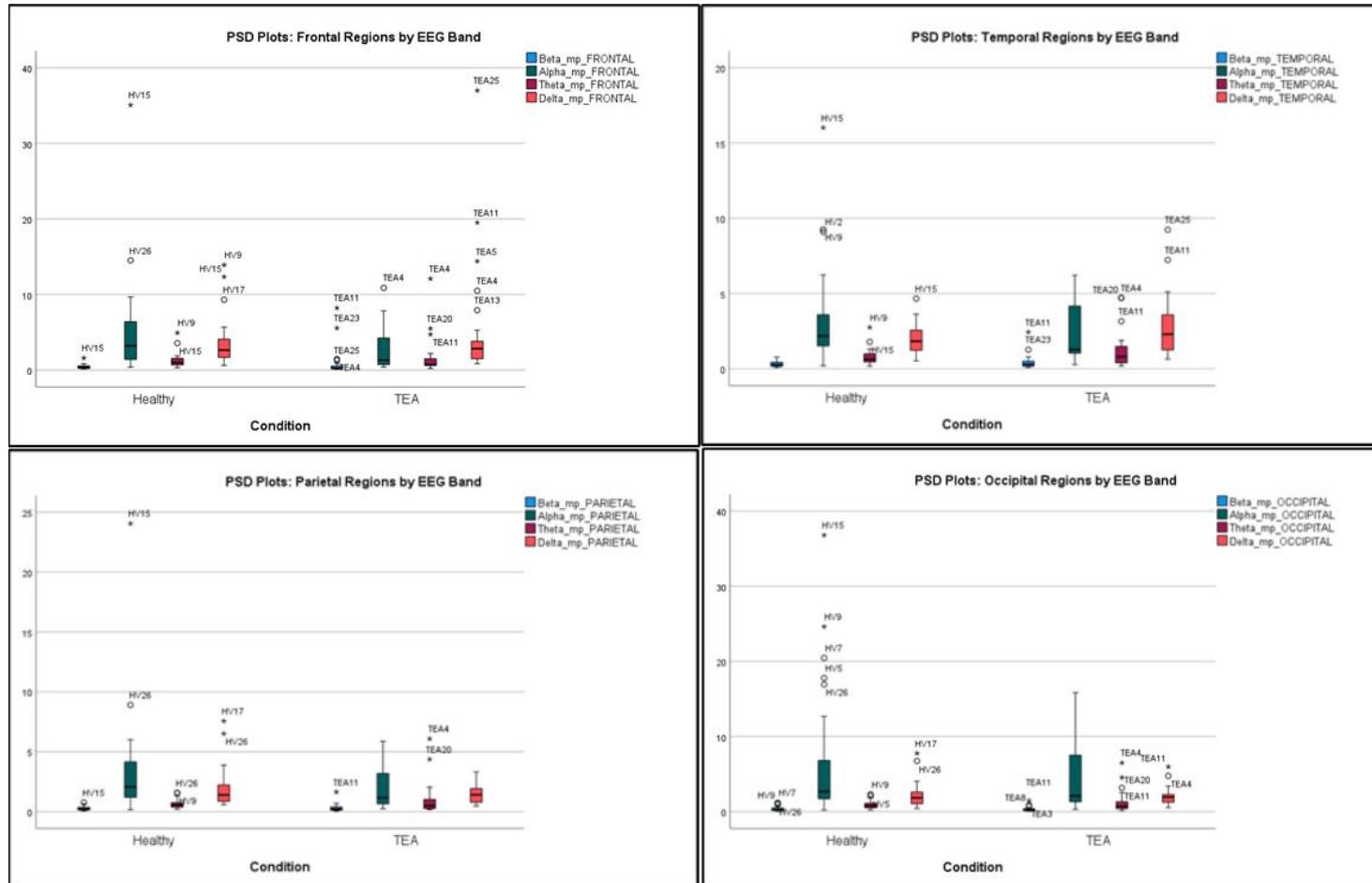


Figure 72: Boxplots for HV and TEA Regional mPSD within the beta, alpha, theta, and delta EEG bands

Table 57: Regional Datasets – mPSD within EEG Bands, Distribution Descriptors

		Statistics															
		Beta_mp_FRONTAL	Alpha_mp_FRONTAL	Theta_mp_FRONTAL	Delta_mp_FRONTAL	Beta_mp_TEMPORAL	Alpha_mp_TEMPORAL	Theta_mp_TEMPORAL	Delta_mp_TEMPORAL	Beta_mp_PARIETAL	Alpha_mp_PARIETAL	Theta_mp_PARIETAL	Delta_mp_PARIETAL	Beta_mp_OCCIPITAL	Alpha_mp_OCCIPITAL	Theta_mp_OCCIPITAL	Delta_mp_OCCIPITAL
N	Valid	56	56	56	55	56	56	56	56	56	56	56	56	56	56	56	56
	Missing	0	0	0	1	0	0	0	0	0	0	0	0	0	0	0	0
Mean		.64517331	3.91707465	1.46461914	4.40103048	.36636813	2.81892255	1.00527651	2.39411753	.28371220	2.67249263	.79975353	1.68815661	.35155699	5.64319142	1.04946674	2.14141206
Std. Error of Mean		.170624242	.703337124	.244288607	.791051430	.048039140	.364316150	.124330066	.219221328	.033367099	.462536743	.128700099	.174532625	.039189228	.930674038	.144047478	.193815215
Std. Deviation		1.276834909	5.263293092	1.828088545	5.866594417	.359492003	2.726292428	.930401017	1.640502204	.249696503	3.461308040	.963103350	1.306082568	.293265326	6.964526775	1.077952617	1.450380258
Variance		1.630	27.702	3.342	34.417	.129	7.433	.866	2.691	.062	11.981	.928	1.706	.086	48.505	1.162	2.104
Skewness		4.979	4.098	4.110	3.823	3.949	2.608	2.676	1.905	3.211	4.542	4.065	2.695	1.979	2.427	3.228	2.041
Std. Error of Skewness		.319	.319	.319	.322	.319	.319	.319	.319	.319	.319	.319	.319	.319	.319	.319	.319
Kurtosis		26.233	22.255	20.930	17.922	20.387	9.476	8.039	5.216	15.206	26.691	19.053	9.347	3.948	7.070	12.792	4.960
Std. Error of Kurtosis		.628	.628	.628	.634	.628	.628	.628	.628	.628	.628	.628	.628	.628	.628	.628	.628
Percentiles	25	.19578949	.90306804	.62208903	1.54968751	.17213236	1.06938001	.43027982	1.24699122	.13023351	.72605375	.32772002	.82753819	.16727306	1.53486532	.44346032	1.14941237
	50	.33458861	2.51442650	.89266543	2.83071350	.28309625	1.86043845	.74602727	2.00737776	.23116217	1.65158838	.54344690	1.39910809	.26234719	2.47991434	.73256441	1.92738231
	75	.55659881	4.74956003	1.60390060	4.14583865	.44990081	3.99764475	1.13678739	3.13946558	.39379193	3.47588612	.92450186	2.05118443	.42017828	7.29229235	1.23611355	2.45226406

All regional mPSD datasets are leptokurtic, with frontal beta and parietal alpha data having the most significant leptokurtosis and occipital beta and delta showing the least. All regional mPSD datasets show a significant positive skew (Table 57).

Frontal delta and occipital alpha frequencies have the highest mPSD, and beta frequencies have the lowest mPSD. (Figure 72, Table 57). Alpha activities in frontal and occipital areas and frontal delta tend to show the highest standard errors for the mean, whilst beta frequencies have the lowest. A similar pattern is seen for standard deviation, variance, and interquartile range. (Figure 72, Table 57).

Only temporal delta data for the HV cohort meets the criteria for normal distribution using Shapiro-Wilk (Table 58). Therefore, all datasets were compared using the non-parametric Mann-Whitney U test. Only frontal alpha activities show a significant p-value ($p=0.03$) however, once multiple comparisons FDR adjustments are made, the resulting q-values are not significant for either the classic one-stage or the two-stage sharpened method (Table 59).

Table 58: Tests for Normality for Regional mPSD Data within EEG Bands

Tests of Normality							
Condition	Statistic	Kolmogorov-Smirnov ^a			Shapiro-Wilk		
		df	Sig.	Statistic	df	Sig.	
Beta_mp_FRONTAL	Healthy	.169	28	.039	.789	28	<.001
	TEA	.369	27	<.001	.441	27	<.001
Alpha_mp_FRONTAL	Healthy	.239	28	<.001	.616	28	<.001
	TEA	.240	27	<.001	.789	27	<.001
Theta_mp_FRONTAL	Healthy	.206	28	.004	.729	28	<.001
	TEA	.309	27	<.001	.530	27	<.001
Delta_mp_FRONTAL	Healthy	.244	28	<.001	.723	28	<.001
	TEA	.334	27	<.001	.561	27	<.001
Beta_mp_TEMPORAL	Healthy	.190	28	.011	.866	28	.002
	TEA	.236	27	<.001	.627	27	<.001
Alpha_mp_TEMPORAL	Healthy	.262	28	<.001	.734	28	<.001
	TEA	.264	27	<.001	.824	27	<.001
Theta_mp_TEMPORAL	Healthy	.173	28	.032	.803	28	<.001
	TEA	.222	27	.001	.726	27	<.001
Delta_mp_TEMPORAL	Healthy	.123	28	.200 [*]	.952	28	.223
	TEA	.152	27	.109	.852	27	.001
Beta_mp_PARIETAL	Healthy	.166	28	.045	.903	28	.013
	TEA	.209	27	.004	.653	27	<.001
Alpha_mp_PARIETAL	Healthy	.239	28	<.001	.572	28	<.001
	TEA	.228	27	<.001	.840	27	<.001
Theta_mp_PARIETAL	Healthy	.182	28	.019	.862	28	.002
	TEA	.325	27	<.001	.571	27	<.001
Delta_mp_PARIETAL	Healthy	.233	28	<.001	.688	28	<.001
	TEA	.129	27	.200 [*]	.921	27	.041
Beta_mp_OCCIPITAL	Healthy	.227	28	<.001	.822	28	<.001
	TEA	.236	27	<.001	.709	27	<.001
Alpha_mp_OCCIPITAL	Healthy	.313	28	<.001	.698	28	<.001
	TEA	.257	27	<.001	.831	27	<.001
Theta_mp_OCCIPITAL	Healthy	.183	28	.018	.889	28	.006
	TEA	.257	27	<.001	.658	27	<.001
Delta_mp_OCCIPITAL	Healthy	.206	28	.004	.789	28	<.001
	TEA	.197	27	.009	.842	27	<.001

*. This is a lower bound of the true significance.
a. Lilliefors Significance Correction

Table 59: Regional mPSD per EEG Band - Multiple Comparisons using False Discovery Rates (FDRs) Adjustments

FDRs		Classical one-stage method*			Two-stage sharpened method†		
Order	Ascending	Hypothesis name	FDR-derived significance thresholds	FDR-adjusted	Stage 1	Stage 2	FDR-adjusted
	p-values			p-values	significance thresholds	significance thresholds	p-values
				a.k.a. q-values			a.k.a. q-values
1	0.03895	Alpha_mp_FRONTAL	0.003125	0.623152	0.0029762	0.0029762	0.6543096
2	0.11953	Alpha_mp_PARIETAL	0.00625	0.795513846	0.0059524	0.0059524	0.835289538
3	0.21299	Delta_mp_TEMPORAL	0.009375	0.795513846	0.0089286	0.0089286	0.835289538
4	0.29429	Alpha_mp_TEMPORAL	0.0125	0.795513846	0.0119048	0.0119048	0.835289538
5	0.35028	Beta_mp_OCCIPITAL	0.015625	0.795513846	0.014881	0.014881	0.835289538
6	0.35880	Beta_mp_TEMPORAL	0.01875	0.795513846	0.0178571	0.0178571	0.835289538
7	0.36744	Beta_mp_FRONTAL	0.021875	0.795513846	0.0208333	0.0208333	0.835289538
8	0.51216	Alpha_mp_OCCIPITAL	0.025	0.795513846	0.0238095	0.0238095	0.835289538
9	0.60002	Theta_mp_PARIETAL	0.028125	0.795513846	0.0267857	0.0267857	0.835289538
10	0.60002	Theta_mp_TEMPORAL	0.03125	0.795513846	0.0297619	0.0297619	0.835289538
11	0.61146	Beta_mp_PARIETAL	0.034375	0.795513846	0.0327381	0.0327381	0.835289538
12	0.63463	Delta_mp_PARIETAL	0.0375	0.795513846	0.0357143	0.0357143	0.835289538
13	0.64636	Theta_mp_FRONTAL	0.040625	0.795513846	0.0386905	0.0386905	0.835289538
14	0.80584	Theta_mp_OCCIPITAL	0.04375	0.920954286	0.0416667	0.0416667	0.967002
15	0.91954	Delta_mp_FRONTAL	0.046875	0.973855	0.0446429	0.0446429	1.02254775
16	0.97386	Delta_mp_OCCIPITAL	0.05	0.973855	0.047619	0.047619	1.02254775

4.2. Interhemispheric mPSD Difference

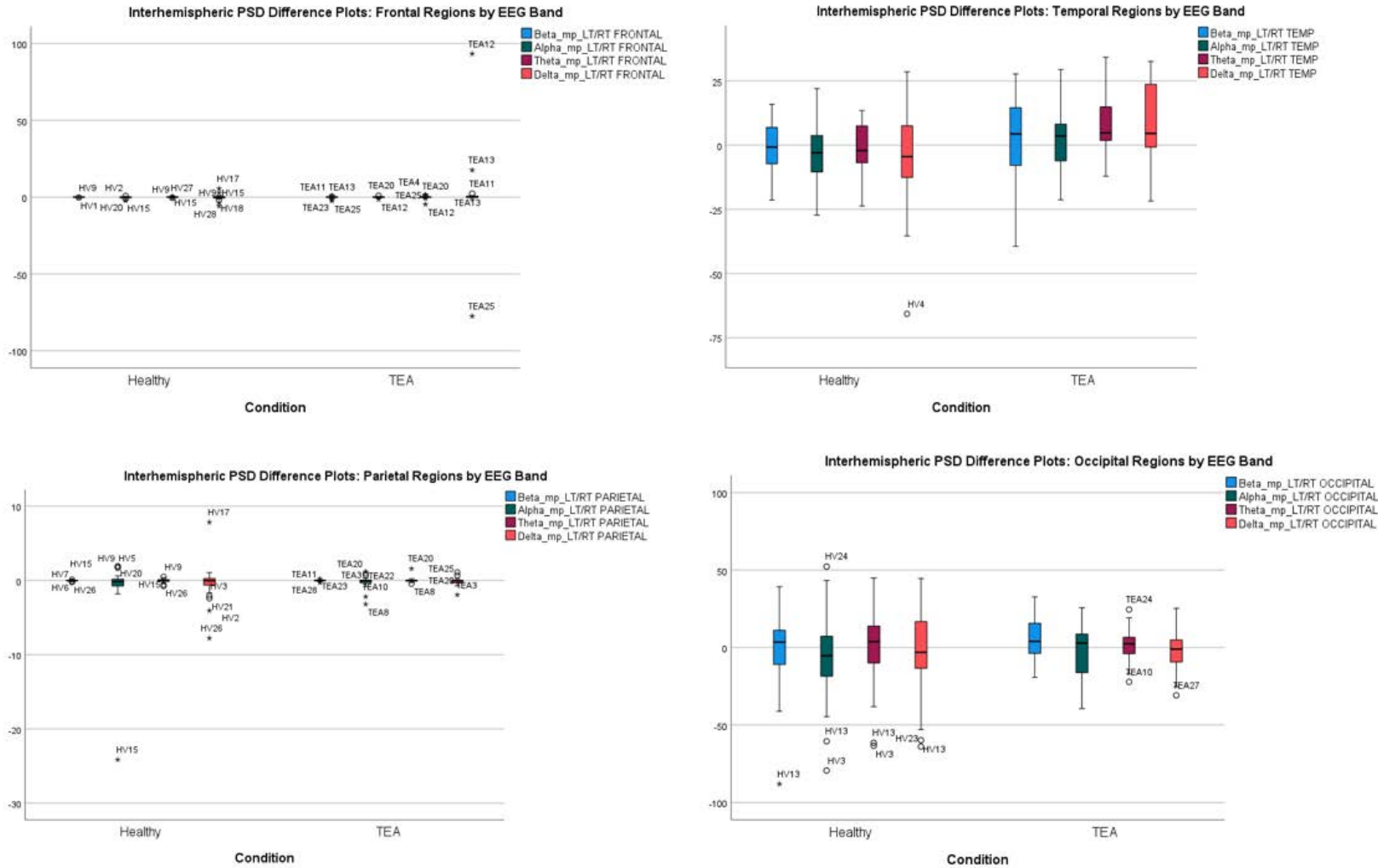


Figure 73: Boxplots for HV and TEA Regional Interhemispheric mPSD Differences within beta, alpha, theta, and delta EEG bands

Table 60: Regional Datasets – Interhemispheric mPSD Difference within EEG Bands, Distribution Descriptors

		Statistics															
		Beta_mp_LT/RT FRONTAL	Alpha_mp_LT/RT FRONTAL	Theta_mp_LT/RT FRONTAL	Delta_mp_LT/RT FRONTAL	Beta_mp_LT/RT TEMP	Alpha_mp_LT/RT TEMP	Theta_mp_LT/RT TEMP	Delta_mp_LT/RT TEMP	Beta_mp_LT/RT PARIETAL	Alpha_mp_LT/RT PARIETAL	Theta_mp_LT/RT PARIETAL	Delta_mp_LT/RT PARIETAL	Beta_mp_LT/RT OCCIPITAL	Alpha_mp_LT/RT OCCIPITAL	Theta_mp_LT/RT OCCIPITAL	Delta_mp_LT/RT OCCIPITAL
N	Valid	56	56	56	56	56	56	56	56	56	56	56	56	56	56	56	56
	Missing	0	0	0	0	0	0	0	0	0	0	0	0	0	0	0	0
Mean		-.064527	-.098695	-.061165	.552620	1.125843	-.493468	3.666806	2.068633	-.024114	-.572991	-.025154	-.250007	2.229037	-3.258820	.083472	-1.881935
Std. Error of Mean		.0545459	.0640121	.0947312	2.2144065	1.7957907	1.5316332	1.6096902	2.4090279	.0116294	.4430288	.0405804	.2290434	2.6477406	3.2314240	2.6113501	2.9186565
Std. Deviation		.4081844	.4790226	.7089037	16.5711006	13.4384668	11.4616931	12.0458187	18.0275138	.0870261	3.3153242	.3036762	1.7140041	19.8138762	24.1817632	19.5415546	21.8412250
Variance		.167	.229	.503	274.601	180.592	131.370	145.102	324.991	.008	10.991	.092	2.938	392.590	584.758	381.872	477.039
Skewness		-3.932	-1.789	-4.703	1.356	-.303	.080	.325	-.814	-.560	-6.754	2.410	.105	-1.804	-.472	-1.002	-.535
Std. Error of Skewness		.319	.319	.319	.319	.319	.319	.319	.319	.319	.319	.319	.319	.319	.319	.319	.319
Kurtosis		21.966	6.900	32.755	26.693	.407	.399	.739	2.450	2.567	48.635	14.261	15.050	6.960	1.319	2.991	1.265
Std. Error of Kurtosis		.628	.628	.628	.628	.628	.628	.628	.628	.628	.628	.628	.628	.628	.628	.628	.628
Percentiles	25	-.053799	-.204450	-.102177	-.353049	-7.602712	-7.216186	-3.579040	-7.121500	-.050757	-.413749	-.118080	-.405286	-5.648268	-16.905739	-6.552755	-10.418493
	50	-.009797	-.040650	-.008006	.001245	2.292825	-.307526	3.700158	.223996	-.012103	-.107391	-.017829	-.054188	3.682258	-1.123699	2.594205	-1.137403
	75	.026988	.116975	.074328	.409042	11.431807	6.525821	11.427894	13.982130	.013206	.089579	.056957	.140405	14.674871	8.227588	9.348891	9.871448

All regional interhemispheric mPSD difference datasets are leptokurtic, with frontal beta and parietal alpha data having the most significant leptokurtosis and occipital beta and delta showing the least. All regional interhemispheric mPSD difference datasets show significant positive skew (Table 60).

Temporal theta activities have the highest left hemisphere mPSD difference (3.67) whilst occipital alpha shows the highest right hemisphere mPSD difference (-3.26). Parietal beta and theta activities show the lowest interhemispheric mPSD difference i.e., are the most symmetric between the hemispheres (Figure 73, Table 60). Frequency bands on occipital regions tend to show the highest standard errors for the mean, standard deviation, variance, and interquartile range. (Figure 73, Table 60).

Both TEA and HV datasets for temporal beta, alpha, theta, and delta interhemispheric mPSD, and alpha, theta and delta occipital datasets meet the criteria for normal distribution using Shapiro-Wilk (Table 61). These datasets were compared using an independent samples parametric T-test, whilst the rest of the datasets were compared using the non-parametric Mann-Whitney U test.

Table 61: Tests for Normality for Regional Interhemispheric mPSD Difference Data within EEG Bands

Tests of Normality							
	Condition	Kolmogorov-Smirnov ^a			Shapiro-Wilk		
		Statistic	df	Sig.	Statistic	df	Sig.
Beta_mp_LT/RT FRONTAL	Healthy	.196	28	.007	.858	28	.001
	TEA	.306	28	<.001	.604	28	<.001
Alpha_mp_LT/RT FRONTAL	Healthy	.201	28	.005	.797	28	<.001
	TEA	.150	28	.110	.900	28	.011
Theta_mp_LT/RT FRONTAL	Healthy	.176	28	.026	.862	28	.002
	TEA	.387	28	<.001	.518	28	<.001
Delta_mp_LT/RT FRONTAL	Healthy	.227	28	<.001	.799	28	<.001
	TEA	.418	28	<.001	.433	28	<.001
Beta_mp_LT/RT TEMP	Healthy	.130	28	.200 [*]	.955	28	.267
	TEA	.075	28	.200 [*]	.967	28	.514
Alpha_mp_LT/RT TEMP	Healthy	.093	28	.200 [*]	.980	28	.855
	TEA	.093	28	.200 [*]	.982	28	.901
Theta_mp_LT/RT TEMP	Healthy	.140	28	.172	.936	28	.087
	TEA	.173	28	.032	.942	28	.122
Delta_mp_LT/RT TEMP	Healthy	.134	28	.200 [*]	.931	28	.065
	TEA	.141	28	.166	.953	28	.238
Beta_mp_LT/RT PARIETAL	Healthy	.174	28	.029	.932	28	.070
	TEA	.170	28	.037	.890	28	.007
Alpha_mp_LT/RT PARIETAL	Healthy	.389	28	<.001	.348	28	<.001
	TEA	.276	28	<.001	.747	28	<.001
Theta_mp_LT/RT PARIETAL	Healthy	.188	28	.013	.955	28	.271
	TEA	.332	28	<.001	.556	28	<.001
Delta_mp_LT/RT PARIETAL	Healthy	.247	28	<.001	.737	28	<.001
	TEA	.167	28	.044	.857	28	.001
Beta_mp_LT/RT OCCIPITAL	Healthy	.132	28	.200 [*]	.892	28	.007
	TEA	.089	28	.200 [*]	.989	28	.986
Alpha_mp_LT/RT OCCIPITAL	Healthy	.148	28	.120	.963	28	.418
	TEA	.184	28	.016	.947	28	.165
Theta_mp_LT/RT OCCIPITAL	Healthy	.159	28	.068	.934	28	.076
	TEA	.085	28	.200 [*]	.982	28	.898
Delta_mp_LT/RT OCCIPITAL	Healthy	.117	28	.200 [*]	.954	28	.255
	TEA	.124	28	.200 [*]	.982	28	.885

*. This is a lower bound of the true significance.
a. Lilliefors Significance Correction

Significant inter-hemisphere mPSD differences for theta, delta and alpha activities were seen over temporal regions, with p-values of $p=0.002$, $p=0.006$, and $p=0.043$ respectively.

Once multiple comparisons FDR adjustments are made, both interhemispheric differences for temporal theta and delta activities remain significant for classic one-stage, two-stage sharpened and graphically sharpened methods (theta $q=0.032$, delta $q=0.048$) (Table 65).

Examining the hemispheric mean power mean/median values in more depth, the delta frequency range mPSD is significantly higher on the left, when compared to the right as well as the mean inter-hemisphere difference is significantly higher in TEA (Table 62, Table 64).

For the theta frequency band, only the mean inter-hemisphere difference shows significance, with higher values seen in the TEA cohort (Table 62, Table 63).

Table 62: Mean and Median values for TEA and HV cohorts - mPSD temporal inter-hemisphere analysis. Right: Theta frequencies. Left: Delta frequencies.

Report: mPSD IHD TEMPORAL, Theta					Report: mPSD IHD TEMPORAL, Delta				
Condition		psdRIGHT	psdLEFT	psdDIFF/SUM	Condition		psdRIGHT	psdLEFT	psdDIFF/SUM
Healthy	Mean	.82100291	.80435433	-1.18241622	Healthy	Mean	2.11493004	1.90019762	-4.38045868
	Median	.63219854	.64327573	-2.08402223		Median	1.78250190	1.59353225	-4.46613274
TEA	Mean	1.08738277	1.30836605	8.51602792	TEA	Mean	2.49475149	3.06659098	8.51772510
	Median	.73490175	.80043257	4.77459245		Median	2.06466897	2.34686102	4.58472686
Total	Mean	.95419284	1.05636019	3.66680585	Total	Mean	2.30484076	2.48339430	2.06863321
	Median	.71371181	.71485054	3.70015840		Median	1.93579591	1.91394794	.22399643

Table 63: Mann Whitney-U test results for mPSD temporal inter-hemisphere analysis, theta frequencies.

Hypothesis Test Summary: mPSD IHD TEMPORAL, Theta				
	Null Hypothesis	Test	Sig. ^{a,b}	Decision
1	The distribution of psdRIGHT is the same across categories of Condition.	Independent-Samples Mann-Whitney U Test	.806	Retain the null hypothesis.
2	The distribution of psdLEFT is the same across categories of Condition.	Independent-Samples Mann-Whitney U Test	.232	Retain the null hypothesis.
3	The distribution of psdDIFF/SUM is the same across categories of Condition.	Independent-Samples Mann-Whitney U Test	.004	Reject the null hypothesis.

a. The significance level is .050.
b. Asymptotic significance is displayed.

Table 64: T- test results for mPSD temporal inter-hemisphere analysis, delta frequencies.

Independent Samples Test: mPSD IHD TEMPORAL, Delta										
		Levene's Test for Equality of Variances		t-test for Equality of Means						
		F	Sig.	t	df	Sig. (2-tailed)	Mean Difference	Std. Error Difference	95% Confidence Interval of the Difference	
									Lower	Upper
psdRIGHT	Equal variances assumed	2.411	.126	-.951	54	.346	-.379821450	.399326979	-1.180423840	.420780939
	Equal variances not assumed			-.951	47.607	.346	-.379821450	.399326979	-1.182893224	.423250324
psdLEFT	Equal variances assumed	7.563	.008	-2.323	54	.024	-1.166393360	.502058565	-2.172960179	-1.159826541
	Equal variances not assumed			-2.323	38.420	.026	-1.166393360	.502058565	-2.182393293	-1.150393427
psdDIFF/SUM	Equal variances assumed	.099	.754	-2.844	54	.006	-12.89818378	4.534616268	-21.9895420	-3.806825547
	Equal variances not assumed			-2.844	50.784	.006	-12.89818378	4.534616268	-22.0027452	-3.793622328

Table 65: Regional Interhemispheric mPSD Difference per EEG Band - Multiple Comparisons using False Discovery Rates (FDRs) Adjustments

FDRs			Classical one-stage method*		Two-stage sharpened method†			Graphically sharpened method‡				
Order	Ascending p-values	Hypothesis name	Parametric	FDR-derived significance thresholds	FDR-adjusted p-values a.k.a. q-values	Stage 1 significance thresholds	Stage 2 significance thresholds	FDR-adjusted p-values a.k.a. q-values	Point estimates of no. of H ₀ s	Best estimate	FDR-derived significance thresholds	FDR-adjusted p-values a.k.a. q-values
1	0.00200	TEMPORAL Theta psdDIFF/SUM	NP	0.003125 *	0.032	0.0029762	0.0031746 *	0.0315	16.0000		0.003125 *	0.032
2	0.00600	TEMPORAL Delta psdDIFF/SUM	P	0.00625 *	0.048	0.0059524	0.0063492 *	0.04725	15.0905		0.00625 *	0.048
3	0.04300	TEMPORAL Alpha psdDIFF/SUM	NP	0.009375	0.229333333	0.0089286	0.0095238	0.22575	14.6290		0.009375	0.229333333
4	0.09500	FRONTAL Delta psdDIFF/SUM	P	0.0125	0.38	0.0119048	0.0126984	0.3740625	14.3646		0.0125	0.38
5	0.14000	FRONTAL Alpha psdDIFF/SUM	NP	0.015625	0.448	0.014881	0.015873	0.441	13.9535		0.015625	0.448
6	0.20900	TEMPORAL Beta psdDIFF/SUM	NP	0.01875	0.557333333	0.0178571	0.0190476	0.548625	13.9064		0.01875	0.557333333
7	0.35900	FRONTAL Beta psdDIFF/SUM	NP	0.021875	0.6976	0.0208333	0.0222222	0.6867	15.6006	True	0.021875	0.6976
8	0.39400	OCCIPITAL Beta psdDIFF/SUM	P	0.025	0.6976	0.0238095	0.0253968	0.6867	14.8515		0.025	0.6976
9	0.42200	FRONTAL Theta psdDIFF/SUM	NP	0.028125	0.6976	0.0267857	0.0285714	0.6867	13.8408		0.028125	0.6976
10	0.43600	OCCIPITAL Alpha psdDIFF/SUM	P	0.03125	0.6976	0.0297619	0.031746	0.6867	12.4113		0.03125	0.6976
11	0.63300	OCCIPITAL Theta psdDIFF/SUM	NP	0.034375	0.797866667	0.0327381	0.0349206	0.7854	16.0000		0.034375	0.797866667
12	0.67000	PARIETAL Alpha psdDIFF/SUM	P	0.0375	0.797866667	0.0357143	0.0380952	0.7854	15.1515		0.0375	0.797866667
13	0.69400	PARIETAL Theta psdDIFF/SUM	NP	0.040625	0.797866667	0.0386905	0.0412698	0.7854	13.0719		0.040625	0.797866667
14	0.70600	PARIETAL Delta psdDIFF/SUM	P	0.04375	0.797866667	0.0416667	0.0444444	0.7854	10.2041		0.04375	0.797866667
15	0.74800	OCCIPITAL Delta psdDIFF/SUM	NP	0.046875	0.797866667	0.0446429	0.047619	0.7854	7.9365		0.046875	0.797866667
16	0.98700	PARIETAL Beta psdDIFF/SUM	P	0.05	0.987	0.047619	0.0507937	0.971578125	16.0000		0.05	0.987

Second Phase – Connectivity Analysis – Imaginary Coherence (iCoh)

The analysis aimed to determine the effects TEA may have on the communication within and between brain regions, at the global and regional levels, considering variation within the frequency band. The coherence-based measure Imaginary Coherence (iCoh) was used to assess the linear, functional connectivity, recognising its benefits and disadvantages (i.e. while iCoh effectively minimises the effects of volume conduction, it is affected by phase (connectivity with $\frac{1}{4}$ of a cycle lag is best detected), and signal amplitude (Jia, 2019; Nolte *et al.*, 2004).

Regional and interhemispheric iCoh were computed for the full frequency spectrum and within frequency bands (beta, alpha, theta, delta), for both global and regional spectra.

Dataset distributions were assessed using SPSS explore and Shapiro-Wilk tests were performed to check for normality. Comparison of TEA and HV cohorts was undertaken using a parametric Independent Samples T-Test for normal distributions; otherwise, a non-parametric Independent Samples Mann-Whitney U test was performed. Statistical significance was set at $p = <0.05$. To control for type I errors generated by the false rejection of the null hypothesis through multiple comparisons within the regional, and frequency band analysis, False Discovery Rate (FDR) adjustments using the classic one-stage, and two-stage sharpened methods were undertaken (Benjamini and Hochberg, 1995; Benjamini and Hochberg, 2000; Benjamini *et al.*, 2006; Pike, 2011; Nichols, 2007) with before p -values, and after correction q -values being reported within the results.

1. Global iCoh, All Frequencies

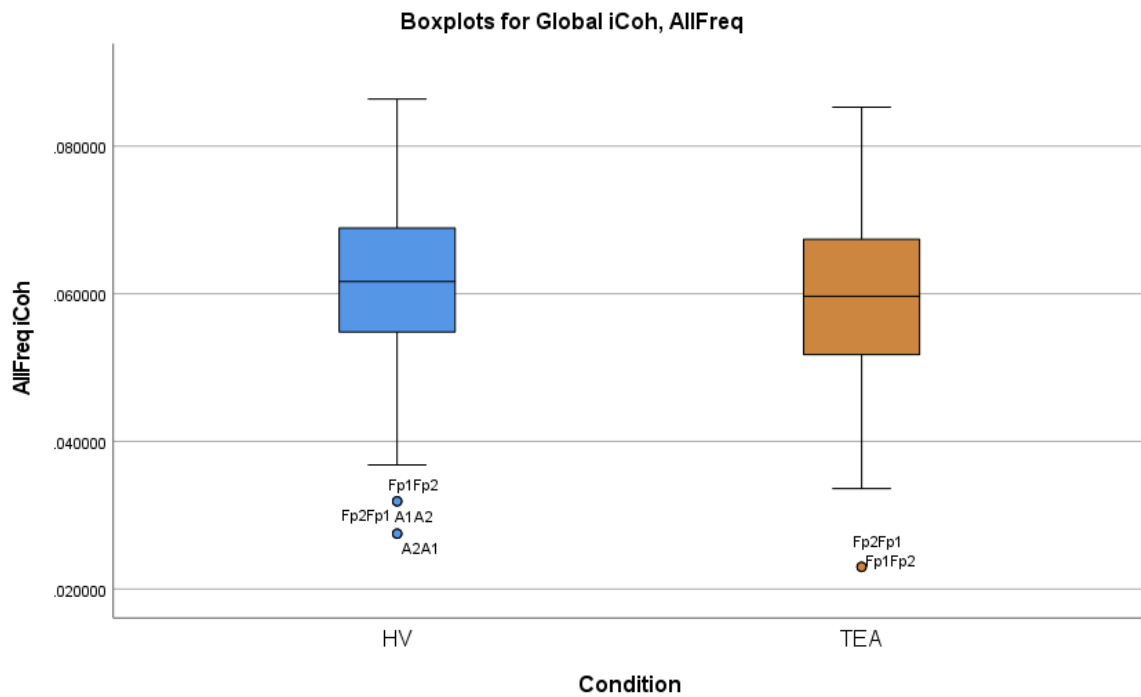


Figure 74: Boxplots for TEA and HV iCoh at Global level, all frequencies (1-40Hz)

Global iCoh has a platykurtic data distribution with a slight positive skew (Table 67). The mean across all data is 0.061, with a standard error (SE) of 0.0004 and a standard deviation (SD) of 0.011. The interquartile range is 0.0156, and the range is 0.063 (Table 67, Figure 74).

As both cohorts do not show a normal distribution (Table 66), the non-parametric Mann-Whitney U test was performed demonstrating a significant difference in iCoh profiles between the cohorts at a global level ($p = 0.004$), with lower mean/median values seen in the TEA cohort (Table 68, Table 69).

Table 66: Tests of Normality for global iCoh, all frequencies (1-40Hz)

Tests of Normality - Global iCoh, AllFreq							
Condition	Kolmogorov-Smirnov ^a			Shapiro-Wilk			
	Statistic	df	Sig.	Statistic	df	Sig.	
AllFreq HV	.050	420	.014	.991	420	.009	
AllFreq TEA	.051	420	.011	.989	420	.003	

a. Lilliefors Significance Correction

Table 67: Descriptives for global iCoh, all frequencies (1-40Hz)

Statistics - Global iCoh		
AllFreq		
N	Valid	840
	Missing	42
Mean		.06096060
Std. Error of Mean		.000378640
Median		.06086527
Std. Deviation		.010974040
Variance		.000
Skewness		-.101
Std. Error of Skewness		.084
Kurtosis		-.167
Std. Error of Kurtosis		.169
Range		.063382
Percentiles	25	.05301524
	50	.06086527
	75	.06860800

Table 68: Significant Non-Parametric Findings for Global iCoh.

Independent-Samples Mann-Whitney U Test Summary	
Total N	840
Mann-Whitney U	78096.000
Wilcoxon W	166506.000
Test Statistic	78096.000
Standard Error	3516.056
Standardized Test Statistic	-2.874
Asymptotic Sig.(2-sided test)	.004

Report Global iCoh		
AllFreq		
Condition	Mean	Median
HV	.06190880	.06167086
TEA	.06001240	.05966969
Total	.06096060	.06086527

Table 69: Global iCoh Mean/Median values for TEA and HV cohorts, with lower values for TEA (marked in blue).

2. Intra-Regional and Inter-Regional iCoh, All Frequencies

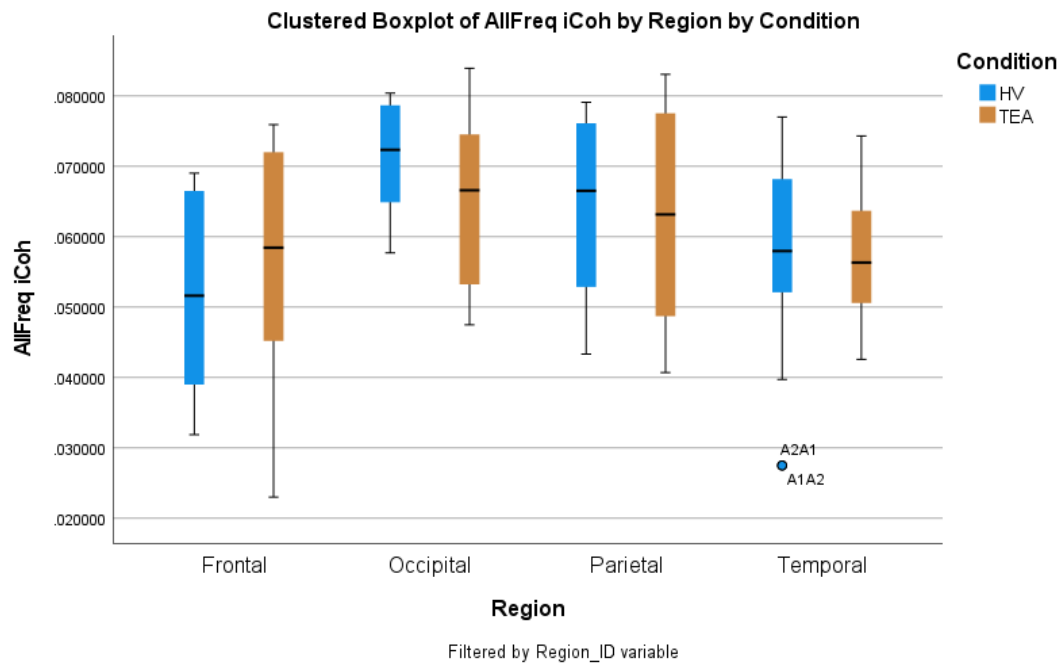


Figure 75: Intra-Regional iCoh Boxplot, all frequencies (1-40Hz)

Regional iCoh data shows a platykurtic data distribution with a slight negative skew, for all regions (frontal, occipital, parietal, temporal) (Table 71). Data descriptives for regions are as follows (Table 71, Figure 75):

- Frontal regions - the mean is 0.0542, with a SE of 0.0024 and an SD of 0.0155. The interquartile range is 0.0272, and the range is 0.0529.
- Occipital regions - the mean is 0.0681, with a SE of 0.0028 and an SD of 0.0114. The interquartile range is 0.0182, and the range is 0.0365.
- Parietal regions - the mean is 0.0629, with a SE of 0.0017 and SD of 0.0132. The interquartile range is 0.0247, and the range is 0.0424.
- Temporal regions - the mean is 0.0579, with a SE of 0.0008 and SD of 0.0097. The interquartile range is 0.0144, and the range is 0.0495.

Only the TEA cohort occipital iCoh data distribution meets the criteria for normality (the TEA temporal distribution is borderline); all other data do not meet normality requirements (Table 70). Therefore, the non-parametric Mann-Whitney U test was utilised. There are no significant differences in intra-regional iCoh between cohorts, for all regions i.e., frontal, occipital, parietal, or temporal - Table 72.

Table 70: Tests for normality for Regional iCoh, all frequencies (1-40Hz).

Tests of Normality: Frontal iCoh, AllFreq							
Condition	Kolmogorov-Smirnov			Shapiro-Wilk			
	Statistic	df	Sig.	Statistic	df	Sig.	
AllFreq HV	.164	20	.162	.900	20	.042	
TEA	.201	20	.033	.887	20	.024	

Tests of Normality: Occipital iCoh, AllFreq							
Condition	Kolmogorov-Smirnov			Shapiro-Wilk			
	Statistic	df	Sig.	Statistic	df	Sig.	
AllFreq HV	.293	8	.042	.842	8	.080	
TEA	.164	8	.200	.926	8	.484	

Tests of Normality: Parietal iCoh, AllFreq							
Condition	Kolmogorov-Smirnov			Shapiro-Wilk			
	Statistic	df	Sig.	Statistic	df	Sig.	
AllFreq HV	.173	30	.023	.888	30	.004	
TEA	.182	30	.013	.920	30	.026	

Tests of Normality: Temporal iCoh, AllFreq							
Condition	Kolmogorov-Smirnov ^a			Shapiro-Wilk			
	Statistic	df	Sig.	Statistic	df	Sig.	
AllFreq HV	.068	74	.200 [*]	.966	74	.043	
TEA	.091	74	.200 [*]	.968	74	.058	

^{*}. This is a lower bound of the true significance.
^a. Lilliefors Significance Correction

Table 71: Data descriptives for regional iCoh, all frequencies (1-40Hz).

Statistics - Frontal iCoh, AllFreq			Occipital iCoh, AllFreq			Parietal iCoh, AllFreq			Temporal iCoh, AllFreq		
AllFreq			AllFreq			AllFreq			AllFreq		
N	Valid	40	N	Valid	16	N	Valid	60	N	Valid	148
	Missing	10		Missing	4		Missing	12		Missing	16
Mean		.05424366	Mean		.06812937	Mean		.06290511	Mean		.05793373
Std. Error of Mean		.002446713	Std. Error of Mean		.002848428	Std. Error of Mean		.001697737	Std. Error of Mean		.000797929
Median		.05331532	Median		.06661080	Median		.06398265	Median		.05775963
Std. Deviation		.015474373	Std. Deviation		.011393712	Std. Deviation		.013150615	Std. Deviation		.009707223
Variance		.000	Variance		.000	Variance		.000	Variance		.000
Skewness		-.234	Skewness		-.444	Skewness		-.092	Skewness		-.174
Std. Error of Skewness		.374	Std. Error of Skewness		.564	Std. Error of Skewness		.309	Std. Error of Skewness		.199
Kurtosis		-1.012	Kurtosis		-.606	Kurtosis		-1.415	Kurtosis		.130
Std. Error of Kurtosis		.733	Std. Error of Kurtosis		1.091	Std. Error of Kurtosis		.608	Std. Error of Kurtosis		.396
Range		.052912	Range		.036457	Range		.042360	Range		.049498
Percentiles	25	.04165299	Percentiles	25	.06048094	Percentiles	25	.05141071	Percentiles	25	.05082146
	50	.05331532		50	.06661080		50	.06398265		50	.05775963
	75	.06882012		75	.07867141		75	.07613300		75	.06524727

Table 72: FDR q-values for Intra-Regional iCoh, AllFreq

Unique rank	OUTPUT AREA	Multiple comparisons using False Discovery Rates (FDRs)		Classical one-stage method*		Two-stage sharpened method [†]		FDR-adjusted p-values a.k.a. q-values
		Order	Ascending p-values	Hypothesis name	FDR-derived significance thresholds	FDR-adjusted p-values a.k.a. q-values	Stage 1 significance thresholds	
1	1	0.13400	AllFreq FRONTAL	0.0125	0.386666667	0.0119048	0.0119048	0.406
3	2	0.24800	AllFreq TEMPORAL	0.025	0.386666667	0.0238095	0.0238095	0.406
4	3	0.29000	AllFreq OCCIPITAL	0.0375	0.386666667	0.0357143	0.0357143	0.406
2	4	0.74500	AllFreq PARIETAL	0.05	0.745	0.047619	0.047619	0.78225

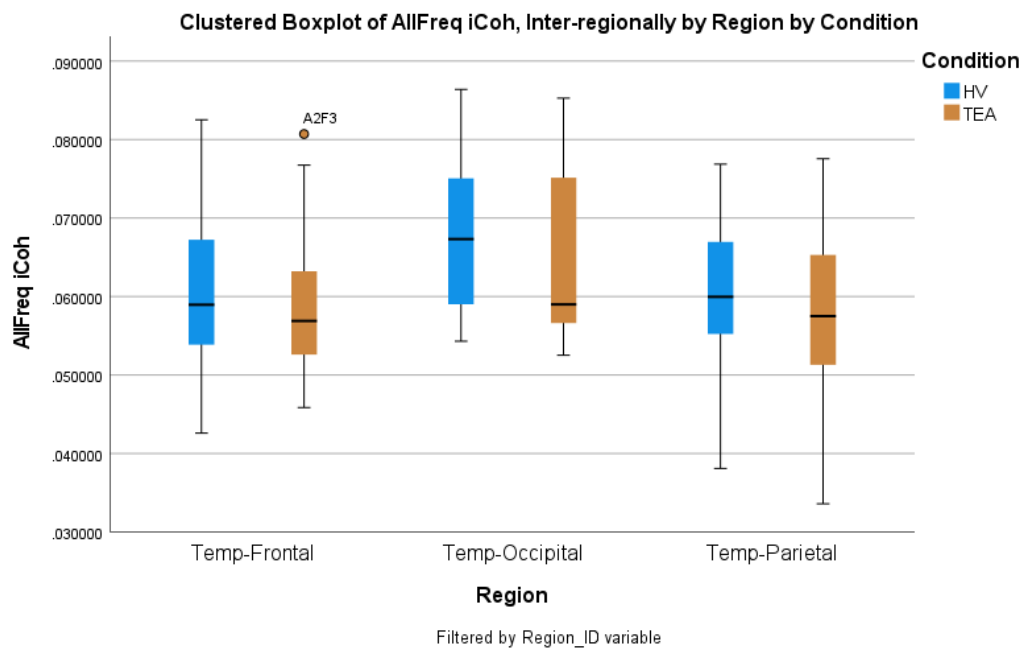


Figure 76: Inter-Regional iCoh Boxplot, all frequencies (1-40Hz)

Inter-regional iCoh data shows a platykurtic data distribution for all regions (frontal, occipital, parietal, temporal); Temporal/frontal and temporal/occipital distributions show a slight positive skew, whilst the temporal/parietal dataset is slightly negatively skewed (Table 73). Data descriptives for regions are as follows (Table 73, Figure 76):

- Temporal/Frontal regions - the mean is 0.0595, with a SE of 0.0010 and SD of 0.0092. The interquartile range is 0.0120, and the range is 0.0399.
- Temporal/Occipital regions - the mean is 0.0664, with a SE of 0.0019 and SD of 0.0108. The interquartile range is 0.0197, and the range is 0.0337.
- Temporal/Parietal regions - the mean is 0.0585, with a SE of 0.0010 and SD of 0.0101. The interquartile range is 0.0147, and the range is 0.0439.

Temporal/frontal and temporal/occipital TEA iCoh datasets do not meet the normal criteria. All other data meet the hypothesis for normality (Table 74). Therefore, the non-parametric Man-Whitney U test was utilised for both temporal/frontal and temporal/occipital data, and an independent samples t-test was used for the temporal-parietal dataset (as both distributions are normal). No significant differences are seen between cohorts, for any of the iCoh inter-regional areas of interest - Table 75.

Table 73: Data descriptives for inter-regional iCoh, all frequencies (1-40Hz).

Statistics: T-F iCoh, AllFreq			Statistics: T-O iCoh, AllFreq			Statistics: T-P iCoh, AllFreq		
AllFreq			AllFreq			AllFreq		
N	Valid	80	N	Valid	32	N	Valid	96
	Missing	0		Missing	0		Missing	0
Mean		.05949634	Mean		.06643893	Mean		.05851602
Std. Error of Mean		.001026091	Std. Error of Mean		.001901841	Std. Error of Mean		.001028132
Median		.05787339	Median		.06336742	Median		.05837990
Std. Deviation		.009177635	Std. Deviation		.010758437	Std. Deviation		.010073593
Variance		.000	Variance		.000	Variance		.000
Skewness		.657	Skewness		.537	Skewness		-.292
Std. Error of Skewness		.269	Std. Error of Skewness		.414	Std. Error of Skewness		.246
Kurtosis		-.034	Kurtosis		-1.129	Kurtosis		-.296
Std. Error of Kurtosis		.532	Std. Error of Kurtosis		.809	Std. Error of Kurtosis		.488
Range		.039928	Range		.033866	Range		.043949
Percentiles	25	.05286190	Percentiles	25	.05707334	Percentiles	25	.05172869
	50	.05787339		50	.06336742		50	.05837990
	75	.06482823		75	.07679903		75	.06646619

Table 74: Tests for normality for inter-regional iCoh, all frequencies (1-40Hz).

Tests of Normality: Temp-Frontal iCoh, AllFreq							
Condition	Kolmogorov-Smirnov			Shapiro-Wilk			Sig.
	Statistic	df	Sig.	Statistic	df	Sig.	
AllFreq HV	.101	40	.200	.960	40	.167	
TEA	.112	40	.200	.938	40	.029	

Tests of Normality: Temp-Occipital iCoh, AllFreq							
Condition	Kolmogorov-Smirnov			Shapiro-Wilk			Sig.
	Statistic	df	Sig.	Statistic	df	Sig.	
AllFreq HV	.170	16	.200	.925	16	.206	
TEA	.234	16	.019	.851	16	.014	

Tests of Normality: Temp-Parietal iCoh, AllFreq							
Condition	Kolmogorov-Smirnov ^a			Shapiro-Wilk			Sig.
	Statistic	df	Sig.	Statistic	df	Sig.	
AllFreq HV	.092	48	.200 [*]	.974	48	.363	
TEA	.062	48	.200 [*]	.983	48	.691	

*. This is a lower bound of the true significance.
^a. Lilliefors Significance Correction

Table 75: FDR q-values for Inter-Regional iCoh, AllFreq

OUTPUT AREA				Classical one-stage method*		Two-stage sharpened method [†]		
Unique rank	Order	Ascending p-values	Hypothesis name	FDR-derived significance thresholds	FDR-adjusted p-values a.k.a. q-values	Stage 1 significance thresholds	Stage 2 significance thresholds	FDR-adjusted p-values a.k.a. q-values
3	1	0.09600	AllFreq Global TEMPORAL-OCCIPITAL	0.01666667	0.1815	0.015873	0.015873	0.190575
1	2	0.12100	AllFreq Global TEMPORAL-PARIETAL	0.03333333	0.1815	0.031746	0.031746	0.190575
2	3	0.33000	AllFreq Global TEMPORAL-FRONTAL	0.05	0.33	0.047619	0.047619	0.3465

3. Global iCoh – Frequency Bands

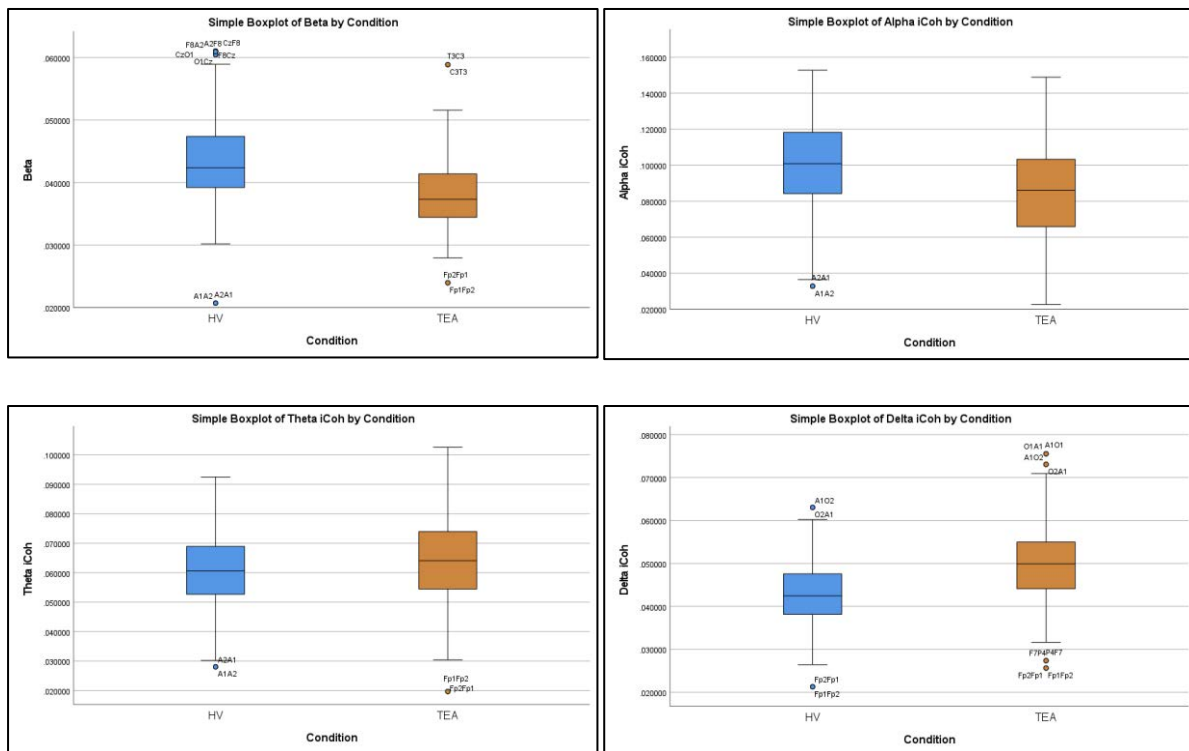


Figure 77: Boxplots for global iCoh, by frequency band. Top left - beta, top right - alpha, bottom left - theta, bottom right - delta.

Global iCoh within frequency bands shows a platykurtic data distribution for all frequency bands with a slight negative skew for beta, theta, and delta bands; the alpha frequency band distribution is symmetric around the mean. (Table 76). Data descriptives for frequency bands are as follows (Table 76, Figure 77):

- Beta frequencies - the mean is 0.0407, with a SE of 0.0002 and SD of 0.0065. The interquartile range is 0.0087, and the range is 0.0403.
- Alpha frequencies - the mean is 0.0938, with a SE of 0.0009 and SD of 0.0256. The interquartile range is 0.0375, and the range is 0.1301.
- Theta frequencies - the mean is 0.0630, with a SE of 0.0005 and SD of 0.0134. The interquartile range is 0.0174, and the range is 0.0828.
- Delta frequencies - the mean is 0.0463, with a SE of 0.0003 and SD of 0.0084. The interquartile range is 0.0111, and the range is 0.0543.

The HV delta and theta iCoh data distributions meet the criteria for normality, with the TEA delta iCoh cohort showing a borderline normal distribution. All other datasets do not meet normality requirements (Table 77). Therefore, the non-parametric Mann-Whitney U test was utilised. There are significant differences in global iCoh between cohorts, for all frequency bands i.e., beta, alpha, theta, and delta, with the delta bands showing significantly higher iCoh in the TEA cohort compared to HV, and beta, alpha, and theta bands showing significantly lower iCoh in TEA (Table 78).

Table 76: Data descriptives for global iCoh, by frequency band.

Statistics: iCoh by Frequency Band					
		Delta	Theta	Alpha	Beta
N	Valid	840	840	840	840
	Missing	42	42	42	42
Mean		.04626500	.06304457	.09378290	.04074994
Std. Error of Mean		.000291062	.000461892	.000884785	.000225459
Median		.04607370	.06265439	.09417724	.04026401
Std. Deviation		.008435776	.013386903	.025643495	.006534427
Variance		.000	.000	.001	.000
Skewness		.299	.152	.006	.554
Std. Error of Skewness		.084	.084	.084	.084
Kurtosis		.349	-.042	-.633	.412
Std. Error of Kurtosis		.169	.169	.169	.169
Range		.054252	.082813	.130075	.040335
Percentiles	25	.04066143	.05370842	.07459478	.03585098
	50	.04607370	.06265439	.09417724	.04026401
	75	.05178238	.07109828	.11209428	.04458644

Table 77: Tests for normality for global iCoh, by frequency band.

Tests of Normality: Global iCoh by Frequency Band							
		Kolmogorov-Smirnov ^a			Shapiro-Wilk		
Condition		Statistic	df	Sig.	Statistic	df	Sig.
Delta	HV	.032	420	.200 [*]	.998	420	.785
	TEA	.041	420	.086	.993	420	.052
Theta	HV	.031	420	.200 [*]	.994	420	.087
	TEA	.048	420	.024	.991	420	.008
Alpha	HV	.036	420	.200 [*]	.991	420	.014
	TEA	.069	420	<.001	.984	420	<.001
Beta	HV	.073	420	<.001	.980	420	<.001
	TEA	.071	420	<.001	.979	420	<.001

^{*}. This is a lower bound of the true significance.
^a. Lilliefors Significance Correction

Table 78: FDR q-values for Global iCoh within Frequency Bands. Lower mean iCoh in the TEA cohort is marked in blue.

OUTPUT AREA				Multiple comparisons using False Discovery Rates (FDRs)	Classical one-stage method*
Unique rank	Order	Ascending p-values	Hypothesis name	FDR-derived significance thresholds	FDR-adjusted p-values a.k.a. q-values
2	1	0.00000	Global iCoh BETA	0.0125 *	0
4	2	0.00000	Global iCoh DELTA	0.025 *	0
3	3	0.00100	Global iCoh ALPHA	0.0375 *	0.001
1	4	0.00100	Global iCoh THETA	0.05 *	0.001

4. Intra-Regional iCoh – Frequency Bands

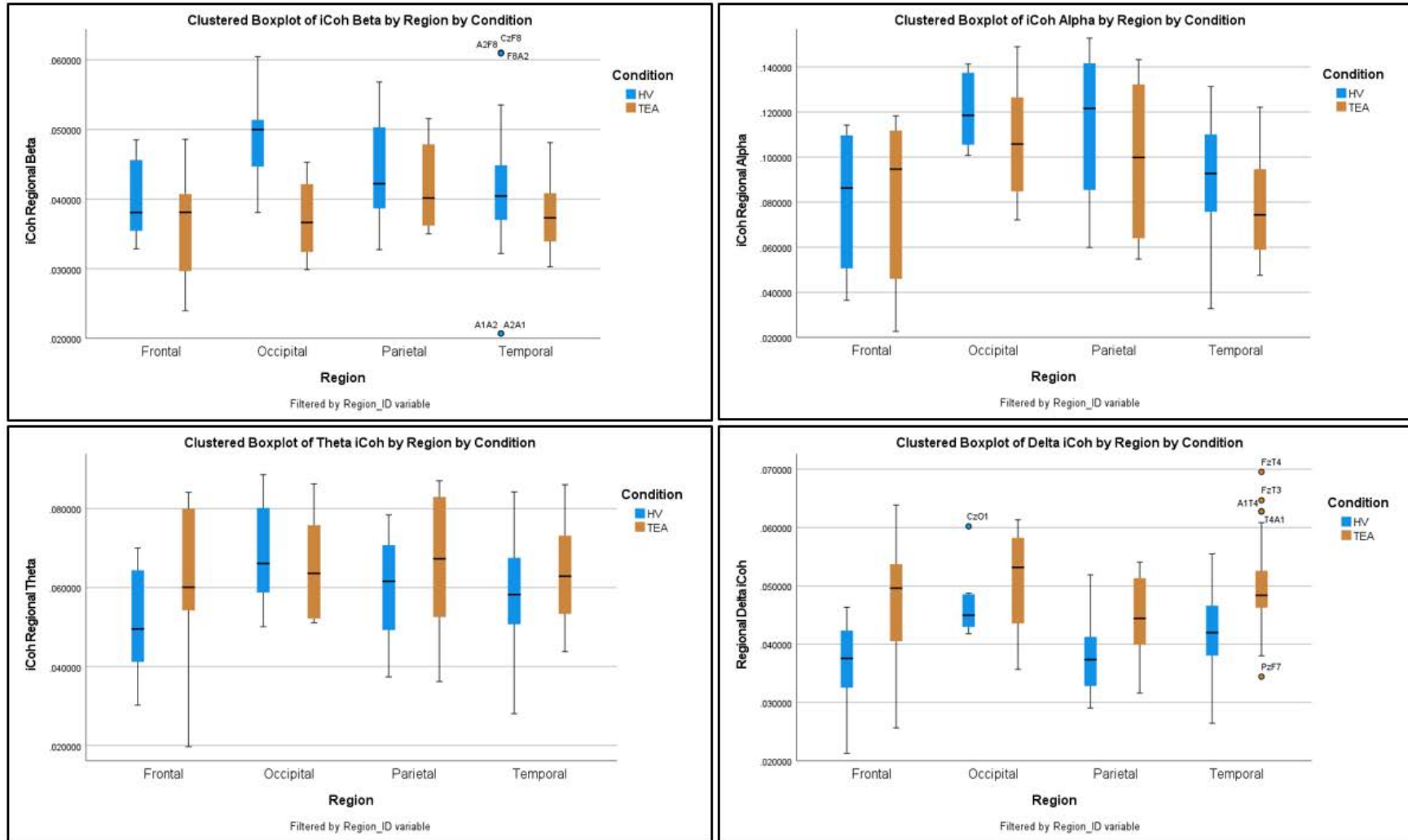


Figure 78: Boxplots for regional iCoh, by frequency band. Top left - beta, top right - alpha, bottom left - theta, bottom right - delta.

4.1. Frontal Regions

Frontal iCoh within frequency bands show a platykurtic data distribution for all frequency bands with a slight negative skew for beta, alpha, and theta; the delta frequency band distribution has a slight positive skew. (Table 79). Data descriptives for frequency bands are as follows (Table 79, Figure 78):

- Beta frequencies - the mean is 0.0381, with a SE of 0.0010 and SD of 0.0065. The interquartile range is 0.0070, and the range is 0.0246.
- Alpha frequencies - the mean is 0.0803, with a SE of 0.0051 and SD of 0.0320. The interquartile range is 0.0641, and the range is 0.0956.
- Theta frequencies - the mean is 0.0561, with a SE of 0.0028 and SD of 0.0178. The interquartile range is 0.0261, and the range is 0.0644.
- Delta frequencies - the mean is 0.0425, with a SE of 0.0017 and an SD of 0.0109. The interquartile range is 0.0161, and the range is 0.0426.

Both cohorts for frontal delta iCoh meet normality tests, as do the theta HV and the beta TEA cohort. Other datasets do not meet normality requirements (Table 80). Therefore, the non-parametric Mann-Whitney U test was utilised for frontal beta, alpha, and theta iCoh, and an independent samples t-test for delta iCoh. Only frontal delta iCoh shows a significant p-value ($p < 0.001$), and with multiple comparisons of FDR adjustments the resulting q-values are significant for both the classic one-stage and the two-stage sharpened method (Table 81). Delta iCoh is significantly higher in the TEA cohort, compared to HV participants.

4.2. Occipital Regions

Occipital iCoh within frequency bands show a platykurtic data distribution for all frequency bands with a slight negative skew for alpha frequencies and a slight positive skew for beta and theta frequencies; the delta frequency band distribution is relatively symmetrical about the mean. (Table 79). Data descriptives for frequency bands are as follows (Table 79, Figure 78):

- Beta frequencies - the mean is 0.0430, with a SE of 0.0021 and SD of 0.0086. The interquartile range is 0.0139, and the range is 0.0306.

- Alpha frequencies - the mean is 0.1138, with a SE of 0.0058 and SD of 0.0232. The interquartile range is 0.0373, and the range is 0.0768.
- Theta frequencies - the mean is 0.0669, with a SE of 0.0034 and SD of 0.0136. The interquartile range is 0.0284, and the range is 0.0385.
- Delta frequencies - the mean is 0.0489, with a SE of 0.0021 and SD of 0.0083. The interquartile range is 0.0124, and the range is 0.0256.

Only the HV occipital delta iCoh data does not meet normality measures (Table 80).

Therefore, the non-parametric Mann-Whitney U test was utilised for occipital delta iCoh and an independent samples t-test for beta, alpha and theta data. Occipital iCoh within the beta range show a significant p-value ($p= 0.003$) and following multiple comparisons FDR adjustments using both the classic one-stage and the two-stage sharpened method (Table 81). Beta iCoh is significantly lower in the TEA cohort, compared to HV participants.

4.3. Parietal Regions

Parietal iCoh within frequency bands show a platykurtic data distribution for all frequency bands with a slight negative skew for theta frequencies, and a slight positive skew for beta and delta frequencies, whilst the alpha frequency band distribution is relatively symmetrical about the mean. (Table 79). Data descriptives for frequency bands are as follows (Table 79, Figure 78):

- Beta frequencies - the mean is 0.0427, with a SE of 0.0008 and SD of 0.0062. The interquartile range is 0.0108, and the range is 0.0241.
- Alpha frequencies - the mean is 0.1049, with a SE of 0.0040 and SD of 0.0312. The interquartile range is 0.0588, and the range is 0.0980.
- Theta frequencies - the mean is 0.0626, with a SE of 0.0019 and SD of 0.0149. The interquartile range is 0.0198, and the range is 0.0509.
- Delta frequencies - the mean is 0.0415, with a SE of 0.0009 and SD of 0.0071. The interquartile range is 0.0097, and the range is 0.0250.

Parietal delta iCoh for both cohorts meet normality measures, whilst all other datasets do not reach normality criteria (Table 80). Therefore, the non-parametric Mann-Whitney U test was utilised for parietal beta, alpha and theta iCoh and an independent samples t-test for

delta iCoh. Parietal iCoh within the alpha and delta ranges show a significant p-value ($p=0.041$, $p<0.001$ respectively). Following multiple comparisons of FDR adjustment, only parietal delta iCoh remains significant using both the classic one-stage and the two-stage sharpened method (Table 81). Delta iCoh is significantly higher in the TEA cohort, compared to HV participants.

4.4. Temporal Regions

Temporal iCoh within frequency bands show a platykurtic data distribution for all frequency bands with, a slight positive skew for beta frequencies, whilst the alpha, theta and delta frequency band distributions are relatively symmetrical about the mean. (Table 79). Data descriptives for regions are as follows (Table 79, Figure 78):

- Beta frequencies - the mean is 0.0396, with a SE of 0.0005 and SD of 0.0064. The interquartile range is 0.0076, and the range is 0.0403.
- Alpha frequencies - the mean is 0.0847, with a SE of 0.0018 and an SD of 0.0223. The interquartile range is 0.0347, and the range is 0.0984.
- Theta frequencies - the mean is 0.0617, with a SE of 0.0010 and SD of 0.0125. The interquartile range is 0.0188, and the range is 0.0580.
- Delta frequencies - the mean is 0.0457, with a SE of 0.0006 and SD of 0.0072. The interquartile range is 0.0085, and the range is 0.0431.

Temporal delta, theta and alpha iCoh meet normality measures within the HV cohort, whilst all other datasets do not reach normality criteria (Table 80). Therefore, the non-parametric Mann-Whitney U test was utilised for all temporal iCoh. Temporal iCoh within the beta, alpha and delta ranges show a significant p-value ($p<0.001$ for all). Following multiple comparisons FDR adjustment, these frequency bands remain significant using both the classic stage, and the two-stage sharpened method, with beta and alpha band frequencies being significantly lower in the TEA cohort compared to healthy volunteers, and delta iCoh significantly higher in the TEA cohort. (Table 81).

Significant findings within all regions show significantly lower iCoh in the TEA cohort compared to HV, within the beta and alpha frequency bands. Within the delta band, all significant differences have higher iCoh in the TEA group compared to HV participants (Table 81).

Table 79: Descriptives for regional iCoh by frequency band. Top left - frontal, top right - occipital, bottom left - parietal, bottom right – temporal.

Statistics: Frontal iCoh by Frequency Band					
		Delta	Theta	Alpha	Beta
N	Valid	40	40	40	40
	Missing	10	10	10	10
Mean		.04245462	.05612729	.08030541	.03808730
Std. Error of Mean		.001730888	.002816876	.005060157	.001023961
Median		.04143922	.05535199	.08911574	.03811771
Std. Deviation		.010947098	.017815490	.032003246	.006476095
Variance		.000	.000	.001	.000
Skewness		.117	-.193	-.357	-.232
Std. Error of Skewness		.374	.374	.374	.374
Kurtosis		-.342	-.674	-1.522	-.199
Std. Error of Kurtosis		.733	.733	.733	.733
Range		.042581	.064446	.095565	.024635
Percentiles	25	.03447574	.04369480	.04707145	.03501442
	50	.04143922	.05535199	.08911574	.03811771
	75	.05054113	.06983235	.11215151	.04201443

Statistics: Occipital iCoh by Frequency Band					
		Delta	Theta	Alpha	Beta
N	Valid	16	16	16	16
	Missing	4	4	4	4
Mean		.04887903	.06685979	.11375847	.04302020
Std. Error of Mean		.002065670	.003403516	.005801284	.002145258
Median		.04857665	.06364179	.11094229	.04325274
Std. Deviation		.008262679	.013614064	.023205137	.008581032
Variance		.000	.000	.001	.000
Skewness		.029	.389	-.254	.181
Std. Error of Skewness		.564	.564	.564	.564
Kurtosis		-.865	-1.347	-.467	-.475
Std. Error of Kurtosis		1.091	1.091	1.091	1.091
Range		.025642	.038514	.076773	.030585
Percentiles	25	.04247800	.05382147	.10121397	.03620463
	50	.04857665	.06364179	.11094229	.04325274
	75	.05483869	.08224450	.13853505	.05010475

Statistics: Parietal iCoh by Frequency Band					
		Delta	Theta	Alpha	Beta
N	Valid	60	60	60	60
	Missing	12	12	12	12
Mean		.04146720	.06256539	.10492312	.04266473
Std. Error of Mean		.000913295	.001917426	.004029311	.000797307
Median		.04121410	.06692527	.10414383	.04116877
Std. Deviation		.007074350	.014852322	.031210908	.006175917
Variance		.000	.000	.001	.000
Skewness		.112	-.193	-.071	.506
Std. Error of Skewness		.309	.309	.309	.309
Kurtosis		-.771	-.839	-1.416	-.760
Std. Error of Kurtosis		.608	.608	.608	.608
Range		.025017	.050861	.098036	.024084
Percentiles	25	.03644986	.05231238	.07575323	.03844310
	50	.04121410	.06692527	.10414383	.04116877
	75	.04612419	.07122880	.13455919	.04919507

Statistics: Temporal iCoh by Frequency Band					
		Delta	Theta	Alpha	Beta
N	Valid	148	148	148	148
	Missing	16	16	16	16
Mean		.04568577	.06174931	.08469738	.03960246
Std. Error of Mean		.000594417	.001024638	.001836254	.000526981
Median		.04661614	.06027655	.08846146	.03883790
Std. Deviation		.007231396	.012465263	.022338995	.006411001
Variance		.000	.000	.000	.000
Skewness		.068	.024	.006	.662
Std. Error of Skewness		.199	.199	.199	.199
Kurtosis		.962	-.525	-.745	1.873
Std. Error of Kurtosis		.396	.396	.396	.396
Range		.043110	.058036	.098422	.040335
Percentiles	25	.04115155	.05171392	.06578119	.03503862
	50	.04661614	.06027655	.08846146	.03883790
	75	.04962277	.07052859	.10045492	.04266354

Table 80: Tests of normality for regional iCoh by frequency band. Top left - frontal, top right - occipital, bottom left - parietal, bottom right – temporal.

Tests of Normality: Frontal iCoh by Frequency Band							
Condition	Kolmogorov-Smirnov ^a			Shapiro-Wilk			Sig.
	Statistic	df	Sig.	Statistic	df	Sig.	
Delta	HV	.126	20	.200*	.921	20	.103
	TEA	.131	20	.200*	.939	20	.228
Theta	HV	.135	20	.200*	.915	20	.081
	TEA	.198	20	.038	.882	20	.019
Alpha	HV	.207	20	.025	.852	20	.006
	TEA	.218	20	.014	.834	20	.003
Beta	HV	.210	20	.021	.868	20	.011
	TEA	.145	20	.200*	.940	20	.237

*. This is a lower bound of the true significance.
^a. Lilliefors Significance Correction

Tests of Normality: Occipital iCoh by Frequency Band							
Condition	Kolmogorov-Smirnov ^a			Shapiro-Wilk			Sig.
	Statistic	df	Sig.	Statistic	df	Sig.	
Delta	HV	.253	8	.141	.799	8	.028
	TEA	.272	8	.084	.835	8	.068
Theta	HV	.258	8	.124	.914	8	.383
	TEA	.197	8	.200*	.864	8	.132
Alpha	HV	.196	8	.200*	.889	8	.228
	TEA	.167	8	.200*	.928	8	.498
Beta	HV	.228	8	.200*	.935	8	.563
	TEA	.153	8	.200*	.917	8	.408

*. This is a lower bound of the true significance.
^a. Lilliefors Significance Correction

Tests of Normality: Parietal iCoh by Frequency Band							
Condition	Kolmogorov-Smirnov ^a			Shapiro-Wilk			Sig.
	Statistic	df	Sig.	Statistic	df	Sig.	
Delta	HV	.098	30	.200*	.950	30	.169
	TEA	.139	30	.144	.935	30	.065
Theta	HV	.180	30	.015	.927	30	.042
	TEA	.196	30	.005	.906	30	.012
Alpha	HV	.203	30	.003	.894	30	.006
	TEA	.170	30	.027	.899	30	.008
Beta	HV	.196	30	.005	.922	30	.030
	TEA	.143	30	.117	.898	30	.007

*. This is a lower bound of the true significance.
^a. Lilliefors Significance Correction

Tests of Normality: Temporal iCoh by Frequency Band							
Condition	Kolmogorov-Smirnov ^a			Shapiro-Wilk			Sig.
	Statistic	df	Sig.	Statistic	df	Sig.	
Delta	HV	.077	74	.200*	.980	74	.275
	TEA	.134	74	.002	.945	74	.003
Theta	HV	.079	74	.200*	.975	74	.156
	TEA	.074	74	.200*	.960	74	.019
Alpha	HV	.074	74	.200*	.975	74	.147
	TEA	.129	74	.004	.941	74	.002
Beta	HV	.100	74	.065	.951	74	.006
	TEA	.098	74	.078	.953	74	.008

*. This is a lower bound of the true significance.
^a. Lilliefors Significance Correction

Table 81: FDR q-values for Intra-Regional iCoh within Frequency Bands. Lower mean iCoh in the TEA cohort is marked in blue.

OUTPUT AREA		Multiple comparisons using False Discovery Rates (FDRs)		Classical one-stage method*		Two-stage sharpened method [†]		
Unique rank	Order	Ascending p-values	Hypothesis name	FDR-derived	FDR-adjusted	Stage 1	Stage 2	FDR-adjusted
				significance thresholds	p-values a.k.a. q-values	significance thresholds	significance thresholds	p-values a.k.a. q-values
5	1	0.00100	Beta TEMPORAL	0.003125 *	0.0032	0.0029762	0.0047619 *	0.0021
8	2	0.00100	Alpha TEMPORAL	0.00625 *	0.0032	0.0059524	0.0095238 *	0.0021
9	3	0.00100	Delta TEMPORAL	0.009375 *	0.0032	0.0089286	0.0142857 *	0.0021
15	4	0.00100	Delta PARIETAL	0.0125 *	0.0032	0.0119048	0.0190476 *	0.0021
13	5	0.00100	Delta FRONTAL	0.015625 *	0.0032	0.014881	0.0238095 *	0.0021
16	6	0.00300	Beta OCCIPITAL	0.01875 *	0.008	0.0178571	0.0285714 *	0.00525
14	7	0.04100	Alpha PARIETAL	0.021875	0.093714286	0.0208333	0.0333333	0.0615
6	8	0.05200	Theta FRONTAL	0.025	0.104	0.0238095	0.0380952	0.06825
4	9	0.08410	Alpha FRONTAL	0.028125	0.144	0.0267857	0.0428571	0.0945
12	10	0.09000	Theta TEMPORAL	0.03125	0.144	0.0297619	0.047619	0.0945
7	11	0.20300	Beta PARIETAL	0.034375	0.285714286	0.0327381	0.052381	0.1875
11	12	0.22500	Theta PARIETAL	0.0375	0.285714286	0.0357143	0.0571429	0.1875
3	13	0.23400	Delta OCCIPITAL	0.040625	0.285714286	0.0386905	0.0619048	0.1875
10	14	0.25000	Alpha OCCIPITAL	0.04375	0.285714286	0.0416667	0.0666667	0.1875
2	15	0.39800	Beta FRONTAL	0.046875	0.424533333	0.0446429	0.0714286	0.2786
1	16	0.62100	Theta OCCIPITAL	0.05	0.621	0.047619	0.0761905	0.40753125

4.5. Inter-hemisphere Analysis of Significant Findings

Further interhemispheric analysis between the TEA and HV cohorts. This was undertaken on significant intra-regional findings, examining the left, right, and interhemispheric networks separately. An independent samples t-test was used for normally distributed datasets and

the non-parametric Mann-Whitney U-test was for those not meeting the criteria for normality.

The highest area of significance is the temporal region. All hemispheric elements within the delta band show a significant difference between cohorts, with TEA iCoh being significantly higher than HV ($p=0.001$, $p=0.001$, $p=0.002$, for right, left, and interhemispheric networks respectively). Temporal region beta frequencies over the right and left hemispheres also show significant differences between cohorts ($p=0.001$, $p=0.010$ respectively), as do the left and inter-hemisphere networks within the alpha band ($p=0.016$, $p=0.036$ respectively); significant data within both beta and theta iCoh show significantly lower iCoh in the TEA group compared to HV.

Frontal and parietal regions also show significant differences within the delta band, with higher iCoh in TEA compared to HV. Significances are seen in the right frontal ($p=0.002$) and parietal inter-hemisphere networks ($p=0.002$). All significant differences remain so following multiple comparisons of FDR adjustment, these frequency bands remain significant using both the classic stage and the two-stage sharpened method (Table 82).

Table 82: FDR q-values for Intra-Regional iCoh within Frequency Bands (split by hemisphere, and inter-hemisphere). Lower mean iCoh in the TEA cohort is marked in blue.

OUTPUT AREA		Multiple comparisons using FDRs		Classical one-stage method*		Two-stage sharpened method†		
Unique rank	Order	Ascending p-values	Hypothesis name	FDR-derived significance thresholds	FDR-adjusted p-values a.k.a. q-values	Stage 1 significance thresholds	Stage 2 significance thresholds	FDR-adjusted p-values a.k.a. q-values
12	1	0.00100	Beta TEMPORAL Right	0.00294118 *	0.005666667	0.0028011	0.0047619 *	0.0035
5	2	0.00100	Delta TEMPORAL Right	0.00588235 *	0.005666667	0.0056022	0.0095238 *	0.0035
17	3	0.00100	Delta TEMPORAL Left	0.00882353 *	0.005666667	0.0084034	0.0142857 *	0.0035
3	4	0.00200	Delta PARIETAL Inter-H	0.01176471 *	0.0068	0.0112045	0.0190476 *	0.0042
2	5	0.00200	Delta FRONTAL Right	0.01470588 *	0.0068	0.0140056	0.0238095 *	0.0042
7	6	0.01000	Beta TEMPORAL Left	0.01764706 *	0.024285714	0.0168067	0.0285714 *	0.015
8	7	0.01000	Delta TEMPORAL Inter-H	0.02058824 *	0.024285714	0.0196078	0.0333333 *	0.015
10	8	0.01600	Alpha TEMPORAL Left	0.02352941 *	0.034	0.022409	0.0380952 *	0.021
9	9	0.03600	Alpha TEMPORAL Inter-H	0.02647059	0.068	0.0252101	0.0428571 *	0.042
6	10	0.06200	Alpha TEMPORAL Right	0.02941176	0.1054	0.0280112	0.047619	0.0651
1	11	0.10500	Delta PARIETAL Right	0.03235294	0.162272727	0.0308123	0.052381	0.100227273
13	12	0.13200	Delta FRONTAL Left	0.03529412	0.187	0.0336134	0.0571429	0.1155
15	13	0.14700	Beta TEMPORAL Inter-H	0.03823529	0.192230769	0.0364146	0.0619048	0.118730769
11	14	0.17200	Beta OCCIPITAL Right	0.04117647	0.208857143	0.0392157	0.0666667	0.129
4	15	0.19000	Delta PARIETAL Left	0.04411765	0.215333333	0.0420168	0.0714286	0.133
16	16	0.20400	Beta OCCIPITAL Left	0.04705882	0.21675	0.0448179	0.0761905	0.133875
14	17	0.23400	Delta FRONTAL Inter-H	0.05	0.234	0.047619	0.0809524	0.144529412
			NR Beta OCCIPITAL Inter-H	NR				NR

5. Inter-Regional iCoh – Frequency Bands

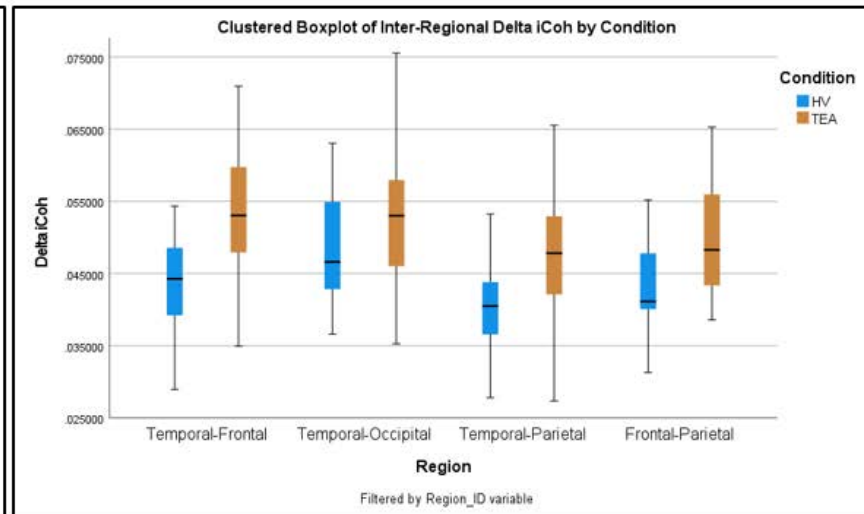
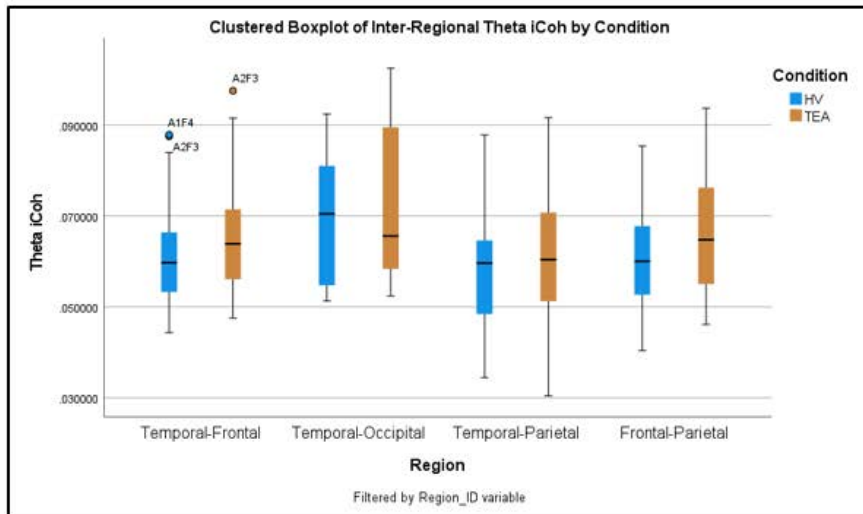
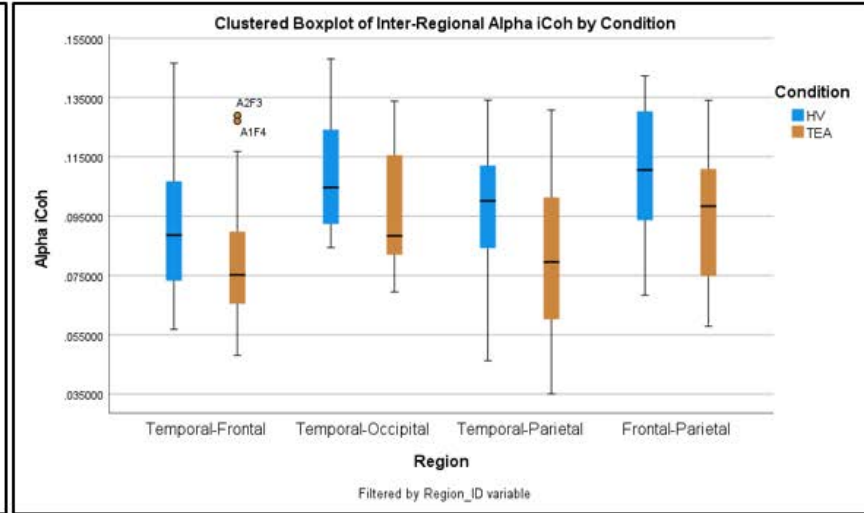
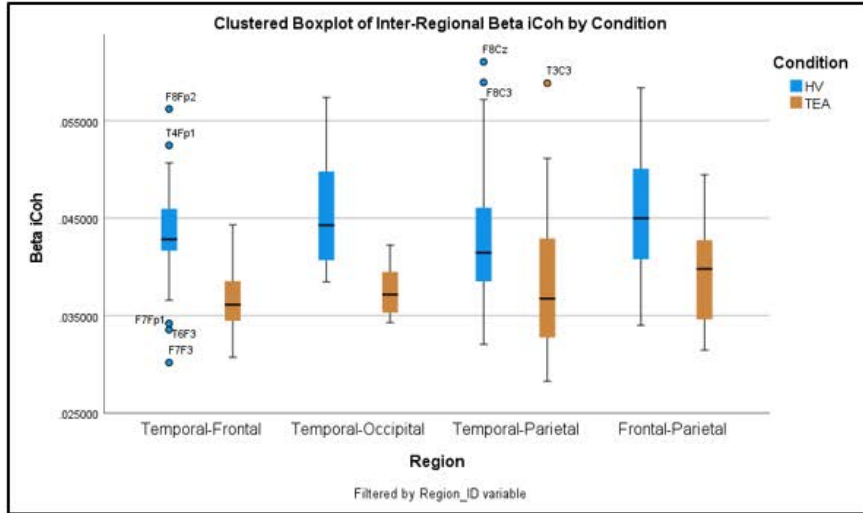


Figure 79: Boxplots for inter-regional iCoh, by frequency band. Top left - beta, top right - alpha, bottom left - theta, bottom right - delta.

5.1. Temporal and Frontal Regions

Temporal-frontal iCoh within frequency bands show a platykurtic data distribution and a positive skew across all frequency bands. (Table 83). Data descriptives for regions are as follows (Table 83, Figure 79):

- Beta frequencies - the mean is 0.0399, with a SE of 0.0006 and SD of 0.0053. The interquartile range is 0.0075, and the range is 0.0260.
- Alpha frequencies - the mean is 0.0858, with a SE of 0.0025 and an SD of 0.0223. The interquartile range is 0.0300, and the range is 0.0985.
- Theta frequencies - the mean is 0.0637, with a SE of 0.0013 and SD of 0.0120. The interquartile range is 0.0163, and the range is 0.0532.
- Delta frequencies - the mean is 0.0485, with a SE of 0.0010 and an SD of 0.0094. The interquartile range is 0.0124, and the range is 0.0420.

Table 83: Data descriptives for inter-regional iCoh between temporal and frontal regions, by frequency band

Statistics: Temporal-Frontal Inter-Regional iCoh by Band					
		Delta	Theta	Alpha	Beta
N	Valid	80	80	80	80
	Missing	0	0	0	0
Mean		.04852958	.06371323	.08583081	.03991174
Std. Error of Mean		.001049767	.001341011	.002489358	.000595345
Median		.04824583	.06307551	.08121226	.04055517
Std. Deviation		.009389401	.011994365	.022265491	.005324932
Variance		.000	.000	.000	.000
Skewness		.355	.690	.812	.380
Std. Error of Skewness		.269	.269	.269	.269
Kurtosis		-.103	.023	.224	.039
Std. Error of Kurtosis		.532	.532	.532	.532
Range		.041967	.053207	.098515	.026033
Percentiles	25	.04131485	.05476483	.06887180	.03550337
	50	.04824583	.06307551	.08121226	.04055517
	75	.05373739	.07103412	.09888131	.04302105

Temporal-frontal theta within the HV cohort and alpha within the TEA cohort do not meet the criteria for normality. All other datasets meet normality requirements (Table 84).

Therefore, the non-parametric Mann-Whitney U test was utilised for temporal-frontal theta and alpha, whilst an independent samples t-test was used to assess beta and delta iCoh. All frequency bands across the temporal-frontal regions have significant p-values ($p < 0.001$ for all bands), and all remain significant after multiple comparisons of FDR adjustments using

both the classic one-stage and the two-stage sharpened method (Table 91, Table 81). iCoh in the delta and theta frequency bands is significantly higher than that of the HV group, while alpha and beta frequencies show a significantly lower iCoh in the TEA group.

Table 84: Tests of normality for inter-regional iCoh between temporal and frontal regions, by frequency band.

Tests of Normality: Temporal-Frontal Inter-Regional iCoh by Band							
	Condition	Kolmogorov-Smirnov ^a			Shapiro-Wilk		
		Statistic	df	Sig.	Statistic	df	Sig.
Delta	HV	.091	40	.200 [*]	.977	40	.571
	TEA	.081	40	.200 [*]	.973	40	.460
Theta	HV	.093	40	.200 [*]	.939	40	.031
	TEA	.107	40	.200 [*]	.956	40	.118
Alpha	HV	.093	40	.200 [*]	.947	40	.061
	TEA	.118	40	.170	.940	40	.034
Beta	HV	.189	40	<.001	.948	40	.066
	TEA	.093	40	.200 [*]	.977	40	.595

^{*}. This is a lower bound of the true significance.
^a. Lilliefors Significance Correction

5.2. Temporal and Occipital Regions

Temporal-occipital iCoh within frequency bands show a platykurtic data distribution and a positive skew in all frequency bands (Table 85, Table 79). Data descriptives for regions are as follows (Table 85, Table 79, Figure 79):

- Beta frequencies - the mean is 0.0416, with a SE of 0.0011 and SD of 0.0061. The interquartile range is 0.0075, and the range is 0.0231.
- Alpha frequencies - the mean is 0.1021, with a SE of 0.0036 and SD of 0.0206. The interquartile range is 0.0360, and the range is 0.0785.
- Theta frequencies - the mean is 0.0713, with a SE of 0.0028 and SD of 0.0157. The interquartile range is 0.0289, and the range is 0.0512.
- Delta frequencies - the mean is 0.0508, with a SE of 0.0017 and an SD of 0.0096. The interquartile range is 0.0138, and the range is 0.0402.

Table 85: Data descriptives for inter-regional iCoh between temporal and occipital regions, by frequency band

Statistics: Temporal-Occipital Inter-Regional iCoh by Band					
		Delta	Theta	Alpha	Beta
N	Valid	32	32	32	32
	Missing	0	0	0	0
Mean		.05079090	.07127134	.10206667	.04162680
Std. Error of Mean		.001700914	.002775637	.003633958	.001069745
Median		.05168297	.06634180	.09902522	.04027608
Std. Deviation		.009621823	.015701372	.020556770	.006051393
Variance		.000	.000	.000	.000
Skewness		.643	.317	.445	.951
Std. Error of Skewness		.414	.414	.414	.414
Kurtosis		.514	-1.368	-.719	.249
Std. Error of Kurtosis		.809	.809	.809	.809
Range		.040246	.051225	.078510	.023105
Percentiles	25	.04302014	.05673863	.08568006	.03693285
	50	.05168297	.06634180	.09902522	.04027608
	75	.05678139	.08567307	.12165380	.04441489

Both TEA and HV temporal-occipital delta iCoh data do not meet normality measures; all other frequency bands have a normal distribution (Table 86, Table 80). Therefore, the non-parametric Mann-Whitney U test was utilised for temporal-occipital theta iCoh and an independent samples t-test for beta, alpha and delta data. Temporal-occipital iCoh within the beta and alpha ranges show significant p-values ($p = <0.001$ and $p = 0.021$ respectively). Following multiple comparisons FDR adjustments both theta and delta temporal-occipital iCoh additionally show significance with q-values when the two-stage sharpened method is employed ($q = 0.039$ and $q = 0.029$ respectively) - Table 91. iCoh in the delta and theta frequency bands is significantly higher than that of the HV group, while alpha and beta frequencies show a significantly lower iCoh in the TEA group.

Table 86: Tests of normality for inter-regional iCoh between temporal and occipital regions, by frequency band

Tests of Normality: Temporal-Occipital Inter-Regional iCoh by Band							
Condition	Kolmogorov-Smirnov ^a			Shapiro-Wilk			
	Statistic	df	Sig.	Statistic	df	Sig.	
Delta	HV	.130	16	.200 [*]	.959	16	.636
	TEA	.146	16	.200 [*]	.942	16	.379
Theta	HV	.191	16	.121	.887	16	.050
	TEA	.234	16	.019	.876	16	.034
Alpha	HV	.178	16	.186	.919	16	.161
	TEA	.209	16	.060	.914	16	.135
Beta	HV	.145	16	.200 [*]	.934	16	.280
	TEA	.158	16	.200 [*]	.920	16	.167

^{*}. This is a lower bound of the true significance.
^a. Lilliefors Significance Correction

4.1. Temporal and Parietal Regions

Temporal-parietal iCoh within frequency bands show a platykurtic data distribution for all frequency bands with a slight negative skew for alpha frequencies, and a slight positive skew for beta, theta, and delta frequencies. (Table 87, Table 79). Data descriptives for regions are as follows (Table 87, Figure 79, Figure 78):

- Beta frequencies - the mean is 0.0403, with a SE of 0.0007 and SD of 0.0070. The interquartile range is 0.0108, and the range is 0.0328.
- Alpha frequencies - the mean is 0.0901, with a SE of 0.0025 and SD of 0.0242. The interquartile range is 0.0588, and the range is 0.0990.
- Theta frequencies - the mean is 0.0596, with a SE of 0.0013 and SD of 0.0126. The interquartile range is 0.0198, and the range is 0.0612.
- Delta frequencies - the mean is 0.0441, with a SE of 0.0008 and SD of 0.0077. The interquartile range is 0.0097, and the range is 0.0382.

Table 87: Data descriptives for inter-regional iCoh between temporal and parietal regions, by frequency band

Statistics: Temporal-Parietal Inter-Regional iCoh by Band					
		Delta	Theta	Alpha	Beta
N	Valid	96	96	96	96
	Missing	0	0	0	0
Mean		.04411830	.05959318	.09006245	.04029016
Std. Error of Mean		.000784619	.001282091	.002472628	.000714367
Median		.04341931	.06029875	.09116922	.03980194
Std. Deviation		.007687664	.012561874	.024226706	.006999334
Variance		.000	.000	.001	.000
Skewness		.305	.115	-.204	.746
Std. Error of Skewness		.246	.246	.246	.246
Kurtosis		-.127	-.085	-.809	.492
Std. Error of Kurtosis		.488	.488	.488	.488
Range		.038174	.061186	.099030	.032775
Percentiles	25	.03816239	.04861374	.07428226	.03493977
	50	.04341931	.06029875	.09116922	.03980194
	75	.04909672	.06688424	.10957443	.04495925

Only TEA and HV beta frequency iCoh within the temporal-parietal regions do not meet the criteria for normality (Table 88, Table 80). Therefore, the non-parametric Mann-Whitney U test was utilised for temporal-parietal beta and an independent samples t-test for alpha, theta, and delta iCoh. Beta, alpha and delta ranges show significant p-values ($p < 0.001$ for all bands). Following multiple comparisons of FDR adjustment, temporal-parietal theta iCoh additionally shows significance when the two-stage sharpened method is utilised ($q = 0.015$) - Table 91, Table 81). Areas of significance show significantly lower iCoh within the beta and alpha bands in TEA compared to HV, and significantly higher iCoh in the theta and delta bands (Table 91).

Table 88: Tests of normality for inter-regional iCoh between temporal and parietal regions, by frequency band

Tests of Normality: Temporal-Parietal Inter-Regional iCoh by Band							
		Kolmogorov-Smirnov ^a			Shapiro-Wilk		
Condition		Statistic	df	Sig.	Statistic	df	Sig.
Delta	HV	.109	48	.200 [*]	.983	48	.708
	TEA	.086	48	.200 [*]	.988	48	.891
Theta	HV	.089	48	.200 [*]	.985	48	.795
	TEA	.072	48	.200 [*]	.990	48	.949
Alpha	HV	.102	48	.200 [*]	.972	48	.312
	TEA	.100	48	.200 [*]	.970	48	.247
Beta	HV	.145	48	.013	.940	48	.017
	TEA	.149	48	.009	.934	48	.010

^{*}. This is a lower bound of the true significance.
^a. Lilliefors Significance Correction

4.1. Frontal and Parietal Regions

Frontal-parietal iCoh within frequency bands shows a platykurtic data distribution for all frequency bands with a slight positive skew for delta, theta and beta frequencies, and alpha frequencies being symmetrical around the mean (Table 89, Table 79). Data descriptives for regions are as follows (Table 89, Figure 79, Figure 78):

- Beta frequencies - the mean is 0.0425, with a SE of 0.0009 and SD of 0.0069. The interquartile range is 0.0086, and the range is 0.0269.
- Alpha frequencies - the mean is 0.1027, with a SE of 0.0031 and SD of 0.0243. The interquartile range is 0.0428, and the range is 0.0844.
- Theta frequencies - the mean is 0.0638, with a SE of 0.0031 and an SD of 0.0243. The interquartile range is 0.0170, and the range is 0.0533.
- Delta frequencies - the mean is 0.0464, with a SE of 0.0010 and an SD of 0.0076. The interquartile range is 0.0113, and the range is 0.0340.

Table 89: Data descriptives for inter-regional iCoh between frontal and parietal regions, by frequency band.

		Delta	Theta	Alpha	Beta
N	Valid	60	60	60	60
	Missing	0	0	0	0
Mean		.04643563	.06375786	.10272767	.04252631
Std. Error of Mean		.000986745	.001606026	.003139416	.000894041
Median		.04513070	.06269562	.10131834	.04171110
Std. Deviation		.007643293	.012440226	.024317808	.006925213
Skewness		.483	.544	-.094	.597
Std. Error of Skewness		.309	.309	.309	.309
Kurtosis		-.249	-.050	-1.080	-.099
Std. Error of Kurtosis		.608	.608	.608	.608
Range		.034010	.053289	.084397	.026912
Percentiles	25	.04078608	.05394973	.08206542	.03721322
	50	.04513070	.06269562	.10131834	.04171110
	75	.05212483	.07091776	.12493063	.04575650

Only HV theta frequency iCoh within the frontal-parietal regions meets the criteria for normality (Table 88, Table 80). Therefore, the non-parametric Mann-Whitney U test was utilised for all frontal-parietal iCoh datasets. All frequency bands show significant p-values ($p < 0.001$ for beta, alpha and delta, $p = 0.027$ for theta frequencies). Following multiple comparisons FDR adjustment, all frequency bands remain significant, with Table 81 lower iCoh within the beta and alpha bands in TEA compared to HV, and higher iCoh in the theta and delta bands (Table 91).

Table 90: Tests of normality for inter-regional iCoh between frontal and parietal regions, by frequency band

Condition	Kolmogorov-Smirnov ^a			Shapiro-Wilk			
	Statistic	df	Sig.	Statistic	df	Sig.	
Delta	HV	.161	60	<.001	.950	60	.016
	TEA	.146	60	.003	.943	60	.008
Theta	HV	.097	60	.200 [*]	.977	60	.310
	TEA	.138	60	.006	.941	60	.006
Alpha	HV	.125	60	.021	.931	60	.002
	TEA	.109	60	.074	.941	60	.006
Beta	HV	.105	60	.098	.949	60	.014
	TEA	.112	60	.058	.955	60	.027
AllFreq	HV	.114	60	.051	.954	60	.025
	TEA	.108	60	.080	.951	60	.018

*. This is a lower bound of the true significance.
a. Lilliefors Significance Correction

Table 91: FDR q-values for Inter-Regional iCoh within Frequency Bands. Lower mean iCoh in the TEA cohort is marked in blue.

OUTPUT AREA			Multiple comparisons using FDRs	Classical one-stage method*		Two-stage sharpened method†		
Unique rank	Order	Ascending p-values	Hypothesis name	FDR-derived significance thresholds	FDR-adjusted p-values a.k.a. q-values	Stage 1 significance thresholds	Stage 2 significance thresholds	FDR-adjusted p-values a.k.a. q-values
10	1	0.00100	Beta FRONTAL-PARIETAL	0.003125 *	0.0016	0.0029762	0.015873 *	0.000315
11	2	0.00100	Alpha FRONTAL-PARIETAL	0.00625 *	0.0016	0.0059524	0.031746 *	0.000315
9	3	0.00100	Delta FRONTAL-PARIETAL	0.009375 *	0.0016	0.0089286	0.047619 *	0.000315
8	4	0.00100	Beta TEMPORAL-PARIETAL	0.0125 *	0.0016	0.0119048	0.0634921 *	0.000315
14	5	0.00100	Alpha TEMPORAL-PARIETAL	0.015625 *	0.0016	0.014881	0.0793651 *	0.000315
16	6	0.00100	Delta TEMPORAL-PARIETAL	0.01875 *	0.0016	0.0178571	0.0952381 *	0.000315
12	7	0.00100	Beta TEMPORAL-OCCIPITAL	0.021875 *	0.0016	0.0208333	0.1111111 *	0.000315
7	8	0.00100	Beta TEMPORAL-FRONTAL	0.025 *	0.0016	0.0238095	0.1269841 *	0.000315
6	9	0.00100	Alpha TEMPORAL-FRONTAL	0.028125 *	0.0016	0.0267857	0.1428571 *	0.000315
15	10	0.00100	Delta TEMPORAL-FRONTAL	0.03125 *	0.0016	0.0297619	0.1587302 *	0.000315
5	11	0.02000	Theta TEMPORAL-FRONTAL	0.034375 *	0.028	0.0327381	0.1746032 *	0.0055125
4	12	0.02100	Alpha TEMPORAL-OCCIPITAL	0.0375 *	0.028	0.0357143	0.1904762 *	0.0055125
3	13	0.02700	Theta FRONTAL-PARIETAL	0.040625 *	0.033230769	0.0386905	0.2063492 *	0.006542308
13	14	0.06000	Delta TEMPORAL-OCCIPITAL	0.04375	0.068571429	0.0416667	0.2222222 !	0.0135
2	15	0.07100	Theta TEMPORAL-PARIETAL	0.046875	0.075733333	0.0446429	0.2380952 !	0.01491
1	16	0.14700	Theta TEMPORAL-OCCIPITAL	0.05	0.147	0.047619	0.2539683 !	0.028940625

4.2. Inter-hemisphere Analysis of Significant Findings

Further interhemispheric analysis between the TEA and HV cohorts. This was undertaken on significant inter-regional findings, examining the left, right, and interhemispheric networks separately. An independent samples t-test was used for normally distributed datasets and the non-parametric Mann-Whitney U-test was for those not meeting the criteria for normality.

4.2.1. Temporal-Frontal iCoh

Left hemisphere temporal-frontal networks show the most marked iCoh differences between the TEA and HV cohorts which affects all frequency bands. Significant differences are seen within the inter-hemisphere networks within beta and delta iCoh data. The only significant differences within right-sided temporal-parietal networks are seen within delta iCoh (Table 92). There is significantly lower iCoh within the beta and alpha bands in TEA compared to HV, and significantly higher iCoh in the theta and delta bands

Table 92: FDR q-values for iCoh between Temporal and Frontal regions, within Frequency Bands (split by hemisphere, and inter-hemisphere). Lower mean iCoh in the TEA cohort is marked in blue.

OUTPUT AREA		Multiple comparisons using False Discovery Rates (FDRs)		Classical one-stage method*		Two-stage sharpened method†		
Unique rank	Order	Ascending p-values	Hypothesis name	FDR-derived significance thresholds	FDR-adjusted p-values a.k.a. q-values	Stage 1 significance thresholds	Stage 2 significance thresholds	FDR-adjusted p-values a.k.a. q-values
7	1	0.00100	Beta iCoh Inter-Hemisphere Temporal/Frontal	0.00416667 *	0.0024	0.0039683	0.0079365 *	0.00126
5	2	0.00100	Beta iCoh Left Temporal/Frontal	0.00833333 *	0.0024	0.0079365	0.015873 *	0.00126
4	3	0.00100	Theta iCoh Left Temporal/Frontal	0.0125 *	0.0024	0.0119048	0.0238095 *	0.00126
12	4	0.00100	Delta iCoh Inter-Hemisphere Temporal/Frontal	0.01666667 *	0.0024	0.015873	0.031746 *	0.00126
3	5	0.00100	Delta iCoh Left Temporal/Frontal	0.02083333 *	0.0024	0.0198413	0.0396825 *	0.00126
8	6	0.00900	Alpha iCoh Left Temporal/Frontal	0.025 *	0.018	0.0238095	0.047619 *	0.00945
10	7	0.03300	Delta iCoh Right Temporal/Frontal	0.02916667	0.056571429	0.0277778	0.0555556 *	0.0297
6	8	0.08900	Theta iCoh Inter-Hemisphere Temporal/Frontal	0.03333333	0.1335	0.031746	0.0634921	0.0700875
11	9	0.21500	Beta iCoh Right Temporal/Frontal	0.0375	0.286666667	0.0357143	0.0714286	0.1505
9	10	0.28900	Alpha iCoh Right Temporal/Frontal	0.04166667	0.3468	0.0396825	0.0793651	0.18207
2	11	0.37000	Alpha iCoh Inter-Hemisphere Temporal/Frontal	0.04583333	0.403636364	0.0436508	0.0873016	0.211909091
1	12	0.53000	Theta iCoh Right Temporal/Frontal	0.05	0.53	0.047619	0.0952381	0.27825

4.2.2. Temporal-Occipital iCoh

Beta iCoh between temporal-occipital regions shows significant differences between cohorts across all hemispheric networks (right, left, and interhemispheric connections). There are no significant differences between cohorts concerning alpha iCoh, when looking at the right, left or inter-hemisphere networks in isolation. Table 93. iCoh in the beta frequency band shows a significantly lower iCoh in the TEA group.

Table 93: FDR q-values for iCoh between Temporal and Occipital regions, within Frequency Bands (split by hemisphere, and inter-hemisphere)

OUTPUT AREA		Multiple comparisons using FDRs		Classical one-stage method*		Two-stage sharpened method†		
Unique rank	Order	Ascending p-values	Hypothesis name	FDR-derived significance thresholds	FDR-adjusted p-values a.k.a. q-values	Stage 1 significance thresholds	Stage 2 significance thresholds	FDR-adjusted p-values a.k.a. q-values
8	1	0.00100	INTER-H TEMPORAL-OCCIPITAL BETA	0.00416667 *	0.006	0.0039683	0.005291 *	0.004725
10	2	0.00100	LEFT TEMPORAL-OCCIPITAL BETA	0.00833333 *	0.006	0.0079365	0.010582 *	0.004725
9	3	0.00400	RIGHT TEMPORAL-OCCIPITAL BETA	0.0125 *	0.016	0.0119048	0.015873 *	0.0126
2	4	0.07300	INTER-H TEMPORAL-OCCIPITAL ALPHA	0.01666667	0.219	0.015873	0.021164	0.1724625
12	5	0.23400	RIGHT TEMPORAL-OCCIPITAL ALPHA	0.02083333	0.4485	0.0198413	0.026455	0.35319375
11	6	0.27900	INTER-H TEMPORAL-OCCIPITAL THETA	0.025	0.4485	0.0238095	0.031746	0.35319375
5	7	0.28800	INTER-H TEMPORAL-OCCIPITAL DELTA	0.02916667	0.4485	0.0277778	0.037037	0.35319375
3	8	0.29900	LEFT TEMPORAL-OCCIPITAL DELTA	0.03333333	0.4485	0.031746	0.042328	0.35319375
7	9	0.44300	LEFT TEMPORAL-OCCIPITAL ALPHA	0.0375	0.59066667	0.0357143	0.047619	0.46515
6	10	0.62400	LEFT TEMPORAL-OCCIPITAL THETA	0.04166667	0.748363636	0.0396825	0.0529101	0.589336364
4	11	0.68600	RIGHT TEMPORAL-OCCIPITAL THETA	0.04583333	0.748363636	0.0436508	0.0582011	0.589336364
1	12	0.88000	RIGHT TEMPORAL-OCCIPITAL DELTA	0.05	0.88	0.047619	0.0634921	0.693

4.2.3. Temporal-Parietal iCoh

Alpha and delta band iCoh between temporal and parietal regions have significant differences between the cohorts in all hemispheric categories (right, left, and inter-hemispheric), with the inter-hemisphere delta iCoh becoming significant utilising the two stages sharpened and the graphically sharpened FDR method (Table 94).

Right temporal-parietal and inter-hemisphere temporal-parietal iCoh show significant cohort differences within the beta band, whilst there are significant changes within the left temporal-parietal iCoh for theta frequencies only (Table 94).

Table 94: FDR q-values for iCoh between Temporal and Parietal regions, within Frequency Bands (split by hemisphere, and inter-hemisphere)

OUTPUT AREA		Multiple comparisons using False Discovery Rates (FDRs)		Classical one-stage method*		Two-stage sharpened method†		Graphically sharpened method‡				
Unique rank	Order	Ascending p-values	Hypothesis name	FDR-derived significance thresholds	FDR-adjusted p-values a.k.a. q-values	Stage 1 significance thresholds	Stage 2 significance thresholds	FDR-adjusted p-values a.k.a. q-values	Point estimates of no. of H ₀ s estimate	Best estimate	FDR-derived significance thresholds	FDR-adjusted p-values a.k.a. q-values
4	1	0.00100	Beta iCoh Right Temporal/Parietal	0.00416667 *	0.003	0.0039683	0.0119048 *	0.00105	12.0000	0.00714286 *	0.00175	0.00175
3	2	0.00100	Alpha iCoh Inter-Hemisphere Temporal/Parietal	0.00833333 *	0.003	0.0079365	0.0238095 *	0.00105	11.0110	0.01428571 *	0.00175	0.00175
9	3	0.00100	Delta iCoh Left Temporal/Parietal	0.0125 *	0.003	0.0119048	0.0357143 *	0.00105	10.0100	0.02142857 *	0.00175	0.00175
12	4	0.00100	Delta iCoh Right Temporal/Parietal	0.01666667 *	0.003	0.015873	0.047619 *	0.00105	9.0090	0.02857143 *	0.00175	0.00175
8	5	0.00700	Beta iCoh Inter-Hemisphere Temporal/Parietal	0.02083333 *	0.014	0.0198413	0.0595238 *	0.0049	8.0564	0.03571429 *	0.00816667	0.00816667
11	6	0.00700	Alpha iCoh Left Temporal/Parietal	0.025 *	0.014	0.0238095	0.0714286 *	0.0049	7.0493	0.04285714 *	0.00816667	0.00816667
7	7	0.01200	Alpha iCoh Right Temporal/Parietal	0.02916667 *	0.020571429	0.0277778	0.0833333 *	0.0072	6.0729	0.05 *	0.012	0.012
6	8	0.01400	Theta iCoh Left Temporal/Parietal	0.03333333 *	0.021	0.031746	0.0952381 *	0.00735	5.0710	0.05714286 *	0.01225	0.01225
2	9	0.06000	Delta iCoh Inter-Hemisphere Temporal/Parietal	0.0375	0.08	0.0357143	0.1071429 !	0.028	4.2553	0.06428571 !	0.04666667	0.04666667
1	10	0.17600	Beta iCoh Left Temporal/Parietal	0.04166667	0.2112	0.0396825	0.1190476	0.07392	3.6408	0.07142857	0.1232	0.1232
10	11	0.38000	Theta iCoh Inter-Hemisphere Temporal/Parietal	0.04583333	0.414545455	0.0436508	0.1309524	0.145090909	3.2258	0.07857143	0.241818182	0.241818182
5	12	0.84800	Theta iCoh Right Temporal/Parietal	0.05	0.848	0.047619	0.1428571	0.2968	6.5789	True	0.08571429	0.494666667

Across all significant differences in the hemisphere elements of inter-regional networks (right, left, and inter-hemisphere iCoh), beta and theta bands show significantly lower iCoh in the TEA cohort compared to HV, and significantly higher TEA iCoh in the theta and delta bands (Table 92, Table 93, Table 94).

4.2.4. Frontal-Parietal iCoh

Right frontal-parietal beta, delta and left frontal-parietal beta iCoh show significant differences between the cohorts (p=0.002, p=0.004, p=0.026 respectively). Following multiple comparisons, FDR adjustment left frontal-parietal beta iCoh no longer shows significance (Table 95). The beta band shows significantly lower iCoh in the TEA cohort compared to HV, delta iCoh is significantly higher in TEA.

Table 95: FDR q-values for iCoh between Frontal and Parietal regions, within Frequency Bands (split by hemisphere, and inter-hemisphere)

OUTPUT AREA				Classical one-stage method*		Two-stage sharpened method†		
Unique rank	Order	Ascending p-values	Hypothesis name	FDR-derived significance thresholds	FDR-adjusted p-values a.k.a. q-values	Stage 1 significance thresholds	Stage 2 significance thresholds	FDR-adjusted p-values a.k.a. q-values
9	1	0.00200	RIGHT FRONTAL-PARIETAL BETA	0.00416667 *	0.024	0.0039683	0.0047619 *	0.021
11	2	0.00400	RIGHT FRONTAL-PARIETAL DELTA	0.00833333 *	0.024	0.0079365	0.0095238 *	0.021
10	3	0.02600	LEFT FRONTAL-PARIETAL BETA	0.0125	0.104	0.0119048	0.0142857	0.091
3	4	0.06700	INTER-H FRONTAL-PARIETAL BETA	0.01666667	0.201	0.015873	0.0190476	0.175875
2	5	0.10800	INTER-H FRONTAL-PARIETAL DELTA	0.02083333	0.253714286	0.0198413	0.0238095	0.222
12	6	0.13700	RIGHT FRONTAL-PARIETAL ALPHA	0.025	0.253714286	0.0238095	0.0285714	0.222
6	7	0.14800	INTER-H FRONTAL-PARIETAL THETA	0.02916667	0.253714286	0.0277778	0.0333333	0.222
1	8	0.19500	INTER-H FRONTAL-PARIETAL ALPHA	0.03333333	0.282666667	0.031746	0.0380952	0.247333333
5	9	0.21200	LEFT FRONTAL-PARIETAL DELTA	0.0375	0.282666667	0.0357143	0.0428571	0.247333333
7	10	0.24300	LEFT FRONTAL-PARIETAL ALPHA	0.04166667	0.2916	0.0396825	0.047619	0.25515
8	11	0.27300	LEFT FRONTAL-PARIETAL THETA	0.04583333	0.297818182	0.0436508	0.052381	0.260590909
4	12	0.62800	RIGHT FRONTAL-PARIETAL THETA	0.05	0.628	0.047619	0.0571429	0.5495

Second Phase – Connectivity Analysis – Weighted Phase Lag Index (wPLI)

The analysis aimed to determine the effects TEA may have on the communication within and between brain regions, at the global and regional levels, considering variation within frequency band. The phase synchronisation-based measure, weighted Phase Lag Index, was used to assess both linear and non-linear functional connectivity, whilst recognising its benefits and disadvantages (Vinck *et al.*, 2011; Jia, 2019; Hardmeier *et al.*, 2014) :

- wPLI is robust at eliminating volume conduction and resolving the common sources problem.
- Unlike iCoh, wPLI can separate the amplitude component from the phase-related component.
- wPLI is more robust than the Phase Lag Index in distinguishing phase lags from phase leads and is less affected by unrelated noise.
- wPLI does not assess effective connectivity (i.e., it does not assess causal relationships between signals or regions).
- wPLI shows good inter-subject reliability when used to estimate functional connectivity from resting state EEG.

Regional and interhemispheric wPLI were computed for the full frequency spectrum and within frequency bands (beta, alpha, theta, delta), for both global and regional spectra.

Dataset distributions were assessed using SPSS explore and Shapiro-Wilk tests were performed to check for normality. Comparison of TEA and HV cohorts was undertaken using a parametric Independent Samples T-Test for normal distributions; otherwise, a non-parametric Independent Samples Mann-Whitney U test was performed. Statistical significance was set at $p < 0.05$. To control for type I errors generated by the false rejection of the null hypothesis through multiple comparisons within the regional, and frequency band analysis, False Discovery Rate (FDR) adjustments using the classic one-stage, and two-stage sharpened methods were undertaken (Benjamini and Hochberg, 1995; Benjamini and Hochberg, 2000; Benjamini *et al.*, 2006; Pike, 2011; Nichols, 2007) with before p -values, and after correction q -values being reported within the results.

1. Global wPLI, All Frequencies

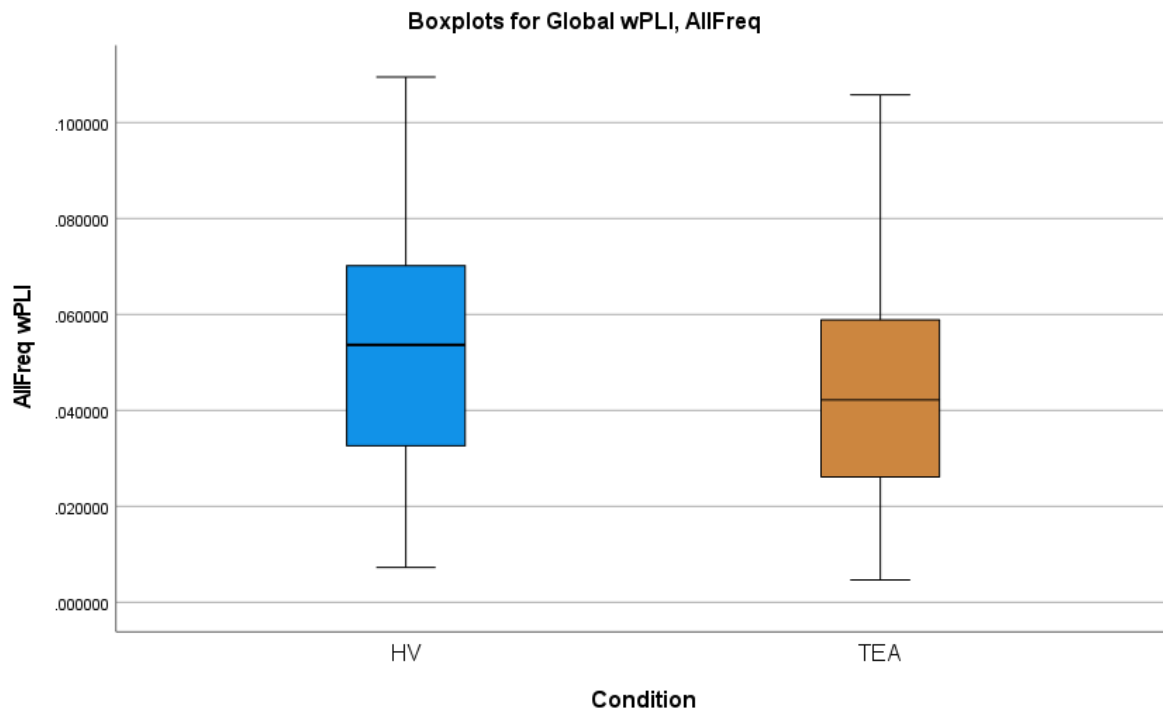


Figure 80: Boxplots for TEA and HV wPLI at Global level, all frequencies (1-40Hz)

Global wPLI has a platykurtic data distribution with a slight positive skew (Table 97). The mean across all data is 0.0475, with a standard error (SE) of 0.0008 and a standard deviation (SD) of 0.022. The interquartile range is 0.0351, and the range is 0.1049. (Table 97, Figure 80).

As neither cohort is normally distributed (Table 96), the non-parametric Man-Whitney U test was performed demonstrating a significant difference in wPLI profiles between the cohorts at a global level ($p < 0.001$), with lower mean/median values seen in the TEA cohort (Table 98, Table 99).

Table 96: Tests of Normality: TEA and HV wPLI at Global level, all frequencies (1-40Hz)

Tests of Normality - Global wPLI, AllFreq							
Condition	Kolmogorov-Smirnov ^a			Shapiro-Wilk			
	Statistic	df	Sig.	Statistic	df	Sig.	
AllFreq HV	.067	420	<.001	.977	420	<.001	
TEA	.055	420	.004	.980	420	<.001	

a. Lilliefors Significance Correction

Table 97: Data descriptives for TEA and HV wPLI at Global level, all frequencies (1-40Hz)

Statistics - Global wPLI		
AllFreq		
N	Valid	840
	Missing	42
Mean		.04747617
Std. Error of Mean		.000759973
Median		.04646030
Std. Deviation		.022026098
Variance		.000
Skewness		.177
Std. Error of Skewness		.084
Kurtosis		-.629
Std. Error of Kurtosis		.169
Range		.104855
Percentiles	25	.02943200
	50	.04646030
	75	.06455771

Report: Global wPLI		
AllFreq		
Condition	Mean	Median
HV	.05135247	.05368242
TEA	.04359987	.04219544
Total	.04747617	.04646030

Table 98: Global wPLI Mean/Median values for TEA and HV cohorts, with lower values for TEA. Lower mean wPLI in the TEA cohort is marked in blue.

Table 99: Significant Non-Parametric Findings for Global wPLI.

Hypothesis Test Summary - wPLI Connectivity measure: GLOBAL, ALLFREQUENCIES				
	Null Hypothesis	Test	Sig. ^{a,b}	Decision
1	The distribution of AllFreq is the same across categories of Condition.	Independent-Samples Mann-Whitney U Test	<.001	Reject the null hypothesis.

a. The significance level is .050.
 b. Asymptotic significance is displayed.

2. Intra-Regional and Inter-Regional wPLI, All Frequencies

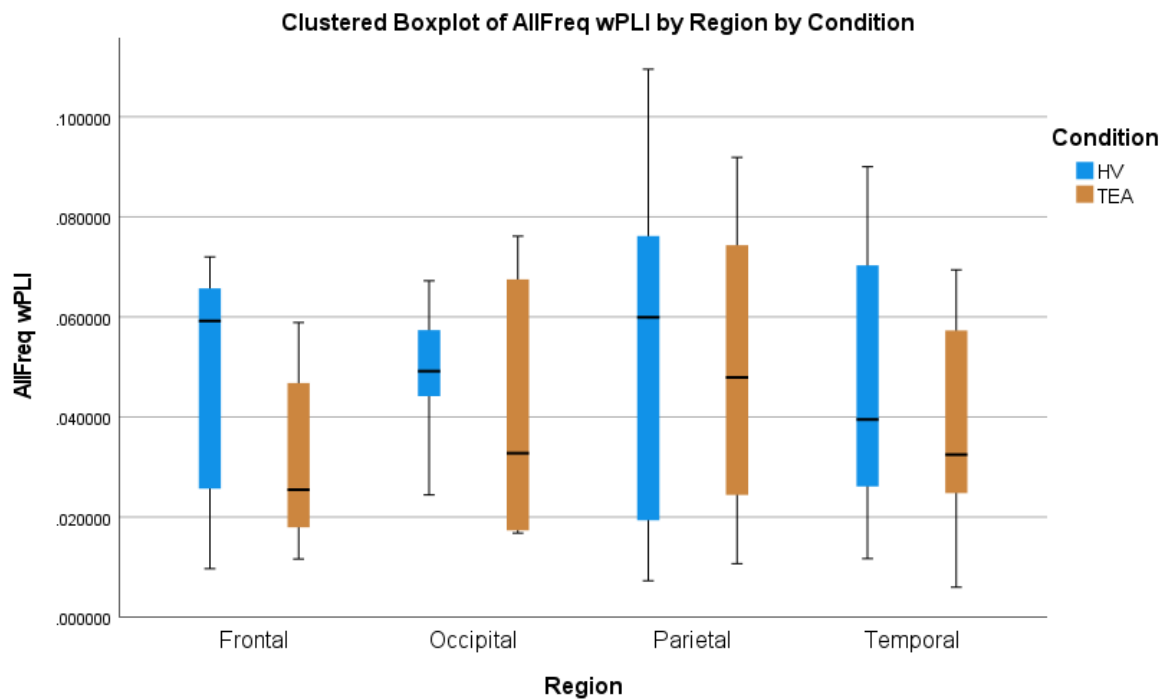


Figure 81: Intra-Regional wPLI Boxplot, all frequencies (1-40Hz)

Regional wPLI data shows a platykurtic data distribution for all regions (frontal, occipital, parietal, temporal), with parietal and temporal regions showing a slight positive skew and frontal and occipital regions being relatively symmetrical around the mean (Table 100). Data descriptives for regions are as follows (Table 100, Figure 81):

- Frontal regions - the mean is 0.0390, with a SE of 0.0035 and SD of 0.0221. The interquartile range is 0.0429, and the range is 0.0623.
- Occipital regions - the mean is 0.0451, with a SE of 0.0050 and an SD of 0.0201. The interquartile range is 0.0347, and the range is 0.0594.
- Parietal regions - the mean is 0.0523, with a SE of 0.0038 and an SD of 0.0295. The interquartile range is 0.0505, and the range is 0.1023.
- Temporal regions - the mean is 0.0423, with a SE of 0.0018 and SD of 0.00218. The interquartile range is 0.0364, and the range is 0.0840.

Only the HV occipital and parietal wPLI data distribution meets the criteria for normality, with all other data not meeting normality requirements (Table 101). Therefore, the non-parametric Mann-Whitney U test was utilised. There are no significant differences in intra-regional wPLI between cohorts, for all regions i.e., frontal, occipital, parietal, or temporal - Table 104.

Table 100: Data descriptives for TEA and HV wPLI at regional level, all frequencies (1-40Hz)

Statistics - Frontal wPLI, AllFreq			Statistics: Occipital wPLI, AllFreq			Statistics: Parietal wPLI, AllFreq			Statistics: Temporal wPLI, AllFreq		
AllFreq			AllFreq			AllFreq			AllFreq		
N	Valid	40	N	Valid	16	N	Valid	60	N	Valid	148
	Missing	10		Missing	4		Missing	12		Missing	16
Mean		.03903911	Mean		.04508197	Mean		.05230108	Mean		.04227065
Std. Error of Mean		.003495127	Std. Error of Mean		.00503102	Std. Error of Mean		.003810677	Std. Error of Mean		.001789799
Median		.03744313	Median		.04689498	Median		.05683420	Median		.03656930
Std. Deviation		.022105125	Std. Deviation		.02012409	Std. Deviation		.029517381	Std. Deviation		.021773840
Variance		.000	Variance		.000	Variance		.001	Variance		.000
Skewness		.070	Skewness		-.014	Skewness		.170	Skewness		.338
Std. Error of Skewness		.374	Std. Error of Skewness		.564	Std. Error of Skewness		.309	Std. Error of Skewness		.199
Kurtosis		-1.628	Kurtosis		-1.133	Kurtosis		-1.072	Kurtosis		-1.029
Std. Error of Kurtosis		.733	Std. Error of Kurtosis		1.091	Std. Error of Kurtosis		.608	Std. Error of Kurtosis		.396
Range		.062310	Range		.059355	Range		.102253	Range		.084022
Percentiles	25	.01813534	Percentiles	25	.02567941	Percentiles	25	.02441936	Percentiles	25	.02537641
	50	.03744313		50	.04689498		50	.05683420		50	.03656930
	75	.06104957		75	.06042260		75	.07496591		75	.06181726

Table 101: Tests of normality for TEA and HV wPLI at regional level, all frequencies (1-40Hz)

Tests of Normality: Frontal wPLI, AllFreq						
Condition	Kolmogorov-Smirnov			Shapiro-Wilk		
	Statistic	df	Sig.	Statistic	df	Sig.
AllFreq HV	.264	20	.001	.817	20	.002
TEA	.223	20	.010	.858	20	.007

Tests of Normality: Occipital wPLI, AllFreq						
Condition	Kolmogorov-Smirnov			Shapiro-Wilk		
	Statistic	df	Sig.	Statistic	df	Sig.
AllFreq HV	.181	8	.200	.958	8	.795
TEA	.200	8	.200	.833	8	.064

Tests of Normality: Parietal wPLI, AllFreq						
Condition	Kolmogorov-Smirnov			Shapiro-Wilk		
	Statistic	df	Sig.	Statistic	df	Sig.
AllFreq HV	.145	30	.110	.935	30	.069
TEA	.127	30	.200	.927	30	.042

Tests of Normality: Temporal wPLI, AllFreq						
Condition	Kolmogorov-Smirnov ^a			Shapiro-Wilk		
	Statistic	df	Sig.	Statistic	df	Sig.
AllFreq HV	.120	74	.010	.929	74	.000
TEA	.165	74	.000	.925	74	.000

a. Lilliefors Significance Correction

Inter-regional wPLI data shows a platykurtic data distribution for all regions (frontal, occipital, parietal, temporal). Temporal/frontal and temporal/occipital distributions show a slight positive skew, whilst the temporal/parietal dataset is reasonably symmetrical around the mean (Table 102). Data descriptives for regions are as follows (Table 102, Figure 82):

- Temporal/Frontal regions - the mean is 0.0431, with a SE of 0.0022 and SD of 0.0194. The interquartile range is 0.0260, and the range is 0.0860.
- Temporal/Occipital regions - the mean is 0.0422, with a SE of 0.0032 and SD of 0.0183. The interquartile range is 0.0275, and the range is 0.0662.
- Temporal/Parietal regions - the mean is 0.0479, with a SE of 0.0022 and SD of 0.0215. The interquartile range is 0.0355, and the range is 0.0910.

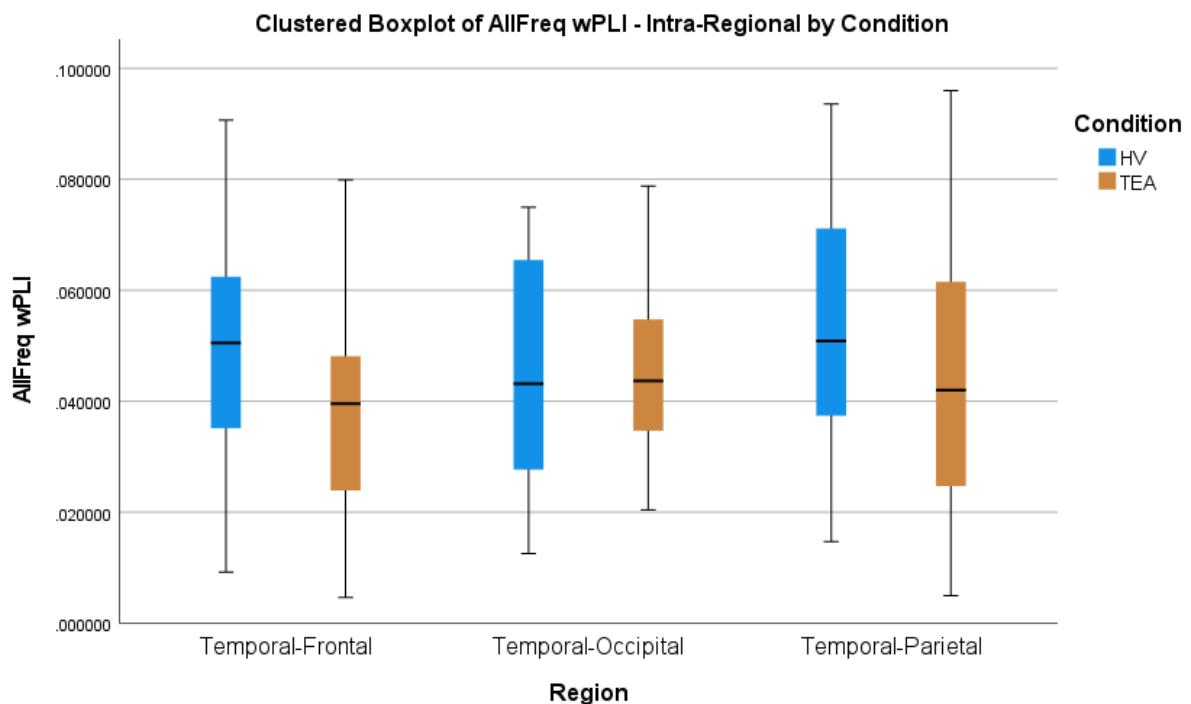


Figure 82: Inter-Regional wPLI Boxplot, all frequencies (1-40Hz)

Table 102: Data descriptives for TEA and HV wPLI at inter-regional level, all frequencies (1-40Hz)

Temporal-Frontal wPLI, AllFreq			Temporal-Occipital wPLI, AllFreq			Temporal-Parietal wPLI, AllFreq		
AllFreq			AllFreq			AllFreq		
N	Valid	80	N	Valid	32	N	Valid	96
	Missing	0		Missing	0		Missing	0
Mean		.04313390	Mean		.04422932	Mean		.04787969
Std. Error of Mean		.002174400	Std. Error of Mean		.003226754	Std. Error of Mean		.002190332
Median		.04106404	Median		.04325308	Median		.04493320
Std. Deviation		.019448425	Std. Deviation		.018253279	Std. Deviation		.021460788
Variance		.000	Variance		.000	Variance		.000
Skewness		.105	Skewness		.180	Skewness		.027
Std. Error of Skewness		.269	Std. Error of Skewness		.414	Std. Error of Skewness		.246
Kurtosis		-.537	Kurtosis		-.938	Kurtosis		-.932
Std. Error of Kurtosis		.532	Std. Error of Kurtosis		.809	Std. Error of Kurtosis		.488
Range		.085994	Range		.066228	Range		.091019
Percentiles	25	.03186131	Percentiles	25	.02803014	Percentiles	25	.03192376
	50	.04106404		50	.04325308		50	.04493320
	75	.05783345		75	.05552644		75	.06744369

All datasets apart from HV temporal/parietal wPLI meet the normal criteria (Table 103). Therefore, a non-parametric Man-Whitney U test was utilised for temporal/parietal data, and an independent samples t-test was used for the temporal-frontal and temporal-occipital datasets. There is a significant difference between TEA and HV cohorts within temporal-parietal and temporal-frontal network connectivity using the wPLI measure (Table 104), with mean/median values being lower in the TEA cohort.

Table 103: Tests for normality for TEA and HV wPLI at inter-regional level, all frequencies (1-40Hz)

Tests of Normality: Temporal-Frontal wPLI, AllFreq							
Kolmogorov-Smirnov ^a				Shapiro-Wilk			
Condition	Statistic	df	Sig.	Statistic	df	Sig.	
AllFreq HV	.072	40	.200	.981	40	.742	
TEA	.116	40	.192	.975	40	.519	
Tests of Normality: Temporal-Occipital wPLI, AllFreq							
Kolmogorov-Smirnov ^a				Shapiro-Wilk			
Condition	Statistic	df	Sig.	Statistic	df	Sig.	
AllFreq HV	.150	16	.200	.927	16	.222	
TEA	.121	16	.200	.964	16	.732	
Tests of Normality: Temporal-Parietal wPLI, AllFreq							
Kolmogorov-Smirnov ^a				Shapiro-Wilk			
Condition	Statistic	df	Sig.	Statistic	df	Sig.	
AllFreq HV	.148	48	.011	.940	48	.017	
TEA	.091	48	.200 [*]	.975	48	.388	

*. This is a lower bound of the true significance.
a. Lilliefors Significance Correction

Table 104: FDR q-values for Intra and Inter-Regional wPLI, AllFreq

OUTPUT AREA				Multiple comparisons using False Discovery Rates (FDRs)		Classical one-stage method*		Two-stage sharpened method†			Graphically sharpened method‡		
Unique rank	Order	Ascending p-values	Hypothesis name	FDR-derived significance thresholds	FDR-adjusted p-values a.k.a. q-values	Stage 1 significance thresholds	Stage 2 significance thresholds	FDR-adjusted p-values a.k.a. q-values	Point estimates of no. of H ₀ s	Best estimate	FDR-derived significance thresholds	FDR-adjusted p-values a.k.a. q-values	
3	1	0.00100	AllFreq TEMPORAL-PARIETAL	0.00714286 *	0.007	0.0068027	0.0095238 *	0.00525	7.0000		0.00833333 *	0.006	
5	2	0.00400	AllFreq TEMPORAL-FRONTAL	0.01428571 *	0.014	0.0136054	0.0190476 *	0.0105	6.0241		0.01666667 *	0.012	
6	3	0.03000	AllFreq FRONTAL	0.02142857	0.07	0.0204082	0.0285714	0.0525	5.1546		0.025	0.06	
4	4	0.05600	AllFreq TEMPORAL	0.02857143	0.098	0.0272109	0.0380952	0.0735	4.2373		0.03333333	0.084	
2	5	0.44000	AllFreq OCCIPITAL	0.03571429	0.536666667	0.0340136	0.047619	0.4025	5.3571	True	0.04166667	0.46	
7	6	0.46000	AllFreq PARIETAL	0.04285714	0.536666667	0.0408163	0.0571429	0.4025	3.7037		0.05	0.46	
1	7	0.78800	AllFreq TEMPORAL-OCCIPITAL	0.05	0.788	0.047619	0.0666667	0.591	4.7170		0.05833333	0.675428571	

3. Global wPLI – Frequency Bands

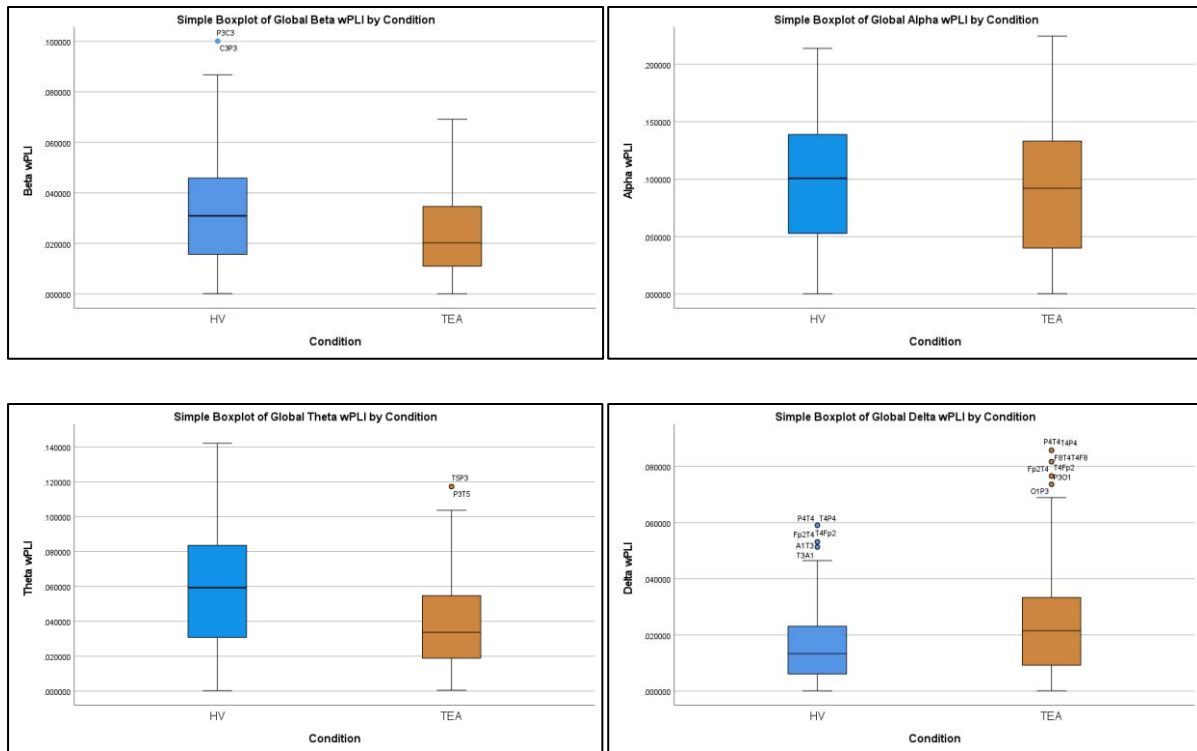


Figure 83: Boxplots for global wPLI, by frequency band. Top left - beta, top right - alpha, bottom left - theta, bottom right - delta.

Global wPLI within frequency bands show a platykurtic data distribution for all frequency bands with a positive skew for beta and theta bands, and a highly positive skew for delta bands, with the alpha frequency band distribution being symmetric around the mean. (Table 105). Data descriptives for regions are as follows (Table 105, Figure 83):

- Beta frequencies - the mean is 0.0282, with a SE of 0.0007 and SD of 0.0194. The interquartile range is 0.0277, and the range is 0.1000.
- Alpha frequencies - the mean is 0.0939, with a SE of 0.0018 and SD of 0.0522. The interquartile range is 0.0906, and the range is 0.2243.
- Theta frequencies - the mean is 0.0479, with a SE of 0.0011 and SD of 0.0305. The interquartile range is 0.0488, and the range is 0.0142.
- Delta frequencies - the mean is 0.0199, with a SE of 0.0005 and SD of 0.00159. The interquartile range is 0.0218, and the range is 0.0856.

No wPLI datasets within frequencies meet the criteria for normality (Table 107). Therefore, the non-parametric Mann-Whitney U test was utilised. There are significant differences in global wPLI between cohorts, for all frequency bands i.e., beta, alpha, theta, and delta. TEA mean/median values are lower for theta, alpha and beta frequencies, but higher within the delta band (Table 106, Table 108).

Table 105: Data descriptives for global wPLI, by frequency band.

Statistics: Global wPLI, Frequency Bands					
		Delta	Theta	Alpha	Beta
N	Valid	840	840	840	840
	Missing	42	42	42	42
Mean		.01989212	.04790997	.09391739	.02818520
Std. Error of Mean		.000548564	.001053744	.001802568	.000668173
Median		.01642426	.04381477	.09731788	.02545811
Std. Deviation		.015898895	.030540393	.052243380	.019365499
Variance		.000	.001	.003	.000
Skewness		1.192	.379	-.045	.696
Std. Error of Skewness		.084	.084	.084	.084
Kurtosis		1.547	-.721	-.975	-.018
Std. Error of Kurtosis		.169	.169	.169	.169
Range		.085646	.141948	.224310	.099995
Percentiles	25	.00745230	.02300754	.04615355	.01244420
	50	.01642426	.04381477	.09731788	.02545811
	75	.02927636	.07181059	.13671427	.04012877

Report: Global wPLI, Frequency Bands					
Condition		Delta	Theta	Alpha	Beta
HV	Mean	.01588661	.05734728	.09921019	.03296582
	Median	.01330460	.05938630	.10071871	.03092193
TEA	Mean	.02389764	.03847267	.08862458	.02340458
	Median	.02150464	.03375147	.09201177	.02028785
Total	Mean	.01989212	.04790997	.09391739	.02818520
	Median	.01642426	.04381477	.09731788	.02545811

Table 106: Mean/Median values for global wPLI, by frequency band. Lower mean wPLI in the TEA cohort is marked in blue.

Table 107: Tests of normality for global wPLI, by frequency band.

Tests of Normality: Global wPLI, Frequency Bands							
Condition		Kolmogorov-Smirnov ^a			Shapiro-Wilk		
		Statistic	df	Sig.	Statistic	df	Sig.
Delta	HV	.108	420	<.001	.924	420	<.001
	TEA	.094	420	<.001	.923	420	<.001
Theta	HV	.061	420	<.001	.974	420	<.001
	TEA	.088	420	<.001	.953	420	<.001
Alpha	HV	.071	420	<.001	.975	420	<.001
	TEA	.080	420	<.001	.960	420	<.001
Beta	HV	.063	420	<.001	.961	420	<.001
	TEA	.092	420	<.001	.954	420	<.001

a. Lilliefors Significance Correction

Table 108: FDR q-values for Global wPLI within Frequency Bands

OUTPUT AREA				Multiple comparisons using FDRs		Classical one-stage method*	
Unique rank	Order	Ascending Hypothesis		FDR-derived significance thresholds	FDR-adjusted p-values a.k.a. q-values		
3	1	0.00000 Theta GLOBAL		0.0125 *	0		
1	2	0.00100 Beta GLOBAL		0.025 *	0.001333333		
4	3	0.00100 Delta GLOBAL		0.0375 *	0.001333333		
2	4	0.00500 Alpha GLOBAL		0.05 *	0.005		

4. Intra-Regional wPLI – Frequency Bands

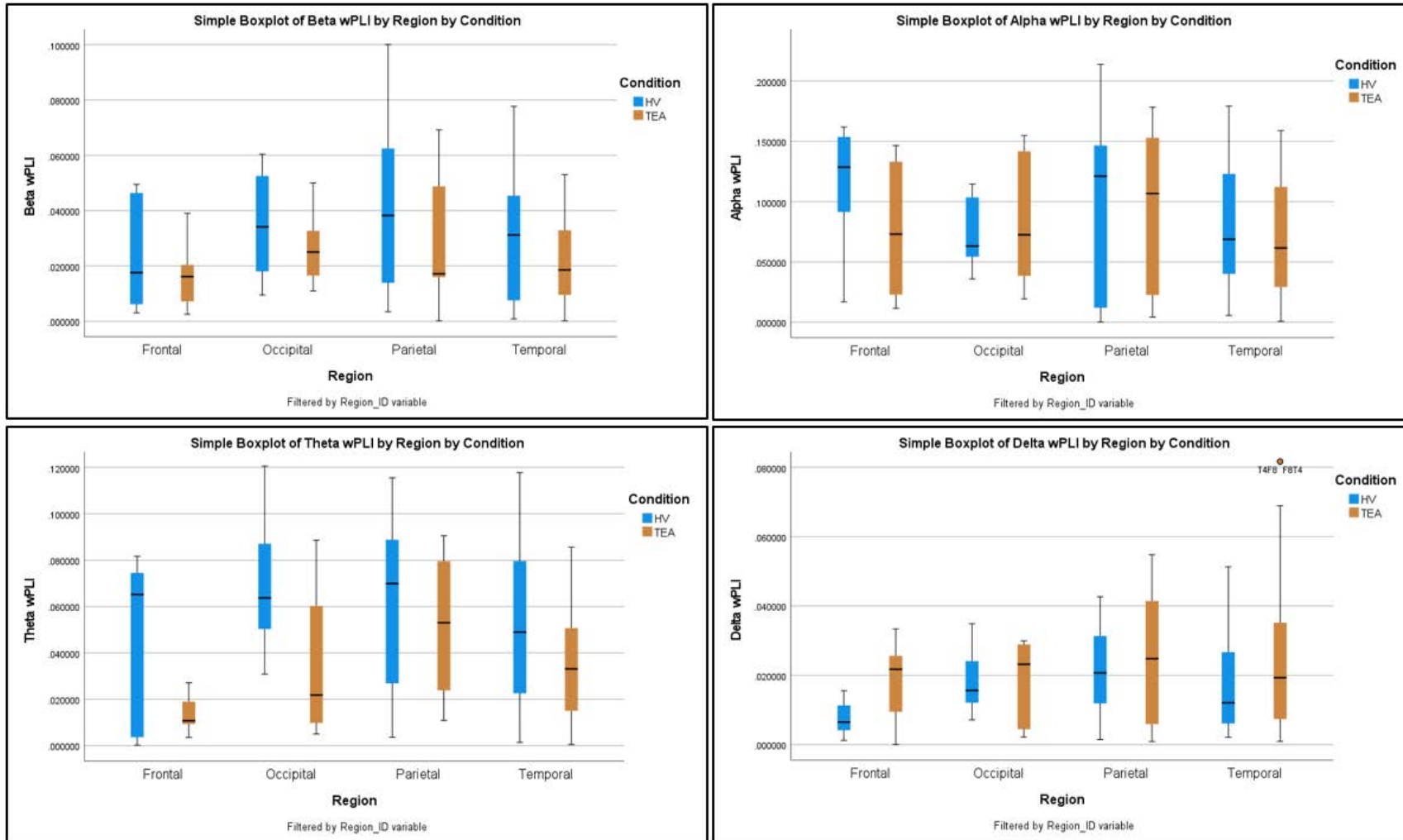


Figure 84: Boxplots for regional wPLI, by frequency band. Top left - beta, top right - alpha, bottom left - theta, bottom right - delta.

4.1. Frontal

Frontal wPLI within frequency bands show a platykurtic data distribution for all frequency bands with a positive skew for beta, theta, and delta, while alpha frequency data has a slight negative skew (Table 109). Data descriptives for frequency bands are as follows (Table 109, Figure 84):

- Beta frequencies - the mean is 0.0200, with an SE of 0.0023 and an SD of 0.0147. The interquartile range is 0.0188, and the range is 0.0469.
- Alpha frequencies - the mean is 0.0947, with a SE of 0.0087 and SD of 0.0553. The interquartile range is 0.1214, and the range is 0.1503.
- Theta frequencies - the mean is 0.0297, with a SE of 0.0047 and SD of 0.0300. The interquartile range is 0.0612, and the range is 0.0815.
- Delta frequencies - the mean is 0.0128, with a SE of 0.0016 and SD of 0.0101. The interquartile range is 0.0179, and the range is 0.0333.

Both cohorts for frontal delta wPLI meet normality tests, as do the theta and beta TEA cohorts. Other datasets do not meet normality requirements (Table 110).

Therefore, the non-parametric Mann-Whitney U test was utilised for frontal beta, alpha, and theta wPLI, and an independent samples t-test for delta wPLI. Frontal delta and alpha wPLI show significant p-values ($p < 0.001$ and $p = 0.040$ respectively). After multiple comparisons FDR adjustment only frontal delta wPLI shows a significant difference between TEA and HV cohorts, using both the classic one-stage and the two-stage sharpened method (Table 111). Delta wPLI means and median values are higher overall in TEA subjects over frontal regions.

4.2. Occipital

Occipital wPLI within frequency bands show a platykurtic data distribution for all frequency bands with a slight negative skew for the delta frequency band and a positive skew for beta, alpha, and theta bands (Table 109). Data descriptives for frequency bands are as follows (Table 109, Figure 84):

- Beta frequencies - the mean is 0.0306, with a SE of 0.0042 and SD of 0.0166. The interquartile range is 0.0266, and the range is 0.0510.

- Alpha frequencies - the mean is 0.0796, with an SE of 0.0107 and an SD of 0.0427. The interquartile range is 0.0724, and the range is 0.1355.
- Theta frequencies - the mean is 0.0520, with a SE of 0.0085 and SD of 0.0341. The interquartile range is 0.0617, and the range is 0.1156.
- Delta frequencies - the mean is 0.0182, with a SE of 0.0027 and SD of 0.0106. The interquartile range is 0.0213, and the range is 0.0327.

Only the occipital delta wPLI data for the TEA cohort does not meet the criteria for normality (Table 110). Therefore, the non-parametric Mann-Whitney U test was utilised for occipital delta wPLI while an independent samples t-test was used for occipital beta, alpha and theta wPLI for delta wPLI. Occipital theta wPLI initially shows a significant p-value ($p=0.038$). After multiple comparisons of FDR adjustment, there are no significant differences seen for wPLI within any of the frequency bands in occipital regions, however (Table 111).

4.3. *Parietal*

Parietal wPLI within frequency bands show a platykurtic data distribution for all frequency bands with a slight negative skew for beta and delta frequencies, while alpha and theta distributions are roughly symmetric around the mean (Table 109). Data descriptives for frequency bands are as follows (Table 109, Figure 84):

- Beta frequencies - the mean is 0.0340, with a SE of 0.0033 and an SD of 0.0254. The interquartile range is 0.0334, and the range is 0.0100.
- Alpha frequencies - the mean is 0.0953, with a SE of 0.0091 and SD of 0.0702. The interquartile range is 0.1241, and the range is 0.2137.
- Theta frequencies - the mean is 0.0569, with a SE of 0.0042 and an SD of 0.0322. The interquartile range is 0.0528, and the range is 0.1187.
- Delta frequencies - the mean is 0.0229, with a SE of 0.0019 and SD of 0.0150. The interquartile range is 0.023, and the range is 0.0539.

Only parietal delta and beta data distributions in the HV cohort satisfy the criteria for normality. All other datasets do not meet normality requirements (Table 110). Therefore, the non-parametric Mann-Whitney U test was utilised for all frequency bands. There are no

significant differences seen for wPLI within any of the frequency bands in parietal regions (Table 111).

4.4. Temporal

Temporal wPLI within frequency bands show a platykurtic data distribution for all frequency bands with a slight positive skew for beta, alpha, and theta; the delta frequency band distribution has a highly positive skew. (Table 109). Data descriptives for frequency bands are as follows (Table 109, Figure 84):

- Beta frequencies - the mean is 0.0272, with a SE of 0.0017 and SD of 0.00202. The interquartile range is 0.0336, and the range is 0.0775.
- Alpha frequencies - the mean is 0.0771, with a SE of 0.0041 and SD of 0.0499. The interquartile range is 0.0791, and the range is 0.1784.
- Theta frequencies - the mean is 0.0437, with a SE of 0.0024 and SD of 0.0297. The interquartile range is 0.0448, and the range is 0.1172.
- Delta frequencies - the mean is 0.0210, with a SE of 0.0015 and SD of 0.0180. The interquartile range is 0.0226, and the range is 0.0807.

Table 109: Descriptives for regional wPLI by frequency band. Top left - frontal, top right - occipital, bottom left - parietal, bottom right – temporal.

Statistics - Frontal wPLI within Frequency Bands						Statistics : Occipital wPLI within Frequency Bands					
		Delta	Theta	Alpha	Beta			Delta	Theta	Alpha	Beta
N	Valid	40	40	40	40	N	Valid	16	16	16	16
	Missing	10	10	10	10		N	Missing	4	4	4
Mean		.01277159	.02867799	.09468718	.02001968	Mean			.01822349	.05195168	.07956563
Std. Error of Mean		.001599045	.004737112	.008747894	.002324796	Std. Error of Mean		.002650535	.008532268	.010681247	.004155386
Median		.01042017	.01254717	.11406708	.01728565	Median		.01788992	.05267079	.06555066	.02672377
Std. Deviation		.010113252	.029960129	.055326539	.014703301	Std. Deviation		.010602140	.034129073	.042724988	.016621545
Variance		.000	.001	.003	.000	Variance		.000	.001	.002	.000
Skewness		.614	.801	-.390	.937	Skewness		-.086	.296	.524	.577
Std. Error of Skewness		.374	.374	.374	.374	Std. Error of Skewness		.564	.564	.564	.564
Kurtosis		-.861	-1.181	-1.530	-.221	Kurtosis		-1.280	-.715	-.937	-.664
Std. Error of Kurtosis		.733	.733	.733	.733	Std. Error of Kurtosis		1.091	1.091	1.091	1.091
Range		.033306	.081455	.150280	.046887	Range		.032688	.115620	.135491	.050964
Percentiles	25	.00446013	.00460777	.02455173	.00720529	Percentiles	25	.00782522	.01948264	.04213812	.01658150
	50	.01042017	.01254717	.11406708	.01728565		50	.01788992	.05267079	.06555066	.02672377
	75	.02233788	.06587656	.14596537	.02603628		75	.02910553	.08122440	.11458700	.04315251

Statistics: Parietal wPLI within Frequency Bands						Statistics: Temporal wPLI within Frequency Bands					
		Delta	Theta	Alpha	Beta			Delta	Theta	Alpha	Beta
N	Valid	60	60	60	60	N	Valid	148	148	148	148
	Missing	12	12	12	12		N	Missing	16	16	16
Mean		.02294929	.05691114	.09534934	.03399457	Mean			.02098813	.04373856	.07712744
Std. Error of Mean		.001932259	.004160499	.009060985	.003282187	Std. Error of Mean		.001477964	.002444786	.004100191	.001659378
Median		.02122330	.05596598	.11808402	.02975461	Median		.01784726	.04260938	.06569525	.02631175
Std. Deviation		.014967218	.032227083	.070186086	.025423711	Std. Deviation		.017980212	.029742107	.049880979	.020187200
Variance		.000	.001	.005	.001	Variance		.000	.001	.002	.000
Skewness		.355	-.030	-.068	.609	Skewness		1.260	.493	.421	.474
Std. Error of Skewness		.309	.309	.309	.309	Std. Error of Skewness		.199	.199	.199	.199
Kurtosis		-.875	-1.003	-1.495	-.255	Kurtosis		1.291	-.464	-.964	-.806
Std. Error of Kurtosis		.608	.608	.608	.608	Std. Error of Kurtosis		.396	.396	.396	.396
Range		.053864	.111864	.213724	.099861	Range		.080689	.117252	.178394	.077519
Percentiles	25	.01007735	.02690543	.02249482	.01603089	Percentiles	25	.00707639	.02014555	.03899902	.00831742
	50	.02122330	.05596598	.11808402	.02975461		50	.01784726	.04260938	.06569525	.02631175
	75	.03334812	.08065860	.14658637	.04942664		75	.02967996	.06498466	.11807455	.04193545

None of the datasets for temporal wPLI meets the criteria for normality (Table 110). Therefore, the non-parametric Mann-Whitney U test was utilised for all temporal wPLI frequency bands. Temporal theta and beta wPLI show significant p-values ($p < 0.001$ and $p = 0.004$ respectively). After multiple comparisons of FDR adjustments, only temporal theta wPLI demonstrates a significant difference between TEA and HV cohorts using both the classic one-stage and the two-stage sharpened method (Table 111). TEA mean/median wPLI is significantly lower than HV for temporal theta activities.

Table 110: Tests of normality for regional wPLI by frequency band. Top left - frontal, top right - occipital, bottom left - parietal, bottom right – temporal.

Tests of Normality - Frontal wPLI within Frequency Bands							Tests of Normality: Occipital wPLI within Frequency Bands								
Condition		Kolmogorov-Smirnov ^a			Shapiro-Wilk			Condition		Kolmogorov-Smirnov ^a			Shapiro-Wilk		
		Statistic	df	Sig.	Statistic	df	Sig.			Statistic	df	Sig.	Statistic	df	Sig.
Delta	HV	.221	20	.012	.910	20	.065	Delta	HV	.219	8	.200*	.912	8	.370
	TEA	.178	20	.097	.914	20	.075	TEA	.261	8	.116	.806	8	.033	
Theta	HV	.307	20	<.001	.729	20	<.001	Theta	HV	.170	8	.200*	.969	8	.888
	TEA	.184	20	.074	.908	20	.057	TEA	.226	8	.200*	.862	8	.126	
Alpha	HV	.190	20	.057	.809	20	.001	Alpha	HV	.229	8	.200*	.893	8	.248
	TEA	.225	20	.009	.834	20	.003	TEA	.184	8	.200*	.885	8	.208	
Beta	HV	.292	20	<.001	.802	20	<.001	Beta	HV	.154	8	.200*	.921	8	.441
	TEA	.172	20	.125	.919	20	.096	TEA	.230	8	.200*	.925	8	.468	

a. Lilliefors Significance Correction

Tests of Normality: Parietal wPLI within Frequency Bands							
Condition		Kolmogorov-Smirnov ^a			Shapiro-Wilk		
		Statistic	df	Sig.	Statistic	df	Sig.
Delta	HV	.108	30	.200*	.970	30	.544
	TEA	.200	30	.004	.891	30	.005
Theta	HV	.139	30	.146	.927	30	.041
	TEA	.131	30	.200*	.915	30	.020
Alpha	HV	.233	30	<.001	.853	30	<.001
	TEA	.210	30	.002	.865	30	.001
Beta	HV	.133	30	.187	.935	30	.067
	TEA	.229	30	<.001	.904	30	.011

*. This is a lower bound of the true significance.
a. Lilliefors Significance Correction

Tests of Normality: Temporal wPLI within Frequency Bands							
Condition		Kolmogorov-Smirnov ^a			Shapiro-Wilk		
		Statistic	df	Sig.	Statistic	df	Sig.
Delta	HV	.191	74	<.001	.886	74	<.001
	TEA	.189	74	<.001	.876	74	<.001
Theta	HV	.078	74	.200*	.959	74	.018
	TEA	.109	74	.030	.948	74	.004
Alpha	HV	.151	74	<.001	.912	74	<.001
	TEA	.112	74	.021	.936	74	.001
Beta	HV	.148	74	<.001	.924	74	<.001
	TEA	.149	74	<.001	.922	74	<.001

*. This is a lower bound of the true significance.
a. Lilliefors Significance Correction

Table 111: FDR q-values for Intra-Regional wPLI within Frequency Bands. Lower mean wPLI in the TEA cohort is marked in blue.

OUTPUT AREA		Multiple comparisons using FDRs		Classical one-stage method ^a		Two-stage sharpened method ^b		Graphically sharpened method ^c				
Unique rank	Order	Ascending p-values	Hypothesis name	FDR-derived significance thresholds	FDR-adjusted p-values a.k.a. q-values	Stage 1 significance thresholds	Stage 2 significance thresholds	FDR-adjusted p-values a.k.a. q-values	Point estimates of no. of H ₀ s	Best estimate	FDR-derived significance thresholds	FDR-adjusted p-values a.k.a. q-values
2	1	0.00100	Theta TEMPORAL	0.003125*	0.008	0.0029762	0.0034014*	0.00735	16.0000		0.00384615*	0.0065
9	2	0.00100	Delta FRONTAL	0.00625*	0.008	0.0059524	0.0068027*	0.00735	15.0150		0.00769231*	0.0065
5	3	0.03800	Theta OCCIPITAL	0.009375	0.128	0.0089286	0.0102041	0.1176	14.5530		0.01153846	0.104
13	4	0.04000	Beta TEMPORAL	0.0125	0.128	0.0119048	0.0136054	0.1176	13.5417		0.01538462	0.104
16	5	0.04000	Alpha FRONTAL	0.015625	0.128	0.014881	0.0170068	0.1176	12.5000		0.01923077	0.104
3	6	0.13100	Beta PARIETAL	0.01875	0.349333333	0.0178571	0.0204082	0.32095	12.6582	True	0.02307692	0.283833333
14	7	0.16400	Theta PARIETAL	0.021875	0.357333333	0.0208333	0.0238095	0.3283	11.9617		0.02692308	0.290333333
11	8	0.17900	Delta TEMPORAL	0.025	0.357333333	0.0238095	0.0272109	0.3283	10.9622		0.03076923	0.290333333
12	9	0.20100	Theta FRONTAL	0.028125	0.357333333	0.0267857	0.0306122	0.3283	10.0125		0.03461538	0.290333333
7	10	0.27300	Alpha TEMPORAL	0.03125	0.4368	0.0297619	0.0340136	0.40131	9.6286		0.03846154	0.3549
15	11	0.31100	Beta OCCIPITAL	0.034375	0.452363636	0.0327381	0.037415	0.415609091	8.7083		0.04230769	0.367545455
6	12	0.57400	Beta PARIETAL	0.0375	0.716571429	0.0357143	0.0408163	0.65835	11.7371		0.04615385	0.582214286
8	13	0.60200	Beta FRONTAL	0.040625	0.716571429	0.0386905	0.0442177	0.65835	10.0503		0.05	0.582214286
1	14	0.62700	Alpha OCCIPITAL	0.04375	0.716571429	0.0416667	0.047619	0.65835	8.0429		0.05384615	0.582214286
10	15	0.70100	Alpha PARIETAL	0.046875	0.747733333	0.0446429	0.0510204	0.68698	6.8890		0.05769231	0.607533333
4	16	1.00000	Delta OCCIPITAL	0.05	1	0.047619	0.0544218	0.91875	#DIV/0!		0.06153846	0.8125

4.5. Inter-hemisphere Analysis of Significant Findings

Further interhemispheric analysis between the TEA and HV cohorts. This was undertaken on significant intra-regional findings, examining the left, right, and interhemispheric networks separately. An independent samples t-test was used for normally distributed datasets and the non-parametric Mann-Whitney U-test was for those not meeting the criteria for normality. All findings were subjected to multiple comparisons of FDR adjustment.

4.5.1. Frontal

Using hemispheric comparisons (for left, right and inter-hemisphere networks) only the left frontal area shows a significant difference in delta wPLI between TEA and HV cohorts (Table 112), with TEA mean/median values being significantly higher than HV subjects overall.

Table 112: FDR q-values for significant Intra-Regional wPLI - FRONTAL (split by hemisphere, and inter-hemisphere). Lower mean wPLI in the TEA cohort is marked in blue.

OUTPUT AREA		Multiple comparisons using False Discovery Rates (FDRs)		Classical one-stage method*		Two-stage sharpened method†		
Unique rank	Order	Ascending p-values	Hypothesis name	FDR-derived significance thresholds	FDR-adjusted p-values a.k.a. q-values	Stage 1 significance thresholds	Stage 2 significance thresholds	FDR-adjusted p-values a.k.a. q-values
1	1	0.00200	LEFT FRONTAL DELTA	0.01666667 *	0.006	0.015873	0.0238095 *	0.0042
3	2	0.10500	INTER-H FRONTAL DELTA	0.03333333	0.1575	0.031746	0.047619	0.11025
2	3	0.39400	RIGHT FRONTAL DELTA	0.05	0.394	0.047619	0.0714286	0.2758

4.5.2. Temporal

Over temporal regions, both the left and right hemisphere wPLI results demonstrate a significant difference within the theta frequency band, with TEA mean and median values being significantly lower than in the HV cohort.

Table 113: FDR q-values for significant Intra-Regional wPLI - TEMPORAL (split by hemisphere, and inter-hemisphere). Lower mean wPLI in the TEA cohort is marked in blue.

OUTPUT AREA		Multiple comparisons using False Discovery Rates (FDRs)		Classical one-stage method*		Two-stage sharpened method†		
Unique rank	Order	Ascending p-values	Hypothesis name	FDR-derived significance thresholds	FDR-adjusted p-values a.k.a. q-values	Stage 1 significance thresholds	Stage 2 significance thresholds	FDR-adjusted p-values a.k.a. q-values
1	1	0.00400	LEFT TEMPORAL THETA	0.01666667 *	0.0105	0.015873	0.047619 *	0.003675
2	2	0.00700	RIGHT TEMPORAL THETA	0.03333333 *	0.0105	0.031746	0.0952381 *	0.003675
3	3	0.30700	INTER-H TEMPORAL THETA	0.05	0.307	0.047619	0.1428571	0.10745

5. Inter-Regional wPLI – Frequency Bands

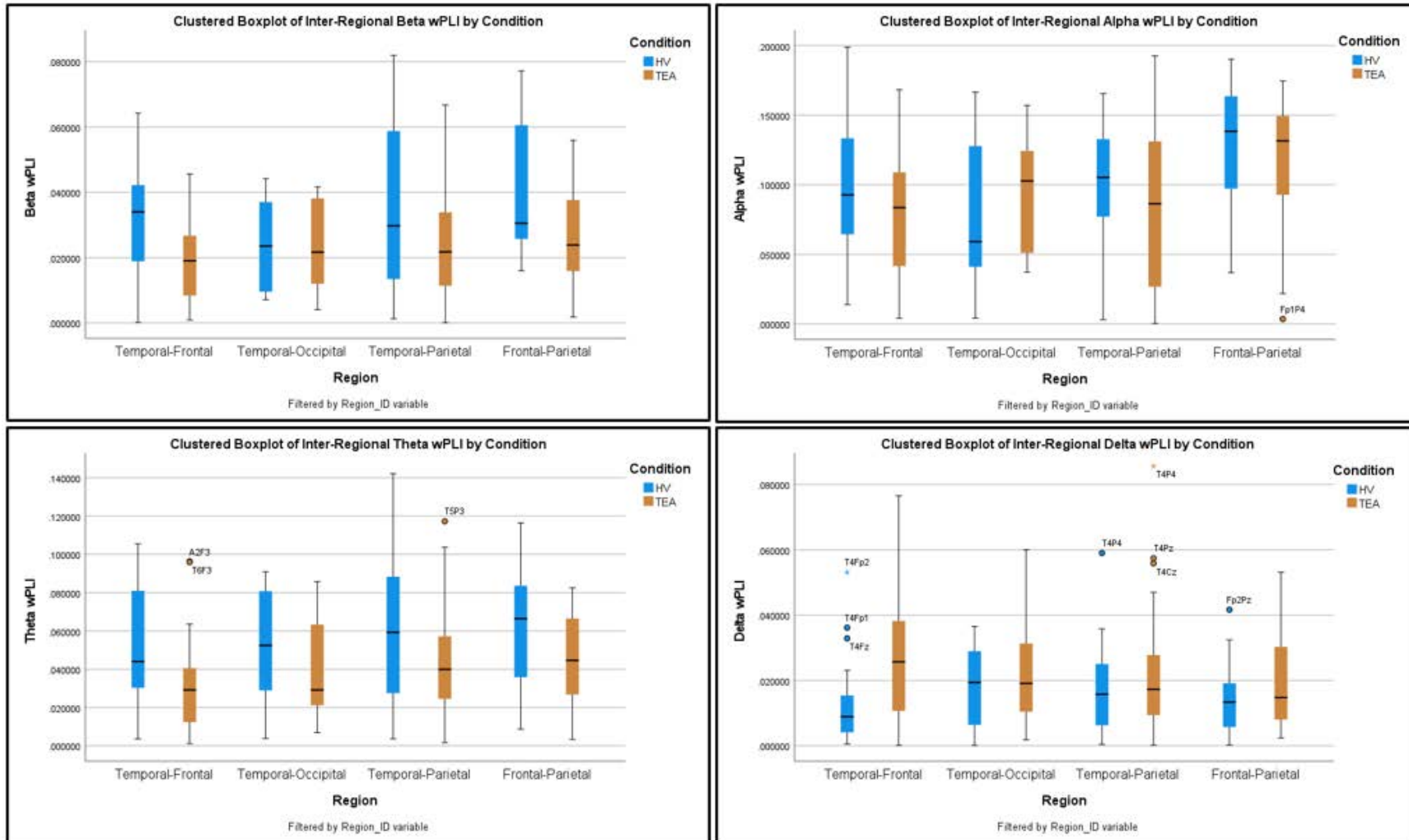


Figure 85: Boxplots for inter-regional wPLI, by frequency band. Top left - beta, top right - alpha, bottom left - theta, bottom right - delta.

5.1. Temporal and Frontal Regions

Temporal-frontal wPLI within frequency bands show a platykurtic data distribution and a positive skew across all frequency bands. (Table 114). Data descriptives for regions are as follows (Table 114, Figure 85):

- Beta frequencies - the mean is 0.0248 with a SE of 0.0018 and SD of 0.0016. The interquartile range is 0.0278, and the range is 0.0641.
- Alpha frequencies - the mean is 0.0878, with a SE of 0.0053 and SD of 0.0472. The interquartile range is 0.0678, and the range is 0.1946.
- Theta frequencies - the mean is 0.0409, with a SE of 0.0033 and SD of 0.0294. The interquartile range is 0.0409, and the range is 0.1043.
- Delta frequencies - the mean is 0.0190, with a SE of 0.0019 and SD of 0.0169. The interquartile range is 0.0220, and the range is 0.0764.

Table 114: Data descriptives for inter-regional wPLI between temporal and frontal regions, by frequency band

Statistics: Temporal-Frontal wPLI within Frequency Bands					
		Delta	Theta	Alpha	Beta
N	Valid	80	80	80	80
	Missing	0	0	0	0
Mean		.01901961	.04086820	.08780346	.02484433
Std. Error of Mean		.001888745	.003285547	.005278175	.001783634
Median		.01343033	.03463542	.08534051	.02264726
Std. Deviation		.016893446	.029386822	.047209429	.015953307
Variance		.000	.001	.002	.000
Skewness		1.260	.674	.256	.312
Std. Error of Skewness		.269	.269	.269	.269
Kurtosis		1.326	-.580	-.578	-.751
Std. Error of Kurtosis		.532	.532	.532	.532
Range		.076416	.104318	.194612	.064087
Percentiles	25	.00532410	.01704283	.04780565	.01124751
	50	.01343033	.03463542	.08534051	.02264726
	75	.02727223	.05786872	.11563737	.03904149

Both cohorts for temporal-frontal alpha wPLI and beta wPLI within the HV cohort meet the criteria for normality. All other datasets fall short of normality requirements (Table 115). Therefore, the non-parametric Mann-Whitney U test was utilised for temporal-frontal beta, theta, and delta bands, whilst an independent samples t-test was used to assess alpha wPLI.

All frequency bands across the temporal-frontal regions show significant p-values ($p < 0.001$ for beta, theta and delta bands, and $p = 0.011$ for alpha frequencies), and all remain significant after multiple comparisons FDR adjustments using both the classic one-stage and the two-stage sharpened method (Table 122, Table 81). Delta band activities within the temporal frontal networks have significantly higher mean/median wPLI in TEA subjects compared to HV, overall. Within the beta, alpha and theta frequency bands within the temporal frontal networks, there are significantly lower mean/median wPLI in the TEA cohort overall.

Table 115: Tests of normality for inter-regional wPLI between temporal and frontal regions, by frequency band

Tests of Normality: Temporal-Frontal wPLI within Frequency Bands							
Condition	Kolmogorov-Smirnov ^a			Shapiro-Wilk			
	Statistic	df	Sig.	Statistic	df	Sig.	
Delta	HV	.155	40	.017	.829	40	<.001
	TEA	.114	40	.200*	.939	40	.033
Theta	HV	.148	40	.027	.925	40	.011
	TEA	.125	40	.115	.906	40	.003
Alpha	HV	.068	40	.200*	.972	40	.422
	TEA	.110	40	.200*	.972	40	.405
Beta	HV	.107	40	.200*	.963	40	.213
	TEA	.104	40	.200*	.945	40	.051

*. This is a lower bound of the true significance.
a. Lilliefors Significance Correction

5.2. Temporal and Occipital Regions

Table 116: Data descriptives for inter-regional wPLI between temporal and occipital regions, by frequency band

Statistics: Temporal-Occipital wPLI within Frequency Bands					
		Delta	Theta	Alpha	Beta
N	Valid	32	32	32	32
	Missing	0	0	0	0
Mean		.01999218	.04702485	.08601416	.02388609
Std. Error of Mean		.002393368	.004826989	.008033327	.002373979
Median		.01911021	.04317711	.09839065	.02355575
Std. Deviation		.013538935	.027305574	.045443358	.013429255
Variance		.000	.001	.002	.000
Skewness		.759	.187	.001	.091
Std. Error of Skewness		.414	.414	.414	.414
Kurtosis		.906	-1.381	-1.350	-1.568
Std. Error of Kurtosis		.809	.809	.809	.809
Range		.059952	.087048	.162159	.040117
Percentiles	25	.00869760	.02280997	.04472486	.01064903
	50	.01911021	.04317711	.09839065	.02355575
	75	.03063077	.07410816	.12822985	.03857643

Temporal-occipital wPLI within frequency bands show a platykurtic data distribution and a positive skew across the delta and theta frequency bands, while alpha and beta data are relatively symmetrical around the mean (Table 116). Data descriptives for regions are as follows (Table 116, Figure 85):

- Beta frequencies - the mean is 0.0239 with a SE of 0.0024 and SD of 0.0134. The interquartile range is 0.0280, and the range is 0.0401.
- Alpha frequencies - the mean is 0.0860, with a SE of 0.0080 and SD of 0.0454. The interquartile range is 0.0835, and the range is 0.1622.
- Theta frequencies - the mean is 0.0470, with a SE of 0.0048 and SD of 0.0273. The interquartile range is 0.0513, and the range is 0.0870.
- Delta frequencies - the mean is 0.0200, with a SE of 0.0024 and SD of 0.0135. The interquartile range is 0.0219, and the range is 0.0560.

All data distributions for temporal-occipital wPLI within bands meet the criteria for normality (Table 117). Therefore, an independent samples t-test was used to assess all wPLI data between these regions.

Table 117: Tests of normality for inter-regional wPLI between temporal and occipital regions, by frequency band

Tests of Normality: Temporal-Occipital wPLI within Frequency Bands							
Condition	Statistic	Kolmogorov-Smirnov ^a			Shapiro-Wilk		
		df	Sig.	Statistic	df	Sig.	
Delta	HV	.130	16	.200*	.934	16	.287
	TEA	.158	16	.200*	.919	16	.163
Theta	HV	.142	16	.200*	.938	16	.321
	TEA	.225	16	.029	.899	16	.078
Alpha	HV	.196	16	.103	.918	16	.156
	TEA	.209	16	.061	.898	16	.074
Beta	HV	.163	16	.200*	.896	16	.068
	TEA	.188	16	.134	.892	16	.061

*. This is a lower bound of the true significance.
a. Lilliefors Significance Correction

Theta frequency wPLI within temporal-occipital networks shows a significant p-value ($p = <0.032$). This remains significant after multiple comparisons of FDR adjustments using both the classic one-stage and the two-stage sharpened method (Table 122, Table 81). Theta

frequency bands within the temporal frontal networks show a significantly lower mean/median wPLI in the TEA group when compared to HV.

5.1. Temporal and Parietal Regions

Table 118: Data descriptives for inter-regional wPLI between temporal and parietal regions, by frequency band

Statistics: Temporal-Parietal wPLI within Frequency Bands					
		Delta	Theta	Alpha	Beta
N	Valid	96	96	96	96
	Missing	0	0	0	0
Mean		.01914139	.05156609	.09161456	.02919672
Std. Error of Mean		.001561239	.003342159	.005065676	.002173564
Median		.01728600	.04545520	.09711676	.02425316
Std. Deviation		.015296952	.032746334	.049633287	.021296494
Variance		.000	.001	.002	.000
Skewness		1.447	.520	-.290	.649
Std. Error of Skewness		.246	.246	.246	.246
Kurtosis		3.181	-.456	-.981	-.578
Std. Error of Kurtosis		.488	.488	.488	.488
Range		.085543	.140570	.192222	.081864
Percentiles	25	.00691593	.02556916	.04322620	.01217540
	50	.01728600	.04545520	.09711676	.02425316
	75	.02577967	.07622727	.13136080	.04258192

Temporal-parietal wPLI within frequency bands show a platykurtic data distribution for beta, alpha, and theta bands; the delta band distribution is mesokurtic. Beta and theta bands have positive skew, while the delta band data is highly positively skewed and alpha frequency distribution is slightly negatively skewed (Table 118). Data descriptives for regions are as follows (Table 118, Figure 85):

- Beta frequencies - the mean is 0.0292 with a SE of 0.0022 and SD of 0.0213. The interquartile range is 0.0304, and the range is 0.0819.
- Alpha frequencies - the mean is 0.0916, with a SE of 0.0051 and SD of 0.0496. The interquartile range is 0.0882, and the range is 0.1922.
- Theta frequencies - the mean is 0.0516, with a SE of 0.0033 and an SD of 0.0327. The interquartile range is 0.0506, and the range is 0.1405.
- Delta frequencies - the mean is 0.0191, with a SE of 0.0016 and SD of 0.0153. The interquartile range is 0.0189, and the range is 0.0855.

Temporal-parietal alpha and theta wPLI within the HV cohort meet the criteria for normality. All other datasets fall short of normality requirements (Table 119). Therefore, the non-parametric Mann-Whitney U test was used to assess all wPLI data between these regions.

Table 119: Tests of normality for inter-regional wPLI between temporal and parietal regions, by frequency band

Tests of Normality: Temporal-Parietal wPLI within Frequency Bands							
Condition	Kolmogorov-Smirnov ^a			Shapiro-Wilk			
	Statistic	df	Sig.	Statistic	df	Sig.	
Delta	HV	.125	48	.060	.919	48	.003
	TEA	.165	48	.002	.878	48	<.001
Theta	HV	.079	48	.200*	.969	48	.241
	TEA	.143	48	.016	.946	48	.029
Alpha	HV	.107	48	.200*	.956	48	.072
	TEA	.153	48	.007	.929	48	.006
Beta	HV	.128	48	.049	.930	48	.007
	TEA	.121	48	.077	.939	48	.015

*. This is a lower bound of the true significance.
a. Lilliefors Significance Correction

Beta, alpha and theta band wPLI across the temporal-parietal regions show significant p-values ($p=0.009$, $p=0.008$, $p=0.002$ respectively), and all remain significant after multiple comparisons FDR adjustments using both the classic one-stage and the two-stage sharpened method (Table 122, Table 81). Beta, alpha, and theta frequency bands within the temporal-parietal networks, there are significantly lower mean/median wPLI in the TEA group.

5.1. Frontal and Parietal Regions

Frontal-parietal wPLI within frequency bands show a platykurtic data distribution for all frequency bands. Beta frequency data have a positive skew, while delta band data is highly positively skewed and alpha frequency distribution is negatively skewed; theta band frequencies are symmetrical around the mean (Table 120). Data descriptives for regions are as follows (Table 120, Figure 85):

- Beta frequencies - the mean is 0.0337 with a SE of 0.0025 and SD of 0.0191. The interquartile range is 0.0263, and the range is 0.0754.
- Alpha frequencies - the mean is 0.1221, with a SE of 0.0057 and an SD of 0.0442. The interquartile range is 0.0626, and the range is 0.1866.
- Theta frequencies - the mean is 0.0531, with a SE of 0.0035 and SD of 0.0272. The interquartile range is 0.0444, and the range is 0.1132.
- Delta frequencies - the mean is 0.0169, with a SE of 0.0017 and SD of 0.0131. The interquartile range is 0.0177, and the range is 0.0529.

Table 120: Data descriptives for inter-regional wPLI between frontal and parietal regions, by frequency band

Statistics: Frontal-Parietal wPLI by Band					
		Delta	Theta	Alpha	Beta
N	Valid	60	60	60	60
	Missing	0	0	0	0
Mean		.01692786	.05312547	.12211994	.03365259
Std. Error of Mean		.001697375	.003505076	.005702663	.002468814
Median		.01379030	.05144012	.13316699	.02906716
Std. Deviation		.013147807	.027150199	.044172634	.019123349
Skewness		.935	.047	-.757	.672
Std. Error of Skewness		.309	.309	.309	.309
Kurtosis		.203	-.830	-.122	-.250
Std. Error of Kurtosis		.608	.608	.608	.608
Range		.052911	.113177	.186629	.075395
Percentiles	25	.00752595	.02998956	.09289064	.01949930
	50	.01379030	.05144012	.13316699	.02906716
	75	.02524155	.07441522	.15554019	.04583231

Frontal-parietal theta wPLI within the HV cohort meets the criteria for normality. All other datasets fall short of normality requirements (Table 121). Therefore, the non-parametric Mann-Whitney U test was used to assess all wPLI data between these regions.

Beta and theta band wPLI across the frontal-parietal regions show significant p-values ($p=0.004$, $p=0.002$ respectively), and these remain significant after multiple comparisons of FDR adjustments using both the classic one-stage and the two-stage sharpened method. Following FDR adjustment, delta frequencies within the frontal-parietal network (initially $p=0.065$) become significant with an adjusted significance of $q=0.043$ (Table 122, Table 81). Beta, and theta frequency bands within the frontal-parietal networks, there are significantly lower mean/median wPLI in the TEA group, whilst delta wPLI is significantly higher in TEA than in the HV cohort.

Table 121: Tests of normality for inter-regional wPLI between frontal and parietal regions, by frequency band

Tests of Normality: Frontal-Parietal wPLI by Band							
Condition	Kolmogorov-Smirnov ^a			Shapiro-Wilk			Sig.
	Statistic	df	Sig.	Statistic	df	Sig.	
Delta	HV	.094	60	.200*	.943	60	.007
	TEA	.156	60	<.001	.899	60	<.001
Theta	HV	.108	60	.081	.967	60	.100
	TEA	.110	60	.069	.948	60	.012
Alpha	HV	.131	60	.012	.927	60	.002
	TEA	.167	60	<.001	.915	60	<.001
Beta	HV	.228	60	<.001	.867	60	<.001
	TEA	.101	60	.200*	.961	60	.051
AllFreq	HV	.161	60	<.001	.936	60	.004
	TEA	.092	60	.200*	.963	60	.069

*. This is a lower bound of the true significance.
a. Lilliefors Significance Correction

Table 122: FDR q-values for Inter-Regional wPLI within Frequency Bands. Lower mean wPLI in the TEA cohort is marked in blue.

OUTPUT AREA		Multiple comparisons using FDRs			Classical one-stage method*		Two-stage sharpened method [†]		
Unique rank	Order	Ascending Hypothesis p-values	Hypothesis name	FDR-derived significance thresholds	FDR-adjusted p-values a.k.a. q-values	Stage 1 significance thresholds	Stage 2 significance thresholds	FDR-adjusted p-values a.k.a. q-values	
3	1	0.00100	Beta TEMPORAL-FRONTAL	0.003125*	0.005333333	0.0029762	0.0068027*	0.00245	
2	2	0.00100	Theta TEMPORAL-FRONTAL	0.00625*	0.005333333	0.0059524	0.0136054*	0.00245	
9	3	0.00100	Delta TEMPORAL-FRONTAL	0.009375*	0.005333333	0.0089286	0.0204082*	0.00245	
1	4	0.00200	Theta FRONTAL-PARIETAL	0.0125*	0.0064	0.0119048	0.0272109*	0.00294	
15	5	0.00200	Theta TEMPORAL-PARIETAL	0.015625*	0.0064	0.014881	0.0340136*	0.00294	
10	6	0.00400	Beta FRONTAL-PARIETAL	0.01875*	0.010666667	0.0178571	0.0408163*	0.0049	
14	7	0.00800	Alpha TEMPORAL-PARIETAL	0.021875*	0.018	0.0208333	0.047619*	0.00826875	
16	8	0.00900	Beta TEMPORAL-PARIETAL	0.025*	0.018	0.0238095	0.0544218*	0.00826875	
12	9	0.01100	Alpha TEMPORAL-FRONTAL	0.028125*	0.019555556	0.0267857	0.0612245*	0.008983333	
5	10	0.03200	Theta TEMPORAL-OCCIPITAL	0.03125	0.0512	0.0297619	0.0680272*	0.02352	
7	11	0.06500	Delta FRONTAL-PARIETAL	0.034375	0.094545455	0.0327381	0.0748299!	0.043431818	
8	12	0.08300	Delta TEMPORAL-PARIETAL	0.0375	0.110666667	0.0357143	0.0816327	0.0508375	
11	13	0.13600	Alpha FRONTAL-PARIETAL	0.040625	0.167384615	0.0386905	0.0884354	0.076892308	
4	14	0.23700	Alpha TEMPORAL-OCCIPITAL	0.04375	0.270857143	0.0416667	0.0952381	0.124425	
13	15	0.45200	Delta TEMPORAL-OCCIPITAL	0.046875	0.482133333	0.0446429	0.1020408	0.22148	
6	16	0.70700	Beta TEMPORAL-OCCIPITAL	0.05	0.707	0.047619	0.1088435	0.324778125	

5.2. Inter-hemisphere Analysis of Significant Findings

Further interhemispheric analysis between the TEA and HV cohorts. This was undertaken on significant inter-regional findings, examining the left, right, and interhemispheric networks separately. An independent samples t-test was used for normally distributed datasets and the non-parametric Mann-Whitney U-test was for those not meeting the criteria for normality.

5.2.1. Temporal-Frontal wPLI

All wPLI hemisphere network elements are significant for delta ($p=0.0001$, $p=0.001$, $p=0.004$ for right, left, and inter-hemisphere connections respectively) and beta frequencies ($p=0.009$, $p=0.016$, $p=0.036$ for right, left, and inter-hemisphere connections respectively) within temporal frontal connectivity. Significant left and inter-hemisphere differences are seen within theta frequencies, and for the alpha band, the left hemisphere shows a significant difference in mean connectivity (Table 123). Mean/median values for all delta hemisphere elements are significantly higher within the TEA cohort compared to HV. For significant theta, alpha and beta changes, TEA mean/median values are significantly lower than those within the HV group.

Table 123: FDR q-values for wPLI between Temporal and Frontal regions, within Frequency Bands (split by hemisphere, and inter-hemisphere). Lower mean wPLI in the TEA cohort is marked in blue.

OUTPUT AREA		Multiple comparisons using False Discovery Rates (FDRs)		Classical one-stage method*		Two-stage sharpened method†		
Unique rank	Order	Ascending p-values	Hypothesis name	FDR-derived significance thresholds	FDR-adjusted p-values a.k.a. q-values	Stage 1 significance thresholds	Stage 2 significance thresholds	FDR-adjusted p-values a.k.a. q-values
2	1	0.00100	INTER-H TEMPORAL-FRONTAL DELTA	0.00416667 *	0.006	0.0039683	0.0095238 *	0.002625
5	2	0.00100	LEFT TEMPORAL-FRONTAL DELTA	0.00833333 *	0.006	0.0079365	0.0190476 *	0.002625
7	3	0.00700	INTER-H TEMPORAL-FRONTAL THETA	0.0125 *	0.0216	0.0119048	0.0285714 *	0.00945
6	4	0.00900	RIGHT TEMPORAL-FRONTAL BETA	0.01666667 *	0.0216	0.015873	0.0380952 *	0.00945
9	5	0.00900	LEFT TEMPORAL-FRONTAL THETA	0.02083333 *	0.0216	0.0198413	0.047619 *	0.00945
12	6	0.01600	LEFT TEMPORAL-FRONTAL BETA	0.025 *	0.029142857	0.0238095	0.0571429 *	0.01275
10	7	0.01700	LEFT TEMPORAL-FRONTAL ALPHA	0.02916667 *	0.029142857	0.0277778	0.0666667 *	0.01275
4	8	0.03600	INTER-H TEMPORAL-FRONTAL BETA	0.03333333	0.053333333	0.031746	0.0761905 *	0.023333333
1	9	0.04000	RIGHT TEMPORAL-FRONTAL DELTA	0.0375	0.053333333	0.0357143	0.0857143 *	0.023333333
3	10	0.25200	RIGHT TEMPORAL-FRONTAL ALPHA	0.04166667	0.3024	0.0396825	0.0952381	0.1323
11	11	0.30300	INTER-H TEMPORAL-FRONTAL ALPHA	0.04583333	0.330545455	0.0436508	0.1047619	0.144613636
8	12	0.34500	RIGHT TEMPORAL-FRONTAL THETA	0.05	0.345	0.047619	0.1142857	0.1509375

5.2.2. Temporal-Occipital wPLI

When split for hemispheric wPLI network analysis (right, left, and interhemispheric networks), no hemispheric element of temporal-occipital theta shows a significant difference between cohorts, in isolation.

5.1.1. Temporal-Parietal wPLI

Data was split for hemispheric wPLI network analysis (right, left, and interhemispheric networks). Within the temporal-parietal alpha, theta and beta bands, no hemispheric element shows a significant difference between cohorts, in isolation.

5.1.1. Frontal-Parietal wPLI

Data was split for hemispheric wPLI network analysis (right, left, and interhemispheric networks). Within the frontal-parietal beta, theta and delta bands, no hemispheric element shows a significant difference between cohorts, in isolation.

Second Phase – Connectivity Analysis – Phase Transfer Entropy (PTE)

The analysis aimed to determine the effects TEA may have on mean frequency, considering variation within frequency band and brain regions. The directed connectivity metric, Phase Transfer Entropy (PTE) was used to assess the network flow, and therefore the causal influence of one brain area upon another, whilst recognising its benefits and disadvantages (Lobier *et al.*, 2014; Wang and Chen, 2021; Wang *et al.*, 2019a; Wang *et al.*, 2019b; Ursino *et al.*, 2020)

- Phase-specific directional connectivity flow/coupling.
- More robust to noise and linear mixing compared to Granger Causality (GC), and therefore better suited for EEG analysis.
- PTE makes no assumptions on either the signal or the interaction structure i.e., PTE is a “model-free” metric.
- Transfer entropy requires large amounts of continuous data; however, PTE can be successfully applied to a concatenation of shorter time series trials.
- PTE is more sensitive for distal regions (those further apart), but less so for proximal regions which show less transfer delay.
- PTE is limited to the exploration of bivariate directed coupling, therefore excluding the possibility of multivariate analysis.

Mean frequency and interhemispheric spectra were computed for global and regional cortical activities. Relative frequency analysis was calculated within frequency bands (beta, alpha, theta, delta) for both global and regional spectra.

Dataset distributions were assessed using SPSS explore and Shapiro-Wilk tests were performed to check for normality. Comparison of TEA and HV cohorts was undertaken using a parametric Independent Samples T-Test for normal distributions; otherwise, a non-parametric Independent Samples Mann-Whitney U test was performed. Statistical significance was set at $p = <0.05$. To control for type I errors generated by the false rejection of the null hypothesis through multiple comparisons within the regional, and frequency band analysis, False Discovery Rate (FDR) adjustments using the classic one-stage, and two-stage sharpened methods were undertaken (Benjamini and Hochberg, 1995; Benjamini and Hochberg, 2000; Benjamini *et al.*, 2006; Pike, 2011; Nichols, 2007) with before p -values, and after correction q -values being reported within the results.

1. Global PTE, All Frequencies

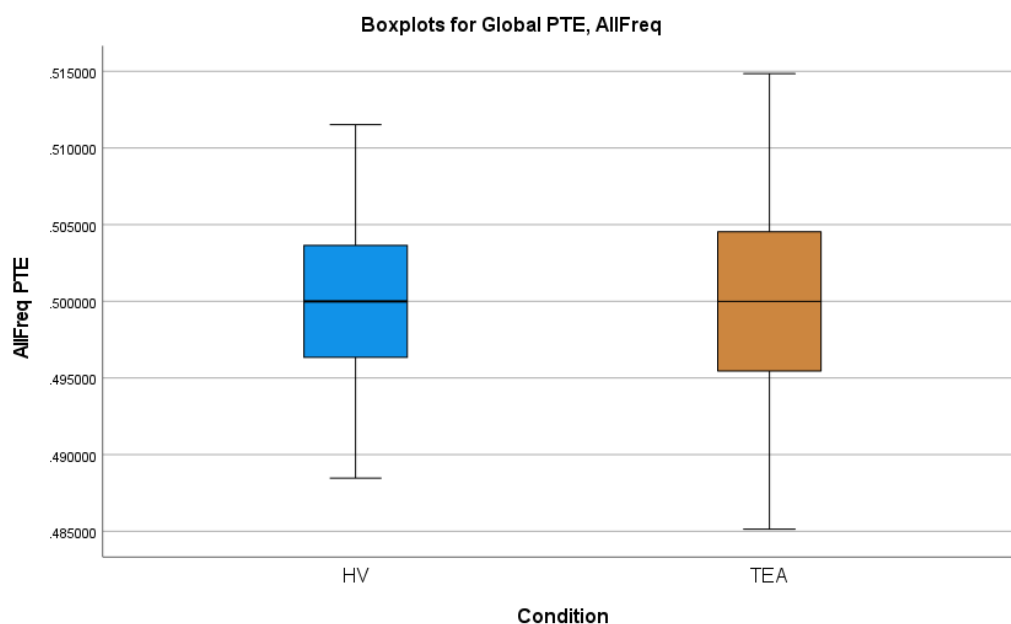


Figure 86: Boxplots for global Phase Transfer Entropy data by condition, all frequencies (1-40Hz)

Global PTE has a platykurtic data distribution and is symmetrical around the mean (Table 124). The mean across all data is 0.500, with a standard error (SE) of 0.0002 and a standard deviation (SD) of 0.0053. The interquartile range is 0.0078, and the range is 0.0297. (Table 124, Figure 86).

Table 124: Data Descriptors for global Phase Transfer Entropy data, all frequencies (1-40Hz)

Descriptives: Global PTE, AllFreq		
AllFreq		
N	Valid	840
	Missing	42
Mean		.50000000
Std. Error of Mean		.000183007
Median		.50000000
Std. Deviation		.005304050
Variance		.000
Skewness		.000
Std. Error of Skewness		.084
Kurtosis		-.436
Std. Error of Kurtosis		.169
Range		.029710
Percentiles	25	.49610314
	50	.50000000
	75	.50389686

Tests of Normality: Global PTE, AllFreq							
AllFreq	Condition	Kolmogorov-Smirnov ^a			Shapiro-Wilk		
		Statistic	df	Sig.	Statistic	df	Sig.
AllFreq	HV	.041	420	.086	.993	420	.035
	TEA	.037	420	.191	.994	420	.069

a. Lilliefors Significance Correction

Table 125: Tests of normality for global Phase Transfer Entropy data, all frequencies (1-40Hz)

As only the TEA global PTE distribution meets the criteria for normality (Table 125), a non-parametric Man-Whitney U test was performed demonstrating no significant difference in PTE profiles between the cohorts at a global level ($p = 1.000$), with identical mean/median values across cohorts (Table 126).

Table 126: Mann-Whitney U Test Findings for Global PTE.

Hypothesis Test Summary - PTE GLOBAL AllFreq				
	Null Hypothesis	Test	Sig. ^{a,b}	Decision
1	The distribution of AllFreq is the same across categories of Condition.	Independent-Samples Mann-Whitney U Test	1.000	Retain the null hypothesis.

a. The significance level is .050.
 b. Asymptotic significance is displayed.

2. Intra-Regional and Inter-Regional PTE, All Frequencies

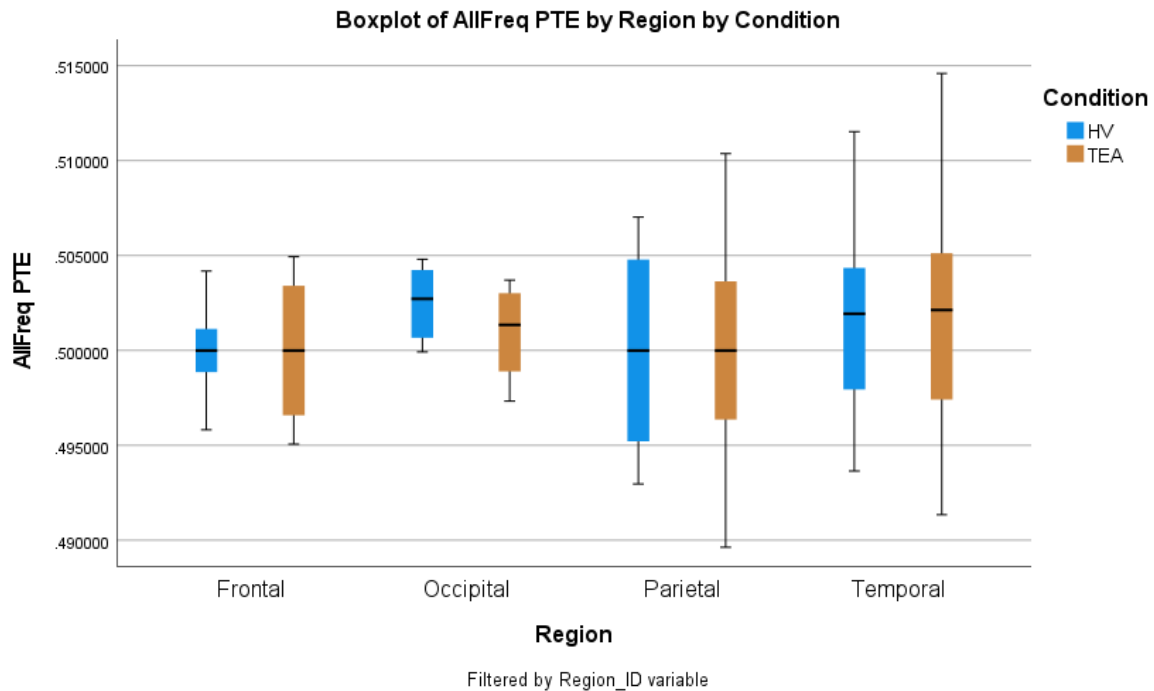


Figure 87: Intra-Regional PTE Boxplot, all frequencies (1-40Hz)

Regional PTE data shows a platykurtic data distribution for all regions (frontal, occipital, parietal, temporal), with temporal regions showing a slight positive skew, occipital regions showing a slight negative skew, and frontal and parietal regions being symmetrical around the mean (Table 127). Data descriptives for regions are as follows (Table 127, Figure 87):

- Frontal regions - the mean is 0.5000, with a SE of 0.0005 and SD of 0.0031. The interquartile range is 0.0056, and the range is 0.0099.
- Occipital regions - the mean is 0.5027, with a SE of 0.0006 and SD of 0.0022. The interquartile range is 0.0036, and the range is 0.0075.
- Parietal regions - the mean is 0.5000, with a SE of 0.0007 and SD of 0.0052. The interquartile range is 0.0090, and the range is 0.0207.
- Temporal regions - the mean is 0.5017, with a SE of 0.0004 and SD of 0.0048. The interquartile range is 0.0070, and the range is 0.0233.

Only the HV parietal PTE data distribution does not meet the normality criteria (Table 128). Therefore, the non-parametric Man-Whitney U test was utilised for parietal PTE and an independent samples t-test was used for frontal, occipital and temporal datasets. There are

no significant differences in intra-regional PTE between cohorts, for all regions i.e., frontal, occipital, parietal, or temporal -Table 129.

Table 127: Data descriptives for intra-regional PTE, AllFreq (1-40Hz)

Statistics: Frontal PTE, AllFreq			Statistics: Occipital PTE, AllFreq			Statistics: Parietal PTE, AllFreq			Statistics: Temporal PTE, AllFreq		
AllFreq			AllFreq			AllFreq			AllFreq		
N	Valid	40	N	Valid	16	N	Valid	60	N	Valid	148
	Missing	10		Missing	4		Missing	12		Missing	16
Mean		.50000000	Mean		.50172160	Mean		.50000000	Mean		.50169570
Std. Error of Mean		.000482723	Std. Error of Mean		.000556668	Std. Error of Mean		.000674067	Std. Error of Mean		.000395999
Median		.50000000	Median		.50187909	Median		.50000000	Median		.50201804
Std. Deviation		.003053010	Std. Deviation		.002226672	Std. Deviation		.005221300	Std. Deviation		.004817538
Variance		.000	Variance		.000	Variance		.000	Variance		.000
Skewness		.000	Skewness		-.428	Skewness		.000	Skewness		.258
Std. Error of Skewness		.374	Std. Error of Skewness		.564	Std. Error of Skewness		.309	Std. Error of Skewness		.199
Kurtosis		-1.164	Kurtosis		-.789	Kurtosis		-.806	Kurtosis		-.335
Std. Error of Kurtosis		.733	Std. Error of Kurtosis		1.091	Std. Error of Kurtosis		.608	Std. Error of Kurtosis		.396
Range		.009873	Range		.007473	Range		.020736	Range		.023253
Percentiles	25	.49717669	Percentiles	25	.49996070	Percentiles	25	.49549979	Percentiles	25	.49764428
	50	.50000000		50	.50187909		50	.50000000		50	.50201804
	75	.50282331		75	.50362873		75	.50450021		75	.50468582

Table 128: Tests of normality for intra-regional PTE, AllFreq (1-40Hz)

Tests of Normality: Frontal PTE, AllFreq						
		Kolmogorov-Smirnov			Shapiro-Wilk	
Condition	Statistic	df	Sig.	Statistic	df	Sig.
AllFreq HV	.125	20	.200	.921	20	.105
TEA	.114	20	.200	.913	20	.074
Tests of Normality: Occipital PTE, AllFreq						
		Kolmogorov-Smirnov			Shapiro-Wilk	
Condition	Statistic	df	Sig.	Statistic	df	Sig.
AllFreq HV	.175	8	.200	.905	8	.323
TEA	.180	8	.200	.924	8	.459
Tests of Normality: Parietal PTE, AllFreq						
		Kolmogorov-Smirnov			Shapiro-Wilk	
Condition	Statistic	df	Sig.	Statistic	df	Sig.
AllFreq HV	.125	30	.200	.922	30	.030
TEA	.088	30	.200	.965	30	.408
Tests of Normality: Temporal PTE, AllFreq						
		Kolmogorov-Smirnov ^a			Shapiro-Wilk	
Condition	Statistic	df	Sig.	Statistic	df	Sig.
AllFreq HV	.073	74	.200*	.976	74	.166
TEA	.067	74	.200*	.985	74	.540

*. This is a lower bound of the true significance.
a. Lilliefors Significance Correction

Table 129: FDR q-values for Intra-Regional PTE, AllFreq.

OUTPUT AREA		Multiple comparisons using FDRs			Classical one-stage method*		Two-stage sharpened method†	
Unique rank	Order	Ascending p-values	Hypothesis name	FDR-derived significance thresholds	FDR-adjusted p-values a.k.a. q-values	Stage 1 significance thresholds	Stage 2 significance thresholds	FDR-adjusted p-values a.k.a. q-values
5	1	0.17100	PTE OCCIPITAL AllFreq	0.01	0.855	0.0095238	0.0095238	0.89775
4	2	0.79800	PTE TEMPORAL AllFreq	0.02	1	0.0190476	0.0190476	1.05
1	3	1.00000	PTE PARIETAL AllFreq	0.03	1	0.0285714	0.0285714	1.05
3	4	1.00000	PTE FRONTAL AllFreq	0.04	1	0.0380952	0.0380952	1.05
2	5	1.00000	PTE GLOBAL AllFreq	0.05	1	0.047619	0.047619	1.05

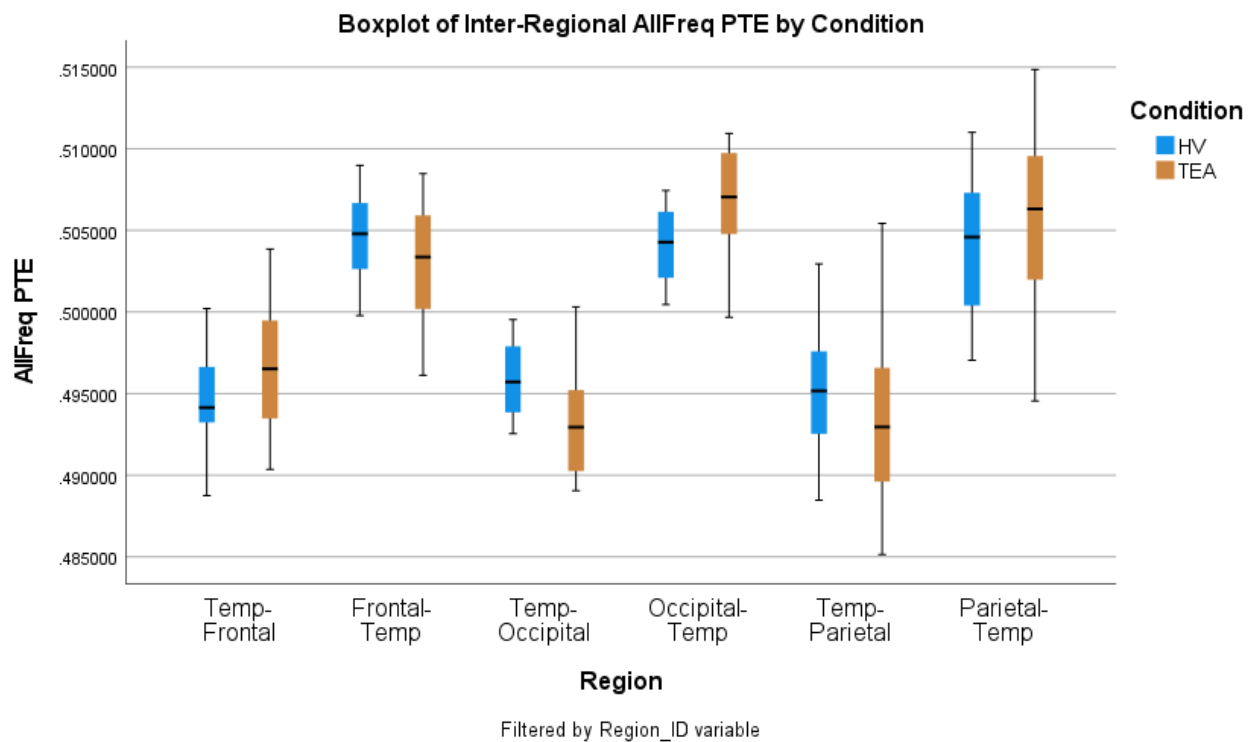


Figure 88: Inter-Regional PTE Boxplot, all frequencies (1-40Hz)

As PTE is a directional connectivity measure, datasets were additionally obtained for frontal-to-temporal, occipital-to-temporal and parietal-to-temporal networks.

Inter-regional wPLI data shows a platykurtic data distribution for all directional measures (temporal to frontal, frontal to temporal, temporal to occipital, occipital to temporal, temporal to parietal, parietal to temporal). Temporal-to-frontal and temporal-to-parietal PTE data have a slight positive skew, whereas frontal-to-temporal, and parietal-to-temporal are slightly negatively skewed. Temporal to occipital, and occipital to temporal PTE distributions are reasonably symmetric around the mean (Table 130). Data descriptives for regions are as follows (Table 130, Figure 88):

- Temporal-frontal region - the mean is 0.4957, with a SE of 0.0004 and SD of 0.0033. The interquartile range is 0.0046, and the range is 0.0151.
- Frontal-temporal region - the mean is 0.5041, with a SE of 0.0004 and SD of 0.0031. The interquartile range is 0.0047, and the range is 0.0128.
- Temporal to the occipital region - the mean is 0.4946 with a SE of 0.0005 and SD of 0.0030. The interquartile range is 0.0042 and the range is 0.0113.

- Occipital to temporal region - the mean is 0.5054, with a SE of 0.0005 and SD of 0.0030. The interquartile range is 0.0042, and the range is 0.0113.
- Temporal to the parietal region - the mean is 0.4943, with a SE of 0.0004 and SD of 0.0044. The interquartile range is 0.0062, and the range is 0.0203.
- Parietal to the temporal region - the mean is 0.5050, with a SE of 0.0005 and SD of 0.0044. The interquartile range is 0.0069, and the range is 0.0203.

Table 130: Data descriptives for inter-regional PTE, AllFreq (1-40Hz)

Temporal-Frontal PTE, AllFreq			Temporal-Occipital PTE, AllFreq			Temporal-Parietal PTE, AllFreq			Frontal-Temporal PTE, AllFreq			Occipital-Temporal PTE, AllFreq			Parietal-Temporal PTE, AllFreq		
AllFreq			AllFreq			AllFreq			AllFreq			AllFreq			AllFreq		
N	Valid	Missing	N	Valid	Missing	N	Valid	Missing	N	Valid	Missing	N	Valid	Missing	N	Valid	Missing
Mean	.49567890		Mean	.49456752		Mean	.49432709		Mean	.50406625		Mean	.50543248		Mean	.50503948	
Std. Error of Mean	.000365089		Std. Error of Mean	.000530841		Std. Error of Mean	.000446575		Std. Error of Mean	.000380442		Std. Error of Mean	.000530841		Std. Error of Mean	.000524085	
Median	.49537138		Median	.49458624		Median	.49370831		Median	.50449908		Median	.50541376		Median	.50553386	
Std. Deviation	.003265454		Std. Deviation	.003002889		Std. Deviation	.004375521		Std. Deviation	.003137202		Std. Deviation	.003002889		Std. Deviation	.004447013	
Variance	.000		Variance	.000		Variance	.000		Variance	.000		Variance	.000		Variance	.000	
Skewness	.455		Skewness	.021		Skewness	.201		Skewness	-.552		Skewness	-.021		Skewness	-.187	
Std. Error of Skewness	.269		Std. Error of Skewness	.414		Std. Error of Skewness	.246		Std. Error of Skewness	.291		Std. Error of Skewness	.414		Std. Error of Skewness	.283	
Kurtosis	-.148		Kurtosis	-.766		Kurtosis	-.341		Kurtosis	-.241		Kurtosis	-.766		Kurtosis	-.545	
Std. Error of Kurtosis	.532		Std. Error of Kurtosis	.809		Std. Error of Kurtosis	.488		Std. Error of Kurtosis	.574		Std. Error of Kurtosis	.809		Std. Error of Kurtosis	.559	
Range	.015110		Range	.011260		Range	.020293		Range	.012849		Range	.011260		Range	.020293	
Percentiles	25	.49319868	Percentiles	25	.49255461	Percentiles	25	.49142591	Percentiles	25	.50190327	Percentiles	25	.50322195	Percentiles	25	.50143329
	50	.49537138		50	.49458624		50	.49370831		50	.50449908		50	.50541376		50	.50553386
	75	.49784750		75	.49677805		75	.49759447		75	.50668371		75	.50744539		75	.50831959

Table 131: Tests of normality for inter-regional PTE, AllFreq (1-40Hz)

Tests of Normality: Temporal-Frontal PTE, AllFreq								Tests of Normality: Frontal-Temporal PTE, AllFreq									
Kolmogorov-Smirnov ^a								Kolmogorov-Smirnov ^a									
Condition	Statistic	df	Sig.	Statistic	df	Sig.		Condition	Statistic	df	Sig.	Statistic	df	Sig.	Statistic	df	Sig.
AllFreq	HV	.120	40	.155	.983	40	.810	AllFreq	HV	.120	34	.200 [*]	.967	34	.374		
	TEA	.091	40	.200 [*]	.965	40	.253		TEA	.100	34	.200 [*]	.954	34	.166		
Tests of Normality: Temporal-Occipital PTE, AllFreq								Tests of Normality: Occipital-Temporal PTE, AllFreq									
Kolmogorov-Smirnov ^a								Kolmogorov-Smirnov ^a									
Condition	Statistic	df	Sig.	Statistic	df	Sig.		Condition	Statistic	df	Sig.	Statistic	df	Sig.	Statistic	df	Sig.
AllFreq	HV	.128	16	.200 [*]	.948	16	.463	AllFreq	HV	.128	16	.200 [*]	.948	16	.463		
	TEA	.138	16	.200 [*]	.934	16	.286		TEA	.138	16	.200 [*]	.934	16	.286		
Tests of Normality: Temporal-Parietal PTE, AllFreq								Tests of Normality: Parietal-Temporal PTE, AllFreq									
Kolmogorov-Smirnov ^a								Kolmogorov-Smirnov ^a									
Condition	Statistic	df	Sig.	Statistic	df	Sig.		Condition	Statistic	df	Sig.	Statistic	df	Sig.	Statistic	df	Sig.
AllFreq	HV	.083	48	.200 [*]	.974	48	.363	AllFreq	HV	.124	36	.173	.956	36	.157		
	TEA	.077	48	.200 [*]	.975	48	.389		TEA	.091	36	.200 [*]	.977	36	.652		

*. This is a lower bound of the true significance.
a. Lilliefors Significance Correction

All inter-regional PTE datasets meet the normal criteria (Table 131). Therefore, the independent samples t-test was used for all comparisons. There is a significant difference between TEA and HV cohorts within temporal-to-occipital, and occipital-to-temporal networks ($p=0.017$ in the case of both datasets). There is also a significant difference between temporal-to-frontal and frontal-to-temporal networks ($p=0.018$ and $p=0.046$ respectively). Within temporal and parietal networks, only temporal to parietal demonstrates a significant difference between cohorts ($p=0.030$) - Table 132. All significant datasets remain so following multiple comparisons FDR adjustments using the two-stage sharpened method (Table 132). Frontal-to-temporal, temporal-to-occipital and temporal-

to-parietal networks show a significantly lower PTE value in the TEA group compared to HV. Temporal to frontal, and occipital to temporal networks have significantly higher PTE values in the TEA cohort (Table 133).

Table 132: FDR q-values for Inter-Regional PTE, AllFreq.

OUTPUT AREA		Multiple comparisons using FDRs		Classical one-stage method*		Two-stage sharpened method†		FDR-adjusted	
Unique rank	Order	Ascending p-values	Hypothesis name	FDR-derived significance thresholds	FDR-adjusted p-values a.k.a. q-values	Stage 1 significance thresholds	Stage 2 significance thresholds	FDR-adjusted p-values	a.k.a. q-values
5	1	0.01700	PTE TEMPORAL to OCCIPITAL AllFreq	0.00833333 *	0.036	0.0079365	0.0119048 *	0.0252	0.0252
3	2	0.01700	PTE OCCIPITAL to TEMPORAL AllFreq	0.01666667 *	0.036	0.015873	0.0238095 *	0.0252	0.0252
2	3	0.01800	PTE TEMPORAL to FRONTAL AllFreq	0.025 *	0.036	0.0238095	0.0357143 *	0.0252	0.0252
1	4	0.03000	PTE TEMPORAL to PARIETAL AllFreq	0.03333333 *	0.045	0.031746	0.047619 *	0.0315	0.0315
6	5	0.04600	PTE FRONTAL to TEMPORAL AllFreq	0.04166667	0.0552	0.0396825	0.0595238 *	0.03864	0.03864
4	6	0.11000	PTE PARIETAL to TEMPORAL AllFreq	0.05	0.11	0.047619	0.0714286	0.077	0.077

Table 133: Mean and median comparisons for inter-regional PTE, AllFreq (1-40Hz). The lower mean PTE in the TEA cohort is marked in blue.

Temporal-Frontal PTE, AllFreq			Temporal-Occipital PTE, AllFreq			Temporal-Parietal PTE, AllFreq		
Condition	Mean	Median	Condition	Mean	Median	Condition	Mean	Median
HV	.49482261	.49414435	HV	.49580688	.49571901	HV	.49529045	.49517695
TEA	.49653460	.49651975	TEA	.49332815	.49294349	TEA	.49336374	.49295558
Total	.49567860	.49537138	Total	.49456752	.49458624	Total	.49432709	.49370831

Frontal-Temporal PTE, AllFreq			Occipital-Temporal PTE, AllFreq			Parietal-Temporal PTE, AllFreq		
Condition	Mean	Median	Condition	Mean	Median	Condition	Mean	Median
HV	.50482406	.50479051	HV	.50419312	.50428099	HV	.50419985	.50459627
TEA	.50330845	.50336767	TEA	.50667185	.50705651	TEA	.50587911	.50632047
Total	.50406625	.50449908	Total	.50543248	.50541376	Total	.50503948	.50553386

3. Global PTE – Frequency Bands

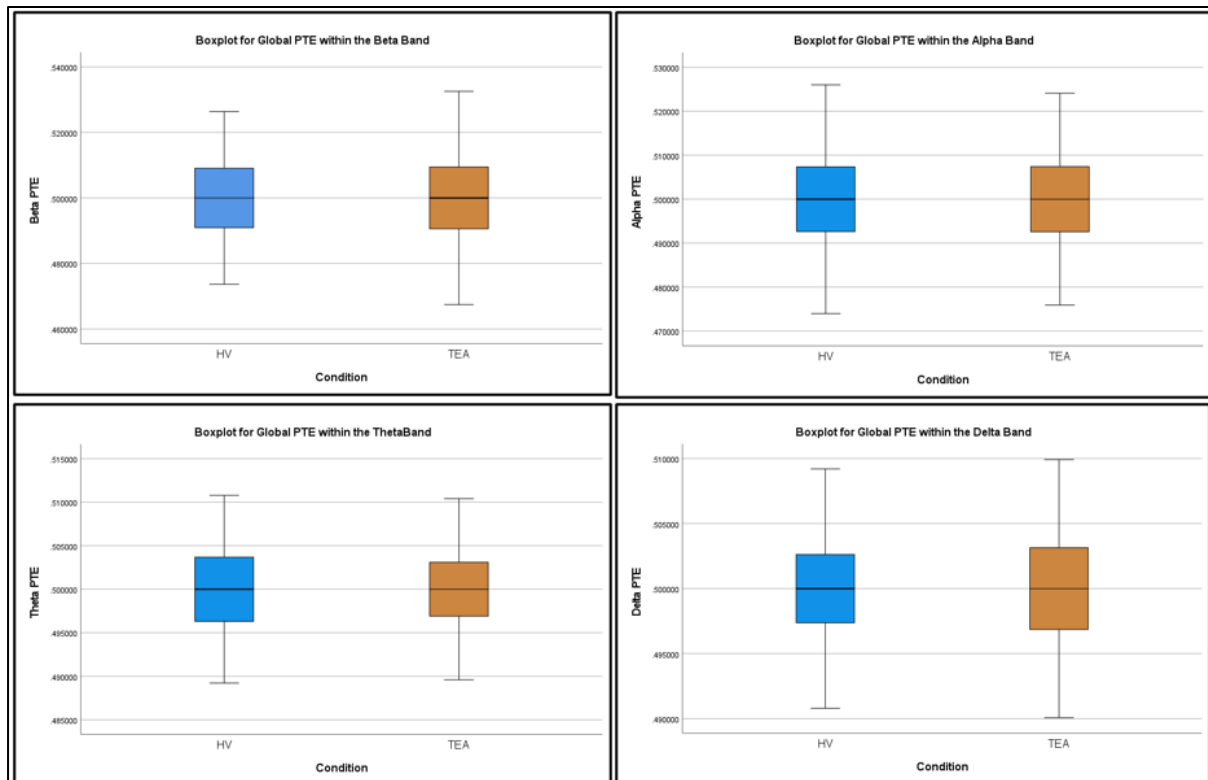


Figure 89: Boxplots for global PTE, by frequency band. Top left - beta, top right - alpha, bottom left - theta, bottom right - delta.

Global PTE within frequency bands show a platykurtic data distribution and is symmetric around the mean across all bands (Table 134). Data descriptives for regions are as follows (Table 134, Figure 89):

- Beta frequencies - the mean is 0.5000, with a SE of 0.0004 and SD of 0.0127. The interquartile range is 0.0184, and the range is 0.0651.
- Alpha frequencies - the mean is 0.5000, with a SE of 0.0003 and SD of 0.0105. The interquartile range is 0.0148, and the range is 0.0520.
- Theta frequencies - the mean is 0.5000, with a SE of 0.0002 and SD of 0.0047. The interquartile range is 0.0068, and the range is 0.0216.
- Delta frequencies - the mean is 0.5000, with a SE of 0.0001 and SD of 0.0039. The interquartile range is 0.0056, and the range is 0.0198.

Table 134: Data descriptives for global PTE, by frequency band.

Statistics: Global PTE within Frequency Bands					
		Delta	Theta	Alpha	Beta
N	Valid	840	840	840	840
	Missing	42	42	42	42
Mean		.50000000	.50000000	.50000000	.50000000
Std. Error of Mean		.000134298	.000160492	.000361950	.000438762
Median		.50000000	.50000000	.50000000	.50000000
Std. Deviation		.003892339	.004651499	.010490309	.012716519
Variance		.000	.000	.000	.000
Skewness		.000	.000	.000	.000
Std. Error of Skewness		.084	.084	.084	.084
Kurtosis		-.499	-.711	-.575	-.396
Std. Error of Kurtosis		.169	.169	.169	.169
Range		.019837	.021578	.052048	.065078
Percentiles	25	.49717938	.49659994	.49256303	.49077168
	50	.50000000	.50000000	.50000000	.50000000
	75	.50282062	.50340006	.50743697	.50922832

The HV global PTE within the delta band, and the TEA global PTE within and alpha bands meet normality criteria; all other datasets do not meet the tests for normality (Table 135). Therefore, the non-parametric Mann-Whitney U test was utilised for all frequency bands. There are no significant differences in PTE within any frequency band at the global level (Table 136).

Table 135: Tests of normality for global PTE, by frequency band.

Tests of Normality: Global PTE within Frequency Bands							
		Kolmogorov-Smirnov ^a			Shapiro-Wilk		
Condition		Statistic	df	Sig.	Statistic	df	Sig.
Delta	HV	.039	420	.131	.994	420	.080
	TEA	.032	420	.200*	.990	420	.006
Theta	HV	.040	420	.109	.986	420	<.001
	TEA	.030	420	.200*	.991	420	.010
Alpha	HV	.034	420	.200*	.988	420	.001
	TEA	.020	420	.200*	.993	420	.057
Beta	HV	.042	420	.078	.989	420	.003
	TEA	.021	420	.200*	.994	420	.095

*. This is a lower bound of the true significance.
a. Lilliefors Significance Correction

Table 136: Mann-Whitney U Test Findings for Global PTE within Frequency Bands.

Hypothesis Test Summary - GLOBAL PTE Freq Bands				
	Null Hypothesis	Test	Sig. ^{a,b}	Decision
1	The distribution of Delta is the same across categories of Condition.	Independent-Samples Mann-Whitney U Test	1.000	Retain the null hypothesis.
2	The distribution of Theta is the same across categories of Condition.	Independent-Samples Mann-Whitney U Test	1.000	Retain the null hypothesis.
3	The distribution of Alpha is the same across categories of Condition.	Independent-Samples Mann-Whitney U Test	1.000	Retain the null hypothesis.
4	The distribution of Beta is the same across categories of Condition.	Independent-Samples Mann-Whitney U Test	1.000	Retain the null hypothesis.
a. The significance level is .050. b. Asymptotic significance is displayed.				

4. Intra-Regional PTE –Frequency Bands

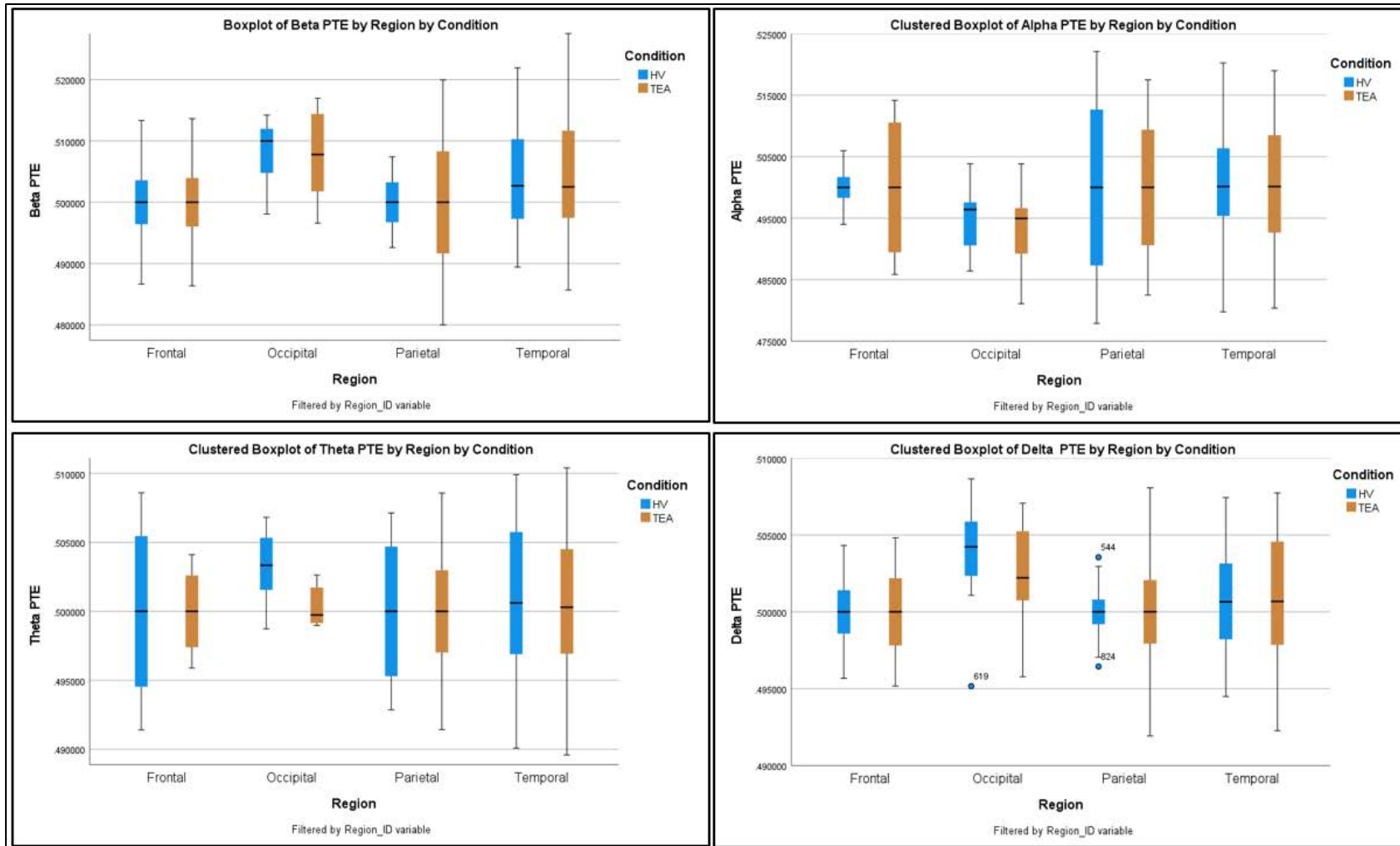


Figure 90: Boxplots for regional PTE, by frequency band. Top left - beta, top right - alpha, bottom left - theta, bottom right - delta.

4.1. *Frontal*

Frontal PTE within frequency bands show a platykurtic data distribution with symmetry around the mean, for all frequency bands (Table 137). Data descriptives for frequency bands are as follows (Table 137, Figure 90):

- Beta frequencies - the mean is 0.5000, with a SE of 0.0011 and SD of 0.0071. The interquartile range is 0.0074, and the range is 0.0273.
- Alpha frequencies - the mean is 0.5000, with a SE of 0.0011 and SD of 0.0071. The interquartile range is 0.0056, and the range is 0.0283.
- Theta frequencies - the mean is 0.5000, with a SE of 0.0007 and SD of 0.0043. The interquartile range is 0.0060, and the range is 0.0172.
- Delta frequencies - the mean is 0.5000, with a SE of 0.0004 and SD of 0.0023. The interquartile range is 0.0034, and the range is 0.0096.

All datasets meet the criteria for normality (Table 138). Therefore, an independent samples t-test was used for all comparisons. There are no significant differences in frontal PTE within frequency bands between TEA and HV cohorts (Table 139).

4.2. *Occipital*

Occipital PTE within frequency bands show a platykurtic data distribution with symmetry around the mean, for all frequency bands (Table 137). Data descriptives for frequency bands are as follows (Table 137, Figure 90):

- Beta frequencies - the mean is 0.5080, with a SE of 0.0016 and SD of 0.0065. The interquartile range is 0.0114, and the range is 0.0204.
- Alpha frequencies - the mean is 0.4941, with a SE of 0.0015 and SD of 0.0061. The interquartile range is 0.0076, and the range is 0.0228.
- Theta frequencies - the mean is 0.5018, with a SE of 0.0006 and SD of 0.0026. The interquartile range is 0.0042, and the range is 0.0081.
- Delta frequencies - the mean is 0.5030, with a SE of 0.0009 and SD of 0.0038. The interquartile range is 0.0049, and the range is 0.0135.

All datasets meet the criteria for normality (Table 138). Therefore, an independent samples t-test was used for all comparisons. There are no significant differences in occipital PTE within frequency bands between TEA and HV cohorts (Table 139).

4.3. *Parietal*

Parietal PTE within frequency bands show a platykurtic data distribution with symmetry around the mean, for all frequency bands (Table 137). Data descriptives for frequency bands are as follows (Table 137, Figure 90):

- Beta frequencies - the mean is 0.5000, with a SE of 0.0011 and SD of 0.0084. The interquartile range is 0.0094, and the range is 0.0399.
- Alpha frequencies - the mean is 0.5000, with a SE of 0.0016 and SD of 0.0126. The interquartile range is 0.0206, and the range is 0.0442.
- Theta frequencies - the mean is 0.5000, with a SE of 0.0006 and SD of 0.0044. The interquartile range is 0.0064, and the range is 0.0172.
- Delta frequencies - the mean is 0.5000, with a SE of 0.0004 and SD of 0.0041. The interquartile range is 0.0036, and the range is 0.0161.

All datasets meet the criteria for normality (Table 138). Therefore, an independent samples t-test was used for all comparisons. There are no significant differences in parietal PTE within frequency bands between TEA and HV cohorts (Table 139).

4.4. *Temporal*

Temporal PTE within frequency bands show a platykurtic data distribution, temporal delta dataset showing a slight positive skew, temporal beta PTE data having a positive skew and theta and alpha data being reasonably symmetrical around the mean (Table 137). Data descriptives for frequency bands are as follows (Table 137, Figure 90):

- Beta frequencies - the mean is 0.5047, with a SE of 0.0008 and SD of 0.0103. The interquartile range is 0.0137, and the range is 0.0453.
- Alpha frequencies - the mean is 0.5006, with a SE of 0.0008 and SD of 0.0095. The interquartile range is 0.0132, and the range is 0.0405.
- Theta frequencies - the mean is 0.5007, with a SE of 0.0004 and SD of 0.0053. The interquartile range is 0.0086, and the range is 0.0208.

- Delta frequencies - the mean is 0.5007, with a SE of 0.0003 and SD of 0.0038. The interquartile range is 0.0058, and the range is 0.0155.

Both HV and TEA temporal alpha band datasets meet the normal criteria, along with TEA theta band data, and HV delta band data. All other datasets fail to meet the parameters for normality (Table 138). Therefore, an independent samples t-test was used for alpha band comparison, and the non-parametric Mann Whitney-U test for beta, theta, and delta bands. There are no significant differences in temporal PTE within frequency bands between TEA and HV cohorts (Table 139).

Table 137: Descriptives for regional PTE by frequency band. Top left - frontal, top right - occipital, bottom left - parietal, bottom right – temporal.

Statistics: Frontal PTE by Frequency Band						Statistics: Occipital PTE by Frequency Band					
		Delta	Theta	Alpha	Beta			Delta	Theta	Alpha	Beta
N	Valid	40	40	40	40	16	16	16	16	16	16
	Missing	10	10	10	10	4	4	4	4	4	4
Mean		.50000000	.50000000	.50000000	.50000000	.50299868	.50180321	.49412462	.50795988		
Std. Error of Mean		.000369913	.000682824	.001119257	.001119501	.000944567	.000646263	.001524350	.001615077		
Median		.50000000	.50000000	.50000000	.50000000	.50361319	.50155867	.49606819	.50999635		
Std. Deviation		.002339532	.004318561	.007078804	.007080344	.003778268	.002585053	.006097399	.006460307		
Variance		.000	.000	.000	.000	.000	.000	.000	.000		
Skewness		.000	.000	.000	.000	-.762	.648	-.405	-.420		
Std. Error of Skewness		.374	.374	.374	.374	.564	.564	.564	.564		
Kurtosis		-.419	-.792	.045	-.162	.322	-.374	.188	-1.203		
Std. Error of Kurtosis		.733	.733	.733	.733	1.091	1.091	1.091	1.091		
Range		.009647	.017181	.028347	.027296	.013493	.008082	.022766	.020375		
Percentiles	25	.49827805	.49699495	.49716609	.49630755	.50112764	.49923621	.48952208	.50208123		
	50	.50000000	.50000000	.50000000	.50000000	.50361319	.50155867	.49606819	.50999635		
	75	.50172195	.50300505	.50283391	.50369245	.50593091	.50337504	.49714185	.51354528		

Statistics: Parietal PTE by Frequency Band						Statistics: Temporal PTE by Frequency Band					
		Delta	Theta	Alpha	Beta			Delta	Theta	Alpha	Beta
N	Valid	60	60	60	60	148	148	148	148	148	148
	Missing	12	12	12	12	16	16	16	16	16	16
Mean		.50000000	.50000000	.50000000	.50000000	.50067271	.50070721	.50060897	.50479390		
Std. Error of Mean		.000395241	.000563432	.001622556	.001081001	.000309106	.000432147	.000779973	.000847633		
Median		.50000000	.50000000	.50000000	.50000000	.50068117	.50045867	.50013815	.50260666		
Std. Deviation		.003061521	.004364322	.012568268	.008373401	.003760438	.005257293	.009488779	.010311896		
Variance		.000	.000	.000	.000	.000	.000	.000	.000		
Skewness		.000	.000	.000	.000	-.126	-.096	-.028	.715		
Std. Error of Skewness		.309	.309	.309	.309	.199	.199	.199	.199		
Kurtosis		1.140	-.950	-1.143	.703	-.747	-.893	-.583	-.147		
Std. Error of Kurtosis		.608	.608	.608	.608	.396	.396	.396	.396		
Range		.016123	.017156	.044236	.039924	.015468	.020807	.040477	.045321		
Percentiles	25	.49824354	.49678332	.48974946	.49530221	.49799912	.49689700	.49413512	.49730502		
	50	.50000000	.50000000	.50000000	.50000000	.50068117	.50045867	.50013815	.50260666		
	75	.50175646	.50321668	.51025054	.50469779	.50376708	.50552196	.50725570	.51100667		

Table 138: Tests of normality for regional PTE by frequency band. Top left - frontal, top right - occipital, bottom left - parietal, bottom right – temporal.

Tests of Normality: Frontal PTE by Frequency Band								Tests of Normality: Occipital PTE by Frequency Band							
		Kolmogorov-Smirnov ^a			Shapiro-Wilk					Kolmogorov-Smirnov ^a			Shapiro-Wilk		
Condition		Statistic	df	Sig.	Statistic	df	Sig.	Condition		Statistic	df	Sig.	Statistic	df	Sig.
Delta	HV	.070	20	.200*	.975	20	.859	Delta	HV	.251	8	.148	.905	8	.322
	TEA	.088	20	.200*	.972	20	.803	Delta	TEA	.148	8	.200*	.957	8	.781
Theta	HV	.118	20	.200*	.925	20	.121	Theta	HV	.143	8	.200*	.955	8	.761
	TEA	.152	20	.200*	.920	20	.097	Theta	TEA	.254	8	.138	.832	8	.062
Alpha	HV	.098	20	.200*	.991	20	.999	Alpha	HV	.212	8	.200*	.955	8	.763
	TEA	.140	20	.200*	.906	20	.053	Alpha	TEA	.167	8	.200*	.961	8	.817
Beta	HV	.101	20	.200*	.973	20	.816	Beta	HV	.207	8	.200*	.892	8	.243
	TEA	.082	20	.200*	.970	20	.747	Beta	TEA	.222	8	.200*	.900	8	.290

*. This is a lower bound of the true significance.
a. Lilliefors Significance Correction

Tests of Normality: Parietal PTE by Frequency Band							
		Kolmogorov-Smirnov ^a			Shapiro-Wilk		
Condition		Statistic	df	Sig.	Statistic	df	Sig.
Delta	HV	.107	30	.200*	.982	30	.884
	TEA	.070	30	.200*	.979	30	.809
Theta	HV	.121	30	.200*	.943	30	.107
	TEA	.073	30	.200*	.983	30	.897
Alpha	HV	.099	30	.200*	.948	30	.149
	TEA	.083	30	.200*	.940	30	.093
Beta	HV	.078	30	.200*	.979	30	.789
	TEA	.054	30	.200*	.973	30	.635

*. This is a lower bound of the true significance.
a. Lilliefors Significance Correction

Tests of Normality: Temporal PTE by Frequency Band							
		Kolmogorov-Smirnov ^a			Shapiro-Wilk		
Condition		Statistic	df	Sig.	Statistic	df	Sig.
Delta	HV	.061	74	.200*	.977	74	.198
	TEA	.086	74	.200*	.961	74	.023
Theta	HV	.107	74	.036	.955	74	.011
	TEA	.057	74	.200*	.983	74	.446
Alpha	HV	.051	74	.200*	.984	74	.469
	TEA	.064	74	.200*	.980	74	.303
Beta	HV	.130	74	.003	.928	74	<.001
	TEA	.117	74	.014	.938	74	.001

*. This is a lower bound of the true significance.
a. Lilliefors Significance Correction

Table 139: FDR q-values for Intra-Regional PTE, within Frequency Bands

OUTPUT AREA		Multiple comparisons using FDRs			Classical one-stage method*		Two-stage sharpened method†		FDR-adjusted
Unique rank	Order	Ascending p-values	Hypothesis name	FDR-derived significance thresholds	FDR-adjusted p-values a.k.a. q-values	Stage 1 significance thresholds	Stage 2 significance thresholds	FDR-adjusted p-values a.k.a. q-values	
16	1	0.01900	PTE OCCIPITAL Theta	0.003125	0.304	0.0029762	0.0029762	0.3192	
2	2	0.55000	PTE OCCIPITAL Delta	0.00625	1	0.0059524	0.0059524	1.05	
15	3	0.61800	PTE OCCIPITAL Alpha	0.009375	1	0.0089286	0.0089286	1.05	
7	4	0.83600	PTE TEMPORAL Beta	0.0125	1	0.0119048	0.0119048	1.05	
14	5	0.86800	PTE TEMPORAL Alpha	0.015625	1	0.014881	0.014881	1.05	
1	6	0.87400	PTE OCCIPITAL Beta	0.01875	1	0.0178571	0.0178571	1.05	
13	7	0.92100	PTE TEMPORAL Delta	0.021875	1	0.0208333	0.0208333	1.05	
8	8	0.93300	PTE TEMPORAL Theta	0.025	1	0.0238095	0.0238095	1.05	
12	9	1.00000	PTE PARIETAL Beta	0.028125	1	0.0267857	0.0267857	1.05	
3	10	1.00000	PTE FRONTAL Beta	0.03125	1	0.0297619	0.0297619	1.05	
11	11	1.00000	PTE PARIETAL Alpha	0.034375	1	0.0327381	0.0327381	1.05	
5	12	1.00000	PTE FRONTAL Alpha	0.0375	1	0.0357143	0.0357143	1.05	
10	13	1.00000	PTE PARIETAL Theta	0.040625	1	0.0386905	0.0386905	1.05	
6	14	1.00000	PTE FRONTAL Theta	0.04375	1	0.0416667	0.0416667	1.05	
9	15	1.00000	PTE PARIETAL Delta	0.046875	1	0.0446429	0.0446429	1.05	
4	16	1.00000	PTE FRONTAL Delta	0.05	1	0.047619	0.047619	1.05	

5. Inter-Regional PTE –Frequency Bands

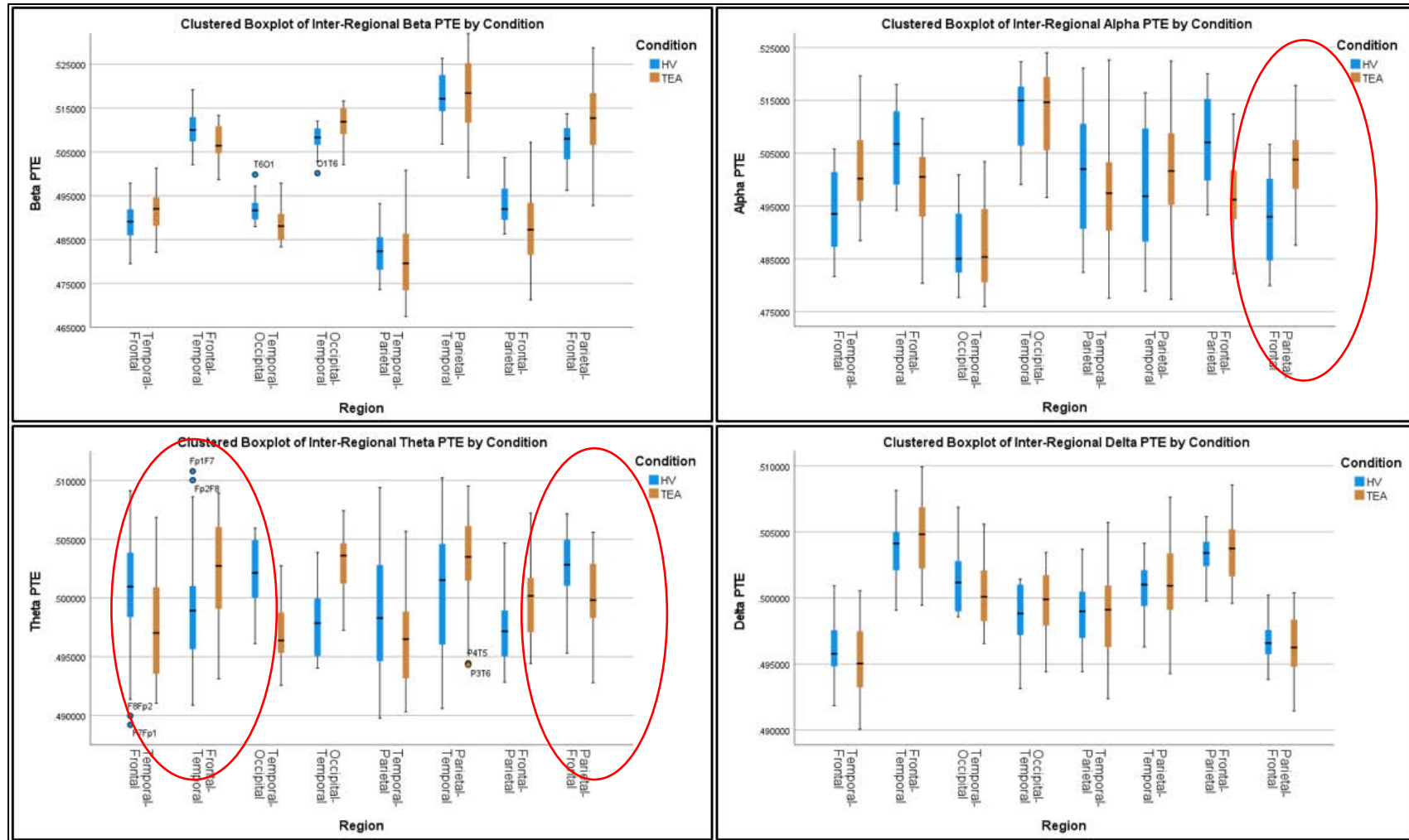
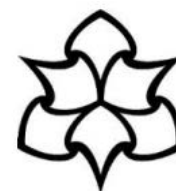


Figure 91: Boxplots for inter-regional PTE, by frequency band. Top left - beta, top right - alpha, bottom left - theta, bottom right - delta.



5.1. *Temporal to Frontal PTE*

Temporal to frontal PTE within frequency bands show a platykurtic data distribution, with the delta data having a slight negative skew, the alpha data having a slight positive skew, and the beta and theta data being relatively symmetrical around the mean (Table 140). Data descriptives for regions are as follows (Table 140, Figure 91):

- Beta frequencies - the mean is 0.4904 with a SE of 0.0006 and SD of 0.0005. The interquartile range is 0.0070, and the range is 0.0218.
- Alpha frequencies - the mean is 0.4978, with a SE of 0.0010 and SD of 0.0089. The interquartile range is 0.0117, and the range is 0.0379.
- Theta frequencies - the mean is 0.4989, with a SE of 0.0005 and SD of 0.0049. The interquartile range is 0.0085, and the range is 0.0199.
- Delta frequencies - the mean is 0.4957, with a SE of 0.0003 and SD of 0.0025. The interquartile range is 0.0037, and the range is 0.0108.

Only the TEA theta and the HV alpha data for temporal-frontal PTE do not achieve the parameters for normality. All other data meet the criteria for a normal distribution (Table 141). Therefore, the non-parametric Mann-Whitney U test was utilised for temporal-frontal theta and alpha bands, while an independent samples t-test was used to assess beta and delta PTE.

Alpha, beta, and theta bands networks between the temporal and frontal regions show significant p -values ($p < 0.001$, $p = 0.004$, $p = 0.006$ respectively). Following multiple comparisons of FDR adjustments using the two-stage sharpened method, the delta band connectivity also shows significance (the unadjusted $p = 0.095$, but the adjusted $q = 0.025$) (Table 142, Table 81). Delta and theta bands within the temporal to frontal networks have significantly lower mean/median PTE in TEA subjects compared to HV. Within the beta and alpha bands within the temporal to frontal networks, mean/median PTE is significantly higher in the TEA cohort overall (Table 143).

5.2. Frontal to Temporal PTE

Frontal to temporal PTE within frequency bands show a platykurtic data distribution, with beta and alpha data having a slight negative skew, delta data having a slight positive skew, and theta data being relatively symmetrical around the mean (Table 140). Data descriptives for regions are as follows (Table 140, Figure 91):

- Beta frequencies - the mean is 0.5085 with a SE of 0.0005 and SD of 0.0045. The interquartile range is 0.0061, and the range is 0.0205.
- Alpha frequencies - the mean is 0.5026, with a SE of 0.0011 and SD of 0.0088. The interquartile range is 0.0116, and the range is 0.0376.
- Theta frequencies - the mean is 0.5009, with a SE of 0.0006 and SD of 0.0050. The interquartile range is 0.0083, and the range is 0.0199.
- Delta frequencies - the mean is 0.5042, with a SE of 0.0003 and SD of 0.0026. The interquartile range is 0.0038, and the range is 0.0108.

Only the HV alpha data for frontal to temporal PTE do not achieve the parameters for normality. All other data meet the criteria for a normal distribution (Table 141). Therefore, the non-parametric Mann-Whitney U test was utilised for the frontal to the temporal alpha band, while an independent samples t-test was used to assess beta, theta, and delta PTE.

Beta, alpha, and theta bands networks between the frontal and temporal regions show significant p-values ($p < 0.003$, $p = 0.004$, $p = 0.012$ respectively). Following multiple comparisons of FDR adjustments using the two-stage sharpened method, the delta band connectivity also showed significance (the unadjusted $p = 0.087$, but the adjusted $q = 0.025$) (Table 142, Table 81). Delta and theta bands within the frontal to temporal networks have significantly higher mean/median PTE in TEA subjects compared to HV. Within the beta and alpha bands within the frontal to temporal networks, mean/median PTE is significantly lower in the TEA cohort overall (Table 143).

Table 140: Data descriptives for directional, inter-regional PTE between temporal and frontal regions, by frequency band

Temporal Frontal PTE within Frequency Bands					Statistics: Frontal Temporal PTE within Frequency Bands						
		Delta	Theta	Alpha	Beta			Delta	Theta	Alpha	Beta
N	Valid	80	80	80	80	N	Valid	68	68	68	68
	Missing	0	0	0	0		Missing	0	0	0	0
Mean		.49565336	.49887585	.49776103	.49042417	Mean		.50422933	.50090593	.50260538	.50852437
Std. Error of Mean		.000274656	.000547747	.001000022	.000573192	Std. Error of Mean		.000310154	.000610506	.001061352	.000545020
Median		.49551620	.49919577	.49803205	.49030791	Median		.50424014	.50068748	.50260796	.50919694
Std. Deviation		.002456596	.004899201	.008944472	.005126781	Std. Deviation		.002557594	.005034362	.008752136	.004494352
Variance		.000	.000	.000	.000	Variance		.000	.000	.000	.000
Skewness		-.112	-.015	.312	-.033	Skewness		.209	.082	-.342	-.192
Std. Error of Skewness		.269	.269	.269	.269	Std. Error of Skewness		.291	.291	.291	.291
Kurtosis		-.392	-.821	-.187	-.278	Kurtosis		-.415	-.800	-.207	-.185
Std. Error of Kurtosis		.532	.532	.532	.532	Std. Error of Kurtosis		.574	.574	.574	.574
Range		.010844	.019918	.037945	.021809	Range		.010844	.019918	.037602	.020532
Percentiles	25	.49393259	.49432224	.49112981	.48711029	Percentiles	25	.50212962	.49702255	.49761152	.50569617
	50	.49551620	.49919577	.49803205	.49030791		50	.50424014	.50068748	.50260796	.50919694
	75	.49759421	.50278919	.50283475	.49414054		75	.50592295	.50534315	.50915249	.51184238

Table 141: Tests of normality for directional, inter-regional PTE between temporal and frontal regions, by frequency band

Tests of Normality: Temporal Frontal PTE within Frequency Bands						Tests of Normality: Frontal Temporal PTE within Frequency Bands									
		Kolmogorov-Smirnov ^a			Shapiro-Wilk					Kolmogorov-Smirnov ^a			Shapiro-Wilk		
Condition		Statistic	df	Sig.	Statistic	df	Sig.	Condition		Statistic	df	Sig.	Statistic	df	Sig.
Delta	HV	.114	40	.200 [*]	.985	40	.872	Delta	HV	.136	34	.115	.981	34	.797
	TEA	.078	40	.200 [*]	.978	40	.607		TEA	.085	34	.200 [*]	.971	34	.479
Theta	HV	.140	40	.047	.968	40	.309	Theta	HV	.141	34	.083	.955	34	.178
	TEA	.143	40	.038	.945	40	.051		TEA	.108	34	.200 [*]	.956	34	.192
Alpha	HV	.137	40	.057	.924	40	.010	Alpha	HV	.138	34	.097	.925	34	.023
	TEA	.098	40	.200 [*]	.953	40	.097		TEA	.112	34	.200 [*]	.948	34	.110
Beta	HV	.085	40	.200 [*]	.970	40	.369	Beta	HV	.066	34	.200 [*]	.983	34	.848
	TEA	.076	40	.200 [*]	.976	40	.530		TEA	.095	34	.200 [*]	.943	34	.075

*. This is a lower bound of the true significance.
a. Lilliefors Significance Correction

Table 142: FDR q-values for Directional Temporal and Frontal PTE within Frequency Bands. The lower mean PTE in the TEA cohort is marked in blue.

OUTPUT AREA				Classical one-stage method*		Two-stage sharpened method [†]		
Unique rank	Order	Ascending p-values	Hypothesis name	FDR-derived significance thresholds	FDR-adjusted p-values a.k.a. q-values	Stage 1 significance thresholds	Stage 2 significance thresholds	FDR-adjusted p-values a.k.a. q-values
7	1	0.00100	Alpha TEMPORAL to FRONTAL	0.00625 *	0.008	0.0059524	0.0238095 *	0.0021
6	2	0.00300	Beta FRONTAL to TEMPORAL	0.0125 *	0.008	0.0119048	0.047619 *	0.0021
4	3	0.00400	Beta TEMPORAL to FRONTAL	0.01875 *	0.008	0.0178571	0.0714286 *	0.0021
2	4	0.00400	Alpha FRONTAL to TEMPORAL	0.025 *	0.008	0.0238095	0.0952381 *	0.0021
8	5	0.00600	Theta TEMPORAL to FRONTAL	0.03125 *	0.0096	0.0297619	0.1190476 *	0.00252
5	6	0.01200	Theta FRONTAL to TEMPORAL	0.0375 *	0.016	0.0357143	0.1428571 *	0.0042
1	7	0.08700	Delta FRONTAL to TEMPORAL	0.04375	0.095	0.0416667	0.1666667 !	0.0249375
3	8	0.09500	Delta TEMPORAL to FRONTAL	0.05	0.095	0.047619	0.1904762 !	0.0249375

Table 143: Mean and Median differences within the temporal to frontal networks, within frequency bands. The lower mean PTE in the TEA cohort is marked in blue.

Temporal Frontal PTE within Frequency Bands					Frontal Temporal PTE within Frequency Bands						
Condition		Delta	Theta	Alpha	Beta	Condition		Delta	Theta	Alpha	Beta
HV	Mean	.49611154	.50035220	.49403754	.48878916	HV	Mean	.50369807	.49939951	.50610611	.51009254
	Median	.49578217	.50096597	.49349135	.48911520		Median	.50412149	.49892450	.50672469	.51002419
TEA	Mean	.49519519	.49739951	.50148451	.49205918	TEA	Mean	.50476059	.50241235	.49910465	.50695619
	Median	.49504553	.49703507	.50020853	.49202891		Median	.50482248	.50273631	.50053135	.50642693
Total	Mean	.49565336	.49887585	.49776103	.49042417	Total	Mean	.50422933	.50090593	.50260538	.50852437
	Median	.49551620	.49919577	.49803205	.49030791		Median	.50424014	.50068748	.50260796	.50919694

There is a further effect in PTE findings within the mid-frequency bands, alpha and theta (encompassing frequencies from 4Hz-12.9Hz). When examining the strength of directional connectivity within cohorts, from temporal to frontal then frontal to temporal, networks from temporal to frontal have less PTE strength than networks in the opposite direction (frontal to temporal). This phenomenon is consistent across cohorts and frequency bands. The TEA alpha-band and HV theta-band networks, however, show a paradoxical effect where temporal-to-frontal networks have higher PTE strength compared to frontal-to-temporal traffic (Figure 92).

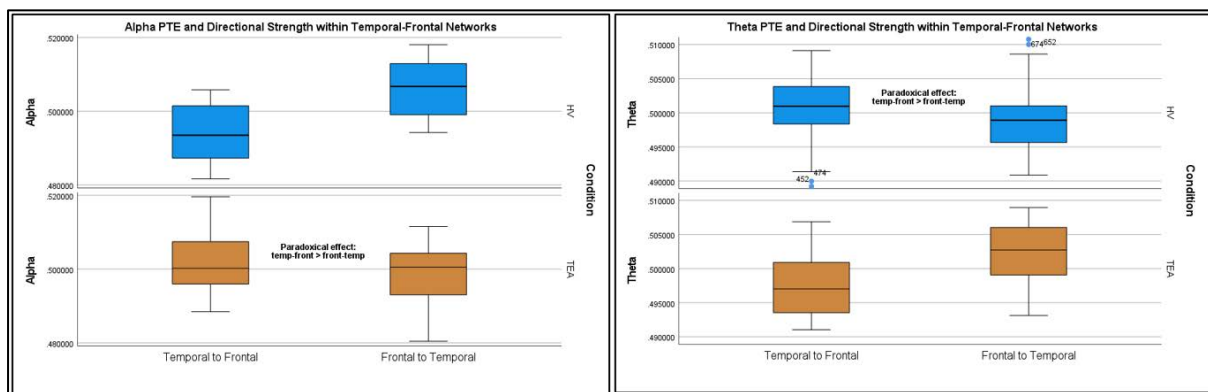


Figure 92: Paradoxical effect of higher PTE magnitude in the temporal to frontal networks, compared to frontal to temporal networks.

5.3. Inter-hemisphere Analysis of Significant Findings within Frontal and Temporal Directional PTE

Further interhemispheric analysis between the TEA and HV cohorts. This was undertaken on significant intra-regional findings, examining the left, right, and interhemispheric networks separately. An independent samples t-test was used for normally distributed datasets and the non-parametric Mann-Whitney U-test was for those not meeting the criteria for normality.

Table 144: FDR q-values for Directional Temporal and Frontal PTE within Frequency Bands (split by hemisphere, and inter-hemisphere)

OUTPUT AREA				Classical one-stage method*		Two-stage sharpened method†		
Unique rank	Order	Ascending p-values	Hypothesis name	FDR-derived significance thresholds	FDR-adjusted p-values a.k.a. q-values	Stage 1 significance thresholds	Stage 2 significance thresholds	FDR-adjusted p-values a.k.a. q-values
3	1	0.01600	Alpha FRONTAL to TEMPORAL INTER-H	0.00277778	0.116	0.0026455	0.0026455	0.1218
9	2	0.01600	Alpha TEMPORAL to FRONTAL INTER-H	0.00555556	0.116	0.005291	0.005291	0.1218
2	3	0.02600	Alpha TEMPORAL to FRONTAL LEFT	0.00833333	0.116	0.0079365	0.0079365	0.1218
8	4	0.03100	Theta TEMPORAL to FRONTAL LEFT	0.01111111	0.116	0.010582	0.010582	0.1218
16	5	0.05300	Beta TEMPORAL to FRONTAL INTER-H	0.01388889	0.116	0.0132275	0.0132275	0.1218
6	6	0.05300	Beta FRONTAL to TEMPORAL INTER-H	0.01666667	0.116	0.015873	0.015873	0.1218
7	7	0.05400	Beta TEMPORAL to FRONTAL LEFT	0.01944444	0.116	0.0185185	0.0185185	0.1218
15	8	0.05500	Beta FRONTAL to TEMPORAL LEFT	0.02222222	0.116	0.021164	0.021164	0.1218
5	9	0.05800	Alpha TEMPORAL to FRONTAL RIGHT	0.025	0.116	0.0238095	0.0238095	0.1218
11	10	0.06700	Theta FRONTAL to TEMPORAL LEFT	0.02777778	0.1206	0.026455	0.026455	0.12663
14	11	0.07900	Alpha FRONTAL to TEMPORAL LEFT	0.03055556	0.129272727	0.0291005	0.0291005	0.135736364
1	12	0.11800	Theta FRONTAL to TEMPORAL INTER-H	0.03333333	0.163384615	0.031746	0.031746	0.171553846
4	13	0.11800	Theta TEMPORAL to FRONTAL INTER-H	0.03611111	0.163384615	0.0343915	0.0343915	0.171553846
17	14	0.14600	Alpha FRONTAL to TEMPORAL RIGHT	0.03888889	0.187714286	0.037037	0.037037	0.1971
13	15	0.17900	Beta TEMPORAL to FRONTAL RIGHT	0.04166667	0.2148	0.0396825	0.0396825	0.22554
10	16	0.23400	Beta FRONTAL to TEMPORAL RIGHT	0.04444444	0.26325	0.042328	0.042328	0.2764125
18	17	0.33300	Theta TEMPORAL to FRONTAL RIGHT	0.04722222	0.352588235	0.0449735	0.0449735	0.370217647
12	18	0.40900	Theta FRONTAL to TEMPORAL RIGHT	0.05	0.409	0.047619	0.047619	0.42945

When split for hemispheric PTE network analysis (right, left, and interhemispheric networks), no hemispheric element of either temporal-to-frontal or frontal-to-temporal networking shows a significant difference between cohorts in isolation (Table 144).

5.4. Temporal to Occipital Connectivity

Temporal to occipital PTE within all frequency bands shows a platykurtic data distribution, with a positive skew (Table 145). Data descriptives for regions are as follows (Table 145, Figure 91):

- Beta frequencies - the mean is 0.4903 with a SE of 0.0007 and SD of 0.0041. The interquartile range is 0.0048, and the range is 0.0165.
- Alpha frequencies - the mean is 0.4877, with a SE of 0.0014 and SD of 0.0080. The interquartile range is 0.0131, and the range is 0.0274.
- Theta frequencies - the mean is 0.4994, with a SE of 0.0007 and SD of 0.0038. The interquartile range is 0.0066, and the range is 0.0134.
- Delta frequencies - the mean is 0.5008, with a SE of 0.0004 and SD of 0.0025. The interquartile range is 0.0039, and the range is 0.0103.

All temporal to occipital PTE data meet the criteria for a normal distribution (Table 146).

Therefore, an independent samples t-test was used to assess all frequency bands.

Theta and beta band networks between the temporal and occipital regions show significant p-values ($p < 0.001$, $p = 0.016$ respectively). These remain significant following multiple comparisons of FDR adjustments (Table 147, Table 81). Theta bands within the temporal to occipital networks have significantly lower mean/median PTE in TEA subjects compared to HV. Within the beta band, mean/median PTE is significantly higher in the TEA cohort overall (Table 148).

5.5. Occipital to Temporal Connectivity

Occipital to temporal PTE within all frequency bands show a platykurtic data distribution, with a negative skew (Table 145). Data descriptives for regions are as follows (Table 145, Figure 91):

- Beta frequencies - the mean is 0.5097 with a SE of 0.0007 and SD of 0.0041. The interquartile range is 0.0048, and the range is 0.0165.
- Alpha frequencies - the mean is 0.5123, with a SE of 0.0014 and SD of 0.0080. The interquartile range is 0.0131, and the range is 0.0274.
- Theta frequencies - the mean is 0.5006, with a SE of 0.0007 and SD of 0.0038. The interquartile range is 0.0066, and the range is 0.0134.
- Delta frequencies - the mean is 0.4992, with a SE of 0.0004 and SD of 0.0025. The interquartile range is 0.0039, and the range is 0.0103.

All occipital to temporal PTE data meet the criteria for a normal distribution (Table 146). Therefore, an independent samples t-test was used to assess all frequency bands.

Theta and beta band networks between the occipital and temporal regions show significant p-values ($p < 0.001$, $p = 0.016$ respectively). These remain significant following multiple comparisons of FDR adjustments (Table 147, Table 81). Theta bands within the occipital to temporal networks have significantly higher mean/median PTE in TEA subjects compared to HV. Within the beta band, mean/median PTE is significantly lower in the TEA cohort overall (Table 148).

Table 145: Data descriptives for directional, inter-regional PTE between temporal and occipital regions, by frequency band.

Statistics: Temporal Occipital PTE within Frequency Bands						Statistics: Occipital Temporal PTE within Frequency Bands					
		Delta	Theta	Alpha	Beta			Delta	Theta	Alpha	Beta
N	Valid	32	32	32	32	N	Valid	32	32	32	32
	Missing	0	0	0	0		Missing	0	0	0	0
Mean		.50080606	.49944067	.48773387	.49028947	Mean		.49919394	.50055933	.51226613	.50971053
Std. Error of Mean		.000447779	.000673732	.001414300	.000723060	Std. Error of Mean		.000447779	.000673732	.001414300	.000723060
Median		.50079312	.49933737	.48504402	.49052203	Median		.49920688	.50066263	.51495598	.50947797
Std. Deviation		.002533018	.003811201	.008000491	.004090245	Std. Deviation		.002533018	.003811201	.008000491	.004090245
Variance		.000	.000	.000	.000	Variance		.000	.000	.000	.000
Skewness		.513	.265	.465	.296	Skewness		-.513	-.265	-.465	-.296
Std. Error of Skewness		.414	.414	.414	.414	Std. Error of Skewness		.414	.414	.414	.414
Kurtosis		-.206	-1.064	-1.018	-1.102	Kurtosis		-.206	-1.064	-1.018	-1.102
Std. Error of Kurtosis		.809	.809	.809	.809	Std. Error of Kurtosis		.809	.809	.809	.809
Range		.010301	.013394	.027388	.016468	Range		.010301	.013394	.027388	.016468
Percentiles	25	.49882366	.49603047	.48103179	.48750187	Percentiles	25	.49728753	.49735409	.50585751	.50774292
	50	.50079312	.49933737	.48504402	.49052203		50	.49920688	.50066263	.51495598	.50947797
	75	.50271247	.50264591	.49414249	.49225708		75	.50117634	.50396953	.51896821	.51249813

Table 146: Tests of normality for directional, inter-regional PTE between temporal and occipital regions, by frequency band.

Tests of Normality: Temporal Occipital PTE within Frequency Bands						Tests of Normality: Occipital Temporal PTE within Frequency Bands									
		Kolmogorov-Smirnov ^a			Shapiro-Wilk					Kolmogorov-Smirnov ^a			Shapiro-Wilk		
Condition		Statistic	df	Sig.	Statistic	df	Sig.	Condition		Statistic	df	Sig.	Statistic	df	Sig.
Delta	HV	.140	16	.200*	.912	16	.123	Delta	HV	.140	16	.200*	.912	16	.123
	TEA	.121	16	.200*	.963	16	.725		TEA	.121	16	.200*	.963	16	.725
Theta	HV	.194	16	.109	.910	16	.115	Theta	HV	.194	16	.109	.910	16	.115
	TEA	.152	16	.200*	.955	16	.570		TEA	.152	16	.200*	.955	16	.570
Alpha	HV	.203	16	.076	.918	16	.154	Alpha	HV	.203	16	.076	.918	16	.154
	TEA	.182	16	.164	.921	16	.178		TEA	.182	16	.164	.921	16	.178
Beta	HV	.216	16	.045	.917	16	.149	Beta	HV	.216	16	.045	.917	16	.149
	TEA	.139	16	.200*	.937	16	.314		TEA	.139	16	.200*	.937	16	.314

*. This is a lower bound of the true significance.
a. Lilliefors Significance Correction

Table 147: FDR q-values for Directional Temporal and Occipital PTE within Frequency Bands. The lower mean PTE in the TEA cohort is marked in blue.

OUTPUT AREA				Classical one-stage method*			Two-stage sharpened method†			Graphically sharpened method‡		
Unique rank	Order	Ascending p-values	Hypothesis name	FDR-derived significance thresholds	FDR-adjusted p-values a.k.a. q-values	Stage 1 significance thresholds	Stage 2 significance thresholds	FDR-adjusted p-values a.k.a. q-values	Point estimates of no. of H ₀ s	Best estimate	FDR-derived significance thresholds	FDR-adjusted p-values a.k.a. q-values
6	1	0.00100	Theta TEMPORAL to OCCIPITAL	0.00625*	0.004	0.0059524	0.0119048*	0.0021	8.0000		0.00833333*	0.003
2	2	0.00100	Theta OCCIPITAL to TEMPORAL	0.0125*	0.004	0.0119048	0.0238095*	0.0021	7.0070		0.01666667*	0.003
8	3	0.01600	Beta TEMPORAL to OCCIPITAL	0.01875*	0.032	0.0178571	0.0357143*	0.0168	6.0976		0.025*	0.024
4	4	0.01600	Beta OCCIPITAL to TEMPORAL	0.025*	0.032	0.0238095	0.047619*	0.0168	5.0813		0.03333333*	0.024
5	5	0.24000	Delta TEMPORAL to OCCIPITAL	0.03125	0.32	0.0297619	0.0595238	0.168	5.2632	True	0.04166667	0.24
1	6	0.24000	Delta OCCIPITAL to TEMPORAL	0.0375	0.32	0.0357143	0.0714286	0.168	3.9474		0.05	0.24
7	7	0.85700	Alpha TEMPORAL to OCCIPITAL	0.04375	0.857	0.0416667	0.0833333	0.449925	8.0000		0.05833333	0.64275
3	8	0.85700	Alpha OCCIPITAL to TEMPORAL	0.05	0.857	0.047619	0.0952381	0.449925	6.9930		0.06666667	0.64275

Table 148: Mean and Median differences within the temporal to occipital networks, within frequency bands. The lower mean PTE in the TEA cohort is marked in blue.

Temporal Occipital PTE within Frequency Bands						Occipital Temporal PTE within Frequency Bands					
Condition		Delta	Theta	Alpha	Beta	Condition		Delta	Theta	Alpha	Beta
HV	Mean	.50133921	.50190027	.48799551	.49199255	HV	Mean	.49866079	.49809973	.51200449	.50800745
	Median	.50117265	.50213435	.48504402	.49167377		Median	.49882735	.49786565	.51495598	.50832623
TEA	Mean	.50027291	.49698106	.48747223	.48858640	TEA	Mean	.49972709	.50301894	.51252777	.51141360
	Median	.50009853	.49638728	.48537416	.48810467		Median	.49990147	.50361272	.51462584	.51189533
Total	Mean	.50080606	.49944067	.48773387	.49028947	Total	Mean	.49919394	.50055933	.51226613	.50971053
	Median	.50079312	.49933737	.48504402	.49052203		Median	.49920688	.50066263	.51495598	.50947797

5.6. *Inter-hemisphere Analysis of Significant Findings within Occipital and Temporal Directional PTE*

Further interhemispheric analysis between the TEA and HV cohorts. This was undertaken on significant inter-regional findings, examining the left, right, and interhemispheric networks separately. An independent samples t-test was used for normally distributed datasets and the non-parametric Mann-Whitney U-test was for those not meeting the criteria for normality.

Table 149: FDR q-values for Directional Temporal and Occipital PTE within Frequency Bands (split by hemisphere, and inter-hemisphere). The lower mean PTE in the TEA cohort is marked in blue.

OUTPUT AREA				Classical one-stage method*		Two-stage sharpened method†		
Unique rank	Order	Ascending p-values	Hypothesis name	FDR-derived significance thresholds	FDR-adjusted p-values a.k.a. q-values	Stage 1 significance thresholds	Stage 2 significance thresholds	FDR-adjusted p-values a.k.a. q-values
2	1	0.00500	Theta TEMPORAL to OCCIPITAL LEFT	0.00416667 *	0.03	0.0039683	0.005291 *	0.023625
8	2	0.00500	Theta OCCIPITAL to TEMPORAL LEFT	0.00833333 *	0.03	0.0079365	0.010582 *	0.023625
4	3	0.01000	Theta TEMPORAL to OCCIPITAL INTER-H	0.0125 *	0.03	0.0119048	0.015873 *	0.023625
6	4	0.01000	Theta OCCIPITAL to TEMPORAL INTER-H	0.01666667 *	0.03	0.015873	0.021164 *	0.023625
11	5	0.04000	Beta TEMPORAL to OCCIPITAL LEFT	0.02083333	0.08	0.0198413	0.026455	0.063
10	6	0.04000	Beta OCCIPITAL to TEMPORAL LEFT	0.025	0.08	0.0238095	0.031746	0.063
1	7	0.11500	Theta TEMPORAL to OCCIPITAL RIGHT	0.02916667	0.1725	0.0277778	0.037037	0.13584375
7	8	0.11500	Theta OCCIPITAL to TEMPORAL RIGHT	0.03333333	0.1725	0.031746	0.042328	0.13584375
3	9	0.18800	Beta TEMPORAL to OCCIPITAL INTER-H	0.0375	0.2256	0.0357143	0.047619	0.17766
5	10	0.18800	Beta OCCIPITAL to TEMPORAL INTER-H	0.04166667	0.2256	0.0396825	0.0529101	0.17766
12	11	0.25300	Beta OCCIPITAL to TEMPORAL RIGHT	0.04583333	0.256	0.0436508	0.0582011	0.2016
9	12	0.25600	Beta TEMPORAL to OCCIPITAL RIGHT	0.05	0.256	0.047619	0.0634921	0.2016

When split for hemispheric PTE network analysis (right, left, and interhemispheric networks), theta PTE values across the left and inter-hemisphere temporal to occipital, and occipital to temporal networks show a significant difference between cohorts. Temporal to occipital connections within the left and inter-hemisphere networks have significantly lower PTE in the TEA group compared to the healthy. In contrast, occipital to temporal connections within the left and inter-hemisphere networks have significantly higher PTE in the TEA group compared to healthy. Other previously significant PTE values do not show any significant differences between TEA and HV cohorts, for isolated hemispheric elements of either temporal to occipital, or the occipital to temporal networks (Table 149).

5.7. *Temporal to Parietal Connectivity*

Temporal to parietal PTE within all frequency bands show a platykurtic data distribution, with a slight positive skew (

Table 150). Data descriptives for regions are as follows (Table 150, Figure 91):

- Beta frequencies - the mean is 0.4812 with a SE of 0.0007 and SD of 0.0070. The interquartile range is 0.0102, and the range is 0.0334.
- Alpha frequencies - the mean is 0.4993, with a SE of 0.0010 and SD of 0.0101. The interquartile range is 0.0163, and the range is 0.0451.
- Theta frequencies - the mean is 0.4979, with a SE of 0.0005 and SD of 0.0050. The interquartile range is 0.0079, and the range is 0.0196.
- Delta frequencies - the mean is 0.4989, with a SE of 0.0003 and SD of 0.0030. The interquartile range is 0.0042, and the range is 0.0133.

Only the TEA theta and beta data for temporal-parietal PTE do not achieve the parameters for normality. All other data meet the criteria for a normal distribution (Table 151).

Therefore, the non-parametric Mann-Whitney U test was utilised for temporal-parietal theta and beta bands, while an independent samples t-test was used to assess alpha and delta PTE.

The theta temporal to parietal PTE shows significance at $p=0.049$. However, following multiple comparisons of FDR adjustments using the two-stage sharpened method, the resulting q -value is not significant. There are no significant differences between TEA and HV cohorts within the temporal to parietal networks, within the beta, alpha, theta, or delta frequency bands (Table 152).

5.8. *Parietal to Temporal Connectivity*

Parietal to temporal PTE within all frequency bands show a platykurtic data distribution, with a negative skew (Table 150). Data descriptives for regions are as follows (Table 150, Figure 91):

- Beta frequencies - the mean is 0.5178 with a SE of 0.0008 and SD of 0.0071. The interquartile range is 0.0104, and the range is 0.0334.
- Alpha frequencies - the mean is 0.4997, with a SE of 0.0012 and an SD of 0.0104. The interquartile range is 0.0179, and the range is 0.0196.
- Theta frequencies - the mean is 0.5018, with a SE of 0.0006 and SD of 0.0050. The interquartile range is 0.0068, and the range is 0.0196.
- Delta frequencies - the mean is 0.5008, with a SE of 0.0003 and SD of 0.0028. The interquartile range is 0.0039, and the range is 0.0133.

Only the TEA theta and the HV alpha data for parietal to temporal PTE do not achieve the parameters for normality. All other data meet the criteria for a normal distribution (Table 151). Therefore, the non-parametric Mann-Whitney U test was utilised for parietal to temporal alpha and theta bands, while an independent samples t-test was used to assess beta and delta PTE.

The theta parietal to temporal PTE shows significance at $p=0.011$. However, following multiple comparisons of FDR adjustments using the two-stage sharpened method, the resulting q -value is not significant. There are no significant differences between TEA and HV cohorts within the parietal to temporal networks, within the beta, alpha, theta, or delta frequency bands (Table 152).

Table 150: Data descriptives for directional, inter-regional PTE between temporal and parietal regions, by frequency band

Statistics: Temporal Parietal PTE within Frequency Bands					Statistics: Parietal Temporal PTE within Frequency Bands						
		Delta	Theta	Alpha	Beta			Delta	Theta	Alpha	Beta
N	Valid	96	96	96	96	N	Valid	72	72	72	72
	Missing	0	0	0	0		Missing	0	0	0	0
Mean		.49894654	.49785357	.49931609	.48119217	Mean		.50085706	.50180165	.49968721	.51781201
Std. Error of Mean		.000308976	.000509940	.001030091	.000710650	Std. Error of Mean		.000330210	.000584767	.001229864	.000831615
Median		.49908369	.49746078	.50011678	.48084179	Median		.50095493	.50235871	.49933787	.51773688
Std. Deviation		.003027331	.004996375	.010092788	.006962918	Std. Deviation		.002801925	.004961915	.010435741	.007056486
Variance		.000	.000	.000	.000	Variance		.000	.000	.000	.000
Skewness		.128	.504	.177	.265	Skewness		-.151	-.572	-.137	-.236
Std. Error of Skewness		.246	.246	.246	.246	Std. Error of Skewness		.283	.283	.283	.283
Kurtosis		-.323	-.651	-.717	-.225	Kurtosis		-.070	-.481	-.849	-.324
Std. Error of Kurtosis		.488	.488	.488	.488	Std. Error of Kurtosis		.559	.559	.559	.559
Range		.013332	.019634	.045063	.033386	Range		.013332	.019634	.045063	.033386
Percentiles	25	.49662781	.49378105	.49059015	.47605357	Percentiles	25	.49918888	.49859124	.49148446	.51288942
	50	.49908369	.49746078	.50011678	.48084179		50	.50095493	.50235871	.49933787	.51773688
	75	.50081112	.50166263	.50689232	.48629273		75	.50312820	.50544034	.50940985	.52323214

Table 151: Tests of normality for directional, inter-regional PTE between temporal and parietal regions, by frequency band

Tests of Normality: Temporal Parietal PTE within Frequency Bands							Tests of Normality: Parietal Temporal PTE within Frequency Bands								
		Kolmogorov-Smirnov ^a			Shapiro-Wilk					Kolmogorov-Smirnov ^a			Shapiro-Wilk		
Condition	Statistic	df	Sig.	Statistic	df	Sig.	Condition	Statistic	df	Sig.	Statistic	df	Sig.		
Delta	HV	.076	48	.200*	.973	48	.342	Delta	HV	.099	36	.200*	.956	36	.163
	TEA	.074	48	.200*	.968	48	.208		TEA	.093	36	.200*	.976	36	.611
Theta	HV	.091	48	.200*	.960	48	.100	Theta	HV	.122	36	.193	.959	36	.201
	TEA	.115	48	.140	.926	48	.005		TEA	.140	36	.074	.926	36	.019
Alpha	HV	.116	48	.119	.954	48	.060	Alpha	HV	.147	36	.047	.933	36	.030
	TEA	.071	48	.200*	.990	48	.956		TEA	.063	36	.200*	.989	36	.966
Beta	HV	.083	48	.200*	.980	48	.578	Beta	HV	.103	36	.200*	.969	36	.412
	TEA	.106	48	.200*	.950	48	.041		TEA	.094	36	.200*	.966	36	.325

*. This is a lower bound of the true significance.
a. Lilliefors Significance Correction

Table 152: FDR q-values for Directional Temporal and Parietal PTE within Frequency Bands. The lower mean PTE in the TEA cohort is marked in blue.

OUTPUT AREA				Classical one-stage method ^a		Two-stage sharpened method ^b			Graphically sharpened method ^c			
Unique rank	Order	Ascending p-values	Hypothesis name	FDR-derived significance thresholds	FDR-adjusted p-values a.k.a. q-values	Stage 1 significance thresholds	Stage 2 significance thresholds	FDR-adjusted p-values a.k.a. q-values	Point estimates of no. of H ₀ s	Best estimate	FDR-derived significance thresholds	FDR-adjusted p-values a.k.a. q-values
				6	1	0.01100	Theta PARIETAL to TEMPORAL	0.00625	0.088	0.0059524	0.0059524	0.0924
1	2	0.04900	Theta TEMPORAL to PARIETAL	0.0125	0.196	0.0119048	0.0119048	0.2058	7.3607		0.0125	0.196
4	3	0.08500	Alpha TEMPORAL to PARIETAL	0.01875	0.226666667	0.0178571	0.0178571	0.238	6.5574		0.01875	0.226666667
8	4	0.14600	Alpha PARIETAL to TEMPORAL	0.025	0.292	0.0238095	0.0238095	0.3066	5.8548		0.025	0.292
7	5	0.20500	Beta TEMPORAL to PARIETAL	0.03125	0.328	0.0297619	0.0297619	0.3444	5.0314		0.03125	0.328
2	6	0.59500	Delta PARIETAL to TEMPORAL	0.0375	0.793333333	0.0357143	0.0357143	0.833	7.4074	True	0.0375	0.793333333
3	7	0.72700	Delta TEMPORAL to PARIETAL	0.04375	0.830857143	0.0416667	0.0416667	0.8724	7.3260		0.04375	0.830857143
5	8	0.90100	Beta PARIETAL to TEMPORAL	0.05	0.901	0.047619	0.047619	0.94605	8.0000		0.05	0.901

5.9. *Frontal to Parietal PTE*

Frontal to parietal PTE within all frequency bands show a platykurtic data distribution, with alpha, delta and theta data showing a slight positive skew, and beta data a slight negative skew (Table 153). Data descriptives for regions are as follows (Table 153, Figure 91):

- Beta frequencies - the mean is 0.4907 with a SE of 0.0010 and SD of 0.0074. The interquartile range is 0.0099, and the range is 0.0360.
- Alpha frequencies - the mean is 0.5021, with a SE of 0.0012 and SD of 0.0092. The interquartile range is 0.0127, and the range is 0.0378.
- Theta frequencies - the mean is 0.4986, with a SE of 0.0004 and SD of 0.0034. The interquartile range is 0.0055, and the range is 0.0144.
- Delta frequencies - the mean is 0.5035, with a SE of 0.0003 and SD of 0.0020. The interquartile range is 0.0024, and the range is 0.0089.

All data meet the criteria for a normal distribution (Table 154). Therefore, the independent samples t-test was utilised for frontal-parietal PTE analysis.

Beta, alpha, and theta parietal to frontal PTE show a significant difference between cohorts ($p=0.008$, $p<0.001$, $p=0.003$ respectively). These all remain significant following multiple comparisons of FDR adjustments (Table 155). TEA beta and alpha band PTE within the parietal to frontal networks are significantly lower than those of HV participants, whilst theta frequency PTE is significantly higher in TEA.

5.10. *Parietal to Frontal PTE*

Parietal to frontal PTE within all frequency bands show a platykurtic data distribution, with alpha, theta and delta bands having a slight negative skew and the beta data a slight positive skew (Table 153). Data descriptives for regions are as follows (Table 153, Figure 91):

- Beta frequencies - the mean is 0.5093 with a SE of 0.0010 and SD of 0.0074. The interquartile range is 0.0099, and the range is 0.0360.
- Alpha frequencies - the mean is 0.4979, with a SE of 0.0012 and SD of 0.0092. The interquartile range is 0.0128, and the range is 0.0378.

- Theta frequencies - the mean is 0.5014, with a SE of 0.0004 and SD of 0.0034. The interquartile range is 0.0055, and the range is 0.0144.
- Delta frequencies - the mean is 0.4965, with a SE of 0.0003 and SD of 0.0020. The interquartile range is 0.0024, and the range is 0.0089.

All data meet the criteria for a normal distribution (Table 154). Therefore, the independent samples t-test was utilised for frontal-parietal PTE analysis.

Beta, alpha, and theta parietal to frontal PTE show a significant difference between cohorts ($p=0.008$, $p<0.001$, $p=0.003$ respectively). These all remain significant following multiple comparisons of FDR adjustments (Table 155). TEA beta and alpha band PTE within the parietal to frontal networks are significantly higher than those of HV participants, whilst theta frequency PTE is significantly lower in TEA.

Table 153: Data descriptives for directional, inter-regional PTE between frontal and parietal regions, by frequency band

Statistics: Frontal-Parietal PTE						Statistics: Parietal-Frontal PTE											
N	Delta		Theta		Alpha		Beta		N	Delta		Theta		Alpha		Beta	
	Valid	Missing	Valid	Missing	Valid	Missing	Valid	Missing		Valid	Missing	Valid	Missing	Valid	Missing	Valid	Missing
	60	0	60	0	60	0	60	0	60	0	60	0	60	0	60	0	60
Mean	.50345833		.49856849		.50212700		.49070883		.49654167		.50143151		.49787300		.50929117		.50929117
Std. Error of Mean	.000262456		.000434676		.001193304		.000958651		.000262456		.000434676		.001193304		.000958651		.000958651
Median	.50344282		.49791038		.50139241		.49059742		.49655718		.50208962		.49860759		.50940258		.50940258
Std. Deviation	.002032974		.003366983		.009243294		.007425680		.002032974		.003366983		.009243294		.007425680		.007425680
Skewness	.271		.469		.108		-.305		-.271		-.469		-.108		.305		.305
Std. Error of Skewness	.309		.309		.309		.309		.309		.309		.309		.309		.309
Kurtosis	.049		-.477		-.582		.205		.049		-.477		-.582		.205		.205
Std. Error of Kurtosis	.608		.608		.608		.608		.608		.608		.608		.608		.608
Range	.008945		.014400		.037842		.035957		.008945		.014400		.037842		.035957		.035957
Percentiles	25	.50207448	49582645	.49551942	.48628324				25	.49552731	.49868383	.49167471	.50380810				
	50	.50344282	.49791038	.50139241	.49059742				50	.49655718	.50208962	.49860759	.50940258				
	75	.50447269	.50131617	.50832529	.49619190				75	.49792552	.50417355	.50448058	.51371676				

Table 154: Tests of normality for directional, inter-regional PTE between frontal and parietal regions, by frequency band

Tests of Normality: Frontal-Parietal PTE								Tests of Normality: Parietal-Frontal PTE							
Condition	Statistic	Kolmogorov-Smirnov ^a			Shapiro-Wilk			Condition	Statistic	Kolmogorov-Smirnov ^a			Shapiro-Wilk		
		df	Sig.		Statistic	df	Sig.			df	Sig.		Statistic	df	Sig.
Delta	HV	.114	30	.200*	.973	30	.613	Delta	HV	.114	30	.200*	.973	30	.613
	TEA	.082	30	.200*	.965	30	.412		TEA	.082	30	.200*	.965	30	.412
Theta	HV	.088	30	.200*	.965	30	.421	Theta	HV	.088	30	.200*	.965	30	.421
	TEA	.132	30	.193	.958	30	.269		TEA	.132	30	.193	.958	30	.269
Alpha	HV	.156	30	.062	.940	30	.089	Alpha	HV	.156	30	.062	.940	30	.089
	TEA	.089	30	.200*	.979	30	.809		TEA	.089	30	.200*	.979	30	.809
Beta	HV	.133	30	.186	.947	30	.144	Beta	HV	.133	30	.186	.947	30	.144
	TEA	.088	30	.200*	.979	30	.798		TEA	.088	30	.200*	.979	30	.798
AllFreq	HV	.193	30	.006	.914	30	.019	AllFreq	HV	.193	30	.006	.914	30	.019
	TEA	.159	30	.052	.953	30	.198		TEA	.159	30	.052	.953	30	.198

*. This is a lower bound of the true significance.
a. Lilliefors Significance Correction

Table 155: FDR q-values for Directional Frontal and Parietal PTE within Frequency Bands. The lower mean PTE in the TEA cohort is marked in blue.

OUTPUT AREA		Multiple comparisons using FDRs		Classical one-stage method*		Two-stage sharpened method†		Graphically sharpened method‡				
Unique rank	Order	Ascending p-values	Hypothesis	FDR-derived significance thresholds	FDR-adjusted p-values a.k.a. q-values	Stage 1 significance thresholds	Stage 2 significance thresholds	FDR-adjusted p-values a.k.a. q-values	Point estimates of no. of H ₀ s	Best estimate	FDR-derived significance thresholds	FDR-adjusted p-values a.k.a. q-values
8	1	0.00100	Alpha PARIETAL to FRONTAL	0.00625 *	0.004	0.0059524	0.0238095 *	0.00105	8.0000		0.0125 *	0.002
4	2	0.00100	Alpha FRONTAL to PARIETAL	0.0125 *	0.004	0.0119048	0.047619 *	0.00105	7.0070		0.025 *	0.002
2	3	0.00300	Theta PARIETAL to FRONTAL	0.01875 *	0.006	0.0178571	0.0714286 *	0.001575	6.0181		0.0375 *	0.003
5	4	0.00300	Theta FRONTAL to PARIETAL	0.025 *	0.006	0.0238095	0.0952381 *	0.001575	5.0150		0.05 *	0.003
7	5	0.00800	Beta FRONTAL to PARIETAL	0.03125 *	0.012	0.0297619	0.1190476 *	0.00315	4.0323		0.0625 *	0.006
3	6	0.00900	Beta PARIETAL to FRONTAL	0.0375 *	0.012	0.0357143	0.1428571 *	0.00315	3.0272		0.075 *	0.006
1	7	0.36500	Delta PARIETAL to FRONTAL	0.04375	0.365	0.0416667	0.1666667	0.0958125	3.1496	True	0.0875	0.1825
6	8	0.36500	Delta FRONTAL to PARIETAL	0.05	0.365	0.047619	0.1904762	0.0958125	1.5748		0.1	0.1825

5.11. Inter-hemisphere analysis of Significant Findings within Frontal and Parietal directional PTE

Further interhemispheric analysis between the TEA and HV cohorts. This was undertaken on significant inter-regional findings, examining the left, right, and interhemispheric networks separately. An independent samples t-test was used for normally distributed datasets and the non-parametric Mann-Whitney U-test was for those not meeting the criteria for normality.

Table 156: FDR q-values for Directional Frontal and Parietal PTE within Frequency Bands (split by hemisphere, and inter-hemisphere).

OUTPUT AREA		Multiple comparisons using FDRs		Classical one-stage method*		Two-stage sharpened method†		Graphically sharpened method‡				
Unique rank	Order	Ascending p-values	Hypothesis name	FDR-derived significance thresholds	FDR-adjusted p-values a.k.a. q-values	Stage 1 significance thresholds	Stage 2 significance thresholds	FDR-adjusted p-values a.k.a. q-values	Point estimates of no. of H ₀ s	Best estimate	FDR-derived significance thresholds	FDR-adjusted p-values a.k.a. q-values
6	1	0.00700	Alpha PARIETAL to FRONTAL LEFT	0.00277778 *	0.045	0.0026455	0.0028011 *	0.044625	18.0000		0.005 *	0.025
14	2	0.00700	Alpha FRONTAL to PARIETAL LEFT	0.00555556 *	0.045	0.005291	0.0056022 *	0.044625	17.1198		0.01 *	0.025
16	3	0.01000	Alpha PARIETAL to FRONTAL RIGHT	0.00833333 *	0.045	0.0079365	0.0084034 *	0.044625	16.1616		0.015 *	0.025
2	4	0.01000	Alpha FRONTAL to PARIETAL RIGHT	0.01111111 *	0.045	0.010582	0.0112045 *	0.044625	15.1515		0.02 *	0.025
4	5	0.02700	Theta PARIETAL to FRONTAL LEFT	0.01388889	0.081	0.0132275	0.0140056	0.080325	14.3885		0.025 *	0.045
8	6	0.02700	Theta FRONTAL to PARIETAL LEFT	0.01666667	0.081	0.015873	0.0168067	0.080325	13.3607		0.03 *	0.045
10	7	0.05900	Alpha PARIETAL to FRONTAL INTER-H	0.01944444	0.1206	0.0185185	0.0196078	0.119595	12.7524		0.035	0.067
12	8	0.05900	Alpha FRONTAL to PARIETAL INTER-H	0.02222222	0.1206	0.021164	0.022409	0.119595	11.6897		0.04	0.067
18	9	0.06700	Beta PARIETAL to FRONTAL LEFT	0.025	0.1206	0.0238095	0.0252101	0.119595	10.7181		0.045	0.067
5	10	0.06700	Beta FRONTAL to PARIETAL LEFT	0.02777778	0.1206	0.026455	0.0280112	0.119595	9.6463		0.05	0.067
13	11	0.18900	Beta PARIETAL to FRONTAL RIGHT	0.03055556	0.264857143	0.0291005	0.0308123	0.26265	9.8644	True	0.055	0.147142857
15	12	0.18900	Beta FRONTAL to PARIETAL RIGHT	0.03333333	0.264857143	0.031746	0.0336134	0.26265	8.6313		0.06	0.147142857
1	13	0.20600	Theta PARIETAL to FRONTAL RIGHT	0.03611111	0.264857143	0.0343915	0.0364146	0.26265	7.5567		0.065	0.147142857
3	14	0.20600	Theta FRONTAL to PARIETAL RIGHT	0.03888889	0.264857143	0.037037	0.0392157	0.26265	6.2972		0.07	0.147142857
7	15	0.32800	Theta PARIETAL to FRONTAL INTER-H	0.04166667	0.369	0.0396825	0.0420168	0.365925	5.9524		0.075	0.205
9	16	0.32800	Theta FRONTAL to PARIETAL INTER-H	0.04444444	0.369	0.042328	0.0448179	0.365925	4.4643		0.08	0.205
11	17	0.58000	Beta PARIETAL to FRONTAL INTER-H	0.04722222	0.58	0.0449735	0.047619	0.575166667	4.7619		0.085	0.322222222
17	18	0.58000	Beta FRONTAL to PARIETAL INTER-H	0.05	0.58	0.047619	0.0504202	0.575166667	2.3810		0.09	0.322222222

There are significant differences between TEA and HV cohorts within alpha PTE in both frontal to parietal, and parietal to frontal networks on the left (in both cases $p=0.007$), and on the right (in both cases $p=0.010$). Theta frequency PTE within the left frontal to parietal, and parietal to frontal connectivity also shows a significant difference between cohorts ($p=0.027$). All remain significant following FDR adjustment using the graphically sharpened method (Table 156). Alpha frontal to parietal PTE is significantly lower in TEA than HV, and in contrast, alpha parietal to frontal PTE is significantly higher in TEA. Theta frontal to parietal PTE is significantly higher in TEA than HV, and in contrast, alpha parietal to frontal PTE is significantly lower in TEA.